

Award Number: W81XWH-06-1-0317

TITLE: Genetic and Environmental Pathways in Type 1 Diabetes Complication

PRINCIPAL INVESTIGATOR: Massimo Trucco, M.D.

CONTRACTING ORGANIZATION: Children's Hospital of Pittsburgh  
Pittsburgh, PA 15213

REPORT DATE: June 2008

TYPE OF REPORT: Annual

PREPARED FOR: U.S. Army Medical Research and Materiel Command  
Fort Detrick, Maryland 21702-5012

DISTRIBUTION STATEMENT: Approved for Public Release;  
Distribution Unlimited

The views, opinions and/or findings contained in this report are those of the author(s) and should not be construed as an official Department of the Army position, policy or decision unless so designated by other documentation.

REPORT DOCUMENTATION PAGE				Form Approved OMB No. 0704-0188	
Public reporting burden for this collection of information is estimated to average 1 hour per response, including the time for reviewing instructions, searching existing data sources, gathering and maintaining the data needed, and completing and reviewing this collection of information. Send comments regarding this burden estimate or any other aspect of this collection of information, including suggestions for reducing this burden to Department of Defense, Washington Headquarters Services, Directorate for Information Operations and Reports (0704-0188), 1215 Jefferson Davis Highway, Suite 1204, Arlington, VA 22202-4302. Respondents should be aware that notwithstanding any other provision of law, no person shall be subject to any penalty for failing to comply with a collection of information if it does not display a currently valid OMB control number. <b>PLEASE DO NOT RETURN YOUR FORM TO THE ABOVE ADDRESS.</b>					
1. REPORT DATE (DD-MM-YYYY) 01/06/08		2. REPORT TYPE Annual		3. DATES COVERED (From - To) 1 June 2007 – 31 May 2008	
4. TITLE AND SUBTITLE  Genetic and Environmental Pathways in Type 1 Diabetes Complication				5a. CONTRACT NUMBER	
				5b. GRANT NUMBER W81XWH-06-1-0317	
				5c. PROGRAM ELEMENT NUMBER	
6. AUTHOR(S) Massimo Trucco, M.D.  E-Mail: <a href="mailto:mnt@pitt.edu">mnt@pitt.edu</a>				5d. PROJECT NUMBER	
				5e. TASK NUMBER	
				5f. WORK UNIT NUMBER	
7. PERFORMING ORGANIZATION NAME(S) AND ADDRESS(ES)  Children's Hospital of Pittsburgh Pittsburgh, PA 15213				8. PERFORMING ORGANIZATION REPORT NUMBER	
9. SPONSORING / MONITORING AGENCY NAME(S) AND ADDRESS(ES) U.S. Army Medical Research and Materiel Command Fort Detrick, Maryland 21702-5012				10. SPONSOR/MONITOR'S ACRONYM(S)	
				11. SPONSOR/MONITOR'S REPORT NUMBER(S)	
12. DISTRIBUTION / AVAILABILITY STATEMENT Approved for Public Release; Distribution Unlimited					
13. SUPPLEMENTARY NOTES					
14. ABSTRACT: Type 1 diabetes is considered an autoimmune disease characterized by the presence of inflammatory cells in the islets of Langerhans. These cells are T lymphocytes, considered responsible for the destruction of the insulin producing beta-cells present in the islets. When the majority of the beta cells are dead, the disease presents, frequently with an abrupt and clinically serious onset. Hyperglycemia can be induced by chemical destruction of the insulin producing beta cells in monkeys. Following diabetes induction, histological examination of the pancreas shows islet cells with virtually null or sporadic immuno-reactivity for insulin. In our pilot studies, monkeys (macaca fascicularis) were rendered diabetic prior to receiving a xenogeneic porcine islet transplantation. A recovery of endogenous C-peptide production was observed in monkey recipients of steadily functioning pig islet grafts, concurrently to improved metabolic control. Histological analysis of the pancreatic tissue of these monkeys showed: increased proliferative (Ki67+) activity in the pancreas; small aggregates of insulin positive cells detached from the pre-existing "damaged" islets; as well as high numbers of CK19+ cells that also showed strong insulin positive immunoreactivity. Such hallmarks were not seen in diabetic animals kept under insulin daily administrations, nor in recipients that experienced early graft loss. It remains to be demonstrated whether islet cell transplantation, in combination with a regimen of a non-diabetogenic immunosuppression, has a role in triggering endogenous insulin production.					
15. SUBJECT TERMS Type 1 diabetes, HLA alleles, regeneration, stem cells, non-humans primates					
16. SECURITY CLASSIFICATION OF:			17. LIMITATION OF ABSTRACT	18. NUMBER OF PAGES	19a. NAME OF RESPONSIBLE PERSON
a. REPORT	b. ABSTRACT	c. THIS PAGE			USAMRMC
U	U	U	UU	165	19b. TELEPHONE NUMBER (include area code)

**Children's Hospital of Pittsburgh**  
**W81XWH-06-1-0317**  
**Annual Report (06/01/2007 – 05/31/2008)**  
**Table of Contents**

<b>Introduction .....</b>	<b>4</b>
<b>Body.....</b>	
<b>First Quarter.....</b>	<b>6</b>
<b>Second Quarter.....</b>	<b>14</b>
<b>Third Quarter.....</b>	<b>20</b>
<b>Fourth Quarter .....</b>	<b>27</b>
<b>Key Research Accomplishments.....</b>	<b>39</b>
<b>Conclusions.....</b>	<b>40</b>

<b>Appendix .....</b>	<b>41</b>
(published papers)	

**Am J Pysiol Endocrinol Metabolism** 293:E293, 2007.

**Pediatric Diabetes** 8:307, 2007.

**Cell Science Reviews** 3:250, 2007.

**Advanced Drug Delivery Reviews** 60:106, 2008.

**Diabetologia** 51:120, 2008.

**Am J Human Genetics** 82:453, 2008.

**Diabetes** 57:1544, 2008.

**Pediatric Diabetes** 9 (Part II):4, 2008.

**Atherosclerosis**, In press, 2008.

**Diabetologia**, In press, 2008.

## INTRODUCTION:

Lesions of the endocrine pancreas, as they occur in Type 1 Diabetes (T1D), were historically considered to be permanent and irreversible since patients, once endogenous insulin production is blunt, require hormone therapy for life. More recently it was proposed that islet beta cells actually retain the ability to heal from an injury, and to proliferate and multiply from precursors into mature beta cells during adult life, in a way similar to that during embryonic development. It was also proposed that possible reparative events affecting the beta cell mass normally occur but in diabetes are opposed by the destructive mechanisms that cause diabetes in first place such as the autoimmune attack (1,2).

In mouse models, evidence was presented that adult animals retain the ability to expand the beta cell mass as a response to various triggers. However, it remains largely unclear through which molecular and cellular mechanism(s) reestablishment of the beta cell mass takes place. Furthermore it was shown in the diabetic prone NOD-mouse that, even after establishment of the clinical diabetic status, it is still possible to recover endogenous pancreatic insulin production. This can be achieved by successfully combining strategies aimed at blocking the autoimmune attack with the use of non-diabetogenic immunosuppressive drugs. Normally an islet transplantation was used in parallel to supply beta cell function for the relatively long periods required to recover beta cell function (3-6).

A spontaneous recovery of the pancreatic beta cell function is also normally reported in patients diagnosed with autoimmune T1D, the so-called “honeymoon” period. Although the honeymoon may vary in duration quite dramatically from one patient to the next, there are also anecdotal cases of complete and permanent recovery. Following diagnosis of T1D and initiation of exogenous insulin treatment these individuals experienced a return of endogenous insulin production, characterized by increased C-peptide secretion, and reduction in the titre of circulating islet auto-antibodies, confirming the return of the immunologic tolerance and a consequent recovery from islet cell destruction (7). Although it is unquestionably proven that some beta cells are still present and able to produce insulin years after the clinical onset of diabetes (8,9), a steady recovery from the diabetic status is quite unique and is worth further investigations. At any rate, the potential for the pancreatic organ to recover substantial endocrine function is quite fascinating and should be exploited for possible clinical applications.

To this aim, the observation that only a limited islet mass is actively engaged in supplying insulin to maintain normoglycemia at a give time point is remarkable. This information seems to indicate that the critical mass required to synthesize and release insulin sufficient for the body's normal needs is far less than that produced by the entire beta cell pool of a healthy pancreas. This observation implicates that even a relatively limited quantity of insulin producing tissue should exert clinically evident effects in patients.

Non-human primates are relevant animal models for pre-clinical studies in general and, in particular, for xenotransplantation experiments. Monkeys and humans present strong similarities although significant metabolic differences do exist. It is therefore of great value to investigate the potentiality of non-human primate pancreatic tissue to resume endogenous insulin production following its destruction, for a better understanding of the human behaviour as well.

In monkeys, a permanent diabetic status can be induced by total pancreatectomy, a major surgical procedure usually not devoid of technical difficulties or, alternatively, by chemical destruction of the insulin producing cells by means of streptozotocin, a potent toxic agent that specifically target the pancreatic beta cells (10).

Our experimental protocol for pig islet xenotransplantation into monkeys involved induction of diabetes in the recipients by streptozotocin, intra-portal transplantation of porcine islets after recipient immunologic pre-conditioning, completed by an adequate non-diabetogenic immunosuppressive therapy. While the majority of recipients exhibited a transitory islet graft function and were sacrificed early after transplantation, in some recipients' islet graft function (indirectly assessed by measurable levels of porcine C-peptide) lasted for months (11). At a certain point in time, concurrently to a gradual reduction of the C-peptide (porcine) graft output, we observed a stepwise increased in endogenous C-peptide (monkey) levels. Metabolic clinical improvement and peculiar histological features of the pancreatic tissue were also found associated to this change. To note, no



spontaneous recovery of endogenous function was observed in transplanted monkeys with transient function of the graft or diabetic monkeys maintained under exogenous insulin for up to 1 year.

Our data provide evidence that the pancreatic tissue is able to re-establish endogenous insulin production after chemically induced beta cell specific injury. Additional investigation is required to understand whether conditions such as improved glucose metabolic control and an appropriate immunosuppressive regimen, in association with functional islet transplantation could play a role in beta cell rescue or regeneration, and if so, through which mechanism(s) (12).

## **REFERENCES to the Introduction**

1. Trucco, M. (2005) Regeneration of the pancreatic beta cell. *J. Clin. Invest.* 115, 5–12
2. von Herrath, M. and Homann, D. (2004) Islet regeneration needed for overcoming autoimmune destruction considerations on the pathogenesis of type 1 diabetes. *Pediatr. Diabetes* 5, 23–28
3. Li, H. et al. (1996) Mixed allogeneic chimerism induced by a sublethal approach prevents autoimmune diabetes and reverses insulinitis in nonobese diabetic (NOD) mice. *J. Immunol.* 156, 380–388
4. Zorina, T.D. et al. (2002) Distinct characteristics and features of allogeneic chimerism in the NOD mouse model of autoimmune diabetes. *Cell Transplant.* 11, 113–123
5. Hess, D. et al. (2003) Bone marrow-derived stem cells initiate pancreatic regeneration. *Nat. Biotechnol.* 21, 763–770
6. Melton, D.A. (2006) Reversal of type 1 diabetes in mice. *N. Engl. J. Med.* 355, 89–90
7. Rood, P.P. et al. (2006) Facilitating physiologic self-regeneration: a step beyond islet cell replacement. *Pharm. Res.* 23, 227–242
8. Meier, J.J. et al. (2005) Sustained beta cell apoptosis in patients with long-standing type 1 diabetes: indirect evidence for islet regeneration? *Diabetologia* 48, 2221–2228
9. Meier, J.J. et al. (2006) Direct evidence of attempted beta cell regeneration in an 89-year-old patient with recent-onset type 1 diabetes. *Diabetologia* 49, 1838–1844
10. Rood PP et al. (2006) Induction of diabetes in cynomolgus monkeys with high-dose Streptozotocin: side effects and early responses. *Pancreas* 33(3):287-295
11. Rood PP et al. (2007) Reduction of early graft loss after intraportal porcine islet transplantation in monkeys. *Transplantation* 83:202-209
12. Pasquali L (2006) Rehabilitation of adaptive immunity and regeneration of beta-cells. *Trends Biotechnol* 24:516-221

## BODY:

Our first quarterly scientific progress report (06/01/07 – 08/31/07) for the second year of this project, detailed the following steps forward in reaching the aims of our study.

In the aim of completing the studies presented in the first year quarterly reports, we characterized the inflammatory response in diabetes by analyzing expression of a panel of activation markers on the surface of peripheral blood monocytes in recently-diagnosed Type 1 diabetes (T1D) patients. Compelling evidence implicates inflammation in the pathogenesis of T1D and associated vascular complications. Obesity is also characterized by a low-grade systemic inflammation. The potential role of glycemic control and of body mass index (BMI) on monocyte phenotype was then investigated by using flow cytometry to analyze the expression of CD11b, CD49d, CD54, CD62L, and CD64 antigens on monocytes in a cohort of 51 T1D patients ( $\leq 2$  months from diagnosis).

We found that circulating monocytes from T1D patients tested at the clinical onset of the disease (i.e., within 1 week from diagnosis) had higher CD11b expression compared to patients analyzed after 2 months from diagnosis ( $p=0.02$ ). The highest CD11b levels were detected in patients with  $HbA_{1c} > 8\%$  ( $p=0.04$  vs. patients with  $HbA_{1c} < 8\%$ ). In T1D children analyzed after 2 months from diagnosis, we found that those overweight (BMI  $\geq 85^{\text{th}}$  percentile) had higher levels of monocyte activation than those not overweight (BMI  $\leq 85^{\text{th}}$  percentile) ( $p=0.03$ ). CD11b and  $HbA_{1c}$  were significantly correlated (correlation coefficient 0.329,  $p=0.02$ ).

From these studies we can conclude that circulating immune cells from T1D patients display many aspects of a proinflammatory state, as indicated by primed or activated monocytes. Obesity is an important factor in monocyte activation during diabetes.

## Introduction

Compelling evidence demonstrates that components of the innate immune system, including natural killer cells (NK) and monocytes are involved in the autoimmune response characteristic of T1D both in humans and in the non-obese diabetic (NOD) mouse [1-4]. The primary role of monocytes in T1D has been demonstrated by showing that these cells are the first to accumulate in the pancreatic islets of prediabetic BB rats [5]. Subsequent T and B lymphocyte infiltration is dependent upon prior monocyte invasion of the islets [5]. These data suggest a role for monocytes in the early stages of T1D pathogenesis [6].

Monocytes are pivotal cells in inflammatory responses as they serve as the principal reservoir of pro-inflammatory cytokines and are the first cells to be engaged in nonspecific immune responses, such as those triggered by environmental factors. Recent studies reported evidence of increased monocytic activity, biomarkers of inflammation and oxidative stress in adult T1D patients well after the onset of diabetes [7,8]. In these patients, monocytes also released higher levels of pro-inflammatory cytokines as compared to non-diabetic subjects, suggesting presence of an inflammatory response in T1D. Interestingly, elevated circulating levels of the pro-inflammatory cytokine interleukin (IL)-8 were found in children with recent-onset T1D ( $< 1$  year) who were also overweight [9]. Other evidence of monocyte involvement in T1D includes studies showing aberrant constitutive and lipopolysaccharide (LPS)-stimulated expression of monocyte cyclooxygenase (COX)-2 expression in monocytes of T1D patients, a defect which may predispose to a chronic inflammatory response in T1D [4,10]. The direct consequences of monocyte activation in T1D are unknown, but theoretically could involve release of pro-inflammatory cytokines, endothelial activation with increased monocyte adherence to the vascular endothelium, such as that of the pancreatic islets or kidney and retina capillaries.

During cellular activation, monocytes undergo phenotypic modifications with changes in expression of adhesion molecules on the cellular surface. These changes allow adhesion to the endothelial cells and movement of the monocytes through the endothelial layer toward inflammatory sites. The integrin Mac-1 (CD11b) is one of the most studied leukocyte adhesion molecules mediating tight binding to endothelial cells and migration through the vascular wall. While it is known that hyperglycemia, as seen in T1D, upregulates the expression of endothelial cell adhesion molecules [11-13], changes in adhesion molecule on the circulating monocytes have not been as well studied as those on the vascular endothelium. One report demonstrates increased expression of monocyte CD11b in adult T1D patients [14]. This increased CD11b expression was associated with higher monocyte adhesion to human aortic endothelial cells (HAEC) *in vitro* [14]. In contrast, other reports show either no increase [7,15] or increased binding of monocytes to endothelial cells compared

to healthy subjects [16].

The mechanism involved in the recruitment of monocytes in the peri islet vasculature during diabetes is not fully understood. This is of particular importance in human subjects because it is not possible to directly follow the different stages of the islet inflammatory process. Changes that affect both the vasculature and the circulating monocytes in the early stages of T1D may play a crucial role in promoting leukocyte adherence to the endothelium and ongoing infiltration of the islets. Another factor that could affect monocyte activation in T1D patients is changes in body weight, as obesity has been associated with the presence of leukocyte abnormalities and inflammation [9,17,18]. In this study, we therefore investigated the potential role of glycemic control and body mass index (BMI) on monocyte expression of a panel of adhesion molecules in recently-diagnosed T1D children ( $\leq 2$  months from diagnosis).

## Results

### *Monocytes from new-onset T1D patients have an activated phenotype*

Analysis of the mean fluorescence intensity (MFI) of the monocyte marker CD11b in children with T1D, showed a higher expression in those who were tested at clinical onset of diabetes ( $n=38$ ; within 1 week from diagnosis) ( $878 \pm 83$  SEM; range 210-2403, median 698) compared to those tested at 2 months from diagnosis ( $n=13$ ) ( $595 \pm 132$  SEM; range 180-1663, median 442), ( $p=0.02$ ) (Figure 1 and Figure 2).

Because diabetes ketoacidosis (DKA) has been described as an inflammatory condition characterized by elevated levels of C-reactive protein, within our cohort of newly-onset T1D patients, we found that monocyte expression of CD11b in the children with DKA tended to be higher ( $1007 \pm 188$  SEM) compared to those without DKA ( $797 \pm 82$  SEM), however this was not statistically significant ( $p=0.67$ ). When we compared those without DKA at onset ( $n=21$ ) with those without DKA at 2 months ( $n=13$ ), monocyte expression of CD11b was statistically significantly different between the two groups ( $797 \pm 82$  versus  $595 \pm 132$  respectively,  $p=0.03$ ).

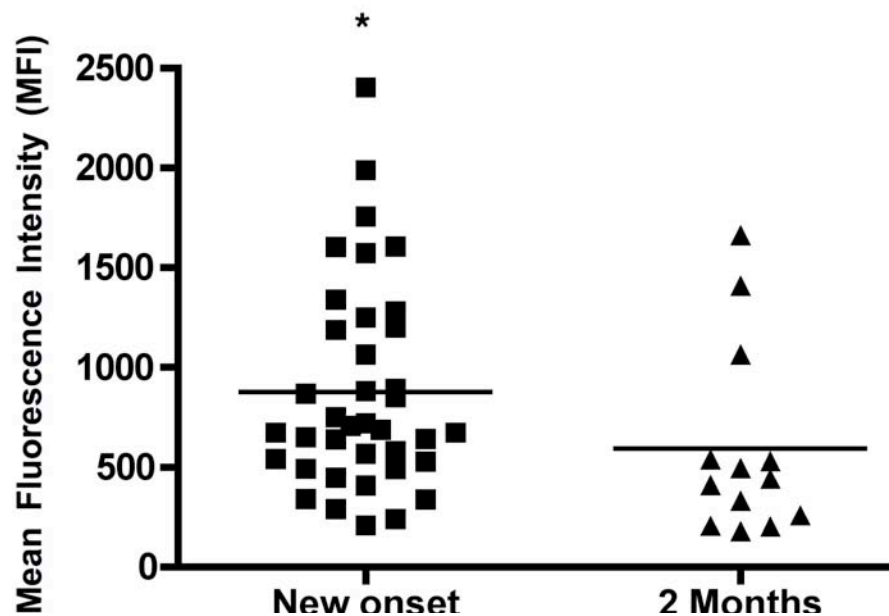


**Figure 1. Expression of CD11b on monocytes of T1D patients.** Column-scatter-plot showing changes in mean fluorescence intensity (MFI) of CD11b expression on circulating monocytes in recently-diagnosed T1D patients. Analysis was performed by flow cytometry. Monocyte from T1D patients at the onset of the disease show ( $n=38$ ) shows higher expression of the adhesion molecule CD11b then T1D patients assayed at 2 months of diabetes ( $n=13$ ) ( $p=0.02$ ). Horizontal bars show mean CD11b values. \*represents significant difference of surface expression for CD11b between the two groups.

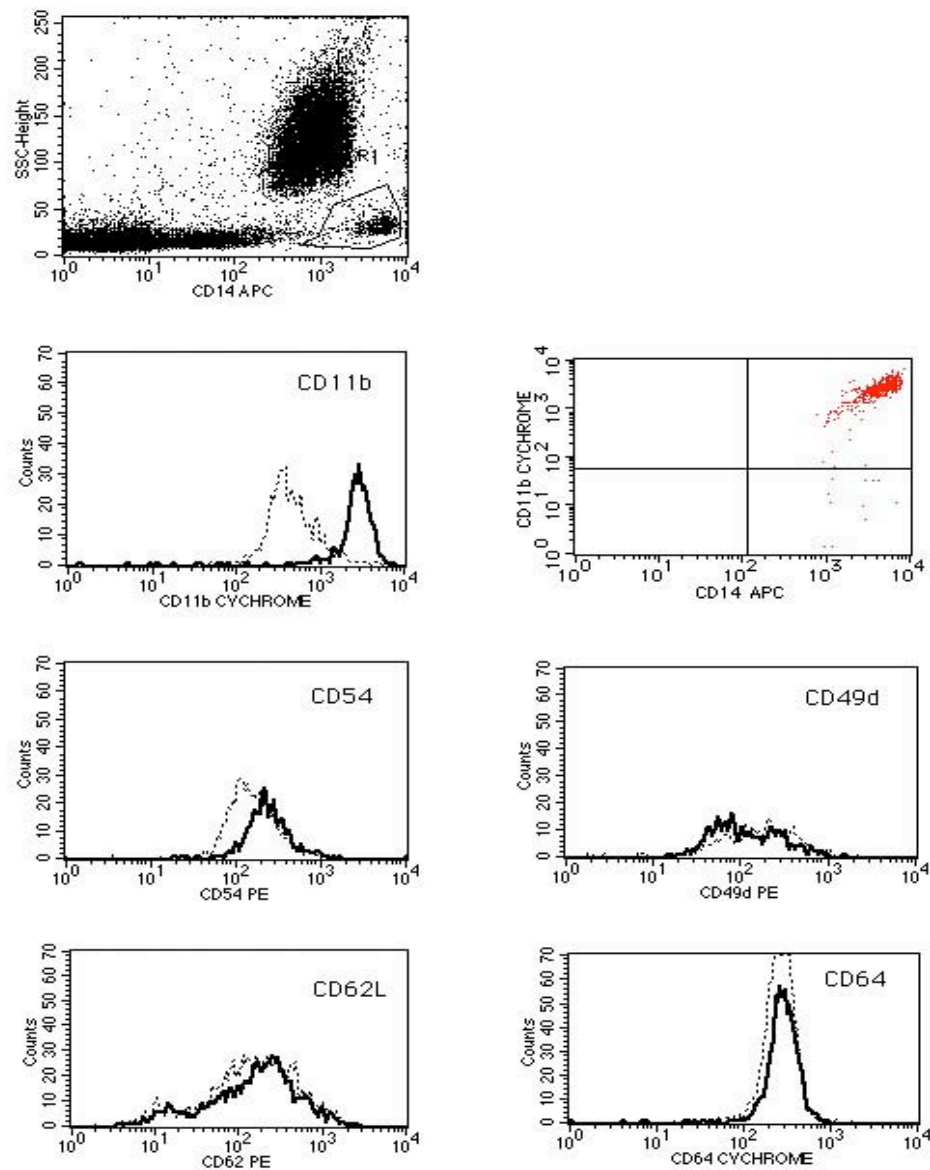


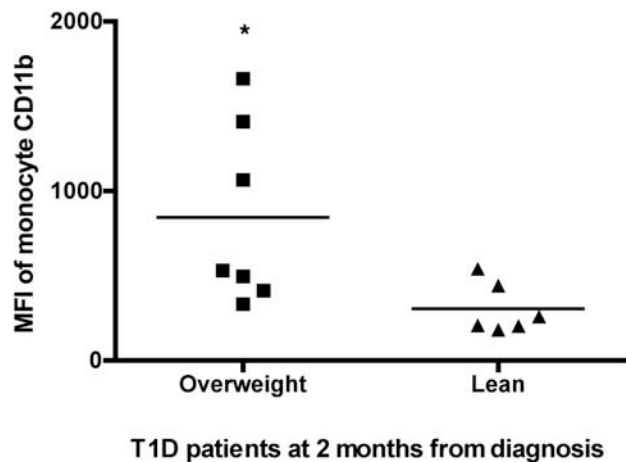
**Figure 2. Representative flow cytometry analysis of CD11b expression in a T1D patient.** In (A) representative dot-plot graph of CD11b expression on circulating monocytes ( $CD14^+$ ) of T1D patients at the onset of the disease. For each sample tested, dot-plot graphs of SSC versus  $CD14^+$  cells were drawn, and a tight gate was created, encompassing the “bright” elements for this specificity. Within the  $CD14$  gate,  $CD14^+$  elements expressing the different adhesion molecules were analyzed by drawing separate dot-plots. Percentage and MFI of positive cells was then defined by setting lower-limits for adhesion molecule positivity from each antibody combination using negative isotype controls. In A it is also shown a representative histogram of CD11b expression in T1D patient at the onset of the disease and after 2 months from diagnosis. Dotted line= T1D patient after 2 months from diagnosis; solid line= T1D patient after 2 months from diagnosis. Expression of CD11b was higher in the T1D patient at the onset of diabetes than after 2 months. In (B) representative histograms of adhesion molecule expression in T1D patient at the onset of the disease and after 2 months from diagnosis. The x axis is fluorescence intensity of the stated adhesion molecule. Dotted line= T1D patient after 2 months from diagnosis; solid line= T1D patient after 2 months from diagnosis. There was no significant differences in expression of CD54, CD49d, CD62L, and CD64 on monocytes between the two studied groups.

As expected, glycemic control measured by HbA<sub>1c</sub> was significantly higher in the onset group compared to the group tested at 2 months ( $11.3\% \pm 2$  versus  $7.4\% \pm 0.9$ ,  $p=0.0001$ ). To test whether patients with higher HbA<sub>1c</sub> had also higher monocyte activation, we compared expression of monocyte CD11b in T1D patients according to HbA<sub>1c</sub> levels. We found that T1D patients with higher HbA<sub>1c</sub> levels (HbA<sub>1c</sub>>8%) ( $n=35$ ) had significantly higher expression of CD11b ( $896 \pm 75$  SEM) as compared to those with lower HbA<sub>1c</sub> levels (HbA<sub>1c</sub>≤8%) ( $563 \pm 103$  SEM) ( $n=12$ ) ( $p=0.04$ ). In addition, CD11b and HbA<sub>1c</sub> were significantly correlated (correlation coefficient 0.329,  $p=0.02$ ).

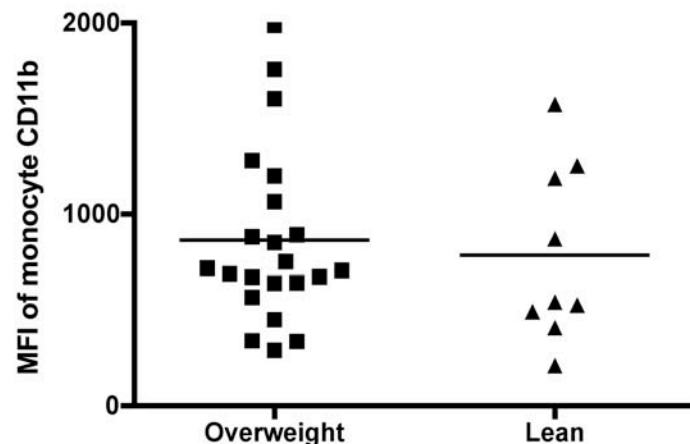
Analysis of the expression of the surface antigens CD49d, CD54, CD62L and CD64 on circulating monocytes in the different subgroups of patients did not show any significant differences. A representative example of the expression of the stated markers in T1D patients at the onset of the disease and after 2 months from diagnosis is shown in **Figure 2**.

### *Overweight children with T1D have high monocyte expression of CD11b*

There is evidence that obesity is associated with a systemic inflammatory process involving both the leukocytes and the body fat [17,18]. We therefore analyzed changes in monocyte CD11b expression in T1D according to BMI. We found that among T1D children who were tested after 2 months from diagnosis ( $n=13$ ), the expression of CD11b was significantly higher overweight children (BMI ≥ 85<sup>th</sup> percentile) ( $n=7$ ) ( $844 \pm 201$  SEM; median 531, range 332-1663) as compared to children who were not overweight (BMI ≤ 85<sup>th</sup> percentile) ( $n=6$ ) ( $305 \pm 61$  SEM; median 233, range 180-540) ( $p=0.03$ ) (**Figure 3A**).



3A



T1D patients at onset

3B

**Figure 3. Monocyte CD11b expression among T1D patients is higher in those who are overweight.** In 3A, column-scatter-plot showing changes in mean fluorescence intensity (MFI) for the molecule CD11b on monocytes according to Body mass index (BMI) in thirteen patients tested at 2 months from diagnosis (Lean  $n=6$ ; Overweight  $n=7$ ). In 3B, same analysis performed in thirty-one T1D patients at the onset of the disease (Lean  $n=22$ ; Overweight  $n=9$ ). Horizontal bars show mean CD11b values. \*represents significant difference of cell surface expression for CD11b between T1D patients who are overweight (BMI≥85<sup>th</sup> percentile) and lean (BMI≤85<sup>th</sup> percentile).

These two groups were not different in terms of their glycemic control as measured by HbA<sub>1c</sub> (7.1%±0.3 in the overweight group versus 7.6%±4.5 in the non-overweight group, p=0.33) and none of them were in DKA at the time of the evaluation.

Same analysis performed in patients at the onset of the disease (n=31) did not show significant differences in monocyte CD11b between overweight (BMI ≥ 85<sup>th</sup> percentile) (n=9) (864±97 SEM; median 713, range 291-1989), and lean (BMI ≤ 85<sup>th</sup> percentile) (784±153 SEM; median 543, range 210-1574) (n=22) patients p=0.66 (Figure 3B). These two groups were not different in terms of their control as measured by HbA<sub>1c</sub> (10.4%±0.5 in the overweight group versus 11.6%±0.4 in the non-overweight group, p=0.33) or the presence of DKA (50 versus 31%, p=0.65). CD11b and BMI percentile were not statistically significantly correlated (correlation coefficient 0.027; p=0.86).

## Conclusions

Little is known about monocyte phenotype and function in children with recently-diagnosed T1D. In this study, we analyzed the expression of a panel of adhesion molecules on circulating monocytes in T1D children within 2 months from clinical diagnosis and evaluated the potential role of glycemic control and BMI on cell phenotype. We found that among the markers analyzed, only the expression of CD11b was significantly higher in the cohort of new-onset diabetic patients (i.e., within 1 week from diagnosis) as compared to subjects tested after 2 months from diagnosis. CD11b is a polypeptide  $\alpha$ -chain linked to the  $\beta_2$ -subunit of CD18 that constitute the CD11/CD18  $\beta_2$ -integrin family. Resting monocytes constitutively express integrins, which are important signal transducers for virtually all monocyte functions by mediating cell adhesion, chemotaxis, migration, phagocytosis, and oxidant production. After monocyte activation, new copies of CD11b/CD18 are rapidly translocated to the cell surface from the intracellular granules [21]. Our finding of increased CD11b expression on monocytes at the onset of T1D suggests presence of immune activation at such an early stage of the disease. This result also supports an earlier finding of increased monocyte CD11b expression in T1D patients [14].

Within the cohort of new-onset T1D patients, children who presented with DKA had the highest levels of monocytes CD11b detected. Although these data did not reach statistical significance most likely due to small numbers, it supports a previous report showing presence of an inflammatory response in T1D children with DKA [22]. However, other factors, besides DKA, appear to be involved in triggering monocyte activation at the onset of diabetes. In fact, significantly higher monocyte CD11b expression was detected in new-onset T1D children without DKA versus those without DKA at 2 months. These results seem to suggest that the onset of diabetes is *per se* an inflammatory condition. Further studies on a larger number of patients at the onset of T1D are required to better define the inflammatory state present in DKA.

We found that diabetic children tested after 2 months from diagnosis who were overweight (BMI ≥ 85<sup>th</sup> percentile) displayed higher CD11b values when compared to lean diabetic children. This finding supports the association between obesity and inflammation [17,18]. Recently, it has been shown that obesity is characterized by abnormalities in peripheral leukocyte counts [17], increased circulating levels of the pro-inflammatory cytokine interleukin(IL)-8 [9], and by an accumulation of immune cells, especially macrophages, in the adipose tissue [18]. The fact that we could not detect the same changes of monocyte CD11b between overweight and lean diabetic children within the cohort of patients tested at the onset of the disease is probably due to the confounding effect of the inflammatory response associated with the onset of the disease.

The factor(s) triggering up-regulation of CD11b on the monocytes in diabetes and its biological significance are not known. One hypothesis would be that the increased expression of CD11b on monocytes in diabetes is simply a marker of an inflammatory response, which becomes more pronounced in overweight children and in children who present with DKA. Alternatively, CD11b up-regulation could reflect an increased monocyte activation in response to poor glycemic control and insulin-deficiency likely present at the onset of diabetes, which is supported by the fact that HbA<sub>1c</sub> levels were significantly higher at the onset than at 2 months and by the fact that there was a significant correlation between the two variables. In addition, diabetic children with higher HbA<sub>1c</sub> (HbA<sub>1c</sub>>8%) also had higher CD11b. A third explanation envisions that intercurrent infections may have precipitated the diagnosis (due to increased insulin requirements) and be responsible for immune activation. At this point, we cannot decide to which extent the inflammatory state is a pathogenic



mechanism contributing to the development of T1D or is the response to a metabolic derangement. In the first case, the inflammatory state should precede overt diabetes and in this context the study of pre-diabetic subjects (i.e., autoantibody-positive individuals) should be characterized in respect to the inflammatory state.

Our findings of increased CD11b on the monocytes of T1D patients at the clinical onset of diabetes would strengthen the idea that these cells have the potential to adhere to the endothelium and exit the circulation at such an early stage of the disease. In fact, current investigations in our laboratory show that monocytes isolated from peripheral blood of recently-diagnosed T1D patients (who were free from any vascular complications) have increased adherence to Human Umbelical Vein Endothelial Cells (HUVEC) *in vitro* (unpublished preliminary findings) (Figure 4).

A

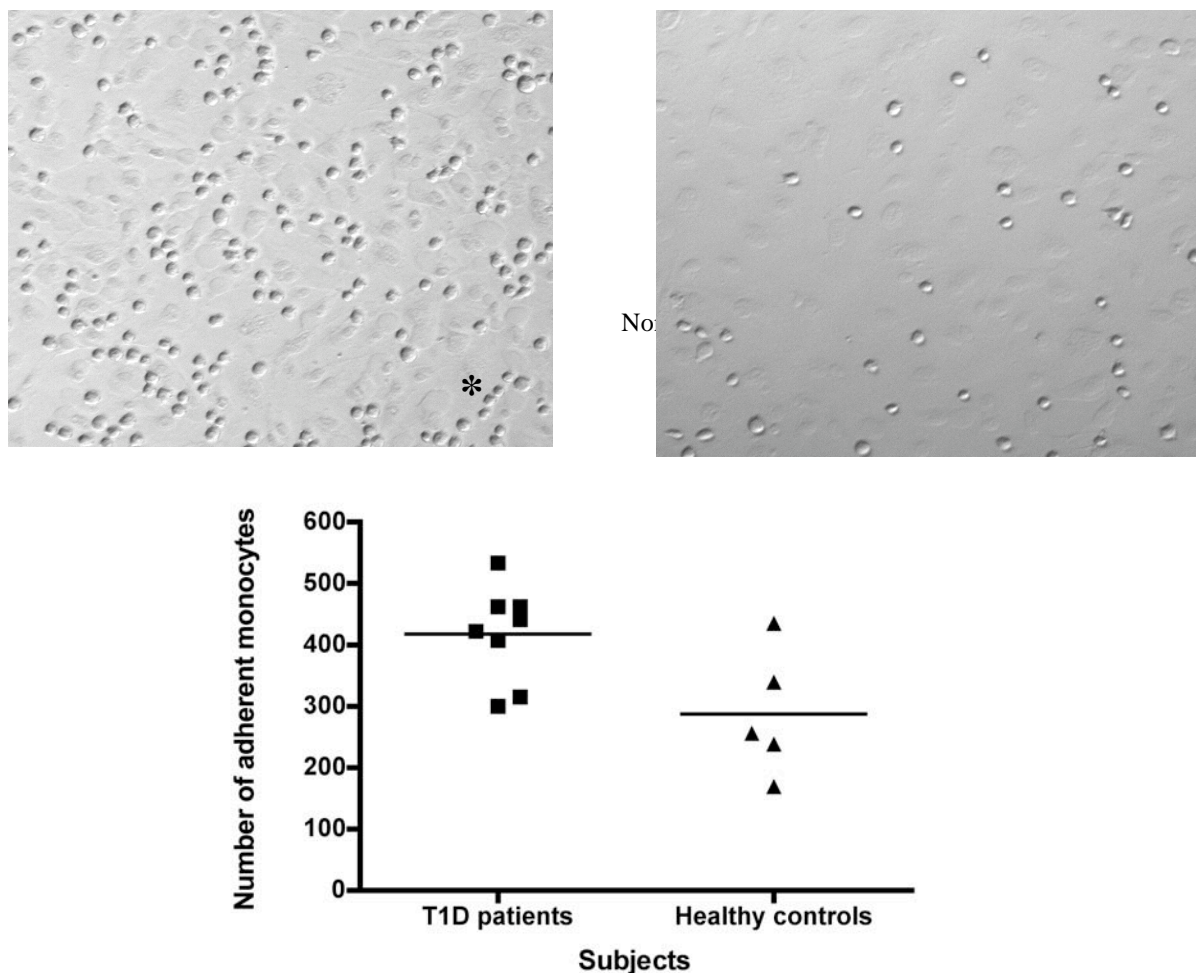


**Figure 4. Monocytes from T1D patients have increased adherence to HUVEC.** Freshly isolated monocytes from new onset T1D patients (n=8) and from healthy controls (n=5) were added to confluent HUVEC and counted, as described in Materials and Methods. In (A) 40x photomicrographs of monocytes adherent to HUVEC. In (B) Columns-scatter-dot-plot showing number of monocytes adherent to HUVEC in 5 random 40x fields per well. Horizontal bars show mean number of monocytes. The number of monocytes of T1D patients adherent to the wells was significantly higher than in normal controls ( $p = 0.04$ ).

These findings, although preliminary, would support the hypothesis that monocytes from recent-onset T1D patients have increased adhesive capacity and the potential to exit the circulation and infiltrate the islets of Langerhans. Protracted inflammation with increased expression of the same adhesion molecules could be the basis for late diabetes-associated atherosclerotic vascular complications.

In conclusion, the clinical onset of T1D is associated with changes in activation-related markers on the circulating monocytes as part of a generalized inflammatory response. We have identified the leukocyte integrin CD11b/CD18 as a crucial molecule up-regulated on circulating monocytes, especially in overweight children. Enhanced monocyte CD11b would support the notion that monocytes of recently-diagnosed T1D patients have the potential to adhere to the endothelium, most likely in the vasculature of the pancreas, and accumulate in the islets.

## References for the first quarterly scientific progress report

1. Goodier MR, Nawroly N, Beyan H, Hawa M, Leslie RD, Londei M. Identical twins discordant for type 1 diabetes show a different pattern of in vitro CD56<sup>+</sup> cell activation. *Diabetes Metab Res Rev* 2006. 22(5):367-375.
2. Wilson SB, Kent SC, Patton KT, Orban T, Jackson RA, Exley M, Porcelli S, Schatz DA, Atkinson MA, Balk SP, et al. Extreme Th1 bias of invariant Valpha24JalphaQ T cells in type 1 diabetes. *Nature* 1998. 391:177-181.
3. Adler T, Akiyama H, Herder C, Kolb H, Burkart V. Heat shock protein 60 elicits abnormal response in macrophages of diabetes-prone non-obese diabetic mice. *Biochem Biophys Res Commun* 2002. 294:592-596.
4. Beyan H, Goodier MR, Nawroly NS, Hawa MI, Bustin SA, Ogunkolade WB, Londei M, Yousaf N, Leslie RDG. Altered monocyte cyclooxygenase response to lipopolysaccharide in type 1 diabetes. *Diabetes* 2006. 55:3439-3445.
5. Hanenberg H, Kolb-Bachofen V, Kantwerk-Funke G, Kolb H. Macrophage infiltration precedes and is a prerequisite for lymphocytic insulinitis in pancreatic islets of pre-diabetic BB rats. *Diabetologia* 1989. 32:126-134.
6. Kolb-Bachofen V, Kolb H. A role for macrophages in the pathogenesis of type 1 diabetes. *Autoimmunity* 1989. 2:145-154.
7. Devaraj S, Glaser N, Griffen S, Wang-Polagruto J, Miguelino E, Jialal I. Increased monocytic activity and biomarkers of inflammation in patients with type 1 diabetes. *Diabetes* 2006. 55:774-779.
8. Plesner A, Greenbaum CJ, Gaur LK, Ernst RK, Lernmark A. Macrophages from high-risk HLA-DQB1\*0201/\*0302 type 1 diabetes mellitus patients are hypersensitive to lipopolysaccharide stimulation. *Scand J Immunol* 2002. 56:522-529.
9. Erbagci AB, Tarakcioglu M, Coskun Y, Sivasli E, Namiduru ES. Mediators of inflammation in children with type 1 diabetes mellitus: cytokines in type 1 diabetic children. *Clinical Biochem* 2001. 34:645-650.
10. Litherland SA, Xie XT, Hutson AD, Wasserfall C, Whittaker DS, She JX, Hofig A, Dennis MA, Fuller K, Schatz D, et al. Aberrant prostaglandin synthase 2 expression defines an antigen-presenting cell defect for insulin-dependent diabetes mellitus. *J Clin Invest* 1999. 104:515-523.
11. Kado S, Wakatsuki T, Yamamoto M, Nagata N. Expression of intercellular adhesion molecule-1 is induced by high glucose concentrations in human aortic endothelial cells. *Life Sci* 2001. 68:727-737.
12. Kim JA, Berliner JA, Natarajan RD, Nadler JL. Evidence that glucose increases monocyte binding to human aortic endothelial cells. *Diabetes* 1994. 43:1103-1107.
13. Morigi M, Angioletti S, Imberti B, Donadelli R, Micheletti G, Figliuzzi M, Remuzzi A, Zoja C, Remuzzi G. Leukocyte-endothelial interaction is augmented by high glucose concentrations and hyperglycemia in a NF-kB-dependent fashion. *J Clin Invest* 1998. 101:1905-1915.
14. Kunt T, Forst T, Fruh B, Flohr T, Schneider S, Harzer O, Pflutzner A, Engelbach M, Lobig M, Beyer J. Binding of monocytes from normolipidemic hyperglycemic patients with type 1 diabetes to endothelial cells is increased in vitro. *Exp Clin Endocrinol Diabetes* 1999. 107:252-256.



15. Hoogerbrugge N, Verkerk A, Jacobs ML, Postema PTE, Jongkind HF. Hypertryglyceridemia enhances Mo binding to Ec in NIDDM. *Diabetes Care* 1996. 19:1122-1126.
16. Setiadi H, Wautier JL, Courillon-Mallet A, Passa P, Caen J. Increased adhesion to fibronectin and Mo-1 expression by diabetic monocytes. *J Immunol* 1987. 138:3230-3234.
17. Zaldivar F, McMurray RG, Nemet D, Galassetti P, Mills PJ, Cooper DM. Body fat and circulating leukocytes in children. *Int J Obes* 2006. 30:906-911.
18. Sbarbati A, Osculati F, Silvagni D, Benati D, Galie' M, Camoglio FS, Rigotti G, Maffei C. Obesity and inflammation: evidence for an elementary lesion. *Pediatrics* 2006. 117:220-223.
19. Pietropaolo M, Becker DJ, LaPorte RE, Dorman JS, Riboni S, Rudert WA, Mazumdar S, Trucco M. Progression to insulin-requiring diabetes in seronegative prediabetic subjects: the role of two HLA-DQ high-risk haplotypes. *Diabetologia* 2002. 45:66-76.
20. Luppi P, Haluszczak C, Trucco M, DeLoia J. Normal pregnancy is associated with peripheral leukocyte activation. *AJRI* 2002. 47:72-81.
21. Miller LJ, Bainton DF, Borregaard N, Springer TA. Stimulated mobilization of monocyte Mac-1 and p150,95 adhesion proteins from an intracellular vesicular compartment to the cell surface. *J Clin Invest* 1987. 80:535-544.
22. Stentz FB, Umpierrez GE, Cuervo R, Kitabchi AE. Proinflammatory cytokines, markers of cardiovascular risks, oxidative stress, and lipid peroxidation in patients with hyperglycemic crisis. *Diabetes* 2004. 53:2079-2086.

In our second quarterly scientific progress report (09/01/07 – 11/30/07, we presented our attempt to use bone marrow (BM) enriched hematopoietic precursor cells, transfected with an MHC class II b chain gene that confers resistance to the disease, to abrogate autoimmunity.

Type 1 diabetes (T1D) is an autoimmune disease the clinical onset of which most frequently presents in children and adolescents who are genetically predisposed. In light of accumulating evidence that: a) the endocrine pancreas has regenerative properties (1-7); b) hematopoietic chimerism can abrogate destruction of  $\beta$  cells in autoimmune diabetes (8,9), so that physiologically-sufficient endogenous insulin production can be restored in non-obese diabetic (NOD) mice, even after the disease clinically presented (10-12) – this strain of mouse spontaneously develops T1D with etiopathogenetic characteristics very similar to the disease in humans; and c) these regeneration properties of the endocrine pancreas have also been seen, even if only sporadically, in humans (13,14), we propose here to test reliable and more clinically translatable alternatives able to achieve these same goals in non-human primates.

T1D is prevented by transfecting a “diabetes-resistant” MHC class II  $\beta$  chain gene allele into the hematopoietic stem cells of genetically susceptible (i.e., carrying a “diabetes-susceptible” allele) mice (15). The expression of the newly formed diabetes-resistant molecule in the re-infused hematopoietic cells, is sufficient to prevent T1D onset in the NOD mouse, even in the presence of the native, diabetogenic molecule. This approach to obtain autoimmunity abrogation facilitates the recovery of autologous insulin production also in the already-diabetic individual. Safe induction of an autoimmunity-free status might become a new promising therapy for T1D.

Our working hypothesis is currently tested by using bone marrow (BM) enriched hematopoietic precursor cells (instead of a non-fractionated BM cell population used by Tian et al.), transfected with an MHC class II  $\beta$  chain gene that confers resistance to the disease, to abrogate autoimmunity. Also, already diabetic -- rather than pre-diabetic -- mice are treated by the re-infusion of transfected BM enriched precursors. The enriched precursors are able to generate the right derivative cells and in sufficient numbers to efficiently repopulate the thymus. By negatively selecting possibly autoreactive T cell clones, and making peripheral tolerance, mediated by T regulatory cells, more efficient, autoimmunity is abrogated. In the absence of autoimmunity and of diabetogenic immunosuppressive protocols, by adopting auxiliary means to correct hyperglycemia, the regenerative property of the autologous endocrine pancreas repopulates the gland with enough insulin-producing cells to restore euglycemia. Also, to avoid the use of radiation to eliminate the activated T cell clones present in the diabetic patient, an antibody-based preconditioning is used instead. Finally, we are determining how long after its onset disease reversal remains possible.

However, the evidence generated in rodents must be confirmed in non-human primates to be allowed to quickly transfer this protocol to humans. Even in a non-human primate that does not spontaneously develop autoimmunity nor T1D, safety and regenerative issues can be properly addressed.

To this goal we have proposed:

**Task 1.** To isolate – using appropriate antibodies and cell sorting – bone marrow (BM) cell precursors from a diabetic (i.e., streptozotocin [STZ] treated) cynomolgus monkey. **The isolated precursors will then be transfected ex vivo with an Mhc class II beta chain gene conferring resistance to the disease, and re-infused in the BM depleted animal to determine the safety of this maneuver.**

a) This protocol will be implemented immediately after diabetes onset, in association with allogeneic islet transplantation to guarantee the diabetic animal's euglycemia until the regenerative process brings about sufficient  $\beta$  cells to make the islet graft obsolete.

b) In parallel experiments, insulin-based therapy will precede transplantation of transfected BM cells and the protocol will be implemented after a protracted insulin therapy. Exogenous insulin administration will continue after protocol's implementation.

**Task 2.** To ascertain the efficacy of engraftment and repopulation capabilities of the engineered hematopoietic precursor cells, following non-radiation based pre-conditioning.

a) We will systematically substitute to irradiation an antibody-based, immuno-reductive conditioning protocol, testing different quantities and well-defined injection schedules.

**Task 3. To utilize phage integrases to guide the stable and irreversible insertion of DNA at specific locations within the genome to satisfy the need for an everlasting synthesis of the b chain conferring resistance, even in the offspring of the successfully transfected BM precursor cells.**

a) Determine if any of the three DirectIt™ recombinases integrate plasmid DNA at pseudo *att* sites in monkey chromosomes.

b) Determine if the best recombinase identified in Task 1 integrates plasmid DNA into mesenchymal stem cells (MSC) of cynomolgus monkey.

c) Identify the pseudo *att* sites in MSC of cynomolgus monkey.

d) Optimize the transfection and gene targeting procedure for integrating plasmid in to CD34<sup>+</sup> cells of cynomolgus monkey.

**Task 4. To infuse *in situ* appropriate factors (e.g., PAX4, EGF, LIF, HGF, GLP, and IGF) able to speed up the physiologic regenerative process.**

a) A topical route via the pancreatic duct by retrograde delivery, similar to a commonly used clinic technique ERCP (endoscopic retrograde cholangio-pancreatography) will be used.

**Task 5. To test with a proteomics approach whether the successfully infused target tissue secrete, during regeneration, the product(s) of the transfected gene(s) and additional, spontaneously-generated, adjuvant factors.**

a) Isolated endocrine and exocrine tissues obtained at the autopsy, will be used any time they become available.

b) The pancreatic fluid will be collected from the duct of the treated monkeys, by using the ERCP technique and its content analyze in detail in terms of relative quantities of each of the proteins present.

In summary our final goal is to obtain autoimmunity abrogation in a diabetic patient *via* an autotransplant of precursor cells transfected with HLA class II b chain genes conferring resistance to the disease and, while correcting his/her hyperglycemia using conventional insulin administrations, leave “nature” to heal the rest. We also propose to speed up the natural process of healing by endoscopic retrograde intraductal delivery of factors known to promote b cell regeneration. Should this approach work satisfactorily, our young patients will be cured for good, without any need for long drug therapies associated with troublesome consequences.

Towards Task #1 we focused on the isolation of “**BM cell precursors from a diabetic (i.e., streptozotocin [STZ] treated) cynomolgus monkey**”.

With regards to the STZ treatment we can say that so far we have accumulated evidence that regeneration of the endogenous pancreas, in a chemically (STZ) induced, diabetic monkey -- transplanted with  $\alpha$ 1,3-galactosyltransferase double knockout (DKO) (26) pig islets, in which these islets can substitute for endogenous islets producing enough insulin (monitored by pig C-peptide) to control the recipient animal glycemia -- starts to take place a few months after the total destruction of the b cells, provided that diabetogenic immunosuppressants are not used. In **Figure 1** we show how after STZ treatment the endocrine pancreas of the monkey is not any longer able to produce sufficient quantities of insulin to satisfy the need of the animal that consequently becomes diabetic.

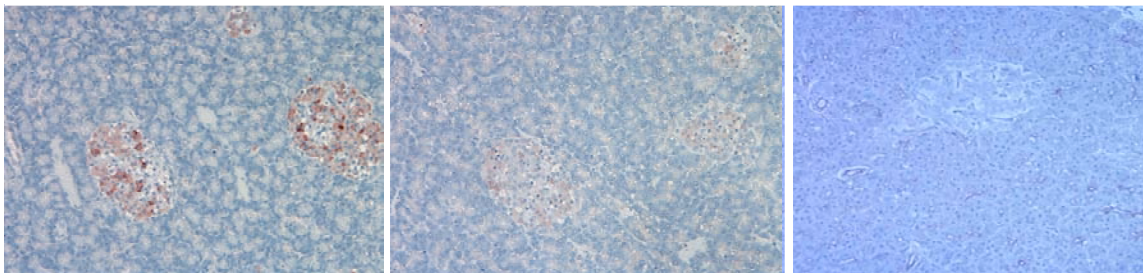


**Figure 1. Monkey pancreas 4 hours, 7 hours, and 4 weeks after 150mg/kg STZ infusion. Insulin in red.**

Regeneration properties are overpowered by the effects of diabetogenic immunosuppressive cocktails: the monkey C peptide levels remained lower than 0.5ng/ml for the entire duration of all these experiments and Arginine-stimulation-test was always blunted when performed during follow-up (Figure 2).

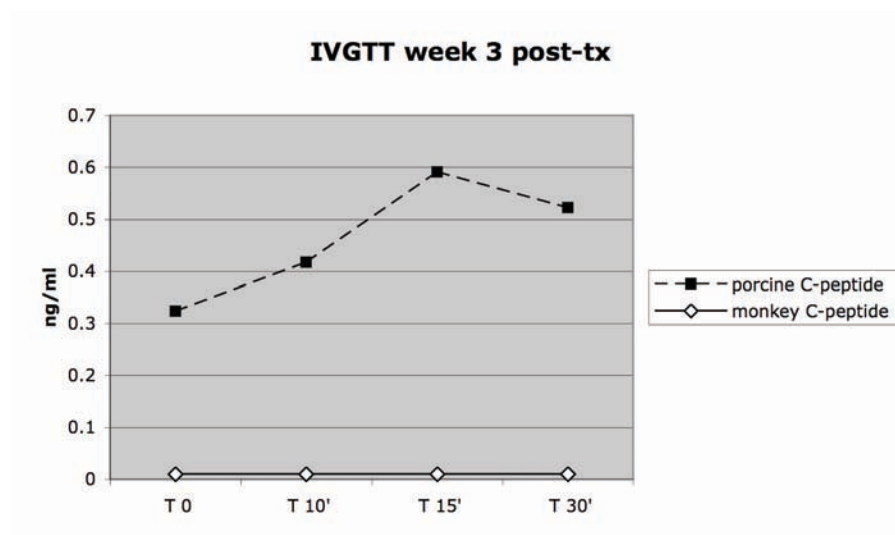


Figure 2. IVGTT carried out on monkey recipient 3 weeks following pig islet xenotransplantation. Porcine (graft) and monkey (endogenous) C peptide levels are shown.

More than three months after STZ treatment -- in the absence of diabetogenic immunosuppressant agents and using instead an anti-CD154 monoclonal antibody to block the recipient's immune system -- the monkeys not only keep producing pig C-peptide but eventually recovered the ability to produce monkey C-peptide. New insulin-producing cells are appearing with time in the monkey endogenous pancreas eventually forming insulin-producing conglomerates of cells (Figure 3).

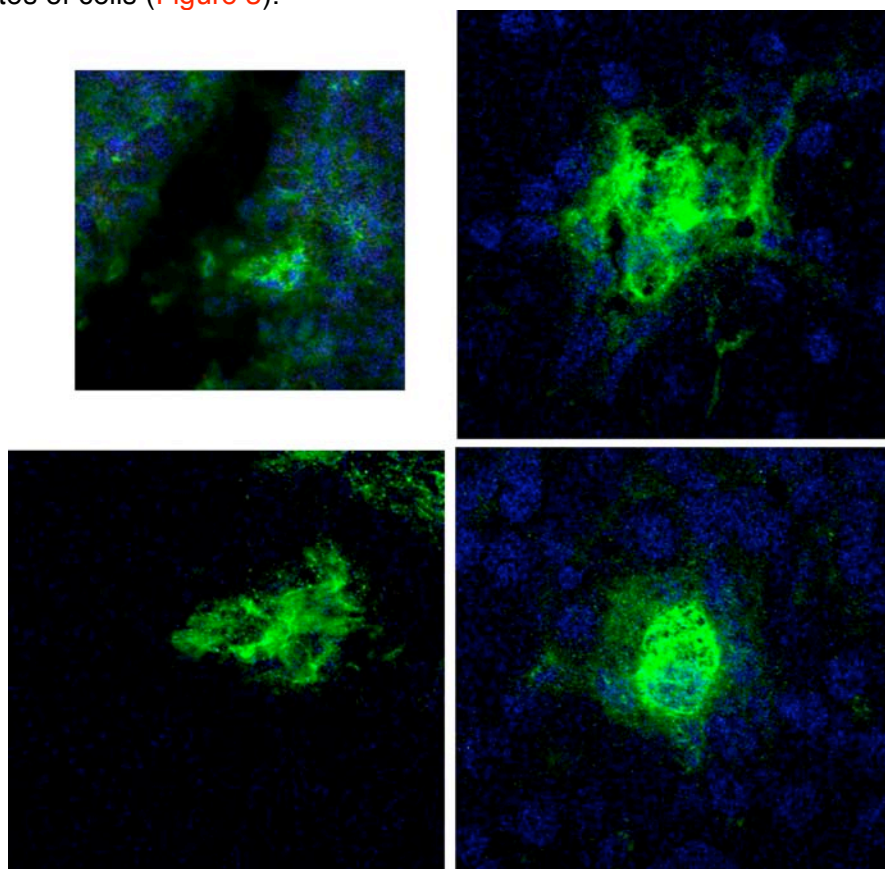
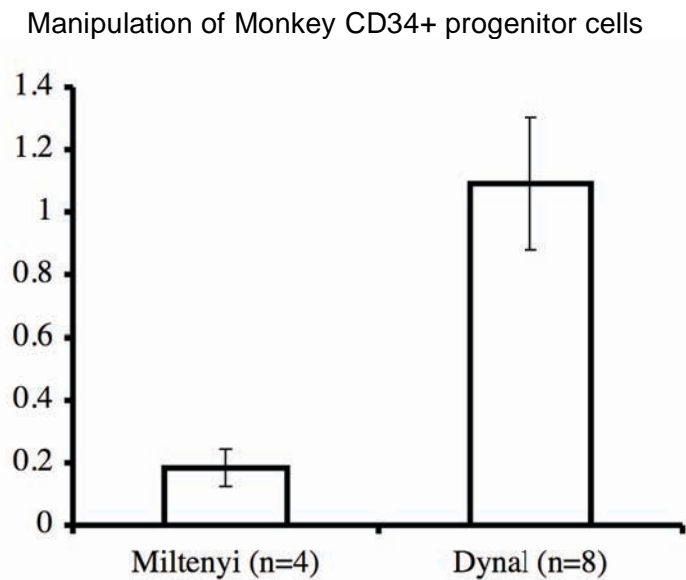


Figure 3. Monkey pancreas four months after transplantation. Insulin in green.

Towards Task #1 we also tested the possibility to isolate BM cell precursors from diabetic (i.e., streptozotocin [STZ] treated) cynomolgus monkeys and our ability to isolate, expand and transfect them.

**Isolation:** Vertebrae were surgically removed from monkeys (*Cynomolgus Macaque*) euthanized for islet transplantation studies. Connective tissues and muscles were removed with scalpel and the cleaned vertebrae were crushed to release the bone marrow cells. Dead cells and red blood cells were further removed by Ficoll-gradient centrifugation. A total of  $5 \pm 2 \times 10^9$  bone marrow cells were harvested from each monkey and subjected to magnetic bead-based progenitor cell isolation. We tested two commercially available CD34+ progenitor cell isolation systems: the DYNAL CD34+ progenitor cell selection system (Invitrogen) and the CD34+ progenitor cell isolation kit from Miltenyi. As shown in **Figure 4**, we were able to isolate hematopoietic progenitor cells from the monkey bone marrow cells at a recovery rate around  $1.1 \pm 0.2\%$  with the DYNAL kit. The isolated progenitor cells were aliquoted and stored in liquid nitrogen for future use.



**Figure 4. Isolation of Monkey CD34+ Progenitor Cells.** Bone marrow cells from monkey vertebrae were harvested and stained with anti-CD34 antibody anchored on magnetic beads. We tested two commercially available systems for the isolation procedure, and found that the DYNAL system is superior to the Miltenyi one, with a much higher recovery rate.

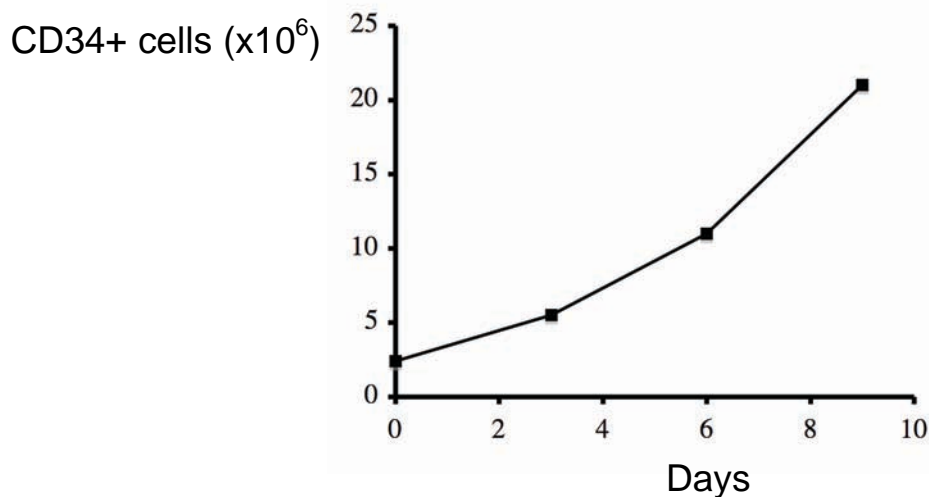


**Figure 5. *In vitro* Culture of Monkey CD34+ Progenitor Cells.** CD34+ progenitor cells harvested were cultured *in vitro*, supplemented with growth factors (human recombinant SCF, TPO and Flt-3). The doubling time is about 72 hours.

**Expansion:** We were able to recover and grow the liquid nitrogen-stored monkey progenitor cells with growth factor supplements (StemSpan CC110 cytokine cocktail from Stemcell Technologies, including 100 ng/mL rh Flt-3 ligand, 100 ng/mL rh stem cell factor and 100 ng/mL rh thrombopoietin). Under such condition, these progenitor cells can expand more than 20 times with a doubling time about 72 hours (Figure 5).

**Transfection:** To further investigate the probability of subjecting the cultured CD34+ monkey bone marrow progenitor cells to therapeutic use, we used the human hematopoietic progenitor Nucleofector kit from AMAXA GmbH to introduce the green fluorescent protein (GFP) expressing plasmid pmaxGFP into these cells. It was shown in previous studies that the Nucleofector technology could be successfully used to introduce transgenes, transiently as well as stably, into a variety of primary stem cell populations, such as adipose progenitor cells, neuronal progenitor cells, and human bone marrow progenitor cells. Seventy-two hours after electroporation, bone marrow cells were analyzed by fluorescein-activated cell sorting (FACS) analysis. More than 50% of bone marrow cells were GFP positive, indicating high-efficient transfection of the pmaxGFP plasmid (Figure 6).

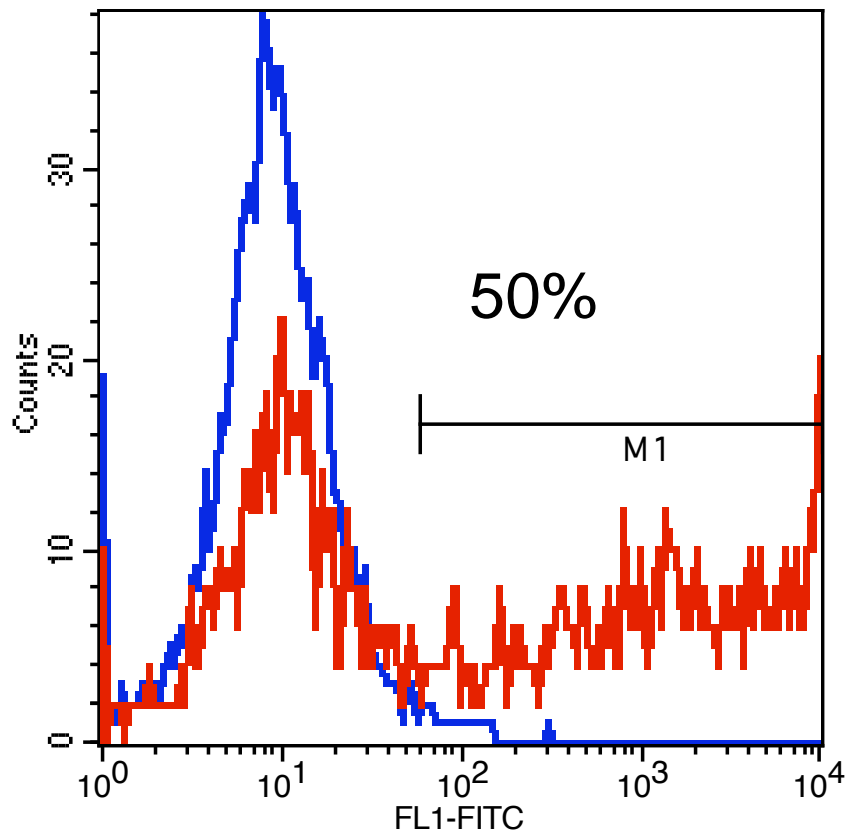


**Figure 6. High Efficient Transfection of Monkey CD34+ Cells.** *In vitro* cultured CD34+ progenitor cells were transfected with pmaxGFP plasmid, using the Amaxa Nucleoprotector system. 72 hours after electroporation, about 50% cells are GFP+.

Taken together, we have overcome all the technical hurdles, and are able to isolate, store, expand and manipulate (introducing transgenes) CD34+ monkey bone marrow progenitor cells *in vitro*.



## References for the second quarterly scientific progress report

1. Lipsett M, Finegood DT: b-cell neogenesis during prolonged hyperglycemia in rats. *Diabetes* 51:1834–1841, 2002.
2. Gu D, Lee MS, Krah T, Sarvetnick N: Transitional cells in the regenerating pancreas. *Development* 120:1873–1881, 1994.
3. Bernard-Kargar C, Ktorza A: Endocrine pancreas plasticity under physiological and pathological conditions. *Diabetes* 50 (Suppl. 1):S30–S35, 2001.
4. Brelje TC, Scharp DW, Lacy PE, Ogren L, Talamantes F, Robertson M, Friesen HG, Sorenson RL: Effect of homologous placental lactogens, prolactins, and growth hormones on islet b-cell division and insulin secretion in rat, mouse, and human islets: implication for placental lactogen regulation of islet function during pregnancy. *Endocrinology* 132:879–887, 1993.
5. Rosenberg L: In vivo cell transformation: neogenesis of beta cells from pancreatic ductal cells. *Cell Transplant* 4:371–383, 1995.
6. Bouwens L: Transdifferentiation versus stem cell hypothesis for the regeneration of islet beta-cells in the pancreas. *Microsc Res Tech* 15:332–336, 1998.
7. Bonner-Weir S, Deery D, Leahy JL, Weir GC: Compensatory growth of pancreatic beta cells in adult rats after short-term glucose infusion. *Diabetes* 38:49–53, 1989.
8. Li H, Kaufman CL, Boggs SS, Johnson PC, Patrene KD, Ildstad ST: Mixed allogeneic chimerism induced by a sublethal approach prevents autoimmune diabetes and reverses insulinitis in nonobese diabetic (NOD) mice. *J Immunol* 156:380–388, 1996.
9. Zorina TD, Subbotin VM, Bertera S, Alexander A, Styche AJ, Trucco M: Distinct characteristics and features of allogeneic chimerism in the NOD mouse model of autoimmune diabetes. *Cell Transplant* 11:113–123, 2002.
10. Ryu S, Kodama S, Ryu K, Schoenfeld DA, Faustman DL: Reversal of established autoimmune diabetes by restoration of endogenous bcell function. *J. Clin. Invest.* 108:63–72. doi:10.1172/JCI200112335, 2001.
11. Hess D, Li L, Martin M, Sakano S, Hill D, Strutt B, Thyssen S, Gray DA, Bhatia M: Bone marrow-derived stem cells initiate pancreatic regeneration. *Nat Biotechnol* 21:763–770, 2003.
12. Zorina TD, Subbotin VM, Bertera S, Alexander A, Haluszczak C, Styche A, Gambrell B, Bottino R, Trucco M: Recovery of the endogenous beta cell function in autoimmune diabetes. *Stem Cells* 21:377–388, 2003.
13. Karges B, Durinovic-Belló I, Heinze E, Boehm BO, Debatin K-M, Karges W: Complete long-term recovery of b-cell function in autoimmune type 1 diabetes after insulin treatment. *Diabetes Care* 27:1207–1208, 2004.
14. Rother KI, Harlan DM: Challenges facing islet transplantation for the treatment of type 1 diabetes mellitus. *J Clin Invest* 114:877–883, 2004.
15. Tian C, Bagley J, Cretin N, Seth N, Wucherpennig KW, Iacomini J: Prevention of type 1 diabetes by gene therapy. *J Clin Invest* 114:969–978, 2004.

In our third quarterly scientific progress report (12/01/07 – 02/29/08) we then reported the possibility of using stem cells of different origins to favor endocrine pancreas cell regeneration.

## INTRODUCTION

Type 1 diabetes is an autoimmune disease characterized by the selective loss of the beta cell mass in the pancreas and the subsequent lack of a single secreted and circulating protein, i.e., insulin (1). As an example of a mono-cellular deficiency state diabetes has tremendous appeal as a target for cell replacement therapy. Whole pancreas and isolated islet transplantation are currently the two available alternatives for beta cell replacement, although their feasibility is severely limited by the shortage of donors and the need for lifelong immunosuppressive therapy (2). In 2000, Shapiro et al. provided the undeniable “proof of principle” that the reestablishment of an adequate beta cell mass via transplantation of isolated human islets can restore euglycemia in patients with insulin-dependent T1D (3). Unfortunately, two or more pancreata per recipient were necessary to achieve insulin independence (4). Thus, many efforts are now aimed at finding alternative sources of insulin-producing cells which satisfy the need for a large number of transplantable cells while preserving the physiological function of the beta cell, i.e. the ability to sense blood glucose levels and consequently release the appropriate amount of hormone. Stem cells, which can be isolated from embryonic, fetal, and adult tissues might represent such an unlimited source because of their ability to self-renew by symmetric division while retaining the potential of differentiating under the proper conditions into the desired phenotype (5).

## EMBRYONIC STEM CELLS

Embryonic stem cells (ESCs) are derived from the inner cell mass of the blastocyst which forms several days after an egg is fertilized (6). ESCs can be defined as totipotent; they are able to generate all of the tissues of the developing organism. Evidence of this property was demonstrated by the injection of mouse ESCs of one strain into the blastocyst of a second strain. Following re-implantation into mice, the ESCs contribute to the formation of all the tissues of the embryo chimera (7). For this reason, human ESCs (hESCs) might represent an excellent source of large numbers of transplantable cells to be used for cell replacement therapies. Human ESCs express telomerase activity and many specific biomarkers such as Oct-4, Nanog, Thy-1, stage specific embryonic antigen-3 and -4, and tumor-rejection antigen-1-60 and -1-81 (8). These markers have been used to characterize hESCs in comparison to other stem cells with less plasticity and more limited differentiation potential. In addition, cultured ESCs can easily be manipulated genetically via ectopic transgene expression or homologous recombination-based approaches, thereby providing powerful model systems for the study of mammalian embryogenesis and disease processes (8). Despite these advantages, the therapeutic use of hESCs has major drawbacks in clinical application, not limited to ethical concerns relative to embryo manipulation (9). Main obstacles are the allogeneic nature of the cells with their consequent chance of immune rejection reactions, and the possibility of teratoma/teratocarcinoma formation after implant in ectopic sites, which is a natural consequence of their broad differentiation potential (8). Therefore, at least to prevent the latter issue, cells derived from ESCs should be depleted of the undifferentiated population before their safe transplantation.

A large number of studies described the derivation of surrogate beta cells from mouse and human ESCs. In 2000, Soria et al. first used the so-called “promoter trapping” approach to enhance the survival of insulin-producing cells taking advantage of spontaneous differentiation of mouse ESCs (10). Spontaneous differentiation was also reported in human ESCs (11). However, the major challenge remained the one of directing *in vitro* the differentiation of ESCs into a specific target cell and at the same time preventing or suppressing all other unnecessary alternatives of the pluripotent repertoire. In 2001 Lumelski et al. claimed that functional islet-like structures could be produced from mouse ESCs using a relatively simple five-step procedure (12). Influenced by the similarities existing between neural and islet cells -- including their shared expression of the intermediate filament protein Nestin and the transcription factors Isl1, Ngn3, Pax6, Pax4, and beta2NeuroD -- their approach was based on protocols developed to differentiate mouse ESCs towards neurons. A major critique, elegantly demonstrated by Melton and his group in 2003, was that insulin positive staining of supposedly differentiated ESCs was an artifact due to absorption of the hormone from the media.



Co-culturing of human ESCs with developing murine pancreas to facilitate their maturation into beta-like cells was another method tested (16). More recently, the dramatic evolution in the discipline of developmental biology and the deeper understanding of the physiologic ontogeny of the pancreas, has led to more precise protocols for directing differentiation of embryonic stem cells towards insulin-producing cells. Achievement of this goal was reported in 2006 using a five-step protocol designed to mimic pancreatic organogenesis (17). The authors were able to differentiate a consistent fraction of hESCs into islet-like cells capable of synthesizing the hormones insulin, glucagon, somatostatin, pancreatic polypeptide, and ghrelin. The insulin content per cell and the frequency with which beta-like cells were obtained was quite remarkable, however glucose responsiveness was not assessed nor were *in vivo* studies performed (18).

## ADULT STEM CELLS AND PROGENITOR CELLS

Somatic or adult stem cells (ASCs) are present within post-natal tissues and are thought to be more limited in their differentiation ability than totipotent ESCs. They are defined as multipotential and they possess some advantages over ESCs, such as their use for autologous transplantation which virtually bypasses the need for immunosuppression, their nearly nonexistent tumorigenic behavior, and the absence of related ethical concerns (19).

The physiologic role of ASCs is to support cell turnover under homeostatic conditions or exceptional circumstances, i.e., regeneration of damaged tissues after severe injuries. ASCs are generally considered not terminally differentiated but pre-committed to only generate cells of the tissue with which they share the embryological origin. However, it has been reported that some ASCs can give rise to cell types other than their default ones. Accumulating lines of evidence revealed for example that bone marrow (BM) harbors not only hematopoietic stem cells, which are committed to differentiate into blood cells, but also the less differentiated mesenchymal stem cells (MSCs) (20). When transplanted in NOD mice, MSCs were reported to be able to differentiate into glucose-competent pancreatic endocrine cells (21), although confirmatory studies resulted in controversial outcomes. Indeed, it has been suggested that MSCs do not become insulin-producing cells *per se*, rather they take part in islet vascularization eventually promoting beta-cell regeneration (22). It has also been proposed that BM cells promote the functional recovery of residual beta cell mass. This is suggested by the fact that allogeneic transplantation of BM cells from autoimmunity-free strains of mice abolishes the autoimmune process in NOD mice before and even after the clinical onset of the disease, creating a hematological chimera that allows the physiologic recovery of sufficient recipient insulin-producing cells to re-establish euglycemia in the treated diabetic animals (23). Transplantation of human MSCs was also shown to induce repair of pancreatic islets and renal glomeruli in NOD/scid mice with STZ-induced diabetes (24).

Since a “resident” expandable stem cell would be an advantageous starting point for the generation of new beta cells, there have been studies which focus on the characterization of possibly-existing pancreatic progenitor cells. In 2000 Ramiya et al. (25) claimed that long-term cultivation of pancreatic ductal epithelial cells isolated from adult NOD mice contained stem cells able to differentiate into islets of Langerhans. These surrogate islets responded *in vitro* to glucose challenge, and reversed insulin-dependent diabetes after being implanted into diabetic NOD mice. Similar observations were reported using more defined culture conditions in which isolated human pancreatic duct preparations led to formation and propagation of human islet-like structures (26). Whether these results can be explained by the existence of proper pancreatic stem cells (and not surviving endocrine contaminants) has not been rigorously determined, although other studies based on selective human duct labeling confirmed that endocrine progenitors might reside in ducts (27). Besides the ductal progenitors, it has been proposed that pancreatic stem cells may also reside within the islets or that the beta cells themselves can regenerate (28).

Progenitor cells found in the liver can be converted into pancreatic endocrine hormone-producing cells (29). Pancreas and liver share the same embryological origin and it has been reported that trans-differentiation of pancreas into liver occurs both naturally *in vivo* and in animal models after a number of experimental treatments. It has been argued that the reverse inter-conversion of liver into pancreas should also be possible (30). Zalzman et al. (31) were able to immortalize a population of human fetal liver epithelial progenitor cells that, once transfected with the *pdx1* gene, gave rise to a stable population of insulin-producing cells. Intra-peritoneal transplantation of these cells into NOD/scid mice led to reversal of diabetes for 80 days. Therapeutically the process of trans-differentiation is very interesting and attractive, since it involves de-differentiation towards a common progenitor-like stage with an associated proliferative potential which can eventually be guided towards a predetermined differentiated cell type. Gershengorn and collaborators first

described such phenomenon as epithelial-to-mesenchymal transition (EMT) of islet-derived tissue cultures, characterized by their extensive proliferation and eventual re-differentiation towards endocrine cells (32). However, many critiques were advanced from other groups claiming that, at least in mouse pancreatic cultures, islet-derived fibroblast-like cells are not derived via EMT from pancreatic beta cells (33, 34). Later Gershengorn confirmed the existence of differences between human and mouse cultures (35).

## FETAL AND UMBILICAL CORD BLOOD STEM CELLS

Fetal (placental, amniotic, trophoblastic) and umbilical cord blood (UCB) stem cells are considered multipotent and share with ASCs the same advantages over ESCs. Fetal and UCB stem cells also possess other characteristics, which make their use a very appealing alternative. UCB is a convenient source of stem cells because of the potentially unlimited donor pool, its easy accessibility, the absence of distress for the donor when harvesting, and the low risk of viral transmission (36). In addition, UCB stem cells seem to have less restrictive transplant requirements in comparison to adult BM cells, possibly due to their low expression of human leukocyte antigens (HLA) (37). Published data about the phenotype of the subpopulation of UCB able to differentiate into non-hematopoietic cells is scarce. Kogler et al. in 2004 first characterized a pluripotent adherent CD45- population of cells, called “unrestricted somatic stem cells” (USSCs), able to differentiate *in vitro* into osteoblasts, chondroblasts, adipocytes, hematopoietic, neural and hepatic cells (38). More recently, other adherent UCB stem cell populations, with both embryonic and hematopoietic characteristics, have been identified (39,40). These cells not only showed several ESC-specific molecular markers, including the transcription factors OCT4 and Nanog and the embryonic antigens SSEA-3 and SSEA-4, but also possessed the ability to differentiate *in vitro* into cells with characteristics of the three embryonic layers. More notably, in our laboratory they were successfully directed to become insulin-producing cells (**Figure 1 and 2**). *In vivo* experiments confirmed these results: once transplanted into an NOD/scid mouse, these same cells were able to generate human insulin (41). However, it has been argued that the demonstrated restoration of metabolic function could merely be the result of cell fusion with host-derived beta cells rather than a true *de novo* cell generation, i.e., neogenesis.

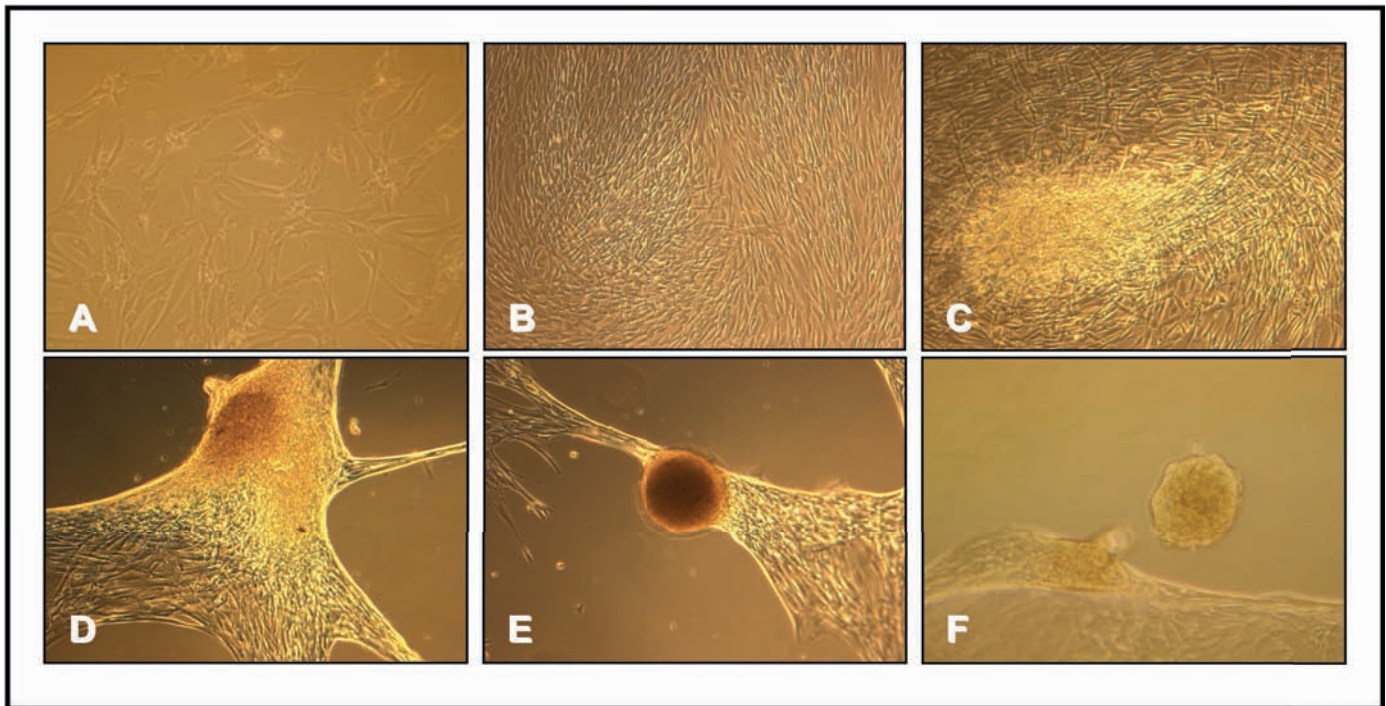


**Fig 1. USSCs in various phases of expansion and differentiation. (A) undifferentiated cells at peak of logarithmic growth; (B) cells at confluency; (C) cells gather and (D) start to form islet-like structures; (E) and (F) show differentiated islet-like bodies. (A): cells cultured in basal media; (B)-(F): cells cultured in differentiation media**

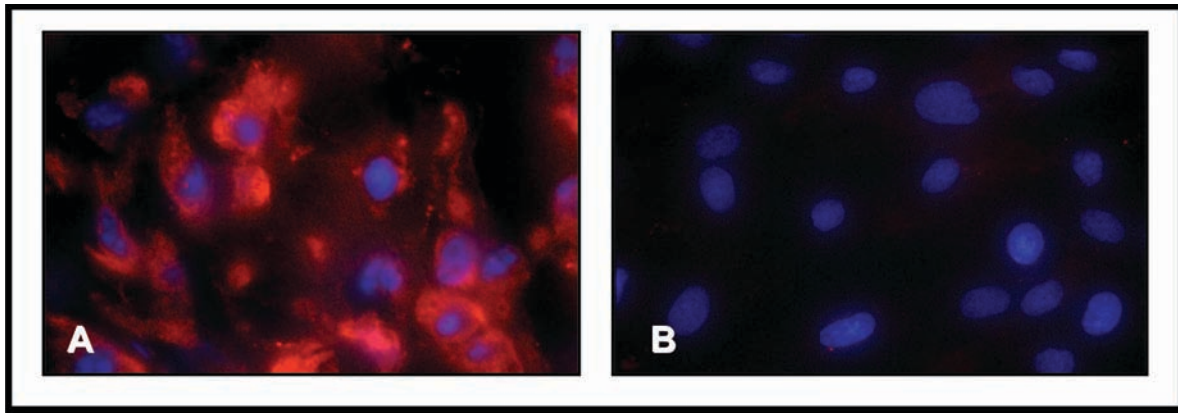


**Fig 2. immunofluorescence analysis of USSCs (A) differentiated islet-like bodies stain positive for insulin; (B) undifferentiated USSCs are negative. Red: insulin; Blue: nuclei**

Stem cells were isolated from amniotic fluid which is known to contain multiple cell types derived from the developing fetus (42). These cells, named AFS, are claimed to be pluripotent, able to give rise to tissue from all of the three germ layers. Recently, stem cells isolated from human placental tissues -- placental-derived multipotent stem cells (PDMSCs) -- were induced to differentiate into insulin positive cells (43). PDMSCs, which express the ESC markers OCT4 and Nanog, were cultured in conditioning media for 4 weeks and gradually formed 3D spheroid bodies. PCR analysis of the bodies revealed the expression of the early pancreatic markers PDX1 and Foxa2, followed by appearance of the mature pancreatic markers insulin, glucagon and somatostatin. When transplanted in STZ-treated mice PDMSCs were able to normalize blood glucose. Insulin secretion was also successfully assessed *in vitro*.

## CONCLUSIONS

Type 1 diabetes is an excellent candidate for cell replacement therapy. The last few years have seen an increase in the publication of experiments carried out to obtain surrogate insulin-producing cells. Stem cells, which have been isolated from embryonic, fetal, and adult tissues, hold great promise for the treatment and potential cure of diabetes. However, despite the enormous scientific potential of human stem cell research, its clinical application is still limited by many challenges.

First, regardless of their nature, the stem cells must be guided efficiently to differentiate into therapeutically relevant cells, i.e., possessing the ability to sense blood glucose levels and consequently release insulin in physiologically appropriate quantities. The primary challenge for ESCs remains the differentiation *in vitro* into a specific target cell while preventing or suppressing all other alternatives of their pluripotent repertoire. Strategies include attempts to recapitulate or exploit the developmental program that orchestrates pancreatic islet ontogeny, as well as directing cells along new pathways not experienced by that cell type *in vivo*. Although promising, the majority of these studies have no immediate clinical applicability because of the low production of insulin or the lack of glucose-regulated secretion even in successfully treated cells.

Second, though ESCs possess the widest differentiation potential and should therefore be the best candidates for cell replacement therapy, they are ethically problematic to some, may give rise to teratomas when implanted outside their physiologic niche, and are by definition only allogeneic. On the other hand, ASCs are ethically acceptable to most people, but lack the pluripotency of ESCs. Furthermore, recent sensational publications suggest that it is possible to approach the otherwise unparalleled pluripotency of the ESCs by reprogramming differentiated human somatic cells (e.g., adult human dermal fibroblasts) by transduction of four defined transcription factors, OCT4 and SOX2, plus either *Klf4*, and *c-Myc* (44) or *Nanog* and *Lin28* (45). These procedures should allow the creation of patient-specific stem cells which would be virtually free of rejection concerns. These studies await full confirmation since the lack of published studies using true clonal analysis raises fundamental scientific concern regarding the legitimacy of attributing extensive pluripotency to these tissue-derived somatic stem cells. However, using these induced pluripotent stem cells (iPS), Hanna et

al. (46) were able to rescue mice from their humanized sickle cell anemia. Autologous iPS were guided *in vitro* to differentiate into hematopoietic progenitors -- after their genetic defect was corrected through homologous recombination -- and then transplanted into the same affected animal which donated the original fibroblasts. The authors of this study correctly added that “problems associated with using retroviruses and oncogenes for reprogramming need to be resolved before iPS cells can be considered for human therapy”.

Finally, in the case of T1D, any suggested cell therapy will also have to deal with the underlying autoimmune disease, since the autoreactive T-lymphocytes will eventually kill new beta cells generated to replace those lost. Cord blood or placental stem cells might address these concerns because they express histocompatibility antigens in very limited amounts.

In conclusion, although human stem cell research carries with it enormous scientific potential in the treatment and possible cure of T1D, it is still hard to say when this approach will be successfully applied in the clinic. However, the rapid progression of science in this particular challenging field of investigation has been especially reassuring.



## References for the third quarterly scientific progress report

1. Bach JF. *Insulin-dependent diabetes mellitus as an autoimmune disease*. Endocr. Rev. 1994;15:516Y542.
2. Sutherland DE, Gruessner R, Kandswamy R, Humar A, Hering B, Gruessner A. *Beta-cell replacement therapy (pancreas and islet transplantation) for treatment of diabetes mellitus: an integrated approach*. Transplant Proc. 2004;36(6):1697-9.
3. Shapiro AM, Lakey JR, Ryan EA, Korbitt GS, Toth E, Warnock GL, et al. *Islet transplantation in seven patients with type 1 diabetes mellitus using a glucocorticoid-free immunosuppressive regimen*. N Engl J Med 2000;343:230–8
4. Shapiro AM, Ricordi C, Hering BJ, et al. *International trial of the Edmonton protocol for islet transplantation*. N Engl J Med. 2006;355(13):1318.
5. Trucco M. *Regeneration of the pancreatic beta cell*. J Clin Invest. 2005;115(1):5-12.
6. Evans MJ, Kaufman MH. *Establishment in culture of pluripotential cells from mouse embryos*. Nature 1981;292:154–6.
7. Dewey MJ, Martin DW Jr, Martin GR, Mintz B. *Mosaic mice with teratocarcinoma-derived mutant cells deficient in hypoxanthine phosphoribosyltransferase*. PNAS 1977;74: 5564-5568.
8. Trounson A. *The production and directed differentiation of human embryonic stem cells*. Endocr Rev 2006;27(2):208-19.
9. Vogel G, Holden C. *Developmental biology. Field leaps forward with new stem cell advances*. Science 2007;318(5854):1224-5.
10. Soria B, Roche E, Berna G, Leon-Quinto T, Reig JA, Martin F. *Insulin-secreting cells derived from embryonic stem cells normalize glycemia in streptozotocin-induced diabetic mice* 39. Diabetes 2000;49: 157–62.
11. Assady S, Maor G, Amit M, Itskovitz-Eldor J, Skorecki KL, Tzukerman M. *Insulin production by human embryonic stem cells*. Diabetes 2001;50:1691–7.
12. Lumelsky N, Blondel O, Laeng P, Velasco I, Ravin R, McKay R. *Differentiation of embryonic stem cells to insulin-secreting structures similar to pancreatic islets*. Science 2001;292:1389–94.
13. Hori Y, Rulifson IC, Tsai BC, Heit JJ, Cahoy JD, Kim SK. *Growth inhibitors promote differentiation of insulin-producing tissue from embryonic stem cells*. PNAS 2002;99:16105–10.
14. Blyszczuk P, Czyz J, Kania G, Wagner M, Roll U, St Onge L, et al. *Expression of Pax4 in embryonic stem cells promotes differentiation of nestin-positive progenitor and insulin-producing cells*. PNAS 2003;100:998–1003.
15. Rajagopal J, Anderson WJ, Kume S, Martinez OI, Melton DA. *Insulin staining of ES cell progeny from insulin uptake*. Science 2003;299:363.
16. Brolen GK, Heins N, Edsbacke J, Semb H. *Signals from the embryonic mouse pancreas induce differentiation of human embryonic stem cells into insulin-producing beta-cell-like cells*. Diabetes 2005;54:2867–74.
17. D'Amour KA, Bang AG, Eliazar S, Kelly OG, Agulnick AD, Smart NG, et al. *Production of pancreatic hormone-expressing endocrine cells from human embryonic stem cells*. Nat Biotechnol 2006;24:1392.
18. Madsen OD, Serup P. *Towards cell therapy for diabetes*. Nat Biotechnol 2006;24:1481–3.
19. Daley GQ, Goodell MA, Snyder EY. *Realistic prospects for stem cell therapeutics*. Hematology Am Soc Hematol Educ Program. 2003; 398-418. .
20. Jiang Y, Jahagirdar BN, Reinhardt RL, Schwartz RE, Keene CD, Ortiz-Gonzalez XR, et al. *Pluripotency of mesenchymal stem cells derived from adult marrow*. Nature 2002;418:41–9.
21. Ianus A, Holz GG, Theise ND, Hussain MA. *In vivo derivation of glucose-competent pancreatic endocrine cells from bone marrow without evidence of cell fusion*. J Clin Invest 2003;111:843–50.
22. Hess D, Li L, Martin M, Sakano S, Hill D, Strutt B, et al. *Bone marrow-derived stem cells initiate pancreatic regeneration*. Nat Biotechnol 2003;21:763–70.
23. Zorina TD, Subbotin VM, Bertera S, Alexander AM, Haluszczak C, Gambrell B, Bottino R, Styche AJ, Trucco M. *Recovery of the endogenous beta cell function in the NOD model of autoimmune diabetes*. Stem Cells. 2003;21(4):377-88.
24. Lee RH, Seo MJ, Reger RL, Spees JL, Pulin AA, Olson SD, Prockop DJ. *Multipotent stromal cells from human marrow home to and promote repair of pancreatic islets and renal glomeruli in diabetic NOD/scid mice*. PNAS 2006;103(46):17438-43. .

25. Ramiya VK, Maraist M, Arfors KE, Schatz DA, Peck AB, Cornelius JG. *Reversal of insulin-dependent diabetes using islets generated in vitro from pancreatic stem cells*. Nat Med 2000;6:278–82.
26. Bonner-Weir S, Taneja M, Weir GC, Tatarkiewicz K, Song KH, Sharma A, et al. *In vitro cultivation of human islets from expanded ductal tissue*. PNAS 2000;97:7999–8004.
27. Gao R, Ustinov J, Pulkkinen MA, Lundin K, Korsgren O, Otonkoski T. *Characterization of endocrine progenitor cells and critical factors for their differentiation in human adult pancreatic cell culture*. Diabetes 2003;52:2007–15.
28. Gu G, Dubauskaite J, Melton DA. *Direct evidence for the pancreatic lineage: NGN3 $\pi$  cells are islet progenitors and are distinct from duct progenitors*. Development 2002;129:2447–57.
29. Yang L, Li S, Hatch H, Ahrens K, Cornelius JG, Petersen BE, Peck AB. *In vitro trans-differentiation of adult hepatic stem cells into pancreatic endocrine hormone-producing cells*. PNAS 2002;99(12):8078.
30. Horb ME, Shen CN, Tosh D, Slack JM. *Experimental conversion of liver to pancreas*. Curr Biol 2003;13:105–15.
31. Zalzman M, Gupta S, Giri RK, Berkovich I, Sappal BS, Karnieli O, et al. *Reversal of hyperglycemia in mice by using human expandable insulin-producing cells differentiated from fetal liver progenitor cells*. PNAS 2003;100:7253–8.
32. Gershengorn MC, Hardikar AA, Wei C, Geras- Raaka E, Marcus-Samuels B, Raaka BM. *Epithelial- to-mesenchymal transition generates proliferative human islet precursor cells*. Science 2004;306:2261–4.
33. Atouf F, Park CH, Pechhold K, Ta M, Choi Y, Lumelsky NL. *No evidence for mouse pancreatic beta-cell epithelial-mesenchymal transition in vitro*. Diabetes 2007;56(3):699-702.
34. Chase LG, Ulloa-Montoya F, Kidder BL, Verfaillie CM. *Islet-Derived Fibroblast-Like Cells Are Not Derived via Epithelial-Mesenchymal Transition From Pdx-1 or Insulin-Positive Cells*. Diabetes. 2007;56(1):3-7.
35. Morton RA, Geras-Raaka E, Wilson LM, Raaka BM, Gershengorn MC. *Endocrine precursor cells from mouse islets are not generated by epithelial-to-mesenchymal transition of mature beta cells*. Mol Cell Endocrinol. 2007;30;270(1-2):87-93.
36. Rubinstein P, Carrier C, Scaradavou A, et al. *Outcomes among 562 recipients of placental-blood transplants from unrelated donors*. N Engl J Med. 1998;339:1565–1577.
37. Gluckman E, Koegler G, Rocha V. *Human leukocyte antigen matching in cord blood transplantation*. Semin Hematol 2005; 42: 85–90.
38. Kogler G, Sensken S, Airey JA, et al. *A new human somatic stem cell from placental cord blood with intrinsic pluripotent differentiation potential*. J Exp Med. 2004;200:123–135.
39. McGuckin CP, Forraz N, Baradez MO, Navran S, Zhao J, Urban R, Tilton R, Denner L. *Production of stem cells with embryonic characteristics from human umbilical cord blood*. Cell Prolif. 2005;38(4):245.
40. Y Zhao, H Wang, T Mazzone. *Identification of stem cells from human umbilical cord blood with embryonic and hematopoietic characteristics*. Exp Cell Res. 2006 Aug 1;312(13):2454-64.
41. Yoshida S, Ishikawa F, Kawano N, Shimoda K, Nagafuchi S, Shimoda S, Yasukawa M, Kanemaru T, Ishibashi H, Shultz LD, Harada M. *Human cord blood--derived cells generate insulin-producing cells in vivo*. Stem Cells. 2005;23(9):1409-16.
42. De Coppi P, Bartsch G Jr, Siddiqui MM, Xu T, Santos CC, Perin L, Mostoslavsky G, Serre AC, Snyder EY, Yoo JJ, Furth ME, Soker S, Atala A. *Isolation of amniotic stem cell lines with potential for therapy*. Nat Biotechnol. 2007;25(1):100-6.
43. Chang CM, Kao CL, Chang YL, Yang MJ, Chen YC, Sung BL, Tsai TH, Chao KC, Chiou SH, Ku HH. *Placenta-derived multipotent stem cells induced to differentiate into insulin-positive cells*. Biochem Biophys Res Commun. 2007;357(2):414-20.
44. Takahashi K, Tanabe K, Ohnuki M, Narita M, Ichisaka T, Tomoda K, Yamanaka S. *Induction of pluripotent stem cells from adult human fibroblasts by defined factors*. Cell 2007;131;861-872.
45. Yu J, Vodyanik MA, Smuga-Otto K, Antosiewicz-Bourget J, Fane JL, Tian S, Nie J, Jonsdottir GA, Ruotti V, Stewart R, Slukvin II, Thomson JA. *Induced pluripotent stem cell lines derived from human somatic cells*. Science 2007;318:1917-1920.
46. Hanna J, Wernig M, Markoulaki S, Sun C-W, Meissner A, Cassady JP, Beard C, Brambrink T, Wu L-C, Townes TM, Jaenisch R. *Treatment of sickle cell anemia mouse model with iPS cells generated from autologous skin*. Science 2007;318:1920-1923.

In the fourth and final quarterly scientific progress report (3/01/08 – 05/30/08) of Year 02 we now report on direct evidence of regeneration in the monkey tissue.

## Introduction

Until a few years ago, lesions of the endocrine pancreas, as they occur in Type 1 Diabetes (T1D), were thought to be permanent and irreversible since diabetic patients require hormone replacement therapy for life (1). Despite the clinical evolution of the disease, it is still unknown whether the islet beta cells preserve, at least in part, the ability to heal from an injury. Moreover, it is not clear whether in T1D a possible recovery of the beta cell mass is contrasted by the destructive mechanisms that cause diabetes in the first place (3).

In mouse models, evidence has accrued that adult animals retain the ability to expand their beta cell mass after stimulation with a variety of triggers (4-7). It has also been shown that in the non-obese diabetic mice (NOD), strategies involving reversal of the autoimmune attack were key to allow recovery of sufficient endogenous insulin production even after diabetes onset (8-12). It remains largely uncertain through which molecular and cellular mechanisms the reparative process works, i.e. if new beta cells are formed via self-proliferation or originate from pancreatic precursors as they do during embryonic development (2).

In humans, the ability of post-natal pancreas to expand beta cell mass after injury is still debated (13-15). Spontaneous recovery of the beta cell function has been reported in only a few cases of patients previously diagnosed with T1D. These individuals experienced a return to endogenous insulin production after diagnosis and initiation of exogenous insulin treatment. Concurrently, the humoral signs of autoimmunity (i.e., autoantibody positivity) eventually vanished (16-19).

It has been reported that in humans some beta cells are still present even years after the clinical onset of diabetes (20). We also know that in the healthy pancreas only a limited islet mass is actively engaged in supplying insulin to maintain normoglycemia, meaning that the critical mass that needs to be functional at a given time point is far less than that of the entire pancreatic beta cell pool (21). This observation may entail that replacement of relatively small numbers of insulin producing cells should exert substantial effects in patients.

The potential for the pancreatic organ to recover the endocrine function is quite fascinating and it is the object of intense focus for possible clinical applications. Non-human primates are important animal models for pre-clinical studies and, in particular, for xenotransplantation experiments. From a physiological point of view, monkeys and humans present strong similarities even though the monkey does not show signs of spontaneous autoimmune diabetes (22). Nonetheless a permanent diabetic status can be induced by total pancreatectomy or by chemical destruction of the beta cells with streptozotocin (STZ) (23). It is therefore of great value to investigate the potential of non-human primate pancreatic tissue to recover endogenous insulin production after injury.

Our experimental protocol involved induction of diabetes in eleven monkeys by high dose of STZ followed, in eight of them, by intra-portal pig islet transplantation. In the pig-to monkey model, endogenous primate C-peptide can be easily distinguished from donor pig C-peptide. No spontaneous recovery of endogenous function was observed in any of the STZ-diabetic monkeys that were not transplanted (n=3) and in those that experienced early graft failure (n=6). In two diabetic recipients in whom pig islet graft functioned for a few weeks, we observed instead increasing endogenous C-peptide levels paralleled by clinical improvement, associated to supportive histological and molecular findings. Interestingly, exceptionally long graft survival time was not associated with recovery of endogenous beta cell function (our unpublished data and 24).

## Results.

### *Recovery of endogenous C-peptide in two STZ-diabetic islet recipients*

All monkeys became hyperglycemic within 48 hours following STZ injection. Diabetic monkeys were administered exogenous insulin to lower blood glucose levels and prevent DKO. Diabetic monkeys that did not undergo transplantation and islet recipients with early graft loss (undetectable porcine C-peptide or detection for less than 2 weeks) showed no significant increase of the autologous C-peptide over the post-STZ basal levels (Figure 1) for more than one year and exogenous insulin requirements remained unchanged (data not shown). The pancreatic tissue showed islets characterized by well-preserved glucagon staining but almost complete absence of insulin positive cells (Figure 2).

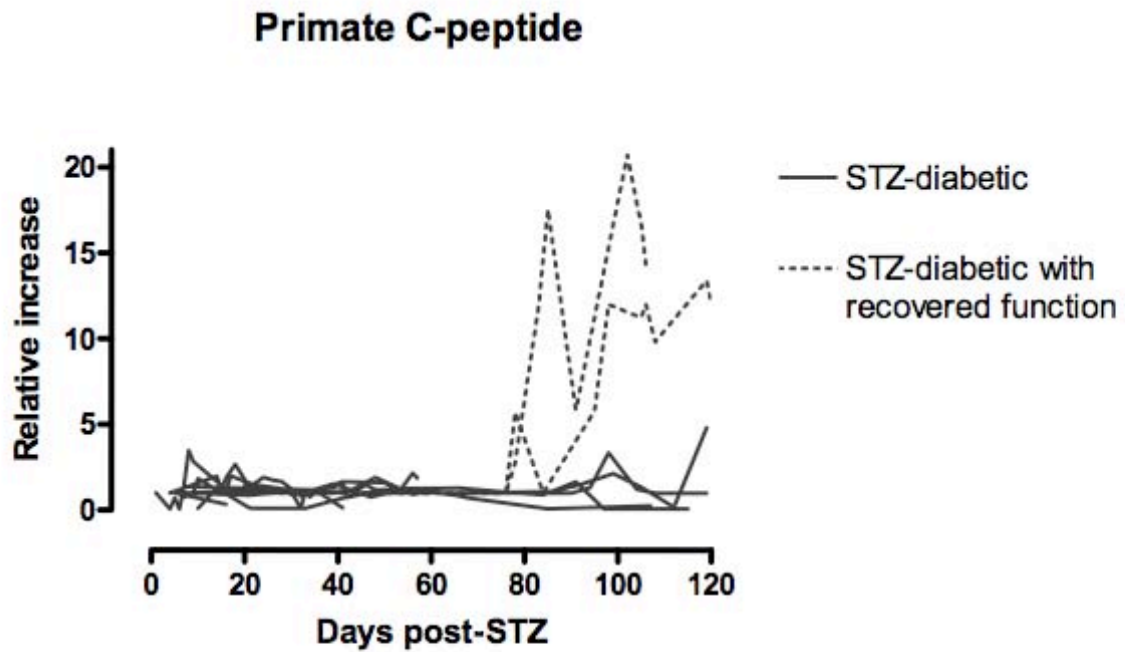


**Figure 1: Relative increase of endogenous C-peptide over basal post-STZ values.** Close lines indicate STZ- diabetic monkeys that were not transplanted (n=3) and STZ-diabetic recipients that experienced early graft loss (n=6). Dotted lines represent the monkeys with recovered beta cell function (n=2).

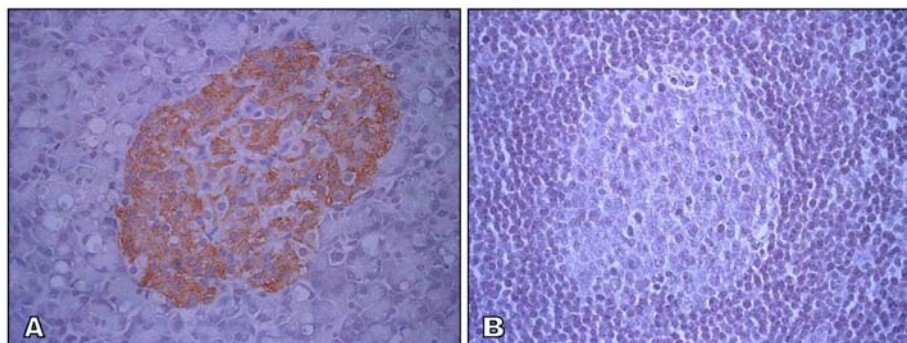


**Figure 2: STZ causes chemical destruction of beta cells.** Pancreatic insulin immunostaining of a non-diabetic control monkey (A) and of a diabetic monkey one year after streptozotocin (B). Magnification: 40x.



In two monkeys (M4804 and M5204), a gradual recovery of basal endogenous C-peptide occurred over time (Figure 1). This increase occurs after a period of islet graft function evidenced by detectable porcine C-peptide levels, but, interestingly, the two curves of endogenous/porcine C-peptide followed an opposite trend (Figure 3 A,C). It appears therefore that graft failure marks a switch in insulin production from the graft to the endogenous pancreas. Graft failure was not followed by a return to severe hyperglycemia and to higher exogenous insulin requirements (Figure 3 B,D). In addition, IVGTT showed that stimulated endogenous C-peptide increased with time, further confirming the progressive recovery of the pancreatic function (Figure 4). In contrast, in all other monkey recipients following islet graft failure, glycemia and insulin requirements returned to pre-transplantation levels (data not shown). Finally, in monkeys with a long-term graft function (3 and 12 months), recovery of endogenous insulin production was not at all observed (our unpublished data).

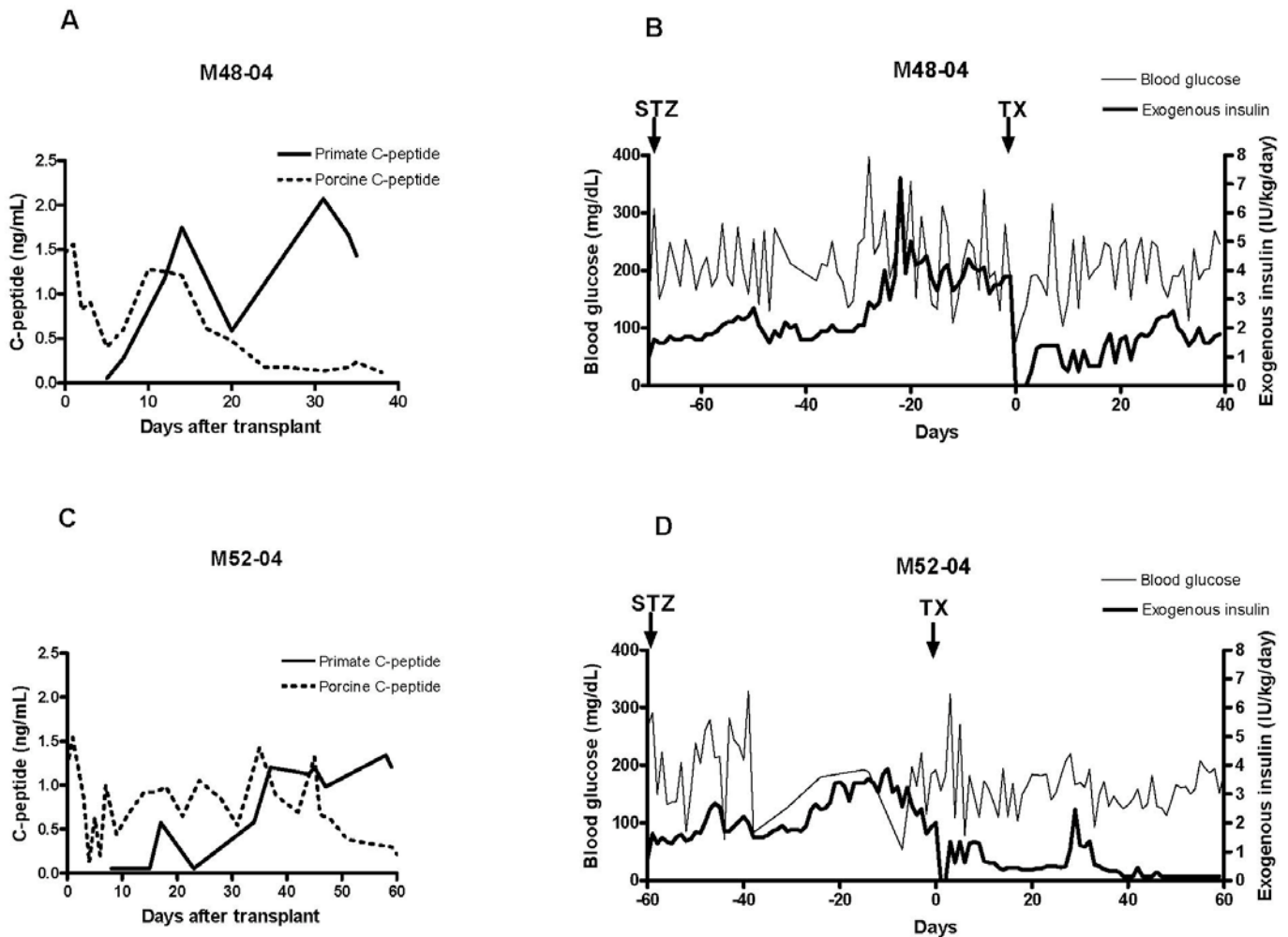


**Figure 3: Metabolic profile of two monkeys recipient of islet grafts recovering endogenous C-peptide. (A-C):** Graft (porcine) and endogenous (primate) C-peptide levels. **(B-D):** Blood glucose and exogenous insulin administration.

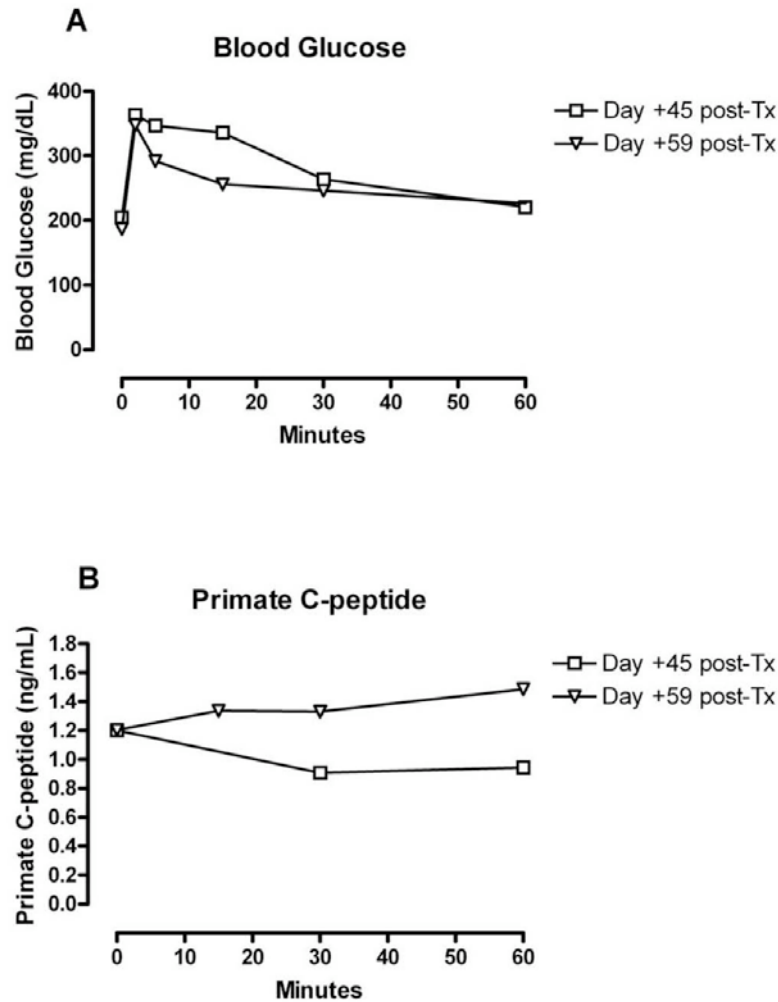


**Figure 4: Improved endogenous beta cell response to glucose stimulation overtime in monkey M5204.** Blood glucose levels (**A**) and endogenous C-peptide (**B**) during IVGTT at day 45 and day 59 following transplantation.

#### *Proinsulin/glucagon immunostaining*

The pancreas of all the monkeys was analysed for the presence of proinsulin positive cells. Pre-existing islets in diabetic monkeys were individuated by glucagon immunostaining.

The two monkeys that re-established endogenous C-peptide production showed several proinsulin positive cells grouped in small aggregates or scattered as single cells throughout the pancreas and/or associated to ducts. They were not part of previously existing islets as demonstrated by the absence of neighbouring glucagon<sup>+</sup> cells (Figure 5). The frequency of proinsulin positive cell clusters with area equal or smaller than 30  $\mu\text{m}^2$  (cell clusters not included in the preformed islets or in the ducts) in the monkeys with recovered endogenous insulin production was higher than in STZ-diabetic controls, with respectively 0.23 and 0.18% positive area/whole section versus  $0.05 \pm 0.0004$  in 4 diabetics, however less than in the pancreas of 3 non diabetic monkeys ( $0.30 \pm 0.01\%$ ).

Proinsulin positive cells also co-stained with PDX-1. Double alpha and beta phenotype (glucagon<sup>+</sup> and proinsulin<sup>+</sup>) was never found (Figure 5A) in any of the groups of animals analysed.

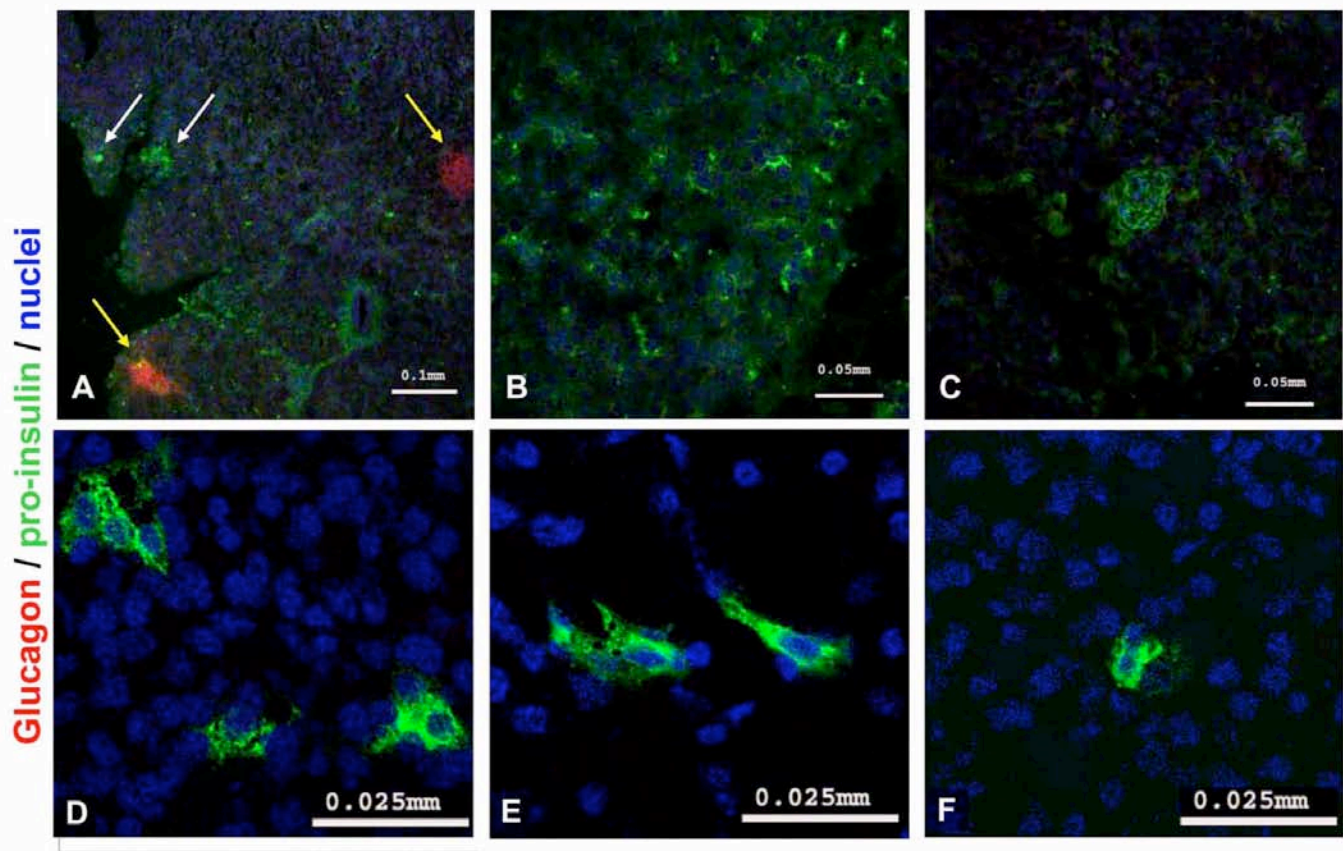


**Figure 5: Proinsulin positive cells in monkeys with recovered endogenous beta cell function.** Proinsulin positive cells in the pancreas are organized in small aggregates (A) or scattered as single cells (B) outside pre-existing islets characterized by glucagon positive staining. White arrows: proinsulin positive cells. Yellow arrows: pre-existing islets. (C-F): different magnifications. Pictures are representative of both monkeys with recovered endogenous beta cell function.

#### *Ductal cells co-stain with proinsulin and PDX-1 in monkeys with recovered function*

Anti-CK19 antibody staining was used to identify the ductal/epithelial cell compartment in the pancreatic tissue. Interestingly, a subpopulation of CK19 cells co-stained with proinsulin in the parenchyma (Figure 6A-D) and in the ducts (Figure 6 E-H) only in the two monkeys with recovered function. The pancreas of the two monkeys with recovered endogenous beta cell function showed stronger expression of CK19 cells (supplemental Figure 2A) in comparison to non-diabetic and STZ-diabetic controls

Additionally, as shown in Figure 7, the monkeys with recovered beta cell function presented double PDX-1<sup>+</sup>/CK19<sup>+</sup> and PDX-1<sup>+</sup>/proinsulin<sup>+</sup> staining. To note, PDX-1<sup>+</sup> cells are found in STZ diabetic monkeys but they do not co-localize with CK19 (Figure 7B) and with proinsulin (data not shown).

ck19 / pro-insulin / nuclei

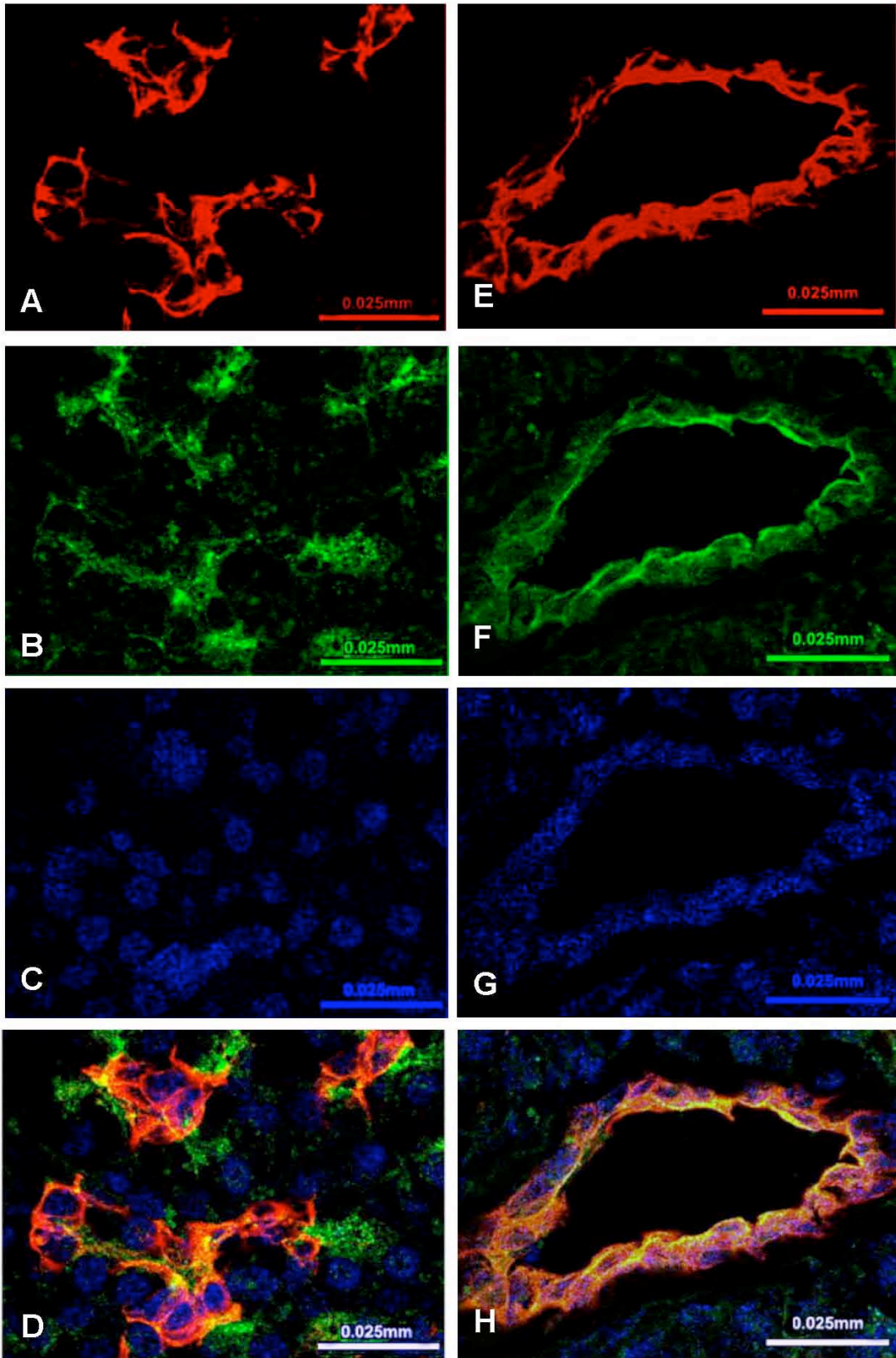


**Figure 6: Presence of double phenotype CK19/proinsulin in monkeys with recovered endogenous beta cell function. (A,B,C,D):** Monkeys with recovered endogenous beta cell function show co-expression of CK19 with proinsulin (yellow). **(E,F,G,H):** Detail of a pancreatic duct.



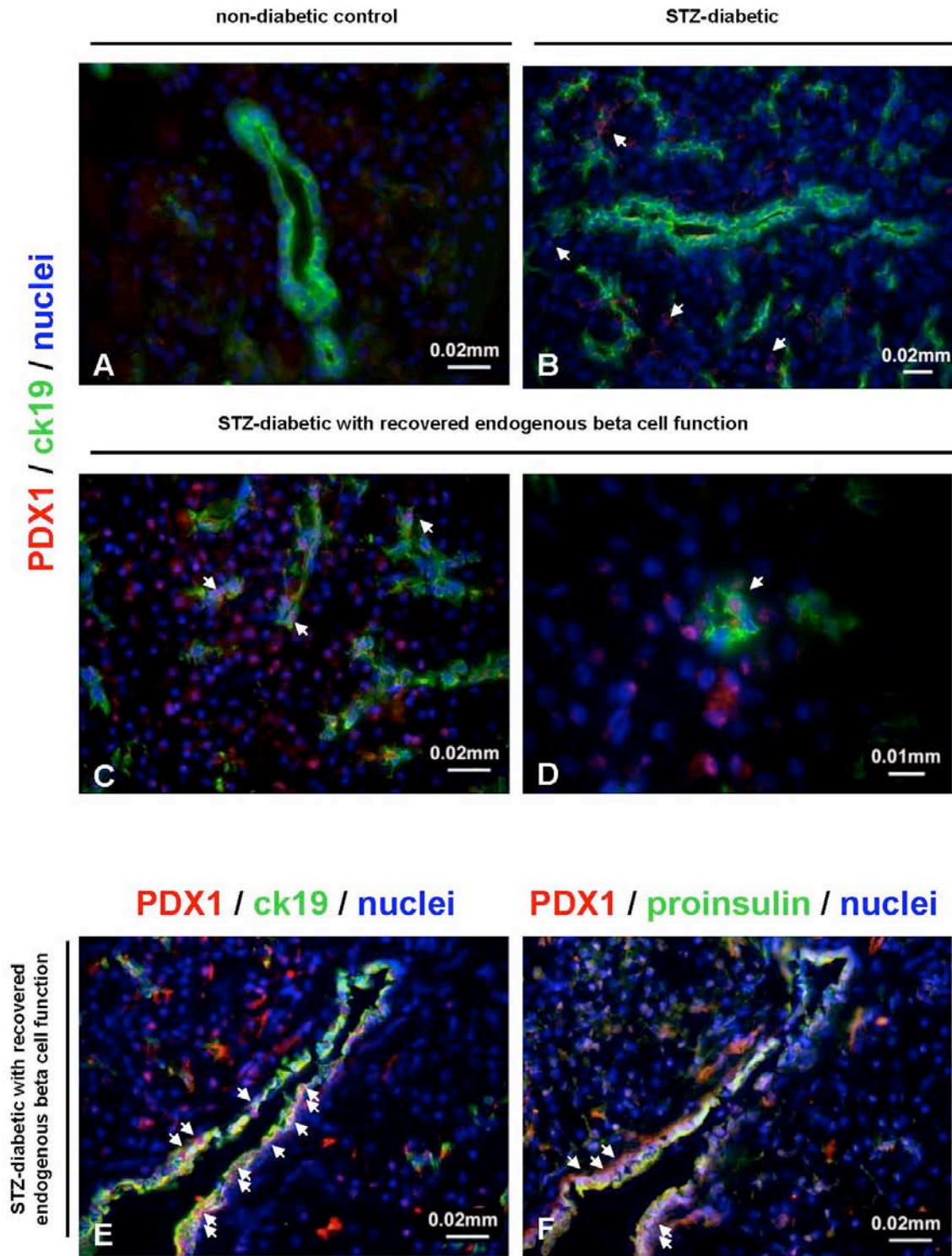


**Figure 7: PDX-1 co-expresses with CK19 in the pancreas of monkeys with recovered function.** CK19 and PDX-1 do not co-stain in the pancreas of non-diabetic healthy monkeys (A); PDX-1 positive cells are found scattered throughout the pancreas of STZ diabetic monkeys, but do not co-localize with CK19 (B); CK19 and PDX-1 co-localization shown in the pancreas of a monkey with recovered beta cell function (C with detail in D). E and F: pancreatic consecutive sections M5204 (monkey with recovered beta cell function) showing CK19<sup>+</sup>/PDX-1<sup>+</sup> (E) and CK19<sup>+</sup>/proinsulin<sup>+</sup> (F) cells respectively. Arrows show PDX-1<sup>+</sup> cells in B, double positive PDX-1<sup>+</sup>/CK19<sup>+</sup> in C, D and E and PDX-1<sup>+</sup>/proinsulin<sup>+</sup> in F.

### Proliferative activity in the pancreas: Ki67 immunostaining

Anti-Ki67 antibody was used as a nuclear marker of active cell proliferation.

Positive cells were observed in pancreatic sections of the monkeys that showed return of endogenous C-peptide (**Figure 8 A,D,E and F**). Ki67<sup>+</sup> cells co-stained with the ductal marker CK19 and with fibroblasts (**Figure 8 D,E**), but not with proinsulin<sup>+</sup> cells (**Figure 8 F**). Pancreatic sections of non-diabetic and STZ-diabetic monkeys contained occasional Ki67<sup>+</sup> cells (**Figure 8 B,C**).

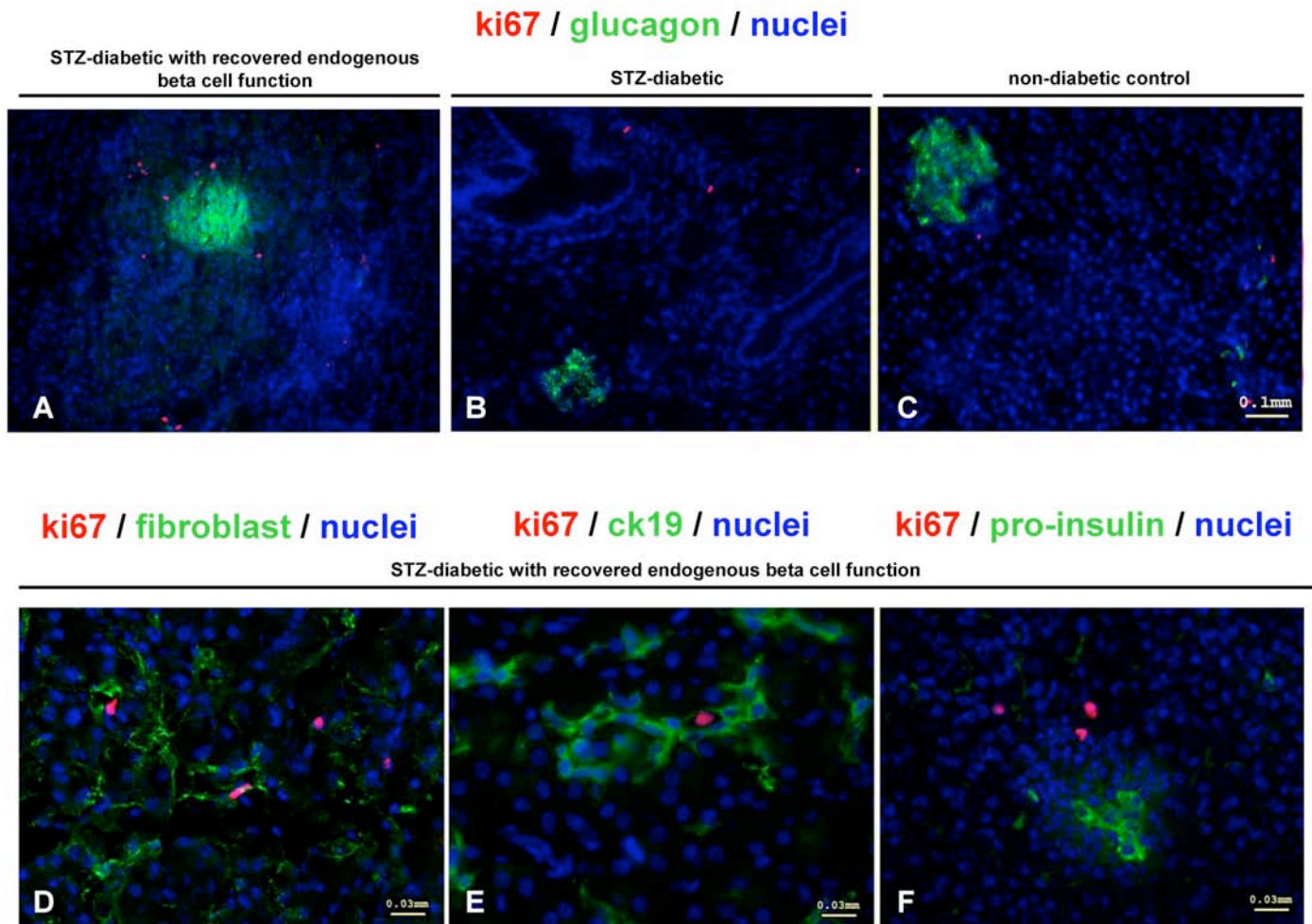


**Figure 8: Proliferative activity in the pancreas.** Ki67 staining is increased in pancreas of STZ-diabetic monkeys with recovered endogenous beta cell function (**A**) in comparison to STZ-diabetic monkeys (**B**) and non-diabetic control (**C**). In STZ-diabetic monkeys with recovered endogenous beta cell function (**D-F**) Ki67 co-stains with fibroblast marker (**D**) and CK19 (**E**) but not with insulin (**F**).

### Analysis of endocrine markers by qRT-PCR

The expression of selected islet-specific nuclear transcription factors was also analyzed in transplanted and non transplanted monkeys (34). Gene expression in the two monkeys with recovered endogenous beta cell function was compared to non-diabetic and STZ- diabetic controls (**Figure 9 A-F**). qRT-PCR of NKX6.1, Pax6, ISL1, Foxa2, Beta2NeuroD, and PDX-1 showed mRNA levels mostly of the same order of magnitude in all monkeys, with only sporadic individual variability. When the expression of each gene was normalized against insulin, in the regenerating monkeys such factors resulted consistently upregulated (**Figure 10**). Ngn3, a master gene regulating early pancreatic endocrine lineage commitment, was not detected in any of the tissues analyzed (data not shown).

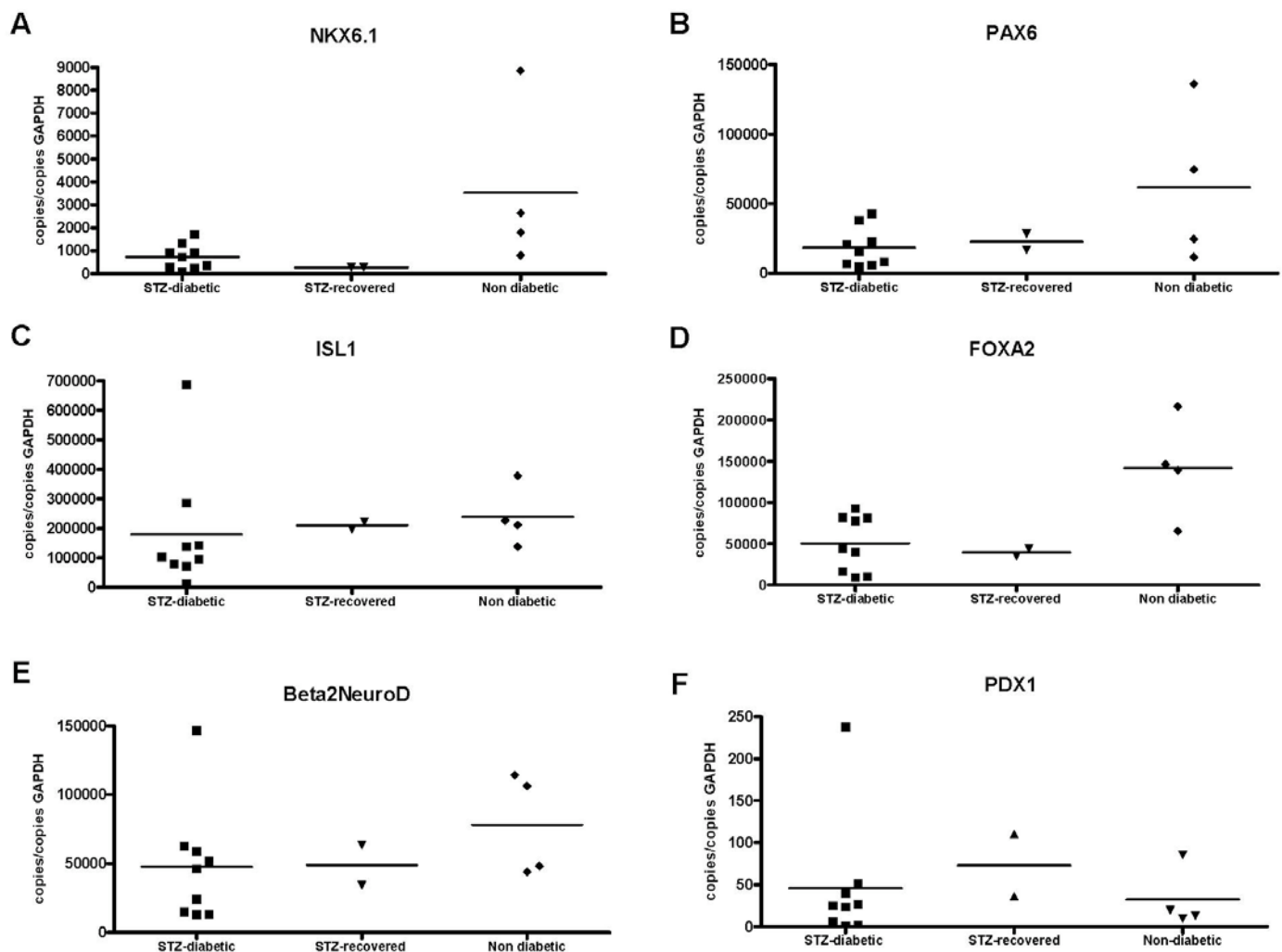


**Figure 9: qRT-PCR analysis of endocrine precursor markers. (A-E):** mRNA expression of the nuclear transcription factors PDX-1, NKX6.1, PAX6, ISL1, FOXA2, Beta2NeuroD in STZ-diabetic monkeys (n=9), monkeys with recovered endogenous C-peptide (n=2) and non-diabetic controls (n=4). Copies are normalized against the housekeeping gene GAPDH. Normalization against HPRT showed no substantial differences

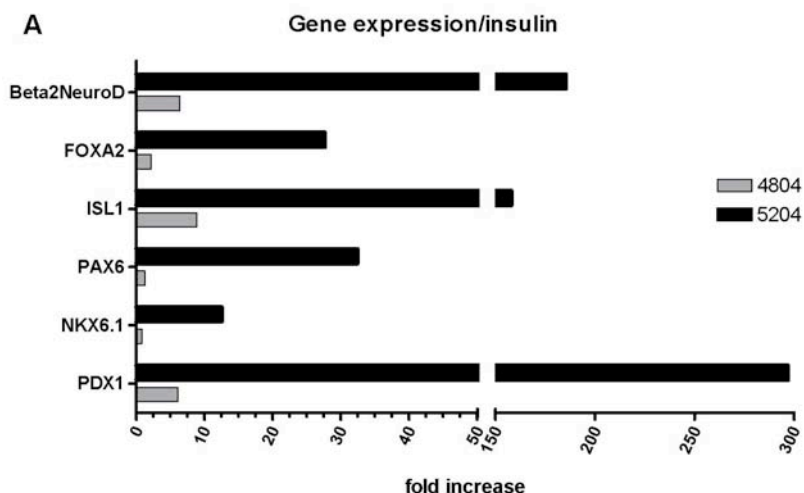


**Figure 10: Normalization of the nuclear transcription factors against insulin in the two monkeys with recovered beta cell function.** Expression levels relative to insulin are consistently upregulated. Values represent fold increase in relation to normal non-diabetic pancreatic tissue (average of n=4 monkeys).

## References

1. Atkinson MA, Eisenbarth GS. Type 1 diabetes: new perspectives on disease pathogenesis and treatment. *Lancet* 2001; 358(9277):221-229
2. Trucco M. Regeneration of the pancreatic beta cell. *J Clin Invest* 2005; 115(1):5-12
3. Rood PP, Bottino R, Balamurugan AN, Fan Y, Cooper DK, Trucco M. Facilitating physiologic self-regeneration: a step beyond islet cell replacement. *Pharm Res* 2006; 23(2):227-242
4. Bonner-Weir S, Baxter LA, Schupp GT, Smith FE. A second pathway for regeneration of adult exocrine and endocrine pancreas. A possible recapitulation of embryonic development. *Diabetes* 1993; 42(12):1715-1720
5. Bowens L, Rorman I. Regulation of pancreatic beta-cell mass. *Physiol Rev* 2005; 85:1255-1270
6. Xu X, D'Hoker J, Stange G, Bonne S, De Leu N, Xiao X et al. b cells can be generated from endogenous progenitors in injured adult mouse pancreas. *Cell* 2008; 132, 197-207
7. Nir T, Melton DA, Dor Y. Recovery from diabetes in mice by beta cell regeneration. *J Clin Invest.* 2007; 117(9):2553-2561
8. Zorina TD, Subbotin VM, Bertera S, Alexander AM, Haluszczak C, Gambrell B et al. Recovery of the endogenous beta cell function in the NOD model of autoimmune diabetes. *Stem Cells* 2003; 21(4):377-388
9. Kodama S, Kühtreiber W, Fujimura S, Dale EA, Faustman DL. Islet regeneration during the reversal of autoimmune diabetes in NOD mice. *Science* 2003; 302(5648):1223-1227
10. Chong AS, Shen J, Tao J, Yin D, Kuznetsov A, Hara M et al. Reversal of diabetes in non-obese diabetic mice without spleen cell-derived beta cell regeneration. *Science* 2006; 311(5768):1774-1775
11. Nishio J, Gaglia JL, Turvey SE, Campbell C, Benoist C, Mathis D. Islet recovery and reversal of murine type 1 diabetes in the absence of any infused spleen cell contribution. *Science* 2006; 311(5768):1775-1778
12. Suri A, Calderon B, Esparza TJ, Frederick K, Bittner P, Unanue ER. Immunological reversal of autoimmune diabetes without hematopoietic replacement of beta cells. *Science* 2006; 311(5768):1778-1780
13. Butler PC, Meier JJ, Butler AE, Bhushan A. The replication of beta cells in normal physiology, in disease and for therapy. *Nat Clin Pract Endocrinol Metab* 2007; 3(11):758-768
14. Butler AE, Galasso R, Meier JJ, Basu R, Rizza RA, Butler PC. Modestly increased beta cell apoptosis but no increased beta cell replication in recent-onset type 1 diabetic patients who died of diabetic ketoacidosis. *Diabetologia* 2007; 50(11):2323-2331
15. Meier JJ, Butler AE, Saisho Y, Monchamp T, Galasso R, Bhushan A et al. Beta-cell replication is the primary mechanism subserving the postnatal expansion of beta-cell mass in humans. *Diabetes* 2008; Mar 11; [Epub ahead of print]
16. Taylor KW. Pathogenesis of diabetes mellitus. *J Clin Path* 1969; 22, suppl, 2:76-81
17. Karges B, Durinovic-Bello I, Heinze E, Boehm B, Debatin K-M, Karges W. Complete long-term recovery of beta cell function in autoimmune type 1 diabetes after insulin treatment. *Diabetes Care* 2004; 27:1207-1208



18. Karges B, Durinovic-Bello' I, Heinze E, Debatin K-M, Boehm B, Karges W. Immunological mechanisms associated with long-term remission of human type 1 diabetes. *Diabetes/Metabolism Res. And Rev* 2006; 22:184-189
19. Meier JJ, Lin JC, Butler AE, Galasso R, Martinez DS, Butler PC. Direct evidence of attempted beta cell regeneration in an 89-year-old patient with recent-onset type 1 diabetes. *Diabetologia* 2006; 49:1838-1844
20. Meier J.J., Bhushan A., Butler A.E., Rizza R.A. and Butler P.C. Sustained beta cell apoptosis in patients with long-standing type 1 diabetes: indirect evidence for islet regeneration? *Diabetologia* 2005; 48:2221-2228
21. Kolb H, Gale EAM. Does partial preservation of residual beta-cell function justify immune intervention in recent onset Type 1 diabetes? *Diabetologia* 2001; 44:1349-1353
22. Casu A, Bottino R, Balamurugan AN, Hara H, van der Windt DJ, Campanile N, et al. Metabolic aspects of pig-to-monkey (*Macaca fascicularis*) islet transplantation: implications for translation into clinical practice. *Diabetologia* 2008; 51(1):120-129
23. Rood PP, Bottino R, Balamurugan AN, Smetanka C, Ezzelarab M, Busch J et al. Induction of diabetes in cynomolgus monkeys with high-dose streptozotocin: adverse effects and early responses. *Pancreas* 2006; 33(3):287-292
24. Hering BJ, Wijkstrom M, Graham ML, Hårdstedt M, Aasheim TC, Jie T, et al. Prolonged diabetes reversal after intraportal xenotransplantation of wild-type porcine islets in immunosuppressed nonhuman primates. *Nat Med* 2006; 12(3):301-303
25. Report of the Expert Committee on the Diagnosis and Classification of Diabetes Mellitus. *Diabetes Care* 1997; 20: 1183-1197
26. Toso C, Brandhorst D, Oberholzer J, Triponez F, Buhler L, Morel P. Isolation of adult porcine islets of Langerhans. *Cell Transplant* 2000; 9: 297-305
27. Yonekawa Y, Matsumoto S, Okitsu T, Arata T, Iwanaga Y, Noguchi H et al. Effective islet isolation method with extremely high islet yields from adult pigs. *Cell Transplant* 2005; 14: 757-762
28. Bottino R, Balamurugan AN, Smetanka C, Bertera S, He J, Rood PP et al. Isolation outcome and functional characteristics of young and adult pig pancreatic islets for transplantation studies. *Xenotransplantation*. 2007; 14(1):74-82
29. Balamurugan AN AJ, Chang Y, Fung JJ, Trucco M, Bottino R. Flexible management of enzymatic digestion improves human islet isolation outcome from sub-optimal donor pancreata. *Am J Transplant* 2003; 3:1135-1142
30. Bottino R, Balamurugan AN, Bertera S, Pietropaolo M, Trucco M, Piganelli JD Preservation of human islet cell functional mass by anti-oxidative action of a novel SOD mimic compound. *Diabetes* 2002; 51: 2561-2567
31. Balamurugan AN, He J, Guo F, Stolz DB, Bertera S, Geng X et al. Harmful delayed effects of exogenous isolation enzymes on isolated human islets: relevance to clinical transplantation. *Am J Transplant* 2005; 5: 2671-2681
32. Bottino R, Balamurugan AN, Tse H, Thirunavukkarasu C, Ge X, Profozich J et al. Response of human islets to isolation stress and the effect of antioxidant treatment. *Diabetes* 2004; 53: 2559-2568
33. Knosalla C, Ryan DJ, Moran K, Gollackner B, Schuler W, Sachs DH et al. Initial experience with the human anti-human CD154 monoclonal antibody, ABI793, in pig-to-baboon xenotransplantation. *Xenotransplantation* 2004; 11: 353-360

34. Servitja JM, Ferrer J. Transcriptional networks controlling pancreatic development and beta cell function. *Diabetologia* 2004; 47(4):597-613
35. Dor Y, Brown J, Martinez OI, Melton DA. Adult pancreatic beta-cells are formed by self-duplication rather than stem-cell differentiation. *Nature* 2004; 429(6987):41-46
36. Bonner-Weir S, Weir GC. New sources of pancreatic beta-cells. *Nat Biotechnol* 2005; 23(7):857-861
37. Ablamunits V, Sherry NA, Kushner JA, Herold KC. Autoimmunity and beta cell regeneration in mouse and human type 1 diabetes: the peace is not enough. *Ann N Y Acad Sci* 2007; 1103:19-32
38. Sherry NA, Kushner JA, Glandt M, Kitamura T, Brillantes AM, Herold KC. Effects of autoimmunity and immune therapy on beta-cell turnover in type 1 diabetes. *Diabetes*. 2006; 55(12):3238-3245
39. Bonner-Weir S, Taneja M, Weir GC, Tatarkiewicz K, Song KH, Sharma A, et al. In vitro cultivation of human islets from expanded ductal tissue. *Proc Natl Acad Sci U S A* 2000; 97(14):7999-8004
40. Gao R, Ustinov J, Korsgren O, Otonkoski T. In vitro neogenesis of human islets reflects the plasticity of differentiated human pancreatic cells. *Diabetologia* 2005; 48(11):2296-2304
41. Pang K, Mukonoweshuro C, Wong G. Beta cells arise from glucose transporter type 2 (Glut2)-expressing epithelial cells of the developing rat pancreas. *Proc. Natl. Acad. USA* 1994; 91:9559-9563
42. Herrera PL. Adult insulin-and glucagon producing cells differentiate from two independent cell lineages. *Development* 2000; 127:2317-2322
43. Matzinger P. Friendly and dangerous signals: is the tissue in control? *Nat Immunol* 2007; 8(1):11-13
44. Rother KI, Harlan D M. Challenges facing islet transplantation for the treatment of type 1 diabetes mellitus. *JCI* 2004; 114:877-883
45. Shapiro AM, Ricordi C, Hering BJ, Auchincloss H, Lindblad R, Robertson RP et al. International trial of the Edmonton protocol for islet transplantation. *N Engl J Med* 2006; 355(13):1318-1330
46. Bonner-Weir S, Deery D, Leahy JL, Weir GC. Compensatory growth of pancreatic beta-cells in adult rats after short-term glucose infusion. *Diabetes* 1989; 38(1):49-53
47. Bernard C, Berthault MF, Saulnier C, Ktorza A. Neogenesis vs. apoptosis as main components of pancreatic beta cell mass changes in glucose-infused normal and mildly diabetic adult rats. *FASEB J* 1999; 13(10):1195-1205

## KEY RESEARCH ACCOMPLISHMENTS

- Diabetes induction is characterized by the establishment of a hyperglycemic status that, in non-human primates, requires exogenous insulin treatment to prevent fatal cheto-acidosis. Streptozotocin successfully induces hyperglycemia following administration in rodents as well as in non-human primates. Following streptozotocin administration, a drastic reduction of endogenous circulating C-peptide is observed, and histologic analysis of the pancreas shows virtual absence of insulin positive cells. Even in those monkeys where low but detectable C-peptide levels were measured after streptozotocin, histological findings confirmed the destruction of insulin positive cells, and in vivo functional studies suggested that any residual insulin producing mass is not responsive. We consequently observed that hyperglycemia and diabetes management were not influenced by the residual C-peptide amounts.
- In the absence of the autoimmune mechanisms (no evidence of autoimmunity is accrued in streptozotocin diabetic monkeys), our experiments suggest that diabetic monkeys -- that receive xenogeneic islet support with sustained detectable biological activity for sometime -- may recover a self-driven endocrine function. Such function is evidenced not only by stepwise increasing levels of endogenous C-peptide, but also by amelioration of the metabolic control, not simply explained by the effect of the graft. No report of a spontaneous remission of the hyperglycaemic status in diabetic monkeys even months after streptozotocin administration was found. It appears therefore that in non-human primates, similarly to rodents, exogenous insulin itself does not trigger a healing process of the pancreatic beta cell mass, even in the absence of a autoimmune contest, thus after chemically-induced diabetes.
- In our experiments no direct evidence that an external, donor origin cell source is really needed, supporting the concept that the pancreatic organ can potentially heal itself. It remains scope for investigations the metabolic effect of the islet graft, that in addition to providing insulin, essential to maintain the animal alive, may further provide additional factors able to affect/trigger the recovery of endocrine function. In this contest, the xenotransplantation model offers the advantage to allow discernment between graft and endogenous insulin production. In two monkey recipients, following transplantation and graft function for at least two months, we observed an increased in endogenous C-peptide levels. Two recipients maintained graft function for even one year but a substantial recovery of endogenous C-peptide didn't occurred.
- This recovery of the endogenous insulin production was associated with quite peculiar histological features of the pancreatic tissue. We found a generalized augmented proliferative activity in the pancreatic tissue, spread throughout the organ and associated to fibroblast positive, ductal and endothelial phenotype, but not specifically to insulin positive cells. We also observed that in monkeys that exhibited endogenous production of C-peptide, pancreatic ducts were hypertrophic. Interestingly, substantial numbers of ductal cells (CK19+) showed also co-staining with proinsulin. More close analysis of the pancreas in the monkey that presented double CK19-proinsulin phenotype, indicated the presence of small size insulin positive cell aggregates. Such clusters appeared not even partially damaged, and differed morphologically from those that clearly showed regressed signs of injury, commonly associated with undamaged alpha cells (glucagon positive cells). Moreover proinsulin positive aggregates were often found not in correspondence of glucagon positive cells suggesting that they were not part of pre-existing islet of Langerhans.
- Since such effects were not found in monkeys that did not receive a transplant, monkeys recipient of non functional graft, or monkeys with long lasting graft, but certainly present in monkeys with a survival time of the graft of roughly two months, we hypothesize that the transplantation may play a role. Whether a functional graft is exerting an effect on recover, it remains unclear but in this line there are reports in human clinical islet allografts that indicate an amelioration of the metabolic conditions, often accompanied by increased endogenous C-peptide production, in patients that received a transplant, even if the graft was rejected or insufficient to establish normoglycemia.

## CONCLUSION

Overall our data suggest that the monkey pancreas retains the ability to recover even after a chemical damage that specifically destroys the islet beta cells inducing a irreversible status of hyperglycemia. Such ability seems to be associated with activation of proliferative events in the pancreatic organ, and hypertrophy of the ductal cells. Double phenotype, epithelial and endocrine on the same pancreatic cells further indicate that a direct relation exists between these two cell types. Recovery of the insulin producing function, in association with the histological findings may provide indirect supportive evidence that epithelial/ductal cells play a role in the generation of insulin producing beta cells. The metabolic enhancement achieved by even partially functioning islet transplantations compared to mere exogenous insulin administration may contribute to promote return of endogenous production of C-peptide and it is desirable to further investigate the multiple biological events that accompany engraftment. Further studies will clarify whether the reparative events involve ex-novo generation of endocrine tissue from pancreatic precursor cells, or, alternatively it involves the recovery of previously damaged cells. In both cases, considering that monkeys are the closest animal species to humans, useful information can be accrued on the dynamic properties of the endocrine pancreas in men.

## APPENDICES

- Geng X, Li L, Bottino R, Balamurugan AN, Bertera S, Densmore E, Su A, Chang Y, **Trucco M**, Drain P: Anti-diabetic sulfonylurea stimulates insulin secretion independent of plasma membrane  $K_{ATP}$  channels. **Am J Physiol Endocrinol Metabolism** 293:E293, 2007.
- Pasquali L, **Trucco M**, Ringquist S: Navigating pathways affecting type 1 diabetic kidney disease. **Pediatric Diabetes** 8:307, 2007.
- Giannoukakis N, Rudert WA, **Trucco M**: Dendritic cells for immunotherapy of type 1 diabetes. **Cell Science Reviews** 3:250, 2007.
- Pasquali L, Giannoukakis N, **Trucco M**: Induction of immune tolerance to facilitate  $\beta$  cell regeneration in type 1 diabetes. **Advanced Drug Delivery Reviews** 60:106, 2008.
- Casu A, Bottino R, Balamurugan AN, Hara H, van der Windt D, Campanile N, Smetanka C, Cooper D, **Trucco M**: Metabolic aspects of pig-to-monkey islet xenotransplantation: implications for translation into clinical practice. **Diabetologia** 51:120, 2008.
- Luca D, Ringquist S, Klei L, Lee AB, Gieger C, Wichmann H-E, Schreiber S, Krawczak M, Lu, Y, Styche A, Devlin B, Roeder K, **Trucco M**: On the use of general control samples for genome-wide association studies: genetic matching highlights causal variants. **Am J Human Genetics** 82:453, 2008.
- Phillips B, Nylander K, Harnaha J, Machen J, Lakomy R, Styche A, Gillis K, Brown L, Gallo M, Knox J, Hogeland K, **Trucco M**, Giannoukakis N: A microsphere-based vaccine prevents and reverses new-onset autoimmune diabetes. **Diabetes** 57:1544, 2008.
- Giannoukakis N, Phillips B, **Trucco M**: Towards a cure for type 1 diabetes mellitus: diabetes-suppressive dendritic cells and beyond. **Pediatric Diabetes** 9 (Part II):4, 2008.
- Cifarelli V, Luppi P, Tse HM, He J, Piganelli J, **Trucco M**: Human proinsulin C-peptide reduces high glucose-induced proliferation and NF- $\kappa$ B activation in vascular smooth muscle cells. **Atherosclerosis**, In press, 2008.
- Luppi P, Cifarelli V, Tse H, Piganelli J, **Trucco M**: Human C-peptide antagonizes high glucose-induced endothelial dysfunction through the NF- $\kappa$ B pathway. **Diabetologia**, In press, 2008.

# Antidiabetic sulfonylurea stimulates insulin secretion independently of plasma membrane $K_{ATP}$ channels

Xuehui Geng,<sup>1</sup> Lehong Li,<sup>1</sup> Rita Bottino,<sup>2</sup> A. N. Balamurugan,<sup>2,3</sup> Suzanne Bertera,<sup>2</sup> Erik Densmore,<sup>1</sup> Anjey Su,<sup>1</sup> Yigang Chang,<sup>2</sup> Massimo Trucco,<sup>2</sup> and Peter Drain<sup>1</sup>

<sup>1</sup>Department of Cell Biology and Physiology, University of Pittsburgh School of Medicine, Pittsburgh;

<sup>2</sup>Department of Pediatrics, University of Pittsburgh School of Medicine, Division of Immunogenetics, Diabetes

Institute, Rangos Research Center, Children's Hospital of Pittsburgh, Pittsburgh; <sup>3</sup>Department of Surgery,

Thomas E. Starzl Transplantation Institute, University of Pittsburgh School of Medicine, Pittsburgh, Pennsylvania

Submitted 8 January 2007; accepted in final form 2 April 2007

**Geng X, Li L, Bottino R, Balamurugan AN, Bertera S, Densmore E, Su A, Chang Y, Trucco M, Drain P.** Antidiabetic sulfonylurea stimulates insulin secretion independently of plasma membrane  $K_{ATP}$  channels. *Am J Physiol Endocrinol Metab* 293: E293–E301, 2007. First published April 3, 2007; doi:10.1152/ajpendo.00016.2007.—Understanding mechanisms by which glibenclamide stimulates insulin release is important, particularly given recent promising treatment by glibenclamide of permanent neonatal diabetic subjects. Antidiabetic sulfonylureas are thought to stimulate insulin secretion solely by inhibiting their high-affinity ATP-sensitive potassium ( $K_{ATP}$ ) channel receptors at the plasma membrane of  $\beta$ -cells. This normally occurs during glucose stimulation, where ATP inhibition of plasmalemmal  $K_{ATP}$  channels leads to voltage activation of L-type calcium channels for rapidly switching on and off calcium influx, governing the duration of insulin secretion. However, growing evidence indicates that sulfonylureas, including glibenclamide, have additional  $K_{ATP}$  channel receptors within  $\beta$ -cells at insulin granules. We tested nonpermeabilized  $\beta$ -cells in mouse islets for glibenclamide-stimulated insulin secretion mediated by granule-localized  $K_{ATP}$  channels by using conditions that bypass glibenclamide action on plasmalemmal  $K_{ATP}$  channels. High-potassium stimulation evoked a sustained rise in  $\beta$ -cell calcium level but a transient rise in insulin secretion. With continued high-potassium depolarization, addition of glibenclamide dramatically enhanced insulin secretion without affecting calcium. These findings support the hypothesis that glibenclamide, or an increased ATP/ADP ratio, stimulates insulin secretion in part by binding at granule-localized  $K_{ATP}$  channels that functionally contribute to sustained second-phase insulin secretion.

$\beta$ -cells; glibenclamide; permanent neonatal diabetes; exocytosis; endocytosis; adenosine 5'-triphosphate-sensitive potassium channels

TO UNDERSTAND THE MECHANISMS underlying insulin secretion by glibenclamide, its functional sites of action in the  $\beta$ -cell of the endocrine pancreas must be identified. The plasmalemmal ATP-sensitive potassium ( $K_{ATP}$ ) channel site for glibenclamide-stimulated insulin release is well studied (3). In glucose-stimulated insulin secretion (GSIS), the plasmalemmal  $K_{ATP}$  channel transduces the signal of elevated glucose metabolism into calcium influx across the plasmalemma. The calcium then completes the final exocytic step by fusing previously primed insulin granules to the plasmalemma, experimentally observed as a transient first-phase insulin release (36).

Generally,  $K_{ATP}$  channels couple glucose metabolism and membrane electrical signaling (1, 2, 10, 16, 27).  $K_{ATP}$  channels are ideal receptors for ligands signaling changes in glucose metabolism, because they are designed as sensors of adenine nucleotide levels. ATP binding to the  $K_{ir}6.2$  subunit of the  $K_{ATP}$  channel inhibits the potassium efflux that otherwise maintains the electrically negative resting state of the cell. ADP binding to the sulfonylurea receptor 1 (SUR1) subunit of the  $K_{ATP}$  channel can antagonize the inhibition gating and restore the resting state. Thus the inhibition gating by ATP and its antagonism by ADP allow glucose metabolism to tightly regulate the  $\beta$ -cell plasmalemmal potential, allowing L-type calcium channels and calcium influx to be rapidly switched on or off. This calcium-controlled signaling pathway initiating GSIS is the  $\beta$ -cell's initial but transient response to curb rises in blood glucose levels.

A prolonged duration of high blood glucose levels, however, requires sustained insulin secretion. Experimentally, this sustained regulatory phase is observed as second-phase insulin release (36). Relatively little is known about the mechanisms coupling rates of high glucose metabolism to the second phase, even though the second phase is disrupted in most forms of diabetes. What is known is that calcium plays different roles in second-phase than it does in first-phase insulin secretion (36, 19, 40). In response to glucose stimulation, first-phase release is initiated by a rise in calcium level but is terminated by rapid depletion of a limited supply of calcium-releasable secretory granules at the plasmalemma. Importantly, the calcium level remains elevated, and after a characteristic delay, a second signal from high glucose metabolism stimulates the resupply of the calcium-releasable secretory granule pool at the plasmalemma. As for the first phase, ATP and ADP are candidate signals coupling high glucose metabolism and second-phase secretion (11, 14, 20, 38), but their receptor proteins in the  $\beta$ -cell are unknown.

Plasmalemmal  $K_{ATP}$  channels are unlikely candidate receptors by which glucose stimulates second phase. If another signaling pathway is used to elevate intracellular calcium level, for example, raising extracellular KCl from 4.8 to 30 mM, then second-phase insulin secretion becomes plasmalemmal  $K_{ATP}$  channel independent (19, 20, 40). Under these conditions, high glucose stimulates further increases in insulin release without further increasing intracellular calcium level (36). These stud-

Address for reprint requests and other correspondence: P. Drain, Dept. of Cell Biology and Physiology, Starzl Biomedical Science Tower South Rm. 323, Univ. of Pittsburgh School of Medicine, 3500 Terrace St., Pittsburgh, PA 15261 (e-mail: drain@pitt.edu).

The costs of publication of this article were defrayed in part by the payment of page charges. The article must therefore be hereby marked "advertisement" in accordance with 18 U.S.C. Section 1734 solely to indicate this fact.



ies raise the question of whether additional  $K_{ATP}$  channels other than plasmalemmal  $K_{ATP}$  channels couple glucose metabolism to the resupply of calcium-releasable secretory granules for sustained second-phase release.

Glibenclamide also appears to have binding sites within the  $\beta$ -cell, in addition to its plasmalemmal  $K_{ATP}$  channel sites. Glibenclamide is distinguished from other antidiabetic sulfonylureas, not only by its superior secretagogue potency but also by its exceptional ability to be internalized within  $\beta$ -cells (23, 25, 26). Furthermore, glibenclamide has been shown to localize to high-affinity sites of the insulin secretory granule membrane (7, 34), which recently have been identified as  $K_{ATP}$  channel subunits (21, 47, 50). Of functional relevance, SUR1 knockout mice, which have no  $K_{ATP}$  channels, exhibit chronically elevated  $\beta$ -cell calcium level yet no detectable second-phase insulin release by high glucose, unless cholinergic modulatory pathways are stimulated (15, 44). These findings predict a second  $K_{ATP}$  channel-dependent pathway, beyond calcium influx and at insulin secretory granules, that resupplies the calcium-releasable granule pool. Otherwise, the high-glucose stimulation, in the permissive high  $\beta$ -cell calcium, would stimulate insulin release.

In this study, we determined whether glibenclamide, which mimics ATP inhibition of  $K_{ATP}$  channels, has an effect on insulin secretion independent of plasmalemmal  $K_{ATP}$  channels. To bypass the signaling pathway involving the plasmalemmal  $K_{ATP}$  channel, we applied high-potassium depolarization of the  $\beta$ -cell plasmalemma, which activates the L-type channels, and monitored  $\beta$ -cell calcium level using either rhod-2 (12) or GCaMP2 fluorescent indicators (46). Insulin release was assayed by both dynamic perfusion and live-cell imaging of fluorescently labeled insulin. The results show that in the presence of high-potassium depolarization, glibenclamide stimulates a sustained insulin secretion without further increasing calcium levels.

## MATERIALS AND METHODS

**Islet preparation and culture.** Murine islets were isolated from male BALB/c mice (20–25 g; Taconic, Germantown, NY). Islets were isolated by intraductal collagenase injection, as previously described (6), and cultured in RPMI 1640 medium supplemented with 10% heat-inactivated fetal calf serum, 7.5 mM glucose, 100  $\mu$ g/ml streptomycin, 100 U/ml penicillin, and 2 mM L-glutamine (Life Technologies, Grand Island, NY) in a humidified 5%  $CO_2$  incubator at 37°C.

**Islet dynamic perfusion and ELISA assay.** Groups of 75–100 isolated hand-picked and size-matched islets (diameter 100–125  $\mu$ m) were used for each perfusion experiment, as previously reported (6). The islets were washed in Krebs-Ringer bicarbonate buffer (KRBB), pH 7.35, containing 20 mM HEPES, 0.1% bovine serum albumin (BSA), 7.5 mM glucose, and 4.8 mM KCl, except where indicated otherwise. Low glucose was set at 7.5 mM because it gave more sustained stimulated insulin release rates with glibenclamide stimulation compared with 5.6 mM glucose. After a 45-min equilibration with KRBB containing 7.5 mM glucose, elution fractions were collected for basal secretion. KRBB buffer containing 7.5 mM glucose and 30 mM KCl was then used to perfuse the islets, during which time elution fractions were collected for high potassium-stimulated first-phase secretion. Finally, islets were perfused with the following: KRBB with 7.5 mM glucose and 30 mM KCl (mock addition negative control); KRBB with 20 mM glucose, KRBB with 7.5 mM glucose, 30 mM KCl, and 4  $\mu$ M glibenclamide (glibenclamide experiment); or 20 mM glucose (high-glucose positive control), during which time elution fractions were collected and stimulated and control second-

phase secretion determined. High extracellular potassium first-phase secretory responses were comparable with and without diazoxide ( $n = 9$ ; unpublished results), consistent with the highly effective depolarization of the  $\beta$ -cell plasmalemma by high potassium. Since diazoxide is known to have deleterious alterations in mitochondrial respiration (24, 37, 41) quite apart from the  $K_{ATP}$  channel, diazoxide was omitted. Insulin concentration of the elution samples was measured using ELISA (ALPCO, Windham, NH) with rat insulin as standard. At the end of the experiment, insulin was extracted from the islets and quantified to determine the insulin content remaining in the islets as well as the insulin in the secretory fractions. The average maximal insulin secretory rate was 125  $pg \cdot min^{-1} \cdot islet^{-1}$  or 0.25%/min of total islet insulin. The insulin secretory rates are given as fractions of the maximal rate observed in each experiment, to emphasize comparison of the time courses across experiments.

**Effective glibenclamide dose.** BSA was used at 0.1%, where it blocks nonspecific binding sites for insulin. BSA, however, also is well known to bind glibenclamide (25, 26). Therefore, for perfusion, we titrated glibenclamide to the minimum final total concentration in the superfusate (4  $\mu$ M) that rapidly achieved secretory response rate amplitudes that were comparable to those achieved by 20 mM glucose. The actual glibenclamide within the  $\beta$ -cells in these transient experiments is therefore far less than 4  $\mu$ M, due to binding to the BSA present, slow partitioning from peripheral to interior  $\beta$ -cells of the islet, and slow partitioning into the  $\beta$ -cell cytosol. For the confocal experiments, we obviated these problems by not using BSA and studying cells on the islet surface. Under these conditions, 400 nM glibenclamide maximally stimulated release, which better estimates the effective glibenclamide dose.

**No calcium control perfusions.** Extracellular calcium was removed by adding no calcium and buffering residual calcium with 1 mM EGTA in the KRBB, used during preincubation periods of 45 min and continued during the application of glibenclamide or high-potassium stimuli in the indicated experiments. Free extracellular calcium level was restored by the addition of 3.5 mM  $CaCl_2$ .

**Confocal monitored release of Ins-C-GFP-labeled insulin secretory granules.** Islets were infected with Ins-C-GFP, a live-cell fluorescent reporter of insulin granules, and, within 2 days, assayed in KRBB at 37°C as described previously (48). Solution changes were performed by superfusion using the BioLogic RSC-160 sewer pipe solution changer, pressurized by its associated BioLogic MS-4 four-syringe module (Molecular Kinetics, Pullman, WA). Glucose concentration was stepped from 7.5 to 20 mM, or glibenclamide was stepped from 0 to 400 nM in KRBB at 37°C with glucose maintained at 7.5 mM. Confocal microscopy was performed using an Olympus Fluoview 300 confocal laser scanning head with an Olympus IX70 inverted microscope (Melville, NY) as described previously (21, 48). Excitation of green fluorescent protein (GFP) was done using the 488-nm argon laser line at  $\sim 2\%$  maximum power. Emission was detected using a 510IF long-pass and BA530RIF short-pass filter. All images were obtained by using a Plan Apo  $\times 60$  oil, NA 1.4, objective lens. Images were recorded from the bottom plasma membrane of a  $\beta$ -cell in an intact islet. Cytoplasmic regions were monitored using MetaMorph v6.1 analysis software from Universal Imaging (Downingtown, PA). Time course decay analyses were performed using Igor Pro v5.05A (WaveMetrics, Lake Oswego, OR).

**Calcium level monitoring by rhod-2 and by GCaMP2.** Membrane-permeant rhod-2 AM (2.5  $\mu$ M; Ref. 12) was superfused onto islets at 37°C typically for 5 min or less, while Ins-C-GFP was initially imaged to identify peripherally located  $\beta$ -cells by their green fluorescent insulin granules. The  $\beta$ -cells were then monitored with the 543-nm excitation laser at  $< 5\%$  power until sufficient basal intracellular red rhod-2 fluorescence was clearly detectable, and then all extracellular rhod-2 AM was washed out by superfusion and the experiment initiated. In a minority of  $\beta$ -cells, significant nonuniform mitochondrial staining was detected, and these cells were not monitored. Three



~0.5- $\mu$ m-thick cytoplasmic sections just below, at midplane of, and just above the nucleus in each of the  $\beta$ -cells were imaged every 30 s using a BA610IF long-pass filter. Immediately after the 5-min time point, KCl was stepped from 4.8 to 30 mM by switching superfusion buffers, resulting in a dramatic increase in red rhod-2 fluorescence that rapidly reached a plateau value that was maintained for the remainder of the recording period. Immediately after the 12-min time point, glibenclamide was stepped from 0 to 4  $\mu$ M by switching superfusion buffers, with no change in fluorescence intensity. Calcium fluorescence intensity was determined using MetaMorph (Universal Imaging) and then averaged for each of the three optical sections of a given time point and normalized to the maximum average intensity for each  $\beta$ -cell studied. Intracellular calcium level was also monitored using GCamp2 (46), expressed in  $\beta$ -cells from an adenovirus-associated virus, AAV6-GCamp2, using methods similar to those described above. After the GCamp2 fluorescence time course  $F(t)$  was measured in the experiments, the islets were treated with ionomycin in 2.5 mM  $CaCl_2$  in KRBB, and  $F_{max}$  was measured. Next, 10 mM EGTA in KRBB with no calcium was added, and  $F_{min}$  was measured. Intracellular calcium concentration ( $[Ca^{2+}]_i$ ) was then determined using the equation  $[Ca^{2+}]_i = K_{d,Ca} \times [F(t) - F_{min}] / [F_{max} - F(t)]$ , where  $K_{d,Ca}$  is 290 nM (46).

**Statistical tests and data display.** Pairwise statistical comparison of the perfusion time courses were performed using the parametric unpaired  $t$ -test and the nonparametric Kolmogorov-Smirnov test (9) with highly similar significance results in each experiment reported. For simplicity, only the results of the more popular  $t$ -test are shown. Mean ( $\pm$ SE) and box-plot time courses were constructed using IGOR Pro (v5.05A) and displayed using Adobe Illustrator (v11.0.0; Adobe Systems, San Jose, CA).

## RESULTS

**Glibenclamide in 7.5 mM glucose stimulates insulin release following maintained KCl stimulation.** Figure 1 shows the results of experiments where live intact mouse islets were perfused in 7.5 mM glucose. The islets responded to a high-potassium stimulus with a transient first-phase insulin release, which then decayed toward basal levels. As the first secretory response subsided, the mouse islets were stimulated with either 4  $\mu$ M glibenclamide or mock (no addition) control. The islets responded to 4  $\mu$ M glibenclamide with a second-phase insulin release ( $n = 6$  islet preparations) but not to the mock addition control ( $n = 6$ ). The peak amplitudes of the first phase of the secretory response to the high-potassium depolarization and insulin islet content were within 30% of one another in all 12 perfusions. The rapid transient first-phase insulin secretory response to the high-potassium stimulus likely results from a rise in  $\beta$ -cell calcium level.

**High-potassium depolarization but not subsequent glibenclamide stimulates a rapid and sustained rise in  $\beta$ -cell calcium level.** Figure 2 shows the results of eight control experiments showing that the rhod-2 does not saturate in response to stepping extracellular potassium from 4.8 to 30 mM and then from 30 to 100 mM. In each of the experiments, rhod-2 fluorescence increased not only in response to the step from 4.8 to 30 mM but again in response to the step from 30 to 100 mM. This is consistent with the  $K_d$  for calcium of rhod-2 (500–700 nM; Ref. 25) and that stimulated  $\beta$ -cell intracellular calcium generally transits to within twofold on either side of these values. With one-to-one binding stoichiometry of calcium and rhod-2, 0.90 saturation would occur at ~5  $\mu$ M, an order of magnitude above the peak  $\beta$ -cell calcium level.

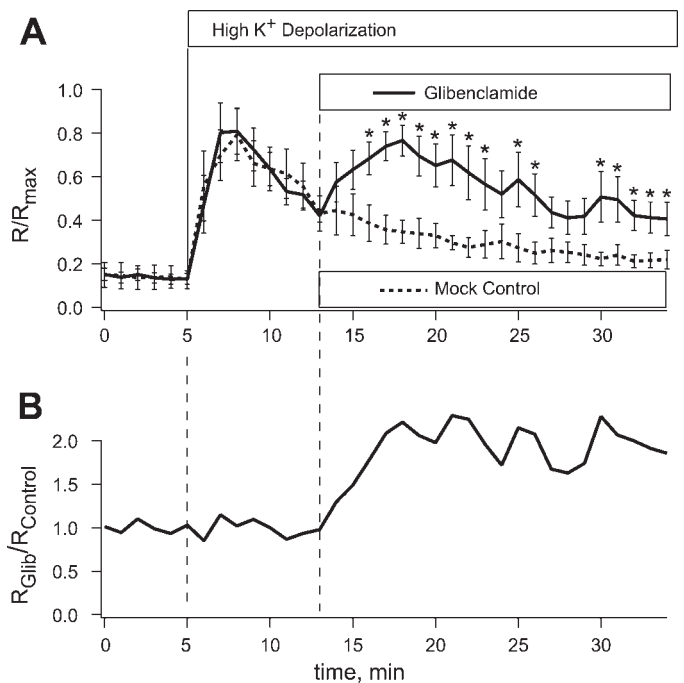


Fig. 1. Glibenclamide stimulation of insulin secretion beyond that elicited by high- $K^+$  depolarization. A: time course of fractional peak insulin secretory rate of mouse islets ( $R/R_{max}$ ) in Krebs-Ringer bicarbonate buffer (KRBB) in 7.5 mM glucose with the stimuli indicated. First stimulus was 30 mM  $K^+$  depolarization to all perfusions beginning at 5 min and continued through the remainder of the perfusions. Second stimulus was 4  $\mu$ M glibenclamide (solid line;  $n = 6$ ) or mock addition negative control (dashed line;  $n = 6$ ) and continued through the remainder of the perfusions with the 30 mM  $K^+$  depolarization. B: relative effect of glibenclamide compared with mock addition control ( $R_{Glib}/R_{Control}$ ). In all experiments, a baseline secretory rate was measured for each perfusion from 0 to 5 min. The secretory rate in response to increasing KCl from 4.8 to 30 mM KCl was then measured for each perfusion from 6 to 12 min. The secretory rate in response to a 4  $\mu$ M glibenclamide stimulus or mock addition control stimulus, in the continued presence of the high- $K^+$  depolarization, was then measured from 13 to 35 min. ELISA was used to determine the insulin content in the fractions of the collected secretion medium at the time points indicated, and results are the fraction of the maximal secretory rate obtained within each perfusion, for easy comparison of time courses. Statistical comparison of the glibenclamide vs. mock control perfusions showed no significant difference ( $P > 0.1$ ) during the basal or 30 mM KCl stimulus periods. The insulin secretory rate after the glibenclamide stimulus, however, was significantly increased ( $*P < 0.05$ ) compared with the mock addition controls at the time points indicated.

In nine experiments, we then monitored  $\beta$ -cell calcium responses of rhod-2 to the same high-potassium first stimulus, followed by the second glibenclamide stimulus used in the insulin secretory assays.  $\beta$ -Cell calcium level rapidly rose immediately after the high-potassium stimulus but was not further changed by the subsequent glibenclamide stimulus. The results indicate that the initial high-potassium and subsequent glibenclamide stimulation are distinguished not only by transient vs. sustained insulin secretion but also by rapidly rising vs. unchanging  $\beta$ -cell calcium levels.

To corroborate that the high potassium was maintaining a constant  $\beta$ -cell calcium level, we independently monitored  $\beta$ -cell calcium responses of the fluorescent protein GCamp2 (46) to the same high-potassium and glibenclamide stimulus protocol. GCamp2 is a genetically encoded calcium sensor directed exclusively to the  $\beta$ -cell cytosol. In the five experiments performed, the  $\beta$ -cell calcium level sharply rose in

response to the first high-potassium depolarization. In the presence of sustained high potassium, subsequent glibenclamide stimulation did not alter the elevated  $\beta$ -cell calcium level. Thus, by two distinct measures under the same high-potassium conditions, glibenclamide stimulated insulin secretion without further raising  $\beta$ -cell calcium levels clamped by 30 mM potassium depolarization.

*Glibenclamide-stimulated insulin release in 7.5 mM glucose mimics 20 mM glucose-stimulated insulin release following maintained high- $K^+$  stimulation.* Figure 3 shows results with 20 mM glucose used as second stimulus instead of glibenclamide. The high-potassium depolarization stimulated a transient first phase of insulin release, as before, and the second 20-mM glucose stimulus evoked a second-phase insulin secretory response ( $n = 4$  islet preparations) that was similar in time course and amplitude to that obtained with glibenclamide.

The results so far suggest a model in which the glibenclamide stimulus and increased ATP from the high-glucose

stimulus might each be acting through the same mechanism, binding to their granule  $K_{ATP}$  channel receptors. This interpretation is consistent with the observation that each stimulus applied alone results in secretory rates of similar amplitude and time course. However, an alternative model is that each stimulus acts through nonoverlapping mechanisms that coincidentally give rise to the similar secretory responses observed. These two models can be distinguished by experiments identical to those previously performed except with simultaneous application of glibenclamide and high glucose. As controls, experiments were performed in parallel in which each stimulus was applied alone. If the same mechanism is involved, the secretory response rates should be nonadditive. If separate mechanisms are brought into play, then the rates with both stimuli applied should be up to twice the rates with either stimulus applied alone. Figure 4 shows that the insulin secretory rates in response to simultaneous application of the glibenclamide and 20 mM glucose are nonadditive. In all pairwise comparisons (glibenclamide and glucose vs. glibenclamide, glibenclamide and glucose vs. glucose, and glibenclamide vs. glucose), there was no significant difference in insulin secretory response ( $P > 0.1$ ;  $n = 3$ ).

*Glibenclamide-stimulated insulin release following sustained KCl stimulation by confocal monitoring of Ins-C-GFP expressed in mouse islets.* The perfusion experiments provide an excellent population sample of the average behavior of  $\beta$ -cells but fail to provide single-cell information. From the perfusion assays alone, we cannot know whether  $\beta$ -cell re-

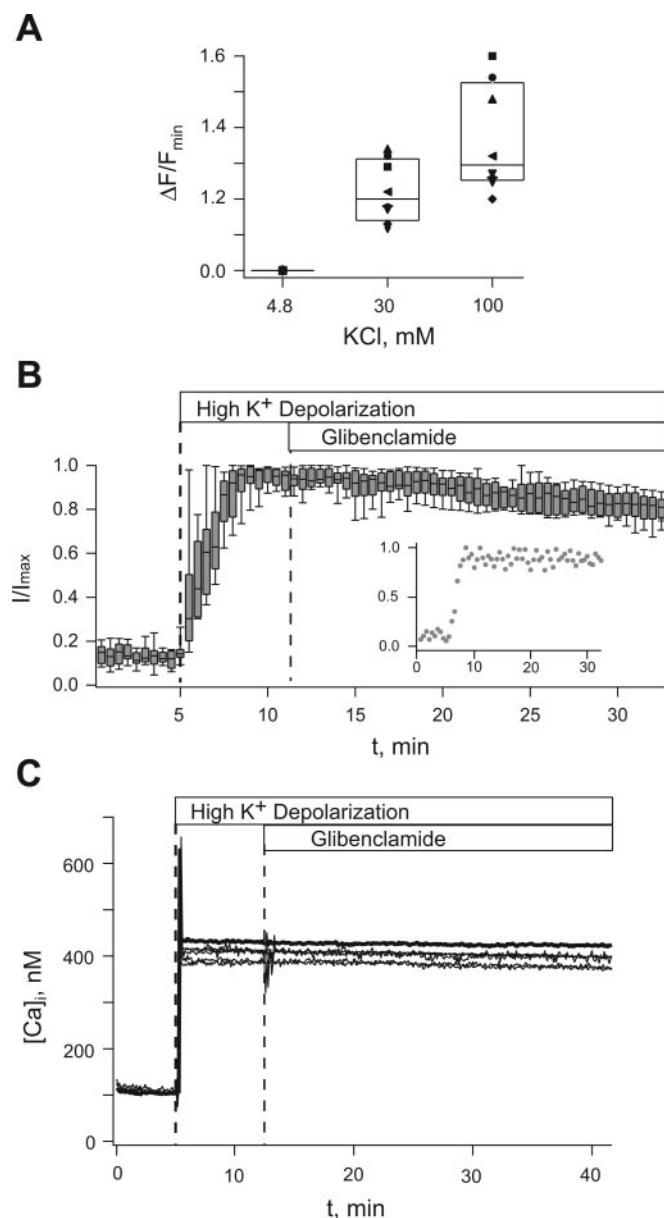


Fig. 2.  $\beta$ -Cell  $Ca^{2+}$  responses to high KCl monitored by the fluorescent indicator rhod-2. Three  $\beta$ -cells from each of 3 separate mouse islets were loaded with the fluorescent  $Ca^{2+}$  indicator rhod-2 AM until a basal fluorescence was easily detectable at  $<5\%$  laser excitation, and then cells were washed ( $n = 9$ ). A minority of cells in each experiment showed nonuniform, more intense rhod-2 fluorescence in mitochondria and were excluded from analysis. **A:** 8 control experiments were done under conditions similar to those described below except that the initial high- $K^+$  depolarization by raising the extracellular  $[K^+]$  to 30 mM was then followed by further depolarization by raising the extracellular  $[K^+]$  to 100 mM. Within each experiment, fluorescence intensity was normalized to the minimal intensity ( $\Delta F/F_{min}$ ), which was the initial baseline intensity observed when the extracellular  $[K^+]$  was 4.8 mM. Upon the 30 mM  $K^+$  depolarization, rhod-2 fluorescence increased  $\sim 1.2$ -fold, and upon subsequent 100 mM  $K^+$  depolarization, rhod-2 fluorescence increased an additional 1.1-fold. Individual experiments are marked by different symbols to emphasize that in each experiment, the initial 30 mM and subsequent 100 mM  $K^+$  stimuli each incremented the rhod-2 fluorescence. The increases in  $\beta$ -cell rhod-2 fluorescence in response to raising extracellular  $[K^+]$  demonstrate that the  $Ca^{2+}$  indicator fluorescence was not saturated by the 30 mM  $K^+$  depolarization and that further increases in intracellular  $Ca^{2+}$  level ( $[Ca^{2+}]_i$ ), were they to occur, could be easily detected in these experiments. **B:**  $\beta$ -cell calcium rose rapidly in response to the initial 30 mM  $K^+$  depolarization but was not markedly altered by subsequent glibenclamide stimulus. The results show single-cell fluorescence changes for all 9 cells studied with time points ( $t$ ) taken every minute. After the 5-min time point, 30 mM  $K^+$  depolarization was applied and continued throughout the remainder of each experiment. After the 12-min time point, 4  $\mu$ M glibenclamide was applied and continued throughout the remainder of each experiment. Data in the  $Ca^{2+}$  experiments are summarized by a box plot in which the shaded box indicates the 25th to 75th percentile range of data, the horizontal bar within each box is the median, and the capped whiskers indicate the 0 to 100th percentile range of data. The results show single-cell fluorescence changes for all 9 cells in 3 islet preparations. *Insert* shows a single cell response. **C:**  $\beta$ -cell cytosolic  $[Ca^{2+}]_i$  changes measured by GCamp2. Similar  $[Ca^{2+}]_i$  responses are shown to the initial 30 mM KCl stimulation and lack of response to the subsequent glibenclamide stimulation. The results are from all 6 cells studied from 3 islet preparations.

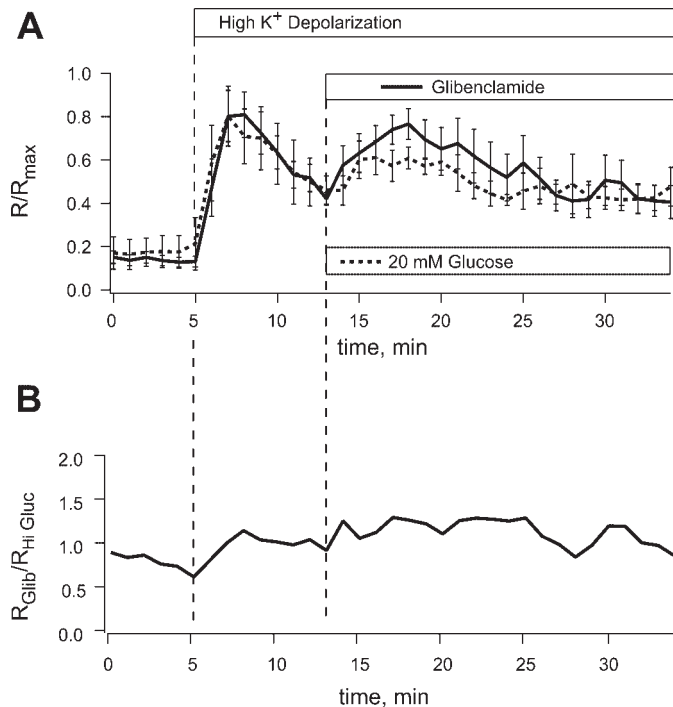


Fig. 3. Glibenclamide stimulation of insulin secretion mimics that of high glucose following high- $K^+$  depolarization. *A*: time course of fractional peak insulin secretory rate of mouse islets in KRBB in 7.5 mM glucose with the stimuli indicated. First stimulus was 30 mM  $K^+$  depolarization to all perfusions beginning at 5 min and continued through the remainder of the perfusions. Second stimulus was 4  $\mu$ M glibenclamide (solid line;  $n = 6$ ; from Fig. 1) or 20 mM glucose positive control (dashed line;  $n = 4$ ) and continued through the remainder of the perfusions along with the 30 mM potassium depolarization. *B*: relative effect of glibenclamide, compared with the 20 mM glucose positive control ( $R_{Glib}/R_{Hi\ Gluc}$ ). As in Fig. 1, baseline secretory rate was measured for each perfusion from 0 to 5 min. The secretory rate in response to increasing KCl from 4.8 to 30 mM KCl was then measured for each perfusion from 6 to 12 min. The 30 mM KCl was continued in each perfusion throughout the remainder of the perfusions. The secretory rate in response to a second 4  $\mu$ M glibenclamide stimulus or a second 20 mM glucose stimulus was then measured from 13 to 35 min, as indicated. ELISA was used to determine the insulin content in the fractions of the collected secretion medium, and results are the fraction of the maximal secretory rate obtained within each perfusion, for easy comparison of time courses. Statistical comparison of the glibenclamide vs. 20 mM glucose positive control perfusions showed no significant difference ( $P > 0.1$ ) during any of the basal or stimulus periods.

sponses to the glibenclamide following high-potassium stimulation occur heterogeneously or homogeneously within a single islet. For example, most  $\beta$ -cells might be refractory to the second glibenclamide stimulus, whereas a few  $\beta$ -cells might suddenly and completely degranulate. Alternatively, most  $\beta$ -cells might be incrementally responding to the glibenclamide stimulation, wherein each  $\beta$ -cell releases a minority fraction of its insulin secretory granules. In eight experiments, we therefore studied individual  $\beta$ -cell responses to glibenclamide after high-potassium depolarization by using the live-cell fluorescent reporter of insulin granules (Ins-C-GFP) and confocal microscopy (21, 48).

$\beta$ -Cells expressing Ins-C-GFP were superfused with low-potassium control (4.8 mM), high potassium (30 mM), or high potassium (30 mM) and glibenclamide (400 nM). First, in control experiments, we maintained the low-potassium KRBB secretion buffer throughout a series of experiments, taking 50

images (every 20 s for 1,000 s) from the 0.5- $\mu$ m optical section ( $n = 5$ ). Figure 5 shows that over the entire time course of the low-potassium experiments, the fluorescence decay in single  $\beta$ -cells was  $\sim 0.05$  that of the initial value. This is a measure of secretagogue-independent fluorescence decay (bleaching), which occurs initially with this fluorophore (43) and is minimal because of the high signal-to-noise property of the Ins-C-emGFP reporter and consequent low excitation intensity used. Second, we switched from low potassium after five images, to high potassium for the remaining 45 images ( $n = 5$ ). In this series of experiments, the fluorescence decayed more rapidly upon the switch to high potassium than in the controls and then paralleled the control fluorescence. This is a measure of first-phase release response to the potassium depolarization and elevation of  $\beta$ -cell calcium. Third, we switched from low potassium after five images, to high potassium after an additional five images, and then to high potassium plus 400 nM glibenclamide for the remaining 40 images ( $n = 8$ ). In this series of experiments, the fluorescence decayed more rapidly than the control, first in response to the switch to high potassium and then in response to the switch to glibenclamide. The time constants show that the first- and second-response components are kinetically distinct and mimic the faster first and slower second phases in response to high glucose. Overall, the results indicate that  $\beta$ -cells rather uniformly responded to the high-potassium and glibenclamide secretagogues, as they do to high-glucose stimulation, with a gradual time-dependent release of a fraction of their insulin secretory content.

We next asked to what extent does the time course of decay in single  $\beta$ -cell fluorescence reflect insulin secretion. The time course of fluorescence decay in the stimulated  $\beta$ -cell should most closely relate to cumulative insulin release in the extra-

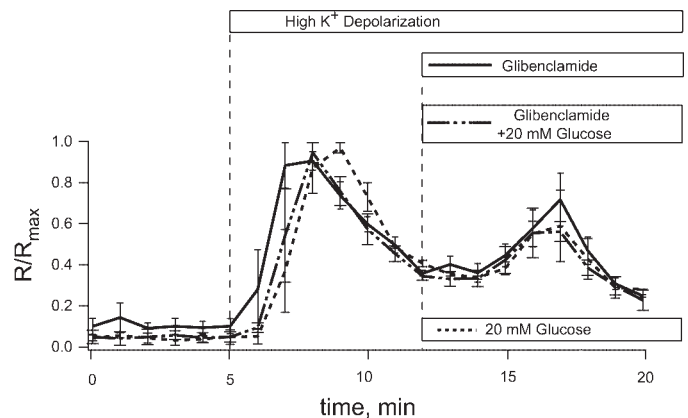


Fig. 4. Simultaneous stimulation of insulin secretion by glibenclamide and glucose is similar to that by either stimulus alone. Time course of fractional peak insulin secretory rate of mouse islets in KRBB in 7.5 mM glucose was determined in response to the stimuli indicated. As before, the first stimulus was 30 mM  $K^+$  depolarization at 5 min and continued throughout the experiments. The second stimulus was simultaneous application of 4  $\mu$ M glibenclamide and 20 mM glucose (dashed-solid line;  $n = 3$ ), 4  $\mu$ M glibenclamide alone as control (solid line;  $n = 3$ ), or 20 mM glucose alone as control (dashed line;  $n = 3$ ) and continued through the remainder of the perfusions. All 3 experimental stimulus conditions were performed in parallel on each of 3 independent sets of islet preparations. ELISA was used as before to determine the insulin content in the perfusion fractions, and the results are the fraction of the maximal secretory rate obtained within each perfusion. Error bar cap widths increase from glibenclamide or glucose alone to glibenclamide and glucose combined stimulus conditions for clarity. Statistical comparisons showed no significant difference ( $P > 0.1$ ) between any pairwise comparisons.



cellular medium. Therefore, the time derivative of the fluorescence decay should be more closely related to the rate of insulin release than the decay itself. Differentiation of the high potassium alone and high potassium plus glibenclamide time courses, after the secretagogue-independent control decay is subtracted, resulted in transient and sustained components of C-emGFP fluorescence decay rates. Most, notably, the high-potassium depolarization evoked a rapid transient rate of fluorescence decay, whereas the further glibenclamide application evoked a more prolonged rate of fluorescence decay.

Figure 6 shows representative experiments on imaging the islet  $\beta$ -cell response to high-potassium depolarization and to the subsequent glibenclamide stimulation. For the response to the high-potassium depolarization, Fig. 6A presents images from one of the eight experiments showing the minor decays in cellular fluorescence and release of one to a few fluorescent granules. For the glibenclamide response, Fig. 6B presents images from an additional three of the eight experiments showing the time-dependent loss of insulin granules labeled by Ins-C-emGFP in response to glibenclamide. Importantly, the images indicate that the glibenclamide stimulus does not elicit

any sudden massive loss of insulin granules. Rather, gradual, time-dependent loss of fluorescent granules was observed from the  $\beta$ -cells in all eight experiments. The results exclude the possibility that glibenclamide stimulates complete degranulation from a minority of  $\beta$ -cells with little or no effect on the majority of cells.

**Glibenclamide-stimulated release depends on calcium.** Glibenclamide-stimulated release might also share with glucose-stimulated release the property of calcium dependence. Alternatively, glibenclamide might be working by a calcium-independent, nonphysiological pathway, altogether distinct from what happens during GSIS. To further compare the stimuli, we studied the extracellular calcium dependence of glibenclamide-stimulated release. Extracellular calcium was omitted, and the calcium chelator EGTA was added at 1 mM to KRBB. The 1.6 mM  $Mg^{2+}$  as a divalent normally present in KRBB should suffice for maintenance of the  $\beta$ -cell membrane. Figure 7 shows the results of three experiments where glibenclamide-stimulated release failed to proceed without free calcium. Insulin secretion returned once free calcium was restored in the secretory buffer, indicating that the islets were competent for release. Therefore, glibenclamide and high extracellular potassium are insufficient for insulin secretion in the absence of calcium.

## DISCUSSION

Under conditions of sustained high-potassium depolarization and elevated  $\beta$ -cell calcium, we found that glibenclamide stimulated a second-phase release of insulin that mimicked second-phase release of insulin by high glucose. Insulin secretion and calcium levels were each measured in intact islet  $\beta$ -cells by using distinct and direct methods. Together with the identification of  $K_{ATP}$  channels at insulin granules (21, 47, 50), the results provide evidence for a second, granule-localized

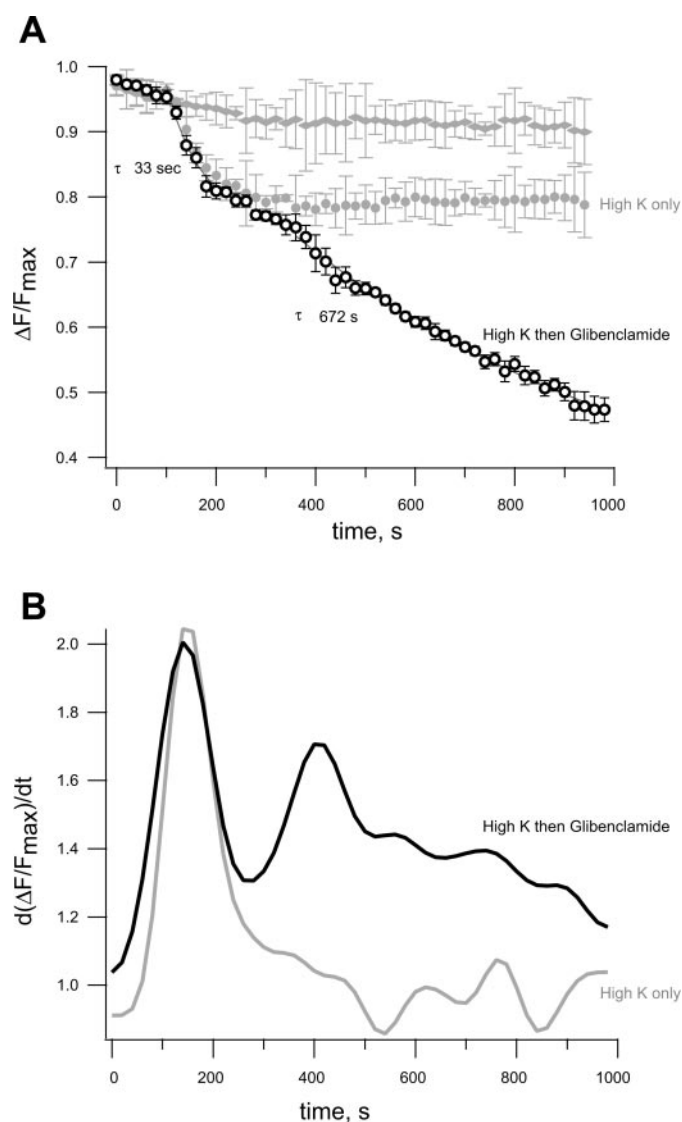


Fig. 5. Slow time-dependent release of C-GFP (green fluorescent protein) insulin granule fluorescence in response to glibenclamide stimulus. **A:** changes in C-GFP fluorescence expressed in the  $\beta$ -cell were monitored following high- $K^+$  depolarization, followed by high  $K^+$  plus glibenclamide ( $n = 8$ ). Images were taken every 20 s or more frequently for 1,000 s. Two classes of control experiments were performed. To identify any stimulatory effect of glibenclamide, we simply omitted the glibenclamide from the superfusion solution in the first class of controls (shaded circles;  $n = 5$ ) by comparing the rate of fluorescence decay with and without the second glibenclamide stimulus. To identify any effect of fluorescence loss independent of secretagogues, both the high  $K^+$  and glibenclamide were omitted (shaded diamonds;  $n = 5$ ). The high- $K^+$  depolarization followed by glibenclamide elicited 2 distinct components of decay. The initial decay was similar to that elicited by high  $K^+$  alone and could be adequately fit by an exponential with  $\tau$  of 33 s. The decay component subsequent to the second glibenclamide stimulus could be adequately fit by an exponential with  $\tau$  of 672 s. In the absence of secretagogues, initial fluorescence decayed a total of 0.05 on average. The fluorescence decay after the glibenclamide stimulus, however, was significantly increased ( $P < 0.05$ ) compared with the mock addition controls shortly after the 400-s time point through the end of the time course. **B:** Time derivative of the fluorescence decay approximates the insulin secretory rate.  $\beta$ -Cells within an islet were infected by adenoviral vector Ins-C-GFP. Mouse islets were maintained in KRBB with 30 mM KCl and 7.5 mM glucose. Time course values are means  $\pm$  SE of the mean fractional fluorescence intensity change, where approximately the first 0.5- $\mu$ m  $\beta$ -cell membrane proximal optical section was imaged over the time points indicated [ $d(F/F_{max})/dt$ ]. Fluorescence intensity changes of entire cell region of interest were analyzed, and values were normalized to the maximum fluorescence value obtained for a given experimental time series, obtained using a Plan Apo  $\times 60$  oil, NA 1.4, objective, Fluoview 300 confocal microscope.

$K_{ATP}$  channel-dependent pathway underlying insulin secretion that can be stimulated by either glibenclamide or high-glucose metabolism. The results expand on previous experiments indicating that, at high glucose concentrations, calcium is not the sole controlling parameter for insulin secretion (36, 19, 20, 40) and further implicate ATP and ADP signals as candidate coupling factors (13, 14, 30, 38).

Previous support for granule-localized  $K_{ATP}$  channels include observations that high-affinity sulfonylurea receptors cosegregated with insulin secretory granules through sucrose

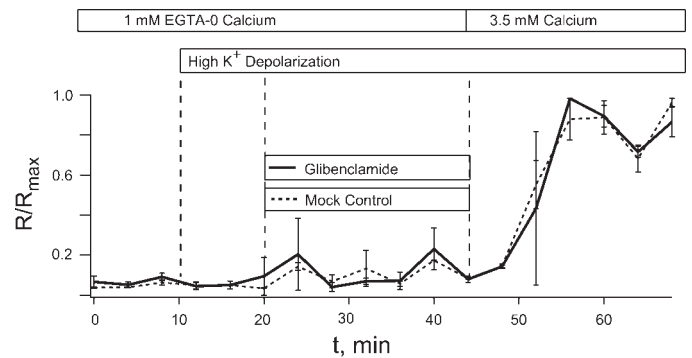
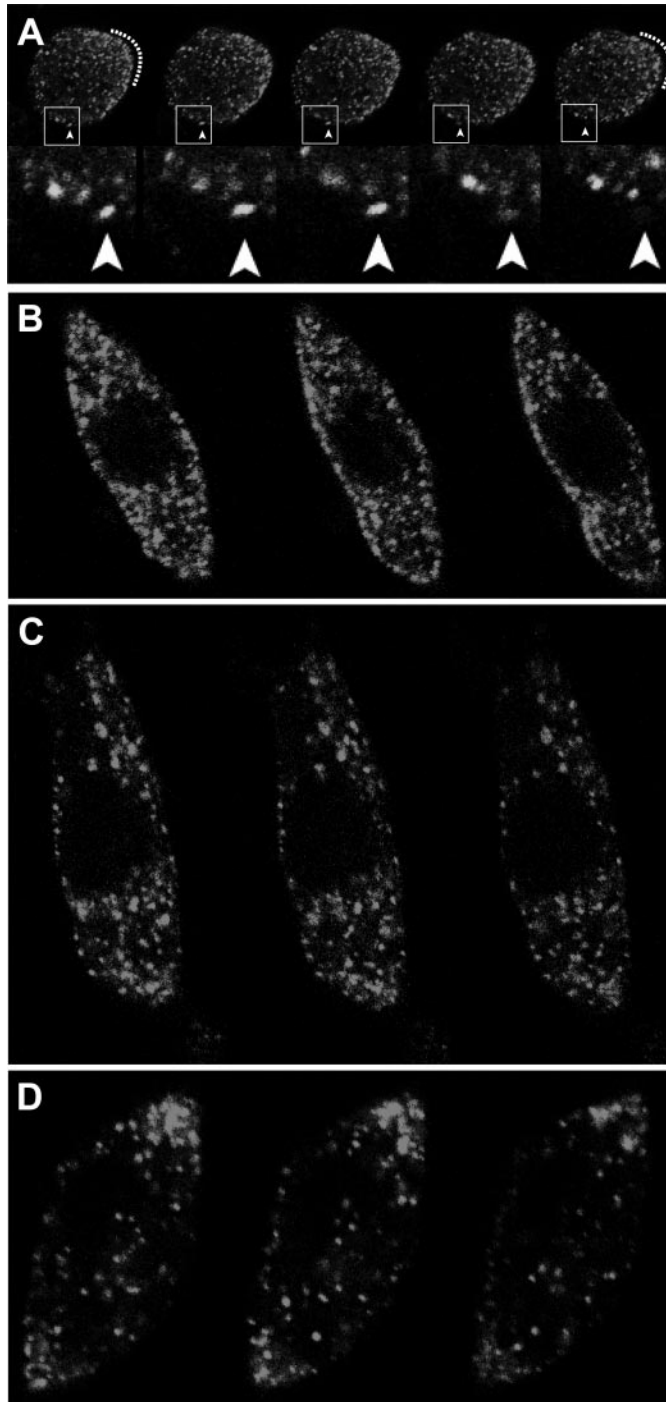


Fig. 7. Calcium dependence of glibenclamide stimulation of insulin secretory rate beyond that elicited by elevated  $KCl$ . Parallel perfusions were performed in EGTA-0  $Ca^{2+}$  KRRB with 7.5 mM glucose. At 10 min,  $KCl$  was stepped from 4.8 to 30 mM in each perfusion for another 10 min. After this, the perfusions were treated differently. To one perfusion at 20–45 min, 4  $\mu M$  glibenclamide was added to the buffer with 30 mM  $KCl$  (solid line). To the other perfusion at 20–45 min, nothing was added (dashed line). Next, to both perfusions at 45 min, 3.5 mM  $CaCl_2$  was added. ELISA was used to determine insulin content in the fractions of the collected secretion medium, as indicated. At the end of the perfusions,  $Ca^{2+}$  was added back to demonstrate that the islets were otherwise secretion competent. Statistical comparison of the glibenclamide vs. mock addition control perfusions showed no significant difference ( $P > 0.1$ ) during any of the basal or stimulus periods with or without extracellular free  $Ca^{2+}$ .



gradient purification (7, 34). These reports also show that glibenclamide localized to insulin dense core granules, as revealed by immunoelectron microscopy, and cross-linked to 140-kDa granule receptor proteins. More recent findings have demonstrated that the major site for  $K_{ATP}$  channels, which comprise the 140-kDa SUR1 and the 43-kDa Kir6.2 subunits, reside on insulin secretory granules (21, 47, 50). The evidence reported included localization of fluorescent glibenclamides to insulin granules and not to other intracellular membranous organelles or the  $\beta$ -cell plasmalemma. Together with the functional evidence reported presently, the observations suggest models in which granule  $K_{ATP}$  channels functionally couple high-glucose metabolism, or glibenclamide stimulation, to speeding the resupply of calcium-releasable secretory granules at sites for exocytic release.

Fig. 6. Single  $\beta$ -cells stimulated by glibenclamide show incremental time-dependent loss of insulin granule fluorescence. A: response to high- $K^+$  stimulation. Top row of images are from an experiment showing the relatively minor decays in cellular fluorescence immediately after the high- $K^+$  stimulation and before glibenclamide addition ( $n = 8$ ). Dashed lines in the first and last images highlight a region of general cellular fluorescence loss. Boxes with arrowheads indicate single fluorescent granule loss. Bottom row of images are the boxed regions from the row above enlarged to better show single fluorescent granule release. B–D: responses to glibenclamide stimulation. Images in each row are shown from each of 3 experiments in which glibenclamide was used as the second stimulus. Each row shows a  $\beta$ -cell with fluorescently labeled granules at 0 (left), 200 (middle), and 400 s (right) after the glibenclamide stimulation. All  $\beta$ -cells responded similarly with an overall net loss in fluorescently labeled granules ( $n = 8$ ). In no case did the glibenclamide stimulus elicit a sudden dramatic loss of granules. Note that for the stationary granules in these experiments, fluorescence intensity typically decremented  $<0.05$ , which was comparable with the decrement in unstimulated whole cell fluorescence. All optical  $z$  planes are immediately proximal to the coverslip to maximize the ability to observe granules that potentially could release. Images were viewed using a Plan Apo  $\times 60$  oil, NA 1.4, objective, Fluoview 300 confocal microscope.



Mouse  $K_{ATP}$  channel knockout models (15, 32, 44) and an additional knockdown model (31), but not another knockout model (33, 42), are consistent with a granule-localized  $K_{ATP}$  channel-dependent pathway. In  $K_{ir6.2}$  and SUR1 knockout models, isolated islets show elevated  $\beta$ -cell calcium levels in low glucose (2.8 mM), yet in high glucose (16.7 mM), they show neither changes in the high calcium levels nor significant GSIS (15, 32, 44). In the knockdown model, in which  $K_{ir6.2}$  expression was disrupted by hammerhead ribozymes, high glucose also failed to stimulate second-phase insulin release despite chronically elevated calcium (31). Another SUR1 knockout model, however, in earlier studies showed islets with dramatically slowed insulin secretory responses to glucose regulation (42), whereas more recent results showed surprisingly normalized GSIS (33). In this model, either the  $K_{ATP}$  channel is dispensable for normal GSIS or compensatory factors have come into play (33).

An intracellular role for sulfonylureas has been previously suggested based on in vitro results showing that intracellular injection of tolbutamide into whole cell clamped  $\beta$ -cells increased its cell capacitance as a measure of insulin secretion (4, 18). Intracellular injection of ADP was also shown to block the  $\beta$ -cell capacitance increase. The results reported presently extend these findings to intact islets and show glibenclamide-stimulated secretion associated with second phase measured directly by insulin assay. In the confocal measurements reported presently, the overall decrease in membrane fluorescence observed indicates that any stimulated rate of granule cargo arrival at the membrane is less than the rates of the exocytic release and endocytic internalization. The sustained stimulated secretory rate observed by insulin assay, together with the decrease in membrane cargo fluorescence, is consistent with a stimulated arrival rate, but one that is more than offset by the other two departure rates.

The actions of glibenclamide on insulin secretion reported presently are consistent with models in which decreased ADP and increased ATP binding to the granule-localized  $K_{ATP}$  channels contributes to insulin granule trafficking or priming mechanisms resupplying calcium-releasable granules for second-phase release. Thus two  $K_{ATP}$  channel-dependent pathways regulating insulin secretion can be distinguished at least in part by their plasmalemmal and granule locations in the  $\beta$ -cell. Our results in no way indicate that adenine nucleotides are exclusive signals from high-glucose metabolism that govern second-phase insulin secretion (28). In the case of adenine nucleotides, we speculate their binding to granule  $K_{ATP}$  channels might regulate priming of the granules to a calcium-releasable state by an ionic mechanism (5, 45), stimulate trafficking to release sites, or enhance interactions there with exocytic and endocytic proteins (11, 17, 29, 35). Further investigation of these regulatory pathways will be important to more fully understand the role of  $K_{ATP}$  channels in the treatment of diabetic subjects (8, 22, 39, 49).

#### ACKNOWLEDGMENTS

We thank Drs. Guy Salama, Michael Kotlikoff, Xiaodong Zhu, and Barry London for expertise in calcium fluorescence measurements and the gift of the GCaMP2 vectors.

#### GRANTS

This study was supported by National Institutes of Health (NIH) Grant R21 DK064383-02 (to P. Drain), American Diabetes Association Grant 1-06-RA-39 (to P. Drain), and NIH Grant U19 AI056374-01 (to M. Trucco).

#### REFERENCES

1. Aguilar-Bryan L, Nichols CG, Weschler SW, Clement IVJP, Boyd IIIAE, Gonzalez G, Herrera-Sosa H, Nguy K, Bryan J, Nelson DA. Cloning of the  $\beta$  cell high-affinity sulfonylurea receptor: a regulator of insulin secretion. *Science* 268: 423–426, 1995.
2. Ashcroft FM, Harrison DE, Ashcroft SJ. Glucose induces closure of single potassium channels in isolated rat pancreatic beta-cells. *Nature* 312: 446–448, 1984.
3. Ashcroft FM. Adenosine 5'-triphosphate-sensitive potassium channels. *Annu Rev Neurosci* 11: 97–118, 1988.
4. Barg S, Renstrom E, Berggren PO, Bertorello A, Bokvist K, Braun M, Eliasson L, Holmes WE, Kohler M, Rorsman P, Thevenod F. The stimulatory action of tolbutamide on  $Ca^{2+}$ -dependent exocytosis in pancreatic  $\beta$  cells is mediated by a 65-kDa mdr-like P-glycoprotein. *Proc Natl Acad Sci USA* 96: 5539–5544, 1999.
5. Barg S, Huang P, Eliasson L, Nelson DJ, Obermuller S, Rorsman P, Thevenod F, Renstrom E. Priming of insulin granules for exocytosis by granular  $Cl^{-}$  uptake and acidification. *J Cell Sci* 114: 2145–2154, 2001.
6. Bertera S, Crawford ML, Alexander AL, Papworth GD, Watkins SC, Robbins PD, Trucco M. Gene transfer of manganese superoxide dismutase extends islets graft function in a model of autoimmune diabetes. *Diabetes* 52: 387–393, 2003.
7. Carpentier JL, Sawano F, Ravazzola M, Malaisse WJ. Internalization of  $^3H$ -glibenclamide in pancreatic islet cells. *Diabetologia* 29: 259–261, 1986.
8. Codner E, Flanagan S, Ellard S, Garcia H, Hattersley AT. High-dose glibenclamide can replace insulin therapy despite transitory diarrhea in early-onset diabetes caused by a novel R201L Kir6.2 mutation. *Diabetes Care* 28: 758–759, 2005.
9. Conover WJ. *Practical Nonparametric Statistics* (2nd ed.). New York: John Wiley & Sons, 1980, p. 344–376.
10. Cook DL, Hales CN. Intracellular ATP directly blocks  $K^{+}$  channels in pancreatic beta-cells. *Nature* 311: 271–273, 1984.
11. Cui N, Kang Y, He Y, Leung YM, Xie H, Pasyk EA, Gao X, Sheu L, Hansen JB, Wahl P, Tsuchima RG, Gaisano HY. H3 domain of syntaxin 1A inhibits  $K_{ATP}$  channels by its actions on the sulfonylurea receptor 1 nucleotide-binding folds-1 and -2. *J Biol Chem* 279: 53259–53265, 2004.
12. Del Nido PJ, Glynn P, Buenaventura PP, Salama G, Koretsky AP. Fluorescence measurement of calcium transients in perfused rabbit heart using rhod 2. *Am J Physiol Heart Circ Physiol* 274: H728–H741, 1998.
13. Detimary P, Berghe VD, Henquin JC. Concentration dependence and time course of the effects of glucose on adenine and guanine nucleotides in mouse pancreatic islets. *J Biol Chem* 271: 20559–20565, 1996.
14. Detimary P, Dejonghe S, Ling Z, Pipeleers D, Schuit F, Henquin JC. The changes in adenine nucleotides measured in glucose-stimulated rodent islets occur in beta cells but not in alpha cells and are also observed in human islets. *J Biol Chem* 273: 33905–33908, 1998.
15. Doliba NM, Qin W, Vatamaniuk MZ, Li C, Zelent D, Najafi H, Buettger CW, Collins HW, Carr RD, Magnuson MA, Matschinsky FM. Restitution of defective glucose-stimulated insulin release of sulfonylurea type 1 receptor knockout mice by acetylcholine. *Am J Physiol Endocrinol Metab* 286: E834–E843, 2004.
16. Drain P, Li L, Wang J.  $K_{ATP}$  channel inhibition by ATP requires distinct functional domains of the cytoplasmic C terminus of the pore-forming subunit. *Proc Natl Acad Sci USA* 95: 13953–13958, 1998.
17. Eliasson L, Ma X, Renstrom E, Barg S, Berggren PO, Galvanovskis J, Gromada J, Jing X, Lundquist I, Salehi A, Sewing S, Rorsman P. SUR1 regulates PKA-independent cAMP-induced granule priming in mouse pancreatic B-cells. *J Gen Physiol* 121: 181–197, 2003.
18. Eliasson L, Renstrom E, Ammala C, Berggren PO, Bertorello AM, Bokvist K, Chibalin A, Deeney JT, Flatt PR, Gabel J, Gromada J, Larsson O, Lindstrom P, Rhodes CJ, Rorsman P. PKC-dependent stimulation of exocytosis by sulfonylureas in pancreatic  $\beta$  cells. *Science* 271: 813–815, 1996.
19. Gembal M, Gilon P, Henquin JC. Evidence that glucose can control insulin release independently from its action on ATP-sensitive  $K^{+}$  channels in mouse beta cells. *J Clin Invest* 89: 1288–1295, 1992.

20. Gembal M, Detimary P, Gilon P, Gao ZY, Henquin JC. Mechanism by which glucose can control insulin release independently from its action on adenosine triphosphate-sensitive  $K^+$  channels in mouse  $\beta$  cells. *J Clin Invest* 91: 871–880, 1993.
21. Geng X, Li L, Watkins S, Robbins PD, Drain P. The insulin secretory granule is the major site of  $K_{ATP}$  channels of the endocrine pancreas. *Diabetes* 52: 767–776, 2003.
22. Gloyn AL, Pearson ER, Antcliff JF, Proks P, Bruining GJ, Slingerland AS, Howard N, Srinivasan S, Silva JM, Molnes J, Edghill EL, Frayling TM, Temple IK, Mackay D, Shield JP, Sumnik Z, van Rhijn A, Wales JK, Clark P, Gorman S, Aisenberg J, Ellard S, Njolstad PR, Ashcroft FM, Hattersley AT. Activating mutations in the gene encoding the ATP-sensitive potassium-channel subunit  $K_{ir}6.2$  and permanent neonatal diabetes. *N Engl J Med* 350: 1838–1849, 2004.
23. Gylfe E, Hellman B, Sehlin J, Taljedal B. Interaction of sulfonylurea with the pancreatic B-cell. *Experientia* 40: 1126–1134, 1984.
24. Hanley PJ, Mickel M, Loffler M, Brandt U, Daut J.  $K_{ATP}$  channel-independent targets of diazoxide and 5-hydroxydecanoate in the heart. *J Physiol* 542: 735–741, 2002.
25. Hellman B. Factors affecting the uptake of glibenclamide in microdissected pancreatic islets rich in  $\beta$  cells. *Pharmacology* 11: 257–267, 1974.
26. Hellman B, Sehlin J, Taljedal IB. Glibenclamide is exceptional among hypoglycaemic sulphonylureas in accumulating progressively in  $\beta$ -cell-rich pancreatic islets. *Acta Endocrinol* 105: 385–390, 1984.
27. Inagaki N, Gono T, Clement JPT, Namba N, Inazawa J, Gonzalez G, Aguilar-Bryan L, Seino S, Bryan J. Reconstitution of  $I_{KATP}$ : an inward rectifier subunit plus the sulfonylurea receptor. *Science* 270: 1166–1170, 1995.
28. Joseph JW, Jensen MV, Ilkayeva O, Palmieri F, Alarcon C, Rhodes CJ, Newgard CB. The mitochondrial citrate/isocitrate carrier plays a regulatory role in glucose-stimulated insulin secretion. *J Biol Chem* 281: 35624–35632, 2006.
29. Kang Y, Leung YM, Manning-Fox JE, Xia F, Xie H, Sheu L, Tsushima RG, Light PE, Gaisano HY. Syntaxin-1A inhibits cardiac  $K_{ATP}$  channels by its actions on nucleotide binding folds 1 and 2 of sulfonylurea receptor 2A. *J Biol Chem* 279: 47125–47131, 2004.
30. Kawazu S, Sener A, Couturier E, Malaisse WJ. Metabolic, cationic and secretory effects of hypoglycemic sulfonylureas in pancreatic islets. *Nauyn Schmiedeberg Arch Pharmacol* 312: 277–283, 1980.
31. Li L, Rojas A, Wu J, Jiang C. Disruption of glucose sensing and insulin secretion by ribozyme  $K_{ir}6.2$ -gene targeting in insulin-secreting cells. *Endocrinology* 145: 4408–4414, 2004.
32. Miki T, Nagashima K, Tashiro F, Kotake K, Yoshitomi H, Tamamoto A, Gono T, Iwanaga T, Miyazaki J, Seino S. Defective insulin secretion and enhanced insulin action in  $K_{ATP}$  channel-deficient mice. *Proc Natl Acad Sci USA* 95: 10402–10406, 1998.
33. Nenquin M, Szollosi A, Aguilar-Bryan L, Bryan J, Henquin JC. Both triggering and amplifying pathways contribute to fuel-induced insulin secretion in the absence of sulfonylurea receptor-1 in pancreatic  $\beta$ -cells. *J Biol Chem* 279: 32316–32324, 2004.
34. Ozanne SE, Guest PC, Hutton JC, Hales CN. Intracellular localization and molecular heterogeneity of the sulphonylurea receptor in insulin-secreting cells. *Diabetologia* 38: 277–282, 1995.
35. Pasyk EA, Kang Y, Huang X, Cui N, Sheu L, Gaisano HY. Syntaxin-1A binds the nucleotide-binding folds of sulphonylurea receptor 1 to regulate the  $K_{ATP}$  channel. *J Biol Chem* 279: 4234–4240, 2004.
36. Ravier MA, Henquin JC. Time and amplitude regulation of pulsatile insulin secretion by triggering and amplifying pathways in mouse islets. *FEBS Lett* 530: 215–219, 2002.
37. Rodrigo GC, Davies NW, Standen NB. Diazoxide causes early activation of cardiac sarcolemmal  $K_{ATP}$  channels during metabolic inhibition by an indirect mechanism. *Cardiovasc Res* 61: 570–579, 2004.
38. Ronner P, Naumann CM, Friel E. Effects of glucose and amino acids on free ADP in  $\beta$ HC9 insulin-secreting cells. *Diabetes* 50: 291–300, 2001.
39. Sagen JV, Raeder H, Hathout E, Shehadeh N, Gudmundsson K, Baevre H, Abuelo D, Phornphutkul C, Molnes J, Bell GI, Gloyn AL, Hattersley AT, Molven A, Sovik O, Njolstad PR. Permanent neonatal diabetes due to mutations in *KCNJ11* encoding  $K_{ir}6.2$ : patient characteristics and initial response to sulfonylurea therapy. *Diabetes* 53: 2713–2718, 2004.
40. Sato Y, Aizawa T, Komatsu M, Okada N, Yamada T. Dual functional role of membrane depolarization/ $Ca^{2+}$  influx in rat pancreatic  $\beta$  cell. *Diabetes* 41: 438–443, 1992.
41. Schafer G, Portenhaus R, Trolp R. Inhibition of mitochondrial metabolism by the diabetogenic thiazide diazoxide. I. Action on succinate dehydrogenase and TCA-cycle oxidations. *Biochem Pharmacol* 20: 1271–1280, 1971.
42. Seghers V, Nakazaki M, DeMayo F, Aguilar-Bryan L, Bryan J. SUR1 knockout mice. A model for  $K_{ATP}$  channel-independent regulation of insulin secretion. *J Biol Chem* 275: 9270–9277, 2000.
43. Shaner NC, Steinbach PA, Tsien RY. A guide to choosing fluorescent proteins. *Nat Methods* 2: 905–909, 2005.
44. Shiota C, Larsson O, Shelton KD, Shiota M, Efanov AM, Hoy M, Lindner J, Kooptiwut S, Juntti-Berggren L, Gromada J, Berggren PO, Magnusson MA. Sulfonylurea receptor type 1 knock-out mice have intact feeding-stimulated insulin secretion despite marked impairment in their response to glucose. *J Biol Chem* 277: 37176–37183, 2002.
45. Stienet P, Guiot Y, Gilon P, Henquin JC. Glucose acutely decreases pH of secretory granules in mouse pancreatic islets: mechanisms and influence on insulin secretion. *J Biol Chem* 281: 22142–22151, 2006.
46. Tallini YN, Ohkura M, Choi BR, Ji G, Imoto K, Doran R, Lee J, Plan P, Wilson J, Xin HB, Sanbe A, Gulick J, Mathai J, Robbins J, Salama G, Nakai J, Kotlikoff MI. Imaging cellular signals in the heart in vivo: cardiac expression of the high-signal  $Ca^{2+}$  indicator GCaMP2. *Proc Natl Acad Sci USA* 103: 4753–4758, 2006.
47. Varadi A, Grant A, McCormack M, Nicolson T, Magistri M, Mitchell KJ, Halestrap AP, Yuan H, Schwappach B, Rutter GA. Intracellular ATP-sensitive  $K^+$  channels in mouse pancreatic  $\beta$  cells: against a role in organelle cation homeostasis. *Diabetologia* 49: 1567–1577, 2006.
48. Watkins S, Geng X, Li L, Papworth G, Robbins PD, Drain P. Imaging secretory vesicles by fluorescent protein insertion in propeptide rather than mature secreted peptide. *Traffic* 3: 461–471, 2002.
49. Zung A, Glaser B, Nimri R, Zadik Z. Glibenclamide treatment in permanent neonatal diabetes mellitus due to an activating mutation in  $K_{ir}6.2$ . *J Clin Endocrinol Metab* 89: 5504–5507, 2004.
50. Zunkler BJ, Wos-Maganga M, Panten U. Fluorescence microscopy studies with a fluorescent glibenclamide derivative, a high-affinity blocker of pancreatic  $\beta$ -cell ATP-sensitive  $K^+$  currents. *Biochem Pharmacol* 67: 1437–1444, 2004.

## Review Article

# Navigating pathways affecting type 1 diabetic kidney disease

Pasquali L, Trucco M, Ringquist S. Navigating pathways affecting type 1 diabetic kidney disease.  
*Pediatric Diabetes* 2007; 8: 307–322.

**Lorenzo Pasquali<sup>a,b</sup>,  
Massimo Trucco<sup>a</sup> and  
Steven Ringquist<sup>a</sup>**

<sup>a</sup>Division of Immunogenetics, Department of Pediatrics, Rangos Research Center, Children's Hospital of Pittsburgh, University of Pittsburgh School of Medicine, Pittsburgh, PA, USA; and <sup>b</sup>Department of Pediatrics, Institute G Gaslini, University of Genoa, Genoa, Italy

Key words: diabetes – genetics – insulin – nephropathy – renal disease

Corresponding author:  
Massimo Trucco, MD  
Division of Immunogenetics  
Department of Pediatrics  
Rangos Research Center, Children's Hospital of Pittsburgh  
University of Pittsburgh School of Medicine  
3460 Fifth Avenue  
Pittsburgh, PA 15213  
USA.  
Tel: (412) 692-6570;  
fax: (412) 692-5809;  
e-mail: mnt@pitt.edu

Submitted 4 April 2007. Accepted for publication 10 May 2007

Complications of type 1 diabetes (T1D), even with reduction in risk as a result of better glycemic control, are still the major concern for pediatricians dealing with young patients who during their lifetime will eventually have to face impaired vision, reduced peripheral sensitivity, and kidney disease. T1D is associated with increased risk of nephropathy, a clinical syndrome usually accompanied by other diabetic-related complications such as retinopathy and neuropathy. Blood pressure elevation, cerebrovascular disease and high risk of cardiovascular morbidity and mortality accompany the renal symptoms, completing the picture of the syndrome (1). An estimated 20–40% of T1D patients will develop diabetic nephropathy (DN), clinically first evidenced by microalbuminuria, during their lifetime. If untreated, nearly all T1D

patients experiencing microalbuminuria will progress to overt nephropathy, evidenced by macroalbuminuria, followed by declining kidney function, and culminating in end-stage renal disease (ESRD) (2, 3). In addition to frequent morbidity linked to treating complications of the kidney (e.g., dialysis and kidney transplantation), patients experience a high rate of mortality, with a 5-yr survival rate of 21% once ESRD has developed. An estimated 45% of new patients requiring dialysis and kidney transplant are diabetic (T1D and T2D), and diabetes is the most common and rapidly increasing cause of ESRD in the US and European populations.

The prevalence and course of DN are similar in T1D and T2D patients when matched for duration of the disease (4). T2D incidence is increasing in children



and has become a major concern for pediatricians. DN follows an established natural history. The cardinal clinical feature of the syndrome is the progressive increase in urine protein excretion rate (2). The clinical course starting with microalbuminuria through proteinuria and azotemia culminates with ESRD. Before the onset of overt nephropathy, a prolonged period of clinical silence hides various changes in renal function such as hyperfiltration, hyperinfusion, and increasing capillary permeability to macromolecules.

A progressive rise in arterial blood pressure and albuminuria accompanies glomerular filtration rate (GFR) decline. T1D patients predominantly develop diastolic hypertension, whereas T2D patients typically manifest systolic hypertension (1). Microalbuminuria remains the best predictor of DN in both T1D and T2D patients (5). Risk factors correlated with disease progression are poor glycemic control, hypertension, dyslipidemia, elevated serum cholesterol, and smoking (6–8). ESRD is the major cause of mortality in T1D patients and is the dominant indicator of fatality as a result of cardiovascular disease (9, 10).

Changes in kidney structure described in diabetic patients (T1D and T2D) include nodular glomerular sclerosis (Kimmelstiel–Wilson nodular disease) (11) and a diffuse, generalized process of mesangial expansion (diffuse diabetic glomerulosclerosis). In addition, ultrastructural changes such as thickening of the tubular and the glomerular basement membrane (GBM), arteriolar hyalinosis (afferent and efferent) and increase of mesangial matrix component have been observed in both T1D and T2D. Changes in the GBM and the mesangium already can be detected after 2 yr of diabetes during a period of clinical silence (12). However, in some T2D patients, a more heterogeneous renal pathology has been described (13, 14). The latter includes superimposed changes observed in T2DM such as chronic vascular (arteriosclerotic type) and tubulointerstitial lesions or glomerular changes unrelated to diabetes such as proliferative glomerulonephritis or membranous nephropathy (15). The atypical pattern in renal pathology described for T2D may underline the interplay of different factors acting as promoters of progression in the disease other than hyperglycemia.

### Genetic risk of DN and ESRD

It is widely accepted that poorly controlled blood glucose while closely correlated with T1DN is insufficient to fully account for the incidence of kidney disease in this population. Approximately half of the patients with poor glycemic control do not develop nephropathy (16–18). Epidemiologic study of the disease has provided evidence supporting the hypothesis that there is a genetic predisposition. Among T1D patients who have healthy kidney

function 30 yr after onset of diabetes, the incidence of T1DN decreases, even among individuals experiencing retinopathy. New cases of T1DN are few among individuals with long-lasting T1D (3, 19, 20). Studies of siblings concordant for T1D have demonstrated familial clustering of DN. The increased familial incidence of T1DN allowed the estimation of the genetic risk ratio for a sibling ranging between roughly twofold for T1DN and threefold for T1D–ESRD (21–24).

T1DN is a complex genetic disease indicating that synergy among several genes, with varying individual effects, are contributing to the disease. Models of genetic susceptibility to T1DN are based primarily on the analysis of Rogus et al. (25) who used the data reported by Quinn et al. (23) to simulate the incidence of T1DN among siblings. Their analysis modeled the occurrence of T1DN assuming co-occurrence of 71.5% when the index case exhibited T1DN and 25.4% when the index case presented T1D but with normal kidney function. Comparison of these observations, when overlaid onto a genetic model of an autosomal dominant gene with 20% disease allele frequency and 100% penetrance, implied a 36% lifetime risk of developing nephropathy in the individuals with T1D. Risks of 66.2 and 19.0% were predicted for T1D siblings of the index cases with and without T1DN, respectively. In contrast, an autosomal recessive model assuming 60% disease allele frequency in the Caucasian population also accounted for the observed lifetime risk of T1DN and similar sibling risks of 64.0 and 23.3% for an index case with siblings who are T1DN or T1D, respectively.

Genome-wide mapping aimed at understanding the basis for inherited risk of diseases coincident with T1DN (i.e., T1D and hypertension) have identified genetic elements consistent with their etiology (Table 1). For example, T1D has been strongly linked to inheritance of histocompatibility leukocyte antigen (HLA) class II DRB1 and DQB1 loci expressing a non-aspartate residue at amino acid 57 (26, 27). An estimated 95% of T1D patients have inherited at least one copy of the DRB1\*0301,DQB1\*0201 or the DRB1\*04,DQB1\*0302 haplotype (28). Between 30 and 40% of T1D patients are heterozygous for the combined haplotype despite the expected frequency of 2% in their respective populations (29–31). However, HLA is estimated to account for only 40% of the genetic risk of developing T1D (32–34). Genetic analyses of affected individuals have identified additional T1D susceptibility loci, reproducibly implicating chromosomal regions 11p15.5 (insulin-dependent diabetes mellitus [IDDM]2, INS), 2q33 (IDDM12, CTLA4 region), and 1p13 (PTPN22) (34–36).

Comparison of biopsy tissues from the kidneys of T1DN patients supports the hypothesis that familial factors affect severity of the glomerular lesion. In fact

Table 1. Confirmed genetic elements influencing susceptibility to type 1 diabetes

Locus symbol	IDDM region	Cytogenetic band	Odds ratio	Sibling risk ratio	Description
HLA-DQB1	IDDM1	6p21.3	95	2.5–3.6	HLA class II locus DQB1 accounts for greater than 40% of the relative genetic risk associated with T1D
INS	IDDM2	11p15.5	2.7	1.29	Association between a VNTR marker located immediately 5' of the insulin gene locus
CTLA4	IDDM12	2q33	1.2	1.01	The CTLA4 locus along with ICOS and CD28 are each strong candidates for IDDM12-associated risk
PTPN22	–	1p13	1.8	1.23	The PTPN22 locus encodes a tyrosine phosphatase and is linked with an increased risk for T1D as well as other autoimmune diseases, e.g., rheumatoid arthritis, systemic lupus erythematosus, and thyroiditis

HLA, histocompatibility leukocyte antigen; ICOS, inducible t-cell costimulator; IDDM, insulin dependent diabetes mellitus; INS, insulin; T1D, type 1 diabetes; VNTR, variable number of tandem repeat. Data are summarized from genetic linkage analysis described by Onengut-Gumuscu and Concannon (36) and Motzo et al. (147).

significant similarities between glomerular lesions were identified even when sibling T1D patients were discordant for glycemic control (37). The correlation in severity of glomerular lesions among T1D siblings independent of hemoglobin A1C (HbA1C) levels is consistent with an underlying genetic predisposition. Development of lesions in normal kidneys transplanted into diabetic patients has been described in a long-term study of recipients 6–14 yr after transplantation. Wide variation in the rate of development of lesions in different kidneys was observed independently from the history of blood glucose levels. This suggests that in addition to glycemic control *per se* risk factors intrinsic to the kidney itself are present (38, 39).

In addition to T1D, hypertension is an inheritable risk factor linked to development of kidney disease,

indicating that the genetics of T1DN and essential hypertension may be linked (Tables 2 and 3). By controlling blood volume, the kidney is responsible for long-term blood pressure control. Impaired kidney function is a principal component underlying the physiology of essential hypertension (40, 41). Family-based studies have reported an increased incidence of hypertension, 30–40% higher in patients who develop T1DN (42, 43), whereas patients with uncomplicated T1D exhibit relatively lower blood pressures (41). Parents of T1DN patients frequently exhibit increased blood pressure when compared with parents of unaffected T1D patients, suggesting a familial basis linking hypertension with impaired kidney function (43). Studies designed to deconstruct the role of genetics on hypertension have indicated that different

Table 2. Genes linked to Mendelian hypertensive disorders

Locus symbol(s)	Mendelian disorder	Physiological role	Description
HSB11B1	Apparent mineralocorticoid excess	Salt–water homeostasis	11-beta-hydroxysteroid dehydrogenase, type I (autosomal recessive trait)
CYP11B1, CYP11B2	Glucocorticoid-remediable aldosteronism	Salt–water homeostasis	Cytochrome P450, subfamily XIB, polypeptide 1 and cytochrome P450, subfamily XIB, polypeptide 2 (autosomal dominant trait)
SCNN1B, SCNN1G	Liddle syndrome	Salt–water homeostasis	Sodium channel, nonvoltage-gated 1, beta subunit and sodium channel, nonvoltage-gated 1, gamma subunit (autosomal dominant trait)
NR3C2	Mutations in mineralocorticoid receptor	Salt–water homeostasis	Nuclear receptor subfamily 3, group C, member 2 (autosomal dominant trait)
WNK1, WNK4	Pseudohypoaldosteronism type II	Salt–water homeostasis	Protein kinase, lysine-deficient 1 and protein kinase, lysine-deficient 4 (autosomal dominant trait)

Data are summarized from Mullins et al. (45), Lifton et al. (119), and Cowley (148).



Table 3. Candidate loci influencing susceptibility to essential hypertension

Locus symbol	Cytogenetic band	Physiological role	Description
Candidate genes located on chromosome 1q			
AGT	1q42–q43	RAS	Angiotensin I
AVPR1B	1q32	Salt–water homeostasis	Arginine vasopressin receptor 1B
HSD11B1	1q32–q41	Steroid metabolism	11-beta-hydroxysteroid dehydrogenase, type I
NPR1	1q21–q22	Salt–water homeostasis	Natriuretic peptide A type receptor
REN	1q32	RAS	Renin
Candidate genes located on chromosome 3q			
AGTR1	3q21–q25	RAS	Angiotensin II receptor, type 1
CLCN2	3q27–q28	Salt–water homeostasis	Chloride channel 2
DRD3	3q13.3	adrenergic system	Dopamine receptor D3
ECE2	3q28–q29	Endothelin related	Endothelin-converting enzyme 2
KNG1	3q27	Kallikrein–Kinin system	Kininogen 1
MME	3q25.1–q25.2	Salt–water homeostasis	Membrane metallo-endopeptidase (neutral endopeptidase, enkephalinase)

RAS, renin–angiotensin system. Data are summarized from DeWan et al. (44), Hamet et al. (149), and Jeunemaitre et al. (150).

genes may contribute to increased incidence of hypertension in different ethnic groups (44, 45). Genome-wide scans have implicated different regions of chromosome 3 in Caucasian and African-American populations as well as genetic markers on chromosome 1 and 6 among Caucasians (43, 45, 46) (Table 3). Improved understanding of the inherited basis of T1DN may lead to deeper understanding of the molecular mechanisms underlying the disease, leading to improved therapeutic intervention as well as improved understanding of why the majority of T1D patients maintain normal kidney function while a substantial minority go on to exhibit T1DN.

A number of genome-wide linkage scans have been performed in order to evaluate the genetics underlying impaired kidney phenotype. The first genome scans were performed in a Pima Indian cohort with T2D and proteinuria. Genetic analysis of sib pairs identified significant linkage on chromosome 7. Additional loci were identified on chromosomes 3q and 9. Genome scans performed in an African-American cohort affected by T2D and ESRD revealed evidence for susceptibility on chromosomes 3q, 7p, and 18q (Table 4). However, as these studies were performed using DNA obtained from affected sib pairs concordant for both T2D and proteinuria or ESRD, positive signals may have cosegregated with T2D or nephropathy. Following nephropathy only, a study performed using a cohort of 18 large Turkish families with T2D and proteinuria showed strong linkage with chromosome 18q. A recent genome-wide association study has been performed genotyping greater than 80 000 single nucleotide polymorphisms (SNPs) using a cohort of T2DN (case) and T2D (control) patients, identifying genetic association with the engulfment and cell motility 1 gene (*ELMO1*) and a *p* value of less than  $8 \times 10^{-6}$  on chromosome 7p (47). Osterholm et al. (48) have recently performed a genome-wide

linkage analysis using T1D sib pairs discordant for nephropathy. The study identified five genomic regions with possible linkage to T1DN, implicating chromosomes 3q, 4p, 9p, 16q, and 22p. The overlap between chromosome 3q identified from this study and those performed with T2DN cohorts suggests a possible area of focus for future genetic analyses.

The complex etiology of DN reflects the intricate nature of the disease, requiring a combination of alleles of several genes in addition to exposure to environmental factors. The role of shared environmental risk factors has been extensively evaluated, and while their exact nature is unclear, it is likely that similar lifestyles such as eating and smoking habits are more prevalent among siblings compared with unrelated T1D patients. Glycemic control has been proposed to be a risk factor for nephropathy (49). Studies on diabetic twins have indicated that HbA1C levels are at least partially genetically determined, accounting for greater than 60% of the population variance of glycosylated hemoglobin (50). Individuals with good glycemic control, whether through genetics or as a result of rigorous testing and adjustment of insulin doses to control blood glucose levels, are able to reduce their risk of developing diabetic complications, including T1DN as was shown in the Diabetes Control and Complications Trial (DCCT), as explained later in this text.

### Risk factors associated with the progression of T1DN

What factors contribute to onset of nephropathy as a complication in T1D patients? Early age of T1D onset may be linked to the increased risk of T1DN (51), but this conclusion has been controversial (52, 53). The observation that the risk for T1DN reaches a peak incidence at ages 25–29 yr and occurs equally in both males and females may indicate that the triggering

Table 4. Candidate loci influencing susceptibility to diabetic nephropathy

Locus symbol	Cytogenetic band	Physiological role	Description
Candidate genes located on chromosome 3q			
NCK1	3q21	Growth factor/cytokine/signal transduction	NCK adaptor protein 1
RAB7	3q21.3	GTP-binding protein related	RAB7, member RAS oncogene family
SLC2A2	3q26.1–q26.3	Carbohydrate transport/metabolism	GLUT2 (solute carrier family 2 (facilitated glucose transporter), member 2)
SUCNR1	3q24–q25.1	Metabolism	Succinate receptor 1
Candidate genes located on chromosome 4p			
ADD1	4p16.3	Cytoskeletal component	Adducin 1
Candidate genes located on chromosome 7p			
ELMO1	7p14.2	Apoptosis related	Engulfment and cell motility 1
IGFBP1	7p14–p12	Growth factor/cytokine/signal transduction	Insulin-like growth factor-binding protein 1
IL6	7p21	Growth factor/cytokine/signal transduction	Interleukin 6
NXPH1	7p22	Cell adhesion	Neurexophilin 1
RAC1	7p22	GTP-binding protein related	Ras-related C3 botulinum toxin substrate 1 (rho family, small GTP-binding protein Rac 1)
Candidate genes located on chromosome 16q			
BCAR1	16q23.1	Cell adhesion	Breast cancer anti-estrogen resistance 1
CDH1	16q22.1	Tight junction component	Cadherin 1, type 1, E-cadherin (epithelial)
CDH3	16q22.1	Tight junction component	Cadherin 3, type 1, P-cadherin (placental)
CETP	16q21	Fatty acid/cholesterol transport/metabolism	Cholesteryl ester transfer protein, plasma
CYBA	16q24	Reactive oxygen species metabolism	Cytochrome <i>b</i> -(245), alpha subunit
MAPK3	16q11.2	Growth factor/cytokine/signal transduction	Mitogen-activated protein kinase 3
MMP2	16q13	Extracellular matrix component	Matrix metalloproteinase 2
Candidate genes located on chromosome 18q			
BCL2	18q21.3	Apoptosis related	B-cell CLL/lymphoma 2
DSC2	18q12.1	Cell adhesion	Desmocollin 2
SERPINB7	18q21.33	Extracellular matrix component	Serpin peptidase inhibitor, clade b(ovalbumin), member 7
SMAD7	18q21.1	Growth factor/cytokine/signal transduction	SMAD family member 7

CLL, chronic lymphocytic leukemia; GLUT, glucose transporter; RAB, RAS-associated protein; RAS, renin-angiotensin system; SMAD, homolog of mothers against decapentaplegic. Data are summarized from Shimazaki et al. (47), Osterholm et al. (48), He et al. (143), and Ewens et al. (90).

event(s) may be independent of differences in T1D onset. The triggering event may, however, be linked to puberty and the beginning of adolescence. Puberty-associated deterioration in glycemic control, hormonal changes, as well as psychosocial pressures have come under increased scrutiny for their influence in patients who fail to maintain good blood glucose control (54). Glycemic control often deteriorates during adolescence in individuals with T1D and may result from developmental changes, especially increased growth hormone secretion during puberty, as well as the transition to more autonomous lifestyle typified by adulthood. In some female patients, there is also the emergence of eating disorders and the misuse of insulin as a means to control weight gain (54, 55).

### Constitutional factors

Predisposition to the development of DN can be because of genetic susceptibility as well as factors operating *in utero*. Intra-uterine malnutrition has been associated with a reduced number of nephrons (56), increasing the risk of kidney diseases and hypertension in adult life (57). Exposure to unfavorable intra-uterine environment leading to intra-uterine growth retardation (IUGR) was proposed as a risk factor for DN progression. This conclusion follows from the hypothesis that reduced nephron number observed in IUGR patients (58) may lead to reduced functional reserve in those kidneys subjected to potentially toxic agents (e.g., hyperglycemia or smoking). Rossing et al. (59)

observed an increased risk of DN in women with IUGR and T1D. This was confirmed for both sexes in a cohort of Pima Indian type 2 diabetic patients (60). In contrast, the conclusion failed to be reproduced according to observations reported by Eshoj et al. (61) and in a recent study on Finnish T1D patients (62). Contradictory results from different studies have not yet clarified if there is a correlation between IUGR and DN; however, individuals with essential hypertension were shown to have a markedly reduced number of nephrons in addition to an inverse correlation between birth weight and adult systolic blood pressure (63). It is possible that intra-uterine factors may have a direct effect on DN progression later in life although the effect may be indirect, e.g., via hypertension.

### Hyperglycemia

Rates of decline in GFR have been linked in T1D patients to increased levels of blood glucose and occur at a rate of roughly 10–14 ml/min/yr in patients with persistent albuminuria (64). This observation has been confirmed in several independent studies, indicating that HbA1C levels are predictive of the risk of subsequent onset of ESRD. In the absence of therapeutic intervention, the majority of patients with sustained microalbuminuria progress to overt nephropathy over a period of 10–15 yr (65–69).

Control of blood glucose levels is critical to the development of the characteristic complications of diabetes, including DN, as has been demonstrated by the outcome of the DCCT. The DCCT was carried out from 1983 to 1993 and assessed the relative effects of intensive and conventional insulin therapy treatments on preventing development and progression of complications (16). Enrolling greater than 1400 adult patients with T1D, the DCCT showed that HbA1C levels could be reduced from 9.1% to 7.2% with a corresponding reduction in progression of renal complications (16). At the end of the study, the incidence of microalbuminuria was reduced by 34% in a cohort in which no evidence of retinopathy or nephropathy was present at baseline. In a second cohort, mild and early complications were present and the DCCT reported a 43% reduction in the incidence of microalbuminuria. The success of intensive insulin therapy for the treatment of diabetes was confirmed by a follow-up study showing persistent long-term reduction in the incidence of T1DN (70).

Compliance with the intensive insulin therapy regime 2 yr after conclusion of the study indicated that 95% of the intensive therapy group reported following intensive therapy regime and 70% of the conventional treatment group now reported following intensive therapy regime. This means that 30% of the conventional treatment patients failed to adopt intensive therapy despite knowledge of the results.

Comparison of HbA1C levels after 2 yr post-DCCT indicated that the intensive therapy group experienced HbA1C levels of 7.2% during DCCT and 7.9% 2 yr after conclusion of the trial. Of these patients, 46% continued to monitor blood glucose four or more times a day. Patients from the conventional treatment group who converted to intensive therapy demonstrated HbA1C levels of 8.1% post-DCCT. Of these patients, 36% reported monitoring blood glucose four or more times a day. The benefits of intensive therapy 5 yr post-DCCT were disappointing in that both cohorts reported average HbA1C levels exceeding 8%. One conclusion of the study is that in the absence of a strong research motivation and monthly visits with a health care provider, the degree of intensive treatment shown in the DCCT was not maintained. Moreover, the availability of health insurance corresponded to success as measured by reduction of HbA1C levels. Patients receiving intensive therapy 5 yr post-DCCT without health insurance maintained an average HbA1C of 8.6%, while patients with health insurance maintained an average HbA1C of 8.1%.

Unfortunately, patients participating in intensive insulin therapy treatments for diabetes are more likely to experience severe adverse effects resulting from frequent injections of insulin. Severe hypoglycemic events occurred nearly threefold more often in patients enrolled in the intensive therapy regime and were characterized as requiring assistance of another person. This precluded the enrollment of children into the study. Severe hypoglycemic episodes occurred in 25% of the total number of reported cases of hypoglycemia and were manifested by coma or convulsions. Of the adult patients receiving intensive insulin therapy, 22% experienced at least five episodes of severe hypoglycemia vs. 4% of conventionally treated subjects. Life-threatening complications of hypoglycemia are not uncommon, limiting the availability of intensive insulin therapy as a means to prevent onset of DN.

### Hypertension

High blood pressure is prevalent in families in which T1DN is present compared with T1D families without DN (43). Hypertension-associated microalbuminuria is a predictive indicator of overt nephropathy in T1D patients (71). While normalization of blood glucose levels has been linked to healing of microvascular lesions in the kidney, treatment of hypertension has resulted in improved renal outcome by preventing glomerular damage. Clinical studies have indicated a decline in the incidence of nephropathy in T1D patients (72–74). However, many T1D subjects only attain HbA1C levels of 8.5% well in excess of the recommended levels of blood glucose. Regression of microalbuminuria has been observed upon blood pressure control, and remission of overt nephropathy

has been observed in T1D patients treated for hypertension (5, 75).

There is an exponential impact from hypertension on increasing risk for renal disease (76). Maintaining a sustained reduction in blood pressure is the single most influential intervention for reducing progression of nephropathy in T1D as well as T2D patients. Studies of initially normotensive T2D subjects without renal disease who subsequently developed and were treated for hypertension indicated that patients with blood pressure less than 130/80 mm Hg rarely developed nephropathy. In contrast, diabetic patients with blood pressure in the range of 130/80 to 140/90 mm Hg exhibit a significant decline in GFR coincident with 30% of patients progressing to microalbuminuria within 12–15 yr (77). Improvements in blood pressure treatment and glycemic control along with decreased incidence of smoking lead to improved outcomes for T1D patients.

### The kidney structures implicated in the pathogenesis of the disease

#### The glomerular filtration barrier in T1DN

A thorough understanding of the molecular properties of the glomerular filtration barrier (GFB) is crucial to comprehension of the pathology of proteinuria encountered in T1DN. Structurally, the GFB is composed of three layers that mediate the process of ultrafiltration of blood flowing through anastomosing capillary loops leading to the formation of the primary urine in the Bowman's capsule and finally into the tubular system (Fig. 1). The first layer is a highly fenestrated vascular endothelium that covers the wall of the capillaries. It has been suggested that a protein

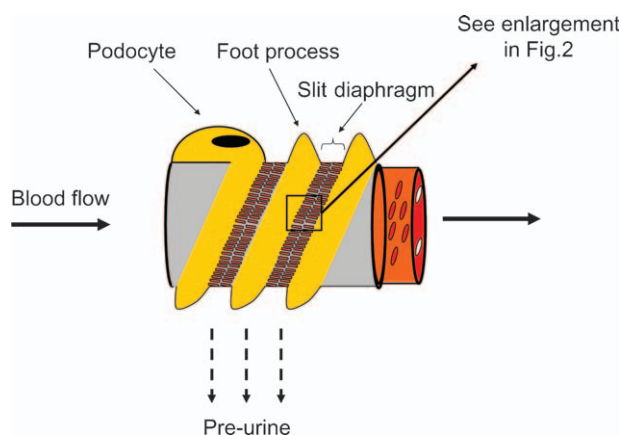


**Fig. 1.** The GFB. Ultrafiltration occurs when the blood flows through the glomerular capillaries. The GFB comprises the fenestrated endothelial cell layer (red) and the glomerular capillary basement membrane (gray). The podocytes (yellow) loop to the capillaries with their pedicles or foot processes. A protein complex forming the slit diaphragm covers the space between the podocytes processes. GFB, glomerular filtration barrier.

filtration role of the endothelium may be critical to proper kidney function because of the barrier properties of glycocalyx coating of the endothelial cells and filling in of the intracellular space (78). The second layer is the GBM, forming the boundary between blood and urine primarily composed of an interconnecting network of type IV collagen (alpha-1 and -2 during fetal development and alpha-3, -4, and -5 in the adult) and laminin-1 (consisting of alpha-1/beta-1/gamma-1 chains in the fetus) and laminin-11 (consisting of alpha-5/beta-2/gamma-1 chains in the adult). The third layer is composed of highly specialized cells, the podocytes whose cytoplasm extends into interdigitating pedicles or foot processes. The area between the podocyte foot processes is the slit diaphragm composed of a number of cell surface proteins including nephrin, neph 1, and P-cadherin. Understanding GFB function has centered on the role of the slit diaphragm formed by these proteins, serving as the ultimate layer ensuring that large macromolecules such as serum albumin and gamma globulin remain in the bloodstream while allowing small molecules such as water, glucose, and ionic salts to pass through (79).

The genesis of albuminuria is consistent with generalized vascular dysfunction, alterations in extracellular matrix components, and impaired basement membrane organization resulting from hyperglycemia (80). Increasing consideration has been given to the GFB and its central role in the filtration of plasma proteins. High-molecular-weight tracer molecules have been used to investigate the molecular sieving properties of the GFB. Ferritin has an estimated Stokes radius (SR) of 61 Å and when injected into healthy rats failed to pass through the GBM (81). In puromycin aminonucleoside-induced nephrosis models, which induce glomerular injury evidenced by flattening of podocyte foot processes, ferritin is only partially retained (82). Smaller proteins have also been used to examine the selective permeability of the GBM. For example, horseradish peroxidase (SR = 30 Å) has been observed to pass through both the GBM and slit diaphragm, while myeloperoxidase (SR = 36 Å) and catalase (SR = 52 Å) are GBM permeable but are captured by the slit diaphragm prior to entering the urine, consistent with the hypothesis that for large proteins, GBM selectivity is the primary barrier separating the blood and urine space (79).

Genetic polymorphisms of extracellular matrix proteins as well as enzymes involved in their metabolism have been suggested as possible explanations for the variation in susceptibility to kidney disease observed in T1D patients (80, 83). Type IV collagens are a principal component of basement membranes (84). In the adult glomerulus, collagens encoded by the COL4A3, COL4A4, and COL4A5 loci replace the fetal collagens COL4A1 and COL4A2 (85). Absence of the adult forms of collagen has been associated with proteinuria



because of Alport syndrome, a genetically determined disease characterized by heavy proteinuria. In these patients, the pathology is sustained by an abnormal basement membrane because of defects and/or absence of adult type IV collagens (86, 87).

SNPs associated with fetal expressed collagen COL4A1 have also been linked with susceptibility to nephropathy. GBM abnormalities characterized by irregularities in the parietal epithelium lining Bowman's capsule have been observed in heterozygous mice containing a single nucleotide mutation in COL4A1, resulting in a Gly627Trp amino acid substitution in exon 26 (83) as well as mice harboring a G to A polymorphism in a COL4A1-encoded splice site resulting in loss of exon 40 from the mRNA transcript (88). Loss of COL4A1 exon 40 has been linked to nearly 100% prevalence of albuminuria in animals by the time they reach 2 yr of age (89). In humans, mutations affecting GBM structure have been linked with hereditary risk of nephropathy (89, 90). While deletion of COL4A1 is lethal, mice die by embryonic day 9.5 (83), and heterozygous individuals may survive to adulthood carrying increased risk of microvascular complications as a result of altered basement membrane structure occurring during early development and organogenesis.

The third layer and ultimate barrier for plasma protein ultrafiltration is the slit diaphragm of the podocytes

Podocytes, highly specialized epithelial cells, lie on the outer surface of GBM to which they affix by cell surface adhesion proteins such as the  $\alpha$ -3  $\beta$ -1

integrin and dystroglycan (91, 92). The podocyte foot process (polypoid extraflections) cover the outer layer of the GBM. The intrapodocyte connections are typified by narrow spaces (30–40 nm) covered by a porous membrane known as the slit diaphragm (Fig. 2). The slit-diaphragm protein complex is an adherens-type junction and presents a dense zipper-like structure composed of the extracellular components of nephrin, neph 1, P-cadherin and FAT tumor suppressor homolog 1 (FAT 1) (93, 94). Podocin and CD2-associated protein (CD2AP) are localized in the intercellular compartment and interact with the intercellular components and interact with the extracellular components of the slit diaphragm anchoring the cytoplasm domain of nephrin to cholesterol-rich regions of the plasma membrane and to the actin filament structure of the podocyte cytoskeleton (79, 95). The protein zona occludens-1 is located at the neph 1 insertion site of the slit diaphragm interacting with the cytoskeleton as well as other components of the cell-cell junction. Recent findings have demonstrated the role of the slit-diaphragm adapter protein NCK (96). NCK binds the cytoplasmic tail of nephrin and following a phosphorylation signal leads to cytoskeletal reorganization. This finding provides evidence that the central role of the cytoplasmic region of the nephrin/NCK complex is to act in a signaling transduction capacity, transmitting antiapoptotic signals (via Akt, a serine-threonine kinase) (96), promoting remodeling of the cytoskeletal structure that drive formation of the actin-based foot processes of the podocyte.

The key role of the slit-diaphragm components in maintaining correct permeability function of the GFB is underscored by the results obtained from animal

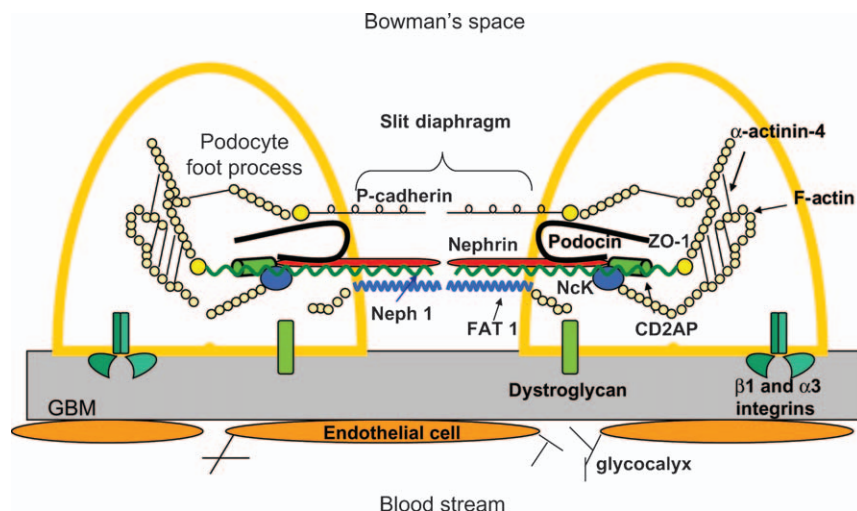


Fig. 2. Schematic view of the molecular anatomy of two podocyte foot processes (yellow) with the interposed slit-diaphragm complex. Interference with proteins that structurally sustain the slit diaphragm (e.g., CD2AP, nephrin, and podocin) can cause foot process effacement resulting in proteinuria. Filtrate from the bloodstream passes through the glycocalyx-filled fenestrae located between endothelial cells lining the GBM. The filtrate then flows through the GBM as well as the slit diaphragm and into the Bowman's space. The image is modified and adapted from Vincenti and Ghiggeri (151) and Johnstone and Holzman (152). CD2AP, CD2-associated protein; FAT 1, FAT tumor suppressor homolog 1; GBM, glomerular basement membrane; NCK, NCK adaptor protein 1; ZO-1, zona occludens-1.



models and human findings. Mutation in genes encoding nephrin, podocin, and  $\alpha$ -actinin proteins leads to severe hereditary forms of nephrotic syndrome in humans (97, 98). Mice lacking CD2AP (99) develop nephrotic syndrome, and mutations in CD2AP were found in two human patients with focal segmental glomerulosclerosis. NCK-deficient animals fail in the formation of podocyte foot processes (96).

Progress in elucidating podocyte biology and signaling have shown that the complex of proteins composing the slit diaphragm is critical to maintaining podocyte architecture as well as supporting the overall function of the glomerular filter of the kidney. For T1D, as well as T2D, nephropathy, there are reports of a reduced number and density of the podocytes and an increase in foot process width (100–105). Steffes et al. (102) has reported loss of podocytes occurring early in T1D, while other authors detected the loss of podocytes continuing later in disease progression (104). The loss of podocytes from the glomerular space has been correlated with increased albumin excretion.

A loss of nephrin along with the onset of microalbuminuria occurs in early stages of DN in T1D patients (106). The loss of nephrin was detected even before the appearance of microalbuminuria, suggesting that damage to the slit diaphragm may occur early in disease pathogenesis. Other studies confirmed reduction of nephrin and other slit-diaphragm proteins in the glomeruli of patients with both T1D and T2D nephropathies (107–109). Koop et al. (108) reported on DN in six patients, observing statistically significant decrease in protein level of nephrin along with reduced expression of podocin and podocalyxin. Nephrin mRNA expression inversely correlated with increasing severity of proteinuria (108).

### The tubular system

T1DN is often considered a glomerular disease; however, progression to end-stage organ failure also correlates with increased level of renal tubulointerstitial fibrosis (110, 111). Changes occurring in the renal tubular system have been implicated as a primary contributor to the process of renal cortex fibrosis observed in DN (112). Increased fibrosis correlates with macroalbuminuria, nephron tubular cell injury, induction of apoptosis, and hypertension (110, 111, 113–117).

Renal tubular system epithelial cells and interstitial tissue undergo changes during progression of T1DN. These include tubulointerstitium alterations, tubular hypertrophy, and basement membrane alterations that precede tubulointerstitial fibrosis. Tubular cell hypertrophy is an early feature of T1DN. Exposure of proximal tubular epithelial cells to hyperglycemia

occurs as a result of glycosuria as well as from high glucose concentration present in interstitial tissue. Cellular response to elevated glucose includes increased tubular basement membrane thickening as a result of increased synthesis of type IV collagen and fibronectin as well as altered matrix protein metabolism as a result of increased expression of metalloproteinase inhibitors tissue inhibitor of metalloproteinase (TIMP)-1 and TIMP-2 (114, 115, 118). Changes to the tubulointerstitium co-occur along with changes to the glomerulus. Poor filtration of the primary urine may lead to presentation of cytotoxic compounds to the nephron tubular cells. Combining the deleterious affects of glycosuria with exposure to cytokines may stimulate cellular responses leading to organ failure.

Primary filtration of urine occurs at the slit diaphragm of the GFB (45); however, glucose and sodium ions are freely filtered. Glucose is entirely reabsorbed in the proximal tubule by a sodium–glucose cotransport system. Recovery of greater than 99% of filtered sodium ion occurs within the nephron via the action of specialized epithelial cells lining the renal tubular system proximal tubule (responsible for 50% sodium absorption), thick ascending loop of Henle (30–40% sodium absorption), distal convoluted tubule (5% sodium absorption), and the collection duct (4% sodium absorption) (Fig. 3). Sodium reuptake by the distal convoluted tubule and collection duct account of a small percentage of total salt reabsorption but are the principal sites at which net salt balance is determined (119). A widely held model for explaining the role of the kidney in blood pressure

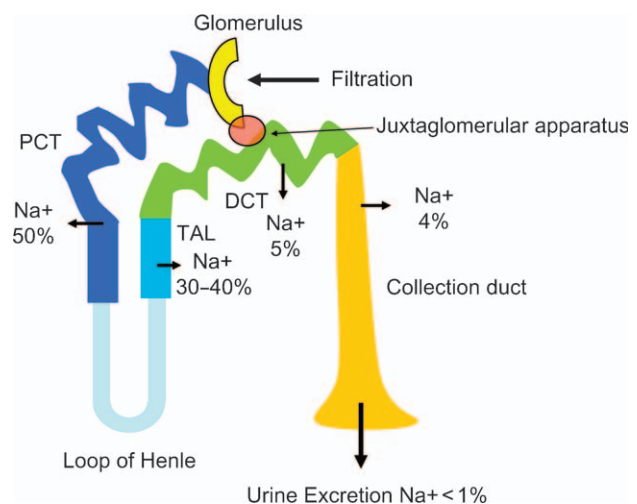


**Fig. 3.** A schematic view of sodium reabsorption along the nephron. Urine is processed via the PCT, TAL, and DCT. The juxtaglomerular apparatus comprises the macula densa cells, which represent specialized tubular cells at the end of the thick ascending limb, comprising cells from the extraglomerular mesangium, vascular smooth muscle cells, and renin-secreting cells in the media of the afferent glomerular arteriole. DCT, distal convoluting tubule; PCT, proximal convoluting tubule; TAL, thick ascending limb.

control is through its role balancing sodium excretion and recovery. Hypertension results from impaired blood pressure control and correlates with changes in the kidney that lead to impaired renal function, i.e., inability to maintain sodium ion homeostasis.

Increased kidney mass is an early feature of DN (120) with expansion of the proximal tubular cells accounting for most of the growth (121, 122). Along with tubular cell expansion there is increased sodium recovery. Vallon et al. (123) have suggested a model in which increased sodium recovery by the proximal convoluted tubule causes glomerular hyperfiltration, leading to nephropathy. The primary increase in proximal tubular reabsorption in early diabetes may be because of proximal tubular reabsorption through enhanced sodium–glucose cotransport. Studies on patients with T1DN have indicated increased sodium recovery occurring primarily within nephron tubular segments upstream from the macula densa in the distal convoluted tubule (124, 125) and have indicated that there is increased tubular recovery of sodium ions occurring in patients with early-stage T1D.

The juxtaglomerular apparatus comprises different structures in functional and structural link: cells of the extraglomerular mesangium, which fill the angle between the afferent and the efferent glomerular arteriole; vascular smooth muscle cells and renin-secreting cells in the media of the afferent glomerular arteriole; and the macula densa. The macula densa is an area of specialized cells lining the region of the distal convoluted tubule next to the glomerular vascular pole. These cells are sensitive to the ionic content and water volume of the fluid in the distal convoluting tubule. An increase or decrease in sodium, chloride, and potassium uptake elicits inverse changes in the single-nephron GFR by altering the vascular tone, predominantly of the afferent arteriole. The mechanism serves to establish an appropriate balance between GFR and tubular reabsorption upstream from the macula densa. As the proximal tubule grows, more of the glomerular filtrate sodium is reabsorbed and less reaches the macula densa at the end of Henle's loop causing GFR to increase through the normal physiologic actions.

The link between increased tubular sodium recovery and diabetic kidney disease is echoed in observations obtained from studies involving hyperfiltering T1D patients in which there is reported a positive correlation between GFR and sodium recovery in the proximal tubular region of the nephron (125). Examination of T1D patients have indicated that hyperfiltration by the nephron may continue even once blood glucose levels are controlled by intensive insulin therapy (126–128) and may continue to progress independent of glucose control as a result of persisting enlargement of the nephron tubular compartment.

## Molecular pathways

### Pathways leading to fibrogenesis

The interplay between glomerular hypertension and hyperglycemia may be linked to the pathological changes seen in T1DN. In non-diabetic individuals, glomeruli are protected from deleterious effects associated with essential hypertension by interacting autoregulatory mechanisms (129). Increased blood pressure is associated with increased preglomerular resistance thus isolating glomerular capillaries from potential damage. However, the ability to regulate glomerular blood flow is impaired when significant ablation of renal mass occurs, resulting in increased single-nephron GFR. Carmine et al. (130) demonstrated that regulatory mechanisms are damaged by hyperglycemia-induced inhibition of voltage-gated calcium channels. Endothelial cell injury as a result of hypertensive glomerular damage may be responsible for initiating glomerulosclerosis, with the process involving increased expression of transforming growth factor (TGF)- $\beta$  and extracellular matrix proteins (131). The accumulation of excess extracellular matrix within the glomerulus and the interstitium is associated, at least in part, with the profibrotic cytokine, TGF- $\beta$  (132–134).

The observation that conditions characterized by a severe but relatively selective albuminuria, such as minimal change nephropathy, do not initiate interstitial fibrosis led to the study of the role of higher molecular weight ultrafiltrated proteins in DN. Ultrafiltrated growth factors, such as insulin-like growth factor 1 (IGF-1), hepatocyte growth factor (HGF), and TGF- $\beta$ , may have a direct effect on the nephron tubular epithelial cells by inducing transcription of genes with profibrogenic effects, whereas other cytokines such as bone morphogenic protein 7 (BMP-7) act as inhibitors of these pathways (135) (Fig. 4). The importance of HGF/IGF-1 action is underscored by the demonstration of a direct effect of these hormones on renal hypertrophy, microalbuminuria, and glomerulosclerosis (136) and that increased excretion rate of both urinary IGF-1 and urinary HGF strongly correlate with microalbuminuria and kidney volume in T1D patients (137).

Pathophysiological mechanisms leading to sclerosis may be related to simultaneous exposure to pro-sclerotic cytokines in glomeruli and tubulointerstitium as well as tubulotoxicity caused by protein contents in filtrate overloading the proximal tubule's absorption ability. Proteinuria is proposed to be more than a highly reliable predictive factor having a causal role during disease progression (138). Ultrafiltrated proteins undergo endocytosis by the proximal tubular cells, resulting in a cytotoxic effect directly leading to tubular damage. The interaction of filtrated protein

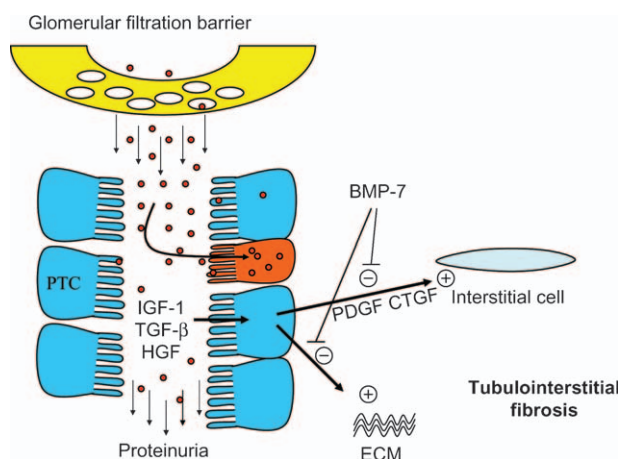


**Fig. 4.** Interstitial fibrogenesis. When glomerular proteinuria occurs, excess filtrated proteins undergo endocytosis by the PTC (in blue), resulting in cytotoxic effects and tubular damage (red PTC). Ultrafiltrated growth factor cytokines (IGF-1, TGF- $\beta$ , and HGF) activate a number of genes, enabling PTC to directly contribute to interstitial fibrosis by producing ECM proteins. Tubular cell interaction with growth factor cytokines elicited production of other cytokine signals (PDGF and CTGF) able to induce ECM production by interstitial cells. Other signals such as BMP-7 act as inhibitors of these pathways. BMP-7, bone morphogenic protein 7; CTGF, connective tissue growth factor; ECM, extracellular matrix; HGF, hepatocyte growth factor; IGF-1, insulin-like growth factor 1; PDGF, platelet-derived growth factor; PTC, proximal tubular cells; TGF- $\beta$ , tissue growth factor-beta.

with proximal tubular cells could be one of the initiating signals enabling a cascade of events leading to changes in extracellular matrix composition and eventually to interstitial fibrogenesis.

### Candidate genes and their pathways

Studies of candidate genes for T1DN have focused on genes controlling the balance between extracellular matrix protein synthesis and degradation, glucose metabolism, as well as those whose products control the interaction between kidney function and blood pressure control. Genes influencing the activity of growth factors, protein kinase C activation, hormones regulating blood pressure, accumulation of advanced glycosylation end products, aldose reductase pathway flux, and altered glucose transport have each been extensively evaluated. The roles of hypertension candidate genes have also been studied, although most of the work has focused on the renin-angiotensin system (RAS).

Candidate gene studies have evaluated both functional (i.e., nonsynonymous codons) and allelic markers linked statistically for their influence on T1DN. However, this approach has as yet to convincingly identify risk factors when replicated in independent cohorts (139). The failure to replicate first-stage results from carefully controlled genetic studies possibly reflects the confounding influence of environmental

factors on statistical power to detect a true positive signal. Strategies for the selection of candidate genes are improved by consideration of linkage scans along with relevant biologic information about the implicated loci. For example, chromosome 3q has been identified in multiple linkage studies for T1DN (48, 140). This region of the genome has also been identified in studies of T2DN in Pima Indians (141) and in African-American families (142). Other chromosomal regions have also been identified by linkage analysis to T1DN, but chromosome 3q is strongly implicated in hypertension (48) and hypertension is frequently found to co-occur with T1DN. A number of candidate genes are contained within the region of chromosome 3q implicated in these studies (Tables 3 and 4). However, one of the possible candidates, the succinate receptor (SUCNR1), has been linked with carbohydrate catabolism and with control of blood pressure. He et al. (143) reported that the orphan G-protein-coupled receptor encoded by the SUCNR1 locus detected succinate, which is a metabolic intermediate produced by the tricarboxylic acid (TCA) cycle during respiration, and increased succinate levels were causal for increased blood pressure in mice. In diabetic patients, it is possible that local mismatch of energy supply and demand, altered metabolism of TCA-cycle intermediates, or injury may lead to mitochondrial dysfunction and the release of succinate into circulation. Succinate molecules activate receptors in the kidney, causing the release of renin and activation of the RAS. The RAS leads to an increase in blood pressure and altered local blood flow. In healthy individuals, this system might act to regulate local blood flow to match metabolic demands. However, in diabetic patients with impaired metabolic control, it might also result in hypertension or altered cellular function and may contribute to renin-mediated constriction of the renal artery (144).

Many other candidate genes have been examined during genetic evaluation of T1DN. For example, Ewens et al. (90) investigated 110 candidate genes by transmission/disequilibrium testing (TDT) (145) using 72 family trios of which the offspring experienced T1DN. Genes were chosen based on the results of previous studies associating various regions of the human genome to the phenotype of T1DN and have implicated proteins expressed within the GFB. Extracellular matrix proteins encoded by the loci COL4A1, LAMA4, and LAMC1 comprise important components of GBM forming the blood-urine barrier in the kidney. Genetic variants linked to different alleles of the COL4A1 locus have been studied by TDT statistical analysis supporting the hypothesis for genetic linkage of COL4A1 (p value = 0.0002) to the nephropathy phenotype along with additional linkage to the laminin-encoding loci, LAMA4 (p value, 0.016) and LAMC1 (p value, 0.026) (90).



## Concluding remarks

The goal of reducing the incidence of T1D complications has been intensively investigated. T1DN is the principal etiology leading to ESRD. The molecular mechanism(s) underlying the disease involve an interplay between genes and gene–environmental exposures. Improved understanding of the disease pathogenesis will lead to better identification of those at risk and by doing so lead to improved treatment regimens.

The evidence for a dominant genetic role in determining susceptibility to kidney disease in T1D patients is primarily the result of epidemiological studies indicating that prevalence of DN increased during the first 15 yr after onset of T1D. After 20 yr duration of diabetes, the incidence of new cases of nephropathy among T1D patients plateaus and in fact may decrease (3, 19, 20). These observations have frequently been interpreted as indicating that there exists a subset of patients susceptible to develop kidney disease. Additional evidence for genetic risk has been obtained from family studies, showing the clustering of DN among T1D siblings (21–24). Siblings experiencing T1D have a significantly increased risk for DN when the T1D proband experiences the disease. Interpretation of the data generated from genetic analysis of T1DN is complicated by the possibility that signals are related to coincident diseases (e.g., hypertension) as well as environmental exposures such as smoking. In order to interpret these results, it is necessary to compare the results of genetic testing of control populations as well as replication of the results in independently recruited case cohorts.

Replication of genome-wide linkage and candidate gene studies for T1DN have been limited by lack of adequate sample size. Recruitment of large independent cohorts for T1DN genetic analysis is required to attain statistical power to detect true genetic signals. Several initiatives are ongoing to address this issue. The most recent of these studies is the genetics of kidneys in diabetes (GoKinD), which has provided a collection of DNA samples and relevant clinical information from greater than 3000 study participants (146). A genome-wide association study of the GoKinD cohort has recently been funded as part of the Genetic Association Information Network's collaborative effort to evaluate genes in complex diseases ([http://www.fnih.org/GAIN/GAIN\\_home.shtml](http://www.fnih.org/GAIN/GAIN_home.shtml)). The initial results of a 500 000 SNP genome-wide association scan based on the GoKinD cohort is due in the fall of 2007. Collection of additional cohorts is ongoing at a number of institutions investigating T1DN genetic risk. Careful collection practices centered on recording relevant health history of participants are essential for success. Knowledge of patient environmental exposures (e.g., history of hypertension, use of anti-hypertensive medications, and smoking) are

as essential as recording T1D history and will greatly aid in stratification of populations when comparing participants recruited at different centers.

## Acknowledgements

This work was supported by grants U19-AI056374-01 Autoimmunity Centers of Excellence (S. R. and M. T.) and RO1DK24021 (M. T.) from the National Institutes of Health and ERMS #00035010 (S. R. and M. T.) from the Department of Defense.

## References

1. PARVING HH. Diabetic nephropathy: prevention and treatment. *Kidney Int* 2001; 60: 2041–2055.
2. REMUZZI G, BENIGNI A, REMUZZI A. Mechanisms of progression and regression of renal lesions of chronic nephropathies and diabetes. *J Clin Invest* 2006; 116: 288–296.
3. PAMBIANCO G, COSTACOU T, ELLIS D, BECKER DJ, KLEIN R, ORCHARD TJ. The 30-year natural history of type 1 diabetes complications: the Pittsburgh Epidemiology of Diabetes Complications Study experience. *Diabetes* 2006; 55: 1463–1469.
4. HASSLACHER C, RITZ E, WAHL P, MICHAEL C. Similar risks of nephropathy in patients with type I or type II diabetes mellitus. *Nephrol Dial Transplant* 1989; 4: 859–863.
5. MOGENSEN CE. Microalbuminuria and hypertension with focus on type 1 and type 2 diabetes. *J Intern Med* 2003; 254: 45–66.
6. ORTH SR, STOCKMANN A, CONRADT C et al. Smoking as a risk factor for end-stage renal failure in men with primary renal disease. *Kidney Int* 1998; 54: 926–931.
7. CHATURVEDI N, FULLER JH, TASKINEN MR. Differing associations of lipid and lipoprotein disturbances with the macrovascular and microvascular complications of type 1 diabetes. *Diabetes Care* 2001; 24: 2071–2077.
8. HOVIND P, TARNOW L, ROSSING P et al. Progression of diabetic nephropathy: role of plasma homocysteine and plasminogen activator inhibitor-1. *Am J Kidney Dis* 2001; 38: 1376–1380.
9. GALL MA, BORCH-JOHNSEN K, HOUGAARD P, NIELSEN FS, PARVING HH. Albuminuria and poor glycemic control predict mortality in NIDDM. *Diabetes* 1995; 44: 1303–1309.
10. RITZ E, STEFANSKI A. Diabetic nephropathy in type II diabetes. *Am J Kidney Dis* 1996; 27: 167–194.
11. KIMMELSTIEL P, WILSON C. Inter-capillary lesions in the glomeruli of the kidney. *Am J Pathol* 1936; 12: 82–97.
12. DRUMMOND K, MAUER M; International Diabetic Nephropathy Study Group. The early natural history of nephropathy in type 1 diabetes: II. Early renal structural changes in type 1 diabetes. *Diabetes* 2002; 51: 1580–1587.
13. FIORETTO P, MAUER M, BROCCO E et al. Patterns of renal injury in NIDDM patients with microalbuminuria. *Diabetologia* 1996; 39: 1569–1576.
14. SCHWARTZ MM, LEWIS EJ, LEONARD-MARTIN T, LEWIS JB, BATLLE D. Renal pathology patterns in type II diabetes mellitus: relationship with retinopathy. The Collaborative Study Group. *Nephrol Dial Transplant* 1998; 13: 2547–2552.
15. GAMBARA V, MECCA G, REMUZZI G, BERTANI T. Heterogeneous nature of renal lesions in type II diabetes. *J Am Soc Nephrol* 1993; 3: 1458–1466.

16. DCCT. THE DIABETES CONTROL AND COMPLICATIONS TRIAL RESEARCH GROUP. The effect of intensive treatment of diabetes on the development and progression of long-term complications in insulin-dependent diabetes mellitus. *N Engl J Med* 1993; 329: 977–986.
17. DCCT. THE DIABETES CONTROL AND COMPLICATIONS TRIAL RESEARCH GROUP. Effect of intensive therapy on the development and progression of diabetic nephropathy in the Diabetes Control and Complications Trial. *Kidney Int* 1995; 47: 1703–1720.
18. KROLEWSKI M, EGGERS PW, WARRAM JH. Magnitude of end-stage renal disease in IDDM: a 35 year follow-up study. *Kidney Int* 1996; 50: 2041–2046.
19. KROLEWSKI AS, WARRAM JH, CHRISTLIEB AR, BUSICK EJ, KAHN CR. The changing natural history of nephropathy in type I diabetes. *Am J Med* 1985; 78: 785–794.
20. DIABETES RESEARCH WORKING GROUP (DRWG). Conquering diabetes: a strategic plan for the 21st century. NIH Publication No. 99–4398. 1999 (available from <http://www.niddk.nih.gov/federal/dwg/fr.pdf>). Accessed 6 June 2007.
21. SEAQUIST ER, GOETZ FC, RICH S, BARBOSA J. Familial clustering of diabetic kidney disease. Evidence for genetic susceptibility to diabetic nephropathy. *N Engl J Med* 1989; 320: 1161–1165.
22. BORCH-JOHNSEN K, NORGAARD K, HOMMEL E et al. Is diabetic nephropathy an inherited complication? *Kidney Int* 1992; 41: 719–722.
23. QUINN M, ANGELICO MC, WARRAM JH, KROLEWSKI AS. Familial factors determine the development of diabetic nephropathy in patients with IDDM. *Diabetologia* 1996; 39: 940–945.
24. HARJUTALO V, KATOH S, SARTI C, TAJIMA N, TUOMILEHTO J. Population-based assessment of familial clustering of diabetic nephropathy in type 1 diabetes. *Diabetes* 2004; 53: 2449–2454.
25. ROGUS JJ, WARRAM JH, KROLEWSKI AS. Genetic studies of late diabetic complications: the overlooked importance of diabetes duration before complication onset. *Diabetes* 2002; 51: 1655–1662.
26. TODD JA, BELL JI, MCDEVITT HO. HLA-DQ beta gene contributes to susceptibility and resistance to insulin-dependent diabetes mellitus. *Nature* 1987; 329: 599–604.
27. MOREL PA, DORMAN JS, TODD JA, MCDEVITT HO, TRUCCO M. Aspartic acid at position 57 of the HLA-DQ beta chain protects against type I diabetes: a family study. *Proc Natl Acad Sci U S A* 1988; 85: 8111–8115.
28. THOMSON G. HLA DR antigens and susceptibility to insulin-dependent diabetes mellitus. *Am J Hum Genet* 1984; 36: 1309–1317.
29. VAN DER AUWERA B, SCHUIT F, LYARUU I et al. Genetic susceptibility for insulin-dependent diabetes mellitus in Caucasians revisited: the importance of diabetes registries in disclosing interactions between HLA-DQ- and insulin gene-linked risk. *Belgian Diabetes Registry. J Clin Endocrinol Metab* 1995; 80: 2567–2573.
30. REWERS M, BUGAWAN TL, NORRIS JM et al. Newborn screening for HLA markers associated with IDDM: diabetes autoimmunity study in the young (DAISY). *Diabetologia* 1996; 39: 807–812.
31. RICH SS, CONCANNON P. Challenges and strategies for investigating the genetic complexity of common human diseases. *Diabetes* 2002; 51 (Suppl. 3): S288–S294.
32. RICH SS. Mapping genes in diabetes. Genetic epidemiological perspective. *Diabetes* 1990; 39: 1315–1319.
33. RONNINGEN KS, KEIDING N, GREEN A; EURODIAB ACE Study Group. Europe and Diabetes. Correlations between the incidence of childhood-onset type I diabetes in Europe and HLA genotypes. *Diabetologia* 2001; 44 (Suppl. 3): B51–B59.
34. CONCANNON P, ERLICH HA, JULIER C et al. Type 1 diabetes: evidence for susceptibility loci from four genome-wide linkage scans in 1,435 multiplex families. *Diabetes* 2005; 54: 2995–3001.
35. CONCANNON P, GOGOLIN-EWENS KJ, HINDS DA et al. A second-generation screen of the human genome for susceptibility to insulin-dependent diabetes mellitus. *Nat Genet* 1998; 19: 292–296.
36. ONENGUT-GUMUSCU S, CONCANNON P. The genetics of type 1 diabetes: lessons learned and future challenges. *J Autoimmun* 2005; 25 (Suppl.): 34–39.
37. FIORETTO P, STEFFES MW, BARBOSA J, RICH SS, MILLER ME, MAUER M. Is diabetic nephropathy inherited? Studies of glomerular structure in type 1 diabetic sibling pairs. *Diabetes* 1999; 48: 865–869.
38. MAUER SM, STEFFES MW, CONNETT J, NAJARIAN JS, SUTHERLAND DE, BARBOSA J. The development of lesions in the glomerular basement membrane and mesangium after transplantation of normal kidneys to diabetic patients. *Diabetes* 1983; 32: 948–952.
39. MAUER SM, GOETZ FC, MCHUGH LE et al. Long-term study of normal kidneys transplanted into patients with type I diabetes. *Diabetes* 1989; 38: 516–523.
40. THE MICROALBUMINURIA COLLABORATIVE STUDY GROUP (MCSG). Predictors of the development of microalbuminuria in patients with Type 1 diabetes mellitus: a seven-year prospective study. The Microalbuminuria Collaborative Study Group. *Diabet Med* 1999; 16: 918–925.
41. STERN M, SOWERS, TUCK ML. Pathophysiology of hypertension in diabetes. In: Le Roith D, Taylor SI, Olefsky JM, eds. *Diabetes Mellitus: A Fundamental and Clinical Text*, 3rd edn. Philadelphia, PA: Lippincott, Williams, and Wilkins, 2004: 1377–1400.
42. VIBERTI GC, KEEN H, WISEMAN MJ. Raised arterial pressure in parents of proteinuric insulin dependent diabetics. *Br Med J* 1987; 295: 515–517.
43. KROLEWSKI AS, CANESSA M, WARRAM JH et al. Predisposition to hypertension and susceptibility to renal disease in insulin-dependent diabetes mellitus. *N Engl J Med* 1988; 318: 140–145.
44. DEWAN AT, ARNETT DK, ATWOOD LD et al. A genome scan for renal function among hypertensives: the HyperGEN study. *Am J Hum Genet* 2001; 68: 136–144.
45. MULLINS LJ, BAILEY MA, MULLINS JJ. Hypertension, kidney, and transgenics: a fresh perspective. *Physiol Rev* 2006; 86: 709–746.
46. FREEDMAN BI, BECK SR, RICH SS et al. A genome-wide scan for urinary albumin excretion in hypertensive families. *Hypertension* 2003; 42: 291–296.
47. SHIMAZAKI A, KAWAMURA Y, KANAZAWA A et al. Genetic variations in the gene encoding ELMO1 are associated with susceptibility to diabetic nephropathy. *Diabetes* 2005; 54: 1171–1178.
48. OSTERHOLM AM, HE B, PITKANENIEMI J et al. Genome-wide scan for type 1 diabetic nephropathy in the Finnish population reveals suggestive linkage to a single locus on chromosome 3q. *Kidney Int* 2007; 71: 140–145.
49. ALAVERAS AE, THOMAS SM, SAGRIOTIS A, VIBERTI GC. Promoters of progression of diabetic nephropathy: the relative roles of blood glucose and blood pressure control. *Nephrol Dial Transplant* 1997; 12 (Suppl. 2): 71–74.
50. SNIEDER H, SAWTELL PA, ROSS L, WALKER J, SPECTOR TD, LESLIE RD. HbA(1c) levels are genetically



- determined even in type 1 diabetes: evidence from healthy and diabetic twins. *Diabetes* 2001; 50: 2858–2863.
51. HARVEY JN, ALLAGOA B. The long-term renal and retinal outcome of childhood-onset type 1 diabetes. *Diabet Med* 2004; 21: 26–31.
52. KOSTRABA JN, DORMAN JS, ORCHARD TJ et al. Contribution of diabetes duration before puberty to development of microvascular complications in IDDM subjects. *Diabetes Care* 1989; 12: 686–693.
53. SVENSSON M, NYSTROM L, SCHON S, DAHLQUIST G. Age at onset of childhood-onset type 1 diabetes and the development of end-stage renal disease: a nationwide population-based study. *Diabetes Care* 2006; 29: 538–542.
54. HAMILTON J, DANEMAN D. Deteriorating diabetes control during adolescence; physiological or psychosocial? *J Pediatr Endocrinol Metab* 2002; 15: 115–126.
55. POLONSKY WH, ANDERSON BJ, LOHRER PA, APONTE JE, JACOBSON AM, COLE CF. Insulin omission in women with IDDM. *Diabetes Care* 1994; 17: 1178–1185.
56. HINCHLIFFE SA, LYNCH MR, SARGENT PH, HOWARD CV, VAN VELZEN D. The effect of intrauterine growth retardation on the development of renal nephrons. *Br J Obstet Gynaecol* 1992; 99: 296–301.
57. LUYCKX VA, BRENNER BM. Low birth weight, nephron number, and kidney disease. *Kidney Int* 2005; 97 (Suppl.): S68–S77.
58. BRENNER BM, CHERTOW GM. Congenital oligonephropathy and the etiology of adult hypertension and progressive renal injury. *Am J Kidney Dis* 1994; 23: 171–175.
59. ROSSING P, TARNOW L, NIELSEN FS, HANSEN BV, BRENNER BM, PARVING HH. Low birth weight. A risk factor for development of diabetic nephropathy? *Diabetes* 1995; 44: 1405–1407.
60. NELSON RG, MORGENSTERN H, BENNETT PH. Birth weight and renal disease in Pima Indians with type 2 diabetes mellitus. *Am J Epidemiol* 1998; 148: 650–656.
61. ESHOJ O, VAAG A, BORCH-JOHNSEN K, FELDT-RASMUSSEN B, BECK-NIELSEN H. Is low birth weight a risk factor for the development of diabetic nephropathy in patients with type 1 diabetes? A population-based case-control study. *J Intern Med* 2002; 252: 524–528.
62. FAGERUDD J, FORSBLOM C, PETTERSSON-FERNHOLM K et al. Low birth weight does not increase the risk of nephropathy in Finnish type 1 diabetic patients. *Nephrol Dial Transplant* 2006; 21: 2159–2165.
63. HUXLEY RR, SHIELL AW, LAW CM. The role of size at birth and postnatal catch-up growth in determining systolic blood pressure: a systematic review of the literature. *J Hypertens* 2000; 18: 815–831.
64. PARVING HH, ROSSING P, HOMMEL E, SMIDT UM. Angiotensin-converting enzyme inhibition in diabetic nephropathy: ten years' experience. *Am J Kidney Dis* 1995; 26: 99–107.
65. PARVING HH, OXENBOLL B, SVENDSEN PA, CHRISTIANSEN JS, ANDERSEN AR. Early detection of patients at risk of developing diabetic nephropathy. A longitudinal study of urinary albumin excretion. *Acta Endocrinol (Copenh)* 1982; 100: 550–555.
66. VIBERTI GC, HILL RD, JARRETT RJ, ARGYROPOULOS A, MAHMUD U, KEEN H. Microalbuminuria as a predictor of clinical nephropathy in insulin-dependent diabetes mellitus. *Lancet* 1982; 1: 1430–1432.
67. MATHIESEN ER, OXENBOLL B, JOHANSEN K, SVENDSEN PA, DECKERT T. Incipient nephropathy in type 1 (insulin-dependent) diabetes. *Diabetologia* 1984; 26: 406–410.
68. MOGENSEN CE, CHRISTENSEN CK. Predicting diabetic nephropathy in insulin-dependent patients. *N Engl J Med* 1984; 311: 89–93.
69. MESSENT JW, ELLIOTT TG, HILL RD, JARRETT RJ, KEEN H, VIBERTI GC. Prognostic significance of microalbuminuria in insulin-dependent diabetes mellitus: a twenty-three year follow-up study. *Kidney Int* 1992; 41: 836–839.
70. WRITING TEAM FOR THE DIABETES CONTROL AND COMPLICATIONS TRIAL/EPIDEMIOLOGY OF DIABETES INTERVENTIONS AND COMPLICATIONS RESEARCH GROUP (EDIC). Effect of intensive therapy on the microvascular complications of type 1 diabetes mellitus. *JAMA* 2002; 287: 2563–2569.
71. MULEC H, BLOHME G, GRANDE B, BJORCK S. The effect of metabolic control on rate of decline in renal function in insulin-dependent diabetes mellitus with overt diabetic nephropathy. *Nephrol Dial Transplant* 1998; 13: 651–655.
72. BOJESTIG M, ARNQVIST HF, HERMANSSON G, KARLBERG B, LUDVIGSSON J. Declining incidence of nephropathy in insulin-dependent diabetes mellitus. *N Engl J Med* 1994; 330: 977–986.
73. HOVIND P, TARNOW L, ROSSING K et al. Decreasing incidence of severe diabetic microangiopathy in type 1 diabetes. *Diabetes Care* 2003; 26: 1258–1264.
74. FAGERUDD J, FORSBLOM C, PETTERSSON-FERNHOLM K, GROOP PH; Finndiane Study Group. Implementation of guidelines for the prevention of diabetic nephropathy. *Diabetes Care* 2004; 27: 803–804.
75. HOVIND P, ROSSING P, TARNOW L, TOFT H, PARVING J, PARVING HH. Remission of nephrotic-range albuminuria in type 1 diabetic patients. *Diabetes Care* 2001; 24: 1972–1977.
76. GIUNTI S, BARIT D, COOPER ME. Mechanisms of diabetic nephropathy: role of hypertension. *Hypertension* 2006; 48: 519–526.
77. RAVID M, SAVIN H, JUTRIN I, BENTAL T, KATZ B, LISHNER M. Long-term stabilizing effect of angiotensin-converting enzyme inhibition on plasma creatinine and on proteinuria in normotensive type II diabetic patients. *Ann Intern Med* 1993; 118: 577–581.
78. DEEN WM, LAZZARA MJ, MYERS BD. Structural determinants of glomerular permeability. *Am J Physiol Renal Physiol* 2001; 281: F579–F596.
79. PAVENSTADT H, KRIZ W, KRETZLER M. Cell biology of the glomerular podocyte. *Physiol Rev* 2003; 83: 253–307.
80. DECKERT T, FELDT-RASMUSSEN B, BORCH-JOHNSEN K, JENSEN T, KOFOED-ENEVOLDSEN A. Albuminuria reflects widespread vascular damage. The Steno hypothesis. *Diabetologia* 1989; 32: 219–226.
81. FARQUHAR MG, WISSIG SL, PALADE GE. Glomerular permeability. I. Ferritin transfer across the normal glomerular capillary wall. *J Exp Med* 1961; 113: 47–66.
82. FARQUHAR MG, PALADE GE. Glomerular permeability. II. Ferritin transfer across the glomerular capillary wall in nephrotic rats. *J Exp Med* 1961; 114: 699–716.
83. VAN AGTMAEL T, SCHLOTZER-SCHREHARDT U, MCKIE L et al. Dominant mutations of Col4a1 result in basement membrane defects which lead to anterior segment dysgenesis and glomerulopathy. *Hum Mol Genet* 2005; 14: 3161–3168.
84. KALLURI R. Basement membranes: structure, assembly and role in tumour angiogenesis. *Nat Rev Cancer* 2003; 3: 422–433.
85. MINER JH, SANES JR. Collagen IV alpha 3, alpha 4, and alpha 5 chains in rodent basal laminae: sequence, distribution, association with laminins, and developmental switches. *J Cell Biol* 1994; 127: 879–891.
86. HUDSON BG, REEDERS ST, TRYGGVASON K. Type IV collagen: structure, gene organization, and role in human diseases. *Molecular basis of Goodpasture and*

- Alport syndromes and diffuse leiomyomatosis. *J Biol Chem* 1993; 268: 26033–26036.
87. MINER JH, SANES JR. Molecular and functional defects in kidneys of mice lacking collagen alpha 3(IV): implications for alport syndrome. *J Cell Biol* 1996; 135: 1403–1413.
  88. GOULD DB, PHALAN FC, BREEDVELD GJ et al. Mutations in Col4a1 cause perinatal cerebral hemorrhage and porencephaly. *Science* 2005; 308: 1167–1171.
  89. GOULD DB, PHALAN FC, VAN MIL SE et al. Role of COL4A1 in small-vessel disease and hemorrhagic stroke. *N Engl J Med* 2006; 354: 1489–1496.
  90. EWENS KG, GEORGE RA, SHARMA K, ZIYADEH FN, SPIELMAN RS. Assessment of 115 candidate genes for diabetic nephropathy by transmission/disequilibrium test. *Diabetes* 2005; 54: 3305–3318.
  91. KOJIMA K, KERJASCHKI D. Is podocyte shape controlled by the dystroglycan complex? *Nephrol Dial Transplant* 2002; 17 (Suppl. 9): 23–24.
  92. TSILIBARY EC. Microvascular basement membranes in diabetes mellitus. *J Pathol* 2003; 200: 537–546.
  93. RUOTSALAINEN V, LJUNGBERG P, WARTIOVAARA J et al. Nephlin is specifically located at the slit diaphragm of glomerular podocytes. *Proc Natl Acad Sci U S A* 1999; 96: 7962–7967.
  94. REISER J, KRIZ W, KRETZLER M, MUNDEL P. The glomerular slit diaphragm is a modified adherens junction. *J Am Soc Nephrol* 2000; 11: 1–8.
  95. SALEEM MA, NI L, WITHERDEN I et al. Co-localization of nephlin, podocin, and the actin cytoskeleton: evidence for a role in podocyte foot process formation. *Am J Pathol* 2002; 161: 1459–1466.
  96. JONES N, BLASUTIG IM, EREMINA V et al. Nck adaptor proteins link nephlin to the actin cytoskeleton of kidney podocytes. *Nature* 2006; 440: 818–823.
  97. KOS CH, LE TC, SINHA S et al. Mice deficient in alpha-actinin-4 have severe glomerular disease. *J Clin Invest* 2003; 111: 1683–1690.
  98. ROSELLI S, HEIDET L, SICH M et al. Early glomerular filtration defect and severe renal disease in podocin-deficient mice. *Mol Cell Biol* 2004; 24: 550–560.
  99. SHIH NY, LI J, KARPITSKII V et al. Congenital nephrotic syndrome in mice lacking CD2-associated protein. *Science* 1999; 286: 312–315.
  100. BERG UB, TORBJORNSDOTTER TB, JAREMKO G, THALME B. Kidney morphological changes in relation to long-term renal function and metabolic control in adolescents with IDDM. *Diabetologia* 1998; 41: 1047–1056.
  101. MEYER TW, BENNETT PH, NELSON RG. Podocyte number predicts long-term urinary albumin excretion in Pima Indians with type II diabetes and microalbuminuria. *Diabetologia* 1999; 42: 1341–1344.
  102. STEFFES MW, SCHMIDT D, MCCREARY R, BASGEN JM; International Diabetic Nephropathy Study Group. Glomerular cell number in normal subjects and in type I diabetic patients. *Kidney Int* 2001; 59: 2104–2113.
  103. PAGTALUNAN ME, MILLER PL, JUMPING-EAGLE S et al. Podocyte loss and progressive glomerular injury in type II diabetes. *J Clin Invest* 1997; 99: 342–348.
  104. WHITE KE, BILOUS RW, MARSHALL SM et al. Podocyte number in normotensive type I diabetic patients with albuminuria. *Diabetes* 2002; 51: 3083–3089.
  105. DALLA VESTRA M, MASIERO A, ROITER AM, SALLER A, CREPALDI G, FIORETTO P. Is podocyte injury relevant in diabetic nephropathy? Studies in patients with type 2 diabetes. *Diabetes* 2003; 52: 1031–1035.
  106. PATARI A, FORSBLOM C, HAVANA M, TAIPALE H, GROOP PH, HOLTHOFER H. Nephlinuria in diabetic nephropathy of type 1 diabetes. *Diabetes* 2003; 52: 2969–2974.
  107. DOUBLIER S, SALVIDIO G, LUPA E et al. Nephlin expression is reduced in human diabetic nephropathy: evidence for a distinct role for glycated albumin and angiotensin II. *Diabetes* 2003; 52: 1023–1030.
  108. KOOP K, EIKMANS M, BAELEDE HJ et al. Expression of podocyte-associated molecules in acquired human kidney diseases. *J Am Soc Nephrol* 2003; 14: 2063–2071.
  109. BENIGNI A, GAGLIARDINI E, TOMASONI S et al. Selective impairment of gene expression and assembly of nephlin in human diabetic nephropathy. *Kidney Int* 2004; 65: 2193–2200.
  110. MAUER SM, STEFFES MW, ELLIS EN, SUTHERLAND DE, BROWN DM, GOETZ FC. Structural-functional relationships in diabetic nephropathy. *J Clin Invest* 1984; 74: 1143–1155.
  111. BOHLE A, WEHRMANN M, BOGENSCHUTZ O, BATZ C, MULLER CA, MULLER GA. The pathogenesis of chronic renal failure in diabetic nephropathy. Investigation of 488 cases of diabetic glomerulosclerosis. *Pathol Res Pract* 1991; 187: 251–259.
  112. PHILLIPS AO. The role of renal proximal tubular cells in diabetic nephropathy. *Curr Diab Rep* 2003; 3: 491–496.
  113. PHILLIPS AO, STEADMAN R, MORRISEY K, MARTIN J, EYNSTONE L, WILLIAMS JD. Exposure of human renal proximal tubular cells to glucose leads to accumulation of type IV collagen and fibronectin by decreased degradation. *Kidney Int* 1997; 52: 973–984.
  114. MORRISEY K, STEADMAN R, WILLIAMS JD, PHILLIPS AO. Renal proximal tubular cell fibronectin accumulation in response to glucose is polyol pathway dependent. *Kidney Int* 1999; 55: 160–167.
  115. PHILLIPS AO, MORRISEY K, STEADMAN R, WILLIAMS JD. Decreased degradation of collagen and fibronectin following exposure of proximal cells to glucose. *Exp Nephrol* 1999; 7: 449–462.
  116. JANSSEN U, RILEY SG, VASSILIADOU A, FLOEGE J, PHILLIPS AO. Hypertension superimposed on type II diabetes in Goto Kakizaki rats induces progressive nephropathy. *Kidney Int* 2003; 63: 2162–2170.
  117. ERKAN E, GARCIA CD, PATTERSON LT et al. Induction of renal tubular cell apoptosis in focal segmental glomerulosclerosis: roles of proteinuria and Fas-dependent pathways. *J Am Soc Nephrol* 2005; 16: 398–407.
  118. FUMO P, KUNCIO GS, ZIYADEH FN. PKC and high glucose stimulate collagen alpha 1 (IV) transcriptional activity in a reporter mesangial cell line. *Am J Physiol* 1994; 267: F632–F638.
  119. LIFTON RP, GHARAVI AG, GELLER DS. Molecular mechanisms of human hypertension. *Cell* 2001; 104: 545–556.
  120. RASCH R, NORGAARD JO. Renal enlargement: comparative autoradiographic studies of 3H-thymidine uptake in diabetic and uninephrectomized rats. *Diabetologia* 1983; 25: 280–287.
  121. SEYER-HANSEN K, HANSEN J, GUNDERSEN HJ. Renal hypertrophy in experimental diabetes. A morphometric study. *Diabetologia* 1980; 18: 501–505.
  122. RASCH R, DORUP J. Quantitative morphology of the rat kidney during diabetes mellitus and insulin treatment. *Diabetologia* 1997; 40: 802–809.
  123. VALLON V, BLANTZ RC, THOMSON S. Glomerular hyperfiltration and the salt paradox in early type 1 diabetes mellitus: a tubulo-centric view. *J Am Soc Nephrol* 2003; 14: 530–537.
  124. BROCHNER-MORTENSEN J, STOCKEL M, SORENSEN PJ, NIELSEN AH, DITZEL J. Proximal glomerulo-tubular balance in patients with type 1 (insulin-dependent) diabetes mellitus. *Diabetologia* 1984; 27: 189–192.

125. HANNEDOUCHE TP, DELGADO AG, GNIONSAHE DA, BOITARD C, LACOUR B, GRUNFELD JP. Renal hemodynamics and segmental tubular reabsorption in early type 1 diabetes. *Kidney Int* 1990; 37: 1126–1133.
126. WISEMAN MJ, SAUNDERS AJ, KEEN H, VIBERTI G. Effect of blood glucose control on increased glomerular filtration rate and kidney size in insulin-dependent diabetes. *N Engl J Med* 1985; 312: 617–621.
127. CHRISTENSEN CK, CHRISTIANSEN JS, CHRISTENSEN T, HERMANSEN K, MOGENSEN CE. The effect of six months continuous subcutaneous insulin infusion on kidney function and size in insulin-dependent diabetes. *Diabet Med* 1986; 3: 29–32.
128. TUTTLE KR, BRUTON JL, PERUSEK MC, LANCASTER JL, KOPP DT, DEFONZO RA. Effect of strict glycemic control on renal hemodynamic response to amino acids and renal enlargement in insulin-dependent diabetes mellitus. *N Engl J Med* 1991; 324: 1626–1632.
129. KEVEN K, EKMEKCI Y. Opposing mechanisms in tubuloglomerular feedback. *Am J Kidney Dis* 2004; 44: 574.
130. CARMINES PK, OHISHI K, IKENAGA H. Functional impairment of renal afferent arteriolar voltage-gated calcium channels in rats with diabetes mellitus. *J Clin Invest* 1996; 98: 2564–2571.
131. LEE LK, MEYER TW, POLLOCK AS, LOVETT DH. Endothelial cell injury initiates glomerular sclerosis in the rat remnant kidney. *J Clin Invest* 1995; 96: 953–964.
132. STEFFES MW, BILOUS RW, SUTHERLAND DE, MAUER SM. Cell and matrix components of the glomerular mesangium in type I diabetes. *Diabetes* 1992; 41: 679–684.
133. LANE PH, STEFFES MW, FIORETTO P, MAUER SM. Renal interstitial expansion in insulin-dependent diabetes mellitus. *Kidney Int* 1993; 43: 661–667.
134. ZIYADEH FN, SHARMA K, ERICKSEN M, WOLF G. Stimulation of collagen gene expression and protein synthesis in murine mesangial cells by high glucose is mediated by autocrine activation of transforming growth factor-beta. *J Clin Invest* 1994; 93: 536–542.
135. WANG S, HIRSCHBERG R. BMP7 antagonizes TGF-beta -dependent fibrogenesis in mesangial cells. *Am J Physiol Renal Physiol* 2003; 284: F1006–F1013.
136. BLANKESTIJN PJ, DERKX FH, BIRKENHAGER JC et al. Glomerular hyperfiltration in insulin-dependent diabetes mellitus is correlated with enhanced growth hormone secretion. *J Clin Endocrinol Metab* 1993; 77: 498–502.
137. CUMMINGS EA, SOCHETT EB, DEKKER MG, LAWSON ML, DANEMAN D. Contribution of growth hormone and IGF-I to early diabetic nephropathy in type 1 diabetes. *Diabetes* 1998; 47: 1341–1346.
138. ZOJA C, MORIGI M, REMUZZI G. Proteinuria and phenotypic change of proximal tubular cells. *J Am Soc Nephrol* 2003; 14: S36–S41.
139. RICH SS. Genetics of diabetes and its complications. *J Am Soc Nephrol* 2006; 17: 353–360.
140. MOCZULSKI DK, ROGUS JJ, ANTONELLIS A, WARRAM JH, KROLEWSKI AS. Major susceptibility locus for nephropathy in type 1 diabetes on chromosome 3q: results of novel discordant sib-pair analysis. *Diabetes* 1998; 47: 1164–1169.
141. IMPERATORE G, HANSON RL, PETTITT DJ, KOBES S, BENNETT PH, KNOWLER WC. Sib-pair linkage analysis for susceptibility genes for microvascular complications among Pima Indians with type 2 diabetes. Pima Diabetes Genes Group. *Diabetes* 1998; 47: 821–830.
142. BOWDEN DW, COLICIGNO CJ, LANGEFELD CD et al. A genome scan for diabetic nephropathy in African Americans. *Kidney Int* 2004; 66: 1517–1526.
143. HE W, MIAO FJ, LIN DC et al. Citric acid cycle intermediates as ligands for orphan G-protein-coupled receptors. *Nature* 2004; 429: 188–193.
144. HEBERT SC. Physiology: orphan detectors of metabolism. *Nature* 2004; 429: 143–145.
145. EWENS WJ, SPIELMAN RS. The transmission/disequilibrium test: history, subdivision, and admixture. *Am J Hum Genet* 1995; 57: 455–464.
146. MUELLER PW, ROGUS JJ, CLEARY PA et al. Genetics of Kidneys in Diabetes (GoKinD) Study: a genetics collection available for identifying genetic susceptibility factors for diabetic nephropathy in type 1 diabetes. *J Am Soc Nephrol* 2006; 17: 1782–1790.
147. MOTZO C, CONTU D, CORDELL HJ et al. Heterogeneity in the magnitude of the insulin gene effect on HLA risk in type 1 diabetes. *Diabetes* 2004; 53: 3286–3291.
148. COWLEY AW Jr. The genetic dissection of essential hypertension. *Nat Rev Genet* 2006; 7: 829–840.
149. HAMET P, MERLO E, SEDA O et al. Quantitative founder-effect analysis of French Canadian families identifies specific loci contributing to metabolic phenotypes of hypertension. *Am J Hum Genet* 2005; 76: 815–832.
150. JEUNEMAITRE X, GIMENEZ-ROQUEPLO A-P, DISSE-NIC-ODEME S, CORVOL P. Molecular basis of human hypertension. In: Rimo DL, Connor JM, Pyeritz RE, Korf BR, eds. *Emery and Rimoin's Principles and Practice of Medical Genetics*, 5th edn. Philadelphia, PA: Churchill Livingstone, 2007: 1283–1300.
151. VINCENTI F, GHIGGERI GM. New insights into the pathogenesis and the therapy of recurrent focal glomerulosclerosis. *Am J Transplant* 2005; 5: 1179–1185.
152. JOHNSTONE DB, HOLZMAN LB. Clinical impact of research on the podocyte slit diaphragm. *Nat Clin Pract Nephrol* 2006; 2: 271–282.



## Dendritic cells for immunotherapy of type 1 diabetes

Nick Giannoukakis<sup>1,2</sup>, William A. Rudert<sup>1,3</sup> and Massimo Trucco<sup>1,3</sup> 

<sup>1</sup>Diabetes Institute, Children's Hospital of Pittsburgh, <sup>2</sup>Dept. of Pathology, University of Pittsburgh School of Medicine, <sup>3</sup>Dept. of Pediatrics, Division of Immunogenetics, University of Pittsburgh School of Medicine, Pittsburgh, PA, USA, 15213

Received 25th October 2006, © Cellscience 2007

**Despite its chronic autoimmune progression, type 1 diabetes mellitus (T1DM) offers a number of windows of opportunity through which immunotherapy may be usefully applied to delay and possibly halt the autoimmune processes. Of even more importance is the recent accomplishment of disease reversal, allowing patients to return to reduced exogenous insulin requirements, or to obviate them altogether. As in almost all cell-specific inflammatory processes, dendritic cells are prominent, if not central, regulators of the onset and progression of the inflammation in T1DM. This realization, along with accumulating data confirming a role for dendritic cells (DC) in maintaining and inducing tolerance in multiple therapeutic settings, has prompted a line of investigation seeking to identify the most effective embodiments of dendritic cells for diabetes immunotherapy. Herein, we provide an overview of where DC lie in the immunopathology of autoimmune T1DM, and how DC-based therapy may be usefully translated to treat and reverse the disease.**

### Dendritic cells in diabetes immunopathology: sentinels gone bad

Dendritic cells (DC) are among the body's most remarkable cell types. As sentinels of the immune system par excellence, their function has evolved to maintain host surveillance against microenvironmental anomalies, sensing damaged tissue architecture, foreign pathogen invasion and infection, and most exquisitely, acting as a central orchestrator of mechanisms of self-tolerance (1-5). DC have a capacity to ingest material as small as simple organic chemicals or as large as cells undergoing apoptosis using diverse uptake mechanisms such as pinocytosis, macropinocytosis, mannose receptor-mediated endocytosis and phagocytosis. Once ingested, molecules-especially proteins, are processed in early vesicles which are at the endosomal stage en route to lysosomes and frequently are eventually loaded onto class I or class II Major Histocompatibility Complex (MHC) molecules (6-8) to reach the cell surface. DC are in steady-state flux throughout all body tissues, constantly sampling molecules from the ever changing environment they encounter. Normally, they then transit through the draining lymphoid organs, where it is believed that they maintain potentially autoreactive immune cells in quiescence either directly or via indirect regulatory immune cell networks (3, 5, 9-16) When DC encounter microenvironmental anomalies, viral

infections for example, the local disruption of tissue architecture along with an increase in the output of pro-inflammatory signals by infected cells, will prime the DC to undergo a series of internal changes that are referred to as "maturation". While conceptually thought of as a series of discrete checkpoint-like events, maturation is rapid and often non-linear (13, 17, 18). The morphology of DC transform from a large monocytic, "spiny" cell type into a smaller, more spherical structure with long protruding veils that are densely-endowed with class I and class II MHC and other accessory molecules critical for inducing the activation of naive antigen-specific immune cells. Maturation is coupled to migration towards the proximal draining lymph node with concomitant production of cytokines like TNF $\alpha$  and chemokines. This production helps to establish a gradient that will be sought and followed by other immune cells, especially T-cells once triggered from their quiescent state (1-5). Within the lymph node, the DC will interact with naive T-cells through class I and class II MHC/peptide/T-cell receptor (TCR) contacts, where this interaction is stabilized by coincident contact between accessory co-receptors on DC and T-cells, collectively termed co-stimulatory molecules (19-24). While the identity of the co-stimulatory molecules has been extensively studied (refer to Table I), what is perhaps underappreciated and not yet well understood, is that the critical aspect of the event is not only the signals provided through the co-stimulatory co-receptors, but also a prolongation of the time of the physical interaction of the presented antigen and the T-cell receptors (25-29). In this regard, any mechanism that interrupts costimulation would be predicted to lead to impaired activation of the responding T-cell, possibly leading to functional anergy or apoptosis. This is indeed the outcome of many strategies aimed at costimulation blockade (19-24).

<u>DC molecule</u>	<u>Co-receptor (and cell type)</u>	<u>Functional outcome of modulation</u>
B7-1	CD28 (constitutive)/CTLA4 (induced)	<b>Blockade:</b> long-term allograft survival (204-213)
B7-2	CD28 (constitutive)/CTLA4 (induced)	<b>Blockade:</b> long-term allograft survival (204-213)
B7-h	ICOS (T-cells, -induced)	<b>Blockade:</b> allo- and xenograft survival-in concert with other regimens (214-216)
PD-L1	PD-1 (T-cells, B-cells, APC, NK cells)	<b>Agonist enhancement:</b> allograft survival-in concert with other regimen (2, 217)
PD-L2	PD-1 (T-cells, B-cells, APC, NK cells)	
B7-H3	?	
4-1BBL	4-1BB (T-cells, -induced)	<b>Blockade:</b> allograft survival { Akbari, 2002 #224; Iwasaki, 1999 #223
OX40L	OX40 (T-cells, -induced)	<b>Blockade:</b> allograft survival (168, 218)
CD40	CD40L (T-cells, NK cells, eosinophils)	<b>Blockade:</b> long-term allograft survival in concert with other regimen (85, 124, 125, 219-221)
CD70	CD27 (T-cells, APC)	<b>Blockade:</b> allograft survival (222)
CD30L		
B7-H2	ICOS (T-cells, -induced)	
B7-H4		
B7-H1	PD-1 (T-cells, B-cells, APC, NK cells)	
HVEM/LIGHT	BTLA (T-cells, B-cells)	

**Table 1A.** DC: Immune cell co-receptor pairs and functional outcome of modulation of interaction/signaling

DC however are equally adept at maintaining tolerance to self-antigens. Accumulating evidence



from transplantation models, autoimmune animals, transgenics and *in vitro* experiments is now solidly in support of a state of affairs where, under steady state, DC that are functionally-immature, capture apoptotic debris (which arise out of naturally-occurring cell turnover) in the interstitium or inside tissues proper and, as they migrate into the draining lymph nodes, induce functional silence directly or indirectly to potentially-autoreactive cells (4). This model, however, has been expanded recently to include the possibility that short-lived migratory DC can transfer tissue-restricted molecules to long-lived specialized DC within the peripheral lymph nodes (30-37).

DC:T-cell interactions	Co-activation outcome (signal)
B7-1/B7-2:CD28	positive
B7h:ICOS	positive
OX40L:OX40	positive
CD40:CD40L	positive
CD70:CD27	positive
B7-1/B7-2:CTLA4	negative
B7-H1:PD-1	negative

**Table 1B.** Functional outcomes of interactions between DC:T-cell receptor pairs on T-cells

The distinction between a functional state of immaturity and the tolerogenic state is not yet clear. Some investigators favor a system where tolerogenic DC possess specific properties, either as a consequence of natural development during ontogeny, or acquired during their lifetime in circulation (refer to Table II). Other investigators offer models where DC are metastable and can acquire a broad spectrum of functional capacities ranging from potently immunostimulatory to highly immunosuppressive, depending on their microenvironmental location (and local effects from tissue-derived soluble factors), or their interactions with other physically-proximal cells; immune and/or non-immune (38, 39). While it is not at all clear which of these models is operative in DC-based tolerance to tissue-restricted antigens, what is clear is that DC are prominent in promoting the breakdown in tolerance; the hallmark of autoimmune diseases (13, 40, 41).

**Table 2.** Phenotypes of characterized human DC subsets

**CD11c+ DC (myeloid DC; DC1):**

- CD13+
- CD14+
- CD33+
- CD11b+
- TLR2+
- TLR3+
- GM-CSF-receptor+

- HLA-DR<sup>HIGH</sup>
- produce TNF $\alpha$ , IL-6, IL-12, IFN $\alpha$ , IFN $\beta$  in response to activation
- poorly-developed dendrites (veils)
- can acquire veiled morphology after a period in culture in absence of exogenous cytokines (132)
- induce vigorous proliferation of allogeneic T-cells *in vitro* (132, 223)
- potent antibacterial responses/highly phagocytic
- mainly immunostimulatory when activated
- tolerogenic potential when engineered *in vitro/ex vivo*

### **CD11c- DC (plasmacytoid DC; DC2):**

- CD4+
- CD13<sup>LOW</sup>
- CD14<sup>LOW</sup>
- CD33<sup>LOW</sup>
- CD11b<sup>LOW</sup>
- TLR7+
- TLR9+
- IL-3-receptor+
- HLA-DR+
- produce IFN $\alpha$ , IFN $\beta$  in response to activation
- exhibit plasmacytoid morphology
- well-developed rough ER and Golgi
- require exogenous cytokines for survival *in vitro*
- can develop into myeloid DC types in presence of monocyte conditioned medium or IL-3 (223)
- induce poor proliferation of allogeneic T-cells *in vitro* (132, 223)
- potent antiviral responses
- potentially tolerogenic

One of the most prevalent autoimmune diseases, with considerable morbidity due to its long-term complications, is type 1 diabetes mellitus (T1DM). T1DM in its totality drains considerable healthcare expenditures annually worldwide (42-44). A disorder of glucose homeostasis, T1DM results due to an insufficient amount of insulin, consequent to a chronic inflammation of the islets of Langerhans in the pancreas. The disease is T-cell mediated, targeting the insulin-producing  $\beta$ -cells for eventual destruction, and clinical onset of hyperglycemia can occur before the entire  $\beta$ -cell mass is eradicated (45-55). In fact, the more advanced inflammation consists of macrophages and T-cells that secrete cytokines which are known to suppress glucose sensing and insulin production even though the  $\beta$ -cell mass remains viable (56-62). In the very early stages however, the inflammation consists of an influx of DC into the islets apparently in response to an as yet undefined anomaly.

The nature of the anomaly is not understood. Finegood and colleagues have proposed that a massive wave of  $\beta$ -cell apoptosis occurs very early in the life of rats which is followed by remodeling as the endocrine mass matures towards its eventual adult architecture and composition. A breakdown of proper apoptosis and remodeling may act as a trigger for increased DC influx and maturation of DC as they migrate towards the pancreatic lymph nodes to interact with potentially autoreactive T-cells (63). In rodents, the timing of the wave of apoptosis closely precedes the earliest inflammatory events. In humans however, the initial inflammation is either undetected or frequently occurs much later in childhood. Another model proposes that  $\beta$ -cell antigens are

acquired by DC in response to molecular mimicry, where autoimmunity is induced consequent to infection by a virus or other microbe whose structure, or antigens, cross-react or share epitopes with  $\beta$ -cell-resident molecules (64-66). Finally, a model presented in the early nineties (67) considers the possible implication of so-called 'super'-antigens in the activation of the autoimmune process. Superantigens are TCR ligands from bacterial and viral sources that are able to activate T-cells in a way quite different than conventional antigens. They bind as unmodified, intact proteins to the MHC class II molecules of the antigen presenting cell, outside their peptide binding groove and simultaneously to the V- $\beta$  segments of the TCR, independently of TCR specificity for the MHC molecule-antigenic peptide complex. Their 'none-too-selective' binding properties result in the activation of a very large proportion of the peripheral T-cells (i.e., in a "super" activation). The frequency of T-cells responding to an initial exposure to certain superantigens can be of the order of 30% of the total peripheral T-cell pool. Among the activated cells, some may be autoreactive T-cells that then find their way to the target tissue carrying previously "ignored" antigens: in our case, the pancreatic  $\beta$ -cells (68).

What is clear is that autoimmunity, especially in the genetically non-obese diabetic (NOD) mouse strain, whose immunopathology is widely-held to parallel that believed to occur in humans, starts very early (3-4 weeks of age) with peri-islet inflammation, followed by a slow and progressive impairment and destruction of  $\beta$ -cells by 4-6 months of age. DC and macrophages are the first immune cells detectable at 3-4 weeks of age in the islets of NOD mice (69-71). These cells have been shown to acquire antigen and very likely present it to T-cells in the pancreatic lymph nodes (72-74). Among a number of transgenic mice, two in particular stand out to demonstrate how a microenvironmental anomaly, which is islet-restricted, requires antigen presenting cells, and DC in particular, to provoke and exacerbate islet autoimmunity. The first is an NOD mouse expressing TNF $\alpha$  inside the  $\beta$ -cells under the control of the rat insulin promoter. These mice exhibit accelerated diabetes with strongly-destructive insulitis (75). Local TNF $\alpha$  expression enhanced the accumulation of DC which then presented antigens from apoptotic cells to CD4+ T-cells (75). Indeed, the accumulating DC produced TNF $\alpha$  which exacerbated apoptosis and amplified a vicious cycle (76). To more precisely determine the relevance of DC in the initiation and maintenance of T1DM, an elegant set of studies were undertaken by Zinkernagel and colleagues (77-79) and by Von Herrath and colleagues (80-83). These studies all point to the central role of DC in acquiring tissue-restricted antigens. In an environment of inflammatory and anomalous 'danger' (84-88), these DC undergo maturation, migrate into the pancreatic lymph nodes and activate self-reactive and specifically,  $\beta$ -cell-targeted T-cells.

Beta cell-reactive T-cells are well characterized from a number of animal models however, although their identity in humans remains unclear (68, 89-91). While all the precise mechanisms involved in the selection process are not yet fully clear, one attractive hypothesis posits that mature T-cells are derived from a randomized pool of immature cells which originate in the bone marrow and individually express unique TCRs. Once in the thymus, these immature cells undergo positive and negative selection via fragments of native molecules (self-peptides) lodged in the peptide binding groove of MHC molecules expressed by specialized thymic epithelial cells, which then interact with the TCR. A T-cell which reacts strongly with the MHC molecule loaded with a self-peptide dies and is thus negatively selected. T-cells which respond poorly, do not receive a positive signal and consequently do not proliferate significantly, and are eventually lost or become anergic. The T-cells, whose individualized T-cell receptors fall between the two extremes (i.e., too strong or

too poor affinity for MHC/self-peptide complex) proliferate modestly and survive, that is they are positively selected, and emerge from the thymus to circulate in the periphery. Eventually, some of these T-cells with specific T-cell receptors encounter MHC molecules bearing foreign antigenic peptides – which happen to interact more strongly than in the case of the self-peptides which enabled their positive selection – and a protective immune response driven by the foreign antigen occurs. The thymic cells, quite likely epithelial in nature and perhaps resident in the Hassall's corpuscle, also contribute to negative and positive selection by expressing self antigens (e.g., insulin) under the control of *cis*-acting proximal promoters, whose levels determine self antigen availability for uptake, processing and presentation by thymic resident DC to developing thymocytes (92-97). The greater the levels of self-antigen, the greater the probability that its epitopes will be presented to developing thymocytes, and the greater the potential for negative selection of that thymocyte. Thus, the pool of available T-cells in the periphery is established by the presentation of antigens in the thymus.

In the case of autoimmune diseases that are associated with specific MHC alleles, it is believed that the molecular interactions that drive positive and negative selection are altered by the disease-associated MHC molecules and self-antigen expression, and that consequently dangerous, more strongly reactive T cells are allowed to escape to the periphery. Another not necessarily mutually exclusive consequence is that T-regulatory cells are not as effectively selected, and in their reduced abundance peripheral reactions to self-peptides are not as well maintained in check. Polychronakos and colleagues have shown that mice with variable numbers of terminal repeats (VNTR) mapping upstream of the insulin gene promoter, can yield different quantities of potentially autoreactive T-cells, further supporting the model at a functional immunologic level (92-97). Indeed, the *cis*-acting polymorphism of the insulin gene has been mapped as the *IDDM2* genetic susceptibility locus in humans and is the only such locus other than the MHC in humans, the HLA (*IDDM1*), whose linkage and association to T1DM has been consistent and replicated in different datasets and population studies worldwide (97-102).

Furthermore, the question has arisen about defective DC in T1DM immunopathogenesis. Some studies suggest that DC derived from the only two genetic strains of naturally-occurring diabetes are functionally abnormal, ranging from observations that DC are hyperactivated (103-106) to those showing evidence that DC are hypofunctional (107-109). Diabetes patients, in contrast, do not exhibit any dramatic impairment in responses to infection, recall to vaccination antigens, or in their ability to mount hypersensitivity reactions (110-112), thereby creating deepening the obscurity as to potential defects in DC development and function, even though some recent reports suggest that potential deficiencies may exist in humans (113-115). What is abundantly clear, however, is that DC are potent regulators of the immune system, and can be mobilized to orchestrate anti-tumor activities as well as to induce hyporesponsiveness in order to facilitate allotransplantation or to prevent autoimmunity (116-123).

### **Therapeutic dendritic cells to induce immune hyporesponsiveness: from transplants to autoimmune disease**

Currently, most investigators favor a model where DC arise from two distinct sources, bone marrow progenitors/stem cells and progenitors in circulation (17). According to the current models, there are multiple DC subtypes which differ with respect to surface molecules and functional activities. Broadly divided among Langerhans DC, interstitial DC, monocyte/myeloid-derived DC

and plasmacytoid DC, it is not clear if these subtypes arise through lineage differences or in response to environmental cues (17, 18, 124, 125). Monocyte/myeloid DC in particular develop from CD11c<sup>+</sup> HLA-DR<sup>+</sup> precursors (1). Plasmacytoid DC are believed to differentiate either from a common monocytic precursor or from a committed lymphoid progenitor. Plasmacytoid DC express CD123, CD4 and CD62 ligand (126). In secondary lymphoid organs, and only in mice, other subtypes include CD8a<sup>+</sup> lymphoid DC, CD8a<sup>+</sup> myeloid DC and Langerhans cell-derived DC (127). Moreover, another distinct DC type, resembling human plasmacytoid DC, has been defined in a B220<sup>+</sup> pool (127). Interstitial DC in human circulation are HLA-DR<sup>+</sup> Lin<sup>-</sup> and are quite likely similar to, if not identical to monocyte/myeloid DC (128, 129).

Examining the development of human DC in particular, a number of studies yield the following phenotypes (refer to Table II). We caution that these phenotypes are not necessarily representative of a committed cell subtype, but may in fact represent one unique cell at different developmental stages and exposed to different environments. Indeed, one can consider the observed phenotypes as a snapshot of the cell at a defined moment in its life. The specific functional capacities and phenotypes associated with a later point in its lifetime, go undetected or destroyed by the isolation methods or analytical techniques used. Functionally immature DC derive from hematopoietic stem cells within the bone marrow and their differentiation likely requires Flt3-ligand and GM-CSF exposure (127). Stem cells differentiate into what are termed common myeloid and common lymphoid progenitor cells inside the bone marrow. Common myeloid progenitors can further develop into CD11c<sup>+</sup> CD1a<sup>+</sup> precursor DC (130). CD11c<sup>+</sup> CD1a<sup>+</sup> will eventually move into skin epidermis to become Langerhans cells while CD11c<sup>+</sup> CD1a<sup>-</sup> cells will migrate into most other tissues to become interstitial DC (131). In addition to these two DC subtypes, CD34<sup>+</sup> stem cells can differentiate into two other DC precursors: pre-DC with monocytic morphology (DC1) and plasmacytoid morphology (DC2; 17, 18). There are differences among these DC subtypes. Largely based on the presence/absence of the  $\beta 2$  integrin CD11c, DC have been hypothesized to exist in functionally immature and mature states as described (132) and as illustrated in Table II. Further, CD11c<sup>+</sup> DC are generally referred to as myeloid DC whereas CD11c<sup>-</sup> DC are generally called plasmacytoid DC. CD11c<sup>+</sup> DC in peripheral blood are considered myeloid and so are their monocytic progenitors that differentiate into mature DC *in vitro* under GM-CSF/IL-4 conditions.

The unresolved consensus regarding the association of maturational state, origin, and function with specific cell surface and intracellular markers, taken together with the experimental parameters of time of tissue harvest, method of analysis, age and sex of subject, delineate a large variety of DC subsets (or different manifestations of a few). It is our view that all these subtypes can in fact be variations of a few (and perhaps one) DC, whose phenotype and function varies with physical environment and state of maturation. In fact, we venture to speculate that all these cell subtypes represent a spectrum of the same cell which can range in function from immature tolerogenic to potentially immunostimulatory. We further propose that the state of DC maturation and the environment in which it will interact with a T-cell expressing TCR specific for MHC/ peptide complex present on its surface, will determine the mechanism that will lead to tolerance or activation. In this regard, the DC diversity is the result of a mechanistic response and is not based on the prior existence of discrete and unique DC subtypes.

With the exception of the observations of Morel and colleagues (133), many other lines of investigation support DC in a functionally-immature state (characterized by low to absent co-



stimulation) as agents of immune hyporesponsiveness (3, 8, 16, 116, 119, 121, 122). Exogenous administration of functionally-immature DC (refer to Table III) achieves long term and stable allograft survival in a variety of mouse and rat models and prevents a number of autoimmune diseases (134-141). Mechanistically, functionally-immature DC act by inducing anergy either via direct cell contact and/or cytokines (122, 142, 143) and, as shown more recently, by upregulating the number and function of immune cell subsets, especially the regulatory populations which include Foxp3<sup>+</sup> CD25<sup>+</sup> T-cells and a class of CD8<sup>+</sup> immunosuppressive T-cells (144-152). Table III lists the models where immature DC administration has been successful and will be the focal point from which potential therapies can emerge as discussed in the next section.

While anergy has been a well-studied mechanism during the past two decades and will not be further considered herein (153-160), we would like to focus on potential networks of immune regulatory cells evoked by DC stabilized in a functionally-immature state. In particular, on the Foxp3<sup>+</sup> CD25<sup>+</sup> T-cells whose number is observed to be increased in many recent studies involving the exogenous supply of tolerogenic DC (161-165). Immature or semi-mature DC can induce the differentiation of naturally-occurring (thymic) T-regulatory cells (CD4<sup>+</sup> CD25<sup>+</sup>) as well as IL-10-producing CD4<sup>+</sup> T-cells *in vitro* and *in vivo* (161, 164). Over expression of Jagged-1 in DC results in the augmentation of antigen-specific TGF  $\beta$ -producing CD4<sup>+</sup> CD25<sup>+</sup> T-cells (166). Functionally-immature DC convert naive T-cells into IL-10-secreting cells *in vitro* and antigen-pulsed DC injected subcutaneously into humans augment the number of IL-10-producing CD8<sup>+</sup> T-cells and trigger a reduction in IFN $\gamma$ <sup>+</sup> T-cells (167, 168). Despite the abundance of data in support of immature DC as functional inducers of regulatory immune cells, other investigators have discovered that the state of maturity may not be relevant for the induction of immunosuppressive endogenous T-cells. For example, similar to the studies by Morel and colleagues (133), mature DC were shown to expand CD4<sup>+</sup> CD25<sup>+</sup> T-cells which were functionally-suppressive and capable of preventing diabetes in the NOD mouse (11, 169, 170). Whether this reflects a restimulation of existing CD4<sup>+</sup> CD25<sup>+</sup> T-cells or their expansion is unknown.

**Table 3.** Models of immunotherapeutic DC administration to prolong graft survival and to treat autoimmunity

## **Autoimmune disease**

### Type 1 diabetes:

- pancreatic lymph node DC (untreated) (224)
- Mature bone marrow-derived DC (GM-CSF/IL-4 propagated); or transduced with IL-4 vector (133, 225)
- NF- $\kappa$ B oligonucleotide decoy propagated (172)
- antisense oligonucleotide (CD40, CD80, CD86)-propagated (173)
- Vitamin D receptor ligands (226)
- other DC embodiments (227-230)

### Thyroiditis:

- *in vitro* generation with TNF $\alpha$  and supernatant of a GM-CSF-transduced cell line (231, 232)
- GM-CSF-generated followed by *in vivo* administration of GM-CSF (233)

### Experimental Encephalomyelitis (Multiple Sclerosis model):

- *in vitro* generation with TNF $\alpha$  and supernatant of a GM-CSF-transduced cell line (231, 232)
- VIP and GM-CSF *in vitro* propagation (234, 235)
- TGF $\beta$  and MBP antigen (236)

#### Arthritis:

- VIP and GM-CSF *in vitro* propagation (234, 235)
- IL-4 or IL-10-expressing bone marrow-derived DC and derivative exosome preparations (237-239)
- CD95 (Fas ligand)-expressing bone marrow-derived DC (240, 241)

### **Allotransplantation/Xenotransplantation:**

#### Administration of bone marrow derived DC from transplant organ donor:

- DC propagated in low concentration GM-CSF (242-244)
- DC propagated in GM-CSF, IL-10, TGF $\beta$  and matured with LPS (245)
- *In vitro* blockade of NF- $\kappa$ B by adding aspirin, vitamin D $_3$  metabolites/analogues, glucosamine, N-acetylcysteine, corticosteroids, cyclosporin A, rapamycin, deoxyspergualin, mycophenolate mofetil (246-261)
- gene-engineering *in vitro*; DC expressing IL-10, TGF $\beta$ , CTLA-4Ig, Indolamine-2,3 dioxygenase, Fas-ligand (262-270)

#### Administration of transplant recipient-derived DC prior to transplantation:

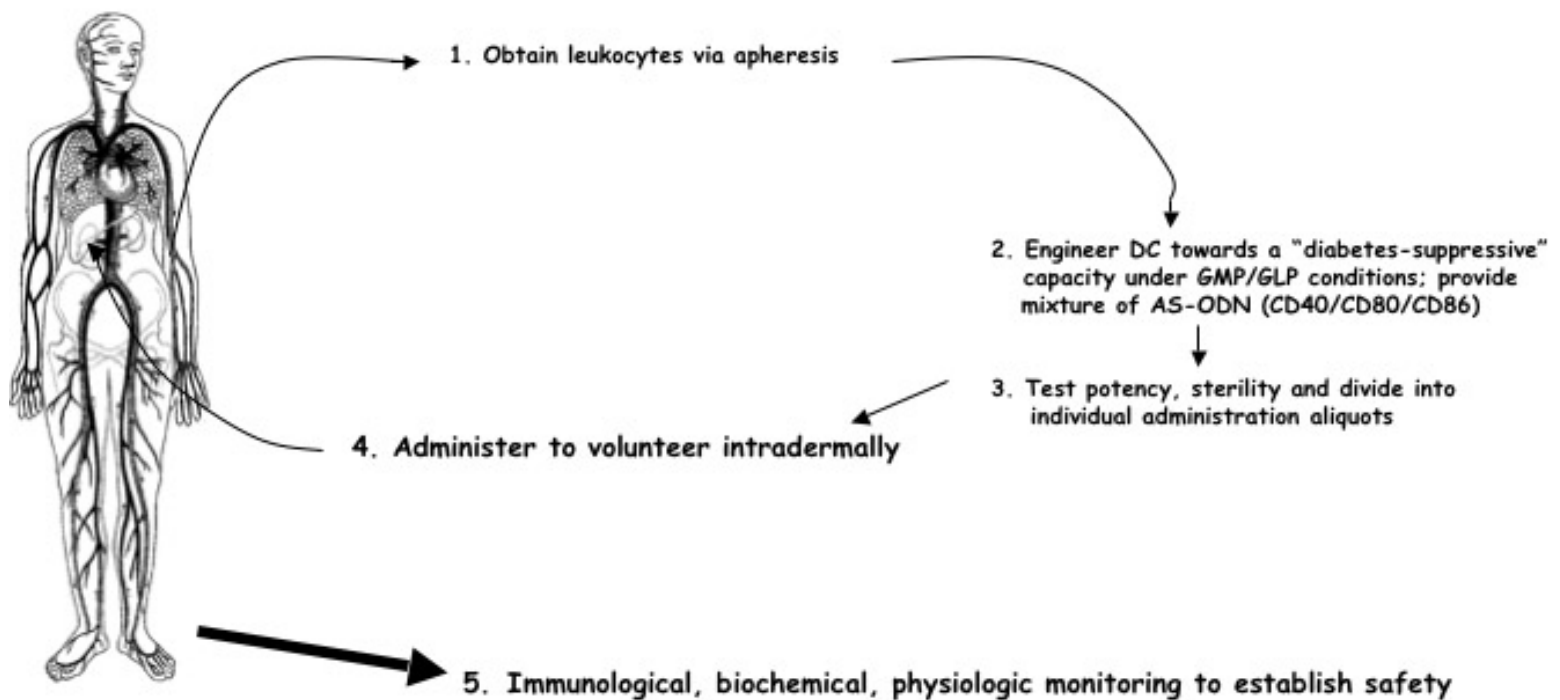
- DC pulsed with class I MHC allopeptide (271)
- rapamycin and donor tissue lysate (272)

CD4 $^{+}$  CD25 $^{+}$  T-regulatory cells expressing the Foxp3 transcription factor (T-reg) are thought to derive from the thymus (natural T-reg) and to differentiate from peripheral CD4 $^{+}$  precursors (peripheral T-reg). Steinman and colleagues have elegantly established that DC are alone capable of augmenting antigen-specific T-reg in diabetic mouse models (11, 170) and that this requires cell contact. Despite their comprehensiveness, these studies did not indicate the precise state of DC maturation and this will be an interesting feature to identify. We have shown that DC maintained in a functionally-immature state following *in vitro* treatment with NF- $\kappa$ B decoys and antisense oligodeoxyribonucleotides (AS-ODN) to the CD40, CD80 and CD86 co-stimulatory molecules are diabetes preventive in the NOD mouse (171-173). This may involve short-range IL-7 signaling, quite likely inside the pancreatic lymph node of NOD mice, and augmentation the number of CD4 $^{+}$  CD25 $^{+}$  T-reg via suppression of apoptosis of a pre-existing pool (171). Multiple injections of AS-ODN-treated DCs in NOD mice maintained the animals as diabetes free without affecting the overall T-cell activity against alloantigens. Furthermore, repeated administrations of co-stimulation deficient DC reverses hyperglycemia in new-onset diabetes NOD mice. The promising results from this study, together with the low risk of the procedure, demonstrated in numerous anti-cancer DC-based treatments, have enabled this NIH-funded protocol to be approved by the Food and Drug Administration (FDA) office as a phase I clinical trial. Adult (18 years or older) volunteers with a documented evidence of insulin-requiring T1DM of at least 5 years duration will be enrolled first, to prove the safety of the procedure. Leukocytes of the patient will be obtained by aphaeresis and DC will be generated *in vitro* and engineered with the addition of AS-ODN. These DCs, which express low levels of CD80, CD86, and CD40 will then be injected into the patient by dermal administration. Attracted to the focus of inflammation, these treated cells will acquire apoptotic cells inside the islets (hence the antigen specificity) and then will migrate into the pancreas-draining

lymph nodes, where they will deliver an anergizing signal to the T-cells they encounter and/or induce regulatory immune cells. The vicious cycle that promotes the T-cell mediated anti-beta-cell-antigen spreading phenomenon will be interrupted this way, enabling the recovery of the physiologic endocrine function of the gland with time. The abrogation of the autoimmune diabetogenic insult should be sufficient to promote rescue or regeneration of the insulin-producing  $\beta$ -cells in the host endocrine pancreas, even after the onset of the disease. Once safety has been demonstrated, a phase II efficacy trial will start, involving new onset diabetic patients (Figure 1).

### *NIH-funded, IRB- and FDA-approved safety study*

**To confirm that intradermal administration of autologous, diabetes-suppressive, dendritic cells (DC) is safe, non-toxic and without side-effects**



**Study begins in January 2007**

**Figure 1. Schema of FDA-approved safety trial administering autologous diabetes-suppressive DC into established type 1 diabetic volunteers (Pittsburgh Study).** The protocol will enroll established type 1 diabetic volunteers between the ages of 18-25 who are otherwise healthy. They must be diabetic >5 years. Autologous DC will be generated *in vitro* from apheresis product. Half of the study group will be administered autologous DC engineered *in vitro* with the mixture of CD40, CD80 and CD86 antisense oligonucleotides and the other half will receive untreated autologous DC. The volunteers will be monitored immunologically, physiologically and biochemically to determine safety of the approach. If the engineered DC are safe, then, the protocol will be submitted for consideration to enroll new-onset diabetics with the objective of determining the effect of the engineered autologous DC on residual functional beta cell mass and markers of autoimmunity.

In Table IV, we list, in a general manner, the current methods by which DC can be maintained in, or induced into, a functionally-tolerogenic state whether this involves their maintenance in stably-

immature state or not. Specific studies are shown in Table III. These lists and methods are growing and based on the differences in methods of choice, the question arises: are all such DC embodiments equivalent and translatable for clinical use?

**Table 4.** Methods to generate/propagate immunotolerogenic DC *in vitro* for *in vivo* administration

- NF $\kappa$ B blockade (peptides blocking signaling, DNA transcriptional decoys)
- targeting co-stimulatory molecule expression specifically (antisense, siRNA, RNAi)
- conferring tolerogenic signals (engineered to produce immunosuppressive cytokines/growth factors/cell surface proteins/soluble costimulation co-receptor decoys)
- Conferring death signals to autoreactive T-cells (apoptosis-inducing cell surface proteins)

### **The growing palette of therapeutic dendritic cells for autoimmune diabetes: are they all equivalent and clinically-translatable?**

It is evident from Tables III and IV that multiple pathways exist to generate tolerogenic DC. Some methods converge upon identical cellular and molecular pathways (augmentation of T-reg numbers, NF- $\kappa$ B inhibition, co-stimulation blockade). Others are not so obvious. First, it is important to understand that transplantation immunobiology may not be identical to autoimmunity and vice versa. Indeed, there are numerous instances where a therapeutic regimen achieving long-term allograft survival has failed to abrogate autoimmunity (174-181). Therefore, DC that are able to suppress donor-specific antigen alloreactivity may not evoke the appropriate regulatory mechanisms capable of controlling and reversing autoimmunity. At the same time, although different DC embodiments may exhibit similar cell surface phenotypes and nuclear proteome signatures, by no means can this be a predictor of mechanism of action. Cell viability has rarely been examined in these embodiments and not all potential mechanisms of action were considered. It is possible that all listed embodiments may intersect at immune regulatory cell levels, but this remains to be determined. Also, the site of action is currently unknown: while it is generally believed that the DC activity will occur inside the pancreatic lymph nodes, there are equally-likely possibilities that the activity of immune tolerance may in fact occur extralymphatically and, in autoimmune diabetes, around the islets. The study by Zinkernagel and colleagues demonstrating a nascent peri-islet lymphoid ultrastructure during diabetes onset is very interesting, instructive and awaits the discovery of a mechanism (79).

Tables III and IV also demonstrate that few studies examined the outcome of diabetes incidence in animals treated with tolerogenic DC pulsed with putative autoantigens. Although the ongoing insulinitis drives migration of exogenously-administered DC into the islets, where they acquire the antigen-specificity to provide  $\beta$ -cell antigens (from apoptotic/necrotic  $\beta$ -cells) to pancreatic lymph node-resident regulatory immune cells like CD25<sup>+</sup> Foxp3<sup>+</sup> T-cells, it is currently unknown if *ex vivo* pulsing with putative autoantigen(s) could stabilize class I MHC to yield more specific T-reg *in vivo*. Our published data, however, indicate that supply of putative autoantigens may not be necessary given the endogenous supply acquired by migratory exogenous DC inside the insulinitic lesion. The critical factor is to maintain the DC in a functionally immature state (136, 138, 171-173).

It is our view that all immunoregulatory DC are not identical for the reasons outlined above. However, we believe that DC, which can reverse new onset disease and which share final common pathways (like low NF- $\kappa$ B activity, low levels of costimulation), can be clinically useful and therefore should be at the forefront of translatability. Clinical translation of diabetes-suppressive DC is an attractive option primarily because DC immunotherapy alone has proven to be a safe protocol in humans (182-203). While institutional review boards (IRBs) should carefully gauge the preclinical animal studies and DC should be generated in facilities with considerable experience with immune cell therapy products (like those involved in generating cancer DC vaccines under GMP/GLP standards), we believe that Table IV provides a tentative list of DC applications to further explore and to translate into safety trials for the eventual remission and perhaps cure of this lifelong disease.

## References

1. Banchereau, J., and R. M. Steinman. 1998. Dendritic cells and the control of immunity. *Nature* 392:245.
2. Lutz, M. B., and G. Schuler. 2002. Immature, semi-mature and fully mature dendritic cells: which signals induce tolerance or immunity? *Trends Immunol* 23:445.
3. Steinman, R. M., D. Hawiger, and M. C. Nussenzweig. 2003. Tolerogenic dendritic cells. *Annu Rev Immunol* 21:685.
4. Steinman, R. M., S. Turley, I. Mellman, and K. Inaba. 2000. The induction of tolerance by dendritic cells that have captured apoptotic cells. *J Exp Med* 191:411.
5. Vlad, G., R. Cortesini, and N. Suciuc-Foca. 2005. License to heal: bidirectional interaction of antigen-specific regulatory T cells and tolerogenic APC. *J Immunol* 174:5907.
6. Mellman, I. 2005. Antigen processing and presentation by dendritic cells: cell biological mechanisms. *Adv Exp Med Biol* 560:63.
7. Mellman, I., and R. M. Steinman. 2001. Dendritic cells: specialized and regulated antigen processing machines. *Cell* 106:255.
8. Steinman, R. M., K. Inaba, S. Turley, P. Pierre, and I. Mellman. 1999. Antigen capture, processing, and presentation by dendritic cells: recent cell biological studies. *Hum Immunol* 60:562.
9. Smits, H. H., E. C. de Jong, E. A. Wierenga, and M. L. Kapsenberg. 2005. Different faces of regulatory DCs in homeostasis and immunity. *Trends Immunol* 26:123.
10. Smits, H. H., A. Engering, D. van der Kleij, E. C. de Jong, K. Schipper, T. M. van Capel, B. A. Zaat, M. Yazdanbakhsh, E. A. Wierenga, Y. van Kooyk, and M. L. Kapsenberg. 2005. Selective probiotic bacteria induce IL-10-producing regulatory T cells in vitro by modulating dendritic cell function through dendritic cell-specific intercellular adhesion molecule 3-grabbing nonintegrin. *J Allergy Clin Immunol* 115:1260.
11. Yamazaki, S., T. Iyoda, K. Tarbell, K. Olson, K. Velinzon, K. Inaba, and R. M. Steinman. 2003. Direct expansion of functional CD25<sup>+</sup> CD4<sup>+</sup> regulatory T cells by antigen-processing dendritic cells. *J Exp Med* 198:235.
12. Inaba, K., J. P. Metlay, M. T. Crowley, and R. M. Steinman. 1990. Dendritic cells pulsed with protein antigens in



vitro can prime antigen-specific, MHC-restricted T cells in situ. *J Exp Med* 172:631.

13. Kubach, J., C. Becker, E. Schmitt, K. Steinbrink, E. Huter, A. Tuettenberg, and H. Jonuleit. 2005. Dendritic cells: sentinels of immunity and tolerance. *Int J Hematol* 81:197.
14. Steinman, R. M. 2003. Some interfaces of dendritic cell biology. *Apmis* 111:675.
15. Steinman, R. M., L. Bonifaz, S. Fujii, K. Liu, D. Bonnyay, S. Yamazaki, M. Pack, D. Hawiger, T. Iyoda, K. Inaba, and M. C. Nussenzweig. 2005. The innate functions of dendritic cells in peripheral lymphoid tissues. *Adv Exp Med Biol* 560:83.
16. Steinman, R. M., and M. C. Nussenzweig. 2002. Avoiding horror autotoxicus: the importance of dendritic cells in peripheral T cell tolerance. *Proc Natl Acad Sci U S A* 99:351.
17. Liu, Y. J. 2001. Dendritic cell subsets and lineages, and their functions in innate and adaptive immunity. *Cell* 106:259.
18. Liu, Y. J., H. Kanzler, V. Soumelis, and M. Gilliet. 2001. Dendritic cell lineage, plasticity and cross-regulation. *Nat Immunol* 2:585.
19. Bluestone, J. A. 1996. Costimulation and its role in organ transplantation. *Clin Transplant* 10:104.
20. Clarkson, M. R., and M. H. Sayegh. 2005. T-cell costimulatory pathways in allograft rejection and tolerance. *Transplantation* 80:555.
21. Kishimoto, K., V. M. Dong, and M. H. Sayegh. 2000. The role of costimulatory molecules as targets for new immunosuppressives in transplantation. *Curr Opin Urol* 10:57.
22. Lenschow, D. J., T. L. Walunas, and J. A. Bluestone. 1996. CD28/B7 system of T cell costimulation. *Annu Rev Immunol* 14:233.
23. Rothstein, D. M., and M. H. Sayegh. 2003. T-cell costimulatory pathways in allograft rejection and tolerance. *Immunol Rev* 196:85.
24. Sayegh, M. H., and L. A. Turka. 1995. T cell costimulatory pathways: promising novel targets for immunosuppression and tolerance induction. *J Am Soc Nephrol* 6:1143.
25. Gakamsky, D. M., I. F. Luescher, and I. Pecht. 2004. T cell receptor-ligand interactions: a conformational preequilibrium or an induced fit. *Proc Natl Acad Sci U S A* 101:9063.
26. Germain, R. N., and I. Stefanova. 1999. The dynamics of T cell receptor signaling: complex orchestration and the key roles of tempo and cooperation. *Annu Rev Immunol* 17:467.
27. Gonzalez, P. A., L. J. Carreno, D. Coombs, J. E. Mora, E. Palmieri, B. Goldstein, S. G. Nathenson, and A. M. Kalergis. 2005. T cell receptor binding kinetics required for T cell activation depend on the density of cognate ligand on the antigen-presenting cell. *Proc Natl Acad Sci U S A* 102:4824.
28. Kalergis, A. M. 2003. Modulation of T cell immunity by TCR/pMHC dwell time and activating/inhibitory receptor pairs on the antigen-presenting cell. *Curr Pharm Des* 9:233.
29. Khilko, S. N., M. T. Jelonek, M. Corr, L. F. Boyd, A. L. Bothwell, and D. H. Margulies. 1995. Measuring interactions of MHC class I molecules using surface plasmon resonance. *J Immunol Methods* 183:77.

30. Belz, G. T., F. R. Carbone, and W. R. Heath. 2002. Cross-presentation of antigens by dendritic cells. *Crit Rev Immunol* 22:439.
31. Carbone, F. R., G. T. Belz, and W. R. Heath. 2004. Transfer of antigen between migrating and lymph node-resident DCs in peripheral T-cell tolerance and immunity. *Trends Immunol* 25:655.
32. Carbone, F. R., C. Kurts, S. R. Bennett, J. F. Miller, and W. R. Heath. 1998. Cross-presentation: a general mechanism for CTL immunity and tolerance. *Immunol Today* 19:368.
33. Heath, W. R., G. T. Belz, G. M. Behrens, C. M. Smith, S. P. Forehan, I. A. Parish, G. M. Davey, N. S. Wilson, F. R. Carbone, and J. A. Villadangos. 2004. Cross-presentation, dendritic cell subsets, and the generation of immunity to cellular antigens. *Immunol Rev* 199:9.
34. Heath, W. R., and F. R. Carbone. 2001. Cross-presentation in viral immunity and self-tolerance. *Nat Rev Immunol* 1:126.
35. Heath, W. R., and F. R. Carbone. 2001. Cross-presentation, dendritic cells, tolerance and immunity. *Annu Rev Immunol* 19:47.
36. Heath, W. R., C. Kurts, J. F. Miller, and F. R. Carbone. 1998. Cross-tolerance: a pathway for inducing tolerance to peripheral tissue antigens. *J Exp Med* 187:1549.
37. Miller, J. F., C. Kurts, J. Allison, H. Kosaka, F. Carbone, and W. R. Heath. 1998. Induction of peripheral CD8+ T-cell tolerance by cross-presentation of self antigens. *Immunol Rev* 165:267.
38. Manz, M. G., D. Traver, K. Akashi, M. Merad, T. Miyamoto, E. G. Engleman, and I. L. Weissman. 2001. Dendritic cell development from common myeloid progenitors. *Ann N Y Acad Sci* 938:167.
39. Manz, M. G., D. Traver, T. Miyamoto, I. L. Weissman, and K. Akashi. 2001. Dendritic cell potentials of early lymphoid and myeloid progenitors. *Blood* 97:3333.
40. Manfredi, A. A., M. G. Sabbadini, and P. Rovere-Querini. 2005. Dendritic cells and the shadow line between autoimmunity and disease. *Arthritis Rheum* 52:11.
41. Suciu-Foca, N., J. S. Manavalan, L. Scotto, S. Kim-Schulze, S. Galluzzo, A. J. Naiyer, J. Fan, G. Vlad, and R. Cortesini. 2005. Molecular characterization of allospecific T suppressor and tolerogenic dendritic cells: review. *Int Immunopharmacol* 5:7.
42. Fenter, T. C., M. J. Naslund, M. B. Shah, M. T. Eaddy, and L. Black. 2006. The cost of treating the 10 most prevalent diseases in men 50 years of age or older. *Am J Manag Care* 12:S90.
43. Lindholm, L. H., B. Kartman, B. Carlberg, M. Persson, A. Svensson, and O. Samuelsson. 2006. Cost implications of development of diabetes in the ALPINE study. *J Hypertens Suppl* 24:S65.
44. Morsanutto, A., P. Berto, S. Lopatriello, R. Gelisio, D. Voinovich, P. P. Cippo, and L. G. Mantovani. 2006. Major complications have an impact on total annual medical cost of diabetes: results of a database analysis. *J Diabetes Complications* 20:163.
45. Komulainen, J., M. Knip, R. Lounamaa, P. Vahasalo, J. Karjalainen, E. Sabbah, and H. K. Akerblom. 1997. Poor beta-cell function after the clinical manifestation of type 1 diabetes in children initially positive for islet cell specific autoantibodies. The Childhood Diabetes in Finland Study Group. *Diabet Med* 14:532.

46. Lampeter, E. F., A. Klinghammer, W. A. Scherbaum, E. Heinze, B. Haastert, G. Giani, and H. Kolb. 1998. The Deutsche Nicotinamide Intervention Study: an attempt to prevent type 1 diabetes. DENIS Group. *Diabetes* 47:980.
47. Larsen, M. O., B. Rolin, C. F. Gotfredsen, R. D. Carr, and J. J. Holst. 2004. Reduction of beta cell mass: partial insulin secretory compensation from the residual beta cell population in the nicotinamide-streptozotocin Gottingen minipig after oral glucose in vivo and in the perfused pancreas. *Diabetologia* 47:1873.
48. Lohmann, T., K. Kellner, H. J. Verlohren, J. Krug, J. Steindorf, W. A. Scherbaum, and J. Seissler. 2001. Titre and combination of ICA and autoantibodies to glutamic acid decarboxylase discriminate two clinically distinct types of latent autoimmune diabetes in adults (LADA). *Diabetologia* 44:1005.
49. Mayer, A., F. Rharbaoui, C. Thivolet, J. Orgiazzi, and A. M. Madec. 1999. The relationship between peripheral T cell reactivity to insulin, clinical remissions and cytokine production in type 1 (insulin-dependent) diabetes mellitus. *J Clin Endocrinol Metab* 84:2419.
50. Papoz, L., F. Lenegre, J. Hors, R. Assan, P. Vague, G. Tchobroutsky, P. Passa, B. Charbonnel, J. Mirouze, G. Feutren, and et al. 1990. Probability of remission in individual in early adult insulin dependent diabetic patients. Results from the Cyclosporine Diabetes French Study Group. *Diabete Metab* 16:303.
51. Petrone, A., A. Galgani, M. Spoletini, I. Alemanno, S. Di Cola, G. Bassotti, A. Picardi, S. Manfrini, J. Osborn, P. Pozzilli, and R. Buzzetti. 2005. Residual insulin secretion at diagnosis of type 1 diabetes is independently associated with both, age of onset and HLA genotype. *Diabetes Metab Res Rev* 21:271.
52. Rasmussen, S. B., T. S. Sorensen, J. B. Hansen, T. Mandrup-Poulsen, L. Hornum, and H. Markholst. 2000. Functional rest through intensive treatment with insulin and potassium channel openers preserves residual beta-cell function and mass in acutely diabetic BB rats. *Horm Metab Res* 32:294.
53. Shimada, A., Y. Imazu, S. Morinaga, O. Funae, A. Kasuga, Y. Atsumi, and K. Matsuoka. 1999. T-cell insulinitis found in anti-GAD65+ diabetes with residual beta-cell function. A case report. *Diabetes Care* 22:615.
54. Sreenan, S., A. J. Pick, M. Levisetti, A. C. Baldwin, W. Pugh, and K. S. Polonsky. 1999. Increased beta-cell proliferation and reduced mass before diabetes onset in the nonobese diabetic mouse. *Diabetes* 48:989.
55. Weets, I., I. Truyen, I. Verschraegen, B. Van der Auwera, J. De Schepper, H. Dorchy, M. C. Lebrethon, L. Van Gaal, P. Van Rooy, D. G. Pipeleers, and F. K. Gorus. 2006. Sex- and season-dependent differences in C-peptide levels at diagnosis of immune-mediated type 1 diabetes. *Diabetologia* 49:1158.
56. Arnush, M., A. L. Scarim, M. R. Heitmeier, C. B. Kelly, and J. A. Corbett. 1998. Potential role of resident islet macrophage activation in the initiation of autoimmune diabetes. *J Immunol* 160:2684.
57. Corbett, J. A., and M. L. McDaniel. 1994. Reversibility of interleukin-1 beta-induced islet destruction and dysfunction by the inhibition of nitric oxide synthase. *Biochem J* 299 (Pt 3):719.
58. Corbett, J. A., J. L. Wang, J. H. Hughes, B. A. Wolf, M. A. Sweetland, J. R. Lancaster, Jr., and M. L. McDaniel. 1992. Nitric oxide and cyclic GMP formation induced by interleukin 1 beta in islets of Langerhans. Evidence for an effector role of nitric oxide in islet dysfunction. *Biochem J* 287 (Pt 1):229.
59. Corbett, J. A., J. L. Wang, T. P. Misko, W. Zhao, W. F. Hickey, and M. L. McDaniel. 1993. Nitric oxide mediates IL-1 beta-induced islet dysfunction and destruction: prevention by dexamethasone. *Autoimmunity* 15:145.
60. Ma, Z., S. Ramanadham, J. A. Corbett, A. Bohrer, R. W. Gross, M. L. McDaniel, and J. Turk. 1996. Interleukin-1 enhances pancreatic islet arachidonic acid 12-lipoxygenase product generation by increasing substrate availability

through a nitric oxide-dependent mechanism. *J Biol Chem* 271:1029.

61. McDaniel, M. L., G. Kwon, J. R. Hill, C. A. Marshall, and J. A. Corbett. 1996. Cytokines and nitric oxide in islet inflammation and diabetes. *Proc Soc Exp Biol Med* 211:24.

62. Scarim, A. L., M. R. Heitmeier, and J. A. Corbett. 1997. Irreversible inhibition of metabolic function and islet destruction after a 36-hour exposure to interleukin-1beta. *Endocrinology* 138:5301.

63. Trudeau, J. D., J. P. Dutz, E. Arany, D. J. Hill, W. E. Fieldus, and D. T. Finegood. 2000. Neonatal beta-cell apoptosis: a trigger for autoimmune diabetes? *Diabetes* 49:1.

64. Oldstone, M. B. 1987. Molecular mimicry and autoimmune disease. *Cell* 50:819.

65. Oldstone, M. B. 1989. Virus-induced autoimmunity: molecular mimicry as a route to autoimmune disease. *J Autoimmun* 2 Suppl:187.

66. Oldstone, M. B. 1989. Molecular mimicry as a mechanism for the cause and a probe uncovering etiologic agent(s) of autoimmune disease. *Curr Top Microbiol Immunol* 145:127.

67. Conrad, B., E. Weidmann, G. Trucco, W. A. Rudert, R. Behboo, C. Ricordi, H. Rodriguez-Rilo, D. Finegold, and M. Trucco. 1994. Evidence for superantigen involvement in insulin-dependent diabetes mellitus aetiology. *Nature* 371:351.

68. Conrad, B., and M. Trucco. 1994. Superantigens as etiopathogenetic factors in the development of insulin-dependent diabetes mellitus. *Diabetes Metab Rev* 10:309.

69. Jansen, A., F. Homo-Delarche, H. Hooijkaas, P. J. Leenen, M. Dardenne, and H. A. Drexhage. 1994. Immunohistochemical characterization of monocytes-macrophages and dendritic cells involved in the initiation of the insulinitis and beta-cell destruction in NOD mice. *Diabetes* 43:667.

70. Jansen, A., J. G. Rosmalen, F. Homo-Delarche, M. Dardenne, and H. A. Drexhage. 1996. Effect of prophylactic insulin treatment on the number of ER-MP23+ macrophages in the pancreas of NOD mice. Is the prevention of diabetes based on beta-cell rest? *J Autoimmun* 9:341.

71. Lo, D., C. R. Reilly, B. Scott, R. Liblau, H. O. McDevitt, and L. C. Burkly. 1993. Antigen-presenting cells in adoptively transferred and spontaneous autoimmune diabetes. *Eur J Immunol* 23:1693.

72. Clare-Salzler, M., and Y. Mullen. 1992. Marked dendritic cell-T cell cluster formation in the pancreatic lymph node of the non-obese diabetic mouse. *Immunology* 76:478.

73. Hoglund, P., J. Mintern, C. Waltzinger, W. Heath, C. Benoist, and D. Mathis. 1999. Initiation of autoimmune diabetes by developmentally regulated presentation of islet cell antigens in the pancreatic lymph nodes. *J Exp Med* 189:331.

74. Shimizu, J., E. Carrasco-Marin, O. Kanagawa, and E. R. Unanue. 1995. Relationship between beta cell injury and antigen presentation in NOD mice. *J Immunol* 155:4095.

75. Green, E. A., E. E. Eynon, and R. A. Flavell. 1998. Local expression of TNFalpha in neonatal NOD mice promotes diabetes by enhancing presentation of islet antigens. *Immunity* 9:733.

76. Dahlen, E., K. Dawe, L. Ohlsson, and G. Hedlund. 1998. Dendritic cells and macrophages are the first and major producers of TNF-alpha in pancreatic islets in the nonobese diabetic mouse. *J Immunol* 160:3585.

77. Ehl, S., J. Hombach, P. Aichele, T. Rulicke, B. Odermatt, H. Hengartner, R. Zinkernagel, and H. Pircher. 1998. Viral and bacterial infections interfere with peripheral tolerance induction and activate CD8<sup>+</sup> T cells to cause immunopathology. *J Exp Med* 187:763.
78. Ludewig, B., S. Ehl, U. Karrer, B. Odermatt, H. Hengartner, and R. M. Zinkernagel. 1998. Dendritic cells efficiently induce protective antiviral immunity. *J Virol* 72:3812.
79. Ludewig, B., B. Odermatt, S. Landmann, H. Hengartner, and R. M. Zinkernagel. 1998. Dendritic cells induce autoimmune diabetes and maintain disease via de novo formation of local lymphoid tissue. *J Exp Med* 188:1493.
80. Christen, U., and M. G. von Herrath. 2002. Transgenic animal models for type 1 diabetes: linking a tetracycline-inducible promoter with a virus-inducible mouse model. *Transgenic Res* 11:587.
81. Christen, U., and M. G. von Herrath. 2004. Manipulating the type 1 vs type 2 balance in type 1 diabetes. *Immunol Res* 30:309.
82. Christen, U., and M. G. von Herrath. 2004. Induction, acceleration or prevention of autoimmunity by molecular mimicry. *Mol Immunol* 40:1113.
83. von Herrath, M. G. 2002. Regulation of virally induced autoimmunity and immunopathology: contribution of LCMV transgenic models to understanding autoimmune insulin-dependent diabetes mellitus. *Curr Top Microbiol Immunol* 263:145.
84. Gallucci, S., and P. Matzinger. 2001. Danger signals: SOS to the immune system. *Curr Opin Immunol* 13:114.
85. Matzinger, P. 1994. Tolerance, danger, and the extended family. *Annu Rev Immunol* 12:991.
86. Matzinger, P. 1998. An innate sense of danger. *Semin Immunol* 10:399.
87. Matzinger, P. 2001. Essay 1: the Danger model in its historical context. *Scand J Immunol* 54:4.
88. Matzinger, P. 2002. An innate sense of danger. *Ann N Y Acad Sci* 961:341.
89. Arif, S., T. I. Tree, T. P. Astill, J. M. Tremble, A. J. Bishop, C. M. Dayan, B. O. Roep, and M. Peakman. 2004. Autoreactive T cell responses show proinflammatory polarization in diabetes but a regulatory phenotype in health. *J Clin Invest* 113:451.
90. Roep, B. O. 2002. Autoreactive T cells in endocrine/organ-specific autoimmunity: why has progress been so slow? *Springer Semin Immunopathol* 24:261.
91. Tree, T. I., G. Duinkerken, S. Willemen, R. R. de Vries, and B. O. Roep. 2004. HLA-DQ-regulated T-cell responses to islet cell autoantigens insulin and GAD65. *Diabetes* 53:1692.
92. Bennett, S. T., A. J. Wilson, L. Esposito, N. Bouzekri, D. E. Undlien, F. Cucca, L. Nistico, R. Buzzetti, E. Bosi, F. Pociot, J. Nerup, A. Cambon-Thomsen, A. Pugliese, J. P. Shield, P. A. McKinney, S. C. Bain, C. Polychronakos, and J. A. Todd. 1997. Insulin VNTR allele-specific effect in type 1 diabetes depends on identity of untransmitted paternal allele. The IMDIAB Group. *Nat Genet* 17:350.
93. Chentoufi, A. A., M. Palumbo, and C. Polychronakos. 2004. Proinsulin expression by Hassall's corpuscles in the mouse thymus. *Diabetes* 53:354.



94. Chentoufi, A. A., and C. Polychronakos. 2002. Insulin expression levels in the thymus modulate insulin-specific autoreactive T-cell tolerance: the mechanism by which the IDDM2 locus may predispose to diabetes. *Diabetes* 51:1383.
95. Durinovic-Bello, I., E. Jelinek, M. Schlosser, T. Eiermann, B. O. Boehm, W. Karges, L. Marchand, and C. Polychronakos. 2005. Class III alleles at the insulin VNTR polymorphism are associated with regulatory T-cell responses to proinsulin epitopes in HLA-DR4, DQ8 individuals. *Diabetes* 54 Suppl 2:S18.
96. Palumbo, M. O., D. Levi, A. A. Chentoufi, and C. Polychronakos. 2006. Isolation and characterization of proinsulin-producing medullary thymic epithelial cell clones. *Diabetes* 55:2595.
97. Vafiadis, P., S. T. Bennett, J. A. Todd, J. Nadeau, R. Grabs, C. G. Goodyer, S. Wickramasinghe, E. Colle, and C. Polychronakos. 1997. Insulin expression in human thymus is modulated by INS VNTR alleles at the IDDM2 locus. *Nat Genet* 15:289.
98. Barratt, B. J., F. Payne, C. E. Lowe, R. Hermann, B. C. Healy, D. Harold, P. Concannon, N. Gharani, M. I. McCarthy, M. G. Olavesen, R. McCormack, C. Guja, C. Ionescu-Tirgoviste, D. E. Undlien, K. S. Ronningen, K. M. Gillespie, E. Tuomilehto-Wolf, J. Tuomilehto, S. T. Bennett, D. G. Clayton, H. J. Cordell, and J. A. Todd. 2004. Remapping the insulin gene/IDDM2 locus in type 1 diabetes. *Diabetes* 53:1884.
99. Bennett, S. T., A. J. Wilson, F. Cucca, J. Nerup, F. Pociot, P. A. McKinney, A. H. Barnett, S. C. Bain, and J. A. Todd. 1996. IDDM2-VNTR-encoded susceptibility to type 1 diabetes: dominant protection and parental transmission of alleles of the insulin gene-linked minisatellite locus. *J Autoimmun* 9:415.
100. Onengut-Gumuscu, S., and P. Concannon. 2002. Mapping genes for autoimmunity in humans: type 1 diabetes as a model. *Immunol Rev* 190:182.
101. Onengut-Gumuscu, S., and P. Concannon. 2005. The genetics of type 1 diabetes: lessons learned and future challenges. *J Autoimmun* 25 Suppl:34.
102. Walter, M., E. Albert, M. Conrad, E. Keller, M. Hummel, K. Ferber, B. J. Barratt, J. A. Todd, A. G. Ziegler, and E. Bonifacio. 2003. IDDM2/insulin VNTR modifies risk conferred by IDDM1/HLA for development of Type 1 diabetes and associated autoimmunity. *Diabetologia* 46:712.
103. Marleau, A. M., and B. Singh. 2002. Myeloid dendritic cells in non-obese diabetic mice have elevated costimulatory and T helper-1-inducing abilities. *J Autoimmun* 19:23.
104. Sen, P., S. Bhattacharyya, M. Wallet, C. P. Wong, B. Poligone, M. Sen, A. S. Baldwin, Jr., and R. Tisch. 2003. NF-kappa B hyperactivation has differential effects on the APC function of nonobese diabetic mouse macrophages. *J Immunol* 170:1770.
105. Weaver, D. J., Jr., B. Poligone, T. Bui, U. M. Abdel-Motal, A. S. Baldwin, Jr., and R. Tisch. 2001. Dendritic cells from nonobese diabetic mice exhibit a defect in NF-kappa B regulation due to a hyperactive I kappa B kinase. *J Immunol* 167:1461.
106. Wheat, W., R. Kupfer, D. G. Gutches, G. R. Rayat, J. Beilke, R. I. Scheinman, and D. R. Wegmann. 2004. Increased NF-kappa B activity in B cells and bone marrow-derived dendritic cells from NOD mice. *Eur J Immunol* 34:1395.
107. Boudaly, S., J. Morin, R. Berthier, P. Marche, and C. Boitard. 2002. Altered dendritic cells (DC) might be responsible for regulatory T cell imbalance and autoimmunity in nonobese diabetic (NOD) mice. *Eur Cytokine Netw* 13:29.
108. Nikolic, T., M. Bunk, H. A. Drexhage, and P. J. Leenen. 2004. Bone marrow precursors of nonobese diabetic mice

develop into defective macrophage-like dendritic cells in vitro. *J Immunol* 173:4342.

109. Strid, J., L. Lopes, J. Marcinkiewicz, L. Petrovska, B. Nowak, B. M. Chain, and T. Lund. 2001. A defect in bone marrow derived dendritic cell maturation in the nonobese diabetic mouse. *Clin Exp Immunol* 123:375.

110. Eibl, N., M. Spatz, G. F. Fischer, W. R. Mayr, A. Samstag, H. M. Wolf, G. Schernthaner, and M. M. Eibl. 2002. Impaired primary immune response in type-1 diabetes: results from a controlled vaccination study. *Clin Immunol* 103:249.

111. McMahon, M. M., and B. R. Bistrian. 1995. Host defenses and susceptibility to infection in patients with diabetes mellitus. *Infect Dis Clin North Am* 9:1.

112. Wheat, L. J. 1980. Infection and diabetes mellitus. *Diabetes Care* 3:187.

113. Peng, R., Y. Li, K. Brezner, S. Litherland, and M. J. Clare-Salzler. 2003. Abnormal peripheral blood dendritic cell populations in type 1 diabetes. *Ann N Y Acad Sci* 1005:222.

114. Summers, K. L., M. T. Behme, J. L. Mahon, and B. Singh. 2003. Characterization of dendritic cells in humans with type 1 diabetes. *Ann N Y Acad Sci* 1005:226.

115. Summers, K. L., A. M. Marleau, J. L. Mahon, R. McManus, I. Hramiak, and B. Singh. 2006. Reduced IFN- $\alpha$  secretion by blood dendritic cells in human diabetes. *Clin Immunol* 121:81.

116. Coates, P. T., and A. W. Thomson. 2002. Dendritic cells, tolerance induction and transplant outcome. *Am J Transplant* 2:299.

117. Davis, I. D., M. Jefford, P. Parente, and J. Cebon. 2003. Rational approaches to human cancer immunotherapy. *J Leukoc Biol* 73:3.

118. Di Nicola, M., A. Anichini, R. Mortarini, M. Bregni, G. Parmiani, and A. M. Gianni. 1998. Human dendritic cells: natural adjuvants in antitumor immunotherapy. *Cytokines Cell Mol Ther* 4:265.

119. Hackstein, H., A. E. Morelli, and A. W. Thomson. 2001. Designer dendritic cells for tolerance induction: guided not misguided missiles. *Trends Immunol* 22:437.

120. Hardin, J. A. 2005. Dendritic cells: potential triggers of autoimmunity and targets for therapy. *Ann Rheum Dis* 64 Suppl 4:iv86.

121. Morelli, A. E., and A. W. Thomson. 2003. Dendritic cells: regulators of alloimmunity and opportunities for tolerance induction. *Immunol Rev* 196:125.

122. Nouri-Shirazi, M., and A. W. Thomson. 2006. Dendritic cells as promoters of transplant tolerance. *Expert Opin Biol Ther* 6:325.

123. Paul, S., B. Calmels, and R. B. Acres. 2002. Improvement of adoptive cellular immunotherapy of human cancer using ex-vivo gene transfer. *Curr Gene Ther* 2:91.

124. Ardavin, C. 2003. Origin, precursors and differentiation of mouse dendritic cells. *Nat Rev Immunol* 3:582.

125. Shortman, K., and Y. J. Liu. 2002. Mouse and human dendritic cell subtypes. *Nat Rev Immunol* 2:151.

126. Colonna, M., G. Trinchieri, and Y. J. Liu. 2004. Plasmacytoid dendritic cells in immunity. *Nat Immunol* 5:1219.

127. Pulendran, B., J. Banchereau, E. Maraskovsky, and C. Maliszewski. 2001. Modulating the immune response with dendritic cells and their growth factors. *Trends Immunol* 22:41.
128. Willmann, K. 2003. Flow-cytometric immune function methodology for human peripheral blood dendritic cells. *Methods Mol Biol* 215:41.
129. Willmann, K., and J. F. Dunne. 2000. A flow cytometric immune function assay for human peripheral blood dendritic cells. *J Leukoc Biol* 67:536.
130. Strunk, D., C. Egger, G. Leitner, D. Hanau, and G. Stingl. 1997. A skin homing molecule defines the langerhans cell progenitor in human peripheral blood. *J Exp Med* 185:1131.
131. Ito, T., M. Inaba, K. Inaba, J. Toki, S. Sogo, T. Iguchi, Y. Adachi, K. Yamaguchi, R. Amakawa, J. Valladeau, S. Saeland, S. Fukuhara, and S. Ikehara. 1999. A CD1a<sup>+</sup>/CD11c<sup>+</sup> subset of human blood dendritic cells is a direct precursor of Langerhans cells. *J Immunol* 163:1409.
132. O'Doherty, U., M. Peng, S. Gezelter, W. J. Swiggard, M. Betjes, N. Bhardwaj, and R. M. Steinman. 1994. Human blood contains two subsets of dendritic cells, one immunologically mature and the other immature. *Immunology* 82:487.
133. Feili-Hariri, M., X. Dong, S. M. Alber, S. C. Watkins, R. D. Salter, and P. A. Morel. 1999. Immunotherapy of NOD mice with bone marrow-derived dendritic cells. *Diabetes* 48:2300.
134. Bottino, R., P. Lemarchand, M. Trucco, and N. Giannoukakis. 2003. Gene- and cell-based therapeutics for type I diabetes mellitus. *Gene Ther* 10:875.
135. Chen, D., R. Sung, and J. S. Bromberg. 2002. Gene therapy in transplantation. *Transpl Immunol* 9:301.
136. Giannoukakis, N., W. A. Rudert, P. D. Robbins, and M. Trucco. 1999. Targeting autoimmune diabetes with gene therapy. *Diabetes* 48:2107.
137. Giannoukakis, N., A. Thomson, and P. Robbins. 1999. Gene therapy in transplantation. *Gene Ther* 6:1499.
138. Giannoukakis, N., and M. Trucco. 2005. Gene therapy for type 1 diabetes. *Am J Ther* 12:512.
139. Tarner, I. H., and C. G. Fathman. 2002. The potential for gene therapy in the treatment of autoimmune disease. *Clin Immunol* 104:204.
140. Tarner, I. H., A. J. Slavin, J. McBride, A. Levicnik, R. Smith, G. P. Nolan, C. H. Contag, and C. G. Fathman. 2003. Treatment of autoimmune disease by adoptive cellular gene therapy. *Ann N Y Acad Sci* 998:512.
141. Trucco, M., P. D. Robbins, A. W. Thomson, and N. Giannoukakis. 2002. Gene therapy strategies to prevent autoimmune disorders. *Curr Gene Ther* 2:341.
142. Chen, W. 2006. Dendritic cells and (CD4<sup>+</sup>)CD25<sup>+</sup> T regulatory cells: crosstalk between two professionals in immunity versus tolerance. *Front Biosci* 11:1360.
143. Hugues, S., A. Boissonnas, S. Amigorena, and L. Fetler. 2006. The dynamics of dendritic cell-T cell interactions in priming and tolerance. *Curr Opin Immunol* 18:491.

144. Beissert, S., A. Schwarz, and T. Schwarz. 2006. Regulatory T cells. *J Invest Dermatol* 126:15.
145. Enk, A. H. 2006. DCs and cytokines cooperate for the induction of tregs. *Ernst Schering Res Found Workshop*:97.
146. Huber, S., and C. Schramm. 2006. TGF-beta and CD4+CD25+ regulatory T cells. *Front Biosci* 11:1014.
147. Lohr, J., B. Knoechel, and A. K. Abbas. 2006. Regulatory T cells in the periphery. *Immunol Rev* 212:149.
148. Roncarolo, M. G., S. Gregori, M. Battaglia, R. Bacchetta, K. Fleischhauer, and M. K. Levings. 2006. Interleukin-10-secreting type 1 regulatory T cells in rodents and humans. *Immunol Rev* 212:28.
149. Shevach, E. M., R. A. DiPaolo, J. Andersson, D. M. Zhao, G. L. Stephens, and A. M. Thornton. 2006. The lifestyle of naturally occurring CD4+ CD25+ Foxp3+ regulatory T cells. *Immunol Rev* 212:60.
150. Tang, Q., and J. A. Bluestone. 2006. Regulatory T-cell physiology and application to treat autoimmunity. *Immunol Rev* 212:217.
151. Verhagen, J., K. Blaser, C. A. Akdis, and M. Akdis. 2006. Mechanisms of allergen-specific immunotherapy: T-regulatory cells and more. *Immunol Allergy Clin North Am* 26:207.
152. Zhang, L., H. Yi, X. P. Xia, and Y. Zhao. 2006. Transforming growth factor-beta: an important role in CD4+CD25+ regulatory T cells and immune tolerance. *Autoimmunity* 39:269.
153. Anderson, C. C., and W. F. Chan. 2004. Mechanisms and models of peripheral CD4 T cell self-tolerance. *Front Biosci* 9:2947.
154. Balomenos, D., and A. C. Martinez. 2000. Cell-cycle regulation in immunity, tolerance and autoimmunity. *Immunol Today* 21:551.
155. Brennan, P. J., S. J. Saouaf, M. I. Greene, and Y. Shen. 2003. Anergy and suppression as coexistent mechanisms for the maintenance of peripheral T cell tolerance. *Immunol Res* 27:295.
156. Goodnow, C. C., J. Sprent, B. Fazekas de St Groth, and C. G. Vinuesa. 2005. Cellular and genetic mechanisms of self tolerance and autoimmunity. *Nature* 435:590.
157. Lechler, R., J. G. Chai, F. Marelli-Berg, and G. Lombardi. 2001. The contributions of T-cell anergy to peripheral T-cell tolerance. *Immunology* 103:262.
158. Lechler, R., J. G. Chai, F. Marelli-Berg, and G. Lombardi. 2001. T-cell anergy and peripheral T-cell tolerance. *Philos Trans R Soc Lond B Biol Sci* 356:625.
159. Saouaf, S. J., P. J. Brennan, Y. Shen, and M. I. Greene. 2003. Mechanisms of peripheral immune tolerance: conversion of the immune to the unresponsive phenotype. *Immunol Res* 28:193.
160. Singh, N. J., and R. H. Schwartz. 2006. Primer: mechanisms of immunologic tolerance. *Nat Clin Pract Rheumatol* 2:44.
161. Battaglia, M., S. Gregori, R. Bacchetta, and M. G. Roncarolo. 2006. Tr1 cells: from discovery to their clinical application. *Semin Immunol* 18:120.
162. Mennechet, F. J., and G. Uze. 2006. Interferon-lambda-treated dendritic cells specifically induce proliferation of FOXP3-expressing suppressor T cells. *Blood* 107:4417.

163. Rutella, S., G. Bonanno, A. Procoli, A. Mariotti, D. G. de Ritis, A. Curti, S. Danese, G. Pessina, S. Pandolfi, F. Natoni, A. Di Febo, G. Scambia, R. Manfredini, S. Salati, S. Ferrari, L. Pierelli, G. Leone, and R. M. Lemoli. 2006. Hepatocyte growth factor favors monocyte differentiation into regulatory interleukin (IL)-10<sup>++</sup>IL-12<sup>low</sup>/neg accessory cells with dendritic-cell features. *Blood* 108:218.
164. Vigouroux, S., E. Yvon, E. Biagi, and M. K. Brenner. 2004. Antigen-induced regulatory T cells. *Blood* 104:26.
165. Watanabe, N., Y. H. Wang, H. K. Lee, T. Ito, Y. H. Wang, W. Cao, and Y. J. Liu. 2005. Hassall's corpuscles instruct dendritic cells to induce CD4<sup>+</sup>CD25<sup>+</sup> regulatory T cells in human thymus. *Nature* 436:1181.
166. Yvon, E. S., S. Vigouroux, R. F. Rousseau, E. Biagi, P. Amrolia, G. Dotti, H. J. Wagner, and M. K. Brenner. 2003. Overexpression of the Notch ligand, Jagged-1, induces alloantigen-specific human regulatory T cells. *Blood* 102:3815.
167. Dhodapkar, M. V., R. M. Steinman, J. Krasovsky, C. Munz, and N. Bhardwaj. 2001. Antigen-specific inhibition of effector T cell function in humans after injection of immature dendritic cells. *J Exp Med* 193:233.
168. Jonuleit, H., E. Schmitt, G. Schuler, J. Knop, and A. H. Enk. 2000. Induction of interleukin 10-producing, nonproliferating CD4(+) T cells with regulatory properties by repetitive stimulation with allogeneic immature human dendritic cells. *J Exp Med* 192:1213.
169. Brinster, C., and E. M. Shevach. 2005. Bone marrow-derived dendritic cells reverse the anergic state of CD4<sup>+</sup>CD25<sup>+</sup> T cells without reversing their suppressive function. *J Immunol* 175:7332.
170. Tarbell, K. V., S. Yamazaki, K. Olson, P. Toy, and R. M. Steinman. 2004. CD25<sup>+</sup> CD4<sup>+</sup> T cells, expanded with dendritic cells presenting a single autoantigenic peptide, suppress autoimmune diabetes. *J Exp Med* 199:1467.
171. Harnaha, J., J. Machen, M. Wright, R. Lakomy, A. Styche, M. Trucco, S. Makaroun, and N. Giannoukakis. 2006. Interleukin-7 is a survival factor for CD4<sup>+</sup> CD25<sup>+</sup> T-cells and is expressed by diabetes-suppressive dendritic cells. *Diabetes* 55:158.
172. Ma, L., S. Qian, X. Liang, L. Wang, J. E. Woodward, N. Giannoukakis, P. D. Robbins, S. Bertera, M. Trucco, J. J. Fung, and L. Lu. 2003. Prevention of diabetes in NOD mice by administration of dendritic cells deficient in nuclear transcription factor-kappaB activity. *Diabetes* 52:1976.
173. Machen, J., J. Harnaha, R. Lakomy, A. Styche, M. Trucco, and N. Giannoukakis. 2004. Antisense oligonucleotides down-regulating costimulation confer diabetes-preventive properties to nonobese diabetic mouse dendritic cells. *J Immunol* 173:4331.
174. Gordon, E. J., L. S. Wicker, L. B. Peterson, D. V. Serreze, T. G. Markees, L. D. Shultz, A. A. Rossini, D. L. Greiner, and J. P. Mordes. 2005. Autoimmune diabetes and resistance to xenograft transplantation tolerance in NOD mice. *Diabetes* 54:107.
175. Markees, T. G., D. V. Serreze, N. E. Phillips, C. H. Sorli, E. J. Gordon, L. D. Shultz, R. J. Noelle, B. A. Woda, D. L. Greiner, J. P. Mordes, and A. A. Rossini. 1999. NOD mice have a generalized defect in their response to transplantation tolerance induction. *Diabetes* 48:967.
176. Pearson, T., T. G. Markees, D. V. Serreze, M. A. Pierce, M. P. Marron, L. S. Wicker, L. B. Peterson, L. D. Shultz, J. P. Mordes, A. A. Rossini, and D. L. Greiner. 2003. Genetic disassociation of autoimmunity and resistance to costimulation blockade-induced transplantation tolerance in nonobese diabetic mice. *J Immunol* 171:185.
177. Pearson, T., T. G. Markees, D. V. Serreze, M. A. Pierce, L. S. Wicker, L. B. Peterson, L. D. Shultz, J. P. Mordes,



- A. A. Rossini, and D. L. Greiner. 2003. Islet cell autoimmunity and transplantation tolerance: two distinct mechanisms? *Ann N Y Acad Sci* 1005:148.
178. Pearson, T., T. G. Markees, L. S. Wicker, D. V. Serreze, L. B. Peterson, J. P. Mordes, A. A. Rossini, and D. L. Greiner. 2003. NOD congenic mice genetically protected from autoimmune diabetes remain resistant to transplantation tolerance induction. *Diabetes* 52:321.
179. Rossini, A. A. 2004. Autoimmune diabetes and the circle of tolerance. *Diabetes* 53:267.
180. Rossini, A. A., J. P. Mordes, D. L. Greiner, and J. S. Stoff. 2001. Islet cell transplantation tolerance. *Transplantation* 72:S43.
181. Seung, E., J. P. Mordes, D. L. Greiner, and A. A. Rossini. 2003. Induction of tolerance for islet transplantation for type 1 diabetes. *Curr Diab Rep* 3:329.
182. Karnes, R. J., C. M. Whelan, and E. D. Kwon. 2006. Immunotherapy for prostate cancer. *Curr Pharm Des* 12:807.
183. Kikuchi, T. 2006. Genetically modified dendritic cells for therapeutic immunity. *Tohoku J Exp Med* 208:1.
184. Pinzon-Charry, A., C. Schmidt, and J. A. Lopez. 2006. Dendritic cell immunotherapy for breast cancer. *Expert Opin Biol Ther* 6:591.
185. Riker, A. I., R. Jove, and A. I. Daud. 2006. Immunotherapy as part of a multidisciplinary approach to melanoma treatment. *Front Biosci* 11:1.
186. Saito, H., D. Frleta, P. Dubsky, and A. K. Palucka. 2006. Dendritic cell-based vaccination against cancer. *Hematol Oncol Clin North Am* 20:689.
187. Xia, D., T. Moyana, and J. Xiang. 2006. Combinational adenovirus-mediated gene therapy and dendritic cell vaccine in combating well-established tumors. *Cell Res* 16:241.
188. Butterfield, L. H., A. Ribas, V. B. Dissette, Y. Lee, J. Q. Yang, P. De la Rocha, S. D. Duran, J. Hernandez, E. Seja, D. M. Potter, W. H. McBride, R. Finn, J. A. Glaspy, and J. S. Economou. 2006. A phase I/II trial testing immunization of hepatocellular carcinoma patients with dendritic cells pulsed with four alpha-fetoprotein peptides. *Clin Cancer Res* 12:2817.
189. Dillman, R., S. Selvan, P. Schiltz, C. Peterson, K. Allen, C. Depriest, E. McClay, N. Barth, P. Sheehy, C. de Leon, and L. Beutel. 2004. Phase I/II trial of melanoma patient-specific vaccine of proliferating autologous tumor cells, dendritic cells, and GM-CSF: planned interim analysis. *Cancer Biother Radiopharm* 19:658.
190. Hersey, P., S. W. Menzies, G. M. Halliday, T. Nguyen, M. L. Farrelly, C. DeSilva, and M. Lett. 2004. Phase I/II study of treatment with dendritic cell vaccines in patients with disseminated melanoma. *Cancer Immunol Immunother* 53:125.
191. Kyte, J. A., L. Mu, S. Aamdal, G. Kvalheim, S. Dueland, M. Hauser, H. P. Gullestad, T. Ryder, K. Lislerud, H. Hammerstad, and G. Gaudernack. 2006. Phase I/II trial of melanoma therapy with dendritic cells transfected with autologous tumor-mRNA. *Cancer Gene Ther* 13:905.
192. Lodge, P. A., L. A. Jones, R. A. Bader, G. P. Murphy, and M. L. Salgaller. 2000. Dendritic cell-based immunotherapy of prostate cancer: immune monitoring of a phase II clinical trial. *Cancer Res* 60:829.
193. Lou, E., J. Marshall, M. Aklilu, D. Cole, D. Chang, and M. Morse. 2006. A phase II study of active

immunotherapy with PANVAC or autologous, cultured dendritic cells infected with PANVAC after complete resection of hepatic metastases of colorectal carcinoma. *Clin Colorectal Cancer* 5:368.

194. Marten, A., D. Flieger, S. Renoth, S. Weineck, P. Albers, M. Compes, B. Schottker, C. Ziske, S. Engelhart, P. Hanfland, L. Krizek, C. Faber, A. von Ruecker, S. Muller, T. Sauerbruch, and I. G. Schmidt-Wolf. 2002. Therapeutic vaccination against metastatic renal cell carcinoma by autologous dendritic cells: preclinical results and outcome of a first clinical phase I/II trial. *Cancer Immunol Immunother* 51:637.

195. Morse, M. A., S. K. Nair, D. Boczkowski, D. Tyler, H. I. Hurwitz, A. Proia, T. M. Clay, J. Schlom, E. Gilboa, and H. K. Lyerly. 2002. The feasibility and safety of immunotherapy with dendritic cells loaded with CEA mRNA following neoadjuvant chemoradiotherapy and resection of pancreatic cancer. *Int J Gastrointest Cancer* 32:1.

196. O'Rourke, M. G., M. Johnson, C. Lanagan, J. See, J. Yang, J. R. Bell, G. J. Slater, B. M. Kerr, B. Crowe, D. M. Purdie, S. L. Elliott, K. A. Ellem, and C. W. Schmidt. 2003. Durable complete clinical responses in a phase I/II trial using an autologous melanoma cell/dendritic cell vaccine. *Cancer Immunol Immunother* 52:387.

197. Pecher, G., A. Haring, L. Kaiser, and E. Thiel. 2002. Mucin gene (MUC1) transfected dendritic cells as vaccine: results of a phase I/II clinical trial. *Cancer Immunol Immunother* 51:669.

198. Slingluff, C. L., Jr., G. R. Petroni, G. V. Yamshchikov, D. L. Barnd, S. Eastham, H. Galavotti, J. W. Patterson, D. H. Deacon, S. Hibbitts, D. Teates, P. Y. Neese, W. W. Grosh, K. A. Chianese-Bullock, E. M. Woodson, C. J. Wiernasz, P. Merrill, J. Gibson, M. Ross, and V. H. Engelhard. 2003. Clinical and immunologic results of a randomized phase II trial of vaccination using four melanoma peptides either administered in granulocyte-macrophage colony-stimulating factor in adjuvant or pulsed on dendritic cells. *J Clin Oncol* 21:4016.

199. Tjoa, B. A., S. J. Simmons, V. A. Bowes, H. Ragde, M. Rogers, A. Elgamal, G. M. Kenny, O. E. Cobb, R. C. Ireton, M. J. Troychak, M. L. Salgaller, A. L. Boynton, and G. P. Murphy. 1998. Evaluation of phase I/II clinical trials in prostate cancer with dendritic cells and PSMA peptides. *Prostate* 36:39.

200. Tjoa, B. A., S. J. Simmons, A. Elgamal, M. Rogers, H. Ragde, G. M. Kenny, M. J. Troychak, A. L. Boynton, and G. P. Murphy. 1999. Follow-up evaluation of a phase II prostate cancer vaccine trial. *Prostate* 40:125.

201. Weihrach, M. R., S. Ansen, E. Jurkiewicz, C. Geisen, Z. Xia, K. S. Anderson, E. Gracien, M. Schmidt, B. Wittig, V. Diehl, J. Wolf, H. Bohlen, and L. M. Nadler. 2005. Phase I/II combined chemoimmunotherapy with carcinoembryonic antigen-derived HLA-A2-restricted CAP-1 peptide and irinotecan, 5-fluorouracil, and leucovorin in patients with primary metastatic colorectal cancer. *Clin Cancer Res* 11:5993.

202. Yamanaka, R., T. Abe, N. Yajima, N. Tsuchiya, J. Homma, T. Kobayashi, M. Narita, M. Takahashi, and R. Tanaka. 2003. Vaccination of recurrent glioma patients with tumour lysate-pulsed dendritic cells elicits immune responses: results of a clinical phase I/II trial. *Br J Cancer* 89:1172.

203. Yamanaka, R., J. Homma, N. Yajima, N. Tsuchiya, M. Sano, T. Kobayashi, S. Yoshida, T. Abe, M. Narita, M. Takahashi, and R. Tanaka. 2005. Clinical evaluation of dendritic cell vaccination for patients with recurrent glioma: results of a clinical phase I/II trial. *Clin Cancer Res* 11:4160.

204. Cella, M., M. Salio, Y. Sakakibara, H. Langen, I. Julkunen, and A. Lanzavecchia. 1999. Maturation, activation, and protection of dendritic cells induced by double-stranded RNA. *J Exp Med* 189:821.

205. d'Ostiani, C. F., G. Del Sero, A. Bacci, C. Montagnoli, A. Spreca, A. Mencacci, P. Ricciardi-Castagnoli, and L. Romani. 2000. Dendritic cells discriminate between yeasts and hyphae of the fungus *Candida albicans*. Implications for initiation of T helper cell immunity in vitro and in vivo. *J Exp Med* 191:1661.

206. De Smedt, T., M. Van Mechelen, G. De Becker, J. Urbain, O. Leo, and M. Moser. 1997. Effect of interleukin-10

on dendritic cell maturation and function. *Eur J Immunol* 27:1229.

207. Gagliardi, M. C., F. Sallusto, M. Marinaro, A. Langenkamp, A. Lanzavecchia, and M. T. De Magistris. 2000. Cholera toxin induces maturation of human dendritic cells and licenses them for Th2 priming. *Eur J Immunol* 30:2394.
208. Macatonia, S. E., N. A. Hosken, M. Litton, P. Vieira, C. S. Hsieh, J. A. Culpepper, M. Wyszocka, G. Trinchieri, K. M. Murphy, and A. O'Garra. 1995. Dendritic cells produce IL-12 and direct the development of Th1 cells from naive CD4<sup>+</sup> T cells. *J Immunol* 154:5071.
209. Rescigno, M., F. Granucci, S. Citterio, M. Foti, and P. Ricciardi-Castagnoli. 1999. Coordinated events during bacteria-induced DC maturation. *Immunol Today* 20:200.
210. Verdijk, R. M., T. Mutis, B. Esendam, J. Kamp, C. J. Melief, A. Brand, and E. Goulmy. 1999. Polyribonucleosinic polyribocytidylic acid (poly(I:C)) induces stable maturation of functionally active human dendritic cells. *J Immunol* 163:57.
211. Vieira, P. L., E. C. de Jong, E. A. Wierenga, M. L. Kapsenberg, and P. Kalinski. 2000. Development of Th1-inducing capacity in myeloid dendritic cells requires environmental instruction. *J Immunol* 164:4507.
212. Whelan, M., M. M. Harnett, K. M. Houston, V. Patel, W. Harnett, and K. P. Rigley. 2000. A filarial nematode-secreted product signals dendritic cells to acquire a phenotype that drives development of Th2 cells. *J Immunol* 164:6453.
213. Winzler, C., P. Rovere, V. S. Zimmermann, J. Davoust, M. Rescigno, S. Citterio, and P. Ricciardi-Castagnoli. 1997. Checkpoints and functional stages in DC maturation. *Adv Exp Med Biol* 417:59.
214. Herrera, O. B., D. Golshayan, R. Tibbott, F. Salcido Ochoa, M. J. James, F. M. Marelli-Berg, and R. I. Lechler. 2004. A novel pathway of alloantigen presentation by dendritic cells. *J Immunol* 173:4828.
215. Jiang, S., O. Herrera, and R. I. Lechler. 2004. New spectrum of allorecognition pathways: implications for graft rejection and transplantation tolerance. *Curr Opin Immunol* 16:550.
216. Zitvogel, L., A. Regnault, A. Lozier, J. Wolfers, C. Flament, D. Tenza, P. Ricciardi-Castagnoli, G. Raposo, and S. Amigorena. 1998. Eradication of established murine tumors using a novel cell-free vaccine: dendritic cell-derived exosomes. *Nat Med* 4:594.
217. Finkelman, F. D., A. Lees, R. Birnbaum, W. C. Gause, and S. C. Morris. 1996. Dendritic cells can present antigen in vivo in a tolerogenic or immunogenic fashion. *J Immunol* 157:1406.
218. Akbari, O., R. H. DeKruyff, and D. T. Umetsu. 2001. Pulmonary dendritic cells producing IL-10 mediate tolerance induced by respiratory exposure to antigen. *Nat Immunol* 2:725.
219. Sornasse, T., V. Flamand, G. De Becker, H. Bazin, F. Tielemans, K. Thielemans, J. Urbain, O. Leo, and M. Moser. 1992. Antigen-pulsed dendritic cells can efficiently induce an antibody response in vivo. *J Exp Med* 175:15.
220. Stumbles, P. A., J. A. Thomas, C. L. Pimm, P. T. Lee, T. J. Venaille, S. Proksch, and P. G. Holt. 1998. Resting respiratory tract dendritic cells preferentially stimulate T helper cell type 2 (Th2) responses and require obligatory cytokine signals for induction of Th1 immunity. *J Exp Med* 188:2019.
221. Wykes, M., A. Pombo, C. Jenkins, and G. G. MacPherson. 1998. Dendritic cells interact directly with naive B lymphocytes to transfer antigen and initiate class switching in a primary T-dependent response. *J Immunol* 161:1313.

222. Weiner, H. L. 2001. Induction and mechanism of action of transforming growth factor-beta-secreting Th3 regulatory cells. *Immunol Rev* 182:207.
223. Grouard, G., M. C. Rissoan, L. Filgueira, I. Durand, J. Banchereau, and Y. J. Liu. 1997. The enigmatic plasmacytoid T cells develop into dendritic cells with interleukin (IL)-3 and CD40-ligand. *J Exp Med* 185:1101.
224. Clare-Salzler, M. J., J. Brooks, A. Chai, K. Van Herle, and C. Anderson. 1992. Prevention of diabetes in nonobese diabetic mice by dendritic cell transfer. *J Clin Invest* 90:741.
225. Feili-Hariri, M., D. H. Falkner, A. Gambotto, G. D. Papworth, S. C. Watkins, P. D. Robbins, and P. A. Morel. 2003. Dendritic cells transduced to express interleukin-4 prevent diabetes in nonobese diabetic mice with advanced insulinitis. *Hum Gene Ther* 14:13.
226. Adorini, L. 2003. Tolerogenic dendritic cells induced by vitamin D receptor ligands enhance regulatory T cells inhibiting autoimmune diabetes. *Ann N Y Acad Sci* 987:258.
227. Kared, H., A. Masson, H. Adle-Biassette, J. F. Bach, L. Chatenoud, and F. Zavala. 2005. Treatment with granulocyte colony-stimulating factor prevents diabetes in NOD mice by recruiting plasmacytoid dendritic cells and functional CD4(+)CD25(+) regulatory T-cells. *Diabetes* 54:78.
228. Morin, J., B. Faideau, M. C. Gagnerault, F. Lepault, C. Boitard, and S. Boudaly. 2003. Passive transfer of flt-3L-derived dendritic cells delays diabetes development in NOD mice and associates with early production of interleukin (IL)-4 and IL-10 in the spleen of recipient mice. *Clin Exp Immunol* 134:388.
229. Papaccio, G., F. Nicoletti, F. A. Pisanti, K. Bendtzen, and M. Galdieri. 2000. Prevention of spontaneous autoimmune diabetes in NOD mice by transferring in vitro antigen-pulsed syngeneic dendritic cells. *Endocrinology* 141:1500.
230. Steptoe, R. J., J. M. Ritchie, L. K. Jones, and L. C. Harrison. 2005. Autoimmune diabetes is suppressed by transfer of proinsulin-encoding Gr-1+ myeloid progenitor cells that differentiate in vivo into resting dendritic cells. *Diabetes* 54:434.
231. Menges, M., S. Rossner, C. Voigtlander, H. Schindler, N. A. Kukutsch, C. Bogdan, K. Erb, G. Schuler, and M. B. Lutz. 2002. Repetitive injections of dendritic cells matured with tumor necrosis factor alpha induce antigen-specific protection of mice from autoimmunity. *J Exp Med* 195:15.
232. Verginis, P., H. S. Li, and G. Carayanniotis. 2005. Tolerogenic semimature dendritic cells suppress experimental autoimmune thyroiditis by activation of thyroglobulin-specific CD4+CD25+ T cells. *J Immunol* 174:7433.
233. Gangi, E., C. Vasu, D. Cheatem, and B. S. Prabhakar. 2005. IL-10-producing CD4+CD25+ regulatory T cells play a critical role in granulocyte-macrophage colony-stimulating factor-induced suppression of experimental autoimmune thyroiditis. *J Immunol* 174:7006.
234. Chorny, A., E. Gonzalez-Rey, A. Fernandez-Martin, D. Ganea, and M. Delgado. 2006. Vasoactive intestinal peptide induces regulatory dendritic cells that prevent acute graft-versus-host disease while maintaining the graft-versus-tumor response. *Blood* 107:3787.
235. Chorny, A., E. Gonzalez-Rey, A. Fernandez-Martin, D. Pozo, D. Ganea, and M. Delgado. 2005. Vasoactive intestinal peptide induces regulatory dendritic cells with therapeutic effects on autoimmune disorders. *Proc Natl Acad Sci U S A* 102:13562.
236. Faunce, D. E., A. Terajewicz, and J. Stein-Streilein. 2004. Cutting edge: in vitro-generated tolerogenic APC induce CD8+ T regulatory cells that can suppress ongoing experimental autoimmune encephalomyelitis. *J Immunol*

237. Kim, S. H., S. Kim, C. H. Evans, S. C. Ghivizzani, T. Oligino, and P. D. Robbins. 2001. Effective treatment of established murine collagen-induced arthritis by systemic administration of dendritic cells genetically modified to express IL-4. *J Immunol* 166:3499.
238. Kim, S. H., E. R. Lechman, N. Bianco, R. Menon, A. Keravala, J. Nash, Z. Mi, S. C. Watkins, A. Gambotto, and P. D. Robbins. 2005. Exosomes derived from IL-10-treated dendritic cells can suppress inflammation and collagen-induced arthritis. *J Immunol* 174:6440.
239. Whalen, J. D., A. W. Thomson, L. Lu, P. D. Robbins, and C. H. Evans. 2001. Viral IL-10 gene transfer inhibits DTH responses to soluble antigens: evidence for involvement of genetically modified dendritic cells and macrophages. *Mol Ther* 4:543.
240. Hoves, S., S. W. Krause, D. Halbritter, H. G. Zhang, J. D. Mountz, J. Scholmerich, and M. Fleck. 2003. Mature but not immature Fas ligand (CD95L)-transduced human monocyte-derived dendritic cells are protected from Fas-mediated apoptosis and can be used as killer APC. *J Immunol* 170:5406.
241. Hoves, S., S. W. Krause, H. Herfarth, D. Halbritter, H. G. Zhang, J. D. Mountz, J. Scholmerich, and M. Fleck. 2004. Elimination of activated but not resting primary human CD4<sup>+</sup> and CD8<sup>+</sup> T cells by Fas ligand (FasL/CD95L)-expressing Killer-dendritic cells. *Immunobiology* 208:463.
242. Fu, F., Y. Li, S. Qian, L. Lu, F. Chambers, T. E. Starzl, J. J. Fung, and A. W. Thomson. 1996. Costimulatory molecule-deficient dendritic cell progenitors (MHC class II<sup>+</sup>, CD80dim, CD86<sup>-</sup>) prolong cardiac allograft survival in nonimmunosuppressed recipients. *Transplantation* 62:659.
243. Lutz, M. B., R. M. Suri, M. Niimi, A. L. Ogilvie, N. A. Kukutsch, S. Rossner, G. Schuler, and J. M. Austyn. 2000. Immature dendritic cells generated with low doses of GM-CSF in the absence of IL-4 are maturation resistant and prolong allograft survival in vivo. *Eur J Immunol* 30:1813.
244. Rastellini, C., L. Lu, C. Ricordi, T. E. Starzl, A. S. Rao, and A. W. Thomson. 1995. Granulocyte/macrophage colony-stimulating factor-stimulated hepatic dendritic cell progenitors prolong pancreatic islet allograft survival. *Transplantation* 60:1366.
245. Sato, K., N. Yamashita, N. Yamashita, M. Baba, and T. Matsuyama. 2003. Regulatory dendritic cells protect mice from murine acute graft-versus-host disease and leukemia relapse. *Immunity* 18:367.
246. Gregori, S., M. Casorati, S. Amuchastegui, S. Smiroldo, A. M. Davalli, and L. Adorini. 2001. Regulatory T cells induced by 1 alpha,25-dihydroxyvitamin D3 and mycophenolate mofetil treatment mediate transplantation tolerance. *J Immunol* 167:1945.
247. Griffin, M. D., W. Lutz, V. A. Phan, L. A. Bachman, D. J. McKean, and R. Kumar. 2001. Dendritic cell modulation by 1alpha,25 dihydroxyvitamin D3 and its analogs: a vitamin D receptor-dependent pathway that promotes a persistent state of immaturity in vitro and in vivo. *Proc Natl Acad Sci U S A* 98:6800.
248. Hackstein, H., A. E. Morelli, A. T. Larregina, R. W. Ganster, G. D. Papworth, A. J. Logar, S. C. Watkins, L. D. Faló, and A. W. Thomson. 2001. Aspirin inhibits in vitro maturation and in vivo immunostimulatory function of murine myeloid dendritic cells. *J Immunol* 166:7053.
249. Hackstein, H., T. Taner, A. F. Zahorchak, A. E. Morelli, A. J. Logar, A. Gessner, and A. W. Thomson. 2003. Rapamycin inhibits IL-4--induced dendritic cell maturation in vitro and dendritic cell mobilization and function in vivo. *Blood* 101:4457.



250. Hackstein, H., and A. W. Thomson. 2004. Dendritic cells: emerging pharmacological targets of immunosuppressive drugs. *Nat Rev Immunol* 4:24.
251. Lee, J. I., R. W. Ganster, D. A. Geller, G. J. Burckart, A. W. Thomson, and L. Lu. 1999. Cyclosporine A inhibits the expression of costimulatory molecules on in vitro-generated dendritic cells: association with reduced nuclear translocation of nuclear factor kappa B. *Transplantation* 68:1255.
252. Ma, L., W. A. Rudert, J. Harnaha, M. Wright, J. Machen, R. Lakomy, S. Qian, L. Lu, P. D. Robbins, M. Trucco, and N. Giannoukakis. 2002. Immunosuppressive effects of glucosamine. *J Biol Chem* 277:39343.
253. Matasic, R., A. B. Dietz, and S. Vuk-Pavlovic. 2000. Cyclooxygenase-independent inhibition of dendritic cell maturation by aspirin. *Immunology* 101:53.
254. Matyszak, M. K., S. Citterio, M. Rescigno, and P. Ricciardi-Castagnoli. 2000. Differential effects of corticosteroids during different stages of dendritic cell maturation. *Eur J Immunol* 30:1233.
255. Mehling, A., S. Grabbe, M. Voskort, T. Schwarz, T. A. Luger, and S. Beissert. 2000. Mycophenolate mofetil impairs the maturation and function of murine dendritic cells. *J Immunol* 165:2374.
256. Nouri-Shirazi, M., and E. Guinet. 2002. Direct and indirect cross-tolerance of alloreactive T cells by dendritic cells retained in the immature stage. *Transplantation* 74:1035.
257. Penna, G., and L. Adorini. 2000. 1 Alpha,25-dihydroxyvitamin D3 inhibits differentiation, maturation, activation, and survival of dendritic cells leading to impaired alloreactive T cell activation. *J Immunol* 164:2405.
258. Piemonti, L., P. Monti, P. Allavena, M. Sironi, L. Soldini, B. E. Leone, C. Socci, and V. Di Carlo. 1999. Glucocorticoids affect human dendritic cell differentiation and maturation. *J Immunol* 162:6473.
259. Roelen, D. L., D. H. Schuurhuis, D. E. van den Boogaardt, K. Koekkoek, P. P. van Miert, J. J. van Schip, S. Laban, D. Rea, C. J. Melief, R. Offringa, F. Ossendorp, and F. H. Claas. 2003. Prolongation of skin graft survival by modulation of the alloimmune response with alternatively activated dendritic cells. *Transplantation* 76:1608.
260. Thomas, J. M., J. L. Contreras, X. L. Jiang, D. E. Eckhoff, P. X. Wang, W. J. Hubbard, A. L. Lobashevsky, W. Wang, C. Asiedu, S. Stavrou, W. J. Cook, M. L. Robbin, F. T. Thomas, and D. M. Neville, Jr. 1999. Peritransplant tolerance induction in macaques: early events reflecting the unique synergy between immunotoxin and deoxyspergualin. *Transplantation* 68:1660.
261. Vosters, O., J. Neve, D. De Wit, F. Willems, M. Goldman, and V. Verhasselt. 2003. Dendritic cells exposed to nacystelyn are refractory to maturation and promote the emergence of alloreactive regulatory t cells. *Transplantation* 75:383.
262. Bonham, C. A., L. Peng, X. Liang, Z. Chen, L. Wang, L. Ma, H. Hackstein, P. D. Robbins, A. W. Thomson, J. J. Fung, S. Qian, and L. Lu. 2002. Marked prolongation of cardiac allograft survival by dendritic cells genetically engineered with NF-kappa B oligodeoxyribonucleotide decoys and adenoviral vectors encoding CTLA4-Ig. *J Immunol* 169:3382.
263. Coates, P. T., R. Krishnan, S. Kireta, J. Johnston, and G. R. Russ. 2001. Human myeloid dendritic cells transduced with an adenoviral interleukin-10 gene construct inhibit human skin graft rejection in humanized NOD-scid chimeric mice. *Gene Ther* 8:1224.
264. Gorczynski, R. M., J. Bransom, M. Cattral, X. Huang, J. Lei, L. Xiaorong, W. P. Min, Y. Wan, and J. Gauldie. 2000. Synergy in induction of increased renal allograft survival after portal vein infusion of dendritic cells transduced to express TGFbeta and IL-10, along with administration of CHO cells expressing the regulatory molecule OX-2. *Clin*

265. Lu, L., A. Gambotto, W. C. Lee, S. Qian, C. A. Bonham, P. D. Robbins, and A. W. Thomson. 1999. Adenoviral delivery of CTLA4Ig into myeloid dendritic cells promotes their in vitro tolerogenicity and survival in allogeneic recipients. *Gene Ther* 6:554.
266. Min, W. P., R. Gorczynski, X. Y. Huang, M. Kushida, P. Kim, M. Obataki, J. Lei, R. M. Suri, and M. S. Cattral. 2000. Dendritic cells genetically engineered to express Fas ligand induce donor-specific hyporesponsiveness and prolong allograft survival. *J Immunol* 164:161.
267. O'Rourke, R. W., S. M. Kang, J. A. Lower, S. Feng, N. L. Ascher, S. Baekkeskov, and P. G. Stock. 2000. A dendritic cell line genetically modified to express CTLA4-IG as a means to prolong islet allograft survival. *Transplantation* 69:1440.
268. Takayama, T., A. E. Morelli, P. D. Robbins, H. Tahara, and A. W. Thomson. 2000. Feasibility of CTLA4Ig gene delivery and expression in vivo using retrovirally transduced myeloid dendritic cells that induce alloantigen-specific T cell anergy in vitro. *Gene Ther* 7:1265.
269. Takayama, T., Y. Nishioka, L. Lu, M. T. Lotze, H. Tahara, and A. W. Thomson. 1998. Retroviral delivery of viral interleukin-10 into myeloid dendritic cells markedly inhibits their allostimulatory activity and promotes the induction of T-cell hyporesponsiveness. *Transplantation* 66:1567.
270. Terness, P., T. M. Bauer, L. Rose, C. Dufter, A. Watzlik, H. Simon, and G. Opelz. 2002. Inhibition of allogeneic T cell proliferation by indoleamine 2,3-dioxygenase-expressing dendritic cells: mediation of suppression by tryptophan metabolites. *J Exp Med* 196:447.
271. Garroville, M., A. Ali, and S. F. Oluwole. 1999. Indirect allorecognition in acquired thymic tolerance: induction of donor-specific tolerance to rat cardiac allografts by allopeptide-pulsed host dendritic cells. *Transplantation* 68:1827.
272. Taner, T., H. Hackstein, Z. Wang, A. E. Morelli, and A. W. Thomson. 2005. Rapamycin-treated, alloantigen-pulsed host dendritic cells induce ag-specific T cell regulation and prolong graft survival. *Am J Transplant* 5:228.

# Induction of immune tolerance to facilitate $\beta$ cell regeneration in type 1 diabetes<sup>☆</sup>

Lorenzo Pasquali<sup>a,b</sup>, Nick Giannoukakis<sup>a,c</sup>, Massimo Trucco<sup>a,\*</sup>

<sup>a</sup> Division of Immunogenetics, Department of Pediatrics, University of Pittsburgh School of Medicine, Pittsburgh, Pennsylvania 15213, USA

<sup>b</sup> Department of Pediatrics, University of Genoa, Institute G. Gaslini, 16174 Genoa, Italy

<sup>c</sup> Department of Pathology, University of Pittsburgh School of Medicine, Pittsburgh, Pennsylvania 15213, USA

Received 21 May 2007; accepted 1 August 2007

Available online 9 October 2007

## Abstract

A definitive cure for type 1 diabetes is currently being pursued with enormous effort by the scientific community. Different strategies are followed to restore physiologic production of insulin in diabetic patients. Restoration of self-tolerance remains the milestone that must be reached in order to move a step further and recover a cell source capable of independent and functional insulin production. Multiple strategies aimed at modulation of both central and peripheral immunity must be considered. Promising results now show that the immune system can be modulated in a way that acquisition of a “diabetes-suppressive” phenotype is possible. Once self-tolerance is achieved, reversal of the disease may be obtained by simply allowing physiologic rescue and/or regeneration of the  $\beta$  cells to take place. Given that these outcomes have already been confirmed in humans, refinement of existing protocols along with novel methods adapted to T1DM reversal will allow translation into clinical trials.

© 2007 Published by Elsevier B.V.

**Keywords:** Diabetes; Dendritic cells; Histocompatibility; Gene therapy; Regeneration

## Contents

1. Introduction . . . . .	107
2. The autoimmune nature of T1DM . . . . .	107
3. Immune modulation . . . . .	108
3.1. Restoration of central tolerance . . . . .	108
3.1.1. Solving the problem from the root . . . . .	108
3.2. Restoration of peripheral tolerance . . . . .	109
3.2.1. Dendritic cells as Trojan horses . . . . .	109
4. Restoration of $\beta$ cell mass . . . . .	110
5. Conclusions . . . . .	111
References . . . . .	111

**Abbreviations:** APC, antigen-presenting cells; AS-ODN, antisense oligodeoxyribonucleotides; BM, bone marrow; DC, dendritic cell; DP-BB, diabetes-prone BioBreeding rat; HLA, human leukocyte antigen; MHC, major histocompatibility complex; NOD, non-obese diabetic; TCR, T-cell receptor; T1D, type 1 diabetes; VNTR, variable number of tandem repeats.

<sup>☆</sup> This review is part of the *Advanced Drug Delivery Reviews* theme issue on “Emerging Trends in Cell-Based Therapeutics”.

\* Corresponding author. Division of Immunogenetics, Children’s Hospital of Pittsburgh, Rangos Research Center, 3460 Fifth Avenue, Pittsburgh, Pennsylvania 15213, USA. Tel.: +1 412 692 6570; fax: +1 412 692 5809.

E-mail address: [mnt@pitt.edu](mailto:mnt@pitt.edu) (M. Trucco).

## 1. Introduction

Type 1 diabetes mellitus (T1DM) can best be characterized as a disorder of glucoregulation due to the insufficient production of a single critical hormone: insulin. Since the middle of the last century, the pharmacologic solution has been to administer daily recombinant variants of the hormone with increasingly sophisticated dosing schedules, which have succeeded in granting normal lifespan to type 1 diabetics [1]. Nevertheless, no matter the degree of sophistication, the current regimens have not proven capable of faithfully recapitulating what the endogenous insulin-producing  $\beta$  cells of the pancreas normally perform in response to glucose. This leads to the inevitable principal causes of morbidity and mortality associated with T1DM, namely the complications of kidney, ocular and neural disease [2–4].

While insulin replacement continues to be the primary treatment, the need to establish physiologic glucoregulation in order to avoid the complications has led to multiple avenues of alternative interventions, most of which are at the experimental stage. Some fulfilled this requirement by allotransplantation of  $\beta$  cell mass or surrogate insulin-producing cells [5–7]. Others are aimed at abrogating the cause of the disease itself, the autoimmunity, which culminates in the destruction of  $\beta$  cell mass [8,9]. An additional tier of interventions is aimed at re-establishment of adequate  $\beta$  cell mass able to provide physiologic euglycemia, through methods that promote  $\beta$  cell preservation and/or regeneration in diabetic individuals [10,11]. What all of these interventions have in common, however, is the hurdle imposed by the immune system at the level of ongoing autoimmunity and, in some cases, at the level of transplant rejection by the host.

## 2. The autoimmune nature of T1DM

T1DM is an autoimmune disease characterized by an inflammatory response against the insulin-producing  $\beta$  cells of the pancreas. A strong genetic susceptibility is essential to T1DM etiopathogenesis [12]. While the genetic associations to functional biochemical and cellular networks are beginning to be unraveled, it is clear that the genetics of susceptibility affect the ontogeny and survival of immune cell subsets at the level of the thymus and in the periphery [13]. In humans, at the thymic level, for example, the *IDDM2* locus, a variable number of tandem repeats (VNTR) polymorphism upstream of the insulin gene promoter, acts in cis to regulate the amount of proinsulin expressed in its tissue [14,15]. Insulin is an antigen against which T-cell reactivity and autoantibodies have been demonstrated to be present in rodent models and in humans and therefore represents the most relevant candidate autoantigen. In the course of the disease, a number of other autoantigens provoke T-cell reactivity and autoantibodies as well (for example GAD, IA2; [16–18]) during the process known as “antigen spreading”. Nonetheless, insulin remains the most specific candidate because it is a gene only expressed in the cells that are specifically targeted by autoimmunity in T1DM. *IDDM2* is one of two loci that have unquestionably demonstrated linkage to and association with T1DM [12]. The other locus is the Major Histocompatibility

Complex (MHC or HLA in humans) class II region which confers the strongest linkage and association with T1DM [12].

Although genetic susceptibility is a “conditio sine qua non” for the disease to occur, it is widely believed that environmental factors trigger the cellular/biochemical networks that are the activating events. Such triggers have, from time to time, included viral infections and diet components [19–24]. Viral infections may trigger  $\beta$  cell-specific T-cells through molecular mimicry where a viral epitope shares sequence homology or identity with candidate autoantigens expressed in pancreatic  $\beta$  cells or by other possible mechanisms [21,25].

Beta cell destruction is the end point of a chronic inflammation around and in the pancreatic islets of Langerhans termed “peri-

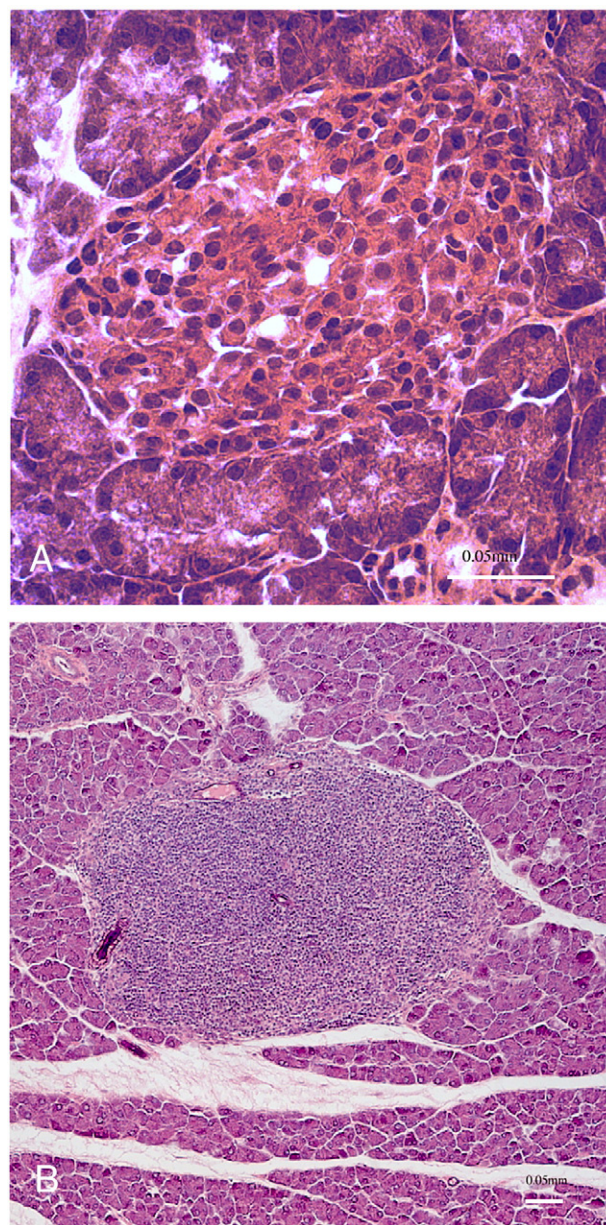


Fig. 1. A) A normal islet of Langerhans. B) The presence of mononuclear, autoreactive T-cells in the islet of the pancreas (i.e., insulinitis) is the most convincing evidence we can get about the autoimmune destruction of the insulin producing cells.



insulinitis” and “insulitis”, respectively. As studied in the two classic rodent models of the disease (diabetes-prone BioBreeding rat, DP-BB, and non-obese diabetic prone, NOD, mouse), early on in the acute phase of the immune attack the islets exhibit an abundant cell infiltration by mononuclear cells, macrophages and dendritic cells (DC) [26]. With time, T-cells become the major constituent of the insulitis and are responsible for the greatest  $\beta$  cell damage and destruction (Fig. 1). T-cells induce apoptosis of  $\beta$  cells either directly (perforin/granzyme B and Fas/Fas ligand) or indirectly through cytokines (TNF $\alpha$ /IFN $\gamma$ ) [27,28]. B-cells are late constituents of the insulitic lesion. This may explain why autoantibodies produced by B lymphocytes are thought to be only epiphenomena not directly involved in the destruction of the  $\beta$  cells. Based on this, T1DM was classically defined as a T-cell-mediated disease and for many years scientists tended to have a “T-cell centric” vision of the disease. There is now more interest and a growing belief that antigen-presenting cells (APC), and in particular DC may play a central role in either initiating or orchestrating the autoimmune response [29].

DCs are considered the body’s sentinels and play a primary role as scouts and reporters of abnormal microenvironmental changes to the immune systems as they migrate from the damaged target tissues to the lymphoid organs [30]. As scavengers, DC captures proteins and processes them into small peptides, as they move towards the draining lymphoid organs (Fig. 2). Once in a secondary lymphoid organ, DCs may present the processed peptides via both class I and class II MHC to the T-cell receptor (TCR) of naïve T-cells. If the DC migrates from a site of steady-state “normal” microphysiology, it will maintain an immune cell network refractory to the source of the acquired

antigen(s). This network generally includes a class of T-cells called regulatory T-cells, the best characterized of which express the Foxp3 transcription factor [31]. In contrast, if the DC migrated from a site of “abnormal” microphysiology, or a site of damage/foreign pathogen invasion, it will (during migration) undergo a series of phenotypic changes, both at the cell surface and the transcriptional level, termed “maturation” as it lays down a gradient of chemokines and other pro-inflammatory molecules [30]. Once a mature DC enters the lymphoid organs will engage T-cells whose TCRs recognize the acquired peptide antigens. The interaction is strengthened by co-receptor interactions (costimulation), so that the T-cell will begin to be activated and to proliferate, with the progeny eventually trafficking back to the site of “danger” as effectors. In the instance in which the T-cells are of an auto-reactive phenotype (i.e. escaped negative thymic selection and recognize antigens whose expression is normal in an organism), this DC/T-cell interaction becomes “the engine” of autoimmunity [32]. It is obvious then why DC is critical in maintaining tolerance to self-antigens and in initiating responses against antigens from foreign pathogens.

### 3. Immune modulation

#### 3.1. Restoration of central tolerance

##### 3.1.1. Solving the problem from the root

In the late 1980s the most influential single hereditary susceptibility factor in T1DM was identified and mapped to the HLA (MHC in mice) gene cluster [33,34]. An allelic form of the HLA-DQ molecule that lacks a charged amino acid at position 57

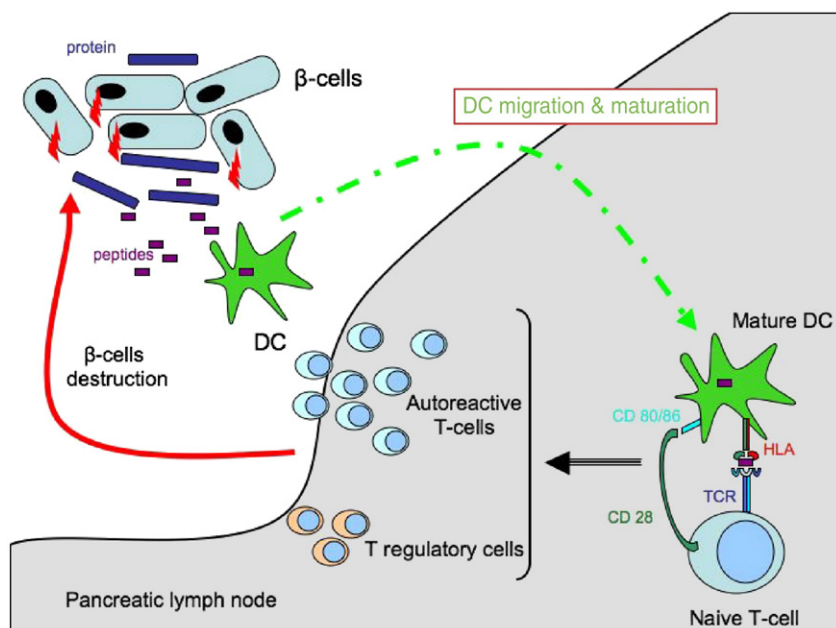


Fig. 2. Islet-resident DC responds to a microenvironmental anomaly ( $\beta$  cell death or apoptosis) by migrating out of the islets into the peripheral pancreatic lymph nodes and initiating a maturation process. By presenting the  $\beta$  cell antigens they have acquired, DCs interact with  $\beta$  cell-reactive T-cells escaped from thymic negative selection triggering their activation and proliferation. Once activated, T-cells are responsible for the greatest  $\beta$  cell damage and destruction by inducing  $\beta$  cells apoptosis either directly (perforin/granzyme B) or indirectly through cytokines (TNF $\alpha$ /IFN $\gamma$ ). Regulatory T-cells may also be involved in modulating this unstable equilibrium but ultimately the process ends in favour of the  $\beta$  cell-reactive T-cells, which eventually will destroy enough  $\beta$  cells to render the patient insulin-dependent.



of its  $\beta$  chain was shown to be strongly correlated with the development of the autoimmune disease. Conversely, resistance to the disease was found to be associated with the inheritance of an HLA-DQ allelic form with an aspartic residue at the same position (Asp57). The importance of this amino acid change has to do with the physical structure of the non-Asp57 alleles constituting class II molecules with a permissive groove [35]. MHC class II molecules are expressed in the thymus where, anchored in the cell membrane of antigen-presenting cells or thymic epithelial cells, constitute pockets containing self-antigens to be presented to developing T-cell clones. The interaction between TCR and MHC/self-antigen complex forms the basis of central tolerance. In the instance where the developing thymocyte interacts strongly with the MHC/self-antigen complex, it will undergo an intrinsic suicide program (i.e. negative selection). This mechanism of central selection ensures that the only adult T-cells let go into the periphery are those that do not react to self-antigens. Indeed, the thymus is now known to express a wide array of self-antigens including insulin, thyroperoxidase, thyroglobulin, myelin basic protein (all of which are produced by cells targeted in a number of autoimmune disorders including T1DM, Hashimoto's thyroiditis and multiple sclerosis; [36]). On the contrary, developing thymocytes that do not efficiently interact with the self-peptide present in the combining site of the MHC molecule will exit the thymus and eventually constitute the "mature" adult T-cell repertoire. At some point in an individual's lifetime, the mature T-cells will be engaged by an APC in the periphery and eventually with a foreign invader. The absence of Asp57 changes the MHC molecule (e.g., HLA-DQ8) antigen binding site in a way that self-antigens may be incorrectly positioned, thus an impaired presentation to T-cells occurs reducing the efficiency of thymic negative selection against possibly-autoreactive T-cell clones [35,37]. The structural feature that characterizes HLA-DQ8 in T1DM susceptibility in humans is identical to the homologous molecule I-Ag<sup>7</sup> present in the NOD mouse strain [38].

The importance of the MHC and the thymic antigen-presenting environment was confirmed in many different studies: 1) in transgenic NOD mice that express class II genes other than I-Ag<sup>7</sup>, the mice were shown to be refractory to diabetes [39,40]; 2) autoimmunity was prevented in NOD mice by transplanting all or part of bone marrow cells derived from diabetes resistant strains [10,11,41,42]. Instead of relying on allogeneic bone marrow transplantation, Tian et al. successfully prevented diabetes in NOD mice by reconstituting sublethally-irradiated NOD mice with its own bone marrow cells genetically-engineered *ex vivo* to express a resistance MHC class II  $\beta$  chain [8]. The reconstituted mice possessed bone marrow-derived cells that coexpressed both their own diabetogenic I-Ag<sup>7</sup> and the transfected non-Asp57  $\beta$  chain. They were diabetes-free without the need of immunosuppressive drugs. The authors suggested a mechanism whereby thymus was repopulated by the engineered bone marrow cells which differentiated into APC promoting proper negative selection due to the stronger affinity of the TCR for the self-antigen bound to the newly-expressed MHC molecule versus the I-Ag<sup>7</sup>, thus eliminating T-cells potentially autoreactive to  $\beta$  cells [43]. This approach may be transferable to clinical trials in the near-future once alternatives to sublethal irradiation are found. They could

consist of myeloablating drugs or antilymphocyte globulins like anti-CD3/CD8, used to induce bone marrow chimerism in mice [44].

### 3.2. Restoration of peripheral tolerance

#### 3.2.1. Dendritic cells as Trojan horses

Classically thought of as a T-cell-driven disease, much of the initial effort to prevent progression of T1DM aimed to target the T-cells. Various immunosuppressive agents were used to extinguish the inflammatory process including azathioprine [45], prednisone [46], and cyclosporine [47], resulting in short-term preservation of insulin production unfortunately associated with a significant toxicity for the patients. This kind of approach was better tolerated once an anti-CD3 antibody was used to prevent and reverse new-onset T1DM. Indeed, this therapy is now in phase II clinical trials [9]. CD3 is part of the TCR signaling complex on T-cells involved in transduction of the activating signals to the cytoplasm of the T-cell, when antigen binds to the TCR. Although unclear, one of the proposed corollary mechanisms that provide a protracted effect of the antibody-based therapy involves the activation of CD4<sup>+</sup> CD25<sup>+</sup> T regulatory cells [48]. Since the native form of anti-CD3 antibodies is highly toxic in humans, the synthesis of two modified proteins (hOKT31 and ChAglyCD3) permitted to test this approach in several clinical trials [9,49]. Reversibility of new-onset T1DM by immunomodulation was demonstrated and residual  $\beta$  cell mass was rescued [50]. More recently, Voltarelli and colleagues demonstrated a prolongation of the "honeymoon" period (i.e., the limited in time re-establishment of glycemia immediately following the clinical onset of the disease) by treating new-onset diabetics with autologous hematopoietic stem cells following non-myeloablative preparation of the patients [51]. However, all these approaches have limits: 1) safety is the first concern: risks from T-cell depletion and a cytokine release "storm-like" symptoms; 2) some patients were not responsive; 3) the majority of patients eventually became refractory to the treatment and T1DM reappeared. Despite these limitations, these studies now pave the way to rescue residual  $\beta$  cell mass as a means of "reversing" the disease through intervening in the autoimmune process and cell networks.

The central role of DC in the immune process and their capacity to shape T-cell responses has recently promoted a new field of immunotherapeutics including cancer immunotherapy and autoimmunity. Clare-Salzler et al. first used DCs to prevent T1DM in NOD mice [52]. These investigators conferred protection to NOD mice by transferring DCs obtained from pancreatic lymph nodes of older syngeneic donors. Feili-Hariri et al. observed similar results in NOD recipients of bone marrow-derived syngeneic DC [53] and more recently autoimmune diabetes was prevented in NOD mice by transferring myeloid progenitor cells expanded *in vitro* but inhibited in the terminal DC differentiation steps. The latter was obtained by culturing bone marrow (BM) in granulocyte macrophage colony-stimulating factor (GM-CSF) and transforming growth factor- $\beta$  1 [54]. Others obtained similar results employing DC induced by vitamin D receptor [55] or pulsed *ex vivo* with disease-specific-antigens

[56] or non-disease-specific proteins such as gamma-globulin [57]. In our group, Machen et al. used antisense oligodeoxynucleotides (AS-ODN) targeting the CD40, CD80 and CD86 primary transcripts to impair the expression of these genes and the presentation of the encoded molecules at the surface of NOD-derived DC. In the absence of a substantial interaction between these three key costimulatory molecules on DC (CD80/86 or CD40) and their co-receptors on putatively autoreactive T-cells (CD28 or CD152, respectively), T-cell engaged in antigen presentation undergo functional silence (anergy) or are primed for apoptosis (Fig. 3). Furthermore, multiple injections of AS-ODN-treated DCs into NOD mice were able to maintain the animals diabetes free without affecting the overall T-cell activity against alloantigens [58]. An additional mechanism shared by all the DC-based interventions is that the host exhibits increased numbers of CD4<sup>+</sup> CD25<sup>+</sup> putative T regulatory cells which alone have been shown to prevent T1DM or via redirection of TH1 to TH2-type responses [59]. The promising results obtained by using AS-ODN targeting the costimulatory signals in DC's, and the low risk of the procedure, have enabled us to proceed with a phase I clinical trial approved by the Food and Drug Administration (FDA).

Our group has recently developed an alternative strategy, targeting migratory DC *in vivo* by injection subcutaneously of microcapsules containing AS-ODN. It is anticipated that migratory DC will acquire the microcapsules with the AS-ODN and will undergo the same phenotypical changes required to acquire a “diabetes-suppressive” feature as they do following *ex vivo* AS-ODN exposure and uptake. The microcapsules may be a simpler, yet still effective treatment, bypassing the cumbersome aphaeresis procedure necessary to obtain autologous DC to be re-injected as engineered DC's into the diabetic donor, who this

way also becomes the recipient (N.G. and M.T., manuscript submitted).

#### 4. Restoration of $\beta$ cell mass

Abrogation of autoimmunity without an adequate residual  $\beta$  cell mass will not restore normoglycemia. Therefore, methods of reconstituting normal, physiologic insulin production must be part of any therapy aimed at restoring normoglycemia. Transplantation of  $\beta$  cells in the form of allografts has historically been the proposed method that recently, in the form of allogeneic islet transplantation, has entered the clinic [60–62]. In 2000, Shapiro and colleagues made islet transplantation a viable clinical reality largely by using a steroid-free immunosuppression cocktail [63]. Despite the initial enthusiasm, and the positive outcomes in a high percentage of patients, after 5 years of follow up, less than 10% of the treated patients remained insulin-independent [64].

Although one may suggest modifications to existing immunosuppressive drug cocktails, almost all currently-approved agents exhibit toxic side effects. The immunosuppressive drugs necessary to avoid allojection are toxic not only to the recipient kidney but also to the transplanted  $\beta$  cells themselves [65]. Furthermore, the need to use multiple cadaveric donors are not only associated with considerable logistic and ethical impediments, but also with the consequent immunization of the recipients against a variety of HLA alleles making an eventually-needed kidney transplant virtually impossible.

An alternative has been to engineer intact islets *ex vivo* with gene delivery vectors encoding cytoprotective, immunomodulatory genes. The limitations to this approach are the recipient's immune responses to the vector and the requirement for multiple gene delivery [66].

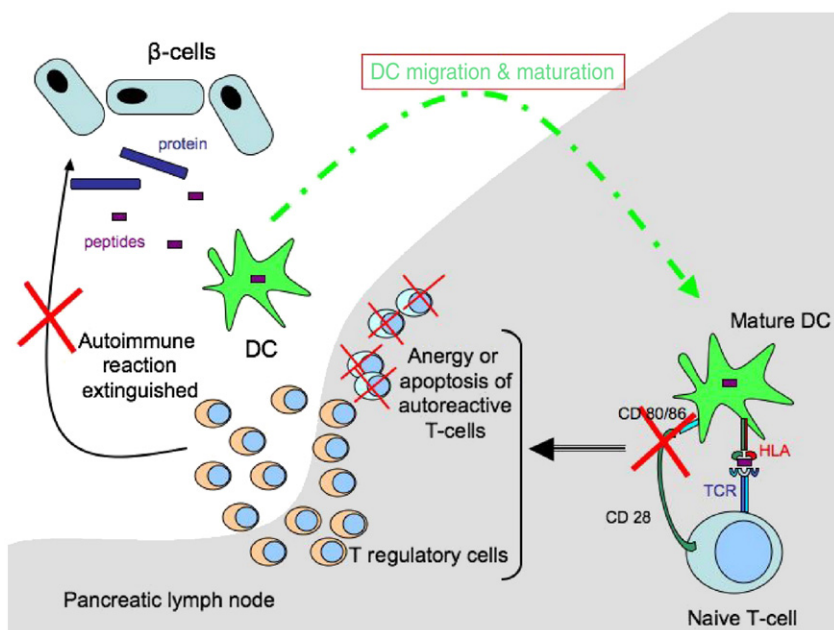


Fig. 3. In the absence of a substantial interaction between CD80 and CD86 costimulatory molecules on DC and CD28 coreceptor on putatively autoreactive T-cells, T-cell engaged in antigen presentation, undergo functional silence (anergy) or apoptosis. Additionally, all DC-based interventions seem to induce expansion of T regulatory cells clones. The result is the acquisition of a new equilibrium in the dynamic autoreactive process that ensures a “diabetes protective” phenotype and further destruction of  $\beta$  cells will be prevented.

Taken together, all these factors necessitate the identification of methods to grow  $\beta$  cells or their surrogates *in vitro* or *in vivo* in a manner that “expands” progenitors into bona fide insulin-secreting cells.

A number of efforts have recently been aimed at finding optimal methods of generating insulin producing cells *ex vivo* from multiple progenitors which eventually become suitable for transplantation [67]. In particular much attention has been directed upon stem cells. D’Amour et al. recently reported a five-step protocol able to convert human embryonic stem cells into insulin producing cells [68]. Although the latter cells do not release insulin functionally in a physiologic way (e.g. under glucose stimulation), this represent a remarkable progress towards the achievement of an inexhaustible source of  $\beta$  cells that could substitute the limited pool obtained from human cadaveric donors.

T1DM pathogenesis is a dynamic process. Once self-tolerance is lost and  $\beta$  cells begin to be destroyed, the system reaches a new equilibrium in which the newly-differentiated  $\beta$  cells are in turn eliminated by the ongoing autoimmune process. The demonstration of persisting autoreactive T-cells in diabetic patients, even after a long time from diabetes onset, shows that latent autoreactive T-cells can be sensitized upon *in vivo* regeneration of  $\beta$  cells from progenitors. It was shown that healthy islets transplanted into syngenic long-term diabetic mice or from the healthy to the diabetic monozygotic twin were quickly eliminated by autoreactive T-cells [69]. Thus, any physiologic reparative attempt to regenerate the lost  $\beta$  cells will eventually be defeated by the more effective autoimmune attack.

Evidence of  $\beta$  cell regeneration promoted by bone marrow or stem cell allotransplantation in new-onset disease NOD mice has been observed by several groups [10,11,70]. In support are three recent publications where in diabetic NOD mice, abrogation of autoimmunity by spleen cell transplantation in the presence of Freund’s complete adjuvant resulted in  $\beta$  cell regeneration which was capable of normalizing hyperglycemia and to reverse the disease [71–73]. While it remains debatable whether bone marrow or spleen cells themselves promote the regenerative process, the recipient origin of the newly generated  $\beta$  cell was confirmed in these studies just as our group had previously demonstrated [10] as had others [10].

A germane question regards the source of the regenerating  $\beta$  cells. Cell lineage tracing studies in transgenic mice revealed that the endoderm provides the progenitor cell populations which eventually migrate into, or develop into pancreatic parenchyma including structures like the pancreatic ducts, acini and the islets [74].

Indeed, a large body of evidence supports the hypothesis that adult pancreas possesses stem cells capable of differentiating into endocrine cells. These endocrine progenitors may be located close to the duct without being components of the ductal epithelium. Experiments performed by Seaberg et al. [75] and Suzuky et al. [76] demonstrated the potential of a single murine adult pancreatic precursor cell to generate daughter cells with characteristics of pancreatic cells, including  $\beta$  cells. One interpretation is that precursor “stem” cells normally present during embryonic development persist in adult tissues. The

putative progenitor cells could be mesenchymal in origin, or derive from a dedifferentiation of an epithelial cell [77–79]. Conclusions and interpretations from these studies must be balanced by the observations made by Dor et al. [80]. These investigators presented evidence that in mice, the already existing  $\beta$  cells are able to regulate their own homeostasis by self-duplication, expanding themselves when necessary. Their data apparently did not support the existence of endocrine “stem” cells capable of differentiation inside adult pancreas. The obvious question that arose from the studies of Dor and colleagues is whether human adult endocrine cells also possess an intrinsic capacity to self-duplicate under certain conditions and whether abrogation of autoimmunity in T1DM might relieve impediments to such endocrine cell division. Indeed, if this process was viable in adult humans, would it be amenable to *in vivo* manipulation to expand existing residual  $\beta$  cell mass to reconstitute euglycemia?

Meier et al. analyzed pancreatic sections from 42 T1DM patients with different duration of the disease to ascertain the presence of  $\beta$  cells. Beta cells were identified in 88% of sections which also exhibited evidence of ongoing apoptosis. The suggestion was made that the presence of  $\beta$  cells despite ongoing apoptosis was indirect evidence of an active regeneration process [81]. Direct evidence of  $\beta$  cell replication was suggested by the same group when pancreas tissue from a lean 89-year-old patient with recent-onset type 1 diabetes was examined [82]. It is quite likely that the ability of  $\beta$  cells to regenerate may be more efficient during the early stages of autoimmunity when the insulinitis is not dense, therefore explaining why some immunomodulation interventions are most successful in patients exhibiting suboptimal (but not abnormally low) C-peptide levels [83].

## 5. Conclusions

The search for a definitive cure for T1DM is being pursued vigorously by the scientific community. A wide variety of strategies has been, and continues to be employed to restore physiologic insulin production in diabetic patients. An important milestone to be reached is the restoration of self-tolerance along with the discovery of insulin-producing cell surrogates. Promising results from animal models demonstrate that the immune system can be modulated in a way that “diabetes-suppressive” status is possible. Self-tolerance re-establishment can be targeted to central or peripheral cell networks and molecular pathways. Some of these strategies are readily translatable to the clinic and others are already in safety and efficacy clinical trials. As self-tolerance is re-established, it will be possible to restore normoglycemia by preservation of endogenous  $\beta$  cell mass where an adequate amount remains in new-onset disease or to restore physiologic glucoregulation by transplantation of surrogate insulin-producing cells or induction of regeneration of undifferentiated endocrine cell precursors *in vivo*.

## References

- [1] I.B. Hirsch, Insulin analogues, *N. Engl. J. Med.* 352 (2005) 174–183.
- [2] The Diabetes Control and Complications Trial Research Group, The effect of intensive treatment of diabetes on the development and progression of long-



- term complications in insulin-dependent diabetes mellitus, *N. Engl. J. Med.* 329 (1993) 977–986.
- [3] The Diabetes Control and Complications Trial/Epidemiology of Diabetes Interventions and Complications Research Group, Retinopathy and nephropathy in patients with type 1 diabetes four years after a trial of intensive therapy, *N. Engl. J. Med.* 342 (2000) 381–389.
  - [4] G. Pambianco, T. Costacou, D. Ellis, D.J. Becker, R. Klein, T.J. Orchard, The 30-year natural history of type 1 diabetes complications: the Pittsburgh Epidemiology of Diabetes Complications Study experience, *Diabetes* 55 (2006) 1463–1469.
  - [5] M.A. Lipes, E.M. Cooper, R. Skelly, C.J. Rhodes, E. Boschetti, G.C. Weir, A.M. Davalli, Insulin-secreting non-islet cells are resistant to autoimmune destruction, *PNAS* 93 (1996) 8595–8600.
  - [6] A.T. Cheung, B. Dayanandan, J.T. Lewis, G.S. Korbitt, R.V. Rajotte, M.O. Boylan, M.M. Wolfe, T.J. Kieffer, Glucose-dependent insulin release from genetically engineered K cells, *Science* 290 (2000) 1959–1962.
  - [7] R.P. Robertson, Islet transplantation as a treatment for diabetes — a work in progress, *N. Engl. J. Med.* 350 (2004) 694–705.
  - [8] C. Tian, J. Bagley, N. Cretin, N. Seth, K.W. Wucherpfennig, J. Iacomini, Prevention of type 1 diabetes by gene therapy, *J. Clin. Invest.* 114 (2004) 969–978.
  - [9] B. Keymeulen, E. Vandemeulebroucke, A.G. Ziegler, C. Mathieu, L. Kaufman, G. Hale, F. Gorus, M. Goldman, M. Walter, S. Candon, L. Schandene, L. Crenier, C. De Block, J.-M. Seigneurin, P. De Pauw, D. Pierard, I. Weets, P. Rebello, P. Bird, E. Berrie, M. Frewin, H. Waldmann, J.-F. Bach, D. Pipeleers, L. Chatenoud, Insulin needs after CD3-antibody therapy in new-onset type 1 diabetes, *N. Engl. J. Med.* 352 (2005) 2598–2608.
  - [10] D. Hess, L. Li, M. Martin, S. Sakano, D. Hill, B. Strutt, S. Thyssen, D.A. Gray, M. Bhatia, Bone marrow-derived stem cells initiate pancreatic regeneration, *Nat. Biotechnol.* 21 (2003) 763–770.
  - [11] T.D. Zorina, V.M. Subbotin, S. Bertera, A. Alexander, C. Haluszczak, A. Styche, B. Gambrell, R. Bottino, M. Trucco, Recovery of the endogenous beta cell function in the NOD model of autoimmune diabetes, *Stem Cells* 21 (2003) 377–388.
  - [12] J.L. Davies, Y. Kawaguchi, S.T. Bennett, J.B. Copeman, H.J. Cordell, L.E. Pritchard, P.W. Reed, S.C.L. Gough, S.C. Jenkins, S.M. Palmer, K.M. Balfour, B.R. Rowe, M. Farrall, A.H. Barnett, S.C. Bain, J.A. Todd, A genome-wide search for human type 1 diabetes susceptibility genes, *Nature* 371 (1994) 130–136.
  - [13] C.E. Egwuagu, P. Charukamnoetkanok, I. Gery, Thymic expression of autoantigens correlates with resistance to autoimmune disease, *J. Immunol.* 159 (1997) 3109–3112.
  - [14] A. Pugliese, M. Zeller, A. Fernandez Jr., L.J. Zalcberg, R.J. Bartlett, C. Ricordi, M. Pietropaolo, G.S. Eisenbarth, S.T. Bennett, D.D. Patel, The insulin gene is transcribed in the human thymus and transcription levels correlated with allelic variation at the INS VNTR-IDD2 susceptibility locus for type 1 diabetes, *Nat. Genet.* 15 (1997) 293–297.
  - [15] P. Vafiadis, S.T. Bennett, J.A. Todd, J. Nadeau, R. Grabs, C.G. Goodyer, S. Wickramasinghe, E. Colle, C. Polychronakos, Insulin expression in human thymus is modulated by INS VNTR alleles at the IDDM2 locus, *Nat. Genet.* 15 (1997) 289–292.
  - [16] G.F. Bottazzo, A. Florin-Christensen, D. Doniach, Islet-cell antibodies in diabetes mellitus with autoimmune polyendocrine deficiencies, *Lancet* 2 (1974) 1279–1283.
  - [17] R. Giorda, M. Peakman, K.C. Tan, D. Vergani, M. Trucco, Glutamic acid decarboxylase expression in islet and brain, *Lancet* 338 (1991) 1469–1470.
  - [18] D.L. Kaufman, M.G. Erlander, M. Clare-Salzler, M.A. Atkinson, N.K. Maclaren, A.J. Tobin, Autoimmunity to two forms of glutamate decarboxylase in insulin-dependent diabetes mellitus, *J. Clin. Invest.* 89 (1992) 283–292.
  - [19] W.L. Clarke, K.A. Shaver, G.M. Bright, A.D. Rogol, W.E., Autoimmunity in congenital rubella syndrome, *J. Pediatr.* 104 (1984) 370–373.
  - [20] J. Karjalainen, J.M. Martin, M. Knip, J. Ilonen, B.H. Robinson, E. Savilahti, H.K. Akerblom, H.M. Dosch, A bovine albumin peptide as a possible trigger of insulin-dependent diabetes mellitus, *N. Engl. J. Med.* 327 (1992) 302–307.
  - [21] B. Conrad, E. Weidmann, G. Trucco, W.A. Rudert, C. Ricordi, H. Rodriguez-Rilo, R. Behboo, D. Finegold, M. Trucco, Evidence for superantigen involvement in insulin-dependent diabetes mellitus etiology, *Nature* 371 (1994) 351–355.
  - [22] J.M. Norris, K. Barriga, G. Klingensmith, M. Hoffman, G.S. Eisenbarth, H.A. Erlich, M. Rewers, Timing of initial cereal exposure in infancy and risk of islet autoimmunity, *JAMA* 290 (2003) 1713–1720.
  - [23] H. Hyoty, Environmental causes: viral causes, *Endocrinol. Metab. Clin. N. Am.* 33 (2004) 27–44.
  - [24] M. Knip, R. Veijola, S.M. Virtanen, H. Hyoty, O. Vaarala, H.K. Akerblom, Environmental triggers and determinants of type 1 diabetes, *Diabetes* 54 (Suppl 2) (2005) S125–S136.
  - [25] L.J. Albert, R.D. Inman, Molecular mimicry and autoimmunity, *N. Engl. J. Med.* 341 (1999) 2068–2074.
  - [26] J.F. Bach, Insulin-dependent diabetes mellitus as an autoimmune disease, *Endocr. Rev.* 15 (1994) 516–542.
  - [27] N.N. Shehadeh, F. LaRosa, K.J. Lafferty, Altered cytokine activity in adjuvant inhibition of autoimmune diabetes, *J. Autoimmun.* 6 (1993) 291–300.
  - [28] W. Suarez-Pinzon, R.V. Rajotte, T.R. Mosmann, A. Rabinovitch, Both CD4+ and CD8+ T-cells in syngeneic islet grafts in NOD mice produce interferon-gamma during beta-cell destruction, *Diabetes* 45 (1996) 1350–1357.
  - [29] P.A. Morel, A.C. Vasquez, M. Feili-Hariri, Immunobiology of DC in NOD mice, *J. Leukoc. Biol.* 66 (1999) 276–280.
  - [30] K. Shortman, S.H. Naik, Steady-state and inflammatory dendritic-cell development, *Nat. Rev. Immunol.* 7 (2007) 19–30.
  - [31] J.D. Fontenot, M.A. Gavin, A.Y. Rudensky, Foxp3 programs the development and function of CD4+CD25+ regulatory T cells, *Nat. Immunol.* 4 (2003) 330–336.
  - [32] J.F. Bach, L. Chatenoud, Tolerance to islet autoantigens in type 1 diabetes, *Annu. Rev. Immunol.* 19 (2001) 131–161.
  - [33] J.A. Todd, J.I. Bell, H.O. McDewitt, HLA-DQ beta gene contributes to susceptibility and resistance to insulin-dependent diabetes mellitus, *Nature* 329 (1987) 599–604.
  - [34] P.A. Morel, J.S. Dorman, J. Todd, H. McDewitt, M. Trucco, Aspartic acid at position 57 of the HLA-DQ beta chain protects against type I diabetes: a family study, *PNAS* 85 (1988) 8111–8115.
  - [35] M. Trucco, To be or not to be Asp 57, that is the question, *Diabetes Care* 15 (1992) 705–715.
  - [36] B. Kyewski, J. Derbinski, Self-representation in the thymus: an extended view, *Nat. Rev. Immunol.* 4 (2004) 688–698.
  - [37] H. McDewitt, The role of MHC class II molecules in the pathogenesis and prevention of type I diabetes, *Adv. Exp. Med. Biol.* 490 (2001) 59–66.
  - [38] H. Acha-Orbea, H.O. McDewitt, The first external domain of the nonobese diabetic mouse class II I-A beta chain is unique, *PNAS* 84 (1987) 2435–2439.
  - [39] T. Lund, L. O'Reilly, P. Hutchings, O. Kanagawa, E. Simpson, R. Gravely, P. Chandler, J. Dyson, J.K. Picard, A. Edwards, D. Kioussis, A. Cooke, Prevention of insulin-dependent diabetes mellitus in non-obese diabetic mice by transgenes encoding modified I-A beta-chain or normal I-E alpha-chain, *Nature* 345 (1990) 727–729.
  - [40] M.S. Hanson, M. Cetkovic-Cvrlje, V.K. Ramiya, M.A. Atkinson, N.K. Maclaren, B. Singh, J.F. Elliott, D.V. Serreze, E.H. Leiter, Quantitative thresholds of MHC class II I-E expressed on hemopoietically derived antigen-presenting cells in transgenic NOD/Lt mice determine level of diabetes resistance and indicate mechanism of protection, *J. Immunol.* 157 (1996) 1279–1287.
  - [41] H. Li, C.L. Kaufman, S.S. Boggs, P.C. Johnson, K.D. Patrene, S.T. Ildstad, Mixed allogeneic chimerism induced by a sublethal approach prevents autoimmune diabetes and reverses insulinitis in nonobese diabetic (NOD) mice, *J. Immunol.* 156 (1996) 380–388.
  - [42] T.D. Zorina, V.M. Subbotin, S. Bertera, A. Alexander, A.J. Styche, M. Trucco, Distinct characteristics and features of allogeneic chimerism in the NOD mouse model of autoimmune diabetes, *Cell Transplant* 11 (2002) 113–123.
  - [43] M. Trucco, N. Giannoukakis, Type 1 diabetes: MHC tailored for diabetes cell therapy, *Gene. Ther.* 12 (2005) 553.
  - [44] C. Zhang, I. Todorov, C.L. Lin, M. Atkinson, F. Kandeel, S. Forman, D. Zeng, Elimination of insulinitis and augmentation of islet beta cell regeneration

- via induction of chimerism in overtly diabetic NOD mice, *PNAS* 104 (2007) 2337–2342.
- [45] J. Silverstein, N. Maclaren, W. Riley, R. Spillar, D. Radjenovic, S. Johnson, Immunosuppression with azathioprine and prednisone in recent-onset insulin-dependent diabetes mellitus, *N. Engl. J. Med.* 319 (1988) 599–604.
- [46] R.B. Elliott, J.R. Crossley, C.C. Berryman, A.G. James, Partial preservation of pancreatic beta-cell function in children with diabetes, *Lancet* 2 (1981) 631–632.
- [47] P.F. Bougneres, P. Landais, C. Boisson, J.C. Carel, N. Frament, C. Boitard, J.L. Chaussain, J.F. Bach, Limited duration of remission of insulin dependency in children with recent overt type I diabetes treated with low-dose cyclosporin, *Diabetes* 39 (1990) 1264–1272.
- [48] M. Belghith, J.A. Bluestone, S. Barriot, J. Megret, J.F. Bach, L. Chatenoud, TGF-beta-dependent mechanisms mediate restoration of self-tolerance induced by antibodies to CD3 in overt autoimmune diabetes, *Nat. Med.* 9 (2003) 1202–1208.
- [49] K.C. Herold, W. Hagopian, J.A. Auger, E. Poumian-Ruiz, L. Taylor, D. Donaldson, S.E. Gitelman, D.M. Harlan, D. Xu, R.A. Zivin, J.A. Bluestone, Anti-CD3 monoclonal antibody in new-onset type 1 diabetes mellitus, *N. Engl. J. Med.* 346 (2002) 1692–1698.
- [50] K.C. Herold, S.E. Gitelman, U. Masharani, W. Hagopian, B. Bisikirska, D. Donaldson, K. Rother, B. Diamond, D.M. Harlan, J.A. Bluestone, A single course of anti-CD3 monoclonal antibody hOKT3gamma1(Ala-Ala) results in improvement in C-peptide responses and clinical parameters for at least 2 years after onset of type 1 diabetes, *Diabetes* 54 (2005) 1763–1769.
- [51] J.C. Voltarelli, C.E. Couri, A.B. Stracieri, M.C. Oliveira, D.A. Moraes, F. Pieroni, M. Coutinho, K.C. Malmegrim, M.C. Foss-Freitas, B.P. Simoes, M.C. Foss, E. Squiers, R.K. Burt, Autologous nonmyeloablative hematopoietic stem cell transplantation in newly diagnosed type 1 diabetes mellitus, *JAMA* 297 (2007) 1568–1576.
- [52] M.J. Clare-Salzler, J. Brooks, A. Chai, K. Van Herle, C. Anderson, Prevention of diabetes in nonobese diabetic mice by dendritic cell transfer, *J. Clin. Invest.* 90 (1992) 741–748.
- [53] M. Feili-Hariri, X. Dong, S.M. Alber, S.C. Watkins, R.D. Salter, P.A. Morel, Immunotherapy of NOD mice with bone marrow-derived dendritic cells, *Diabetes* 48 (1999) 2300–2308.
- [54] R.J. Steptoe, J.M. Ritchie, L.K. Jones, L.C. Harrison, Autoimmune diabetes is suppressed by transfer of proinsulin-encoding Gr-1+ myeloid progenitor cells that differentiate in vivo into resting dendritic cells, *Diabetes* 54 (2005) 434–442.
- [55] L. Adorini, G. Penna, N. Giarratana, M. Uskokovic, Tolerogenic dendritic cells induced by vitamin D receptor ligands enhance regulatory T cells inhibiting allograft rejection and autoimmune diseases, *J. Cell. Biochem.* 88 (2003) 227–233.
- [56] J. Lo, R.H. Peng, T. Barker, C.Q. Xia, M.J. Clare-Salzler, Peptide-pulsed immature dendritic cells reduce response to beta cell target antigens and protect NOD recipients from type I diabetes, *Ann. N. Y. Acad. Sci.* 1079 (2006) 153–156.
- [57] G. Papaccio, F. Nicoletti, F.A. Pisanti, K. Bendtzen, M. Galdieri, Prevention of spontaneous autoimmune diabetes in NOD mice by transferring in vitro antigen-pulsed syngeneic dendritic cells, *Endocrinology* 141 (2000) 1500–1505.
- [58] J. Machen, J. Harnaha, R. Lakomy, A. Styche, M. Trucco, N. Giannoukakis, Antisense oligonucleotides down-regulating costimulation confer diabetes-preventive properties to nonobese diabetic mouse dendritic cells, *J. Immunol.* 173 (2004) 4331–4341.
- [59] M. Feili-Hariri, D.H. Falkner, P.A. Morel, Regulatory Th2 response induced following adoptive transfer of dendritic cells in prediabetic NOD mice, *Eur. J. Immunol.* 32 (2002) 2021–2030.
- [60] R. Bottino, A.N. Balamurugan, M. Trucco, T.E. Starzl, Pancreas and islet cell transplantation, *Best. Pract. Res. Clin. Gastroenterol.* 16 (2002) 457–474.
- [61] K.I. Rother, D.M. Harlan, Challenges facing islet transplantation for the treatment of type 1 diabetes mellitus, *J. Clin. Invest.* 114 (2004) 877–883.
- [62] P.G. Stock, J.A. Bluestone, Beta-cell replacement for type I diabetes, *Annu. Rev. Med.* 55 (2004) 133–156.
- [63] A.M. Shapiro, J.R. Lakey, E.A. Ryan, G.S. Korbutt, E. Toth, G.L. Warnock, N.M. Kneteman, R.V. Rajotte, Islet transplantation in seven patients with type 1 diabetes mellitus using a glucocorticoid-free immunosuppressive regimen, *N. Engl. J. Med.* 343 (2000) 230–238.
- [64] E.A. Ryan, B.W. Paty, P.A. Senior, D. Bigam, E. Alfadhli, N.M. Kneteman, J.R. Lakey, A.M. Shapiro, Five-year follow-up after clinical islet transplantation, *Diabetes* 54 (2005) 2060–2069.
- [65] P.A. Senior, M. Zeman, B.W. Paty, E.A. Ryan, A.M.J. Shapiro, Changes in renal function after clinical islet transplantation: four-year observational study, *Am. J. Transplant.* 7 (2007) 91–98.
- [66] N. Giannoukakis, M. Trucco, Gene therapy for type 1 diabetes: a proposal to move to the next level, *Curr. Opin. Mol. Ther.* 7 (2005) 467–475.
- [67] S. Bonner-Weir, G.C. Weir, New sources of pancreatic beta-cells, *Nat. Biotechnol.* 23 (2005) 857–861.
- [68] K.A. D'Amour, A.G. Bang, S. Eliazar, O.G. Kelly, A.D. Agulnick, N.G. Smart, M.A. Moorman, E. Kroon, M.K. Carpenter, E.E. Baetge, Production of pancreatic hormone-expressing endocrine cells from human embryonic stem cells, *Nat. Biotechnol.* 24 (2006) 1392–1401.
- [69] D.E. Sutherland, R. Sibley, X.Z. Xu, A. Michael, A.M. Srikanta, F. Taub, J. Najarian, F.C. Goetz, Twin-to-twin pancreas transplantation: reversal and reenactment of the pathogenesis of type I diabetes, *Trans. Assoc. Am. Physicians* 97 (1984) 80–87.
- [70] S. Kodama, W. Kuhlreiter, S. Fujimura, E.A. Dale, D.L. Faustman, Islet regeneration during the reversal of autoimmune diabetes in NOD mice, *Science* 302 (2003) 1223–1227.
- [71] A.S. Chong, J. Shen, J. Tao, D. Yin, A. Kuznetsov, M. Hara, L.H. Philipson, Reversal of diabetes in non-obese diabetic mice without spleen cell-derived beta cell regeneration, *Science* 311 (2006) 1774–1775.
- [72] J. Nishio, J.L. Gaglia, S.E. Turvey, C. Campbell, C. Benoist, D. Mathis, Islet recovery and reversal of murine type 1 diabetes in the absence of any infused spleen cell contribution, *Science* 311 (2006) 1775–1778.
- [73] A. Suri, B. Calderon, T.J. Esparza, K. Frederick, P. Bittner, E.R. Unanue, Immunological reversal of autoimmune diabetes without hematopoietic replacement of beta cells, *Science* 311 (2006) 1778–1780.
- [74] G. Gu, J. Dubauskaite, D.A. Melton, Direct evidence for the pancreatic lineage: NGN3+ cells are islet progenitors and are distinct from duct progenitors, *Development* 129 (2002) 2447–2457.
- [75] R.M. Seaberg, S.R. Smukler, T.J. Kieffer, G. Enikolopov, Z. Asghar, M.B. Wheeler, G. Korbutt, D. van der Kooy, Clonal identification of multipotent precursors from adult mouse pancreas that generate neural and pancreatic lineages, *Nat. Biotechnol.* 22 (2004) 1115–1124.
- [76] A. Suzuki, H. Nakauchi, H. Taniguchi, Prospective isolation of multipotent pancreatic progenitors using flow-cytometric cell sorting, *Diabetes* 53 (2004) 2143–2152.
- [77] S. Bonner-Weir, E. Toschi, A. Inada, P. Reitz, S.Y. Fonseca, T. Aye, A. Sharma, The pancreatic ductal epithelium serves as a potential pool of progenitor cells, *Pediatr. Diabetes* 5 (Suppl 2) (2004) 16–22.
- [78] M.C. Gershengorn, A.A. Hardikar, C. Wei, E. Geras-Raaka, B. Marcus-Samuels, B.M. Raaka, Epithelial-to-mesenchymal transition generates proliferative human islet precursor cells, *Science* 306 (2004) 2261–2264.
- [79] E. Hao, B. Tyrberg, P. Itkin-Ansari, J. Lakey, I. Geron, E. Monosov, M. Barcova, M. Mercola, F. Levine, Beta-cell differentiation from none-endocrine epithelial cells of the adult human pancreas, *Nat. Med.* 12 (2006) 310–316.
- [80] Y. Dor, J. Brown, O.I. Martinez, D.A. Melton, Adult pancreatic beta-cells are formed by self-duplication rather than stem-cell differentiation, *Nature* 429 (2004) 41–46.
- [81] J.J. Meier, A. Bhushan, A.E. Butler, R.A. Rizza, P.C. Butler, Sustained beta cell apoptosis in patients with long-standing type 1 diabetes: indirect evidence for islet regeneration? *Diabetologia* 48 (2005) 2221–2228.
- [82] J.J. Meier, J.C. Lin, A.E. Butler, R. Galasso, D.S. Martinez, P.C. Butler, Direct evidence of attempted beta cell regeneration in an 89-year-old patient with recent-onset type 1 diabetes, *Diabetologia* 49 (2006) 1838–1844.
- [83] M. Trucco, Regeneration of the cell, *J. Clin. Invest.* 115 (2005) 5–12.



# Metabolic aspects of pig-to-monkey (*Macaca fascicularis*) islet transplantation: implications for translation into clinical practice

A. Casu · R. Bottino · A. N. Balamurugan · H. Hara ·  
D. J. van der Windt · N. Campanile · C. Smetanka ·  
D. K. C. Cooper · M. Trucco

Received: 19 June 2007 / Accepted: 30 August 2007 / Published online: 25 October 2007  
© Springer-Verlag 2007

## Abstract

**Aims/hypothesis** Attempts to use an alternative source of islets to restore glucose homeostasis in diabetic patients require preclinical islet xenotransplantation models to be tested. These models raise questions about metabolic compatibility between species and the most appropriate metabolic parameters to be used to monitor graft function. The present study investigated and compared relevant gluco-metabolic parameters in pigs, monkeys and the pig-to-monkey islet transplantation model to gain insight into the potential clinical outcome of pig-to-human islet transplantation.

**Methods** Basal and IVGTT-stimulated blood glucose, C-peptide, insulin and glucagon levels were assessed in non-diabetic pigs and monkeys. The same parameters were used to evaluate the performance of porcine islet xenografts in diabetic monkeys.

**Results** Non-diabetic cynomolgus monkeys showed lower levels of fasting and stimulated blood glucose but higher levels of C-peptide and insulin than non-diabetic pigs. The

reported levels in humans lie between those of monkeys and pigs, and differences in metabolic parameters between pigs and humans appear to be smaller than those between pigs and cynomolgus monkeys. The transplantation data indicated that the degree of graft function (evaluated by the measurement of C-peptide levels) necessary to normalise blood glucose in the recipient was determined by the recipient levels rather than by the donor levels.

**Conclusions/interpretation** The differences between donor and recipient species may affect the transplantation outcome and need to be considered when assessing graft function in xenotransplantation models. Given the differences between monkeys and humans as potential recipients of pig islets, it should be easier to reach glucose homeostasis in pig-to-human than in pig-to-non-human primate islet xenotransplantation.

**Keywords** Diabetes · Non-human primates · Pancreatic islets · Pigs · Xenotransplantation

## Abbreviations

ACR <sub>Arg</sub>	acute C-peptide response after arginine
AIR <sub>Arg</sub>	acute insulin response after arginine
AST	arginine stimulation test
GGT1-DKO	GGT1 double-knockout
K <sub>G</sub>	glucose disappearance rate
MMT	mixed meal test

## Introduction

Despite the partial success of clinical islet allotransplantation in long-term follow-up, patients with type 1 diabetes

---

A. Casu and R. Bottino contributed equally to this study.

---

A. Casu (✉) · R. Bottino · A. N. Balamurugan ·  
D. J. van der Windt · N. Campanile · M. Trucco  
Division of Immunogenetics, Department of Pediatrics,  
Children's Hospital of Pittsburgh, Rangos Research Centre,  
Rm 6103, 3460 Fifth Avenue,  
Pittsburgh, PA 15213, USA  
e-mail: anc22@pitt.edu

A. N. Balamurugan · H. Hara · N. Campanile · C. Smetanka ·  
D. K. C. Cooper  
Thomas E. Starzl Transplantation Institute,  
University of Pittsburgh,  
Pittsburgh, PA, USA

may benefit from islet cell replacement therapy [1]. If less aggressive yet effective immunosuppressive protocols were found, islet transplantation could become a valid therapeutic alternative to insulin injections. The source of human islets for transplantation, however, remains limited. The use of animal islets, such as from the pig, offers a possible alternative that deserves consideration. As a preclinical experimental model, pig islet transplantation in non-human primate recipients is currently under investigation by different groups [2–4].

Intraportal injection of porcine islets, as recently reported by the groups of Larsen and Hering, allows a period of insulin independence in immunosuppressed diabetic monkey recipients [2, 3]. This model represents a good prototype to study the immunological aspects of islet xenotransplantation. However, as islet recipients, monkeys, in particular cynomolgus monkeys (*Macaca fascicularis*), display metabolic peculiarities which are only partially characterised [5–8]. Pigs, as a source of islet grafts, show a metabolic performance in vivo and in vitro which differs dramatically from that of monkeys [9–11]. These differences should be taken into consideration when engaging in xenotransplantation studies.

Successful pig-to-monkey islet xenotransplantation makes it possible to investigate how these differences influence the glucose metabolism of this combined model and to directly assess the behaviour of islets characterised by different functionalities within their physiological environment.

The aims of the present study were to define the metabolic compatibility between pigs and cynomolgus monkeys, to determine how it influences the pig-to-monkey islet transplantation model, and, more importantly, to help predict the performance of the islet graft based on the recipient's metabolic demand. Our data suggest that xenogeneic pig-to-human grafting has greater potential for success than pig-to-cynomolgus monkey grafting.

## Methods

**Animals** Twenty healthy male cynomolgus monkeys (*Macaca fascicularis*; Spring Scientific, Perkasie, PA, USA), 2–4 years of age and weighing 2.4–4.7 kg (median 3.6 kg), were studied. Catheters were placed into the jugular vein, carotid artery and stomach.

Seven wild-type outbred Large White female pigs (Wally Whippo, Enon Valley, PA, USA), 2–3 months of age and weighing 12–35 kg (median 24 kg) were used for metabolic studies. Two jugular vein catheters were placed for blood withdrawal and drug infusion.

For islet isolation we used pancreases from wild-type large white adult female pigs (Wally Whippo) and adult female pigs that were double-knockouts for *GGT1*, which encodes  $\alpha 1$ ,

3-galactosyltransferase gene (*GGT1*-DKO pigs; Revivicor, Blacksburg, VA, USA) [12], all weighing >180 kg.

All procedures were in accordance with the Principles of Laboratory Animal Care (National Society for Medical Research) and the Guide for the Care and Use of Laboratory Animals (NIH publication No. 86-23, revised 1985), and were approved by the University of Pittsburgh Animal Care and Use Committee.

**Metabolic parameters** Blood glucose (mmol/l) was measured in whole blood with a portable glucometer (Freestyle; Abbott Laboratories, Abbott Park, IL, USA). Serum levels of porcine and primate C-peptide (nmol/l) were measured by radioimmunoassay (Linco Research, St Charles, MO, USA) using species-specific antibodies. Aprotinin 0.05 kIU/l (Trasylol; Bayer Pharmaceuticals, West Haven, CT, USA) was added at the time of sampling. Primate and porcine insulin levels (pmol/l) in plasma or serum were measured by ELISA using species-specific assays (Mercodia, Uppsala, Sweden). Glucagon (pmol/l) was measured in serum by radioimmunoassay (Linco Research).

To summarise the metabolic status of each monkey before induction of diabetes, after induction of diabetes, and after islet transplantation until euthanasia or until vascular catheters were removed (8–120 days after transplantation), we recorded (1) mean blood glucose (mmol/l); (2) the prevalence of blood glucose readings >11.1 mmol/l (%); (3) the mean exogenous insulin requirement ( $\text{IU kg}^{-1} \text{ day}^{-1}$ ); and (4) mean porcine C-peptide levels.

**Intravenous glucose tolerance test** After an overnight fast, 0.5 g/kg of a 25% dextrose solution was infused i.v. over 1 min. Blood glucose was measured in the monkeys before and 2, 5, 15, 30, 60 and 90 min after infusion. Insulin, C-peptide and glucagon were measured before and 5, 15 and 90 min after infusion. In the pigs, blood glucose, C-peptide, insulin and glucagon were measured before and 5, 15, 30, 60 and 120 min after glucose infusion.

IVGTTs were performed in seven non-diabetic monkeys, five diabetic monkeys, four diabetic monkey recipients of functional porcine islet grafts, and seven non-diabetic pigs. The glucose disappearance rate ( $K_G$ ), which represents the log-linear (ln) decline in the glucose level during the first 30 min of the IVGTT, was calculated using the following formula [13]:

$$K_G = [\ln(\text{glucose level at 5 min}) - \ln(\text{glucose level at 30 min})] / 25 \times 100.$$

The mean of the ratios between C-peptide and insulin values at 5 and 15 min was expressed as a fold increase over the prechallenge value (time 0).

**Oral glucose tolerance test** Tests were performed in eight non-diabetic and two diabetic monkeys. After an overnight fast, 2 g/kg of glucose in a 50% dextrose solution was administered through the indwelling gastric catheter. Blood glucose was measured before and 15, 30, 60 and 90 min after the infusion. Primate C-peptide, insulin and glucagon were measured before and 15, 30, and 90 min after glucose infusion.

**Arginine stimulation test** Arginine stimulation tests (ASTs) were performed in seven non-diabetic and seven diabetic monkeys. After an overnight fast, 70 mg/kg of 10% arginine solution (Pharmacia & Upjohn Company, Kalamazoo, MI, USA) was administered and i.v. samples were drawn before and 2, 3, 4 and 5 min after the infusion for measurement of blood glucose, C-peptide, insulin and glucagon levels. The acute insulin response ( $AIR_{Arg}$ ) and the acute C-peptide response ( $ACR_{Arg}$ ) after the arginine stimulus were calculated as the difference between the mean at 2, 3, 4 and 5 min after stimulus and the corresponding prechallenge value of C-peptide and insulin [14, 15].

**Mixed meal test** Mixed meal tests (MMTs) were performed in three non-diabetic and three diabetic monkeys. After an overnight fast, a mixed meal (four Purina biscuits + half an apple [carbohydrate 30 g, fat 4 g, protein 6 g]) was administered orally, and serum samples were taken before and 60 and 120 min after the meal for determination of blood glucose, C-peptide, insulin and glucagon levels.

**Induction of diabetes** Diabetes was induced in ten monkeys by i.v. injection of streptozotocin 125–150 mg/kg (Zanosar; Sicor Pharmaceuticals, Irvine, CA, USA) in a single dose, as described in [16].

Diabetes was confirmed by persistent hyperglycaemia ( $>11.1$  mmol/l on at least two occasions) and by the need for insulin to prevent ketosis [17]. IVGTTs, OGTTs, ASTs and MMTs were performed 8–35 days (median 11 days) after induction of diabetes. Immunohistochemical analyses of pancreatic sections from four diabetic monkeys showed  $<1\%$  of insulin-positive cells compared with  $\sim 70\%$  of insulin-positive cells in healthy controls, as reported previously [16].

Diabetic monkeys were treated by continuous i.v. infusion of insulin (Humulin R; Eli Lilly, Indianapolis, IN, USA) to maintain the blood glucose level  $<11.1$  mmol/l and to prevent the development of ketosis. Insulin therapy was stopped 1.5 h before stimulation tests.

#### *Porcine islet isolation and transplantation into monkeys*

Nine monkeys underwent porcine islet transplantation. Porcine islets were isolated and purified according to a

standard procedure that involved low enzyme concentration, low digestion temperature and minimal mechanical digestion [18]. The overall quality of the islet preparations was evaluated as described in [18]: viability was  $>95\%$ , purity  $82.1 \pm 4.5\%$  ( $n=5$ ) islets/whole tissue, and the mean stimulation index was  $4.6 \pm 1.7$  ( $n=5$ ). A total of 40,000–100,000 islet equivalents (IEq)/kg was infused into the portal vein under direct vision at laparotomy under general anaesthesia. Transplantation was performed at least 2 weeks after diabetes induction (range 15–71 days, median 22 days). Insulin infusion was discontinued 2 h before islet infusion. In three monkeys (monkeys 8, 9 and 10), insulin was administered at  $0.03$ – $0.06$  IU  $\text{kg}^{-1} \text{h}^{-1}$  for 3 h after meals for 2 weeks following islet transplantation to minimise metabolic stress of the graft. Continuous insulin infusion was restored if blood glucose was consistently  $>11.1$  mmol/l.

The immunosuppressive regimen was based on antithymocyte globulin (Thymoglobulin; Genzyme Polyclonals, Lyon, France; 10 mg/kg i.v. on days  $-3$  and  $-1$ ), costimulatory blockade with a humanised anti-CD154 monoclonal antibody (ABI 793, a gift from Novartis, Basel, Switzerland; 25 mg/kg i.v. at days  $-1$ , 0, 4, 7, 10 and 14 and then every 5–7 days), and mycophenolate mofetil (Cellcept i.v. or oral suspension; Roche Laboratories, Nutley, NJ;  $75$ – $150$  mg  $\text{kg}^{-1} \text{day}^{-1}$  i.v. or twice daily orally beginning on day  $-4$ ), as previously described [4]. They also received dextran sulphate (Fluka Chemie, Buchs, Switzerland) 2 mg/h for 5 h after transplantation, aspirin 40 mg/kg every other day, and prostacyclin (Flolan; GlaxoSmithKline, Research Triangle Park, NC, USA)  $20$  mg  $\text{kg}^{-1} \text{min}^{-1}$  for 5 h after transplantation.

Islet graft function was monitored by measuring porcine C-peptide. An IVGTT was also performed in monkeys that showed an improvement in metabolic control 2 weeks after transplantation or when the clinical condition of the animal allowed it (range 14–45 days after transplantation, median 27 days).

**Statistical analyses** Experimental data are presented as means  $\pm$  SE. Human data obtained from the literature are presented as the range of values or mean of the published data [19, 20]. Student's *t* test was used to compare means. For ease of comparison, human data obtained from the literature are reported in the “Results” section rather than in the “Discussion”.

## Results

**Comparison of metabolic parameters between non-diabetic monkeys and pigs** Fasting blood glucose, C-peptide, insulin

**Table 1** Fasting blood glucose, C-peptide, insulin and glucagon levels in monkeys, pigs and humans

	Cynomolgus monkeys	Pigs	Humans
Blood glucose (mmol/l)	2.2–4.1 ( $3.2 \pm 0.1$ , $n=29$ ) <sup>a</sup>	4.0–5.2 ( $4.8 \pm 0.2$ , $n=7$ )	3.9–5.6 [20]
C-peptide (nmol/l)	0.47–3.14 ( $1.39 \pm 0.09$ , $n=37$ ) <sup>a</sup>	0.11–0.32 ( $0.16 \pm 0.04$ , $n=5$ )	0.17–0.66 [19]
Insulin (pmol/l)	15–201 ( $109 \pm 11$ , $n=27$ ) <sup>b</sup>	7–12 ( $9 \pm 1$ , $n=3$ )	34–138 [19]
Glucagon (pmol/l)	18.7–179.4 ( $54.3 \pm 6.9$ , $n=27$ ) <sup>a</sup>	11.3–13.8 ( $12.5 \pm 1.0$ , $n=3$ )	5.7–28.7 [19]

Data are ranges, with means $\pm$ SE and number of measurements in parentheses. Human data were obtained from the literature and were measured in venous plasma [19, 20]. C-peptide, insulin and glucagon levels in monkeys were significantly higher than corresponding levels in the pig, while blood glucose levels in monkeys were significantly lower than those in pigs (monkey vs pig, <sup>a</sup> $p<0.001$ ; <sup>b</sup> $p=0.021$ )

and glucagon values in monkeys, pigs and humans are presented in Table 1. Blood glucose in fasting non-diabetic monkeys ranged from 2.2 to 4.1 mmol/l and was significantly lower than the corresponding values in pigs (4.0–5.2 mmol/l;  $p<0.001$ ). Mean serum C-peptide and insulin values in monkeys were ten times higher than in pigs (C-peptide,  $1.39 \pm 0.09$  nmol/l in monkeys vs  $0.16 \pm 0.04$  nmol/l in pigs,  $p<0.001$ ; insulin,  $109 \pm 11$  pmol/l in monkeys vs  $9 \pm 1$  pmol/l in pigs,  $p=0.01$ ). Fasting glucagon values were significantly higher ( $p=0.001$ ) in monkeys ( $18.7$ – $179.4$  pmol/l) compared with pigs ( $11.3$ – $13.8$  pmol/l).

The data for healthy monkeys were also compared with the human data to better characterise similarities and differences that may help in predicting the metabolic performance of pig islets if considered for xenotransplantation in humans, even though the comparisons are limited by the difference in the testing conditions. Human fasting blood glucose values (Table 1) [20] appeared to be higher than those in monkeys, even after correction for the type of sample tested (i.e. whole blood in monkeys and plasma in humans) [21–23]. Human C-peptide [19] were consistently lower than monkey C-peptide levels and resembled the values seen in the pigs. The range of human glucagon levels [19] was lower than that in the monkeys, and again more closely resembled levels in the pigs.

Figure 1 shows the differences in blood glucose, C-peptide, insulin and glucagon values between monkeys and pigs after an i.v. glucose stimulus. Elicited insulin secretion was able to reduce blood glucose values in both monkeys and pigs (Fig. 1a). However, after the initial rise, blood glucose fell more slowly in pigs than in monkeys, as indicated by lower  $K_G$  values [monkeys,  $3.27$ – $8.22$  mmol  $l^{-1}$  min $^{-1}$  (mean  $6.17$  mmol  $l^{-1}$  min $^{-1}$ ); pigs,  $2.75$ – $6.70$  mmol  $l^{-1}$  min $^{-1}$  (mean  $3.64$  mmol  $l^{-1}$  min $^{-1}$ );  $p=0.04$ ].

As expected, the absolute C-peptide and insulin-stimulated values were higher in monkeys (mean at 5 min: C-peptide  $3.12 \pm 0.55$  nmol/l, insulin  $706 \pm 164$  pmol/l) than in pigs (mean at 5 min: C-peptide  $0.46 \pm 0.03$  nmol/l, insulin  $25 \pm 6$  pmol/l; Fig. 1b,c).

Nevertheless, the fold increases in C-peptide between time 0 and 5 min and between time 0 and 15 min were

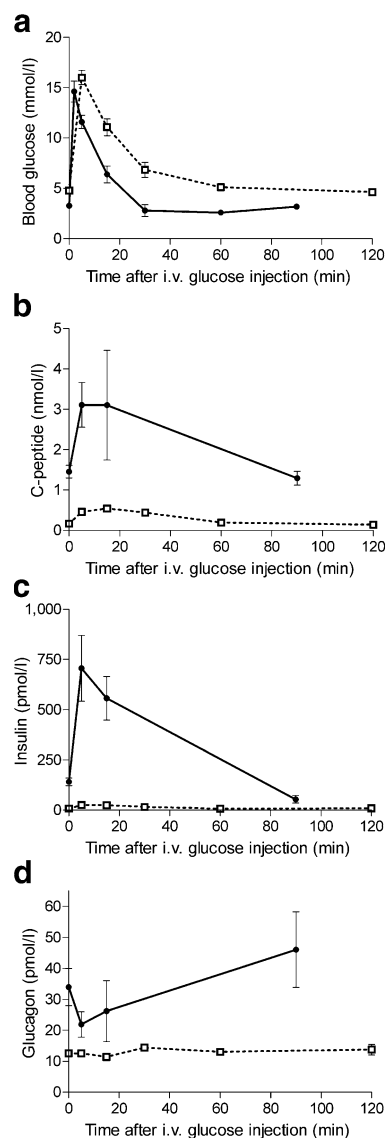


**Fig. 1** Comparison of metabolic parameters during IVGTT between healthy non-diabetic monkeys and pigs. Mean $\pm$ SE of blood glucose (a), C-peptide (b), insulin (c) and glucagon (d) during an IVGTT in non-diabetic monkeys (solid lines) and non-diabetic pigs (broken lines). (The SE is too small to be seen in the figure if below 10% of the mean value). Blood glucose concentrations decreased faster in monkeys than in pigs. The C-peptide and insulin concentrations after the stimulus were significantly higher in monkeys than in pigs



respectively  $3.2 \pm 0.5$  and  $3.9 \pm 0.7$  in pigs,  $2.4 \pm 0.8$  and  $2.9 \pm 1.2$  in monkeys (Fig. 1b). The fold increases in insulin between time 0 and 5 min and between time 0 and 15 min were  $3.5 \pm 0.7$  and  $2.9 \pm 0.7$  in pigs,  $5.6 \pm 1.8$  and  $4.8 \pm 2.1$  in monkeys (Fig. 1c).

Published data on IVGTTs performed in humans after i.v. injection of glucose at 0.3 or 0.5 g/kg showed C-peptide and insulin levels intermediate between those of pigs and monkeys. The fold increases between time 0 and 5 min and between time 0 and 15 min were (range) 2.5–3.5 and 2.1–3.0 respectively for C-peptide and 6.3–11.4 and 4.0–5.0 for insulin [24–30].

In both monkeys and pigs, glucagon fell after the stimulus (Fig. 1d); the fall was more pronounced in monkeys than in pigs.

**Comparison of metabolic parameters between non-diabetic and diabetic monkeys** The metabolic profile of the streptozotocin-treated monkeys was compared with that obtained before streptozotocin treatment. As expected, during the IVGTT the peak glucose concentration was significantly higher ( $p=0.03$ , 2 min after glucose infusion) in diabetic monkeys than in non-diabetic monkeys (Fig. 2a). Thereafter, the glucose levels decreased at a slower rate in diabetic than in non-diabetic monkeys, as shown by the lower  $K_G$  (mean  $1.01 \pm 0.12 \text{ mmol l}^{-1} \text{ min}^{-1}$ ,  $p<0.001$ ). The C-peptide increase, seen in non-diabetic monkeys, was absent in diabetic monkeys, with a slight fall 5 and 15 min after the glucose stimulus (Fig. 2b).

During the OGTT in non-diabetic monkeys, the increase in blood glucose was minimal (mean  $4.3 \pm 0.4 \text{ mmol/l}$  at 15 min), whereas blood glucose continued to rise in diabetic monkeys (Fig. 2c). In the non-diabetic monkeys, C-peptide (Fig. 2d) and insulin (not shown) reached a maximum at 30 min (C-peptide  $2.71 \pm 0.45 \text{ nmol/l}$ , insulin  $571 \pm 158 \text{ pmol/l}$ ), whereas there was no significant increase in diabetic monkeys. From the literature, C-peptide and insulin concentrations following stimulation in non-diabetic humans [31] are not very different from those detected in non-diabetic monkeys. In non-diabetic monkeys, the glucagon response was the mirror image of the C-peptide and insulin responses, with the lowest point at 30 min ( $25.1 \pm 9.2 \text{ pmol/l}$ ; not shown).

During the AST in non-diabetic monkeys (Fig. 2e,f), blood glucose remained stable while C-peptide (as insulin and glucagon) values rose at 2 min and then returned to prestimulus values at 5 min. The  $\text{AIR}_{\text{Arg}}$  ranged from 57 to 328 pmol/l and the  $\text{ACR}_{\text{Arg}}$  ranged from 0.20 to 0.89 nmol/l. Published data show that the human  $\text{AIR}_{\text{Arg}}$  is higher than the monkey  $\text{AIR}_{\text{Arg}}$ , whereas  $\text{ACR}_{\text{Arg}}$  is similar to that in monkeys; however, the absolute basal and stimulated values are lower in humans than in monkeys [15, 32, 33]. In diabetic monkeys during the AST, blood glucose remained

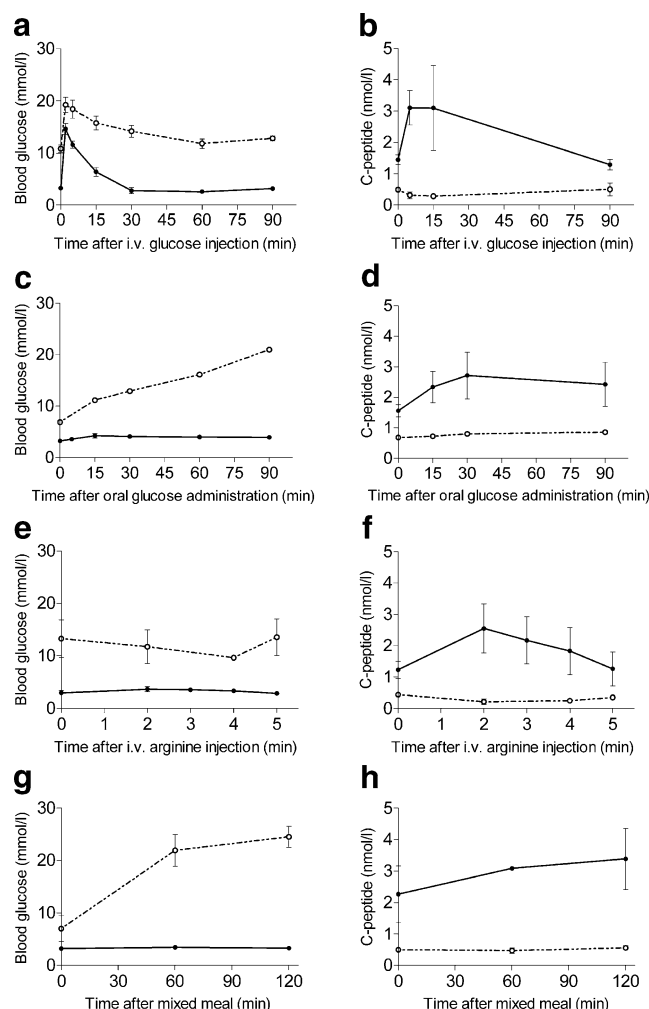


**Fig. 2** Comparison of metabolic parameters between non-diabetic and diabetic monkeys. Mean  $\pm$  SE of blood glucose levels (a, c, e, g) and primate C-peptide levels (b, d, f, h) during IVGTT (a, b), OGTT (c, d), AST (e, f) and MMT (g, h) in non-diabetic (solid lines) and diabetic (broken lines) monkeys. (SE was not calculated when fewer than three measurements were available). The primate C-peptide response to physiological stimuli was completely abolished in diabetic monkeys, and this was associated with a prolonged increase in the blood glucose level

stable at approximately 13.9 mmol/l and C-peptide showed no response ( $\text{ACR}_{\text{Arg}} -0.40$ – $0.02 \text{ nmol/l}$ ).

During the MMT (Fig. 2g,h), in non-diabetic monkeys blood glucose was stable and C-peptide and insulin (not shown) rose slowly, with a peak 120 min after the meal ( $3.39 \pm 0.97 \text{ nmol/l}$  and  $611 \pm 253 \text{ pmol/l}$ , respectively). In diabetic monkeys, blood glucose rose to its highest value ( $24.5 \pm 2.0 \text{ mmol/l}$ ) 120 min after the meal. No increase in monkey C-peptide was seen. In non-diabetic humans, data from the literature show that mean insulin and C-peptide values after meals increase but correspond to lower values in non-diabetic monkeys [31, 33, 34].



In summary, following streptozotocin treatment in monkeys blood glucose levels increased above 15 mmol/l and fasting levels of endogenous C-peptide declined to values corresponding to 12–33% of the C-peptide levels before diabetes induction. Insulin was needed to maintain blood glucose <11 mmol/l and to prevent ketosis. Any residual endogenous C-peptide did not respond to physiological stimuli, as shown by the results of the dynamic tests and by the absence of correlation between endogenous C-peptide and blood glucose levels at the times of sampling. Furthermore, while attempting to maintain blood glucose <11 mmol/l in diabetic monkeys, no correlation was found between endogenous C-peptide levels and the mean daily requirement of exogenous insulin per kg of body weight (data not shown).

*Metabolic parameters in diabetic monkeys following porcine islet transplantation* Following porcine islet transplantation, five monkeys (monkeys 2, 7, 8, 9 and 10) improved their metabolic control of glucose (Tables 2 and 3). This was defined as a mean blood glucose level of <8.9 mmol/l accompanied by a reduction in the requirement for exogenous insulin therapy ( $\leq 0.50$  IU kg<sup>-1</sup> day<sup>-1</sup>). In two of the five monkeys (monkeys 8 and 10), insulin therapy was unnecessary for 34 and 16 days, respectively. On average, porcine C-peptide during the follow-up period after islet transplantation (8–120 days) in these five monkeys was >0.20 nmol/l.

Figure 3a shows the porcine C-peptide levels in monkeys with improved metabolic control compared with those that did not experience any improvement. The porcine C-peptide values were mainly above the established threshold of 0.20 nmol/l. Similarly, the daily insulin requirement in monkeys that had a mean porcine C-peptide level

>0.20 nmol/l was below the threshold of 0.50 IU kg<sup>-1</sup> day<sup>-1</sup> (Fig. 3b). In the monkeys that experienced an improvement in metabolic control, the exogenous insulin requirement was reduced to less than half of that necessary before islet transplantation (Tables 2 and 3). In contrast, the insulin requirement remained stable or increased in those that did not show improved metabolic control (1.2- to 5.2-fold increase compared with before transplantation). Any increase in requirement may have been associated with the stress induced by the surgical procedure and the immunosuppressive therapy. Monkey 1, with only a partial improvement in metabolic parameters (mean blood glucose 10.9 mmol/l, mean porcine C-peptide 0.18 nmol/l) had a reduction in mean insulin requirement to 52% of the pretransplantation requirement (1.38 IU kg<sup>-1</sup> day<sup>-1</sup>).

The monkeys with improved metabolic control also demonstrated more stable glucose values, as indicated by a lower frequency of blood glucose levels >11 mmol/l (23–63% before islet transplantation, 0–21% after transplantation).

Achievement of better metabolic control after islet transplantation appeared to be mainly influenced by the islet mass infused, and it seemed to be independent of donor characteristics (Table 3) or of residual endogenous C-peptide, the level of which did not correlate with the reduction in insulin requirement or with insulin independence until the porcine graft was functional.

The negative response of primate C-peptide to metabolic challenges, with a fall after the stimulus, as seen in diabetic monkeys (Fig. 2), also suggests that the residual islet mass was not able to contribute to the metabolic improvement. This was shown by the analysis of the IVGTTs performed after transplantation in four of the monkeys with a

**Table 2** Mean metabolic values in monkeys before streptozotocin (healthy non-diabetic) and during the diabetic state

Monkey no.	Before streptozotocin: non-diabetic state	After streptozotocin: diabetic state		
	Mean glucose <sup>a</sup> (mmol/l)	Mean glucose <sup>a</sup> (mmol/l)	Glucose >11.1 mmol/l <sup>b</sup> (%)	Mean insulin dosage (IU kg <sup>-1</sup> day <sup>-1</sup> )
1	3.4 (n=1)	12.0±0.5 (n=121)	55 (n=121)	2.67±0.14 (n=70)
3	3.2 (n=1)	13.1±0.3 (n=185)	77 (n=185)	2.17±0.11 (n=95)
4	2.2 (n=2)	11.5±0.6 (n=46)	47 (n=46)	1.03±0.03 (n=23)
5	2.9 (n=2)	10.2±0.8 (n=37)	51 (n=37)	0.58±0.03 (n=21)
6	3.3 (n=2)	13.0±0.9 (n=30)	73 (n=30)	0.75±0.05 (n=15)
2 <sup>c</sup>	4.6 (n=1)	10.7±0.7 (n=54)	48 (n=54)	2.25±0.10 (n=60)
7 <sup>c</sup>	3.9 (n=1)	13.4±1.6 (n=28)	59 (n=28)	0.46±0.02 (n=14)
8 <sup>c</sup>	3.9±0.2 (n=5)	9.1±1.0 (n=28)	32 (n=28)	0.96±0.03 (n=14)
9 <sup>c</sup>	2.9±0.2 (n=4)	8.2±0.5 (n=86)	23 (n=86)	0.80±0.02 (n=43)
10 <sup>c</sup>	3.0±0.1 (n=6)	12.9±0.9 (n=30)	63 (n=30)	1.04±0.07 (n=15)

Data are means±SE, with number of observations in parentheses.

<sup>a</sup> Mean glucose is the average of morning and evening levels.

<sup>b</sup> Percentage of glucose measurements above 11.1 mmol/l for each animal.

<sup>c</sup> Monkeys 2, 7, 8, 9 and 10 showed an improvement in metabolic control.

**Table 3** Mean metabolic values in monkeys after porcine islet transplantation

Monkey no.	Type of donor pig	IEq/kg	Mean glucose <sup>a</sup> (mmol/l)	Glucose >11.1 mmol/l <sup>b</sup> (%)	Mean insulin <sup>c</sup> (IU kg <sup>-1</sup> day <sup>-1</sup> )	Porcine C-peptide (nmol/l)	Follow-up after transplantation (days)
1	Wild-type	40 000	10.9±0.4 (n=79)	46 (n=79)	1.38±0.10 (52%) (n=39)	0.18±0.04 (n=16)	39 <sup>g</sup>
3 <sup>f</sup>	—	—	—	—	—	—	—
4	<i>GGT1</i> -DKO	40 000	9.4±1.0 (n=15)	27 (n=15)	1.28±0.29 (124%) (n=8)	0.11±0.02 (n=5)	8 <sup>i</sup>
5	<i>GGT1</i> -DKO	47 000	9.8±0.8 (n=36)	35 (n=36)	3.05±0.51 (521%) (n=19)	0.07±0.02 (n=11)	19 <sup>h</sup>
6	<i>GGT1</i> -DKO	40 000	15.8±0.4 (n=236)	76 (n=236)	2.20±120 (293%) (n=120)	0.04±0.01 (n=21)	120 <sup>h</sup>
2 <sup>e</sup>	Wild-type	46 000	8.8±0.3 (n=118)	21 (n=118)	0.50±0.06 (22%) (n=60)	0.26±0.03 (n=25)	60 <sup>g</sup>
7 <sup>e</sup>	Wild-type	100 000	6.8±2.1 (n=13)	7 (n=13)	0.06±0.05 (13%) (n=8)	0.93±0.19 (n=5)	8 <sup>i</sup>
8 <sup>d,e</sup>	Wild-type	95 000	5.3±0.16 (n=84)	0 (n=84)	0.04±0.01 (4%) (n=43) <sup>d</sup>	0.21±0.05 (n=13)	43 <sup>h</sup>
9 <sup>e</sup>	<i>GGT1</i> -DKO	77 000	8.5±0.3 (n=40)	7 (n=40)	0.35±0.03 (44%) (n=21)	0.32±0.03 (n=6)	21 <sup>h</sup>
10 <sup>d,e</sup>	<i>GGT1</i> -DKO	100 000	6.8±0.4 (n=73)	7 (n=73)	0.15±0.07 (14%) (n=39) <sup>d</sup>	0.28±0.07 (n=8)	39 <sup>i</sup>

Data are means±SE, with number of observations in parentheses.

<sup>a</sup> Mean glucose represents the average of morning and evening levels.

<sup>b</sup> Percentage of glucose measurements above 11.1 mmol/l obtained in each animal.

<sup>c</sup> Mean insulin dosage after transplantation is the absolute value; percentage of the dosage before transplantation is given in parentheses.

<sup>d</sup> Insulin therapy was discontinued 2 weeks after porcine islet transplantation in monkeys 8 and 10.

<sup>e</sup> Monkeys 2, 7, 8, 9 and 10 showed an improvement in metabolic control.

<sup>f</sup> Monkey 3 was not transplanted because of intolerance to immunosuppressive drugs.

Reasons for end of follow-up: <sup>g</sup> electively killed for undetectable graft function; <sup>h</sup> loss of vascular lines; <sup>i</sup> killed for clinical reasons (severe anaemia, gastric dilatation)

functioning graft. On the contrary, although none of these IVGTTs were completely normal [ $K_G$  ranged from 1.09–3.04 mmol l<sup>-1</sup> min<sup>-1</sup> (mean 1.60±0.30 mmol l<sup>-1</sup> min<sup>-1</sup>), below the normal values ( $p<0.001$ )], a clear porcine C-peptide response was indeed seen (Fig. 4).

## Discussion

During the last 6 years, clinical trials of allotransplantation of pancreatic islets from deceased donors have supplied sufficient insulin to abrogate the need for exogenous insulin in patients with type 1 diabetes, at least for a limited period [1]. Even if the control of diabetes was not complete, islet transplantation was able to improve the management of unstable type 1 diabetes [1, 35].

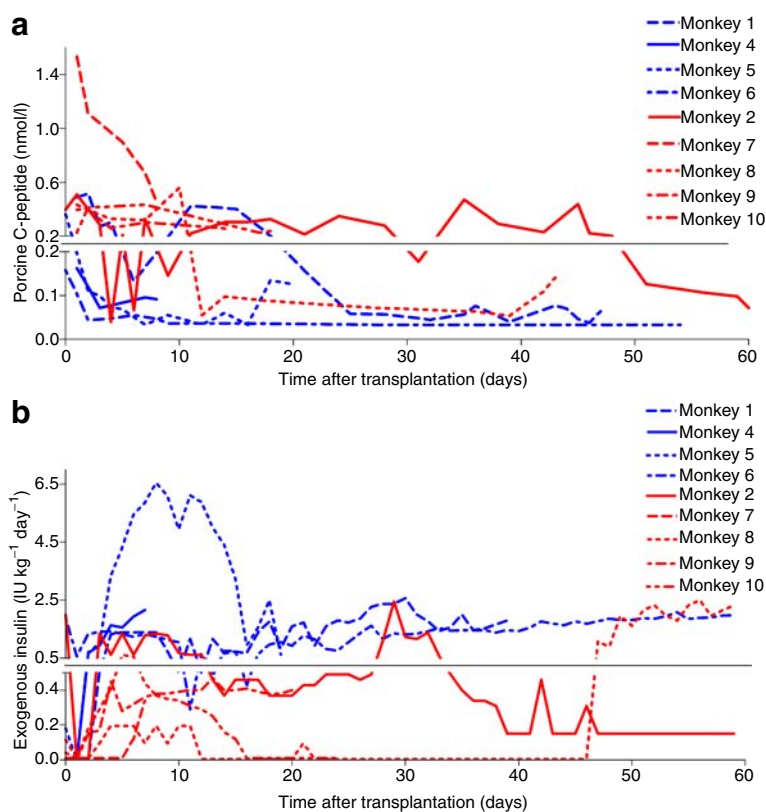
One of the problems presented by these recent clinical trials is that two to three pancreases are needed to provide an islet mass sufficient to establish normal metabolic control in the majority of patients. Furthermore, following transplantation, a number of mechanisms, only partially

understood, contribute to a gradual but eventually complete loss of islet mass [1, 35]. Both of these observations render the availability of deceased organ donors even more insufficient in relation to the number of diabetic patients who might benefit from this therapy. Besides the attention being devoted to the search for strategies to reduce human islet cell loss after transplantation, thus prolonging their function, it would be beneficial to be able to transplant animal islets, as these would provide a virtually unlimited source for clinical needs.

Pigs have been considered as possible sources of islets for transplantation because of the similarity between human and porcine insulin, the number of available islets per animal, and ethical acceptability [36, 37].

Preclinical studies are necessary to test the ability of pig islets to work in vivo in a recipient of a species similar to humans. In this regard, recent data indicate that wild-type neonatal or adult pig islets can survive for weeks in monkey recipients [2, 3]. One of these studies [3], as well as our own studies [4, 16], were performed in cynomolgus monkeys. These Old World monkeys represent a good model for islet transplantation studies [3, 7, 36]. They can

**Fig. 3** Porcine C-peptide levels and exogenous insulin requirements in diabetic monkeys after porcine islet transplantation. **a** Porcine C-peptide levels in most monkeys with improved metabolic control (red lines) were higher than in monkeys that demonstrated no improvement in metabolic control (blue lines). The C-peptide level in monkeys with improved metabolic control was generally  $>0.20$  nmol/l. **b** Insulin requirement in transplanted monkeys with mean porcine C-peptide  $>0.20$  nmol/l (red lines) was lower than that in monkeys with mean porcine C-peptide  $<0.20$  nmol/l (blue lines). The insulin requirement in the majority of monkeys with a mean porcine C-peptide level of  $>0.20$  nmol/l was  $<0.5$  IU  $\text{kg}^{-1} \text{day}^{-1}$



be rendered diabetic by the administration of streptozotocin [7, 16, 38, 39] or by total pancreatectomy [2, 40], and prior to islet transplantation the induced diabetes can be controlled by insulin injections for long periods of time.

The pig-to-monkey transplantation model presents immunological incompatibilities and it therefore remains a good model to study the immunological aspects of islet xenotransplantation. On the other hand, relevant metabolic differences between the two animal species may have an impact on the outcome of islet transplantation, not only in this model but also, more importantly, in clinical applications of the future. This appears to be particularly important when parameters such as blood glucose levels, C-peptide levels and insulin levels are used to monitor the xenograft function.

In the present study we investigated differences in metabolism relating to glucose homeostasis in monkeys and pigs and in the pig-to-monkey islet transplantation setting. The purpose was to identify metabolic parameters that can aid in monitoring and evaluating the success of islet xenotransplantation, and thus aid in translating this model into clinical practice. The data we present clearly demonstrate differences in metabolic parameters between cynomolgus monkeys and pigs. Monkeys are characterised by high circulating C-peptide and insulin levels and by low glucose levels, observations that concur with those reported previously by others [5–8]. On the other hand, pigs exhibit low C-peptide and insulin levels and

higher blood glucose levels [9, 10]. Although both species responded to glucose and food stimulation, differences in insulin output and glucose homeostasis were also noted. The relatively poor response of pig islets to glucose is well known *in vitro*, where, however, it does not seem to be due to alterations in glucose sensing or metabolism [11]. The molecular differences in porcine and monkey C-peptide and insulin are not substantial, but these differences may interfere in their kinetics and *in vivo* activity. Human and porcine insulins, however, have demonstrated equivalent therapeutic activity [41].

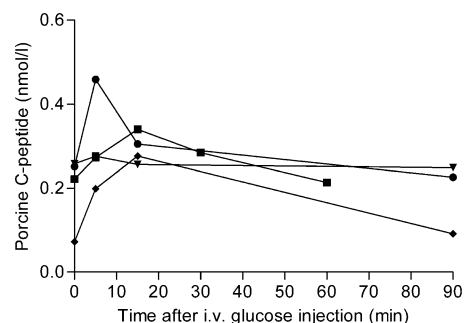


**Fig. 4** Porcine C-peptide responses to IVGTT in four monkeys that showed an improvement in metabolic control after porcine islet transplantation. The IVGTTs were performed on postoperative day 46 in monkey 2 (squares), 27 in monkey 8 (diamonds), 21 in monkey 9 (triangles) and 24 in monkey 10 (circles)

When target glucose levels were similar and the same insulin formulation used, we observed that exogenous s.c. insulin requirements in diabetic pigs ( $0.67 \pm 0.05 \text{ IU kg}^{-1} \text{ day}^{-1}$ ) to maintain a mean blood glucose of  $12.4 \pm 2.3 \text{ mmol/l}$ ;  $n=3$ ) were lower than in diabetic monkeys ( $1.92 \pm 0.20 \text{ IU kg}^{-1} \text{ day}^{-1}$  to maintain a mean blood glucose concentration of  $14.7 \pm 1.0 \text{ mmol/l}$   $n=4$ ). In this respect, human requirements are between those of pigs and monkeys. This may be of importance in respect to the eventual transfer of pig islet transplantation into clinical practice, since human insulin demands are lower than those of the monkeys [42].

Sustained normoglycaemia in the monkey is associated with endogenous C-peptide levels ranging from 0.47 to 3.14 nmol/l; in pigs the range is between 0.11 and 0.32 nmol/l. In the pig-to-monkey islet transplantations, monkeys with porcine C-peptide levels within the normal range for non-diabetic pigs but below normal for monkeys showed an improvement in gluco-metabolism, with insulin independence seen in some cases. Nevertheless, beta cell function associated with higher porcine C-peptide levels should be expected to stably normalise a diabetic monkey. Based on the metabolic performance of porcine islet grafts in our monkey recipients, we estimate that porcine C-peptide levels of at least 0.47 nmol/l should be reached to achieve protracted normalisation. Again, since the normal C-peptide range in a non-diabetic human is lower than that in a monkey, the metabolic demand on pig islet grafts should be lower in a clinical application. The improved metabolic control obtained in monkey recipients following pig islet transplantation was associated with relatively low levels of porcine C-peptide. In particular, we found that a concentration of porcine C-peptide of 0.20 nmol/l provided a threshold for significant improvement. Thus, low levels may be sufficient to prevent chronic complications, as also observed in diabetic patients with residual C-peptide production or in partially functioning islet transplants [1, 43–45].

The data suggest that the level of graft function (evaluated by the measurement of C-peptide levels) necessary to normalise blood glucose in the recipient is determined by the recipient levels rather than by the donor levels. Considering the metabolic target of humans and the performance of pig islets in primates, whose metabolic demand is higher than that of pigs and, more importantly, higher than that of humans, we can conclude that a good metabolic outcome could be reached in humans.

Islet xenotransplantation is still in an experimental phase and requires further exploration. Observations from pre-clinical models suggest that, in addition to immunological aspects linked to species differences, metabolic differences between donor and recipient species are important matters for further investigation and may be key to the success of islet xenotransplantation. An in-depth study of this will aid our understanding of the dynamics of insulin-producing

islet cells and may facilitate the translation of islet xenotransplantation into clinical trials.

**Acknowledgements** We gratefully acknowledge the help of P.P.M. Rood, C. Knoll, A. Sands, A. Funair and A. Styche. We also thank the following surgeons: N. Murase, X. Zhu, Y. Zhu, M. Ezzelarab, H.-C. Tai and Y. J. Lin. This work was supported in part by Juvenile Diabetes Research Foundation grant no. 4-2004-786, Department of Defense grant no. W81XWH-06-1-0317 and American Diabetes Association grant no. 1-04-RA-15.

**Duality of interest** The authors declare that there is no duality of interest associated with this manuscript.

## References

1. Shapiro AM, Ricordi C, Hering BJ et al (2006) International trial of the Edmonton protocol for islet transplantation. *N Engl J Med* 355:1318–1330
2. Cardona K, Korbitt GS, Milas Z et al (2006) Long-term survival of neonatal porcine islets in nonhuman primates by targeting costimulation pathways. *Nat Med* 12:304–306
3. Hering BJ, Wijkstrom M, Graham ML et al (2006) Prolonged diabetes reversal after intraportal xenotransplantation of wild-type porcine islets in immunosuppressed nonhuman primates. *Nat Med* 12:301–303
4. Rood P, Bottino R, Balamurugan AN et al (2007) Reduction of early graft loss after intraportal porcine islet transplantation in monkeys. *Transplantation* 83:202–210
5. Cameron JL, Koerker DJ, Steiner RA (1985) Metabolic changes during maturation of male monkeys: possible signals for onset of puberty. *Am J Physiol* 249:E385–E391
6. Honjo S, Kondo Y, Cho F (1976) Oral glucose tolerance test in the cynomolgus monkey (*Macaca fascicularis*). *Lab Anim Sci* 26:771–776
7. Koulmanda M, Qipo A, Chebrolo S, O'Neil J, Auchincloss H, Smith RN (2003) The effect of low versus high dose of streptozotocin in cynomolgus monkeys (*Macaca fascicularis*). *Am J Transplant* 3:267–272
8. Litwak KN, Cefalu WT, Wagner JD (1998) Streptozotocin-induced diabetes mellitus in cynomolgus monkeys: changes in carbohydrate metabolism, skin glycation, and pancreatic islets. *Lab Anim Sci* 48:172–178
9. Kobayashi K, Kobayashi N, Okitsu T et al (2004) Development of a porcine model of type 1 diabetes by total pancreatectomy and establishment of a glucose tolerance evaluation method. *Artif Organs* 28:1035–1042
10. Shokouh-Amiri MH, Rahimi-Saber S, Andersen HO, Jensen SL (1996) Pancreas autotransplantation in pig with systemic or portal venous drainage. Effect on the endocrine pancreatic function after transplantation. *Transplantation* 61:1004–1009
11. Rabuazzo AM, Davalli AM, Buscema M et al (1995) Glucose transport, phosphorylation, and utilization in isolated porcine pancreatic islets. *Metabolism* 44:261–266
12. Phelps CJ, Koike C, Vaught TD et al (2003) Production of alpha 1,3-galactosyltransferase-deficient pigs. *Science* 299:411–414
13. Tigno XT, Gerzanich G, Hansen BC (2004) Age-related changes in metabolic parameters of nonhuman primates. *J Gerontol A Biol Sci Med Sci* 59:1081–1088
14. McCulloch DK, Koerker DJ, Kahn SE, Bonner-Weir S, Palmer JP (1991) Correlations of in vivo beta-cell function tests with beta-cell mass and pancreatic insulin content in streptozotocin-administered baboons. *Diabetes* 40:673–679



15. Ward WK, Bolgiano DC, McKnight B, Halter JB, Porte D Jr (1984) Diminished B cell secretory capacity in patients with noninsulin-dependent diabetes mellitus. *J Clin Invest* 74:1318–1328
16. Rood PP, Bottino R, Balamurugan AN et al (2006) Induction of diabetes in cynomolgus monkeys with high-dose streptozotocin: adverse effects and early responses. *Pancreas* 33:287–292
17. Expert Committee on the Diagnosis and Classification of Diabetes Mellitus (1997) Report of the Expert Committee on the Diagnosis and Classification of Diabetes Mellitus. *Diabetes Care* 20:1183–1197
18. Bottino R, Balamurugan AN, Smetanka C et al (2007) Isolation outcome and functional characteristics of young and adult pig pancreatic islets for transplantation studies. *Xenotransplantation* 14:74–82
19. Greenspan FS, Gardner DG (2006) Normal hormone reference ranges. In: Greenspan FS, Gardner DG (eds) *Basic and clinical endocrinology*, 7th edn. McGraw-Hill Companies, New York, pp 920–938
20. Genuth S, Alberti KG, Bennett P et al (2003) Follow-up report on the diagnosis of diabetes mellitus. *Diabetes Care* 26:3160–3167
21. World Health Organization (1999) Definition, diagnosis and classification of diabetes mellitus and its complications. Report of a WHO consultation. Part 1: diagnosis and classification of diabetes mellitus. Available from [http://www.staff.ncl.ac.uk/philip.home/who\\_dmc.htm](http://www.staff.ncl.ac.uk/philip.home/who_dmc.htm), last accessed in September 2007
22. Alberti KG, Zimmet PZ (1998) Definition, diagnosis and classification of diabetes mellitus and its complications. Part 1: diagnosis and classification of diabetes mellitus. Provisional report of a WHO consultation. *Diabet Med* 15:539–553
23. D'Orazio P, Burnett RW, Fogh-Andersen N et al (2005) Approved IFCC recommendation on reporting results for blood glucose (abbreviated). *Clin Chem* 51:1573–1576
24. Bakalov VK, Cooley MM, Quon MJ et al (2004) Impaired insulin secretion in the Turner metabolic syndrome. *J Clin Endocrinol Metab* 89:3516–3520
25. Breda E, Cobelli C (2001) Insulin secretion rate during glucose stimuli: alternative analyses of C-peptide data. *Ann Biomed Eng* 29:692–700
26. Kjems LL, Volund A, Madsbad S (2001) Quantification of beta-cell function during IVGTT in type II and non-diabetic subjects: assessment of insulin secretion by mathematical methods. *Diabetologia* 44:1339–1348
27. Monauni T, Zenti MG, Cretti A et al (2000) Effects of glucosamine infusion on insulin secretion and insulin action in humans. *Diabetes* 49:926–935
28. Nyholm B, Porksen N, Juhl CB et al (2000) Assessment of insulin secretion in relatives of patients with type 2 (non-insulin-dependent) diabetes mellitus: evidence of early beta-cell dysfunction. *Metabolism* 49:896–905
29. Overgaard RV, Jelic K, Karlsson M, Henriksen JE, Madsen H (2006) Mathematical beta cell model for insulin secretion following IVGTT and OGTT. *Ann Biomed Eng* 34:1343–1354
30. Vicini P, Zachwieja JJ, Yarasheski KE, Bier DM, Caumo A, Cobelli C (1999) Glucose production during an IVGTT by deconvolution: validation with the tracer-to-tracee clamp technique. *Am J Physiol* 276:E285–E294
31. Dalla Man C, Campioni M, Polonsky KS et al (2005) Two-hour seven-sample oral glucose tolerance test and meal protocol: minimal model assessment of beta-cell responsivity and insulin sensitivity in nondiabetic individuals. *Diabetes* 54:3265–3273
32. Larsson H, Ahren B (1998) Glucose-dependent arginine stimulation test for characterization of islet function: studies on reproducibility and priming effect of arginine. *Diabetologia* 41:772–777
33. Rickels MR, Schutta MH, Markmann JF, Barker CF, Naji A, Teff KL (2005)  $\beta$ -Cell function following human islet transplantation for type 1 diabetes. *Diabetes* 54:100–106
34. Marena S, Montegrosso G, De Michieli F, Pisu E, Pagano G (1992) Comparison of the metabolic effects of mixed meal and standard oral glucose tolerance test on glucose, insulin and C-peptide response in healthy, impaired glucose tolerance, mild and severe non-insulin-dependent diabetic subjects. *Acta Diabetol* 29:29–33
35. Ryan EA, Paty BW, Senior PA et al (2005) Five-year follow-up after clinical islet transplantation. *Diabetes* 54:2060–2069
36. Rood PP, Buhler LH, Bottino R, Trucco M, Cooper DK (2006) Pig-to-nonhuman primate islet xenotransplantation: a review of current problems. *Cell Transplant* 15:89–104
37. Rother KI, Harlan DM (2004) Challenges facing islet transplantation for the treatment of type 1 diabetes mellitus. *J Clin Invest* 114:877–883
38. Tal MG, Hirshberg B, Neeman Z et al (2004) Induction of diabetes in nonhuman primates by means of temporary arterial embolization and selective arterial injection of streptozotocin. *Radiology* 230:163–168
39. Theriault BR, Thistlethwaite JR Jr, Levisetti MG et al (1999) Induction, maintenance, and reversal of streptozotocin-induced insulin-dependent diabetes mellitus in the juvenile cynomolgus monkey (*Macaca fascicularis*). *Transplantation* 68:331–337
40. Ericzon BG, Wijnen RM, Kubota K, vd Bogaard A, Kootstra G (1991) Diabetes induction and pancreatic transplantation in the cynomolgus monkey: methodological considerations. *Transpl Int* 4:103–109
41. Richter B, Neises G (2003) 'Human' insulin versus animal insulin in people with diabetes mellitus. *Cochrane Database Syst Rev*: CD003816
42. International Society for Pediatric and Adolescent Diabetes (2000) ISPAD consensus guidelines for the management of type 1 diabetes mellitus in children and adolescents. Consensus guidelines 2000. Available from <http://www.diabetesguidelines.com/health/dwk/pro/guidelines/ISPAD/ispad.asp>, last accessed in September 2007
43. Diabetes Control and Complications Trial Research Group (1998) Effect of intensive therapy on residual beta-cell function in patients with type 1 diabetes in the diabetes control and complications trial. A randomized, controlled trial. The Diabetes Control and Complications Trial Research Group. *Ann Intern Med* 128:517–523
44. Fiorina P, Folli F, Bertuzzi F et al (2003) Long-term beneficial effect of islet transplantation on diabetic macro-/microangiopathy in type 1 diabetic kidney-transplanted patients. *Diabetes Care* 26:1129–1136
45. Fiorina P, Gremizzi C, Maffi P et al (2005) Islet transplantation is associated with an improvement of cardiovascular function in type 1 diabetic kidney transplant patients. *Diabetes Care* 28:1358–1365



# On the Use of General Control Samples for Genome-wide Association Studies: Genetic Matching Highlights Causal Variants

Diana Luca,<sup>1,7</sup> Steven Ringquist,<sup>2,7</sup> Lambertus Klei,<sup>3</sup> Ann B. Lee,<sup>1</sup> Christian Gieger,<sup>4,5</sup> H.-Erich Wichmann,<sup>4,5</sup> Stefan Schreiber,<sup>6</sup> Michael Krawczak,<sup>6</sup> Ying Lu,<sup>2</sup> Alexis Styche,<sup>2</sup> Bernie Devlin,<sup>3</sup> Kathryn Roeder,<sup>1,7,\*</sup> and Massimo Trucco<sup>2,7</sup>

Resources being amassed for genome-wide association (GWA) studies include “control databases” genotyped with a large-scale SNP array. How to use these databases effectively is an open question. We develop a method to match, by genetic ancestry, controls to affected individuals (cases). The impact of this method, especially for heterogeneous human populations, is to reduce the false-positive rate, inflate other spuriously small p values, and have little impact on the p values associated with true positive loci. Thus, it highlights true positives by downplaying false positives. We perform a GWA by matching Americans with type 1 diabetes (T1D) to controls from Germany. Despite the complex study design, these analyses identify numerous loci known to confer risk for T1D.

## Introduction

Systematic GWA studies are critically dependent on the availability of very large and well-characterized control populations. With a different degree of structure in modern populations, ideally, multiple, diverse, and large control populations will be used. As platforms for GWA become standardized, numerous sources of pregenotyped control individuals are becoming available. Typically, many more controls are available than cases, and we believe these controls can be advantageous for discovering risk loci and for controlling the false-positive rate. For example, the data analyzed here include 416 Americans of European descent diagnosed with T1D (MIM 222100) and a control database of 2159 individuals from different regions of Germany.

Ancestry matching based on nongenetic variables<sup>1</sup> and SNP genotypes<sup>2</sup> for genetic-association studies has been proposed previously. Our approach, which we call genetic matching or GEM, goes further in that we show how to systematically obtain favorable matching by using a panel of genetic markers and how to determine outlying individuals as well as individuals that cannot be successfully matched to others in the available registry. By simulations, we will contrast matching to a commonly used method for controlling the confounding of ancestry, namely the use of eigenvector analysis<sup>3</sup> via Eigenstrat<sup>4</sup> to identify predictors of ancestry; for the real data, we contrast matching to both Eigenstrat and identification of common ancestry, such as European American.

We propose matching on the basis of genetic similarities derived from eigenvector decomposition (EVD), making our initial analyses similar to that taken in Eigenstrat.<sup>4</sup> The best known form of matching is matched pairs (pMatch); however, assuming the criterion for matching are sufficient to remove the effects of unmeasured confounding, an alternative to matched pairs known as full matching (fMatch) is optimal.<sup>5</sup> Consider a scenario in which three cases (a, b, and c) and three controls (x, y, and z) fall into two distinct ancestral clusters (a, x, and y) and (b, c, and z). Matching pairs creates three strata, (a and x), (c and z), and (b and y), but the pair (b and y) does not define a homogeneous strata. Alternatively, fMatch minimizes the total distance between individuals within strata with the constraint being that each stratum includes a single case and one or more controls, or vice versa, i.e., clusters (a, x, and y) and (b, c, and z). Of the two, fMatch is optimal because case and control samples are unlikely to have identical distributions of ancestry, and in this situation, forcing each case to match a unique control leads to suboptimal matches. (pMatch can be very useful, however, in designing follow-up studies that require preselection of case and control samples.)

In large association studies, the sample typically includes some individuals with widely varying ancestry. EVD is highly sensitive to outlying observations. A few points lying far from the majority of the data can determine multiple principal axes of the representation. Indeed, outliers can obscure the discovery of axes that potentially separate the data into distinct types. For this reason, individuals

<sup>1</sup>Department of Statistics, Carnegie Mellon University; Pittsburgh, PA 15213, USA; <sup>2</sup>Division of Immunogenetics, Department of Pediatrics, Children's Hospital, Pittsburgh, PA 15213, USA; <sup>3</sup>Department of Psychiatry, University of Pittsburgh School of Medicine, Pittsburgh, PA 15213, USA; <sup>4</sup>GSF National Research Center for Environment and Health, Institute of Epidemiology, Neuherberg 85764, Germany; <sup>5</sup>Ludwig-Maximilians-University Munich, IBE, Chair of Epidemiology, Munich 85764, Germany; <sup>6</sup>Institute of Clinical Molecular Biology and PopGen biobank, Christian Albrechts University, Kiel 24105, Germany

<sup>7</sup>These authors contributed equally to this work.

\*Correspondence: [roeder@stat.cmu.edu](mailto:roeder@stat.cmu.edu)

DOI 10.1016/j.ajhg.2007.11.003. ©2008 by The American Society of Human Genetics. All rights reserved.

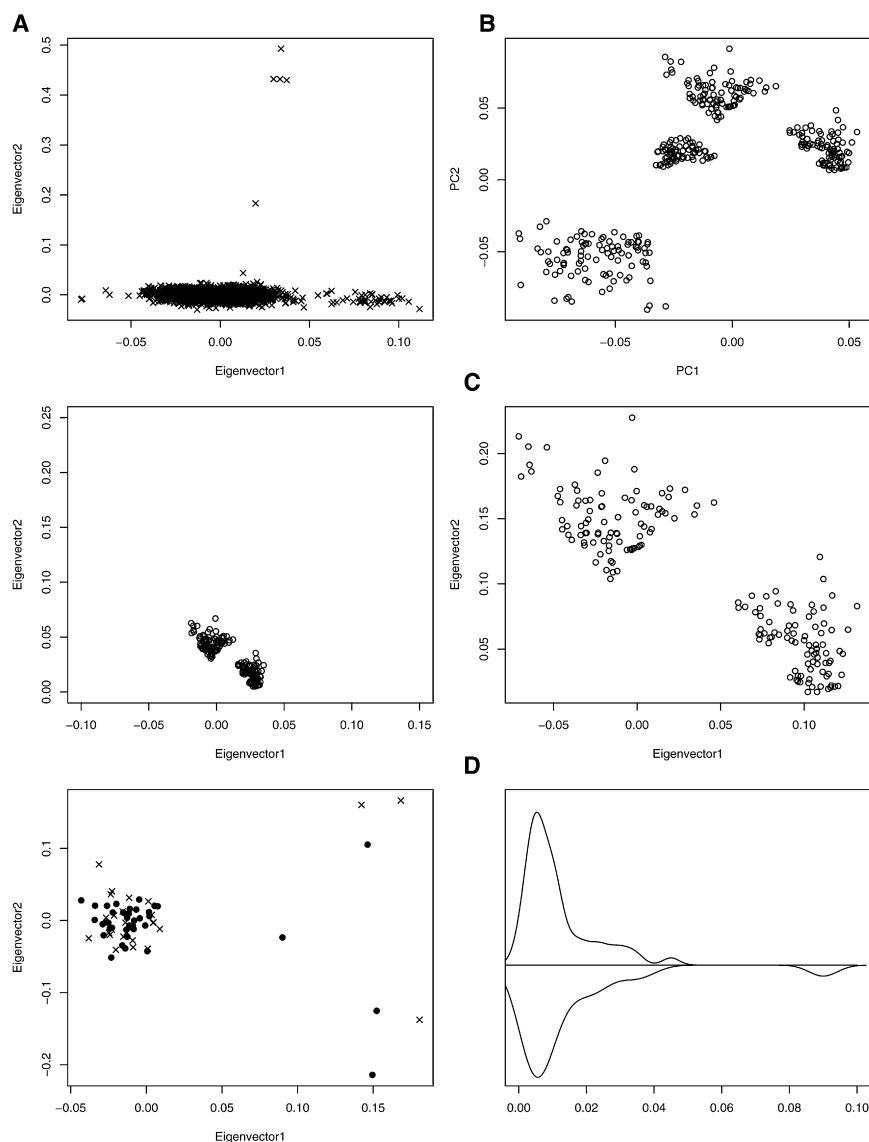


**Figure 1. Flowchart for Genetic-Matching Algorithm Illustrated with Portions of the T1D Data**

Distances between individuals are determined by the major axes of variation in the EVD representation. Outlier removal, illustrated by (A), is critical for revealing the subtle variability between individuals of similar ancestry. After major outliers are removed, clustering is used for discovery of homogeneous clusters; four distinct clusters are displayed here (B), plotted as principal component axes. Two of these clusters are displayed before ([C], left) and after ([C], right) rescaling of axes. Some observations are not outliers, but they are unmatchable ([D], left); for example, the isolated case in the center of the plot. Rescaled distances are compared to distances expected in homogeneous samples ([D], right) to identify cases and controls that can not be successfully matched. Association analysis is performed on matched strata so that the effects of population structure could be removed (not shown).

$D$  dimensional map describing the “ancestry” of each individual, i.e., the mapping of the  $i$ th subject in each dimension is determined by the  $i$ th element in the  $d$ th eigenvector. The  $d$ th eigenvalue determines the importance of the  $d$ th dimension in the new representation of the data. Individuals of similar ancestry map to similar values in the eigenvectors associated with large eigenvalues (Figure 1). Eigenvectors associated with small eigenvalues have little or no genetic interpretation.

having highly unusual measures on any of the major eigenvectors are removed.<sup>4</sup> Likewise, with matching it is necessary to determine which strata span an unusual distance leading to “unmatchable individuals.” If the controls are more numerous than the cases, they typically span a larger range of ancestries than cases, and it should be possible to find one or more controls similar to each case. Conversely, some cases may have to be removed to account for the effects of structure. In this work, we formalize the notions of outlying and unmatchable individuals and propose a method to discover the key axes that describe the population structure.

## Material and Methods

### A Sketch of the Matching Procedure Employed by GEM and Displayed in Figure 1

The illustration (Figure 1) shows the steps involved in matching genotyped cases and controls. To begin, create an  $L$  SNPs and  $N$  individuals matrix of scaled allele counts from which the EVD is computed (see Appendix). The top  $D$  eigenvectors form a

For a homogeneous population, the largest eigenvalues provides the basis for a significance test for population structure (see Patterson<sup>6</sup> and Appendix). Applying this test with significance level  $\alpha = 0.01$ , we determine the number of dimensions  $D$  to be used in the eigenvector representation. The EVD determines the distance between individuals on the basis of the top  $D$  eigenvectors, serving as coordinates or dimensions, and eigenvalues serving as weights to exaggerate differences in dimensions of greater importance (see Appendix).

If the data have many outliers,  $D$  will be relatively large, and the principal eigenvectors will be poorly estimated.<sup>7</sup> Outliers (Figure 1A) can be removed with visual diagnostics or the criterion from Eigenstrat;<sup>4</sup> namely, remove any individuals with ancestry coefficients greater than 6 SDs in at least one of the  $D$  eigenvector axes. After removing outliers, the EVD should be recomputed. If the estimated dimension,  $D$ , is still greater than two or three, we suggest finding the distance between nearest pairs of controls and cases. A subject with ancestry that does not lend itself to matching will appear as an outlier via this criterion and should be removed (see the T1D example).

To determine how to match and which individuals are unmatchable, we rely on the distribution of distances between individuals

in a homogeneous population. For a homogeneous sample, the distribution of distances will depend on sample size  $N$  and the number of loci  $L$ . By using simulations, we can find the distribution of distances for a homogeneous population. These simulations also yield the distribution of eigenvalues for a homogeneous sample of size  $N$ .

Real populations are heterogeneous but can be modeled as mixtures of relatively homogeneous subpopulations (Figure 1B). We wish to represent these subpopulations so that the between-subject distances within a homogeneous subpopulation are comparable to expectation if the entire sample were homogeneous. To do so, we need to model the underlying population substructure and adjust real data so that they are scaled properly (Figure 1C); otherwise, the between subpopulation variance will cause distances between individuals to be poorly calibrated (Figure 1C). We do this via a two-stage algorithm involving clustering and scaling. In stage one, we cluster individuals that appear to have common ancestry. This is done iteratively, by addition of clusters and then testing for structure (see Appendix for testing) until each cluster is homogeneous. We use Ward's algorithm<sup>8,9</sup> to form hierarchical groups of mutually exclusive subsets based on the first  $D$  axes of the EVD. We need a stopping rule for choosing  $K$ , the number of clusters. Start with  $K = 2$  and apply the test for population structure on each of the clusters ( $\alpha = 0.001$ ). Homogeneous clusters, as judged by the significance test, are set aside, and Ward's algorithm is applied only to the remaining data. Repeat this process, increasing  $K$  until all the clusters are homogeneous or consisting of too few observations ( $\sim 20$ ). Finally, we rescale interindividual distances as described in the Appendix so that they are comparable to distances found in a homogeneous population. At this rescaling step, unmatched individuals are uncovered and removed (Figure 1D).

After outliers and unmatched individuals are removed from the sample, recalculate the EVD and determine  $D$ . Reverting back to unscaled eigenvectors, find the distance between cases and controls on the basis of the Euclidean distance with  $D$  dimensions as described in the Appendix. Match strata with either full match or pair match. Software implementing matching algorithms is widely available (e.g., we use the `optmatch` function in the statistical package R). Then, the data can be analyzed for disease and SNP association by conditional logistic regression. Other covariates can be entered into the model at this point.

## T1D Analyses

Purified samples of genomic DNA were obtained from the Genetics of Kidneys in Diabetes (GoKinD) study<sup>10</sup> and from T1D patients recruited at the Children's Hospital of Pittsburgh (CHP) and University of Pittsburgh Medical Center. The study employed a human gene-chip microarray (Affymetrix, Santa Clara, CA) for evaluation of genetic variants with DNA samples from T1D (case) participants with genetic typing data obtained from the KORA<sup>11</sup> and PopGen<sup>12</sup> "control" cohorts.<sup>13</sup> Genotyping results were obtained with the same Affymetrix 500K SNP typing array; however, assays for case and control cohorts were performed independently. Case participants ( $n = 416$ ) were recruited in the U.S., with self-declared European ancestry and T1D; control participants ( $n = 2159$ ) were citizens of Germany recruited independent of phenotype (Table 1). Recruitment of participants at CHP was governed by the human subjects protocol approved by the University of Pittsburgh Institutional Review Board (IRB #011052: New Advanced Technology to Improve Prediction of Type 1 Diabetes). CHP patients ( $n = 28$ ) consented to providing 10 ml blood obtained by vein puncture as well as a brief medical history relating to onset of T1D. The GoKinD

**Table 1. Characteristics of Case and Control Participants**

Demographic Characteristics	Case Participants		Control Participants	
	CHP	GoKinD	KORA	POPGEN
Number of singletons	28	394	1644	500
Nominal European American (%)	100%	100%	—	—
German residents (%)	—	—	100%	100%
Male gender (%)	50%	46.7%	49.5%	51.8%
History of Diabetes				
Type 1 diabetes (%)	100%	100%	—	—
Mean age at T1D	12.7 $\pm$ 7.9	12.2 $\pm$ 7.1	—	—
Diagnosis (yr)				

cohort ( $n = 394$ ) was recruited independently from the CHP cohort by collaborative efforts of the Juvenile Diabetes Research Foundation, National Institutes of Health, and U.S. Center of Disease Control.<sup>10</sup> Material from the GoKinD cohort was provided as solutions of DNA, purified from lymphoblastoid cell lines or from whole blood. DNA solutions were provided as 50  $\mu$ l aliquots containing  $\sim 100$  ng/ $\mu$ l DNA per aliquot dissolved in 20 mM NaCl and 1 mM EDTA (pH 7.5). DNA from the CHP samples were obtained from whole blood with methods described in Ringquist,<sup>14</sup> and genotyping was performed by Affymetrix Services Laboratory (Affymetrix) with GeneChip 500K arrays. All of the genotype data from GoKinD samples generated by this project will be submitted to an accessible database, such as dbGaP or T1Dbase (see Web Resources).

All T1D samples had a sufficient completion rate ( $>95\%$ ) for inclusion, as did almost all KORA and PopGen samples. Initially, genotypes for all three samples were called with the BRLMM algorithm.<sup>15</sup> By using three criteria for genotype QC per SNP—greater than 90% genotype calls, test statistic for Hardy-Weinberg yields  $p$  value  $> 0.005$ , and minor allele frequency  $\geq 0.05$ —we removed  $\sim 140,000$  SNPs and retained 360,000 for the T1D sample, similar to other studies. When we contrasted the T1D samples to the control samples, we noted SNPs with very different allele frequencies that were not in or near known T1D loci. Inspection of the allele frequencies showed that the control allele frequencies were remarkably similar to HapMap frequencies (see Web Resources), but the corresponding genotype clusters for the T1D samples had undesirable features.

We tried various ways to improve the genotype calls. First, we looked for substantial differences between the calls by using the two algorithms employed by Affymetrix, namely DM and BRLMM. Although some discrepancies were noted, we did not see a material improvement in the data by eliminating this small set of loci. Next, because we had the Affymetrix "cel" files for the PopGen control sample, we called all of these genotypes for PopGen and T1D together by using both the DM and BRLMM algorithms. Again, this process eliminated some problematic loci, but the results were not compelling. Finally, we tried the new Bayesian calling algorithm, CHIAMO.<sup>16</sup> This algorithm led to a marked improvement for the genotype calls, as determined by inspection of the genotype clusters. For our data, we found that analyzing the PopGen and T1D data together (batch) yielded slightly better results than analyzing the two data sets as complementary strata, so these were the data we reported. Because we had greater confidence in the BRLMM calls for chromosome X, we reported those calls for X-linked SNPs. Because the KORA sample came to us only with

genotypes called by the BRLMM algorithm, we used those genotypes for that data set.

Preliminary quality control consisted of a six-step process that reduced the number of cases to 415, controls to 2112, and SNPs to 284,216. Step 1: Removed a case who was a clear outlier. Step 2: Removed 32 controls who had greater than 5% missing genotypes. Step 3: Removed 90,732 SNPs with >5% noncall rate in at least one of the three samples. Step 4: Removed 105,658 SNPs with minor allele frequencies less than 0.05 in either control sample. Step 5: Removed 1972 SNPs with  $F_{ST} > 0.02$  (estimated for the two German control samples). Step 6: Removed 18,427 SNPs that violated Hardy-Weinberg equilibrium ( $p < 0.005$ ) in either of the control samples.

## Results

### Simulations

We compare three approaches to correct for the effects of structure: Eigenstrat and GEM with fMatch and pMatch. Although we compare their size (i.e., rate of false positives) and power, these approaches are not direct competitors. The GEM methods are designed to limit analysis to strata that are chosen a priori, whereas Eigenstrat aims to remove the effects of structure in the analysis stage.

Allele frequencies for the subpopulations were generated with the “Balding-Nichols” model<sup>17</sup> (see [Appendix](#)), with allele frequencies varying uniformly between 0.05 and 0.5. To correct for structure,  $L$  reference SNPs were generated. Of these SNPs, 99% had a minor amount of variability across subpopulations ( $F_{ST} = 0.01$ ), and 1% had substantial differentiation ( $F_{ST} = 0.1$ ). Null or causal candidate SNPs of three levels of  $F_{ST}$  were generated: Model (1) strongly differentiated SNPs,  $F_{ST} = 0.1$ ; Model (2) moderately differentiated SNPs with  $F_{ST} = 0.03$ ; and Model (3), modestly differentiated SNPs with  $F_{ST} = 0.01$ .

Ten panels of independent reference SNPs, with  $L$  ranging from 96 to 100,000, were generated. For each of these panels, we simulated 1000 independent causal SNPs and 1000 independent null candidate SNPs. We repeated this analysis for models (1), (2) and (3) and for six choices of  $L$ . Causal SNPs with relative risk  $R = 2$  were generated with the approach described in Price<sup>4</sup> for power calculations.

Our first battery of simulations is based on SNPs sampled from two subpopulations, with 200 individuals per subpopulation. Case status was assigned to 80 and 20 of the individuals from subpopulations 1 and 2, respectively. The remaining individuals were assigned control status. For the matched-pairs analysis, we paired each case to the closest control until we obtained 100 matched pairs. For the other two methods of analyses, we analyzed all 400 individuals. Each method readily detects population substructure and achieves the desired type I error rate as  $L$  increases ([Table 2](#)). pMatch and fMatch successfully remove the effect of structure with a smaller panel of reference SNPs than Eigenstrat does ([Figure 2A](#)). Indeed, when a large panel of reference SNPs is available, the GEM proce-

dures are overly conservative; consequently, Eigenstrat is slightly more powerful than both matching procedures ([Table 2](#)) under these conditions. For SNPs with less information about population membership than present in our simulated reference panels, greater numbers of SNPs would be required to remove the effects of structure.<sup>4</sup>

Our second battery of simulations is based on nine subpopulations distributed along a gradient, designed to simulate a cline such as the north to south cline observed in western Europe. The 100 cases are distributed with 2, 4, 6, 7, 9, 12, 15, 20, and 25 individuals in populations 1–9, respectively. The 300 controls are distributed randomly across the nine subpopulations. Results from this simulation are qualitatively similar to those shown in [Figure 2A](#) ([Table 2](#)). The first two batteries of simulations illustrate that when the case and control samples are drawn from the same subpopulations, but with different frequencies, the effects of substructure can be removed with any of the three methods described. Even the effects of highly differentiated SNPs can be removed provided the reference panel is sufficiently informative.

Our third battery of simulations is also based on a nine population gradient; however, the cases and controls are apportioned in a manner that simulates the complexity of human populations and GWA designs. As in the previous simulation, we simulate nine populations and draw 300 controls randomly. In contrast, all 50 of the cases are drawn from populations 6–9. Because of the nature of this third battery, namely the presence of unmatchable observations, we analyze the data in two ways: Unmatchable observations are removed as described previously; or unmatchable observations are retained. In choosing only a single control for each case, pMatch includes only 50 of the controls in the study regardless of the treatment of outliers. Provided the reference panel is sufficiently informative, many of these controls will be derived from populations 6–9. Eigenstrat, on the other hand, uses all of the data, as will fMatch when unmatchable observations are retained. For fMatch, this means that cases drawn from population 6 will tend to have many controls in their strata sampled from populations 1–5. The remaining cases will tend to have only one or two controls in their strata. By grouping the outlying observations, fMatch attempts to minimize the effect of unmatchable observations. Eigenstrat must account for controls sampled from populations 1–5 with regression techniques, which are well known to suffer adverse consequences when they are extrapolating beyond the range of the data.

When unmatchable observations are retained, pMatch corrects for the effects of substructure with fewer reference SNPs than the other two methods ([Table 3](#) and [Figure 2B](#)). Indeed, Eigenstrat fails to remove the effects of population substructure. By comparing pMatch and fMatch, we see that the latter has greater power. This makes sense because fMatch is using more of the data ([Table 3](#)).

On the basis of the clustering and rescaling process, most of the controls from populations 1–5 are unmatchable, and

**Table 2. Size and Power of Tests at Level 0.05**

Statistic	Design	No. of Markers	Eigenstrat with $F_{ST}$			pMatch with $F_{ST}$			fMatch with $F_{ST}$				
			0.01	0.03	0.1	0.01	0.03	0.1	0.01	0.03	0.1		
Size													
	Two Populations		96	.069	.106	.211	.062	.100	.202	.065	.101	.206	
		386	.055	.061	.085	.044	.045	.051	.047	.049	.054		
		1536	.052	.054	.055	.046	.045	.045	.047	.047	.046		
		6144	.053	.052	.051	.044	.045	.045	.047	.047	.046		
		12000	.053	.052	.052	.044	.044	.045	.047	.045	.047		
		24000	.053	.050	.051	.043	.042	.041	.046	.046	.045		
	Gradient		96	.069	.109	.221	.049	.067	.109	.061	.097	.201	
		386	.054	.058	.071	.043	.046	.048	.048	.052	.063		
		1536	.052	.051	.050	.045	.044	.044	.047	.047	.046		
		6144	.052	.051	.050	.045	.045	.044	.046	.045	.047		
		12000	.052	.052	.052	.044	.044	.045	.047	.047	.047		
		24000	.052	.052	.052	.044	.045	.044	.047	.046	.046		
	Power												
		Two Populations		96	.783	.710	.683	.693	.635	.620	.754	.685	.659
			386	.767	.701	.682	.682	.632	.621	.735	.673	.653	
			1536	.766	.702	.677	.683	.635	.622	.736	.674	.653	
			6144	.765	.694	.676	.684	.630	.623	.735	.671	.653	
			12000	.765	.697	.676	.684	.633	.624	.735	.673	.653	
		24000	.763	.696	.677	.684	.632	.624	.734	.671	.653		
Gradient		96	.939	.917	.833	.886	.872	.804	.922	.900	.814		
		386	.924	.891	.796	.877	.857	.782	.902	.869	.775		
		1536	.917	.876	.774	.876	.850	.775	.894	.856	.754		
		6144	.913	.874	.768	.873	.849	.773	.892	.853	.747		
		12000	.915	.873	.771	.874	.849	.774	.891	.850	.749		
		24000	.912	.874	.768	.873	.849	.771	.892	.852	.747		

Columns depict the results as  $F_{ST}$  varies (0.01, 0.03, and 0.1) in the candidate markers. Results are shown for two scenarios: a two-population mixture and a nine-population gradient. For the size, the expected number of p values smaller than 0.05 is 50.

such a result is desirable because cases were only drawn from populations 6–9. In this instance, the size of the matched analyses is now closer to the nominal level even when  $L$  is small, as expected. Interestingly, there is the considerable enhancement in power for fMatch and pMatch when unmatchable individuals are removed, as recommended by our methods, as opposed to when they are forced to be retained (Table 3). This occurs because removal of the outliers leads to improved performance of the EVD and hence superior choices of matches in the analysis. In addition, for fMatch the removal of controls from populations 1–5 leads to a more homogeneous sample that tends to increase power.

Eigenstrat defines outliers without specific reference to cases and controls; thus, none of the observations are unmatchable observations. Nevertheless, if the regression approach is applied after removal of those observations declared unmatchable by the fMatch procedure, the type I error is successfully controlled, and the power is slightly greater than it is for fMatch (Table 3). This hybrid approach to analysis has some potential for further development.

#### GWA of Type 1 Diabetes Data with fMatch

We analyzed 416 cases of T1D,<sup>18</sup> derived from the GoKinD<sup>10</sup> cohort ( $n = 394$ ) and T1D patients recruited from the Children's Hospital of Pittsburgh ( $n = 28$ ). Samples were genotyped with the Affymetrix 500K GeneChip. All identified their ancestors as European. The mean age of onset for T1D was 12.2 and 12.7 years of age for the GoKinD and Pittsburgh cohorts, respectively. Controls genotyped by the same chip were obtained from the PopGen and KORA repositories, which consist of 500 individuals from north Germany (PopGen) and 1644 individuals from southern Germany (KORA).<sup>11–13,19</sup> The four cohorts were recruited independently of one another. The relevant characteristics of these cohorts are summarized in Table 1.

Stringent quality control reduced the number of SNPs to 284,216 and the number of controls to 2112 (samples were removed if the rate of missing genotypes exceeded 5%). To reconstruct ancestry, we chose 23,552 independent or “tag” SNPs by using the H-clust algorithm<sup>20</sup> with an  $r^2$  cut-off value of 0.04. Both case and control individuals exhibit complex population heterogeneity. For example, individuals were included in the PopGen and KORA registry on



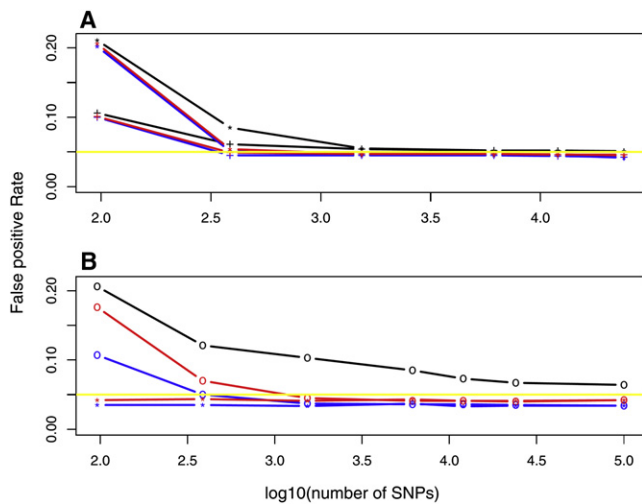


**Figure 2. False-Positive Rate versus Log of the Number of Markers Available for Estimating Structure**

Results are for Eigenstrat (black), pMatch (blue), and fMatch (red). The desired nominal rate of 0.05 is plotted as a yellow line. In (A), a sample derived from two simulated populations is shown. Results are displayed for markers with two levels of differentiation  $F_{ST} = 0.1$  (\*) and 0.03 (+). The former exhibits a higher rate of errors than the latter for small numbers of markers. In (B), a sample derived from a gradient of simulated populations is shown. Results are displayed for the full sample (plotting character "o") and with unmatchable individuals removed (plotting character "\*"; this applies to the matching methods only).

the basis of residence rather than known German ancestry. We removed one case individual who had very different ancestry from the other 415. For 415 cases and 2112 controls,  $D = 22$  dimensions were required to explain the significant axes of genetic variation. Many of these axes exhibited extreme outliers (Figure 1A). After removing 53 controls, only three important axes of variation remained. On the basis of the first two eigenvectors, a cluster of cases that differs in ancestry from the control sample was clearly evident (Figure 3A). To identify unmatchable individuals more completely, we computed the distance between each case and the nearest control and vice versa on the basis of three axes of the EVD map. The resulting distribution of distances indicated that 21 cases could not be matched to a control with similar ancestry (Figure 4). By repeating this process of finding the significant eigenvalues and the corresponding minimum distances between cases and controls in the corresponding axes, we subsequently removed an additional one case and 15 controls. After excluding these outliers, only two significant eigenvalues remain when a significance level of 0.01 was used.

Next, with cluster analysis to identify homogeneous strata, 2136 individuals were clustered into 26 strata, each with 20 or more elements and no significant structure within cluster ( $p > 0.001$ ). The remaining 301 individuals were clustered into 24 small clusters. On the basis of these strata, the data were rescaled and the distance between cases and matched controls was determined. Those that

**Table 3. Size and Power of the Tests before and after Removing Outliers, with Eigenstrat, pMatch, and fMatch**

		Outliers Present								
		Eigenstrat with $F_{ST}$			pMatch with $F_{ST}$			fMatch with $F_{ST}$		
Statistic	No. of Markers	.01	.03	.1	.01	.03	.1	.01	.03	.1
Size										
	96	.064	.097	.206	.044	.056	.107	.056	.082	.176
	386	.057	.068	.121	.038	.040	.050	.045	.051	.070
	1536	.056	.062	.103	.037	.037	.037	.043	.042	.045
	6144	.056	.061	.085	.037	.037	.035	.041	.042	.041
	12000	.058	.058	.073	.037	.036	.036	.042	.040	.041
	24000	.057	.058	.067	.037	.037	.035	.042	.042	.040
	100000	.055	.057	.064	.037	.037	.034	.043	.043	.042
Power										
	96	.804	.753	.650	.590	.579	.511	.770	.726	.623
	386	.784	.731	.630	.583	.566	.489	.721	.686	.583
	1536	.771	.716	.615	.581	.567	.482	.671	.642	.548
	6144	.762	.711	.604	.583	.566	.485	.639	.620	.531
	12000	.751	.704	.595	.582	.564	.485	.637	.615	.528
	24000	.746	.699	.593	.584	.565	.484	.637	.613	.529
	100000	.748	.694	.592	.588	.565	.484	.639	.612	.528
Outliers Removed										
Size										
	96	.061	.090	.195	.037	.036	.035	.044	.043	.042
	386	.057	.060	.095	.036	.036	.035	.043	.041	.043
	1536	.054	.053	.057	.035	.038	.033	.040	.044	.041
	6144	.054	.053	.056	.040	.037	.037	.044	.044	.043
	12000	.052	.053	.054	.038	.035	.033	.041	.042	.041
	24000	.052	.052	.053	.036	.039	.034	.041	.045	.041
	100000	.052	.052	.053	.037	.035	.034	.042	.042	.042
Power										
	96	.906	.931	.927	.706	.713	.656	.772	.776	.719
	386	.873	.885	.870	.698	.713	.656	.771	.769	.726
	1536	.856	.857	.834	.700	.716	.660	.771	.774	.727
	6144	.849	.850	.829	.703	.716	.666	.771	.774	.729
	12000	.843	.843	.818	.703	.713	.663	.769	.767	.726
	24000	.840	.840	.817	.701	.715	.667	.771	.775	.726
	100000	.835	.834	.813	.700	.719	.669	.772	.776	.728

Columns depict the results as  $F_{ST}$  varies (.01, .03, and .1) in the candidate markers. The simulated data are a gradient with nine subpopulations; controls are drawn from 1–9 and cases are only from 6–9.

were considered unmatchable individuals on the basis of the simulation results were removed (see Appendix). With this process, an additional 20 cases and 48 controls are removed from the dataset for fMatch. The resulting distance between the remaining cases and controls in fMatch is consistent with expectations for cases and controls matched within homogeneous strata (data not shown). In the reduced fMatch sample, two principal axes separate the German control samples by region and define a space, spanned by both cases and controls, that facilitates matching (Figure 3B). These dimensions presumably map onto genetic gradients on the European continent; e.g., the horizontal axis is likely to be related to a north-south gradient

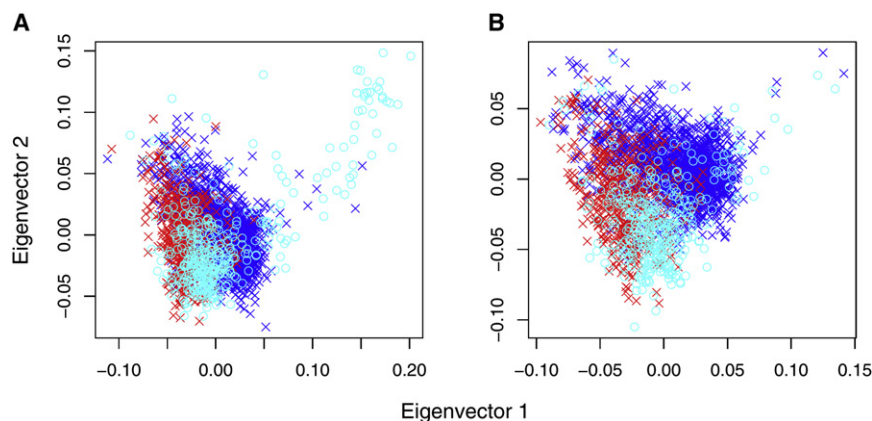


**Figure 3. Plots of the First Two Eigenvector Axes for T1D Data before and after Removing the Unmatchable Individuals after Clustering and Rescaling of the Data**

Each case (light blue) has a matched control (dark blue = South Germany, red = North Germany) in a close neighborhood after removal of unmatchable individuals; compare before (A) with after (B).

because it tends to separate the German samples by north (PopGen)<sup>12</sup> and south (KORA)<sup>11</sup> origin.<sup>21,22</sup> In the pMatch sample, one additional axis is needed to explain important variation (data not shown).

After final removal of outliers and unmatchable individuals for fMatch, cases and controls were stratified on the basis of their genetic ancestry into 298 strata. Most of the strata (159) contain a single case matched to several controls. A single case matched to a single control occurred in 111 strata. A minority of strata (28) contain a single control matched to multiple cases. For example, in the most extreme strata, a single case was matched to 71 controls and a single control was matched to 13 cases. When a single case is matched to a large number of controls (or vice versa), the information gain from the strata is essentially equivalent to that obtained from a single case matched to a moderate number of individuals. Nevertheless, conditional logistic regression is valid regardless of the lack of

balance in the strata. In all, 373 cases were contrasted with 1996 controls by conditional logistic regression (Figure 5, top panel). The results highlight the HLA region, which contains numerous SNPs achieving GWA significance. Variation in the HLA region is well known to account for a large fraction of the risk for T1D.<sup>23–26</sup> No

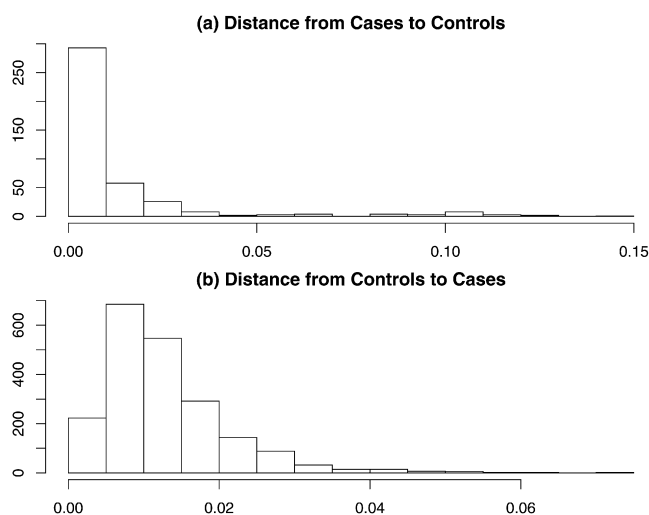


**Figure 4. The Distance between Each Case and the Nearest Control and Vice Versa Based on Three Principal Components Are Computed**

The distributions differ, and we eliminate 34 cases with distances to the nearest control greater than 0.075. (A) shows the histogram of distances between each case and the nearest control. (B) shows the histogram of distances between each control and the nearest case.

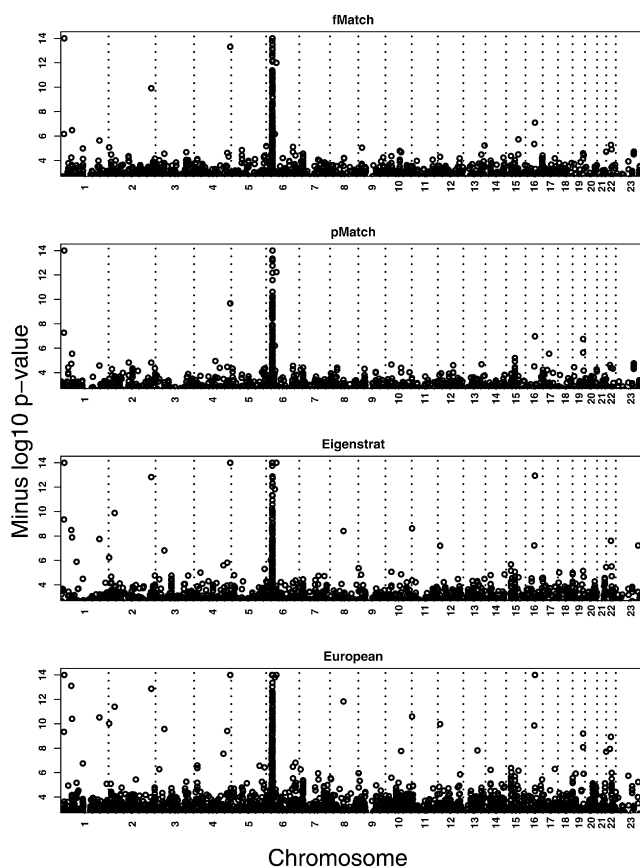


**Figure 5. Transformed p Values after Conditional Logit Regression Was Performed on the Data Stratified with fMatch** Transformed p values (negative of the log, base 10). Results from conditional logistic regression on the data stratified with fMatch (top panel) and pmatch (second panel) are shown. Results obtained with Eigenstrat are shown in the third panel. Results obtained when removing observations with very divergent ancestries (inferred with the Eigenstrat rule for outliers) from the bulk of the sample, which was European, are shown in the bottom panel.

other location in the genome contains SNPs with test statistics meeting reasonable criteria for GWA significance ( $\leq 10^{-7}$ ) after ensuring quality genotype calls by visual inspection of the genotype clusters (see [Figures S1 and S2](#) available online for examples). It should be noted, however, that visual inspection of genotype clusters is essential to interpret this Affymetrix “first-generation” genotype data, a feature other GWA studies with this genotyping platform also report.<sup>27</sup>

Results from fMatch agree with our expectations. Other GWA studies have established that all genetic variation thus far uncovered, aside from variation in the HLA region, account for a modest portion of the risk for T1D.<sup>28,29</sup> For detecting loci of modest effect with good power, either sample sizes must be substantial (i.e., thousands of cases and controls genotyped) or a staged study design must be employed. The staged design typically sets a significance level between 0.01 and 0.001 in stage 1, then genotypes all loci meeting this significance level (and quality-control criteria) in a second, larger sample.<sup>30,31</sup> Treating our study as stage 1 with a significance level of 0.007,<sup>30</sup> results from fMatch would include SNPs for genotyping in stage 2 from six out of ten loci now believed to confer risk to T1D.<sup>29</sup> Of the remaining four loci, only one had more than a few SNPs in the region.

Aside from the HLA region, SNPs in or near *PTPN22* (MIM 600716), *IL2RA* (CD25 [MIM 147730]), and *CTLA4* ([MIM 123890]; window = gene location  $\pm$  40 Kb) showed enough signal to be passed to stage 2. The smallest p value for each gene was 0.000706 (rs2488457), 0.000995 (rs10905669), and 0.000336 (rs231726). The smallest p values for SNPs close to “risk SNPs” rs2292239 and rs12708716 were 0.00667 (rs2292239) and 0.00539 (rs11647011) for window = SNP location  $\pm$  50 Kb. Could it be that the signals in these regions occurred by chance? To answer this question, we performed a simulation experiment. We randomly select from the genome ten intervals that correspond to the same size as the original ten windows (for the HLA region, we assumed a window of 3 Mb). Then, we count the number of intervals in which one or more SNPs have  $p < 0.007$  and would thus be genotyped in stage 2. We perform this random selection  $10^6$  times, counting how many times six or more intervals would have SNPs genotyped in Stage 2. By this experiment, we determined that our results would rarely occur by chance, roughly one in ten thousand times.

A few other observations from these analyses are worth noting. Within the HLA region, Todd<sup>29</sup> cites rs3129934 as the replicated SNP; our independent data and analyses yield a p value for association of  $7.2 \times 10^{-10}$  with this SNP; for the replicated SNP identified in *CTLA4*, rs3087243, our data and analyses yield a p value for association of 0.013, and, as noted above, the replicated SNP rs2292239 produced a p value of 0.00667 from our data. Although the HLA region needs no more support, our results provide further evidence for replication in *CTLA4* and at rs2292239. For genotype cluster plots for the cited SNPs, see [Figure S1](#). In

addition, for all of the loci cited above, we have compared our data to that reported by the Wellcome Trust Case Control Consortium.<sup>27</sup> For these loci, the allele in excess in cases is the same for both data sets (data not shown).

Four loci did not pass stage 1 criteria. None of these SNPs reported by Todd et al.<sup>29</sup> as risk loci were on our Affymetrix genotyping array. Of these four risk SNPs, only rs1893217 in 18p11 was covered well in terms of genotyped SNPs in substantial linkage disequilibrium (LD) with it. This SNP is in almost complete LD with rs2542151 according to HapMap; it passed our QC, but it shows no evidence for association in our data ( $p = 0.51$ ). For the proinsulin precursor gene, *INS* (MIM 176730), only two SNPs on the array pass QC and fall in the region, but HapMap contains no information about their LD with the reported risk SNP, rs689, and they show no association ( $p > 0.35$ ). For the gene encoding interferon-induced helicase C domain-containing protein 1, *IFIH1* (MIM 606951), the reported risk allele shows modest LD with a SNP we genotyped, namely rs7608315, which shows no association ( $p = 0.38$ ). Finally, for the 12q24 region, rs3184504 is identified as the risk SNP. One SNP in this region passed QC for our data, and it is modestly associated with risk for T1D ( $p = 0.046$ ).

The vast majority of the SNPs from this or any relevant GWA are independent of risk for T1D. Many SNPs from the HLA regions of chromosome 6 are associated, however. After eliminating HLA SNPs, ~5% of the association tests are expected to have p values  $< 0.05$ . Of the 284,216 tests, 7.0% were significant at  $\alpha = 0.05$  for fMatch. A moderate excess of false positives occurs for any reasonable choice of  $\alpha$ . Given the success of the GEM method in the simulations, in terms of controlling the false-positive rate, we wondered whether the source of additional false positives could be poor-quality genotype calls. Indeed, by assessing genotype clusters for all SNPs producing p values  $\leq 10^{-4}$ , we find a rate of poor calls of 60%–67% ([Figure S2](#)). The rate of poor-quality genotype calls increases as the p value decreases. Predominantly, the problematic calls occur for the T1D sample. On the basis of our estimated rate of poor-quality genotype calls, we believe the excess false-positive rate is attributable to data-quality issues, not the method.

We also analyzed GWA data by using pMatch and Eigenstrat and by ignoring population substructure after discarding outliers with the Eigenstrat rule (see [Figure 5](#)). As expected, pMatch shows the lowest rates of positive findings, whereas ignoring structure yields the most. Like fMatch, it appears the excess of false positives for pMatch is due to poor-quality genotype calls. The same is predominantly true for Eigenstrat, but we note that an ample number of SNPs producing small p values are not attributable to poor quality, and this problem is amplified by ignoring structure. At significance level 0.0001, after visual inspection of genotypes fMatch has half the false-positive rate of Eigenstrat.

To further validate GEM, we tried a null experiment. We randomly labeled half of the KORA data as cases and half as controls and repeated the matching analysis. Removal of 72 outliers reduced the number of significant eigenvalues

required to explain the variation from 24 to 2. After this simplification, only 12 unmatchable individuals remained. All three methods of analysis (Eigenstrat, Pmatch, and fMatch) produced type I error rates that were on target.

## Discussion

Our GWA analyses of T1D are meant to accomplish two goals. First, they illustrate the utility of ancestry matching in the face of a very difficult problem, that being when cases are sampled in a region quite different from the region of the controls. In our case, the T1D sample comes from any American of nominal European ancestry, whereas the controls were recruited among residents of Germany. Such constellations can also arise even if cases and controls are sampled from the same geographical region. We would expect the example to be especially salient for American samples. Second, we wished to use the results to evaluate reported T1D risk loci and, in later analyses, discover new loci. The results show that genetic or ancestry matching can be an important ingredient in the toolbox of researchers who are performing GWA analyses. Moreover, our results do lend support for previous GWA findings for T1D.<sup>28,29</sup>

We do not yet know whether our analyses have identified any new risk loci for T1D. Although it seems unlikely given the modest sample of cases, a substantial number of controls have been analyzed. Moreover, for a rare disease like T1D, using unscreened instead of screened controls has almost no impact on power.<sup>32</sup> We plan various kinds of stage 2 analyses to assess the association signals from our GWA results. In addition, by agreement the data generated by our project will be reported back to the GoKinD database, and GoKinD will make the data available to qualified investigators. Thus, these data will shortly be available to the research community, and we will be pleased to share detailed results upon request.

We have described how to use genetic matching to enhance a case-control study. We note, however, that these methods can also be used for the analysis of quantitative traits. Once homogeneous clusters are identified, they can be entered into a model as block effects, and the quantitative trait can be analyzed with standard statistical tools, such as analysis of variance.

Theory, simulations, and real-data analyses suggest that genetic matching is useful and powerful for GWA, especially when the samples of cases and controls cannot be guaranteed to be drawn from the same population. It can diminish the false-positive rate, sometimes substantially, and have only modest impact on power. Among others,<sup>33–36</sup> methods similar to Eigenstrat<sup>4</sup> also limit the impact of population structure, but for challenging designs, they cannot be expected to completely control the false-positive rate. Perhaps the gold standard for GWA studies should be to evaluate the data with both regression methods such as Eigenstrat and epidemiological methods such as fMatch. When the results of these methods agree,

researchers have greater assurance of validity; it is when the results diverge that we should be wary.

## Appendix

### EVD of Allele Counts

Using allele counts for SNPs  $l = 1, \dots, L$ , and individuals  $i = 1, \dots, N$ , create an  $N \times L$  matrix  $X$ . For  $p_l$ , the  $l$ th allele frequency, center allele counts in column  $l$  by subtracting  $2p_l$  and scale by dividing by  $(2p_l(1 - p_l))^{1/2}$ . Find the EVD of  $XX^t = U\lambda U^t$ . In the  $D$  dimensional space defined by the top  $D$  eigenvectors, the “ancestry” value for the  $i$ th subject is determined by the  $i$ th row of the eigenvectors  $u_{i1}, \dots, u_{iD}$ . The  $d$ th eigenvalue,  $\lambda_d$ , determines the scaling of distances in the  $d$ th dimension. These coordinates are used for matching.

### Model for Population Stratification

The mean of allele frequencies from a set of populations is assumed to be the allele frequency of an ancestral population. Individual populations have each diverged from the ancestral population over time, with fixation index  $F_{ST}$ , a measure of population differentiation. Within a subpopulation  $j$ , suppose that allele counts are independent and identically distributed and that allele  $a$  is drawn with probability  $p_j$ . If  $X$  is counting allele  $a$ , then  $X \sim \text{Binomial}(2, p_j)$ . Let  $P$  be the random variable that varies across subpopulations, with  $p_j$  as the realized value in subpopulation  $j$ :  $P \sim \text{Beta}(\alpha_1, \alpha_2)$ ,  $\alpha_1 + \alpha_2 = 1/F_{ST} - 1$ . Assume that we have the minor allele frequencies of an ancestral population  $p_{.loci}$  (in our simulations  $p_{.loci}$  is uniform between .05 and .5) at  $L$  loci. From the ancestral population  $J$ , subpopulations have been formed. By knowing  $F_{ST}$ , for each marker  $l$  we can define  $\alpha_{1,l} = p_{.loci_l} \times (1/F_{ST} - 1)$  and  $\alpha_{2,l} = (1 - p_{.loci_l}) \times (1/F_{ST} - 1)$  and generate the alleles as described above. When used in simulation studies, this is often called the Balding-Nichols model.<sup>17</sup> For simulation of a cline (or a gradient), it is enough to order  $p_{jl}$  so that  $p_{j1} \leq \dots \leq p_{jL}$  for each  $l$ .

### Hypothesis Test for Population Structure

A formal significance test for population structure is based on a theoretical result for the eigenvalue distribution of a null sample covariance matrix.<sup>6,37</sup> For a homogeneous population, the largest eigenvalue, properly normed, approximately follows the Tracy-Widom distribution<sup>37</sup>  $W_d = (\lambda_d - \mu_{NL})/\sigma_{NL}$  with centering and scaling parameters that depend on both  $N$  and  $L$ ,  $\mu_{NL} = ((L - 1)^{1/2} + N^{1/2})^2$  and  $\sigma_{NL} = ((L - 1)^{1/2} + N^{1/2})(1/((L - 1)^{1/2}) + 1/N^{1/2})^{1/3}$ . We can test the null hypothesis of population homogeneity against an alternative hypothesis of population heterogeneity. The sample covariance matrix  $S$  follows a  $(N - 1) \times (N - 1)$  Wishart distribution. The test for population structure will be applied iteratively (i.e., the leading eigenvalue, then the second and so on). If we find the first  $d$  eigenvalues  $\lambda_1, \dots, \lambda_d$  to be significant, we test  $\lambda_{d+1}$  as



though  $S$  were an  $(N - d - 1) \times (N - d - 1)$  Wishart matrix. If an eigenvalue is not significant, the smaller eigenvalues will not be significant either.

### Removing Unmatchable Individuals

EVD determines the distance between individuals on the basis of the top  $D$  eigenvectors and eigenvalues. To stabilize the distance metric, we use the normed eigenvalues,  $W_d$ , plus a constant  $a$ , chosen to ensure the weights are positive. The distance between individuals  $i$  and  $i'$  is calculated as  $g(i, i') = \left\{ \sum_{d=1}^D (W_d + a)(u_{id} - u_{i'd})^2 \right\}^{1/2}$ .

To rescale the distances, let  $S_k \subset \{1, 2, \dots, N\}$  be the indices of individuals in the  $k$ 'th cluster. Let  $r_k$  be the number of individuals in the  $k$ 'th cluster. For scaling subject  $i \in S_k$ , we use the eigenvector values  $(u_{i1}, \dots, u_{iD})$  but not the eigenvalues. Assume that the eigenvector representation of each individual consists of an ancestry signal plus random noise:  $u_{id} = \mu_{id} + \varepsilon_{id}$ .

For homogeneous data, because all individuals came from a common source, the ancestry signal is 0 and the representation consists simply of random noise  $u_{id} = \varepsilon_{id}$ . Our target is to identify approximately homogeneous subpopulations that have little or no diversity for ancestry. If the clustering is successful, the signal of each individual in subset  $S_k$  can be approximated by  $\bar{u}_{dk} = \sum_{i \in S_k} u_{id} / r_k$ , and the noise can be approximated by  $u_{id} - \bar{u}_{dk}$ . But notice that EVD automatically scales the eigenvectors so that  $\sum_i u_{id}^2 = 1$  and  $\bar{u}_d = 0$ . A traditional sum of squares decomposition leads to

$$1 = \sum_i u_{id}^2 = \sum_k \sum_{i \in S_k} (u_{id} - \bar{u}_{dk})^2 + \sum_k r_k \bar{u}_{dk}^2,$$

i.e., the total sum of squares (SSTotal) equals the sum of squares attributable to random variation or error (SSError) plus the sum of squares attributable to ancestry differences (SSModel). Unit scaling of SSTotal causes the distances between individuals from heterogeneous populations to be uncomparable to distances in homogeneous populations. For example, if the sample derives from two highly differentiated populations so that SSError = 0.01 and SSModel = 0.99, then the expected distance between two individuals with common ancestry is  $\sim 0.01/n$ . Alternatively, if the populations have identical ancestry, then the expected distance between two individuals is  $\sim 1/n$ . For comparing to a homogeneous scaling, we wish to rescale the random noise so that SSError is 1. It follows that the data will be rescaled equivalently to homogeneous data if we set  $c_d^2 = \sum_k \sum_{i \in S_k} (u_{id} - \bar{u}_{dk})^2$  and rescale the data such that  $u_{id}^* = u_{id} / c_d$ .

In practice,  $\bar{u}_{dk}$  provides a good estimate of the signal only when the cluster size is sufficiently large, say greater than 10. Hence, to compute  $c_d^2$ , include only those clusters  $S_k$  including 10 or more elements in the sum and then multiply by  $n / \sum_k (r_k - 1)$  to account for the missing clusters. Notice that we scale differently for each of the  $d$  dimensions to stretch and shrink accordingly to get the proper scaling of the data.

In the final step, find the distances between individuals with the  $u_{id}^*$  instead of  $u_{id}$  and use the expected value of normed eigenvalues  $W_1, \dots, W_D$  obtained from the simulation, instead of the actual eigenvalues. Match rescaled data with fMatch or pMatch and measure the distances between cases and controls. Any individuals with distances in this metric exceeding the 99.9th quartile of the null distribution of distances are declared unmatchable.

### Supplemental Data

Two figures are available at <http://www.ajhg.org/>.

### Acknowledgments

The Genetics of Kidneys in Diabetes (GoKinD) Study sample collection is supported by the Juvenile Diabetes Research Foundation in collaboration with the Joslin Diabetes Center and George Washington University and by the United States Centers for Disease Control and Prevention. This work was funded by the National Institutes of Health grant MH057881 awarded to B.D. and K.R. and by the Department of Defense (grant W81XWH-07-1-0619) awarded to M.T. The MONICA/KORA Augsburg studies were financed by the GSF-National Research Center for Environment and Health, Neuherberg, Germany, and supported by grants from the German Federal Ministry of Education and Research (BMBF). Part of this work was financed by the German National Genome Research Network (NGFN). The genotypes reported in this publication were generated independently from any other initiatives supported by other organizations.

Received: October 1, 2007

Revised: November 16, 2007

Accepted: November 20, 2007

Published online: January 24, 2008

### Web Resources

The URLs for data presented herein are as follows:

CHIAMO, <http://www.stats.ox.ac.uk/%7Emarchini/software/gwas/chiamo.html>

dbGaP, <http://www.ncbi.nlm.nih.gov/sites/entrez?db=gap>

GEM, <http://wpicr.wpic.pitt.edu/WPICCompGen/>

GoKinD, <http://www.jdrf.org/gokind>

HapMap Frequencies, <http://www.hapmap.org/>

Online Mendelian Inheritance in Man (OMIM), <http://www.ncbi.nlm.nih.gov/Omim>

Optmatch, [http://cran.r-project.org/doc/packages/](http://cran.r-project.org/doc/packages/T1Dbase)

T1Dbase, <http://t1dbase.org/>

### References

1. Lee, W.-C. (2004). Case-control association studies with matching and genomic controlling. *Genet. Epidemiol.* 27, 1–13.
2. Hinds, D.A., Stokowski, R.P., Patil, N., Konvicka, K., Kersheno-bich, D., Cox, D.R., and Ballinger, D.G. (2004). Matching strategies for genetic association studies in structured populations. *Am. J. Hum. Genet.* 74, 317–325.



3. Zhang, S., Zhu, X., and Zhao, H. (2003). On a semiparametric test to detect associations between quantitative traits and candidate genes using unrelated individuals. *Genet. Epidemiol.* 24, 44–56.
4. Price, A.L., Patterson, N.J., Plenge, R.M., Weinblatt, M.E., Shadick, N.A., and Reich, D. (2006). Principal components analysis corrects for stratification in genome-wide association studies. *Nat. Genet.* 38, 904–909.
5. Rosenbaum, P.R. (1995). *Observational Studies* (New York: Springer-Verlag).
6. Patterson, N., Price, A.L., and Reich, D. (2006). Population structure and eigenanalysis. *PLoS Genet.* 2 10.1371/journal.pgen.0020190.
7. Jolliffe, I.T. (2002). *Principal Component Analysis* (New York: Springer).
8. Venables, W.N., and Ripley, B.D. (2002). *Modern Applied Statistics with S, Fourth Edition* (New York: Springer).
9. Everitt, B.S. (1993). *Cluster Analysis* (London: Edward Arnold).
10. Mueller, P.W., Rogus, J.J., Cleary, P.A., Zhao, Y., Smiles, A.M., Steffens, M.W., Bucksa, J., Gibson, T.B., Cordovado, S.K., Krolewski, A.S., et al. (2006). Genetics of Kidneys in Diabetes collection available for identifying genetic susceptibility factors for diabetic nephropathy in type 1 diabetes. *J. Am. Soc. Nephrol.* 17, 1782–1790.
11. Wichmann, H.E., Gieger, C., Illig, T., and MONICA/KORA Study Group. (2006). KORA-gen—resource for population genetics, controls and a broad spectrum of disease phenotypes. *Gesundheitswesen* 67 (Suppl 1), S26–S30.
12. Krawczak, M., Nikolaus, S., von Eberstein, H., Croucher, P.J., El Mokhtari, N.E., and Schreiber, S. (2006). PopGen: Population-based recruitment of patients and controls for the analysis of complex genotype-phenotype relationships. *Community Genet.* 9, 55–61.
13. Steffens, M., Lamina, C., Illig, T., Bettecken, T., Vogler, R., Entz, P., Suk, E.K., Toliat, M.R., Klopp, N., Caliebe, A., et al. (2006). SNP-based analysis of genetic substructure in the German population. *Hum. Hered.* 62, 20–29.
14. Ringquist, S., Styche, A., Rudert, W.A., and Trucco, M. (2007). Pyrosequencing-based strategies for improved allele typing of human leukocyte antigen loci. *Methods Mol. Biol.* 373, 115–134.
15. Rabbee, N., and Speed, T.P. (2006). A genotype calling algorithm for affymetrix SNP arrays. *Bioinformatics* 22, 7–12.
16. Marchini, J., Howie, B., Myers, S., McVean, G., and Donnelly, P. (2007). A new multipoint method for genome-wide association studies via imputation of genotypes. *Nat. Genet.* 39, 906–913.
17. Balding, D.J., and Nichols, R.A. (1995). A method for quantifying differentiation between populations at multi-allelic loci and its implications for investigating identity and paternity. *Genetica* 96, 3–12.
18. Pasquali, L., Fan, Y., Trucco, M., and Ringquist, S. (2006). Rehabilitation of adaptive immunity and regeneration of beta cells. *Trends Biotechnol.* 24, 516–522.
19. Lowel, H., Doring, A., Schneider, A., Heier, M., Thorand, B., and Meisinger, C. (2005). The MONICA Augsburg surveys—basis for prospective cohort studies. *Gesundheitswesen* 67 (Suppl 1), S13–S18.
20. Rinaldo, A., Bacanu, S.-A., Devlin, B., Sonpar, V., Wasserman, L., and Roeder, K. (2005). Characterization of multilocus linkage disequilibrium. *Genet. Epidemiol.* 28, 193–206.
21. Cavalli-Sforza, L.L., Menozzi, P., and Piazza, A. (1994). *The History and Geography of Human Genes* (Princeton, NJ: Princeton University Press).
22. Rosenberg, N.A., Mahajan, S., Ramachandran, S., Zhao, C., Pritchard, J.K., and Feldman, M.W. (2005). Clines, clusters and effect of study design on the inference of human population structure. *PLoS Genetics* 1, e70.
23. Todd, J.A., Bell, J.I., and McDevitt, H.O. (1987). HLA-DQ beta gene contributes to susceptibility and resistance to insulin-dependent diabetes mellitus. *Nature* 329, 599–604.
24. Morel, P.A., Dorman, J.S., Todd, J.A., McDevitt, H.O., and Trucco, M. (1988). Aspartic acid at position 57 of the HLA-DQ beta chain protects against type I diabetes: A family study. *Proc. Natl. Acad. Sci. USA* 85, 8111–8115.
25. Dorman, J.S., LaPorte, R.E., Stone, R.A., and Trucco, M. (1990). Worldwide differences in the incidence of type I diabetes are associated with amino acid variation at position 57 of the HLA-DQ beta chain. *Proc. Natl. Acad. Sci. USA* 87, 7370–7374.
26. Hyttinen, V., Kaprio, J., Kinnunen, L., Koskenvuo, M., and Tuomilehto, J. (2003). Genetic liability of type 1 diabetes and the onset age among 22,650 young Finnish twin pairs: A nationwide follow-up study. *Diabetes* 52, 1052–1055.
27. Wellcome Trust Case Control Consortium (2007). Genome-wide association study of 14,000 cases of seven common diseases and 3,000 shared controls. *Nature* 447, 661–678.
28. Hakonarson, H., Grant, S.F., Bradfield, J.P., Marchand, L., Kim, C.E., Glessner, J.T., Grabs, R., Casalunovo, T., Taback, S.P., Frackelton, E.C., et al. (2007). A genome-wide association study identifies KIAA0350 as a type 1 diabetes gene. *Nature* 448, 591–594.
29. Todd, J.A., Walker, N.M., Cooper, J.D., Smyth, D.J., Downes, K., Plagnol, V., Bailey, R., Nejentsev, S., Field, S.F., and Payne, F. (2007). Robust associations of four new chromosome regions from genome-wide analyses of type 1 diabetes. *Nat. Genet.* 39, 857–864.
30. Wang, H., Thomas, D.C., Pe'er, I., and Stram, D.O. (2006). Optimal two-stage genotyping designs for genome-wide association scans. *Genet. Epidemiol.* 30, 356–368.
31. Skol, A.D., Scott, L.J., Abecasis, G.R., and Boehnke, M. (2007). Optimal designs for two-stage genome-wide association studies. *Genet. Epidemiol.* 31, 776–788.
32. Bacanu, S.A., Devlin, B., and Roeder, K. (2000). The power of genomic control. *Am. J. Hum. Genet.* 66, 1933–1944.
33. Devlin, B., and Roeder, K. (1999). Genomic control for association studies. *Biometrics* 55, 997–1004.
34. Pritchard, J., Stephens, M., and Donnelly, P. (2000). Inference of population structure using multilocus genotype data. *Genetics* 155, 945–959.
35. Devlin, B., Bacanu, S.A., and Roeder, K. (2004). Genomic control to the extreme. *Nat. Genet.* 36, 1129–1130.
36. Epstein, M.P., Allen, A.S., and Satten, G.A. (2007). A simple and improved correction for population stratification in case-control studies. *Am. J. Hum. Genet.* 80, 921–930.
37. Johnstone, I. (2001). On the distribution of the largest eigenvalue in principal components analysis. *Annals of Statistics* 29, 295–327.

# A Microsphere-Based Vaccine Prevents and Reverses New-Onset Autoimmune Diabetes

Brett Phillips,<sup>1</sup> Karen Nylander,<sup>1</sup> Jo Harnaha,<sup>1</sup> Jennifer Machen,<sup>1</sup> Robert Lakomy,<sup>1</sup> Alexis Styche,<sup>1</sup> Kimberly Gillis,<sup>2</sup> Larry Brown,<sup>2</sup> Debra Lafreniere,<sup>2</sup> Michael Gallo,<sup>2</sup> Janet Knox,<sup>2</sup> Kenneth Hogeland,<sup>2</sup> Massimo Trucco,<sup>1</sup> and Nick Giannoukakis<sup>1,3</sup>

**OBJECTIVE**—This study was aimed at ascertaining the efficacy of antisense oligonucleotide-formulated microspheres to prevent type 1 diabetes and to reverse new-onset disease.

**RESEARCH DESIGN AND METHODS**—Microspheres carrying antisense oligonucleotides to CD40, CD80, and CD86 were delivered into NOD mice. Glycemia was monitored to determine disease prevention and reversal. In recipients that remained and/or became diabetes free, spleen and lymph node T-cells were enriched to determine the prevalence of Foxp3<sup>+</sup> putative regulatory T-cells (Treg cells). Splenocytes from diabetes-free microsphere-treated recipients were adoptively cotransferred with splenocytes from diabetic NOD mice into NOD-scid recipients. Live-animal in vivo imaging measured the microsphere accumulation pattern. To rule out nonspecific systemic immunosuppression, splenocytes from successfully treated recipients were pulsed with  $\beta$ -cell antigen or ovalbumin or cocultured with allogeneic splenocytes.

**RESULTS**—The microspheres prevented type 1 diabetes and, most importantly, exhibited a capacity to reverse clinical hyperglycemia, suggesting reversal of new-onset disease. The microspheres augmented Foxp3<sup>+</sup> Treg cells and induced hyporesponsiveness to NOD-derived pancreatic  $\beta$ -cell antigen, without compromising global immune responses to alloantigens and nominal antigens. T-cells from successfully treated mice suppressed adoptive transfer of disease by diabetogenic splenocytes into secondary immunodeficient recipients. Finally, microspheres accumulated within the pancreas and the spleen after either intraperitoneal or subcutaneous injection. Dendritic cells from spleen of the microsphere-treated mice exhibit decreased cell surface CD40, CD80, and CD86.

**CONCLUSIONS**—This novel microsphere formulation represents the first diabetes-suppressive and reversing nucleic acid vaccine that confers an immunoregulatory phenotype to endogenous dendritic cells. *Diabetes* 57:1544–1555, 2008

From the <sup>1</sup>Diabetes Institute, Division of Immunogenetics, Department of Pediatrics, University of Pittsburgh School of Medicine, Pittsburgh, Pennsylvania; <sup>2</sup>Epic Therapeutics, a wholly owned subsidiary of Baxter Healthcare Corporation, Norwood, Massachusetts; and the <sup>3</sup>Department of Pathology, University of Pittsburgh School of Medicine, Pittsburgh, Pennsylvania.

Corresponding author: Nick Giannoukakis, PhD, Department of Pathology, University of Pittsburgh School of Medicine, Diabetes Institute, Rangos Research Center, 3460 Fifth Ave., Pittsburgh, PA 15213. E-mail: ngiann1@pitt.edu.

Received for publication 11 April 2007 and accepted in revised form 22 February 2008.

Published ahead of print at <http://diabetes.diabetesjournals.org> on 26 February 2008. DOI: 10.2337/db07-0507.

Additional information for this article can be found in an online appendix at <http://dx.doi.org/10.2337/db07-0507>.

APC, allophycocyanin; AS-MSP, antisense microsphere; FACS, fluorescence-activated cell sorter; HPLC, high-performance liquid chromatography; IFN- $\gamma$ , interferon- $\gamma$ ; IL, interleukin; PE, phycoerythrin; PEG, polyethylene glycol; PLGA, poly(lactic-co-glycolic acid); PVP, polyvinyl pyrrolidone; SCR-MSP, scrambled control sequences microsphere; TNF- $\alpha$ , tumor necrosis factor- $\alpha$ ; Treg cell, regulatory T-cell.

© 2008 by the American Diabetes Association.

The costs of publication of this article were defrayed in part by the payment of page charges. This article must therefore be hereby marked "advertisement" in accordance with 18 U.S.C. Section 1734 solely to indicate this fact.

Type 1 diabetes is a disorder of glucose homeostasis caused by a chronic autoimmune inflammation of the pancreatic islets of Langerhans (1). The ultimate outcome is the loss of insulin-producing cells to numbers below a threshold that is critically required to maintain physiological glucoregulation. Before this threshold, however, escalating inflammation around (peri-insulitis) and in the islets of Langerhans (insulitis) first renders the insulin-producing  $\beta$ -cells insensitive to glucose and incapable of appropriate insulin production mainly due to the actions of cytokines like interferon- $\gamma$  (IFN- $\gamma$ ), tumor necrosis factor- $\alpha$  (TNF- $\alpha$ ), and interleukin (IL)-1 $\beta$  (2,3).

On clinical confirmation, a large number of type 1 diabetic patients still exhibit evidence of residual  $\beta$ -cell mass that, for a limited time, is functionally responsive to glucose and produces insulin (the so-called "honeymoon period") (4). In fact, patients with a residual  $\beta$ -cell mass manifest better glycemic control and improved prognosis for diabetic complications including retinopathy and nephropathy. These observations have compelled investigation into agents that can be used at the time of clinical diagnosis to preserve residual  $\beta$ -cell mass primarily by intervening with the ongoing autoimmunity. The use of pharmacological systemic immunosuppressive drugs met with initial success in controlling autoimmunity, however, on withdrawal, the autoimmunity recurred, indicating that systemic agents would need to be administered long-term with their associated adverse effects (5,6). More recently, clinical reversal of hyperglycemia has been achieved by anti-CD3 antibody administration, although some questions linger regarding mechanism of action in the transient immunodepletion and associated cytokine-related side effects (7,8). Finally, despite the initial observations in adults, administration of a peptide derived from HSP60 into new-onset diabetic children failed to exhibit any benefit compared with control subjects (9,10). A need therefore remains for a diabetes-suppressive immunotherapeutic agent that does not engender nonspecific systemic immunosuppression.

It is generally accepted that the initial wave of infiltrating immune cells in type 1 diabetes immunopathogenesis consists mainly of antigen-presenting cells homing into the islets in response to an as-yet-unidentified microenvironmental anomaly (11). Although not completely resolved mechanistically and temporally, this anomaly, in a chronic process, compels migratory antigen-presenting cells, and most prominently dendritic cells, to acquire  $\beta$ -cell-resident antigens derived from apoptotic and/or necrotic  $\beta$ -cells. The migratory dendritic cells then undergo an intrinsic "maturation" program that renders them capable

of activating T-cells (including autoreactive,  $\beta$ -cell-specific T-cells) as they accumulate inside the draining pancreatic lymph nodes (12–14).

Dendritic cells, however, also have the capacity to activate and maintain immunoregulatory, “suppressive” cell networks. Apparently, they are regulatory when in a state of functional “immaturity” (15–17). Functional immaturity can be conferred to dendritic cells partly by down-regulating costimulatory pathways using systemic and molecule-specific approaches (18). Numerous studies have confirmed that exogenous administration of functionally immature dendritic cells can facilitate allograft survival and can also prevent autoimmune disease and its recurrence (18). We have shown that administration of dendritic cells from NOD mice with low-level expression of CD40, CD80, and CD86 (induced by *ex vivo* treatment with antisense oligonucleotides targeting the 5′ ends of the respective primary transcripts) into syngeneic recipients can considerably delay and prevent the onset of disease (19,20). This approach is now in a phase I clinical trial in which autologous dendritic cells generated *in vitro* from leukapheresis products are being administered to established type 1 diabetic adult patients to determine safety (M.T. and N.G., personal communication; FDA IND BB-12858). Despite the promise of this study, we have encountered cumbersome logistical requirements to generate these dendritic cell embodiments. We are concurrently pursuing an alternative method to stabilize dendritic cell immaturity directly *in vivo*.

Many studies confirm that microparticle carriers can direct dendritic cells to the administration site, and once phagocytosed, the contents can shape the dendritic cell functional phenotype (21,22). Yoshida and Babensee (22) showed that biodegradable poly-(lactic-co-glycolic acid) (PLGA) microspheres actually induce dendritic cell maturation by upregulating the CD40, CD80, and CD86 costimulatory molecules. Our studies required a nucleic acid delivery system that would be phagocytosed by dendritic cells without upregulating these costimulatory molecules. We therefore chose to incorporate antisense oligonucleotides directed against CD40, CD80, and CD86 into PROMAXX microsphere delivery system (Baxter Healthcare). The inert PROMAXX microsphere technology has been shown to be safe and effective in human trials (23). More importantly, when administered *in vivo*, this technology is neutral with respect to dendritic cell maturation state compared with the known immunostimulatory properties of PLGA-based formulations (22). This neutrality on dendritic cell maturation is a critical criterion in adapting microsphere chemistry for immunosuppressive objectives in which dendritic cells are involved as mediators. Herein, we report a PROMAXX-microsphere-based vaccine in which the antisense oligonucleotides were shown to render dendritic cells diabetes suppressive (19,20) and to prevent and even reverse new-onset autoimmune diabetes.

## RESEARCH DESIGN AND METHODS

**PROMAXX antisense oligonucleotide microsphere formulation and characterization.** Three phosphorothioated (\*) antisense oligonucleotides targeted to the CD40, CD80, and CD86 primary transcripts were synthesized by Integrated DNA Technologies (Coralville, IA). The antisense oligonucleotide sequences are CD40-antisense, 5′ C\* A\* C\* A\* G\* C\* C\* G\* A\* G\* G\* C\* A\* A\* A\* G\* A\* C\* A\* C\* C\* A\* T\* G\* C\* A\* G\* C\* G\* G\* C\* A-3′; CD80-antisense, 5′ -G\* G\* G\* A\* A\* A\* A\* G\* C\* C\* A\* G\* G\* A\* A\* T\* C\* T\* A\* G\* A\* G\* C\* A\* A\* T\* G\* G\* A\* A-3′; and CD86-antisense, 5′ -T\* G\* G\* G\* G\* T\* G\* C\* C\* T\* T\* C\* C\* C\* G\* T\* A\* A\* G\* T\* T\* C\* T\* G\* G\* A\* A\* C\* A\* C\* G\* T\* C-3′. Scrambled antisense oligonucleotides were also

formulated into microspheres and used as nonsense controls in several experiments.

An aqueous solution of the oligonucleotide mixture was prepared by combining aliquots of three oligonucleotide solutions to form a 10 mg/ml solution. Ten milligrams per milliliter poly-L-lysine-HBr in diH<sub>2</sub>O (poly-L-lysine-HBr with an average molecular weight of 50,000 Da; Bachem, King of Prussia, PA) was prepared. Poly-L-lysine-HBr was added to the oligonucleotide solution at a volumetric ratio of 1:1. The mixture was vortexed gently. A 25% polymer solution was prepared containing 12.5% polyvinyl pyrrolidone (PVP; with an average molecular weight of 40,000 Da; Spectrum Chemicals, Gardena, CA) and 12.5% polyethylene glycol (PEG; with an average molecular weight of 3,350 Da; Spectrum Chemicals) in 0.1 mol/l sodium acetate (Spectrum Chemicals) at pH 5.5. The polymer solution was added in a 2:1 volumetric ratio as follows: 750  $\mu$ l antisense oligonucleotides, 750  $\mu$ l poly-L-lysine-HBr, 3.0 ml PEG/PVP, to a final total volume of 4.5 ml.

The 4.5-ml preparation was incubated for 30 min at 70°C and then cooled to 23°C. The solution became turbid on cooling, and a precipitate was formed. The suspension was then centrifuged, and the excess PEG/PVP was aspirated. The resulting pellet was washed by resuspending the pellet in deionized water, followed by centrifugation and removal of the supernatant. The washing process was repeated three times. The aqueous suspension was frozen and lyophilized to form a dry powder of microspheres comprising oligonucleotide and poly-L-lysine. Particle size was determined using dynamic light scattering (LB-550 Nanoparticle Size Analyzer; Horiba, Irvine, CA). Microsphere morphology was examined by scanning electron microscopy (S-4800; Hitachi, Pleasanton, CA).

The weight percent load of the antisense oligonucleotide components in the microsphere was determined using gradient reverse-phase high-performance liquid chromatography (HPLC) with UV detection at 260 nm (Waters, Milford, MA). The microspheres were deformulated using competitive displacement of the DNA oligonucleotides from the poly-L-lysine using an excess of poly-L-aspartic acid sodium salt (molecular weight 5,000–15,000 Da; Sigma) in Tris EDTA buffer (pH 7.8) at 55°C for 24 h. The reverse-phase HPLC was performed on a Waters XTerra MS C18 column (4.6  $\times$  50 mm). Mobile phase A was 8.6 mmol/l tetraethylammonium and 100 mmol/l HFIP, pH 8.2. Mobile phase B was methanol. The oligonucleotides were eluted with a 30-min gradient of 15% B to 18% B at a flow rate of 0.5 ml/min. The column temperature was maintained at 60°C.

Approximately 1.1 mg microspheres was suspended into 1.1 ml 1 $\times$  PBS (pH 7.4) to measure *in vitro* release. The microspheres were centrifuged at several time points, and the release medium was aspirated and measured at UV 260 nm. Fresh release medium was added to the microspheres until the next time point. The release studies were conducted at 22 and 37°C.

**Experimental animals.** Female NOD/LtJ, NOD-scid, C57BL/6, and Balb/c mice were purchased from The Jackson Laboratories (Bar Harbor, ME) and used between the ages of 5 and 22 weeks. Animals were maintained in a specific pathogen-free environment in the Animal Facility of the Rangos Research Center and used in full compliance with experimentation protocols approved by the Animal Research Care Committee of the Children’s Hospital of Pittsburgh.

**Reagents, biochemicals, and cell culture.** All biochemical and cell culture reagents were purchased from Invitrogen (Carlsbad, CA). Antibodies were purchased from BD Biosciences (San Diego, CA) either as directly conjugated fluorescent embodiments or as affinity-purified preparations in concert with fluorescently labeled isotype-matched secondary products. The specific clones used were CD4 clone, RM4-5; and CD25 clone, 7D4. To ascertain the prevalence of Foxp3<sup>+</sup> cells, we used the kit commercially available from eBioscience (San Diego, CA), which includes the FJK-16S Foxp3 clone. Spleen or lymph node–derived cells were enriched into T-cells using column methodology (R&D Systems, Indianapolis, IN). The NIT-1 (NOD insulinoma T-antigen-transformed-1 cell line) insulinoma cell line (CRL-2055; American Type Culture Collection) was maintained in Ham’s F-12K medium with 2 mmol/l L-glutamine and 10% heat-inactivated fetal bovine serum until 70% confluence. The cells were then gently removed by collagenase digestion and made into lysates by repeated freeze-thaw cycles. The lysate was dispensed into aliquots in sterile PBS.

**Antisense microsphere administration.** Microspheres formulated with the mixture of the CD40, CD80, and CD86 antisense oligonucleotides (AS-MSPs) or with scrambled control sequences (SCR-MSP) were dispensed into aliquots of 50- $\mu$ g oligonucleotide formulations in sterile PBS. One hundred microliters of AS-MSP, SCR-MSP, or PBS was injected subcutaneously, at a site anatomically proximal to the pancreatic lymph nodes, into 5- to 8-week-old NOD female mice in the initial prevention study. To determine their efficacy in new-onset diabetic NOD mice, we first treated diabetic mice (determined by two consecutive blood glucose measurements of >300 mg/dl) once daily with 2 units 1:1 Humulin R:Humulin N mix in PBS until nonfasting blood glucose stabilized to below 300 mg/dl. Insulin treatment was immediately stopped, and



the microsphere formulations were injected subcutaneously, at a site anatomically proximal to the pancreatic lymph nodes, three times a week until the mice were killed for further study.

**Adoptive transfer of immune cells into NOD-scid recipients.** To determine whether the microsphere administration induced regulatory immune cell populations, we isolated spleen from diabetes-free NOD mice, administered the AS-MSP, and made single cells. Parallel single-cell preparations were enriched into T-cells. Splenocytes and enriched T-cells were cotransferred in equal numbers ( $1 \times 10^7$ ) into 7- to 10-week-old female NOD-scid recipients by intravenous injection. Diabetes was monitored on consecutive days, twice weekly.

**Fluorescence-activated cell sorter analysis.** Fluorescence-activated cell sorter (FACS) analyses were performed on spleen or lymph node cells of successfully treated NOD mice periodically. These were mice that were treated at <10 weeks of age and remained diabetes free or new-onset diabetic mice that were "reversed." Specifically, cell surface phenotype of the T-cells was assessed by FACS analysis in a FACS Vantage SE instrument using FACSDiva and CellQuest modules (BD Biosciences). In addition to the antibodies described above, relevant isotype-specific, fluorescently conjugated antibodies were used throughout as controls for nonspecific cell surface binding. Cells were incubated with mixtures of specific antibodies, and in parallel, with the isotype controls at titers between 1:100 and 1:500 as per the manufacturer's suggestions. They were also labeled with propidium iodide, 7-AAD, and/or the annexin V-staining reagent (Invitrogen-Molecular Probes) and then used directly for FACS analysis. Percentage of positive cells or mean fluorescence intensity was measured for cells gated on forward and side-scatter properties representing T-lymphocytes. Dead cells and cell clumps were excluded from the analyses, which were performed using the CellQuest software package.

**T-cell proliferation assays in culture.** To ascertain proliferation of T-cells from AS-MSP-treated NOD mice to alloantigens or nominal antigens, spleens were isolated from randomly selected mice and enriched into T-cells. These were then cocultured with equal numbers of irradiated splenocytes ( $1 \times 10^5$ ) from allogeneic mice or syngeneic mice in the presence/absence of 1  $\mu$ g intact ovalbumin. Proliferation was measured 5 days later using the CyQuant fluorometric reagent (Invitrogen-Molecular Probes) as directed by the manufacturer. The coculture supernatants were retained to measure cytokine levels by Luminex-based fluorescence methods (Beadlyte; Upstate Biotechnology). To measure proliferation in response to the NIT-1 cell line-derived lysate,  $1 \times 10^5$  splenocytes from treated NOD mice were cocultured with an equal number of syngeneic and age-matched irradiated splenocytes with or without the addition of 5  $\mu$ g NIT-1 cell lysate. After 5 days, the supernatant was removed for cytokine analysis, and proliferation was measured.

**Histology.** The degree of insulinitis in the pancreata of randomly selected successfully treated NOD mice was ascertained in serial sections of formalin-fixed tissue by hematoxylin-eosin treatment. Additional sections were probed for insulin content using a commercially available method (Vector BioLabs) with an insulin antibody (DakoCytomation, Carpinteria, CA).

**In vivo live-animal imaging.** NOD female mice (8 weeks of age) were anesthetized with isoflurane delivered by the XGI-8 Gas Anesthesia System (Xenogen). Initial isoflurane concentration was set to 2.5% and was reduced to 1.5% once the animal was anesthetized. Mice were imaged before injection on the IVIS Lumina (Xenogen) system using a dsRed filter set. Fluorescent exposure times of 0.8 s were used for in vivo imaging and of 0.1 s for ex vivo imaging. Once imaged for background fluorescence, mice received a 300- $\mu$ l intraperitoneal injection that contained either a mixture of 150  $\mu$ l fluorescent microspheres (FluoSpheres 580 nm/605 nm; Molecular Probes-Invitrogen) and 100  $\mu$ l PBS (control) or a mixture of 150  $\mu$ l fluorescent microspheres (FluoSpheres 580 nm/605 nm) and 0.5  $\mu$ g/ $\mu$ l AS-MSP microspheres. Mice were then imaged just before euthanasia (and organ excision) at 3, 24, and 48 h after injection. The spleen and pancreas were then removed and imaged immediately afterward. In a subsequent study, a PROMAXX formulation of a Cy3-labeled oligonucleotide nontargeting siRNA sequence purchased from Dharmacon (Lafayette, CO) was injected subcutaneously at an anatomically distal and proximal site to the pancreatic lymph nodes (scruff and flank, respectively) and the pancreas and spleen were excised 3 h after the injection. Average radiance of organs was calculated using Living Image version 3.0 (Xenogen-Caliper Life Sciences), and mean values were graphed.

**Determination of costimulatory molecule levels on dendritic cells loaded with AS-MSP in spleen in vivo.** Female NOD mice (8–12 weeks of age) were treated with fluorescent microspheres 0.2  $\mu$ m in diameter with the excitation emission profiles of 505 nm/515 nm (FluoSpheres 505 nm/515 nm; Molecular Probes-Invitrogen). The mice were injected subcutaneously with a mix of either 100  $\mu$ l fluorescent microspheres and 100  $\mu$ l PBS (control) or 100  $\mu$ l fluorescent microspheres and 100  $\mu$ l 0.5  $\mu$ g/ $\mu$ l antisense oligonucleotide mixture (CD40, CD80, and CD86) in a total volume of 300  $\mu$ l. Spleens were excised at 1, 2, 3, and 6 days after injection. Single splenocytes were treated

with Mouse BD Fc block (BD Pharmingen) for 5 min to reduce nonspecific antibody binding. Cells were then treated with anti-mouse CD11c allophycocyanin (APC) and CD40 phycoerythrin (PE), CD80 PE, or CD86 PE for 30 min (BD Pharmingen), after which the cells were washed and fixed in a 2% paraformaldehyde solution. Cells were then gated by FACS into CD11c and fluorescent microsphere double-positive cells, and within this gate, CD40, CD80, and CD86 levels were further ascertained. Control isotypes were used throughout this experiment.

**Statistical analysis.** Student's *t* test, ANOVA, and Kaplan-Meier log-rank analysis where described were facilitated using the Prism version 4 software by GraphPad (San Diego, CA).

## RESULTS

**Characterization of antisense oligonucleotide-formulated PROMAXX microspheres (AS-MSPs).** Scanning electron micrographs of the PROMAXX microspheres exhibited a relatively smooth surface (Fig. 1A). The particle size of the microspheres determined by light scattering was 0.5–4  $\mu$ m in size with an average particle size of  $\sim$ 2.5  $\mu$ m. Thus, the calculated surface area of a single microsphere is  $\sim$ 19.6  $\mu$ m<sup>2</sup>. The loading of oligonucleotides determined by reverse-phase HPLC in the microspheres was  $\sim$ 70% weight by weight. Based on these measurements, the calculated number of copies of antisense oligonucleotide per microsphere was  $\sim$ 1.05  $\times$  10<sup>8</sup>.

The in vitro release kinetics of the antisense oligonucleotides from the microspheres is shown in Fig. 1B at 22 and 37°C. The data show that after a small initial burst effect, the cumulative percent release is proportional to the square root of time. However, after 120 h, <1.1% of the incorporated antisense oligonucleotides have been released at 37°C and <0.8% release was observed at 22°C. This suggests that despite the 70% weight percent loading of oligonucleotide in the microspheres, most of the drug release occurs only after the microsphere has been up-taken by cells in vivo.

**Administration of diabetes-suppressive antisense oligonucleotide-formulated PROMAXX microspheres into pre-diabetic NOD female mice delays/prevents diabetes and reverses it in new-onset diabetic animals.** Our previous studies demonstrated that NOD-derived dendritic cells treated ex vivo with a mixture of phosphorothioated antisense oligonucleotides targeting the 5' end of the CD40, CD80, and CD86 primary transcripts prevented diabetes in syngeneic recipients (19,20). To determine whether the microsphere-formulated antisense mixture was as efficacious, we administered AS-MSP targeting the 5' end of the CD40, CD80, and CD86 primary transcripts into NOD female mice between the ages of 5 and 8 weeks. As controls, we concurrently treated parallel groups with PROMAXX formulation containing SCR-MSP and PBS vehicle. One single injection of AS-MSP, at a site anatomically proximal to the pancreatic lymph nodes, significantly delayed onset of diabetes (Fig. 1C), and eight consecutive injections (Fig. 1D) were very efficacious in preventing the disease altogether. All NOD mice treated with control formulations and untreated NOD mice developed diabetes by 22 weeks of age. We are now determining whether fewer consecutive injections can be as efficacious.

We then proceeded to determine whether the AS-MSP could reverse new-onset hyperglycemia, which could suggest reversal of autoimmunity and mechanisms promoting preservation of residual  $\beta$ -cell mass in NOD mice. NOD mice between 12 and 16 weeks of age developed diabetes confirmed by two consecutive blood glucose readings of >300 mg/dl. These mice were treated with daily insulin

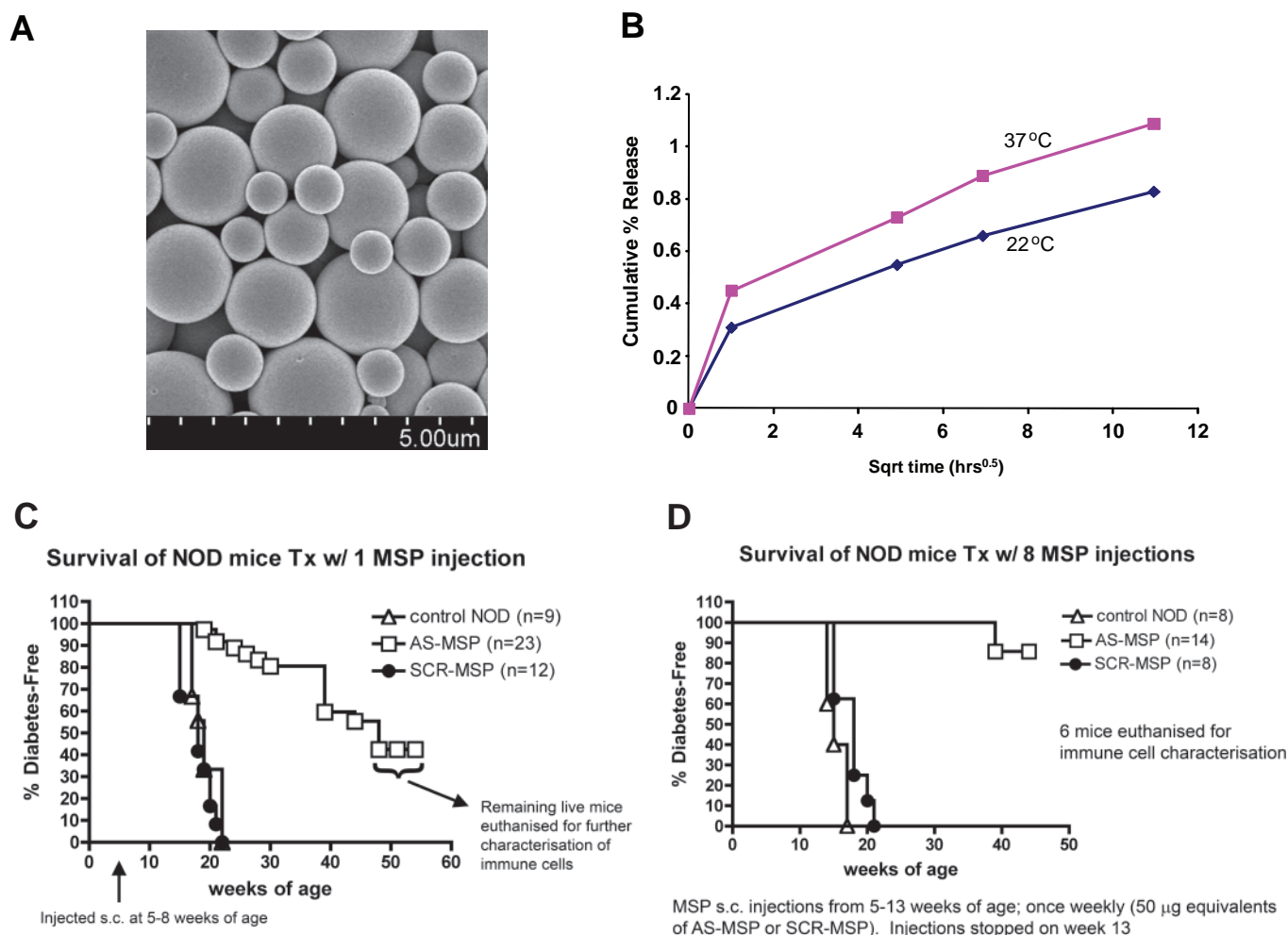


**FIG. 1. A:** Scanning electron micrograph of the AS-MSP. The micrograph exhibits an essentially smooth surface with particle diameters in the 1- to 4-μm size range. Size bar is shown at bottom of the micrograph. **B:** The cumulative percent release of antisense oligonucleotides from the microspheres. The cumulative percent release was observed to be directly proportional to the square root of time. At 22°C, ~0.8% of the oligonucleotide was released, and at 37°C, ~1.1% of the incorporated oligonucleotide was released. The release kinetics appears to conform to matrix diffusion release mechanism. **C:** AS-MSP administration into NOD mice at 5–8 weeks of age delays diabetes onset. Two groups of NOD female mice (5–8 weeks old) were given a single subcutaneous injection of microsphere-formulated antisense oligonucleotides at a site anatomically proximal to the pancreatic lymph nodes. The formulation was injected in the amount of what was considered to contain 50 mg of a 1:1:1 mixture of each antisense oligonucleotide (anti-CD40, anti-CD80, and anti-CD86) or scrambled sequences (SCR-MSP) or PBS vehicle (control). Tail vein blood glucose was measured weekly. Diabetes was confirmed after two consecutive readings of >280–300 mg/dl. The graph shows cumulative survival of two independently treated cohorts.  $P < 0.0001$ , Kaplan-Meier analysis. **D:** Frequent AS-MSP administration into NOD mice at 5–8 weeks of age prevents diabetes onset. NOD female mice (5–8 weeks old) were given eight consecutive single subcutaneous injections, at a site anatomically proximal to the pancreatic lymph nodes (once weekly), of microsphere-formulated antisense oligonucleotides. The formulation was injected in the amount of what was considered to contain 50 μg of a 1:1:1 mixture of each antisense oligonucleotide (anti-CD40, anti-CD80, and anti-CD86; AS-MSP) or scrambled sequences (SCR-MSP) or PBS vehicle (control). Tail vein blood glucose was measured twice weekly. Diabetes was confirmed after two consecutive readings of >280–300 mg/dl.  $P < 0.0001$ , Kaplan-Meier analysis.

injections intraperitoneally until glycemia was stabilized to <300 mg/dl. Decreased blood glucose was generally observed over a 10- to 18-day period of insulin administration. The insulin was then immediately discontinued and AS-MSP, SCR-MSP, or PBS was injected subcutaneously, at a site anatomically proximal to the pancreatic lymph nodes, twice weekly for no more than 25 days after the first microsphere administration (Fig. 2A). Figure 2B and C demonstrate that AS-MSP administration can reverse new-onset hyperglycemia that is stably maintained even after cessation of the microsphere treatment. This outcome is reproducible, and in Fig. 2D, we show the outcome from three additional study groups. An additional 7 of 15 mice exhibited reversal of hyperglycemia and stable maintenance after cessation of the AS-MSP administration.

To ascertain the degree to which pancreatic inflammation was affected in NOD recipients of the AS-MSP that

exhibited long-term protection from diabetes (treated with AS-MSP at <8 weeks of age; cohort shown in Fig. 1D), we isolated pancreata from three randomly selected AS-MSP recipients, SCR-MSP controls, and diabetic NOD mice. Whereas SCR-MSP-treated mice and diabetic controls exhibited significant insulinitis and indistinguishable islet mass, respectively, we observed normal islet architecture with an absence of insulinitis in AS-MSP recipients (Fig. 3). **AS-MSP treatment of NOD female mice augments the prevalence of Foxp3<sup>+</sup> CD25<sup>+</sup> putative regulatory T-cells in vivo.** Our previous data suggested that the ex vivo antisense-treated dendritic cells were suppressive at least in part by augmenting the prevalence of CD4<sup>+</sup> CD25<sup>+</sup> putative regulatory T-cells (Treg cells) (19,20). We have now specifically addressed the question of whether AS-MSP directly augment Treg cells by enumerating the percentage of Foxp3<sup>+</sup> CD25<sup>+</sup> T-cells inside a CD4<sup>+</sup> gate in



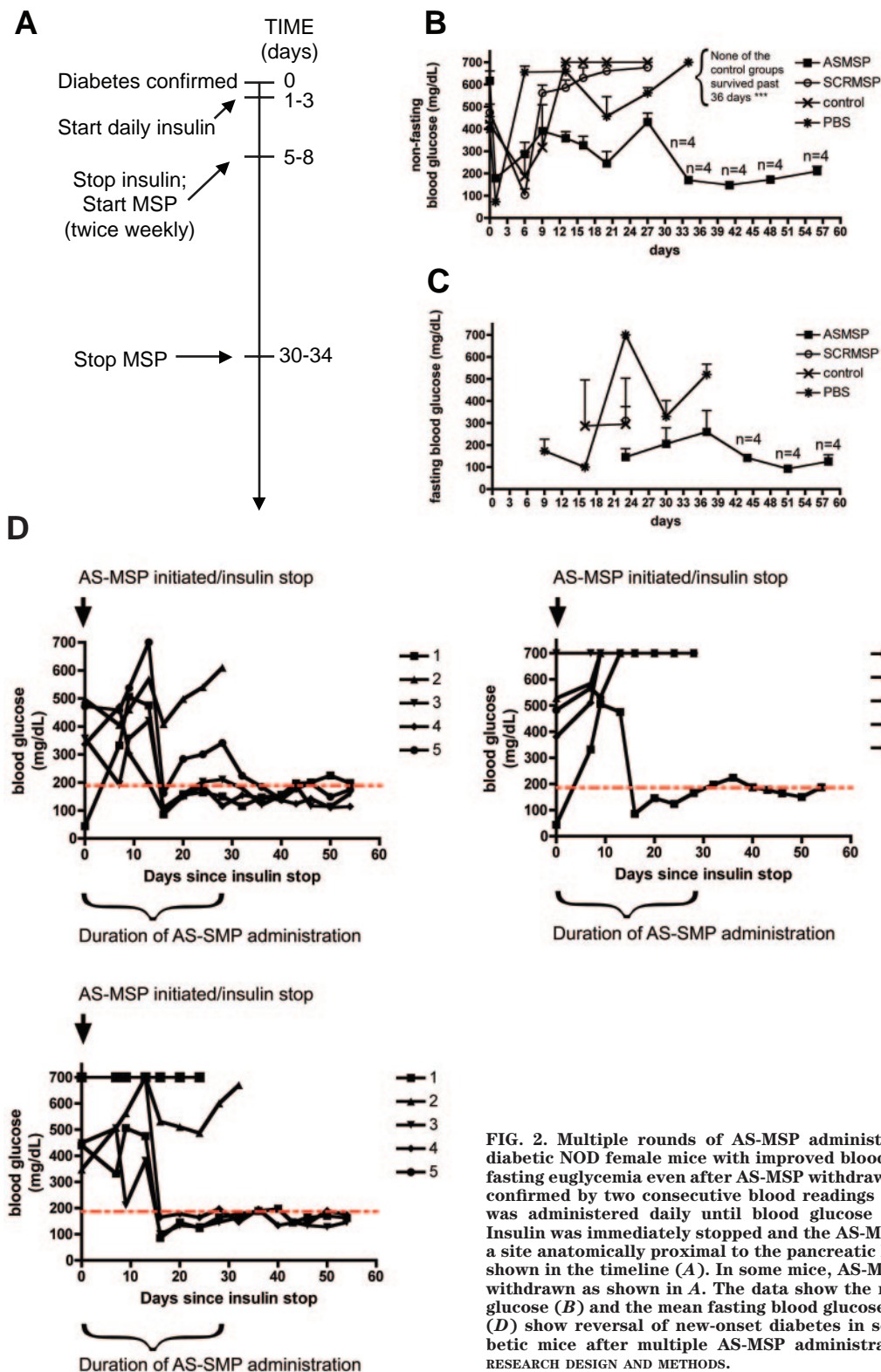
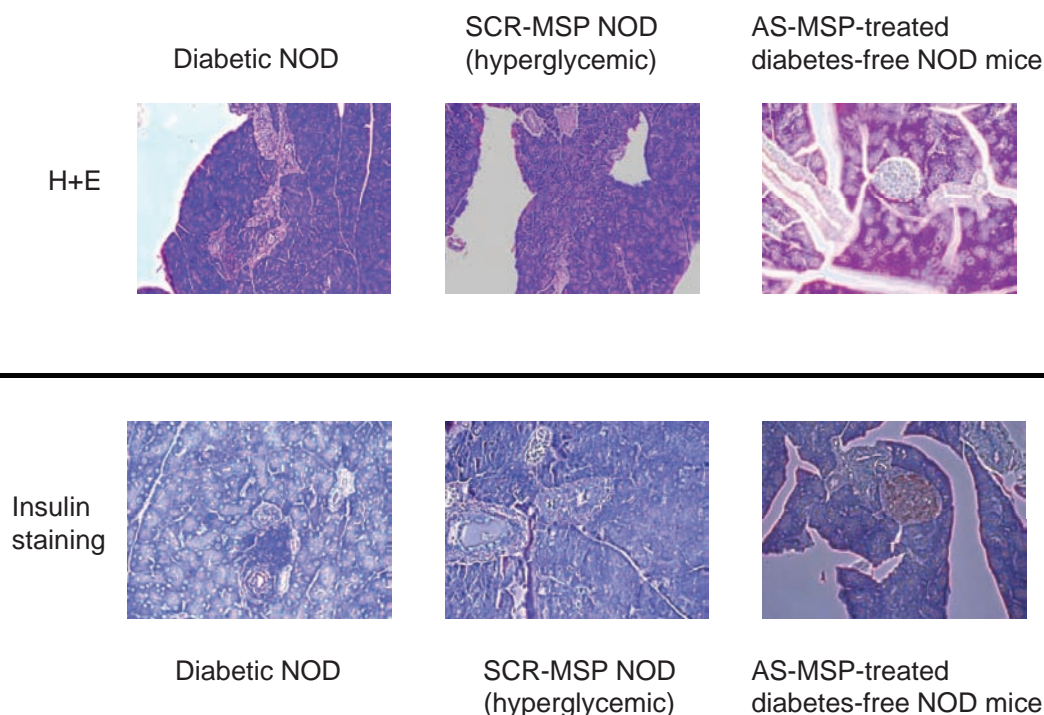


FIG. 2. Multiple rounds of AS-MSP administration into new-onset diabetic NOD female mice with improved blood glucose levels; stable fasting euglycemia even after AS-MSP withdrawal. Diabetes onset was confirmed by two consecutive blood readings of  $>300$  mg/dl. Insulin was administered daily until blood glucose fell below 300 mg/dl. Insulin was immediately stopped and the AS-MSP administrations (at a site anatomically proximal to the pancreatic lymph nodes) began as shown in the timeline (A). In some mice, AS-MSP administration was withdrawn as shown in A. The data show the mean nonfasting blood glucose (B) and the mean fasting blood glucose (C)  $\pm$  SE. The graphs (D) show reversal of new-onset diabetes in separate groups of diabetic mice after multiple AS-MSP administrations as described in RESEARCH DESIGN AND METHODS.

the spleen and lymph nodes of pre-diabetic NOD females. AS-MSP alone, and not the control microspheres or PBS, augmented the prevalence of Foxp3<sup>+</sup> CD25<sup>+</sup> T-cells (Fig. 4).

Given that the AS-MSP treatment yielded augmented numbers of CD4<sup>+</sup> CD25<sup>+</sup> Foxp3<sup>+</sup> putative Treg cells, it was logical to posit that a splenocyte population from

AS-MSP-treated mice should be able to confer some degree of suppression to diabetes inducement in immunodeficient mice administered splenocytes from diabetic NOD mice. Toward this objective, a 1:1 mix of splenocytes from AS-MSP-treated diabetes-free NOD mice and new-onset diabetic NOD mice was injected into female NOD-scid mice between 6 and 10 weeks of age. As controls, a 1:1



**FIG. 3. Absence of insulitis and normal insulin content in pancreata of AS-MSP-treated NOD mice. Top:** Hematoxylin-eosin staining of representative serial sections from diabetic, SCR-MSP diabetic, and diabetes-free AS-MSP recipients. **Bottom:** Insulin staining of representative serial sections from diabetic, SCR-MSP diabetic, and diabetes-free AS-MSP. Sections are representative of three randomly selected NOD mice in each group.

mix of splenocytes from nondiabetic 10-week-old NOD mice was treated with either SCR-MSP (eight consecutive subcutaneous injections spaced every 3 days apart), and splenocytes from diabetic mice were injected into 6- to 10-week-old NOD-scid females. In addition, another control group of NOD-scid mice was injected with splenocytes from new-onset diabetic NOD mice. Each cell population consisted of  $1 \times 10^7$  splenocytes freshly isolated. Blood glucose was monitored twice weekly, and two consecutive readings of nonfasting glucose  $>300$  mg/dl was considered as the diabetic threshold. Figure 5 demonstrates that adoptive transfer of diabetes in NOD-scid recipients was almost completely abrogated in the presence of splenocytes derived from AS-MSP recipients that were diabetes free.

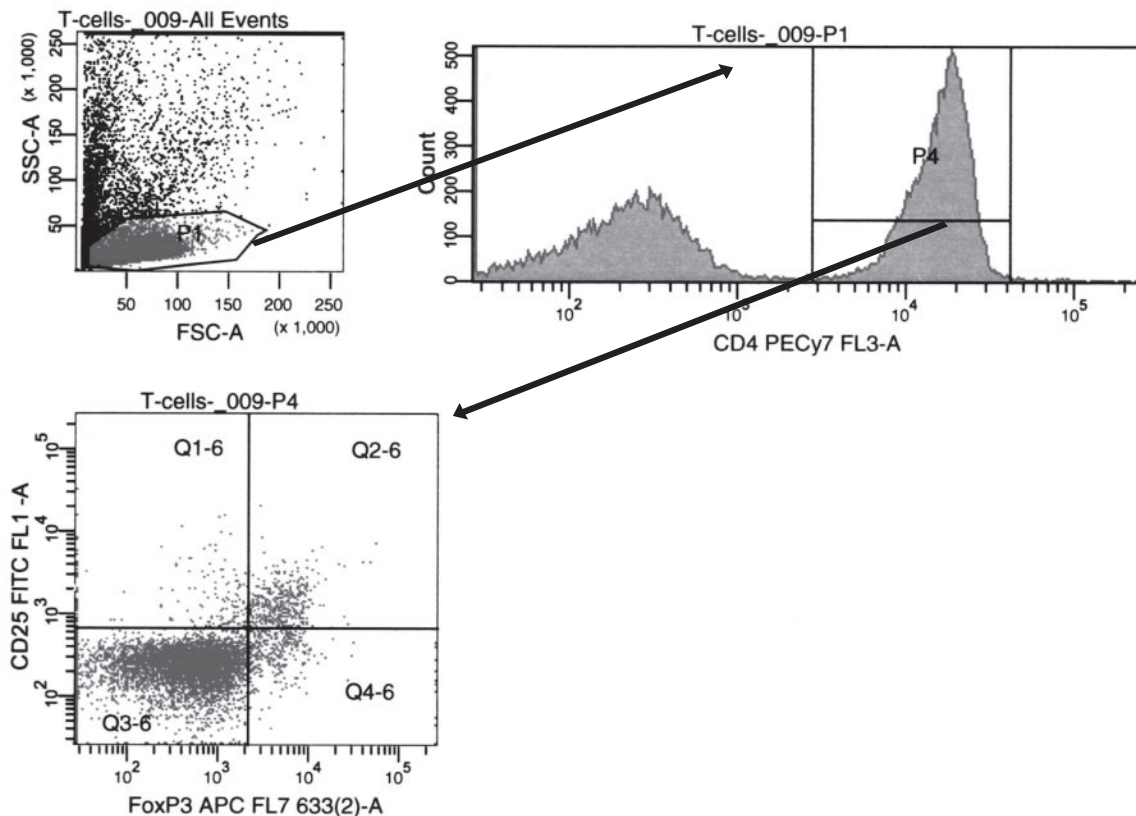
In vivo-injected AS-MSPs accumulate within the pancreatic lymph nodes and spleen and confer decreased costimulatory molecule surface expression on splenic dendritic cells in vivo. To determine the route of migration of the AS-MSP, which could offer insight into the mechanism of immunoregulation and diabetes suppression, we used in vivo imaging technology to observe the temporal accumulation of a 1:1 mix of commercially available fluorescent microspheres and the AS-MSPs. The sizes of the commercially purchased fluorescent microspheres (FluoSpheres) were considerably smaller than the particle size of the AS-MSP. The AS-MSP were  $2.5 \mu\text{m}$  on average and the FluoSpheres were  $0.2 \mu\text{m}$  on average. Thus the FluoSpheres should not interfere with the uptake of the AS-MSP by dendritic cells. In Fig. 6, we show that as early as 3 h after intraperitoneal injection, the fluorescent microspheres accumulated at anatomical sites where the pancreas and the spleen reside (Fig. 6A). The intensity of the fluorescence did not change over a 72-h monitoring period (data not shown). To confirm the accumulation of

the microspheres within the pancreas and spleen, we excised these two organs from the mice that were being monitored live, and in Fig. 6B, we confirm that the fluorescent microspheres accumulated as early as 3 h after injection at distinct foci in pancreas, which we interpret to be the pancreatic lymph nodes, and at distinct foci within the spleen. Although accumulation of fluorescent microspheres was observed in these two organs regardless of whether AS-MSP were included in the mix or not, the actual intensity of the fluorescence was different in organs excised at the times indicated in Fig. 6C and D. The fluorescence was evident in the spleen and pancreata of all mice at all time points studied (from 3 h to 6 days after injection) (Fig. 6; data not shown).

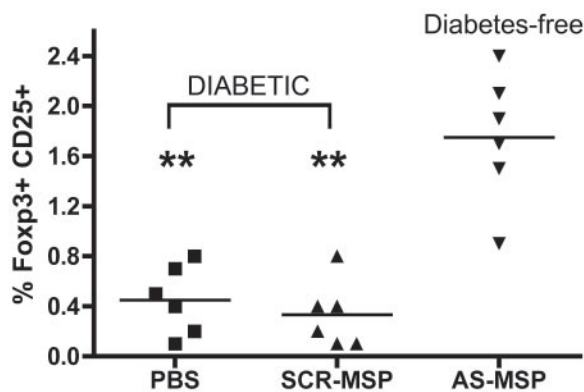
As an additional confirmation that oligonucleotide-formulated microspheres accumulate inside the pancreas and spleen, we injected PROMAXX-formulated Cy3-labeled siRNA to CD86 identically as described above. We also compared the pancreatic accumulation of this Cy3-labeled formulation after intraperitoneal injection, subcutaneous injection at a site distal to the anatomic location of the pancreatic lymph nodes (at the scruff of the mouse), and subcutaneous injection at the site used in the prevention and reversal studies documented herein (flank of the mouse). Figure 6E confirms the pancreatic accumulation of PROMAXX-formulated Cy3-labeled oligonucleotide at 3 h after injection but only when the subcutaneous injection was performed anatomically proximal to the pancreatic lymph nodes.

To confirm that AS-MSP administration conferred a decrease in CD40, CD80, and CD86 in dendritic cells in vivo, we injected NOD mice intraperitoneally with a mixture of the FluoSpheres with PBS as control or with AS-MSP as described in RESEARCH DESIGN AND METHODS. At the times indicated at the top of each graph in Fig. 6F, we

## A Gating for FACS



## B Splenic T-cells



## C Pooled lymph node T-cells

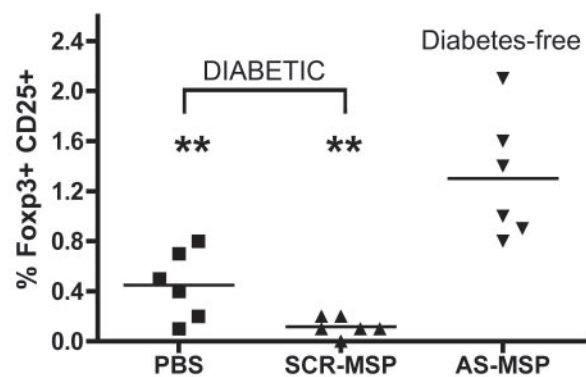


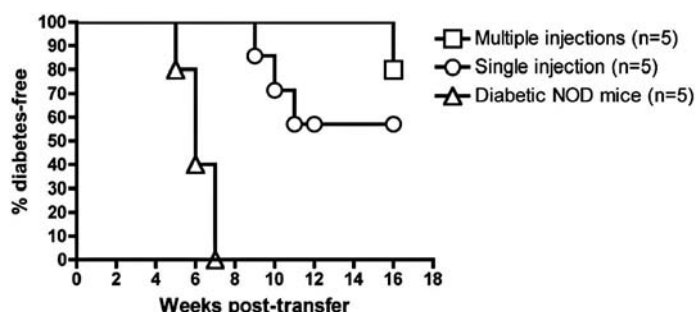
FIG. 4. T-cells from AS-MSP-treated, diabetes-free NOD mice exhibit increased prevalence of Foxp3<sup>+</sup> CD25<sup>+</sup> putative Treg cells. T-cells were enriched from the spleen or the pooled lymph nodes of AS-MSP-treated diabetes-free mice selected at random from the AS-MSP diabetes-free cohort shown in Figure 1D. All mice treated with PBS or SCR-MSP developed diabetes as shown in Figure 1D. At the time of diabetes confirmation, T-cells were harvested from spleen and pooled lymph nodes. The cells were then stained intracellularly for Foxp3 and with CD25, and the percentage of double-positive cells in a lymphocyte population was determined by FACS analysis. An example of the gating is shown in A. The scatter gram in B shows the percentage of double-positive cells in individual mice at the time of euthanasia in spleen, and in C, the percentage of putative Treg cells in pooled lymph node is shown.  $P < 0.001$  between AS-MSP-treated mice and the two controls in both graphs by Mann-Whitney  $U$  test.

excised the spleen and measured CD40, CD80, and CD86 levels in CD11c<sup>+</sup> fluorescence<sup>+</sup> double-positive single cells. We observed a decreased level of all three costimulatory molecules on CD11c<sup>+</sup> cells that had concentrated the mixture of fluorescent microspheres and AS-MSP as early as 1 day after injection with maintenance of these levels compared with CD11c<sup>+</sup> cells from control mix-

treated NOD mice over a 6-day monitoring period. The only exception was seen at day 3 for CD40.

**AS-MSP treatment of NOD pre-diabetic female mice yields T-cells hyporesponsive to NIT-1 cell lysate in vitro without inducing nonspecific immunosuppression.** A major concern for eventual translation of diabetes-suppressive therapies into human trials is the antigen





#### DIABETES INCIDENCE IN NON-SCID RECIPIENTS

- Spl from diabetic NOD mice: 0/5 at 16 weeks post transfer (p.t)
- Spl from single AS-MSP inj. mice: 2/5 at 16 weeks p.t.
- Spl from multiple AS-MSP inj. mice: 4/5 at 16 weeks p.t.

**FIG. 5.** Cotransfer of splenocytes from AS-MSP-treated, diabetes-free NOD mice suppresses the adoptive transfer of diabetes into NOD-scid mice by splenocytes from diabetic NOD donors. Four of five NOD-scid recipients of splenocytes from AS-MSP-treated NOD mice and diabetogenic splenocytes remained diabetes-free at 16 weeks after cell transfer, whereas only two of five and zero of five were diabetes-free after cotransfer of diabetogenic splenocytes and splenocytes from SCR-MSP and PBS-treated NOD mice, respectively. In the graph inset, Spl refers to splenocytes and p.t. refers to the time the mice were killed for further analysis after transfer. Splenocytes from randomly selected diabetes-free AS-MSP-treated mice from the treatment groups shown in Figure 1C and D (single or multiple AS-MSP injections) were cotransferred into female NOD-scid mice of 10 weeks of age along with an equal number of splenocytes ( $1 \times 10^7$ ) from new-onset diabetic NOD female mice (15–18 weeks old). Diabetes was monitored once weekly in tail vein blood. Levels of  $>280$  mg/dl at two consecutive readings were deemed to indicate diabetes. There were five NOD-scid recipients per cotransfer groups as shown below in the graph.  $P = 0.0003$ , between control and AS-MSP splenocyte recipients, Kaplan-Meier analysis.

specificity and therefore the cell specificity of the approach and whether the treatment confers global and nonspecific suppression. To address these issues, we killed randomly selected diabetes-free mice from the cohorts shown in Fig. 1D, and we then proceeded to ascertain the proliferation of splenic and lymph node T-cells to alloantigens, nominal antigens using intact ovalbumin and also using syngeneic  $\beta$ -cell-derived antigen in the form of cell lysate from the NOD-derived insulinoma cell line NIT-1 (24,25). Although insulin and GAD are viable candidate autoantigens with mechanistic and teleological involvement (26), the nature of the initiating autoantigen remains unclear. Nevertheless, it is reasonable to consider that it should be  $\beta$ -cell resident. Therefore, we used the NIT-1 cell line that derives from an NOD insulinoma as a source of  $\beta$ -cell antigen in cocultures of T-cells from diabetes-free NOD mice treated with the AS-MSP to determine the possibility of antigen-specific hyporesponsiveness. Supplementary Fig. 7 (available in an online appendix at <http://dx.doi.org/10.2337/db07-0507>), shows that T-cell proliferation to nominal and alloantigen is maintained, whereas there is T-cell hypoproliferation in cocultures with NIT-1 cell lysate. Furthermore, ascertaining the cytokine profile in the coculture supernatants, we observed a significant decrease in TNF- $\alpha$  production by T-cells from AS-MSP-treated, diabetes-free NOD mice even in the presence of NIT-1 lysate (Supplementary Fig. 7F; from those diabetes-free NOD mice in Fig. 1D). Although IFN- $\gamma$  production was slightly decreased in the cocultures of T-cells from the AS-MSP-treated mice, it was not statistically distinguishable from the cocultures with T-cells from PBS-treated mice in the presence of NIT-1

lysate. The assay, finally, could not detect the presence of IL-4, IL-10, or TGF- $\alpha$  in the supernatants.

#### DISCUSSION

Formulation of bioactive agents into microparticles offers a versatile means of delivering these molecules in vivo especially for the purpose of modulating the immune system (21,27). An important component of the modulatory properties of microspheres is the polymer backbone that often stimulates potent antigen-presenting cell activation, which is beneficial for tumor immunotherapy or antipathogen interventions (28,29). For the purposes of immunosuppression, however, the polymer and the component chemistries should be such that at the very minimum, they should be neutral on antigen-presenting cell state. PROMAXX nucleic acid microspheres offers this versatility (23) as a result of the minimal quantity of formulation excipients. In this regard, we now show its utility as a key component of a diabetes-suppressive vaccine.

The most noteworthy finding in these studies is the capacity of the AS-MSP to reverse new-onset hyperglycemia, which we believe is underlined by preservation of residual  $\beta$ -cell mass. Nevertheless, we cannot yet formally distinguish this from a potential regenerative process of  $\beta$ -cells (division of existing  $\beta$ -cells or differentiation of progenitor/stem cells from ductal epithelium [30–32]). There is, however, considerable support from previous studies for a sufficiency in  $\beta$ -cell mass that is functionally responsive to glucose at the time of diagnosis of type 1 diabetes (32–36). This mass, if permitted to recover from autoimmune attack by modulating the aggressive and  $\beta$ -cell-specific immune cells, may provide the patient with normoglycemic metabolic control.

Although our data herein are not the first to demonstrate small molecule-based diabetes prevention in the NOD mouse, they are the first to show a well-defined microparticle system that can reverse hyperglycemia in new-onset disease whose mechanism of action is decipherable. In preliminary studies, we have observed that when the formulation was injected into NOD-scid immunodeficient mice reconstituted with splenocytes from NOD mice of various diabetes stages (young, 12–15 weeks old where autoimmunity is already established and where  $\beta$ -cell function is impaired, and from new-onset diabetics), the prevalence of CD4 $^{+}$  CD25 $^{+}$  putative Treg cells increased. We have now confirmed herein in a more direct experiment that CD4 $^{+}$  CD25 $^{+}$  Foxp3 $^{+}$  T-cells numbers increase in female NOD mice administered AS-MSP. These findings may explain the capacity of T-cells from AS-MSP-treated NOD mice free of diabetes to prevent the adoptive cotransfer of the disease to NOD-scid recipients. More importantly, T-cells from diabetes-free AS-MSP exhibited poor proliferation to NIT-1 lysate in vitro while proliferating vigorously in cocultures with allogeneic irradiated splenocytes or when pulsed with ovalbumin.

Many lines of evidence conclude that injected microsphere formulations are rapidly taken up by resident and/or migratory antigen-presenting cells, especially dendritic cells, and accumulate inside lymphoid organs anatomically proximal to the site of injection. Our studies in the past have also confirmed this uptake/trafficking (K.N., J.H., N.G., unpublished observations). Herein, we have provided some of these data, which confirm that subcutaneously injected microspheres accumulate as early as 3 h

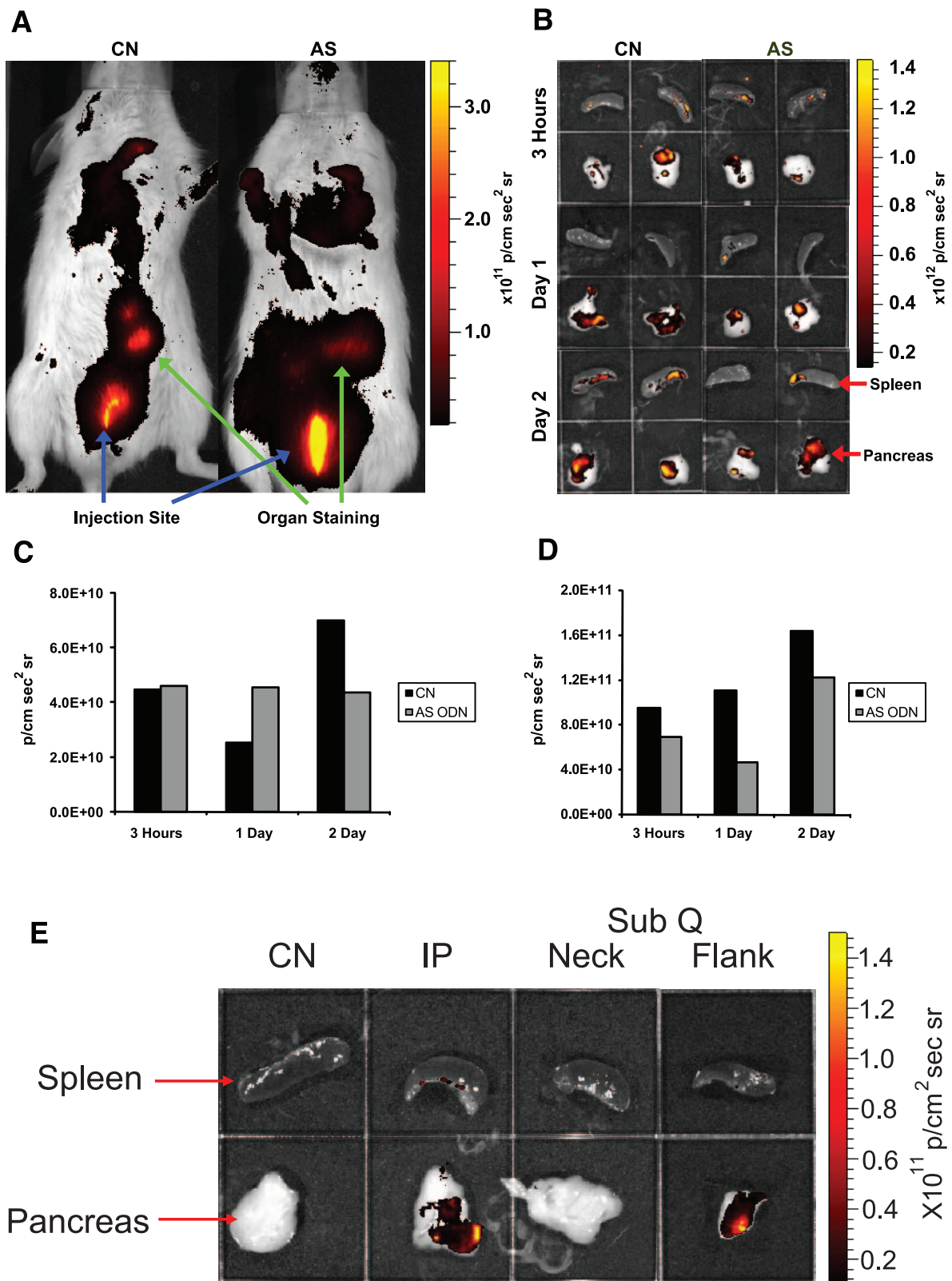
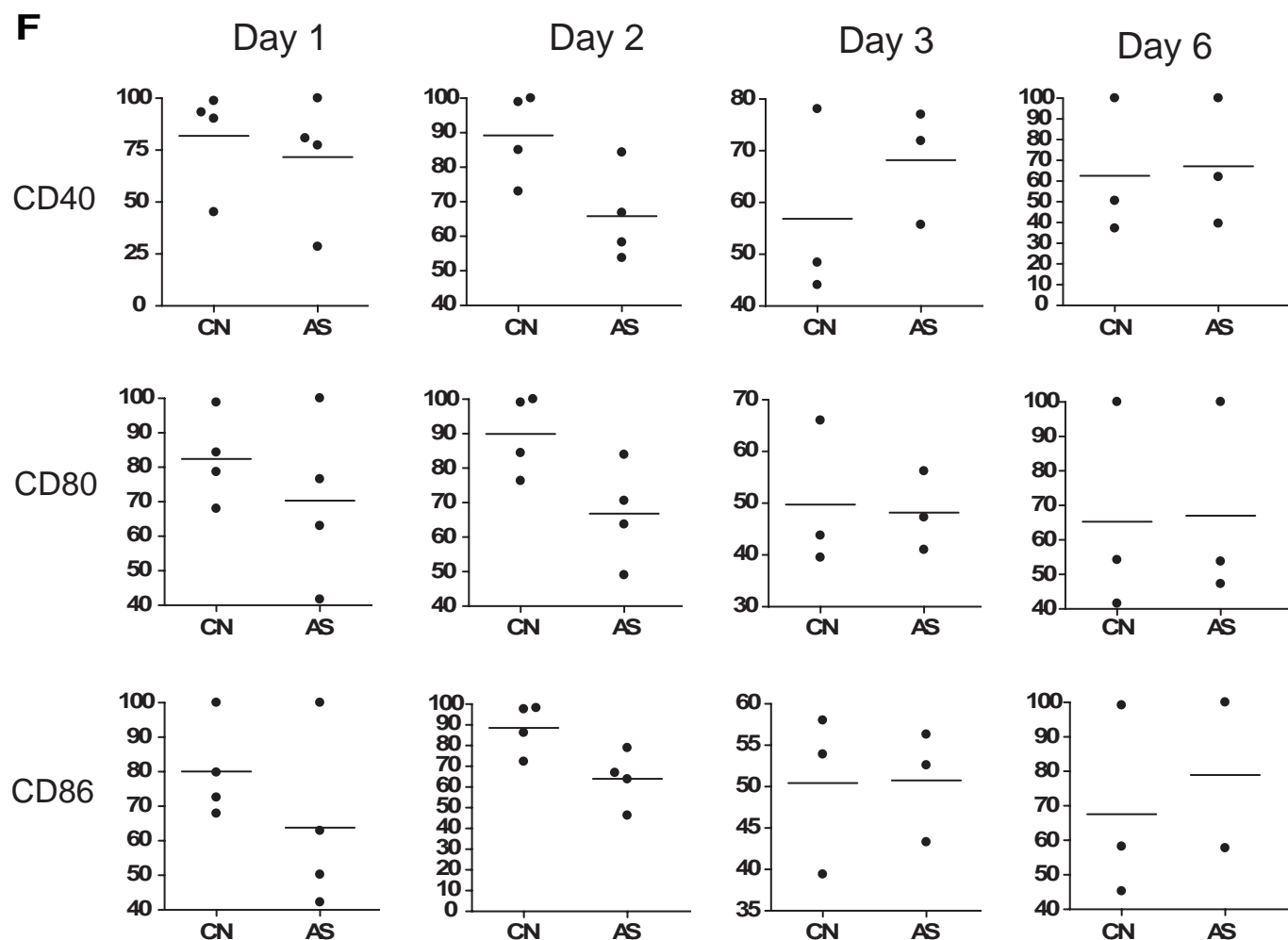


**FIG. 6.** In vivo accumulation of AS-MSP. NOD mice received a subcutaneous injection containing a 1:1 mix of 0.2- $\mu\text{m}$ -diameter fluorescent microspheres and sterile PBS or fluorescent microspheres with 50  $\mu\text{g}$  AS-MSP. **A:** In vivo imaging of mice was performed 3 h after injection. The injection site is clearly visible as well as regions with microsphere accumulation (anatomically located in the area of the pancreas and the spleen). **B:** The spleen and pancreas were removed from animals at 3, 24, and 48 h after injection and imaged. The excised spleens are in the *top two panels* of each quadrant (spleen from mice receiving the fluorescent microspheres+PBS on *left* and spleen from mice receiving the fluorescent microspheres+AS-MSP on the *right*), and the pancreata are shown in the *bottom panels*. **C** and **D:** The mean radiance per area was quantified for the excised spleen and pancreas and graphically shown below the imaging figures. The graphs represent organs from one mouse and the differences in the magnitudes of radiance are representative of organs from three separate mice. **E:** Comparison of intraperitoneal versus subcutaneous administration of directly labeled oligonucleotide microspheres on accumulation inside the pancreas. NOD mice were injected with





after injection within the pancreas, very possibly in the lymph nodes, and eventually in the spleen. Although we do not explicitly demonstrate it, we are very confident that the most likely method of microsphere accumulation inside the pancreas is via dendritic cells. Of wide interest is the mechanism by which antigen and therefore cell/tissue specificity is acquired by the microsphere-loaded dendritic cells. A series of elegant studies (12–14,17) point to a process in which migratory dendritic cells potentially acquire the microspheres that are injected physically proximal to a site of ongoing inflammation and, guided by pro-inflammatory signals deriving from the diabetic pancreas, acquire pancreatic  $\beta$ -cell antigens in the form of apoptotic cells at a site of inflammation. Then, these dendritic cells will exit the inflamed tissue and accumulate within the regional lymphoid organs where they can engage not only effector T-cells but Treg cells as well

(12–14,17,33). It has been shown that dendritic cells that acquire apoptotic cells enter into a state of functional immaturity, which may result in tolerance to the acquired antigens (17,34). We hypothesize that a similar, if not identical, process is occurring immediately after AS-MSP administration in NOD mice. The inflammation inside the pancreas with associated  $\beta$ -cell apoptosis will drive AS-MSP-loaded dendritic cells to acquire  $\beta$ -cell antigen, and immediately thereafter, their accumulation inside the pancreatic lymph nodes will facilitate their interaction with Treg cells, which may, in themselves or in concert with AS-MSP-stabilized dendritic cell or other endogenous dendritic cell subsets, induce  $\beta$ -cell-specific immune hyporesponsiveness or functional tolerance to  $\beta$ -cell-restricted antigens (35–37). We show that microsphere-loaded dendritic cells in the spleen express decreased levels of CD40, CD80, and CD86 at their surface, and we

a PROMAXX formulation of a Cy3-labeled siRNA targeting the CD86 gene via subcutaneous route at a site anatomically distal and proximal to the pancreatic lymph nodes. Three hours after injection, the pancreata and spleens were harvested and imaged as described in RESEARCH DESIGN AND METHODS. CN refers to organs from mice administered PBS vehicle alone, IP refers to animals receiving microsphere-formulated Cy3-conjugated oligonucleotide by intraperitoneal route, and SubQ refers to animals receiving microsphere-formulated Cy3-conjugated oligonucleotide by subcutaneous route. Subcutaneous delivery was made into the scruff of the animal (close to the neck; NECK) and into the flank anatomically proximal to the pancreatic lymph nodes (FLANK). *F*: AS-MSP administration does not increase costimulatory levels on spleen-derived dendritic cells in vivo. NOD mice were treated with a 1:1 mix of fluorescent microspheres and PBS (CN) or with fluorescent microspheres and 50  $\mu$ g antisense oligonucleotide mixture (AS) by subcutaneous injection. Spleens were harvested, and single cells were stained with CD40, CD80, CD86, and CD11c antibodies. The cells were analyzed by flow cytometry at days 1, 2, 3, and 6 after injection. Cell populations that stained positive for CD11c and fluorescent microspheres were then gated to measure the presence and levels of CD40, CD80, or CD86. The graphs show the median of the costimulatory molecule levels of spleen cells from individual mice (horizontal bar) as the percentage of costimulatory molecule inside a CD11c<sup>+</sup> fluorescent bead<sup>+</sup> gate.  $P < 0.05$  by Mann-Whitney  $U$  test between control and AS-MSP mix-treated mice for CD86 on day 1; for CD40, CD80, and CD86 on day 2; for CD40 on day 3

anticipate that this is true for dendritic cells in the pancreatic lymph nodes. Although we do not currently have an explanation for the increase in CD86 levels in fluorescent dendritic cells from the spleen of mice treated with the AS-MSP mixture at day 6 after administration, this could reflect the eventual degradation of the antisense nucleic acid in the dendritic cells by day 6, the disappearance of the migratory dendritic cells and acquisition of the fluorescent particles by endogenous, secondary dendritic cells in a cross-priming mechanism, or both.

What has become apparent in these preliminary accumulation studies is the differential accumulation of microspheres inside the pancreas after subcutaneous injection depending on the proximity of the injection site to the pancreas. When administered subcutaneously at a site that flanks the site of the pancreatic lymph nodes, the microspheres accumulate within 3 h. In contrast, there is no detectable accumulation when the microspheres are administered subcutaneously at a site that does not drain to the pancreatic lymphatics. This observation is relevant for two reasons. First, it offers insight into which administration route may be more clinically useful. Second, it suggests that immunoregulatory interventions, at least those that involve dendritic cells as intermediates, are mechanistically active only when the pancreatic lymph nodes are involved (i.e., the nexus of autoimmune cells and regulatory cells that exhibit antigen specificity). We are, consequently, very interested in identifying the precise mechanism involved in costimulatory protein surface density changes at the dendritic cells in spleen and in pancreatic lymph nodes in response to the AS-MSP treatment. The scarcity of dendritic cells from the pancreatic lymph nodes at the times shown in Fig. 6 did not permit us to pursue an effective enrichment of these cells, but it is one of our objectives in future studies in which the precise mechanisms and temporal sequence of cell migration and interaction with other cells in the pancreatic lymph nodes and/or at the islets of Langerhans remain to be established.

Many investigators support immunotherapy approaches for autoimmunity where putative autoantigen supply provides the antigen, and hence the tissue, specificity (38–41). It is worth noting, however, that suppression of autoimmune disease in animal models need not require antigen supply (37). Mechanistically, such interventions may involve bystander tolerance, linked suppression, or similar phenomena (37,42,43). Although we did not supply autoantigen to the AS-MSP regimen, we did inject diabetic NOD mice with insulin to normalize the glycemia. In one possible mechanism, the exogenous insulin supply (as a well-characterized putative autoantigen) before AS-MSP administration may be acting similar to or in an identical manner as earlier insulin-based tolerance strategies (1,38–41). However, we think a more likely mechanism is that the AS-MSPs stabilized subsets of endogenous dendritic cells toward diabetes-suppressive states by downregulating cell surface CD40, CD80, and CD86. We are currently actively investigating the possible mechanism experimentally. It must be stressed, concurrently, that insulin administration alone cannot account for the AS-MSP effects in its physiological glucoregulatory capacity. No mouse in groups treated with insulin alone was capable of maintaining normoglycemia for more than 1 week after withdrawal of the insulin (Fig. 5). This argues against the possibility that in the AS-MSP-treated animals, new-onset diabetes reversal was due to insulin-induced  $\beta$ -cell rest phenomena (44,45). Taken together, these findings may be readily

translatable clinically with an immediate aim of preserving residual  $\beta$ -cell mass in newly onset or preclinical human autoimmune diabetes.

## ACKNOWLEDGMENTS

This work was supported in part by the National Institutes of Health (grant DK063499 to M.T. and N.G.), the Juvenile Diabetes Research Foundation (grant 17-2007-1066 to N.G.), and a sponsored research agreement from Epic Therapeutics, a wholly owned subsidiary of Baxter Health Care Corporation.

William Fowle at the Electronic Materials Research Institute at Northeastern University (Boston, MA) conducted the scanning electron microscopy studies.

## REFERENCES

- Atkinson MA, Eisenbarth GS: Type 1 diabetes: new perspectives on disease pathogenesis and treatment. *Lancet* 358:221–229, 2001
- Thomas HE, Darwiche R, Corbett JA, Kay TW: Interleukin-1 plus gamma-interferon-induced pancreatic  $\beta$ -cell dysfunction is mediated by  $\beta$ -cell nitric oxide production. *Diabetes* 51:311–316, 2002
- Arnush M, Heitmeier MR, Scarim AL, Marino MH, Manning PT, Corbett JA: IL-1 produced and released endogenously within human islets inhibits beta cell function. *J Clin Invest* 102:516–526, 1998
- Abdul-Rasoul M, Habib H, Al-Khouly M: "The honeymoon phase" in children with type 1 diabetes mellitus: frequency, duration, and influential factors. *Pediatr Diabetes* 7:101–107, 2006
- Bougneres PF, Landais P, Boisson C, Carel JC, Frament N, Boitard C, Chaussain JL, Bach JF: Limited duration of remission of insulin dependency in children with recent overt type 1 diabetes treated with low-dose cyclosporin. *Diabetes* 39:1264–1272, 1990
- Lipton R, LaPorte RE, Becker DJ, Dorman JS, Orchard TJ, Atchison J, Drash AL: Cyclosporin therapy for prevention and cure of IDDM: epidemiological perspective of benefits and risks. *Diabetes Care* 13:776–784, 1990
- Chatenoud L: CD3-specific antibodies restore self-tolerance: mechanisms and clinical applications. *Curr Opin Immunol* 17:632–637, 2005
- Herold KC, Gitelman SE, Masharani U, Hagopian W, Bisikirska B, Donaldson D, Rother K, Diamond B, Harlan DM, Bluestone JA: A single course of anti-CD3 monoclonal antibody hOKT3gamma1(Ala-Ala) results in improvement in C-peptide responses and clinical parameters for at least 2 years after onset of type 1 diabetes. *Diabetes* 54:1763–1769, 2005
- Elias D, Avron A, Tamir M, Raz I: DiaPep277 preserves endogenous insulin production by immunomodulation in type 1 diabetes. *Ann N Y Acad Sci* 1079:340–344, 2006
- Lazar L, Ofan R, Weintrob N, Avron A, Tamir M, Elias D, Phillip M, Josefsberg Z: Heat-shock protein peptide DiaPep277 treatment in children with newly diagnosed type 1 diabetes: a randomised, double-blind phase II study. *Diabet Metab Res Rev* 23:286–291, 2007
- Babaya N, Nakayama M, Eisenbarth GS: The stages of type 1A diabetes. *Ann N Y Acad Sci* 1051:194–204, 2005
- Allan RS, Waithman J, Bedoui S, Jones CM, Villadangos JA, Zhan Y, Lew AM, Shortman K, Heath WR, Carbone FR: Migratory dendritic cells transfer antigen to a lymph node-resident dendritic cell population for efficient CTL priming. *Immunity* 25:153–162, 2006
- Carbone FR, Belz GT, Heath WR: Transfer of antigen between migrating and lymph node-resident DCs in peripheral T-cell tolerance and immunity. *Trends Immunol* 25:655–658, 2004
- Scheinecker C, McHugh R, Shevach EM, Germain RN: Constitutive presentation of a natural tissue autoantigen exclusively by dendritic cells in the draining lymph node. *J Exp Med* 196:1079–1090, 2002
- Steinman RM, Hawiger D, Nussenzweig MC: Tolerogenic dendritic cells. *Annu Rev Immunol* 21:685–711, 2003
- Steinman RM: The control of immunity and tolerance by dendritic cell. *Pathol Biol (Paris)* 51:59–60, 2003
- Steinman RM, Hawiger D, Liu K, Bonifaz L, Bonnyay D, Mahnke K, Iyoda T, Ravetch J, Dhodapkar M, Inaba K, Nussenzweig M: Dendritic cell function in vivo during the steady state: a role in peripheral tolerance. *Ann N Y Acad Sci* 987:15–25, 2003
- McCurry KR, Colvin BL, Zahorchak AF, Thomson AW: Regulatory dendritic cell therapy in organ transplantation. *Transpl Int* 19:525–538, 2006
- Harnaha J, Machen J, Wright M, Lakomy R, Syche A, Trucco M, Makaroun S, Giannoukakis N: Interleukin-7 is a survival factor for CD4<sup>+</sup> CD25<sup>+</sup>

- T-cells and is expressed by diabetes-suppressive dendritic cells. *Diabetes* 55:158–170, 2006
20. Machen J, Harnaha J, Lakomy R, Styche A, Trucco M, Giannoukakis N: Antisense oligonucleotides down-regulating costimulation confer diabetes-preventive properties to nonobese diabetic mouse dendritic cells. *J Immunol* 173:4331–4341, 2004
  21. Waeckerle-Men Y, Allmen EU, Gander B, Scandella E, Schlosser E, Schmidtke G, Merkle HP, Groettrup M: Encapsulation of proteins and peptides into biodegradable poly(D,L-lactide-co-glycolide) microspheres prolongs and enhances antigen presentation by human dendritic cells. *Vaccine* 24:1847–1857, 2006
  22. Yoshida M, Babensee JE: Molecular aspects of microparticle phagocytosis by dendritic cells. *J Biomater Sci Polym Ed* 17:893–907, 2006
  23. Mandal TK: Inhaled insulin for diabetes mellitus. *Am J Health Syst Pharm* 62:1359–1364, 2005
  24. Reid BD, Qin HY, Prange S, Lee-Chan E, Yu Q, Elliott JF, Singh B: Modulation and detection of IDDM by membrane associated antigens from the islet beta cell line NIT-1. *J Autoimmun* 10:27–34, 1997
  25. Hamaguchi K, Gaskins HR, Leiter EH: NIT-1, a pancreatic  $\beta$ -cell line established from a transgenic NOD/Lt mouse. *Diabetes* 40:842–849, 1991
  26. Eisenbarth GS: Type 1 diabetes: molecular, cellular and clinical immunology. *Adv Exp Med Biol* 552:306–310, 2004
  27. Bramwell VW, Perrie Y: Particulate delivery systems for vaccines. *Crit Rev Ther Drug Carrier Syst* 22:151–214, 2005
  28. Keegan ME, Saltzman WM: Surface-modified biodegradable microspheres for DNA vaccine delivery. *Methods Mol Med* 127:107–113, 2006
  29. Davis SS: The use of soluble polymers and polymer microparticles to provide improved vaccine responses after parenteral and mucosal delivery. *Vaccine* 24 (Suppl. 2):S2-7–S2-10, 2006
  30. Zorina TD, Subbotin VM, Bertera S, Alexander AM, Haluszczak C, Gambrell B, Bottino R, Styche AJ, Trucco M: Recovery of the endogenous beta cell function in the NOD model of autoimmune diabetes. *Stem Cells* 21:377–388, 2003
  31. Trucco M: Is facilitating pancreatic beta cell regeneration a valid option for clinical therapy? *Cell Transplant* 15 (Suppl. 1):S75–S84, 2006
  32. Xu X, D'Hoker J, Stange G, Bonne S, DeLeu N, Xiao X, VanDeCastele M, Mellitzer G, Ling Z, Pipeleers D, Bowens L, Scharfmann R, Gradwohl G, Heimberg H: Beta cells can be generated from endogenous progenitors in injured adult mouse pancreas. *Cell* 132:197–207, 2008
  33. Belz GT, Heath WR, Carbone FR: The role of dendritic cell subsets in selection between tolerance and immunity. *Immunol Cell Biol* 80:463–468, 2002
  34. Steinman RM, Turley S, Mellman I, Inaba K: The induction of tolerance by dendritic cells that have captured apoptotic cells. *J Exp Med* 191:411–416, 2000
  35. Yamazaki S, Inaba K, Tarbell KV, Steinman RM: Dendritic cells expand antigen-specific Foxp3+ CD25+ CD4+ regulatory T cells including suppressors of alloreactivity. *Immunol Rev* 212:314–329, 2006
  36. Yamazaki S, Patel M, Harper A, Bonito A, Fukuyama H, Pack M, Tarbell KV, Talmor M, Ravetch JV, Inaba K, Steinman RM: Effective expansion of alloantigen-specific Foxp3+ CD25+ CD4+ regulatory T cells by dendritic cells during the mixed leukocyte reaction. *Proc Natl Acad Sci U S A* 103:2758–2763, 2006
  37. Tarbell KV, Yamazaki S, Steinman RM: The interactions of dendritic cells with antigen-specific, regulatory T cells that suppress autoimmunity. *Semin Immunol* 18:93–102, 2006
  38. Bresson D, Togher L, Rodrigo E, Chen Y, Bluestone JA, Herold KC, von Herrath M: Anti-CD3 and nasal proinsulin combination therapy enhances remission from recent-onset autoimmune diabetes by inducing Tregs. *J Clin Invest* 116:1371–1381, 2006
  39. Alleva DG, Maki RA, Putnam AL, Robinson JM, Kipnes MS, Dandona P, Marks JB, Simmons DL, Greenbaum CJ, Jimenez RG, Conlon PJ, Gottlieb PA: Immunomodulation in type 1 diabetes by NBI-6024, an altered peptide ligand of the insulin B epitope. *Scand J Immunol* 63:59–69, 2006
  40. Martinez NR, Augstein P, Moustakas AK, Papadopoulos GK, Gregori S, Adorini L, Jackson DC, Harrison LC: Disabling an integral CTL epitope allows suppression of autoimmune diabetes by intranasal proinsulin peptide. *J Clin Invest* 111:1365–1371, 2003
  41. Homann D, Dyrberg T, Petersen J, Oldstone MB, von Herrath MG: Insulin in oral immune “tolerance”: a one-amino acid change in the B chain makes the difference. *J Immunol* 163:1833–1838, 1999
  42. Derks R, Jankowska-Gan E, Burlingham WJ: Dendritic cell type determines the mode of linked suppression (TGF- $\beta$  vs. IDO) by adaptive T regulatory cells. *Transplantation* 82: 183, 2006
  43. Frasca L, Carmichael P, Lechler R, Lombardi G: Anergic T cells effect linked suppression. *Eur J Immunol* 27:3191–3197, 1997
  44. Ortvist E, Bjork E, Wallensteen M, Ludvigsson J, Aman J, Johansson C, Forsander G, Lindgren F, Berglund L, Bengtsson M, Berne C, Persson B, Karlsson FA: Temporary preservation of  $\beta$ -cell function by diazoxide treatment in childhood type 1 diabetes. *Diabetes Care* 27:2191–2197, 2004
  45. Palmer JP: Beta cell rest and recovery: does it bring patients with latent autoimmune diabetes in adults to euglycemia? *Ann N Y Acad Sci* 958:89–98, 2002

## Original Article

# Toward a cure for type 1 diabetes mellitus: diabetes-suppressive dendritic cells and beyond

Giannoukakis N, Phillips B, Trucco M. Towards a cure for type 1 diabetes mellitus: diabetes-suppressive dendritic cells and beyond. *Pediatric Diabetes* 2008; 9 (Part II): 4–13.

**Abstract:** Insulin has been the gold standard therapy for diabetes since its discovery and commercial availability. It remains the only pharmacologic therapy for type 1 diabetes (T1D), an autoimmune disease in which autoreactive T cells specifically kill the insulin-producing beta cells. Nevertheless, not even molecularly produced insulin administered four or five times per day can provide a physiologic regulation able to prevent the complications that account for the morbidity and mortality of diabetic patients. Also, insulin does not eliminate the T1D hallmark: beta-cell-specific autoimmunity. In other words, insulin is not a 'cure'. A successful cure must meet the following criteria: (i) it must either replace or maintain the functional integrity of the natural, insulin-producing tissue, the endocrine islets of Langerhans' and, more specifically, the insulin-producing beta cells; (ii) it must, at least, control the autoimmunity or eliminate it altogether; and (iii) it must be easy to apply to a large number of patients. Criterion 1 has been partially realized by allogeneic islet transplantation. Criterion 2 has been partially realized using monoclonal antibodies specific for T-cell surface proteins. Criterion 3 has yet to be realized, given that most of the novel therapies are currently quasi-patient-specific. Herein, we outline the current status of non-insulin-based therapies for T1D, with a focus on cell-based immunomodulation which we propose can achieve all three criteria illustrated above.

**Nick Giannoukakis<sup>a,b</sup>,  
Brett Phillips<sup>a</sup> and  
Massimo Trucco<sup>a</sup>**

<sup>a</sup>Division of Immunogenetics, Department of Pediatrics, University of Pittsburgh School of Medicine, Pittsburgh, PA, USA; and <sup>b</sup>Department of Pathology, University of Pittsburgh School of Medicine, Pittsburgh, PA, USA

**Key words:** diabetes mellitus – dendritic cells – immunotherapy

Corresponding author:  
Dr Massimo Trucco  
Division of Immunogenetics  
Children's Hospital of Pittsburgh  
Rangos Research Center  
3460 Fifth Avenue  
Pittsburgh, PA 15213  
USA.  
Tel: (412) 692-6570;  
fax: (412) 692-5809;  
e-mail: mnt@pitt.edu

Submitted 20 February 2008. Accepted for publication 3 March 2008

## Type 1 diabetes mellitus: nature of the autoimmunity

Type 1 diabetes (T1D) is an autoimmune disorder that culminates in uncontrollable hyperglycemia because of the destruction of the insulin-producing beta cells of the pancreatic islets of Langerhans. The major effectors of beta-cell destruction are T cells reactive to beta-cell-specific antigens. A strong genetic predisposition is a *conditio sine qua non* of T1D and a large body of studies support that key genetic susceptibility loci affect the genesis, function and survival of immune cell subsets including T cells (effectors and putative regulatory T cells) and dendritic cells (DC) (1–4).

To understand the critical role played by the genetic predisposition in T1D, it is necessary to consider the processes that shape the immune system. A randomized pool of immature cells continuously generated in the bone marrow (BM) eventually travel across the thymus.

Once in the thymus, these immature cells, individually expressing unique receptors, undergo positive and negative selection through receptor interaction with fragments of proteins present in our bodies (self-peptides) presented by antigen-presenting cells (APC) once properly inserted in the peptide-binding groove of major histocompatibility complex (MHC) molecules. Indeed, the epithelial thymus is now known to express a wide array of self-antigens including insulin, thyroperoxidase, thyroglobulin, and myelin basic protein, all of which are normally produced by cells targeted in a number of autoimmune disorders including T1D, Hashimoto's thyroiditis and multiple sclerosis. Human leukocyte antigens (HLA), the human MHC molecules, anchored in the cell membrane of thymic epithelial and other APC display HLA/self-peptide complexes for T-cell receptor (TCR) interaction. A cell that interacts strongly with the HLA/self-peptide complex dies in



the thymus and is thus eliminated, i.e., negatively selected. On the contrary, cells that interact poorly with the complex do not proliferate sufficiently or become unable to function (i.e., anergic) and are eventually lost. The cells between these two extremes proliferate modestly, survive (positive selection), and emerge from the thymus to circulate in the periphery. Once in the periphery, the cells that matured in the thymus (T cells) can be engaged by circulating APC. DC are extremely powerful APC that collect foreign or 'ignored' (i.e., not previously exposed to the immune system) material, to present it as 'new' antigens to T cells through their HLA molecule. These T cells interact with the new antigens more strongly than with self-peptides, which enabled their positive selection and consequently the establishment of a T-cell-based protective immune response (5–7). The epitope spreading phenomenon (i.e., the expansion of newly recognized antigens) (8) observed in the islet inflammation is due to both islet-reactive T cells that were generated in the thymus early in ontogeny along with the generation and survival of T cells activated in the periphery by these new antigens.

The pathologic vicious circle of continuous presentation of old and new antigens, collected by the DC from the newly destroyed beta cells, to naive T cells in the pancreatic lymph nodes that eventually go back to the pancreas to kill other beta cells, is illustrated in Fig. 1.

The genetic predisposing background of autoimmune diseases, like T1D, is mainly constituted of specific HLA alleles (9–12). Allelic forms of the HLA-DQ molecule that lack a charged amino acid at position 57 of its beta chain were shown to be strongly correlated with the development of T1D. Conversely, resistance to the disease was found to be associated with the inheritance of an HLA-DQ allelic form with an aspartic residue at the same position (Asp57). The importance of this amino acid change has to do with the physical structure of the non-Asp57 alleles constituting class II molecules with a suboptimal functional groove. In fact, the molecular interactions that normally drive positive and negative selection are altered by the disease-associated HLA molecules so that even strongly self-reactive T-cell clones are allowed to escape to the periphery. HLA structural variations between alleles with Asp 57 and those lacking

### Type 1 diabetes onset the pancreatic environment

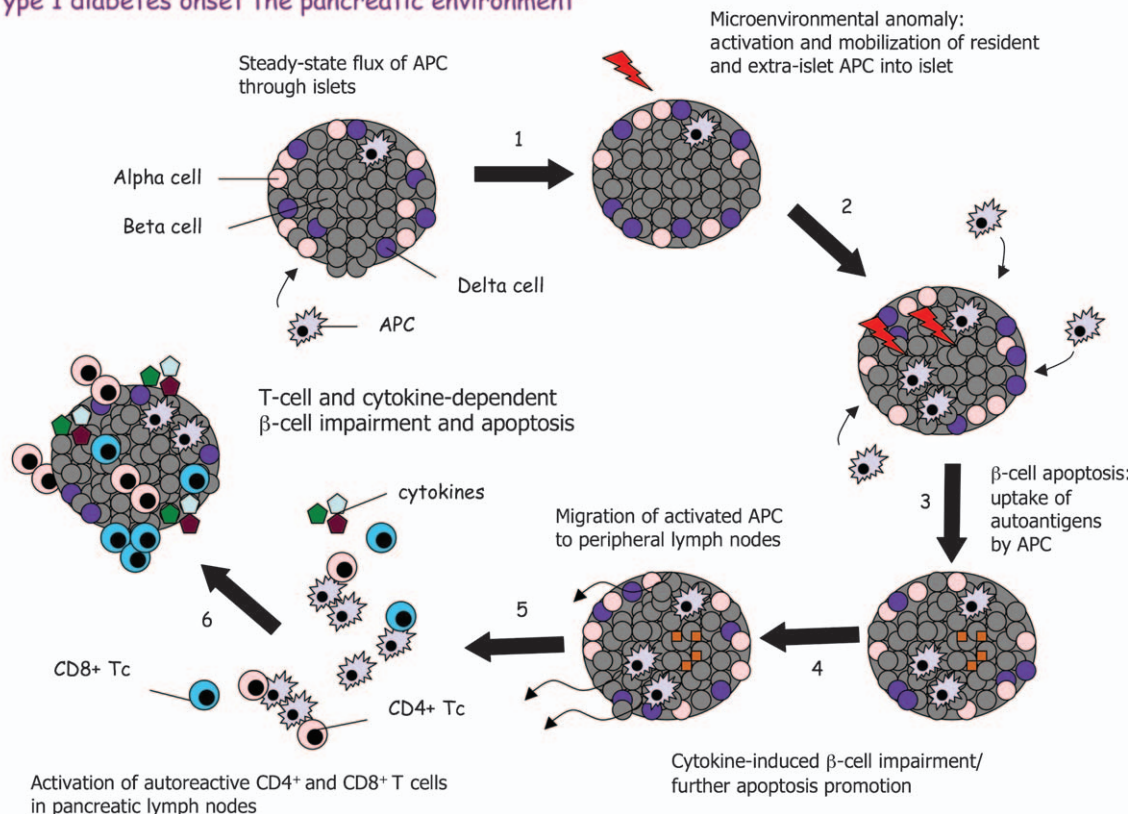


**Fig. 1.** The autoimmune vicious circle favoring the anti-beta-cell epitope spreading. Activated by an environmental stimulus, the autoreactive T cells that escaped thymic censorship, leave the lymph nodes and move into the tissues where eventually they find the self-peptide with which they were originally set up to react. Once the first beta cells are damaged, dendritic cells (DC) come to clean up the scene. Debris from dead cells are brought back to the lymph nodes in which even cytoplasmic markers – thus far not exposed to the immune system – are presented by DC to naive T cells. T cells that were so far 'ignorant' of their existence, recognize these self-antigens as foreign and react against them once back into the islet of Langerhans, killing new beta cells. This constitutes a vicious circle that does not allow the recovery of the insulin-secreting cells, even when the physiologic homeostasis process tries to substitute the lost cells with new cells. APC, antigen-presenting cells.



a charged amino acid at this position (non-Asp57) provide the foundation for HLA-associated diabetic susceptibility and resistance. Susceptibility is closely related to an impaired negative selection of self-reactive T cells. Another not necessarily mutually exclusive consequence is that T-regulatory cells are not as effectively selected and, in their reduced abundance, peripheral reactions to self-peptides are not held in check as well as would occur in a normal immune system.

The importance of the MHC alleles and the thymic antigen-presenting environment was confirmed in studies in which autoimmunity was prevented in non-obese diabetic (NOD) mice by transplanting BM cells derived from diabetes-resistant (Asp57) strains (13, 14). Instead of relying on allogeneic BM transplantation, Tian et al. (15) successfully prevented diabetes by reconstituting sublethally irradiated non-Asp57 NOD mice with their own BM genetically engineered *ex vivo* to express a resistance (Asp57) MHC class II molecule. The reconstituted mice, carrying BM-derived cells that coexpressed both their own diabetogenic (non-Asp57) and the transfected Asp57 beta chain, were diabetes-free. The thymus, repopulated by the engineered BM cells, which differentiated into APC, had restored negative selection and consequently the ability to delete T cells potentially autoreactive to pancreatic beta cells. Autoreactive T-cell clones, which were not found in the treated animals, were eliminated because of the stronger affinity of their TCR for the self-peptide now properly presented by the newly expressed MHC molecule.

Immediately, it became clear to us that once this approach had obtained autoimmunity abrogation also in already diabetic individuals, it could possibly facilitate the recovery of autologous insulin production. Safe induction of an autoimmunity-free status might become a new promising therapy for T1D.

We are working on this aim using a modification of Tian's approach that may be transferable to clinical trials in the near future (16, 17). A reason to believe it comes from the study of Voltarelli et al. in which autologous transplantation of hematopoietic stem cell-enriched BM was used to treat T1D patients (18). The risk of exposing the patient to a non-meloablative yet quite powerful preconditioning was not totally justified, however, by the results obtained. The effects were limited to simple postponement of diabetes recurrence, i.e., just delayed by the time necessary for the transplanted BM to reorganize itself and to reestablish all of its immunocompetent cell subpopulations. The autologous BM did not change the patient's genetic characteristics under which tolerance for the insulin-producing beta cells was not achieved in the first place; in this context, autoimmunity easily recurred. Our approach should safely change the patient's diabetogenic characteristics (16, 17).

New types of intervention are becoming available everyday, which may allow a successful 'take' of the

transplanted BM without the need for a deleterious type of preconditioning (19). Furthermore, new gene therapy approaches that do not involve vector integration at potentially transformative gene loci are continuously discovered (20–22). A protocol that takes into account the choice of the gene transfection vector, any form of safer preconditioning of the patient, and the genetic background of the transplanted BM will significantly improve the one proposed by Voltarelli et al. because efficient negative selection will be reestablished along with central (and possibly also peripheral) tolerance.

The prevalent belief that beta-cell mass is fixed by adulthood and that all adult beta cells are fully differentiated is now being reexamined in light of recent studies showing a regenerative capacity, albeit low, of pancreatic islets of Langerhans during T1D progression. These studies suggest that, although the physiological state of islet cells tends towards a fully differentiated phenotype, the lack of autoimmune aggression, together with the 'danger' signals generated by massive beta-cell destruction may trigger processes inside progenitors (whether islet-resident or ductal epithelium-resident) that result in some degree of islet cell regeneration (14, 23–26).

### Immunomodulation: current state-of-the-art in the clinic

In general, immunomodulation aims at reestablishing central and/or peripheral tolerance to self. The reestablishment of tolerance can include the deletion of autoreactive immune cells, the attenuation of the activity of autoreactive immune cells (T-cell anergy), the generation/augmentation *in vivo* of immunosuppressive cells that can be antigen-specific (T-regulatory cells). Many experimental immunomodulatory interventions have been carried out preclinically in the NOD mouse model and almost all involve treatment of young mice 'prior' to the clinical onset of hyperglycemia. An insightful article by Atkinson and Leiter was instrumental in illustrating the plethora of specific (and sometimes even quite unorthodox) approaches by which diabetes onset was delayed or prevented in this model (27).

As of yet, only one of these methods has shown any significant clinical efficacy. This is the use of a humanized anti-CD3 antibody [TRX-4 (28); and hOKT3g (Ala-Ala) (29)], which can reverse new-onset disease, although for a limited amount of time (30–32).

The manipulation of T-cell responses by autoantigen-derived peptides has been another approach used to attenuate autoimmunity with demonstrated efficacy in rodent models of T1D including the NOD mouse (33–36). The majority of pathogenic CD8+ T-cell clones isolated from pancreata of diabetic NOD mice react specifically with the 9–23 peptide of the insulin B

chain, while approximately 87% of the CD8+ T cells in the islets of young NOD mice are reactive to the 15–23 region of the same B chain (37–43). Similarly, the majority of T1D patients exhibit CD8+ T-cell responses to the 9–23 peptide. Indeed, an altered peptide ligand has been synthesized along these lines (NBI-6024; Neurocrine Biosciences, San Diego, CA, USA) and is currently in phase II studies to see if it can prevent or reverse new-onset disease as a possible vaccine (44, 45).

In addition to the insulin-based peptide, other putative autoantigen-derived peptides exhibit immunoregulatory capacity (46–51) including an Hsp-60-derived peptide (DiaPep277; DeveloGen Inc., Goettingen, Germany) whose most appealing property is its apparent safety. Although laboratory studies suggest that DiaPep277 does not act as an altered peptide ligand, there are no firmly compelling data that it may not act as such in a restricted set of T cells that are critical to the progression, or the attenuation, of diabetes (52–59). A number of similar agents are based on peptides derived from other putative autoantigens such as GAD65, for example, the recombinant alum formulated GAD65 (Diamyd, Stockholm, Germany) in phase III trials with Diamyd Medical AB (60).

Clinical reversal of hyperglycemia achieved by anti-CD3 antibody administration, still poses some questions relative to the mechanism of action in the transient immunodepletion and associated cytokine-related side effects (61, 62). Also, despite the initial observations of improved C-peptide levels in adult diabetics with evidence of T1D-related autoantibodies, administration of DiaPep277 into new-onset T1D children failed to exhibit any benefit compared with controls (53, 56). Both agents (anti-CD3 antibody and DiaPep277) appear to share one potential immunoregulatory mechanism: augmentation of the number of regulatory CD4+ CD25+ T cells expressing the Foxp3 transcription factor. It is now generally accepted that these Foxp3+ regulatory T cells are critical for maintenance of tolerance (63–67). *In vivo*, the activity of these cells appears to be regulated by DC (68, 69).

### **The first clinically adapted immunoregulatory cell therapeutic: diabetes-suppressive autologous DC**

DC are the body's sentinels largely responsible for host surveillance against microenvironmental anomalies including pathogen invasion, infection, and damaged tissue architecture, while coordinating the mechanisms of self-tolerance (70–74). DC continuously traffic throughout all body tissues' sampling molecules from their surroundings, where it is believed they maintain potentially autoreactive immune cells in quiescence either directly or via indirect regulatory immune cell networks (75–82). When DC encounter local disruption

of tissue architecture and elevated proinflammatory signals from infected cells, DC undergo 'maturation' through a series of internal changes. While conceptually thought of as a series of discrete checkpoint-like events, maturation is rapid and often non-linear (63, 83, 84). Concurrent with maturation, DC migrate away from the site of 'danger' and into the anatomically closest lymph nodes. Within the lymph node, the DC, as a powerful APC, initially interacts – using its class I or class II MHC/peptide complex – with the TCR present on a naïve T cell. This will constitute the so-called 'first signal' for T-cell activation. To bring a T cell to full activation, however, a subsequent contact between co-receptors is necessary. Co-stimulatory molecules are so-called because they are present on the APC (e.g., CD80/CD86 or CD40), with their counterparts on the T cell (i.e., CD28 and CD40 ligand, respectively), that, by interacting, further stabilize the signal for activation between the two cells, thus providing the 'second signal'.

Absence of co-stimulatory molecule binding and consequently lack of secondary signal generation has been shown to lead to impaired activation of the responding T cell, eventually bringing it to functional anergy or apoptosis. This is indeed the outcome of many immunosuppressive strategies aimed at co-stimulation blockade (85–90).

Many lines of investigation support the concept that DC in a functionally immature state (characterized by low to absent co-stimulation) are powerful agents of immune hyporesponsiveness (80, 82, 91–95). Exogenous administration of functionally immature DC achieves long-term and stable allograft survival in a variety of mouse and rat models and prevents a number of autoimmune diseases (96–103). Mechanistically, functionally immature DC act by inducing anergy either via direct cell contact and/or cytokines (104–106) and, as described more recently, by up-regulating the number and function of regulatory immune cell subsets, especially CD4+ CD25+ Foxp3+ T cells (Treg) and a class of CD8+ immunosuppressive T cells (106–114).

We have shown that *in vitro* administration of Nuclear Factor-KappaB (NFκB) decoys to DC as well as direct targeting of CD40, CD80, and CD86 with antisense oligodeoxyribonucleotides (AS-ODN), reduce co-stimulatory molecule levels producing functionally immature DC capable of preventing or reversing new-onset diabetes in the NOD mouse (115–117). This was accomplished while maintaining T-cell responsiveness to alloantigens in animals that received repeated injections of modified DC. Co-stimulatory-depleted DC also augmented the number of Treg that were CD4+ CD25+ Foxp3+ through short-range interleukin-7 signaling (115).

Numerous clinical trials have safely used DC-based treatments for cancer therapy providing the basis for

clinical adaptation of DC administration for T1D treatment. A National Institutes of Health-funded protocol approved by the Food and Drug Administration (FDA) is currently underway in phase I clinical trial with an adult (18 yr or older) cohort documented with insulin-requiring T1D of at least 5-yr duration. Leukocytes are obtained from the patient by apheresis and DC are generated *in vitro* and engineered in Good Manufacturing Practice (GMP) facilities with the addition of AS-ODN. These DC, which express low levels of CD40, 80 and CD86 are injected into the patient by intradermal administration at an anatomical site proximal to the pancreas (Fig. 2) (118). DC will migrate to the nearest lymph nodes where they will start to interrupt the vicious circle that maintains islet-specific inflammation, i.e., insulinitis. This therapeutic approach should be more successful when DC injections start close to the clinical onset of the disease. In the pancreas, DC acquire beta-cell-specific antigens from apoptotic cells, leading to the eventual display of these antigens to T cells in the pancreas-draining lymph nodes. The lack of co-stimulatory molecules will result in an anergizing signal to the T cells, induce regulatory immune cells (like Foxp3+ Treg), and interrupt the T-cell-mediated anti-beta-cell epitope spreading phenomenon. The abrogation of the autoimmune diabetogenic insult should be sufficient to promote rescue of still present insulin-producing beta cells and/or neogenesis of other insulin-producing cells in the host endocrine pancreas, even after the onset of the disease. This trial is underway at the time of this writing and once safety has been demonstrated, a phase II efficacy trial will start, involving new-onset diabetic patients.

### Beyond autologous DC: a diabetes-suppressive microsphere vaccine

In spite of the promise of this study, we have encountered cumbersome logistical requirements to generate these diabetes-suppressive DC, which may limit the future enrollment of new-onset diabetic children in the efficacy phase of the trial. Leukopheresis takes 2 or 3 h to provide sufficient precursor cells to generate the number of DC necessary for six to eight injections. The obtained DC should be exposed to AS-ODN in GMP facilities in which the laboratory practices are frequently difficult to reproduce. GMP facilities are frequently located far away from the clinic where the patients are treated. Many DC are lost during the freezing/thawing procedures.

In an effort to avoid these steps, we have been concurrently pursuing an alternative method to stabilize DC immaturity directly *in vivo* using microparticle carriers of immunomodulating agents like AS-ODN.

Many studies confirm that microparticle carriers can direct DC to the administration site and once phagocytosed, the contents can shape the DC functional phenotype (119, 120). We have incorporated the AS-ODN directed against CD40, CD80 and CD86 into Baxter Healthcare's PROMAXX<sup>®</sup> microsphere delivery system. The inert PROMAXX microsphere technology has been shown to be safe and effective in human trials (121). More importantly, when administered *in vivo*, this technology is neutral with respect to DC maturation state compared with the known immunostimulatory properties of other microsphere

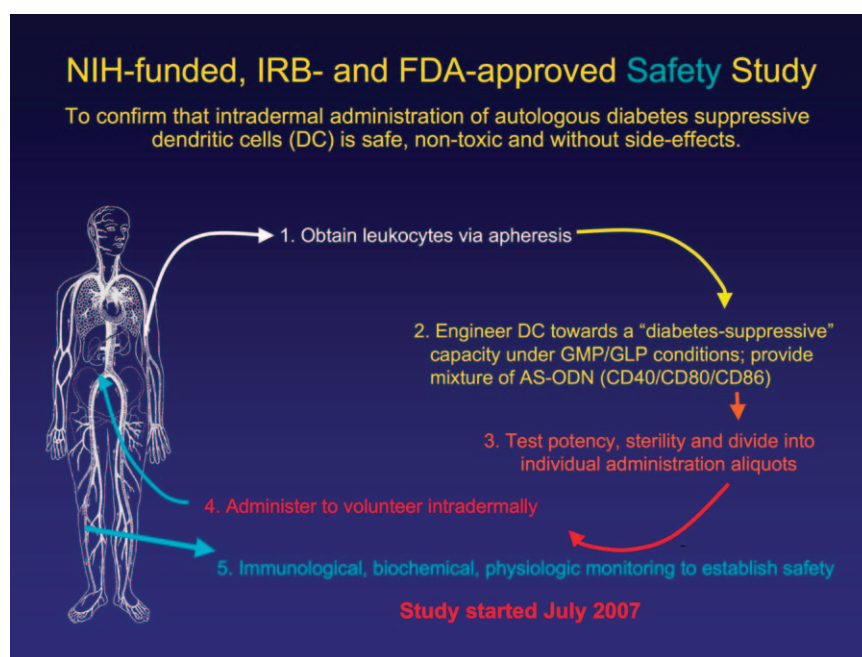


Fig. 2. Living dendritic cells (DC)-based clinical trial for type 1 diabetes. Schematic of the procedures involved in the phase I clinical trial currently underway at the University of Pittsburgh to prove the safety of the living DC-based vaccine [used by permission of Cell Science Reviews, Giannoukakis *et al.* (118)].



formulations. In other words, other polyplex formulations have an inherent capacity to induce the upregulation of co-stimulatory proteins at the DC surface (possibly via Toll-like receptors), whereas the PROMAXX technology does not. This neutrality on DC maturation is a critical criterion in adapting microsphere chemistry for immunosuppressive objectives where DC are involved as mediators. Our very recently developed PROMAXX antisense-formulated vaccine rendered DC diabetes suppressive and newer data show that it can prevent and reverse new-onset autoimmune diabetes in the NOD mouse model (122). This recent study was aimed at ascertaining the efficacy of AS-ODN-formulated PROMAXX microspheres to prevent T1D and to reverse new-onset disease. Microspheres carrying AS-ODN to CD40, CD80 and CD86 were delivered into NOD mice. Glycemia was monitored to determine disease prevention and reversal. In recipients that remained and/or became diabetes free, spleen and lymph node T cells were enriched to determine the prevalence of Foxp3+ putative T-regulatory cells. Splenocytes from diabetes-free microsphere-treated recipients were adoptively cotransferred with splenocytes from diabetic NOD mice into NOD-SCID recipients. To rule out non-specific systemic immunosuppression, splenocytes from successfully treated recipients were pulsed with beta-cell antigen, ovalbumin or cocultured with allogeneic splenocytes. The microspheres prevented T1D and, most importantly, exhibited a capacity to reverse clinical hyperglycemia, suggesting reversal of new-onset disease. The

microspheres augmented Foxp3<sup>+</sup> T-regulatory cells, induced hyporesponsiveness to NOD-derived pancreatic beta-cell antigen, without compromising global immune response to alloantigens and nominal antigens. T cells from successfully treated mice suppressed adoptive transfer of disease by diabetogenic splenocytes into secondary immunodeficient NOD-scid recipients. Finally, microspheres accumulated within the pancreas and the spleen. Live animal *in vivo* imaging measured the microsphere accumulation pattern (Fig. 3). DC from the spleen of the microsphere-treated mice exhibit decreased cell surface CD40, CD80, and CD86. This novel microsphere formulation represents the first diabetes-suppressive and reversing nucleic acid vaccine that confers an immunoregulatory phenotype to endogenous DC (122). We predict that once all preclinical studies are completed, a phase I/II trial can be initiated (Fig. 4). The microspheres are simple to manufacture to clinical grade on a large scale and do not involve the cumbersome logistics outlined earlier that are necessary for the DC-based therapy.

Although we have focused on autoimmune diabetes as a disease target throughout our studies, our microsphere technology can be readily and rapidly applied to producing other immunosuppressive vaccines for other autoimmune conditions in which nucleotides along with disease-specific antigens can be formulated to target the transcripts of other critical molecules involved in immunoregulation inside endogenous DC without affecting their maturation status *in vivo*.

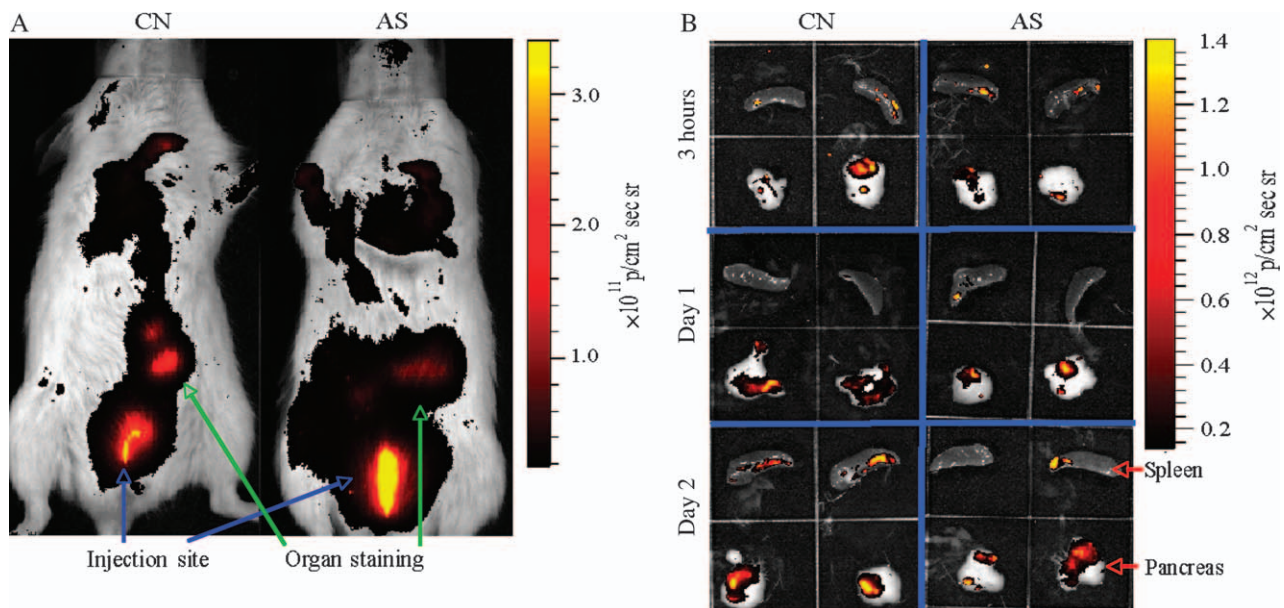
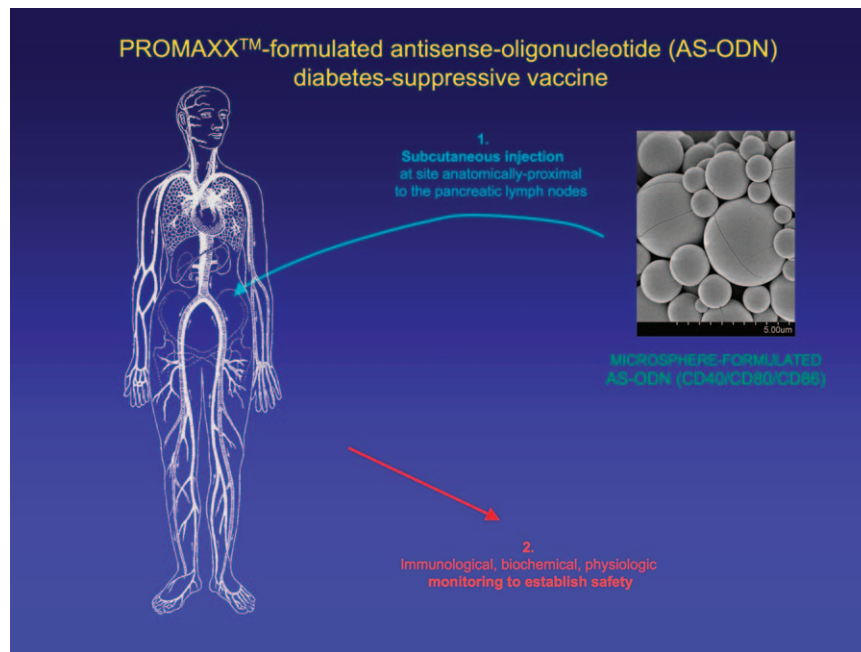


Fig. 3. *In vivo* accumulation of antisense-oligonucleotide-formulated microspheres (AS-MSP). (A) Alive non-obese diabetic (NOD) mice received a subcutaneous injection containing sterile phosphate buffered saline (control, CN) or fluorescent microspheres with 50  $\mu$ g of AS-MSP (AS). Three hours postinjection, the spheres accumulated in the area of the pancreas and spleen. (B) Pancreas and spleen removed at 3, 24, and 48 h postinjection are shown to contain the fluorescently labeled microspheres [used by permission of Diabetes, Phillips *et al.* (122)].





13. ZORINA TD, SUBBOTIN VM, BERTERA S, ALEXANDER A, STYCHE AJ, TRUCCO M. Distinct characteristics and features of allogeneic chimerism in the NOD mouse model of autoimmune diabetes. *Cell Transplant* 2002; 11: 113–123.
14. ZORINA TD, SUBBOTIN VM, BERTERA S et al. Recovery of the endogenous beta cell function in autoimmune diabetes. *Stem Cells* 2003; 21: 377–388.
15. TIAN C, BAGLEY J, CRETIN N, SETH N, WUCHERPFENNIG KW, IACOMINI J. Prevention of type 1 diabetes by gene therapy. *J Clin Invest* 2004; 114: 969–978.
16. ROOD PPM, BOTTINO R, BALAMURUGAN AN, FAN Y, COOPER DKC, TRUCCO M. Facilitating physiologic self-regeneration: a step beyond islet cell replacement. *Pharm Res* 2006; 23: 227–242.
17. PASQUALI L, GIANNOUKAKIS N, TRUCCO M. Induction of immune tolerance to facilitate beta cell regeneration in type 1 diabetes. *Adv Drug Deliv Rev* 2008; 60: 106–111.
18. VOLTARELLI J, COURI C, STRACIERI A et al. Autologous nonmyeloablative hematopoietic stem cell transplantation in newly diagnosed type 1 diabetes mellitus. *JAMA* 2007; 297: 1568–1576.
19. CZECHOWICZ A, KRAFT D, WEISSMAN IL, BHATTACHARYA D. Efficient transplantation via antibody-based clearance of hematopoietic stem cell niches. *Science* 2007; 318: 1296–1299.
20. BEARD BC, DICKERSON D, BEEBE K et al. Comparison of HIV-derived lentiviral and MLV-based gammaretroviral vector integration sites in primate repopulating cells. *Mol Ther* 2007; 15: 1356–1365.
21. CHEN ZY, HE CY, KAY MA. Improved production and purification of minicircle DNA vector free of plasmid bacterial sequences and capable of persistent transgene expression *in vivo*. *Hum Gene Ther* 2005; 16: 126–131.
22. SCLIMENTI CR, NEVIASER AS, BABA EJ, MEUSE L, KAY MA, CALOS MP. Epstein-Barr virus vectors provide prolonged robust factor IX expression in mice. *Biotechnol Prog* 2003; 19: 144–151.
23. CHONG AS, SHEN J, TAO J et al. Reversal of diabetes in non-obese diabetic mice without spleen cell-derived beta cell regeneration. *Science* 2006; 311: 1774–1775.
24. NISHIO J, GAGLIA JL, TURVEY SE, CAMPBELL C, BENOIST C, MATHIS D. Islet recovery and reversal of murine type 1 diabetes in the absence of any infused spleen cell contribution. *Science* 2006; 311: 1775–1778.
25. SURI A, CALDERON B, ESPARZA TJ, FREDERICK K, BITTNER P, UNANUE ER. Immunological reversal of autoimmune diabetes without hematopoietic replacement of beta cells. *Science* 2006; 311: 1778–1780.
26. XU X, D'HOKER J, STANGE G et al. Beta cells can be generated from endogenous progenitors in injured adult mouse pancreas. *Cell* 2008; 132: 197–207.
27. ATKINSON MA, LEITER EH. The NOD mouse model of type 1 diabetes: as good as it gets? *Nat Med* 1999; 5: 601–604.
28. BROWN WM. TRX-4 (TolerRx Inc). *IDrugs* 2006; 9: 283–291.
29. BROWN WM. Anti-CD3 antibody MacroGenics Inc. *Curr Opin Investig Drugs* 2006; 7: 381–388.
30. BISIKIRSKA BC, HEROLD KC. Use of anti-CD3 monoclonal antibody to induce immune regulation in type 1 diabetes. *Ann N Y Acad Sci* 2004; 1037: 1–9.
31. HEROLD KC, HAGOPIAN W, AUGER JA et al. Anti-CD3 monoclonal antibody in new-onset type 1 diabetes mellitus. *N Engl J Med* 2002; 346: 1692–1698.
32. KEYMEULEN B, VANDEMEULEBROUCKE E, ZIEGLER AG et al. Insulin needs after CD3-antibody therapy in new-onset type 1 diabetes. *N Engl J Med* 2005; 352: 2598–2608.
33. BACH JF, CHATENAUD L. Tolerance to islet autoantigens in type 1 diabetes. *Annu Rev Immunol* 2001; 19: 131–161.
34. WEINER HL, ZHANG SJ, KHOURY SJ et al. Antigen-driven peripheral immune tolerance. Suppression of organ-specific autoimmune diseases by oral administration of autoantigens. *Ann N Y Acad Sci* 1991; 636: 227–232.
35. WEINER HL, MILLER A, KHOURY SJ et al. Treatment of autoimmune diseases by oral tolerance to autoantigens. *Adv Exp Med Biol* 1995; 371B: 1217–1223.
36. WHITACRE CC, GIENAPP IE, MEYER A, COX KL, JAVED N. Treatment of autoimmune disease by oral tolerance to autoantigens. *Clin Immunol Immunopathol* 1996; 80: S31–39.
37. EISENBARTH GS, MORIYAMA H, ROBLES DT et al. Insulin autoimmunity: prediction/precipitation/prevention type 1A diabetes. *Autoimmun Rev* 2002; 1: 139–145.
38. NAKAYAMA M, ABIRU N, MORIYAMA H et al. Prime role for an insulin epitope in the development of type 1 diabetes in NOD mice. *Nature* 2005; 435: 220–223.
39. DEVENDRA D, PARONEN J, LIU E et al. Comparative study of oral versus subcutaneous B: 9-23 insulin peptide in Balb/c mice as an experimental model for autoimmune diabetes. *Ann N Y Acad Sci* 2004; 1029: 331–333.
40. DEVENDRA D, PARONEN J, LIU E et al. Differential immune induction with subcutaneous versus oral administration of a diabetogenic insulin peptide in the NOD mouse. *Ann N Y Acad Sci* 2004; 1029: 328–330.
41. LIU E, YU L, MORIYAMA H, EISENBARTH GS. Animal models of insulin-dependent diabetes. *Methods Mol Med* 2004; 102: 195–212.
42. GOTTLIEB PA, EISENBARTH GS. Insulin-specific tolerance in diabetes. *Clin Immunol* 2002; 102: 2–11.
43. WEGMANN DR, EISENBARTH GS. It's insulin. *J Autoimmun* 2000; 15: 286–291.
44. ALLEVA DG, MAKI RA, PUTNAM AL et al. Immunomodulation in type 1 diabetes by NBI-6024, an altered peptide ligand of the insulin B epitope. *Scand J Immunol* 2006; 2006: 59–69.
45. GIANNOUKAKIS N. NBI-6024 (Neurocrine Biosciences). *IDrugs* 2002; 5: 1162–1167.
46. ABIRU N, EISENBARTH GS. Multiple genes/multiple autoantigens role in type 1 diabetes. *Clin Rev Allergy Immunol* 2000; 18: 27–40.
47. ATKINSON MA, MACLAREN NK. Islet cell autoantigens in insulin-dependent diabetes. *J Clin Invest* 1993; 92: 1608–1616.
48. CHRISTIE MR. Islet cell autoantigens in type 1 diabetes. *Eur J Clin Invest* 1996; 26: 827–838.
49. DOTTA F, ANASTASI E, TIBERTI C, DI MARIO U. Autoantigens in type 1 diabetes mellitus. *J Endocrinol Invest* 1994; 17: 497–508.
50. KALLAN AA, DE VRIES RR, ROEP BO. T-cell recognition of beta-cell autoantigens in insulin-dependent diabetes mellitus. *APMIS* 1996; 104: 3–11.
51. YOON JW, JUN HS. Cellular and molecular roles of beta cell autoantigens, macrophages and T cells in the pathogenesis of autoimmune diabetes. *Arch Pharm Res* 1999; 22: 437–447.
52. BRUGMAN S, KLATTER FA, VISSER J, BOS NA, ELIAS D, ROZING J. Neonatal oral administration of DiaPep277, combined with hydrolysed casein diet, protects against Type 1 diabetes in BB-DP rats. An experimental study. *Diabetologia* 2004; 47: 1331–1333.
53. ELIAS D, AVRON A, TAMIR M, RAZ I. DiaPep277 preserves endogenous insulin production by immunomodulation in type 1 diabetes. *Ann N Y Acad Sci* 2006; 1079: 340–344.

54. GIANNOUKAKIS N. DiaPep277 (DeveloGen). *Curr Opin Investig Drugs* 2005; 6: 1043–1050.
55. HUURMAN VA, DECOCHEZ K, MATHIEU C, COHEN IR, ROEP BO. Therapy with the hsp60 peptide DiaPep277 in C-peptide positive type 1 diabetes patients. *Diabetes Metab Res Rev* 2007; 23: 269–275.
56. LAZAR L, OFAN R, WEINTROB N et al. Heat-shock protein peptide DiaPep277 treatment in children with newly diagnosed type 1 diabetes: a randomised, double-blind phase II study. *Diabetes Metab Res Rev* 2007; 23: 286–291.
57. RAZ I, AVRON A, TAMIR M et al. Treatment of new-onset type 1 diabetes with peptide DiaPep277 is safe and associated with preserved beta-cell function: extension of a randomized, double-blind, phase II trial. *Diabetes Metab Res Rev* 2007; 23: 292–298.
58. RAZ I, ELIAS D, AVRON A, TAMIR M, METZGER M, COHEN IR. Beta-cell function in new-onset type 1 diabetes and immunomodulation with a heat-shock protein peptide (DiaPep277): a randomised, double-blind, phase II trial. *Lancet* 2001; 358: 1749–1753.
59. SCHLOOT NC, MEIERHOFF G, LENGUEL C et al. Effect of heat shock protein peptide DiaPep277 on beta-cell function in paediatric and adult patients with recent-onset diabetes mellitus type 1: two prospective, randomized, double-blind phase II trials. *Diabetes Metab Res Rev* 2007; 23: 276–285.
60. AGARDH CD, CILIO CM, LETHAGEN A et al. Clinical evidence for the safety of GAD65 immunomodulation in adult-onset autoimmune diabetes. *J Diabetes Complications* 2005; 19: 238–246.
61. CHATENAUD L. Monoclonal antibody-based strategies in autoimmunity and transplantation. *Methods Mol Med* 2005; 109: 297–328.
62. HEROLD KC, GITELMAN SE, MASHARANI U et al. A single course of anti-CD3 monoclonal antibody hOKT3gamma1(Ala-Ala) results in improvement in C-peptide responses and clinical parameters for at least 2 years after onset of type 1 diabetes. *Diabetes* 2005; 54: 1763–1769.
63. BACCHETTA R, GAMBINERI E, RONCAROLO MG. Role of regulatory T cells and FOXP3 in human diseases. *J Allergy Clin Immunol* 2007; 120: 227–235; quiz 236–227.
64. KIM CH. Molecular targets of FoxP3+ regulatory T cells. *Mini Rev Med Chem* 2007; 7: 1136–1143.
65. OCHS HD, GAMBINERI E, TORGERSON TR. IPEX, FOXP3 and regulatory T-cells: a model for autoimmunity. *Immunol Res* 2007; 38: 112–121.
66. STEPHENS GL, SHEVACH EM. Foxp3+ regulatory T cells: selfishness under scrutiny. *Immunity* 2007; 27: 417–419.
67. VALENCIA X, LIPSKY PE. CD4+CD25+FoxP3+ regulatory T cells in autoimmune diseases. *Nat Clin Pract Rheumatol* 2007; 3: 619–626.
68. LUO X, TARBELL KV, YANG H et al. Dendritic cells with TGF-beta1 differentiate naive CD4+CD25- T cells into islet-protective Foxp3+ regulatory T cells. *Proc Natl Acad Sci U S A* 2007; 104: 2821–2826.
69. YAMAZAKI S, BONITO AJ, SPISEK R, DHODAPKAR M, INABA K, STEINMAN RM. Dendritic cells are specialized accessory cells along with TGF- for the differentiation of Foxp3+ CD4+ regulatory T cells from peripheral Foxp3 precursors. *Blood* 2007; 110: 4293–4302.
70. BANCHEREAU J, STEINMAN RM. Dendritic cells and the control of immunity. *Nature* 1998; 392: 245–252.
71. LUTZ MB, SCHULER G. Immature, semi-mature and fully mature dendritic cells: which signals induce tolerance or immunity? *Trends Immunol* 2002; 23: 445–449.
72. STEINMAN RM, HAWIGER D, NUSSENZWEIG MC. Tolerogenic dendritic cells. *Annu Rev Immunol* 2003; 21: 685–711.
73. STEINMAN RM, TURLEY S, MELLMAN I, INABA K. The induction of tolerance by dendritic cells that have captured apoptotic cells. *J Exp Med* 2000; 191: 411–416.
74. VLAD G, CORTESINI R, SUCIU-FOCA N. License to heal: bidirectional interaction of antigen-specific regulatory T cells and tolerogenic APC. *J Immunol* 2005; 174: 5907–5914.
75. SMITS HH, DE JONG EC, WIERENGA EA, KAPSENBERG ML. Different faces of regulatory DCs in homeostasis and immunity. *Trends Immunol* 2005; 26: 123–129.
76. SMITS HH, ENGERING A, VAN DER KLEIJ D et al. Selective probiotic bacteria induce IL-10-producing regulatory T cells in vitro by modulating dendritic cell function through dendritic cell-specific intercellular adhesion molecule 3-grabbing nonintegrin. *J Allergy Clin Immunol* 2005; 115: 1260–1267.
77. YAMAZAKI S, IYODA T, TARBELL K et al. Direct expansion of functional CD25+ CD4+ regulatory T cells by antigen-processing dendritic cells. *J Exp Med* 2003; 198: 235–247.
78. INABA K, METLAY JP, CROWLEY MT, STEINMAN RM. Dendritic cells pulsed with protein antigens in vitro can prime antigen-specific, MHC-restricted T cells in situ. *J Exp Med* 1990; 172: 631–640.
79. KUBACH J, BECKER C, SCHMITT E et al. Dendritic cells: sentinels of immunity and tolerance. *Int J Hematol* 2005; 81: 197–203.
80. STEINMAN RM. Some interfaces of dendritic cell biology. *APMIS* 2003; 111: 675–697.
81. STEINMAN RM, BONIFAZ L, FUJII S et al. The innate functions of dendritic cells in peripheral lymphoid tissues. *Adv Exp Med Biol* 2005; 560: 83–97.
82. STEINMAN RM, NUSSENZWEIG MC. Avoiding horror autotoxicus: the importance of dendritic cells in peripheral T cell tolerance. *Proc Natl Acad Sci U S A* 2002; 99: 351–358.
83. LIU YJ. Dendritic cell subsets and lineages, and their functions in innate and adaptive immunity. *Cell* 2001; 106: 259–262.
84. LIU YJ, KANZLER H, SOUMELIS V, GILLIET M. Dendritic cell lineage, plasticity and cross-regulation. *Nat Immunol* 2001; 2: 585–589.
85. BLUESTONE JA. Co stimulation and its role in organ transplantation. *Clin Transplant* 1996; 10: 104–109.
86. CLARKSON MR, SAYEGH MH. T-cell costimulatory pathways in allograft rejection and tolerance. *Transplantation* 2005; 80: 555–563.
87. KISHIMOTO K, DONG VM, SAYEGH MH. The role of costimulatory molecules as targets for new immunosuppressives in transplantation. *Curr Opin Urol* 2000; 10: 57–62.
88. LENSCHOW DJ, WALUNAS TL, BLUESTONE JA. CD28/B7 system of T cell costimulation. *Annu Rev Immunol* 1996; 14: 233–258.
89. ROTHSTEIN DM, SAYEGH MH. T-cell costimulatory pathways in allograft rejection and tolerance. *Immunol Rev* 2003; 196: 85–108.
90. SAYEGH MH, TURKA LA. T cell costimulatory pathways: promising novel targets for immunosuppression and tolerance induction. *J Am Soc Nephrol* 1995; 6: 1143–1150.
91. COATES PT, THOMSON AW. Dendritic cells, tolerance induction and transplant outcome. *Am J Transplant* 2002; 2: 299–307.
92. HACKSTEIN H, MORELLI AE, THOMSON AW. Designer dendritic cells for tolerance induction: guided not misguided missiles. *Trends Immunol* 2001; 22: 437–442.

93. MORELLI AE, THOMSON AW. Dendritic cells: regulators of alloimmunity and opportunities for tolerance induction. *Immunol Rev* 2003; 196: 125–146.
94. NOURI-SHIRAZI M, THOMSON AW. Dendritic cells as promoters of transplant tolerance. *Expert Opin Biol Ther* 2006; 6: 325–339.
95. STEINMAN RM, INABA K, TURLEY S, PIERRE P, MELLMAN I. Antigen capture, processing, and presentation by dendritic cells: recent cell biological studies. *Hum Immunol* 1999; 60: 562–567.
96. BOTTINO R, LEMARCHAND P, TRUCCO M, GIANNOUKAKIS N. Gene- and cell-based therapeutics for type I diabetes mellitus. *Gene Ther* 2003; 10: 875–889.
97. CHEN D, SUNG R, BROMBERG JS. Gene therapy in transplantation. *Transpl Immunol* 2002; 9: 301–314.
98. GIANNOUKAKIS N, RUDERT WA, ROBBINS PD, TRUCCO M. Targeting autoimmune diabetes with gene therapy. *Diabetes* 1999; 48: 2107–2121.
99. GIANNOUKAKIS N, THOMSON A, ROBBINS PD. Gene therapy in transplantation. *Gene Ther* 1999; 6: 1499–1511.
100. GIANNOUKAKIS N, TRUCCO M. Gene therapy for type I diabetes. *Am J Ther* 2005; 12: 512–528.
101. TARNER IH, FATHMAN CG. The potential for gene therapy in the treatment of autoimmune disease. *Clin Immunol* 2002; 104: 204–216.
102. TARNER IH, SLAVIN AJ, McBRIDE J et al. Treatment of autoimmune disease by adoptive cellular gene therapy. *Ann N Y Acad Sci* 2003; 998: 512–519.
103. TRUCCO M, ROBBINS PD, THOMSON AW, GIANNOUKAKIS N. Gene therapy strategies to prevent autoimmune disorders. *Curr Gene Ther* 2002; 2: 341–354.
104. CHEN W. Dendritic cells and (CD4+)CD25+ T regulatory cells: crosstalk between two professionals in immunity versus tolerance. *Front Biosci* 2006; 11: 1360–1370.
105. HUGUES S, BOISSONNAS A, AMIGORENA S, FETLER L. The dynamics of dendritic cell-T cell interactions in priming and tolerance. *Curr Opin Immunol* 2006; 18: 491–495.
106. BEISSERT S, SCHWARZ A, SCHWARZ T. Regulatory T cells. *J Invest Dermatol* 2006; 126: 15–24.
107. ENK AH. DCs and cytokines cooperate for the induction of tregs. *Ernst Schering Res Found Workshop* 2006; 56: 97–106.
108. HUBER S, SCHRAMM C. TGF-beta and CD4+CD25+ regulatory T cells. *Front Biosci* 2006; 11: 1014–1023.
109. LOHR J, KNOECHEL B, ABBAS AK. Regulatory T cells in the periphery. *Immunol Rev* 2006; 212: 149–162.
110. RONCAROLO MG, GREGORI S, BATTAGLIA M, BACCHETTA R, FLEISCHHAUER K, LEVINGS MK. Interleukin-10-secreting type 1 regulatory T cells in rodents and humans. *Immunol Rev* 2006; 212: 28–50.
111. SHEVACH EM, DiPAOLO RA, ANDERSSON J, ZHAO DM, STEPHENS GL, THORNTON AM. The lifestyle of naturally occurring CD4+ CD25+ Foxp3+ regulatory T cells. *Immunol Rev* 2006; 212: 60–73.
112. TANG Q, BLUESTONE JA. Regulatory T-cell physiology and application to treat autoimmunity. *Immunol Rev* 2006; 212: 217–237.
113. VERHAGEN J, BLASER K, AKDIS CA, AKDIS M. Mechanisms of allergen-specific immunotherapy: T-regulatory cells and more. *Immunol Allergy Clin North Am* 2006; 26: 207–231.vi.
114. ZHANG L, YI H, XIA XP, ZHAO Y. Transforming growth factor-beta: an important role in CD4+CD25+ regulatory T cells and immune tolerance. *Autoimmunity* 2006; 39: 269–276.
115. HARNAHA J, MACHEN J, WRIGHT M et al. Interleukin-7 is a survival factor for CD4+ CD25+ T-cells and is expressed by diabetes-suppressive dendritic cells. *Diabetes* 2006; 55: 158–170.
116. MA L, QIAN S, LIANG X et al. Prevention of diabetes in NOD mice by administration of dendritic cells deficient in nuclear transcription factor-kappaB activity. *Diabetes* 2003; 52: 1976–1985.
117. MACHEN J, HARNAHA J, LAKOMY R, STYCHE A, TRUCCO M, GIANNOUKAKIS N. Antisense oligonucleotides down-regulating costimulation confer diabetes-preventive properties to nonobese diabetic mouse dendritic cells. *J Immunol* 2004; 173: 4331–4341.
118. GIANNOUKAKIS N, RUDERT WA, TRUCCO M. Dendritic cells for immunotherapy of type I diabetes. *Cell Science Rev* 2007; 3: 250–278.
119. WAECKERLE-MEN Y, ALLMEN EU, GANDER B et al. Encapsulation of proteins and peptides into biodegradable poly(D,L-lactide-co-glycolide) microspheres prolongs and enhances antigen presentation by human dendritic cells. *Vaccine* 2006; 24: 1847–1857.
120. YOSHIDA M, BABENSEE JE. Molecular aspects of microparticle phagocytosis by dendritic cells. *J Biomater Sci Polym Ed* 2006; 17: 893–907.
121. MANDAL TK. Inhaled insulin for diabetes mellitus. *Am J Health Syst Pharm* 2005; 62: 1359–1364.
122. PHILLIPS B, NYLANDER K, HARNAHA J et al. A microsphere-based vaccine prevents and reverses new-onset autoimmune diabetes. *Diabetes* 2008 (in press).



## Human proinsulin C-peptide reduces high glucose-induced proliferation and NF- $\kappa$ B activation in vascular smooth muscle cells

Vincenza Cifarelli<sup>1</sup>, Patrizia Luppi<sup>\*,1</sup>, Hubert M. Tse, Jing He, Jon Piganelli, Massimo Trucco

*Division of Immunogenetics, Department of Pediatrics, University of Pittsburgh, School of Medicine, Pittsburgh, PA 15213, USA*

Received 25 July 2007; received in revised form 27 November 2007; accepted 27 December 2007

### Abstract

Excessive proliferation of vascular smooth muscle cells (VSMCs) is one of the primary lesions in atherosclerosis development during diabetes. High glucose triggers VSMC proliferation and initiates activation of the transcription factor nuclear factor (NF)- $\kappa$ B. Recently, clinical studies have demonstrated that replacement therapy with C-peptide, a cleavage product of insulin, to type 1 diabetic (T1D) patients is beneficial on a variety of diabetes-associated vascular complications. However, the mechanisms underlying the beneficial activity of C-peptide on the vasculature in conditions of hyperglycemia are largely unknown. The effects of C-peptide on the proliferation of human umbilical artery smooth muscle cell (UASMC) and aortic smooth muscle cell (AoSMC) lines cultured under high glucose for 48 h were tested. To gain insights on potential intracellular signaling pathways affected by C-peptide, we analyzed NF- $\kappa$ B activation in VSMCs since this pathway represents a key mechanism for the accelerated vascular disease observed in diabetes. High glucose conditions (25 mmol/L) stimulated NF- $\kappa$ B-dependent VSMC proliferation since the addition of two NF- $\kappa$ B-specific inhibitors, BAY11-7082 and PDTC, prevented proliferation. C-peptide at the physiological concentrations of 0.5 and 1 nmol/L decreased high glucose-induced proliferation of VSMCs that was accompanied by decreased phosphorylation of I $\kappa$ B and reduced NF- $\kappa$ B nuclear translocation. These results suggest that in conditions of hyperglycemia C-peptide reduces proliferation of VSMCs and NF- $\kappa$ B nuclear translocation. In patients with T1D, physiological C-peptide levels may exert beneficial effects on the vasculature that, under high glucose conditions, is subject to progressive dysfunction.

© 2008 Elsevier Ireland Ltd. All rights reserved.

**Keywords:** Diabetes; C-Peptide; Smooth muscle cells; Proliferation; NF- $\kappa$ B

### 1. Introduction

Patients with type 1 diabetes (T1D) exhibit an increased susceptibility to develop a wide range of vascular complications, including microangiopathy and atherosclerosis, which account for the majority of deaths and disability in diabetic patients [1]. Elevated blood glucose levels (hyperglycemia) are considered one of the major causes of vascular complications in T1D patients [2].

Together with endothelial dysfunction, the proliferation of vascular smooth muscle cells (VSMCs) is one of the characteristic features of human atherosclerosis [3]. Under high

glucose conditions, human, porcine and rat VSMC proliferate [4–6] and migrate from the media to the subendothelial space of the vessel wall where early atherosclerotic lesions are localized [3].

In VSMCs, high glucose initiates the activation of the transcription factor NF- $\kappa$ B [7], which leads to the transactivation of a number of genes involved in VSMC proliferation [8]. Several studies have pointed to an involvement of the NF- $\kappa$ B pathway in the process of atherosclerosis by acting at different pathophysiological levels during plaque development. The activated p65 subunit has been found in macrophages, endothelial cells, and VSMCs within human atherosclerotic lesions [9]. Furthermore, administration of anti-sense oligonucleotides to the p65 subunit of NF- $\kappa$ B blocked human VSMC proliferation [10]. Other studies mostly point to a role of NF- $\kappa$ B in regulating apoptosis of VSMCs and fine-tuning of the inflammatory response present in the injured vessel wall [11]. Overall, these studies support

\* Corresponding author at: Children's Hospital of Pittsburgh, Rangos Research Center, 3460 Fifth Avenue, Pittsburgh, PA 15213, USA.  
Tel.: +1 412 692 6570; fax: +1 412 692 5809.

E-mail address: luppi@pitt.edu (P. Luppi).

<sup>1</sup> These two authors contributed equally to this work.



the idea that NF- $\kappa$ B activation in VSMCs represents a key mechanism for the accelerated vascular disease observed in diabetes. Strategies targeting NF- $\kappa$ B pathway activation to inhibit VSMC proliferation for the prevention or the treatment of cardiovascular diseases are emerging [12,13].

Despite intensive insulin treatment and well-controlled glucose levels, vascular complications are still common among T1D patients [2]. As well as reduced endogenous insulin, the level of C-peptide is also decreased in the plasma of T1D patients. This peptide is cleaved from proinsulin and released from the pancreas into the circulation in equimolar amounts to insulin. C-peptide was initially believed to have no biological effects apart from its role in insulin biosynthesis. However, recent evidence suggests that C-peptide may have a physiological role on a variety of cell types including the vasculature [14]. Moreover, results from small clinical trials where C-peptide was administered to T1D patients, showed that C-peptide ameliorates renal dysfunction [15], stimulates skeletal muscle microcirculation [16], and improves functional and structural abnormalities in peripheral nerves [15,17]. It was then proposed that C-peptide may represent an important factor in reversing or preventing microvascular damage associated with diabetes. Supporting this hypothesis, was evidence that T1D patients receiving whole pancreas or islet transplantation exhibited improvement in vascular disease in comparison to patients receiving daily insulin injections to control their hyperglycemia [18,19].

Several studies have focused on the direct effects of C-peptide on the vasculature, often with contradicting results. For example, while there seems to be concordance on the vasodilatory properties of C-peptide [20], it is still controversial whether C-peptide exerts pro-atherogenic effects on the vasculature or vice versa [21]. Other observations point instead to a protective role of C-peptide on vascular dysfunction in diabetes. For example, Kobayashi et al. [22] demonstrated that 3 weeks exposure to C-peptide inhibited high glucose-induced hyperproliferation of rat VSMCs. Another group showed that rat C-peptide inhibits leukocyte–microvascular endothelium interaction *in vivo* [23].

This study evaluated (1) the effects of short-term exposure of C-peptide on high glucose-induced proliferation of human VSMCs *in vitro*, and (2) determined whether the NF- $\kappa$ B pathway is involved in the intracellular signaling events associated with C-peptide in VSMCs, since to date, no data identifies or excludes NF- $\kappa$ B signaling as a molecular event associated with C-peptide effects on VSMCs under high glucose conditions.

## 2. Materials and methods

### 2.1. Cell culture

Human umbilical artery smooth muscle cell (UASMC) and human aortic smooth muscle cell (AoSMC) were obtained from Cambrex (Cambrex Bio Science, Walkersville,

Inc., USA) and grown into 75 cm<sup>2</sup> cell culture flasks (Corning Incorporated, NY, USA) at 37 °C, 5% CO<sub>2</sub> in the presence of smooth muscle cell basal medium-2 (SMGM-2) (Cambrex Bio Science) additioned with 5% of FBS, 0.1% of antibiotics GA-1000 (gentamicyn, amphotericin B), 0.2% of human basic fibroblastic growth factor (hFGF-b), 0.1% insulin, and 0.1% of human epidermal growth factor (hEGF) (Cambrex Bio Science). Cells were used at passage 4–10 for the experiments.

### 2.2. Treatment conditions

SMGM-2 containing 25 mmol/L glucose (Sigma Chemical S. Louis, MO, USA) was used as a high glucose condition in all the experiments, while basal SMGM-2, which contains 5.6 mmol/L glucose, was used as normal glucose control. In all experiments, cells were serum-deprived for 24 h with SMGM-2 containing 1% FBS and 0.1% antibiotics GA-1000. Cells were then replaced with SMGM-2 containing 25 mmol/L glucose in the presence or absence of human C-peptide (0.5 and 1 nmol/L) (Sigma Chemical) for 48 h. Basal SMGM-2 containing 5.6 mmol/L glucose was used as control. Insulin was not added to the culture medium. The effects of two different NF- $\kappa$ B-inhibitors, such as (E)-3-(4-methylphenylsulfonyl)-2-propenenitrile (Bay11-7082; Sigma) (1  $\mu$ M) and pyrrolidine dithiocarbamate (PDTTC, Sigma) (20  $\mu$ M) were also tested in VSMCs. These NF- $\kappa$ B-inhibitors were added to SMGM-2 with 25 mmol/L glucose for 48 h. Separate sets of experiments were performed in which C-peptide (0.5 and 1 nmol/L) was added to medium containing normal glucose. Purity of C-peptide was  $\geq 95\%$  as assessed by the manufacturer by HPLC evaluation. C-peptide concentrations were chosen on the basis of previous reports demonstrating that specific binding of C-peptide to human cell membranes reaches full saturation at low physiological concentrations (0.9 nmol/L) [24]. Human scrambled C-peptide (Sigma-Genosys, Texas, USA) was used as a control. The scrambled C-peptide has an identical amino acid composition to that of the human C-peptide, but the sequence was randomized [23]. Scrambled C-peptide was filtered with 0.2  $\mu$ m filters (Supor Membrane, Life Sciences, Corning) to decrease any chance of bacterial contamination.

## 3. Cell proliferation assays

### 3.1. BrdU measurement of proliferation

Proliferation of VSMCs was evaluated by uptake of bromo-2'-deoxy-uridine (BrdU) using an ELISA kit (Roche Diagnostic, Mannheim, Germany) following manufacturer's instructions. Briefly, UASMC and AoSMC were seeded ( $6 \times 10^3$  cells/100  $\mu$ L) in 96-well flat-bottomed plate (FALCON® Becton Dickinson and Company, Franklin Lakes, NJ) and kept them at 37 °C, 5% CO<sub>2</sub> overnight. Cells were then exposed to the indicated treatment conditions in the



presence of 10  $\mu\text{mol/L}$  of BrdU. Each condition was tested in triplicate. Results were expressed as proliferative response (fold induction vs. 5.6 mmol/L) and final data averaged (mean values  $\pm$  S.D.).

### 3.2. Cell proliferation by cell counting

33,000 UASMC/well were seeded in 6-well plates (Corning Incorporated) and left overnight in an incubator at 37 °C, 5% CO<sub>2</sub>. Cells were then serum-deprived and exposed to the indicated treatment conditions and then counted using a Neubauer Hemocytometer (Hausser Scientific, Horsham, PA), as previously published [4,25].

### 3.3. UASMC Ki-67 staining

As another technique to assess VSMC proliferation, we used Ki-67 immunofluorescence staining for proliferating cells. UASMC were seeded into a glass bottom culture dish (35 mm diameter, poly-d-lysine coated) (MatTek Corporation, Ashland, MA) (~10,000 cells/dish) and then cultured following treatment conditions. Cells were permeabilized with 0.02% of Triton-X100 (Sigma), fixed with 2% paraformaldehyde (PFA) (USB Corporation, Cleveland, OH, USA) and stained with a monoclonal mouse anti-human Ki-67 primary antibody overnight (1:100, DakoCytomation, Denmark). A carboxymethylindocyanine 3(Cy3)-conjugated goat anti mouse secondary antibody (1:500, Jackson Immuno Research Lab INC. West Grove, PA) was then added for 1 h. DAPI stain (Molecular Probes) was used to stain the nuclei. Images were recorded with a confocal laser-scanning microscope (Nikon, Eclipse E800, Japan). The number of Ki67<sup>+</sup> cells was counted in five different fields per dish by one of the investigator blind to the study. A Ki67-labeling index was calculated by dividing the number of Ki67<sup>+</sup> cells by the total number of cells in each of the 5 fields. An averaged Ki-67-labeling index ( $\pm$ S.D.) was then obtained for each section. Four different independent experiments were performed.

## 4. NF- $\kappa$ B analysis assays

### 4.1. Nuclear and cytoplasmic extracts

VSMCs were cultured in SMGM-2 following treatment conditions and then pretreated with 25  $\mu\text{l}$  of protease inhibitor cocktail (Pierce, Rockford, IL). Nuclear and cytoplasmic fractions were separated using NE-PER<sup>®</sup> Nuclear and Cytoplasmic extraction kit (Pierce). Protein concentration was measured using a BCA assay (Pierce).

### 4.2. Immunoblotting

NF- $\kappa$ B p65 immunoblots were performed as previously described [26] with 10  $\mu\text{g}$  of nuclear protein extracts. Densitometry was performed with UN-SCAN-IT gel software

(Silk Scientific, Orem, UT). I $\kappa$ B- $\alpha$  and p-I $\kappa$ B- $\alpha$  immunoblots were performed with 10  $\mu\text{g}$  of cytoplasmic protein extracts [26]. A minimum of three independent experiments was performed.

### 4.3. NF- $\kappa$ B p50 ELISA

Activation of the NF- $\kappa$ B p50 subunit was detected on 3  $\mu\text{g}$  of nuclear extracts using a EZ-Detect<sup>TM</sup> Transcription Factor Kit (Pierce Biotechnology).

### 4.4. Determination of NF- $\kappa$ B p65 translocation by immunofluorescence

UASMC were seeded into a glass bottom culture dish (~10,000 cells/dish) (MatTek Corporation). After the indicated treatments, cells were fixed with 2% PFA (USB Corporation), and stained with a rabbit polyclonal primary antibody against NF- $\kappa$ B p65 (1:150, Santa Cruz Biotechnology, Inc.) at 4 °C overnight. A 3(Cy3)-conjugated goat anti-rabbit secondary antibody (1:500, Jackson Immuno Research Lab Inc.) was then added for 1 h, in the dark, at room temperature. DAPI stain (Molecular Probes) was used to stain the nuclei. Fluorescence staining was evaluated using Nikon, Eclipse E800 epifluorescence microscope connected to a digital camera and interfaced with a computer.

## 5. Statistical analysis

Results from each experiment were averaged and expressed as mean  $\pm$  S.D. Comparisons between 5.6 and 25 mmol/L glucose conditions were performed by paired Student's *t*-test. ANOVA followed by Dunnett's post hoc test was applied to evaluate differences between 25 mmol/L glucose, C-peptide, and NF- $\kappa$ B inhibitors. A *p*-value of *p* < 0.05 was considered statistically significant.

## 6. Results

### 6.1. C-peptide decreases high glucose-induced proliferation of VSMCs

In Fig. 1A, we examined the influence of high glucose on UASMC proliferation by measuring the nuclear incorporation of BrdU (DNA synthesis). We found that exposure of UASMC for 48 h to 25 mmol/L glucose significantly increased BrdU incorporation compared with control cells exposed to 5.6 mmol/L glucose (*p* = 0.002). Administration of C-peptide at a dose of 0.5 (*p* < 0.01), and 1 nmol/L (*p* < 0.01) for 48 h significantly suppressed high glucose-induced increase in BrdU incorporation in UASMC compared to untreated and scrambled C-peptide-treated cells (Fig. 1A). The addition of specific NF- $\kappa$ B inhibitors PDTC or BAY11-7082 under high glucose conditions (25 mmol/L)

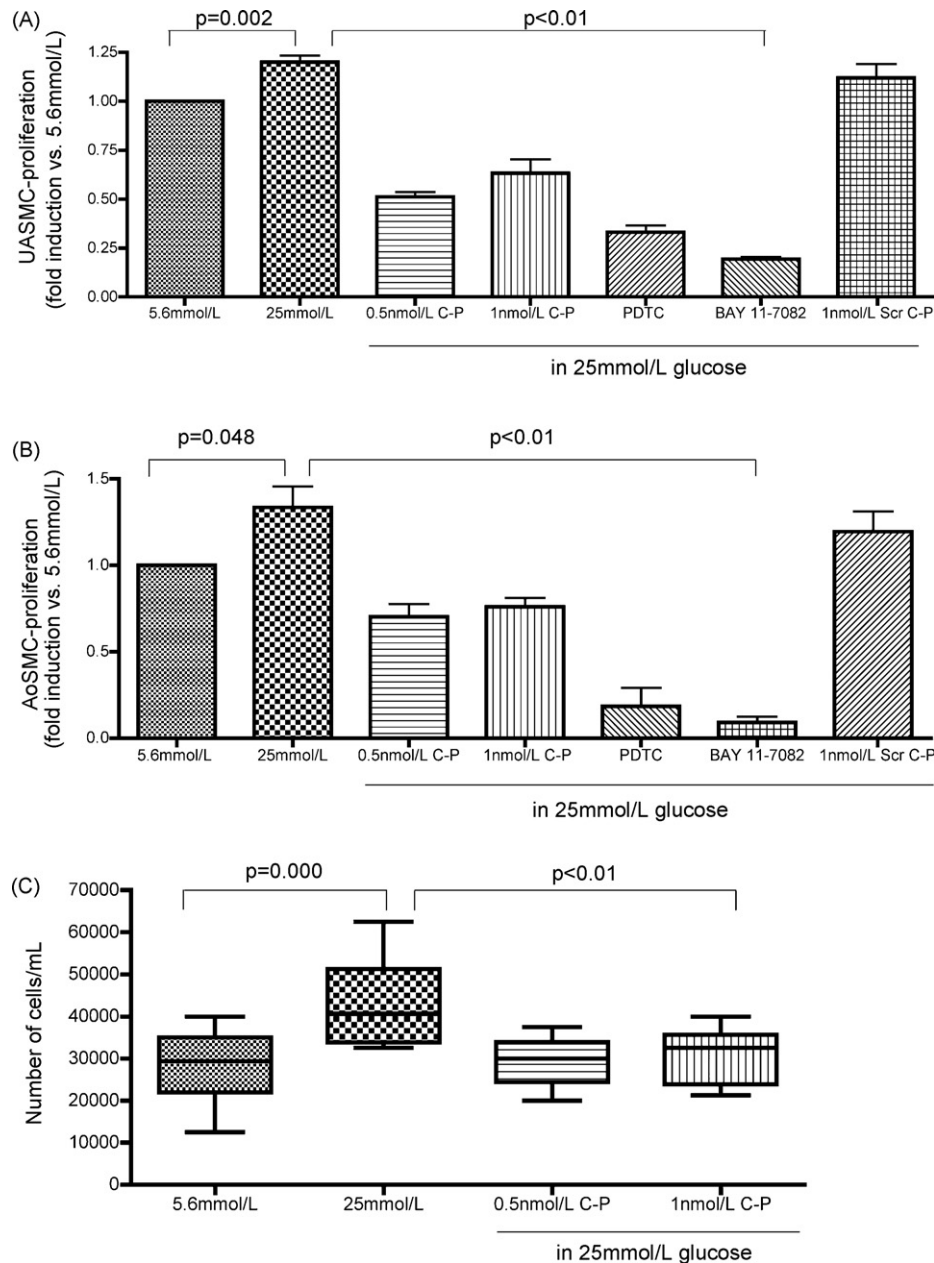


Fig. 1. C-peptide reduces high glucose-induced proliferation of VSMCs. VSMCs were incubated with 25 mmol/L glucose in the presence or in the absence of C-peptide (C-P) for 48 h and assayed for proliferation. In (A), BrdU incorporation shows cellular proliferation in high glucose ( $p=0.002$  vs. 5.6 mmol/L). C-peptide reduced high glucose-induced UASMC proliferation ( $p<0.01$ ), while addition of scrambled C-peptide (Scr C-P) did not have any significant effect. Addition of the NF- $\kappa$ B inhibitors PDTC (20  $\mu$ M) and BAY-11078 (1  $\mu$ M) also showed a decrease in proliferation ( $p<0.01$  vs. 25 mmol/L glucose). In (B), BrdU incorporation in AoSMC demonstrates that high glucose-stimulated cellular proliferation ( $p=0.048$  vs. 5.6 mmol/L). C-peptide significantly reduced high glucose-induced UASMC proliferation ( $p<0.01$  vs. 25 mmol/L), while addition of scrambled C-peptide (Scr C-P) did not have any effect. Addition of PDTC (20  $\mu$ M) and BAY-11078 (1  $\mu$ M) also showed a decrease in proliferation ( $p<0.01$  vs. 25 mmol/L glucose). Values are mean  $\pm$  S.D. of 10 different experiments run in triplicate. In (C), boxplot graphs showing the median values (limits of the lines are 5th and 95th centiles) of number of UASMC counted with a hemocytometer ( $n=10$  experiments) (on the Y-axis). Cell number increased with 25 mmol/L glucose compared to 5.6 mmol/L glucose ( $p=0.000$ ), while 0.5 and 1 nmol/L C-peptide reduced high glucose-induced UASMC proliferation ( $p<0.01$ ).

significantly suppressed UASMC proliferation ( $p<0.01$  vs. 25 mmol/L glucose) (Fig. 1A).

We also tested the effect of C-peptide on the proliferative response of human AoSMC. Similarly to UASMC, exposure to 25 mmol/L glucose for 48 h increased cell proliferation compared to cells exposed to 5.6 mmol/L glucose ( $p=0.048$ )

(Fig. 1B). We observed a decrease in BrdU incorporation when AoSMC were cultured for 48 h with 25 mmol/L glucose in the presence of 0.5 nmol/L ( $p<0.01$ ) and 1 nmol/L ( $p<0.01$ ) C-peptide (Fig. 1B) and the addition of scrambled C-peptide had no effect (Fig. 1B). The NF- $\kappa$ B inhibitors PDTC or BAY11-7082 added to the medium containing

25 mmol/L glucose significantly inhibited AoSMC proliferation ( $p < 0.01$ ) (Fig. 1A).

The increase in high glucose-induced VSMCs cellular proliferation was also confirmed by counting total cell numbers with a hemocytometer (Fig. 1C). UASMC cultured under high glucose (25 mmol/L) increased in number ( $42625 \pm 9672$ ) compared to normal glucose conditions (5.6 mmol/L) ( $28000 \pm 8337$ ) ( $p = 0.000$ ) (Fig. 1C). The addition of C-peptide at concentrations of 0.5 nmol/L ( $p < 0.01$ ) or 1 nmol/L ( $p < 0.01$ ) to high glucose-treated cells, restored cell numbers to the same level as normal glucose conditions (Fig. 1C).

In contrast, when we cultured UASMCs with regular medium (containing 5.6 mmol/L of glucose) in the presence of C-peptide we detected increased BrdU incorporation as compared to regular medium in the absence of C-peptide ( $p < 0.05$ ) (Fig. 2A). We did not detect a significant increase in BrdU incorporation in AoSMC exposed to regular medium in the presence of C-peptide (Fig. 2B).

### 6.2. C-peptide decreases the number of Ki67<sup>+</sup> UASMC exposed to high glucose

As an additional indication of cellular proliferation, immunofluorescence staining of UASMC for the nuclear marker Ki67 was performed under normal (5.6 mmol/L)

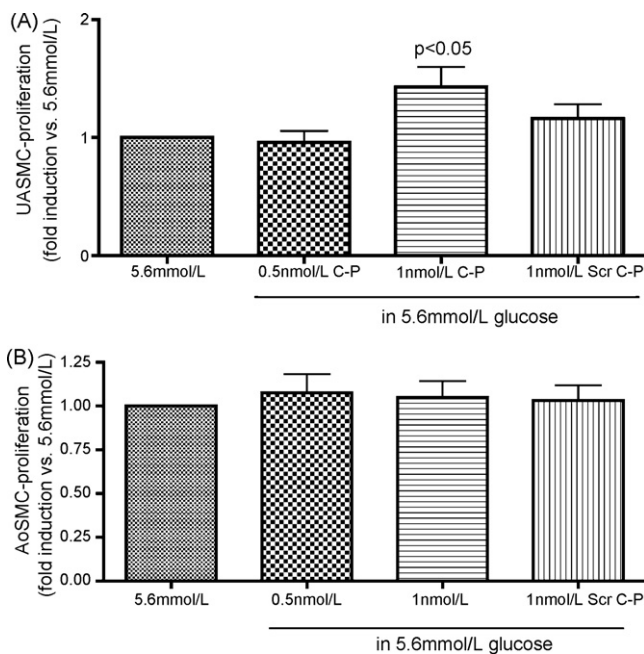


Fig. 2. C-peptide stimulates proliferation of VSMCs under normal glucose. VSMCs were incubated with 5.6 mmol/L in the presence or in the absence of C-peptide (C-P) for 48 h and assayed for proliferation. In (A), BrdU incorporation in UASMC shows increased proliferation in the presence of 1 nmol/L C-peptide ( $p < 0.05$  vs. 5.6 mmol/L glucose), while addition of scrambled C-peptide (Scr C-P) did not have any significant effect. In (B), BrdU incorporation in AoSMC shows no significant effect of C-peptide on cellular proliferation under normal glucose conditions. Values are mean  $\pm$  S.D. of three different experiments run in triplicate.

and high glucose (25 mmol/L) (Fig. 3A) conditions with or without C-peptide (0.5 nmol/L) treatment. We observed a significant increase in Ki67<sup>+</sup> cells under high glucose conditions ( $p = 0.01$  vs. 5.6 mmol/L), while addition of C-peptide reduced Ki67<sup>+</sup> cell number ( $19.8\% \pm 2.88$ ) in comparison to cells exposed to 25 mmol/L glucose only ( $26.8\% \pm 2.91$ ) ( $p = 0.02$ ) (Fig. 3A and B). The increase in Ki67<sup>+</sup> cells from UASMC grown under high glucose conditions was mediated by NF- $\kappa$ B activation since treatment with PDTC (20  $\mu$ M), an NF- $\kappa$ B inhibitor, reduced the number of Ki67<sup>+</sup> cells to basal levels detected in normal glucose conditions ( $p < 0.01$ ) (Fig. 3A and B).

### 6.3. Effect of C-peptide on high glucose-induced NF- $\kappa$ B activation

To determine if high glucose-induced proliferation of UASMC was associated with activation of the NF- $\kappa$ B signaling pathway, immunoblot analysis and NF- $\kappa$ B-specific ELISAs were performed with nuclear extracts from stimulated-UASMC. As shown in Fig. 4A, high glucose (25 mmol/L) induced an increase in NF- $\kappa$ B p65 nuclear translocation in comparison to normal glucose (5.6 mmol/L) stimulated UASMC. The addition of C-peptide to the high glucose cultures decreased NF- $\kappa$ B p65 nuclear translocation to normal glucose levels (Fig. 4A), while the addition of scrambled C-peptide did not suppress NF- $\kappa$ B activity (Fig. 4A). Densitometry of the NF- $\kappa$ B p65 immunoblot demonstrated that high glucose-stimulated NF- $\kappa$ B p65 nuclear translocation ( $p = 0.038$  vs. normal glucose) and that the addition of C-peptide (1 nmol/L) during high glucose exposure reduced NF- $\kappa$ B p65 nuclear translocation by 2-fold as compared to high glucose alone ( $p < 0.05$ ) (Fig. 4B). NF- $\kappa$ B activation was also assessed with a NF- $\kappa$ B p50-specific ELISA with nuclear extracts from glucose-stimulated UASMCs, as shown in Fig. 4C. High glucose-induced a significant increase in NF- $\kappa$ B p50 binding activity in contrast to normal glucose ( $p = 0.02$ ) and was efficiently ablated by the addition of C-peptide ( $p < 0.05$ ).

Similar results were obtained with AoSMC, as shown in Fig. 5. While NF- $\kappa$ B p65 nuclear translocation increased under exposure to high glucose, addition of C-peptide to the high glucose medium reduced NF- $\kappa$ B activation to basal levels observed under 5.6 mmol/L glucose (Fig. 5).

Nuclear translocation of NF- $\kappa$ B p65 was also determined by immunofluorescence staining. UASMC cultured in 25 mmol/L glucose resulted in an increase in NF- $\kappa$ B p65 nuclear translocation as demonstrated by the intense green fluorescence localized in the cell nuclei (Fig. 6) and also from superimposing photomicrographs of DAPI-stained nuclei (blue) (Fig. 6B) with green fluorescence (Fig. 6C). Cells in normal glucose (5.6 mmol/L) retained NF- $\kappa$ B p65 in the cytoplasm (green fluorescence) with very little staining observed in the nuclei (Fig. 6A). The addition of C-peptide (0.5 nmol/L) to high glucose-treated cells prevented NF- $\kappa$ B

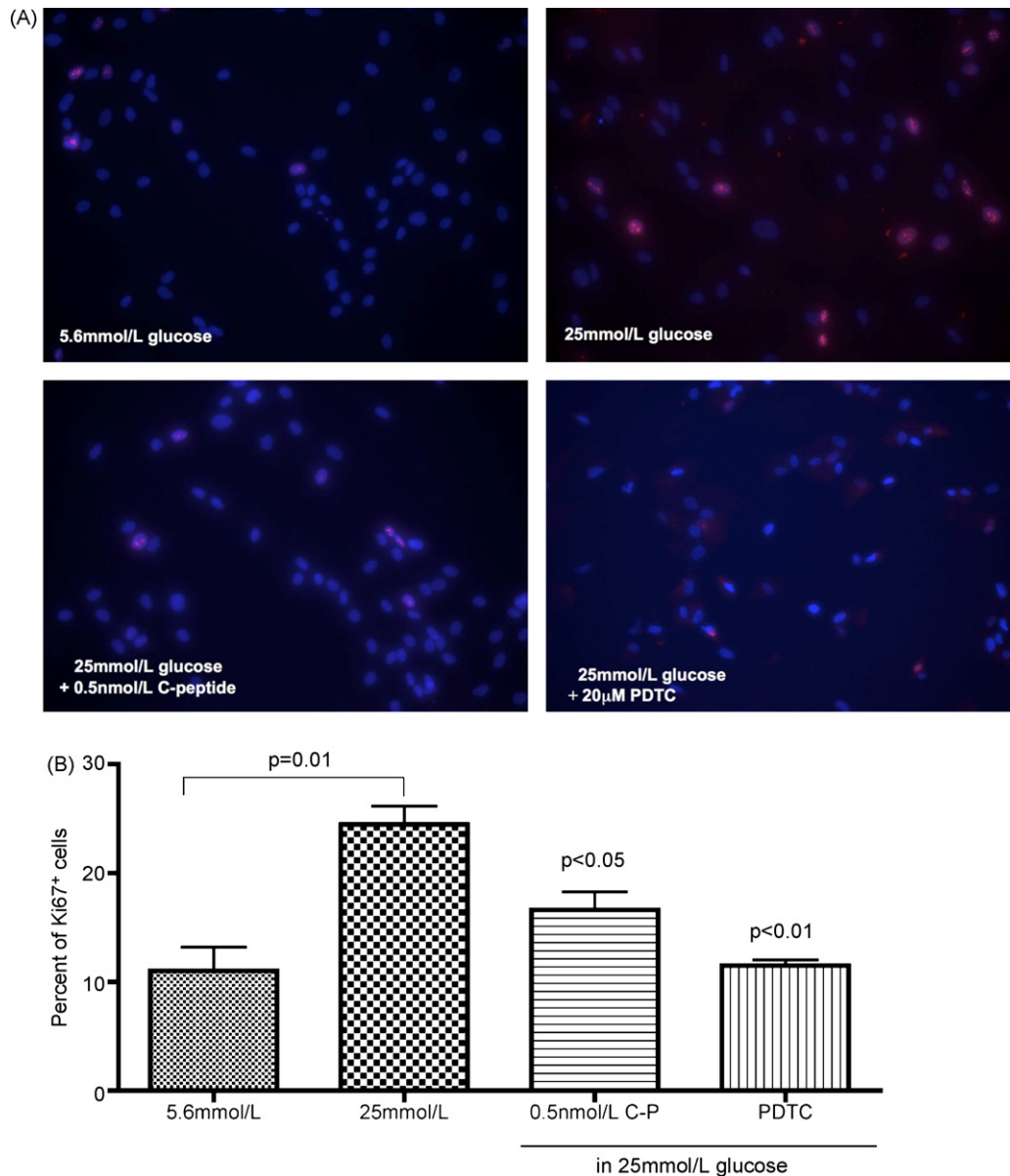


Fig. 3. C-peptide reduces the number of Ki67<sup>+</sup> cells. In (A), images of Ki-67-immunostaining (in red) in UASMC exposed for 48 h to the different conditions, as stated. DAPI staining was used to stain the nuclei (in blue). C-peptide addition to the high glucose medium reduced Ki67<sup>+</sup> cell number. In (B), quantitation of Ki67<sup>+</sup> cells. Bar graph shows percent of Ki-67<sup>+</sup> cells (mean ± S.D.) compared to DAPI staining (blue) from five random fields of four independent experiments. Exposure of UASMC to 25 mmol/L glucose increased number of Ki-67<sup>+</sup> cells compared to normal glucose ( $p = 0.01$ ), while addition of C-peptide significantly reduced the number of Ki-67<sup>+</sup> proliferating cells ( $p < 0.05$  vs. 25 mmol/L glucose). Addition of the NF- $\kappa$ B inhibitor PDTC to the high glucose medium also reduced the number of Ki-67<sup>+</sup> cells ( $p < 0.01$  vs. 25 mmol/L glucose).

p65 nuclear translocation (Fig. 6A), an effect not observed with scrambled C-peptide.

The mechanism underlying NF- $\kappa$ B nuclear translocation from the cytoplasm to the nucleus is based on the phosphorylation of I $\kappa$ B $\alpha$ . We therefore investigated the effects of C-peptide on high glucose-induced phosphorylation of I $\kappa$ B $\alpha$  by Western blotting on cytoplasmic extracts from UASMC (Fig. 7). As expected, an increase in the level of phosphorylated I $\kappa$ B $\alpha$  (p-I $\kappa$ B $\alpha$ ) was observed in the cytoplasmic extracts after UASMC treatment (48 h) with 25 mmol/L glucose as compared to UASMC cultured in low glucose (5.6 mmol/L)

(Fig. 7). Addition of C-peptide to the high glucose medium caused a decrease in the level of p-I $\kappa$ B $\alpha$  as compared to cells exposed to high glucose in the absence of C-peptide (Fig. 7).

## 7. Discussion

T1D patients have an increased risk of developing atherosclerosis compared to the non-diabetic population with lesions marked by endothelial dysfunction and exacerbated VSMC proliferation. Proliferating VSMCs migrate



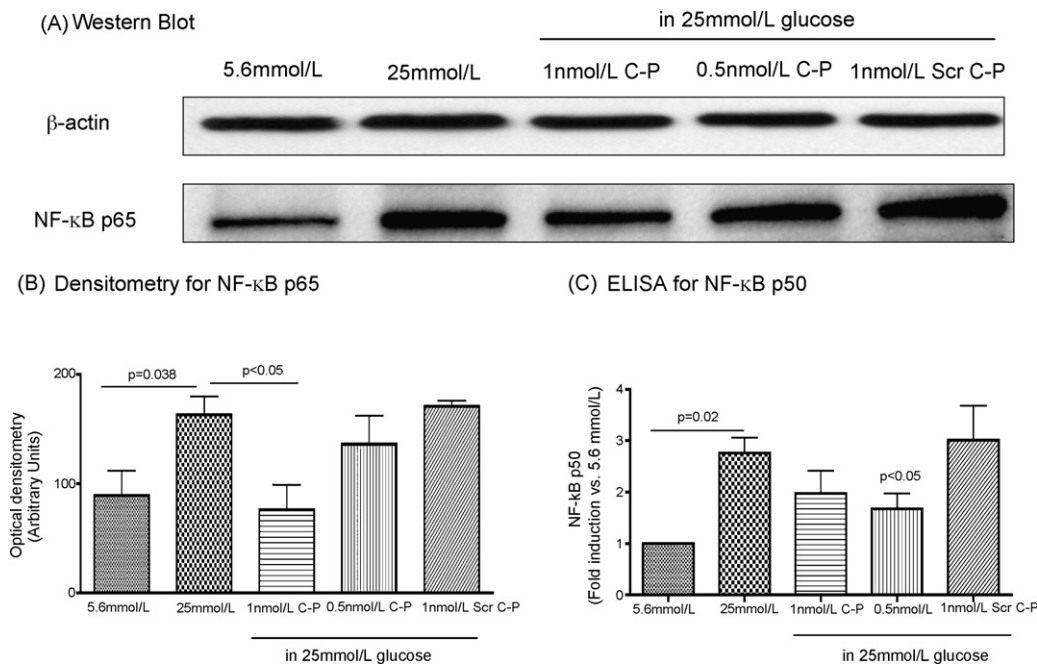


Fig. 4. Expression of p65 subunits of NF-κB in UASMC cultured in high glucose in the presence of C-peptide. UASMC were cultured in 5.6 mmol/L or 25 mmol/L glucose in the presence or absence of C-peptide (C-P) for 48 h. Cellular nuclear extracts were subjected to Western immunoblotting to detect p65 levels using a specific antibody (1:1,000). Scrambled C-peptide (Scr C-P) was used as control. In (A), representative immunoblot depicting the 65-kDa band of the p65 subunit. To show equal loading of the gel, staining for β-actin is also shown. In (B), bar graph showing the densitometric quantitation of the bands ( $n = 4$  different experiments). There is a significant increase in NF-κB p65 nuclear translocation in cells under 25 mmol/L glucose ( $p = 0.038$  vs. 5.6 mmol/L) that is reduced with addition of C-peptide ( $p < 0.05$ ). Results are means  $\pm$  S.D. In (C), NF-κB binding activity of the p50 subunit was examined using a EZ-Detect™ Transcription Factor kit (Pierce Biotechnology). Results were expressed as fold induction of NF-κB p50 activity respect to control at 5.6 mmol/L. High glucose increased NF-κB p50 activation as compared to normal glucose ( $p = 0.02$ ). This activation is decreased by addition of C-peptide to the high glucose medium ( $p < 0.05$  vs. 25 mmol/L glucose alone). Means  $\pm$  S.D. of six independent experiments are shown.

from the media into early atherosclerotic lesions, secrete pro-inflammatory mediators, up-regulate cell adhesion molecules, and promote synthesis of matrix molecules required for the retention of lipoproteins [3]. In advanced human lesions, VSMCs and their secreted product constitutes up to 70–80% of the content of the atherosclerotic plaques. Finally, there is evidence suggesting that VSMCs may also be important for the stability of the atherosclerotic plaque through a formation of a firm fibrous cap [27]. Thus, the involvement of numerous VSMC functional abnormalities in

diabetes, warrant the control of their proliferation to prevent diabetic complications.

In this study, we show that short-term exposure to physiological concentrations of C-peptide inhibited excessive proliferation of UASMC and AoSMC induced by high glucose *in vitro*. Although this evidence in human VSMC is reported here for the first time, a suppressive effect of C-peptide on glucose-induced proliferation of VSMCs has been previously described by Kobayashi et al. in a rat aortic smooth muscle cell line [22]. Our and Kobayashi's results support

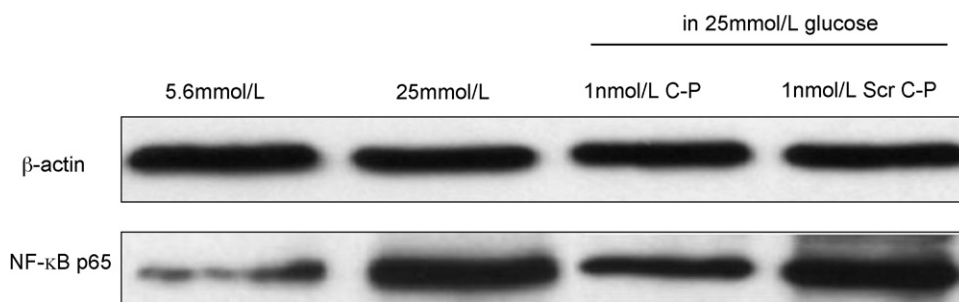


Fig. 5. Expression of p65 subunits of NF-κB in AoSMC cultured in high glucose in the presence of C-peptide. Representative immunoblot (of three independent experiments) depicting the 65-kDa band of the p65 subunit in AoSMC cultured in 5.6 mmol/L or 25 mmol/L glucose in the presence or absence of C-peptide (C-P) for 48 h. Cellular nuclear extracts were subjected to Western immunoblotting to detect p65 levels using a specific antibody (1:1,000). AoSMC cultured in high glucose in the presence of C-peptide showed a decreased NF-κB nuclear translocation as compared to high glucose alone. Scrambled C-peptide (Scr C-P) was used as control. To show equal loading of the gel, staining for β-actin is also shown.



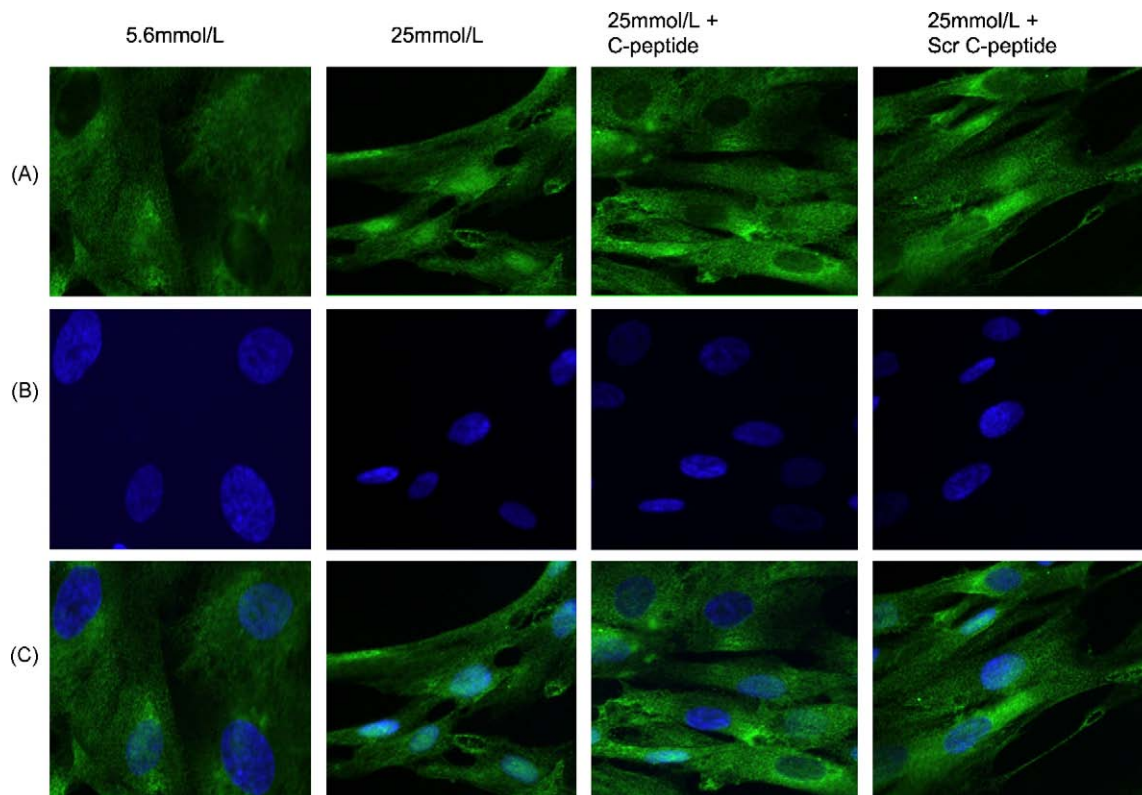


Fig. 6. C-peptide treatment reduces high glucose-induced nuclear translocation of NF- $\kappa$ B p65 subunit in UASMC. UASMC were serum-starved for 24 h and then treated for 48 h with (I) normal glucose; (II) high glucose; (III) high glucose in the presence of either 0.5 nmol/L C-peptide or 0.5 nmol/L scrambled C-peptide (Scr). In (A), localization of NF- $\kappa$ B immunostaining using a monoclonal antibody against the p65 subunit (green fluorescence); (B) UASMC nuclei stained with DAPI; (C) composite images generated by superimposing photographs in A and B. As shown in (A), the green fluorescence corresponding to the p65 subunit was localized mostly in correspondence of the nuclei when cells were treated with 25 mmol/L glucose. This was clearly shown by superimposing the DAPI nuclear staining (in B) with the green fluorescence. On the contrary, UASMC treated with C-peptide showed green fluorescence mostly localized in the cytoplasm, rather than in the cell nuclei. Three independent experiments were performed, and one representative photomicrograph sets (30 $\times$ ) is shown.

the view that physiological concentrations of C-peptide may exert a protective action on VSMCs in conditions of hyperglycemia by targeting the excessive VSMC proliferation. This effect might be specific to conditions of hyperglycemia, as it was not detected under normal glucose. In fact, VSMC cultured in normal glucose in the presence of C-peptide showed an increased proliferation, a result also reported by Walcher et al. [28]. Based on these findings, it is tempting

to speculate that C-peptide effects on proliferative activities of VSMCs *in vitro* is dependent on glucose concentrations in the culture medium, with stimulatory activity under normal glucose and inhibitory one in conditions of hyperglycemia.

Another factor that could affect C-peptide's effect on proliferation of VSMCs *in vitro*, is its concentration in the culture medium. In fact, one possible scenario is that lower, physiological, concentrations of C-peptide produce a beneficial

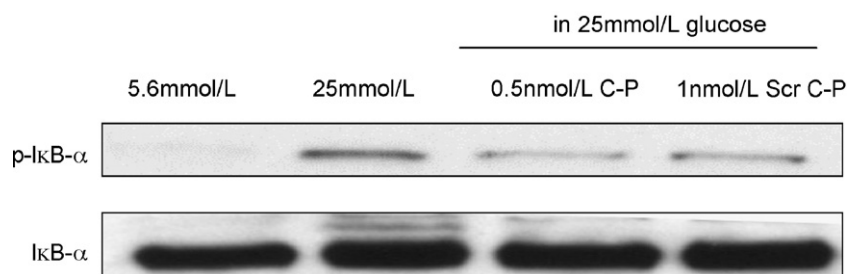


Fig. 7. Inhibitory effect of C-peptide on phosphorylation of I $\kappa$ B $\alpha$  protein in UASMC. UASMC were serum-starved for 24 h and then treated for 48 h with: (1) 5.6 mmol/L glucose; (2) 25 mmol/L glucose; (3) 25 mmol/L glucose + 0.5 nmol/L C-peptide (C-P); and (4) 25 mmol/L glucose + 1 nmol/L C-P. Cellular cytoplasmic extracts were subjected to Western immunoblotting to detect phosphorylated I $\kappa$ B $\alpha$  (p-I $\kappa$ B- $\alpha$ ) using a specific antibody. In this figure, it is shown a representative immunoblotting depicting decreased phosphorylation of I $\kappa$ B- $\alpha$  (p-I $\kappa$ B- $\alpha$ ) with C-peptide. Immunoblot for total I $\kappa$ B- $\alpha$  is also shown. Similar results were obtained in at least two independent experiments.

effect on the vasculature [29], while higher levels of circulating C-peptide, such as those measured in type 2 diabetic patients with hyperinsulinemia associated with insulin resistance, produce deleterious effects on the vasculature. In support of this view is the study by Walcher et al. [21], who found that higher concentrations of C-peptide, mimicking those found in the circulation of type 2 diabetic patients, produced maximal stimulation of lymphocyte chemotaxis *in vitro*. Future studies are required to further elucidate these issues.

The mechanisms underlying the effects of C-peptide on the human vasculature, especially in conditions of hyperglycemia, are still largely unknown. This study investigated C-peptide effects on the NF- $\kappa$ B pathway, since it is known that NF- $\kappa$ B activation in VSMCs represents a key mechanism for the accelerated vascular disease observed in diabetes. In support of a previous study [7], we confirm that high glucose stimulates NF- $\kappa$ B activation in serum-deprived VSMCs, but our work uniquely demonstrates that exogenous addition of C-peptide significantly reduced high glucose-induced nuclear translocation of NF- $\kappa$ B p65 and p50 in both UASMC and AoSMC. Consistently, C-peptide reduced high glucose-induced phosphorylation of I $\kappa$ B $\alpha$  in VSMCs, an upstream signaling event that regulates NF- $\kappa$ B translocation from the cytoplasm to the nucleus.

The suppressive effect of C-peptide on the NF- $\kappa$ B pathway during conditions of hyperglycemia may represent the underlying mechanism for the inhibitory effect of C-peptide on VSMC proliferation. The involvement of NF- $\kappa$ B in VSMC proliferation in high glucose conditions is demonstrated by the fact that addition of PDTC and BAY 11-7082, two specific NF- $\kappa$ B inhibitors, abolished UASMC and AoSMC proliferation *in vitro*. These results are in apparent contrast with the work of Kitazawa et al. [30] who detected a stimulatory activity of C-peptide on the NF- $\kappa$ B pathway in Swiss 3T3 fibroblasts *in vitro*. The reason for the discrepancy between these two studies could lie on the different experimental design and cell types used. In fact, while Kitazawa et al. investigated fibroblast grown in low glucose conditions, our experiments were carried out in VSMC lines exposed to high glucose.

Identification of signal transduction pathways involved in C-peptide functions on VSMCs may have therapeutic implication for the treatment or the prevention of vascular lesions in diabetic patients. It is well known that vascular dysfunction and generalized monocyte activation are very early phenomenon during the progression of T1D, even in patients with recent onset diabetes and in high-risk individuals in the preclinical phase [31]. Our current study emphasize the idea that C-peptide in replacement doses to T1D patients, who lack endogenous C-peptide and are at risk of developing episodes of hyperglycemia, may be beneficial in the prevention and/or progression of vascular compromise associated with diabetes. A beneficial effect of C-peptide replacement therapy has already been demonstrated by clinical studies on T1D patients where C-peptide has been shown to ameliorate chronic myocardial, renal, and neuronal complications

[15–17]. Furthermore, a physiologic anti-inflammatory effect of C-peptide on glucose-induced endothelial dysfunction has also been demonstrated by our group (Luppi P. et al. unpublished results).

In conclusion, our findings support the hypothesis that C-peptide at physiological concentrations inhibits VSMC proliferation under high glucose conditions likely due to suppression of NF- $\kappa$ B activation. These findings underscore a role of C-peptide in VSMC functions, especially in conditions of diabetic insult to the vasculature.

## Acknowledgements

This work was supported in part by the Henry Hillman Endowment Chair in Pediatric Immunology and Department of Defense grant # W81XWH-06-1-0317 to M.T.

## References

- [1] UK Prospective Diabetes Study (UKPDS) Group. Intensive blood-glucose control with sulphonylureas or insulin compared with conventional treatment and risk of complications in patients with type 2 diabetes (UKPDS 33). *Lancet* 1998;352:837–53.
- [2] Diabetes Control, Complications Trial Research Group. The effect of intensive treatment of diabetes on the development and progression of long-term complications in insulin-dependent diabetes mellitus. *N Engl J Med* 1993;329:977–86.
- [3] Ross R. Atherosclerosis—an inflammatory disease. *N Engl J Med* 1999;340:115–26.
- [4] Natarajan R, Gonzales N, Xu L, Nadler JL. Vascular smooth muscle cells exhibit increased growth in response to elevated glucose. *Biochem Biophys Res Commun* 1992;187:552–60.
- [5] Nakamura J, Kasuya Y, Hamada Y, et al. Glucose-induced hyperproliferation of cultured rat aortic smooth muscle cells through polyol pathway hyperactivity. *Diabetologia* 2001;44:480–7.
- [6] Yamamoto M, Acevedo-Duncan M, Chalfant CE, et al. Acute glucose-induced downregulation of PKC- $\beta$  II accelerates cultured VSMC proliferation. *Am J Physiol Cell Physiol* 2000;279:C587–95.
- [7] Kumar K, Yerneni V, Bai W, et al. Hyperglycemia-induced activation of nuclear transcription factor  $\kappa$ B in vascular smooth muscle cells. *Diabetes* 1999;48:855–64.
- [8] Bellas RE, Lee JS, Sonenshein G. Expression of a constitutive NF- $\kappa$ B like activity is essential for proliferation of cultured bovine vascular smooth muscle cells. *J Clin Invest* 1995;96:2521–7.
- [9] Brand K, Page S, Walli AK, Neumeier D, Baeuerle PA. Role of nuclear factor- $\kappa$ B in atherogenesis. *Exp Physiol* 1997;82:297–303.
- [10] Autieri MV, Yue TL, Ferstein GZ, Ohlstein E. Antisense oligonucleotides to the p65 subunit of NF- $\kappa$ B inhibit human vascular smooth muscle cell adherence and proliferation and prevent neointima formation in rat carotid arteries. *Biochem Biophys Res Commun* 1995;213:827–36.
- [11] Merhof FB, Schmidt-Ullrich R, Dietz R, Scheidereit C. Regulation of vascular smooth muscle cell proliferation. Role of NF- $\kappa$ B revisited. *Circ Res* 2005;96:958–64.
- [12] Zuckerbraun BS, McCloskey CA, Mahidhara RS, et al. Overexpression of mutated I $\kappa$ B $\alpha$  inhibits vascular smooth muscle cell proliferation and intimal hyperplasia formation. *J Vasc Surg* 2003;38:812–9.
- [13] Morishita R, Sugimoto T, Aoki M, et al. *In vivo* transfection of *cis* element “decoy” against nuclear factor- $\kappa$ B binding site prevents myocardial infarction. *Nat Med* 1997;3:894–9.

- [14] Marques RG, Fontaine MJ, Rogers J. C-peptide much more than a byproduct of insulin biosynthesis. *Pancreas* 2004;29:231–8.
- [15] Johansson BL, Borg K, Fernqvist-Forbes E, et al. Beneficial effects of C-peptide on incipient nephropathy and neuropathy in patients with type 1 diabetes: a three-month study. *Diabet Med* 2000;17:181–9.
- [16] Johansson BL, Wahren J, Pernow J. C-peptide increases forearm blood flow in patients with type 1 diabetes via a nitric oxide-dependent mechanism. *Am J Physiol Endocrinol Metab* 2003;285:E864–70.
- [17] Ekberg K, Brismar T, Johansson BL, et al. C-peptide replacement therapy and sensory nerve function in type 1 diabetic neuropathy. *Diabetes Care* 2007;30:71–6.
- [18] Lee TC, Barshes NR, Agee EE, et al. The effect of whole organ pancreas transplantation and PIT on diabetic complications. *Curr Diab Rep* 2006;6:323–7.
- [19] Shapiro AM, Ricordi C, Hering BJ, et al. International trial of the Edmonton protocol for islet transplantation. *N Engl J Med* 2006;355:1318–30.
- [20] Lindstrom K, Johansson C, Johansson E, Haraldsson B. Acute effects of C-peptide on the microvasculature of isolated perfused skeletal muscle and kidneys in rat. *Acta Physiol Scand* 1996;156:19–25.
- [21] Walcher D, Aleksie M, Jerg V, et al. C-peptide induces chemotaxis of human CD4-positive cells: involvement of pertussis toxin-sensitive G-proteins and phosphoinositide 3-kinase. *Diabetes* 2004;53(7):1664–70.
- [22] Kobayashi Y, Naruse K, Hamada Y, et al. Human proinsulin C-peptide prevents proliferation of rat aortic smooth muscle cells cultured in high-glucose conditions. *Diabetologia* 2005;48:2396–401.
- [23] Scalia R, Coyle KM, Levin BL, Booth G, Lefer AM. C-peptide inhibits leukocyte endothelium interaction in the microcirculation during acute endothelial dysfunction. *FASEB J* 2000;14:2357–64.
- [24] Rigler R, Pramanik A, Jonasson P, et al. Specific binding of proinsulin C-peptide to human cell membranes. *Proc Natl Acad Sci* 1999;96:13318–23.
- [25] Graier WF, Grubenthal I, Dittrich P, Wascher TC, Kostner GM. Intracellular mechanism of high D-glucose-induced modulation of vascular cell proliferation. *Eur J Pharm* 1995;294:221–9.
- [26] Tse HM, Milton MJ, Piganelli JD. Mechanistic analysis of the immunomodulatory effects of a catalytic antioxidant on antigen-presenting cells: implication for their use in targeting oxidation-reduction reactions in innate immunity. *Free Radic Biol Med* 2004;36:233–47.
- [27] Clarke MC, Figg N, Maguire JJ, et al. Apoptosis of vascular smooth muscle cells induces features of plaque vulnerability in atherosclerosis. *Nat Med* 2006;12:1075–80.
- [28] Walcher D, Babiak C, Poletsek P, et al. C-peptide induces vascular smooth muscle cell proliferation. *Circ Res* 2006;99:1181–7.
- [29] Steffes MW, Sibley S, Jackson M, Thomas W. Beta-cell function and the development of diabetes-related complications in the diabetes control and complications trial. *Diabetes Care* 2003;26(3):832–6.
- [30] Kitazawa M, Shibata Y, Hashimoto S, Ohizumi Y, Yamakuni T. Proinsulin C-peptide stimulates a PKC/I $\kappa$ B/NF- $\kappa$ B signaling pathway to activate COX-2 gene transcription in swiss 3T3 fibroblasts. *J Biochem* 2006;139:1083–6.
- [31] Cifarelli V, Libman IM, DeLuca A, et al. Increased expression of monocyte CD11b (Mac-1) in overweight recent-onset type 1 diabetic children. *Rev Diabet Stud* 2007;4(2):112–7.

# Human C-peptide antagonises high glucose-induced endothelial dysfunction through the nuclear factor- $\kappa$ B pathway

P. Luppi · V. Cifarelli · H. Tse · J. Piganelli · M. Trucco

Received: 11 February 2008 / Accepted: 28 March 2008  
© Springer-Verlag 2008

## Abstract

**Aims/hypothesis** Endothelial dysfunction in diabetes is predominantly caused by hyperglycaemia leading to vascular complications through overproduction of oxidative stress and activation of the transcription factor nuclear factor- $\kappa$ B (NF- $\kappa$ B). Many studies have suggested that decreased circulating levels of C-peptide may play a role in diabetic vascular dysfunction. To date, the possible effects of C-peptide on endothelial cells and intracellular signalling pathways are largely unknown. We therefore investigated the effect of C-peptide on several biochemical markers of endothelial dysfunction in vitro. To gain insights into potential intracellular signalling pathways affected by C-peptide, we tested NF- $\kappa$ B activation, since it is known that inflammation, secondary to oxidative stress, is a key component of vascular complications and NF- $\kappa$ B is a redox-dependent transcription factor. **Methods** Human aortic endothelial cells (HAEC) were exposed to 25 mmol/l glucose in the presence of C-peptide (0.5 nmol/l) for 24 h and tested for expression of the gene encoding vascular cell adhesion molecule-1 (*VCAM-1*) by RT-PCR and flow cytometry. Secretion of IL-8 and monocyte chemoattractant protein-1 (MCP-1) was measured by ELISA. NF- $\kappa$ B activation was analysed by immunoblotting and ELISA. **Results** Physiological concentrations of C-peptide affect high glucose-induced endothelial dysfunction by: (1) decreasing

*VCAM-1* expression and U-937 cell adherence to HAEC; (2) reducing secretion of IL-8 and MCP-1; and (3) suppressing NF- $\kappa$ B activation.

**Conclusions/interpretation** During hyperglycaemia, C-peptide directly affects *VCAM-1* expression and both MCP-1 and IL-8 HAEC secretion by reducing NF- $\kappa$ B activation. These effects suggest a physiological anti-inflammatory (and potentially anti-atherogenic) activity of C-peptide on endothelial cells.

**Keywords** Atherosclerosis · C-peptide · Cytokines · Endothelial cells · Inflammation · Monocytes · NF- $\kappa$ B · Nuclear factor  $\kappa$ B · Vascular smooth muscle cells

## Abbreviations

EBM-2	endothelial basal medium-2
HAEC	human aortic endothelial cells
I $\kappa$ B	inhibitor $\kappa$ B
MCP-1	monocyte chemoattractant protein-1
MFI	mean fluorescence intensity
NF- $\kappa$ B	nuclear factor- $\kappa$ B
PDTC	pyrrolidine dithiocarbamate
ROS	reactive oxygen species
VCAM-1	vascular cell adhesion molecule-1

**Electronic supplementary material** The online version of this article (doi:10.1007/s00125-008-1032-x) contains supplementary material, which is available to authorised users.

P. Luppi (✉) · V. Cifarelli · H. Tse · J. Piganelli · M. Trucco  
Division of Immunogenetics, Department of Pediatrics,  
Rangos Research Center, Children's Hospital of Pittsburgh,  
3460 Fifth Avenue,  
Pittsburgh, PA 15213, USA  
e-mail: luppi@pitt.edu

## Introduction

Diabetes is a well-established risk factor for vascular diseases. Vascular disease in diabetes originates from common functional and structural changes in the tunica media of small (microangiopathy) as well as large vessels (macroangiopathy). In large vessels, these changes increase the probability of developing atherosclerosis, which is one of the major



complications affecting diabetic patients. As a result of the diabetic state, the vascular compromise at small vessels level principally affects the eye, kidney and both peripheral and autonomic nerves, and this dysfunction contributes significantly to the morbidity associated with diabetes [1].

Diabetes causes vascular compromise secondary to endothelial dysfunction, measured by in vivo studies of flow-mediated vasodilation [2] and increased circulating levels of biochemical markers, such as, but clearly not limited to vascular cell adhesion molecule-1 (VCAM-1) [3, 4]. Generally, VCAM-1 is expressed at a low level on endothelial cells and is upregulated upon cellular activation, such as that observed after exposure to inflammatory stimuli or high glucose [5, 6]. VCAM-1 binds to the leucocyte integrin  $\alpha_4\beta_4$  (also called very late antigen-4; CD49d) and has a principal role in the early stages of monocytes adhesion to the vascular endothelium, one of the first steps in atherosclerosis plaque formation. A major hallmark of diabetes is an abnormally elevated blood glucose level, i.e. hyperglycaemia, which has been proposed as one factor causing endothelial dysfunction in diabetes. In endothelial cells, acute and chronic hyperglycaemia works through reactive oxygen species (ROS) production [5, 7, 8] that leads to activation of the transcription factor nuclear factor- $\kappa$ B (NF- $\kappa$ B) [5, 9, 10] and ultimately the production of inflammatory mediators [11].

In the unstimulated state, NF- $\kappa$ B exists in its canonical form as a heterodimer composed of p50 and p65 subunits bound to I $\kappa$ B. Upon activation, I $\kappa$ B is phosphorylated and degraded causing the release of p50/p65 components of NF- $\kappa$ B [12]. The active p50/p65 heterodimer translocates to the nucleus and initiates the transcription of a gamut of genes involved in the inflammatory response, such as those encoding pro-inflammatory cytokines, cell surface adhesion molecules and chemokines, including IL-8 and monocyte chemoattractant protein-1 (MCP-1) [5, 11, 13–15]. IL-8 and MCP-1 production is present in human atherosclerotic plaques [16] and participates in the development of atherosclerosis by recruiting monocytes into the subendothelial cell layer [17].

It has been suggested that proinsulin C-peptide may possess cytoprotective effects on the microvasculature during inflammatory events [18]. In line with this, it has been reported that type 1 diabetic patients with circulating levels of C-peptide closer to the physiological level of 0.5 nmol/l [19] or receiving whole pancreas [20] or allogeneic islet transplantation [21] show a reduced incidence of microvascular complications. The mechanisms able to produce the beneficial effects of C-peptide on vascular dysfunction in diabetes remain largely unknown. One study performed in vivo in a rat inflammatory model of vascular dysfunction showed that a single i.v. dose of C-peptide significantly inhibited leucocyte–endothelium interaction via decreased expression of endothelial cell adhesion molecules [22], a phenomenon

associated with release of nitric oxide [22, 23], which in turn has been shown to inhibit NF- $\kappa$ B [24]. Similar results were obtained in isolated ischaemic and reperfused rat hearts, where addition of C-peptide attenuated polymorphonuclear cell adherence to the vascular endothelium [25]. To date, no data are available on the effects of C-peptide on human endothelial cells exposed to the damaging insult of hyperglycaemia, a common condition in diabetes.

We therefore initiated a study on the direct effects of C-peptide, testing VCAM-1 expression on the cell surface, monocyte adherence and secretion of IL-8 and MCP-1 by human aortic endothelial cells (HAEC) exposed to short-term high glucose. Since activation of the transcription factor NF- $\kappa$ B is involved in these pro-inflammatory responses, we also investigated the direct effect of C-peptide on nuclear translocation of the NF- $\kappa$ B subunits p50/p65 in HAEC. We hypothesised that physiological concentrations of C-peptide protect HAEC from high glucose-induced cellular dysfunction by decreasing NF- $\kappa$ B activation, thus inhibiting NF- $\kappa$ B-dependent genes, such as those encoding VCAM-1, IL-8 and MCP-1.

## Methods

**Cell culture of HAEC** HAEC were obtained from Cambrex (Cambrex Bioscience Walkersville, Walkersville, MD, USA) and grown into 75 cm<sup>2</sup> culture flasks (250,000 per flask) (Corning, Corning, NY, USA) at 37°C, 5% CO<sub>2</sub> and in the presence of endothelial basal medium-2 (EBM-2) supplemented with endothelial growth media SingleQuots (Cambrex). HAEC were used at passages two to six.

**Treatment conditions** EBM-2 containing 25 mmol/l glucose (Sigma Chemical, St Louis, MO, USA) was used as a high glucose condition in all the experiments, while regular EBM-2, which contains 5.6 mmol/l glucose, was used as normal glucose condition. In all experiments, HAEC were used when having reached an 80% to 90% confluency. On the day of the experiment, cells were washed with fresh EBM-2 and then replaced with EBM-2 containing 25 mmol/l glucose in the presence or absence of physiological concentrations of human C-peptide (0.5 and/or 1 nmol/l) (Sigma Chemical) [26] for 4 to 24 h in an incubator at 37°C and 5% CO<sub>2</sub>. As a control for C-peptide activity, C-peptide was heat-inactivated by boiling it for 1 h and then added to the culture. Human recombinant TNF- $\alpha$  (10 ng/ml; R&D Systems, Minneapolis, MN, USA), which activates HAEC, was used as a positive control. The effect of the NF- $\kappa$ B inhibitor pyrrolidine dithiocarbamate (PDTC; 10  $\mu$ mol/l; Sigma) was also tested on HAEC in certain experiments. This inhibitor was added to EBM-2 with 25 mmol/l glucose. Separate sets of experiments were performed in which



C-peptide was added to regular EBM-2 containing 5.6 mmol/l glucose.

**VCAM-1 detection by RT-PCR** HAEC were grown into 75 cm<sup>2</sup> culture flasks (250,000 per flask; Corning) and exposed to the treatment conditions mentioned above. After 4 and 24 h, cells were trypsinised and frozen at −80°C. RNA extraction was performed using the RiboPure-Blood kit (Ambion, Austin, TX, USA). For RT-PCR, 1 µg RNA was used together with Oligo(d)T (RETROscript; Ambion) and 1 µl of cDNA was used to amplify *VCAM-1*. Human *GAPDH*, 18S ribosomal RNA and  $\beta$ -actin were amplified and served as internal controls [5]. Sequences of the oligonucleotides used to amplify these genes and PCR conditions are reported as [Electronic supplementary material \(ESM\)](#). Three independent experiments were performed. Densitometry was performed with UN-SCAN-IT gel software (Silk Scientific, Orem, UT, USA). Data are expressed as median±SD.

**Quantification of VCAM-1 by flow cytometry** HAEC (50,000 per well) were maintained in 6-well plates (Corning) until confluent. On the day of the experiment, cells were exposed to the treatment conditions mentioned above for 24 h. Determination of VCAM-1 expression by surface staining was performed on paraformaldehyde-fixed HAEC monolayers following a methodology shown to preserve single cell integrity [27]. A phycoerythrin-conjugated anti-human monoclonal antibody to CD106 (VCAM-1) or corresponding isotype control (BD Pharmingen, San Diego, CA, USA) were used for staining. Cells were run on a Becton Dickinson FACSCalibur and analysed at a later time (Becton Dickinson, San Jose, CA, USA). For a more detailed description of methodology and data analysis, see [ESM](#). Three sets of independent experiments were performed. Within each experiment, each condition was tested in triplicate. Data are expressed as median±SD.

**Monocyte adhesion assay** HAEC were grown on 48-well plates (12,000 per well; Corning) and exposed to the treatment conditions mentioned above for 4 h. Human monocytic U-937 cells were purchased from the American Type Culture Collection (Rockville, MD, USA) and grown in RPMI 1640 (Cambrex) containing 10% FCS, 100 µl/ml streptomycin, 100 IU/ml penicillin, 250 ng/ml fungizone, 1 mmol/l sodium pyruvate, 10 mmol/l HEPES (all from Gibco Invitrogen, Carlsbad, CA, USA) at 37°C and 5% of CO<sub>2</sub>. On the day of the experiment, medium was removed from each well, cells were washed with PBS and fresh medium containing U-937 cells (1×10<sup>6</sup> cells/ml, 500 µl) was added to each well and incubated for 1 h at room temperature on a rocking plate. Non-adherent U-937 cells were removed and adherent cells fixed in 1% glutaraldehyde.

The number of adherent cells was evaluated by counting three random 40× fields per well by a blinded investigator, avoiding areas of non-confluence and cell clusters. Three experiments were performed. Within each experiment, each condition was tested in triplicate. Results are showed as median±SD.

**IL-8 and MCP-1 detection in culture supernatant fraction by ELISA** HAEC were maintained in 6-well plates (50,000 per well; Corning) in EBM-2 (Cambrex). On the day of the experiment, cells were exposed to the treatment conditions mentioned above for 4 h. The supernatant fraction was collected and kept at −20°C until tested by ELISA (Quantikine; R&D Systems). Three independent experiments were performed, in which each condition was tested in triplicate. Concentration of the chemokines (pg/ml) was assessed by calculating values according to the values obtained in the standard curve. Results from three separate experiments are shown as median±SD.

**NF-κB analysis assays** HAEC were cultured in 75 cm<sup>2</sup> culture flasks (250,000 per flask; Corning) and exposed to the treatment conditions as indicated above. Cells were collected at 4 and 24 h and pretreated with 25 µl of protease inhibitor cocktail (Pierce, Rockford, IL, USA). Nuclear and cytoplasmic fractions were separated using a kit (NE-PER Nuclear and Cytoplasmic Extraction; Pierce). Protein content of the extract was measured using a bicinchoninic acid assay kit (Pierce Biotechnology). For detection of NF-κB p65 subunit by western blot, 10 µg of nuclear protein extracts were used as previously described [28]. Densitometry analysis of the bands was performed with UN-SCAN-IT gel software (Silk Scientific). Activation of the NF-κB p50 subunit was detected on 3 µg of nuclear protein extracts using a kit (EZ-Detect Transcription Factor Kit; Pierce Technology). For each set of data, a minimum of three experiments was performed. Data were averaged and expressed as means±SD.

**Statistics** Paired *t* test (two-tailed) was used to analyse differences between 5.6 and 25 mmol/l glucose. ANOVA with the Dunnett's post hoc test was used to assess differences between 25 mmol/l glucose, C-peptide and PDTC using GraphPad Prism 4 (GraphPad Software, San Diego, CA, USA). Values of *p*<0.05 were considered to be statistically significant.

## Results

**C-peptide reduces VCAM-1 on HAEC exposed to high glucose** In order to determine the effect of C-peptide on high glucose-stimulated VCAM-1 levels on HAEC, cells

were treated in vitro for 24 h with 25 mmol/l glucose alone or in the presence of C-peptide. High glucose increased *VCAM-1* mRNA expression compared with cells cultured in low glucose (Fig. 1a,b;  $p=0.008$ ). C-peptide added to the high glucose medium inhibited *VCAM-1* mRNA expression as compared with high glucose medium alone (Fig. 1a,b). Although both concentrations of C-peptide (0.5 and 1 nmol/l) decreased *VCAM-1* mRNA expression, statistical significance was reached with 0.5 nmol/l C-peptide only ( $p<0.05$ ). Heat-inactivated C-peptide, used as control, did not have a significant effect on *VCAM-1* expression (Fig. 1b). As expected, the cytokine TNF- $\alpha$  induced a dramatic upregulation of *VCAM-1* expression with a threefold increase in comparison to normal glucose (Fig. 1a,b). The inhibitory effect of C-peptide on high glucose-induced stimulation of *VCAM-1* mRNA in HAEC was observed as early as 4 h incubation (Fig. 2).

We obtained similar data by analysing VCAM-1 expression on HAEC by flow cytometry. High glucose significantly ( $p=0.03$ ) changed VCAM-1 levels (average mean fluorescence intensity [MFI]  $117.5\pm 25.5$  SD) compared with cells

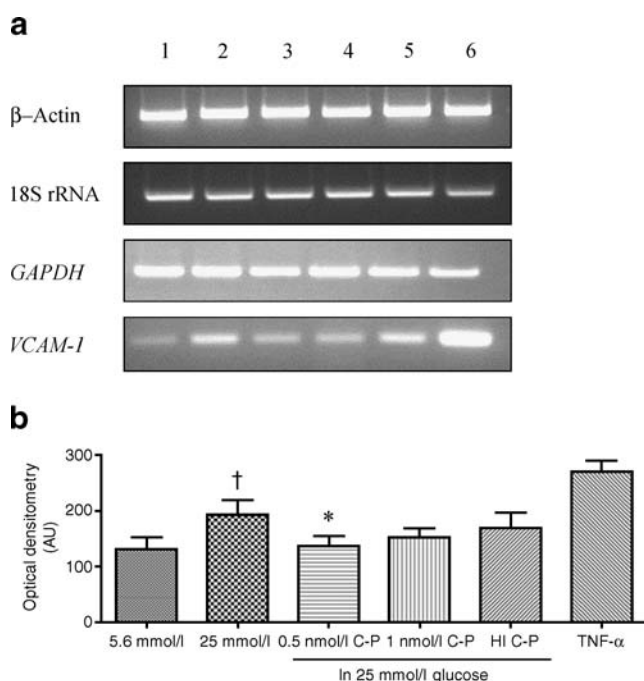


**Fig. 1** C-peptide decreases high glucose-stimulated VCAM-1 mRNA after 24 h. **a** RT-PCR was used to detect VCAM-1 mRNA in HAEC treated for 24 h with: (1) low glucose (5.6 mmol/l; LG); (2) high glucose (25 mmol/l; HG); (3) HG+0.5 nmol/l C-peptide (C-P); (4) HG+1 nmol/l C-P; (5) HG+1 nmol/l heat-inactivated (HI) C-P; (6) LG+TNF- $\alpha$  10 ng/ml). GAPDH, 18S rRNA and  $\beta$ -actin were used as internal controls. **b** Densitometric analysis of *VCAM-1* mRNA expression. Boxplot graphs showing the median values (limits of the lines are the 5th and 95th centiles of arbitrary units [AU]) of *VCAM-1* mRNA in HAEC ( $n=3$  independent experiments). C-peptide decreased high glucose-induced *VCAM-1* mRNA expression compared with high glucose alone.  $^*p<0.05$ ,  $^{\dagger}p=0.008$  vs 5.6 mmol/l

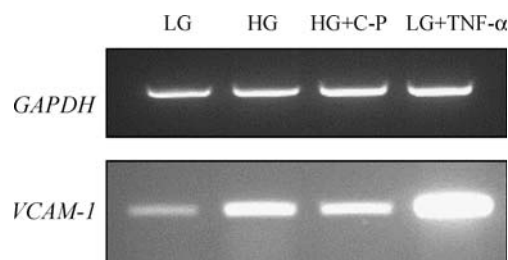


**Fig. 2** C-peptide decreases high glucose-stimulated VCAM-1 mRNA after 4 h. Representative example of RT-PCR to detect VCAM-1 mRNA expression in HAEC treated for 4 h with: (1) low glucose (LG; 5.6 mmol/l glucose); (2) high glucose (HG; 25 mmol/l glucose); (3) HG+0.5 nmol/l C-peptide (C-P); (4) LG+TNF- $\alpha$  00 ng/ml). C-peptide reduced high glucose-stimulated *VCAM-1* mRNA in HAEC. GAPDH was used as an internal control

in 5.6 mmol/l glucose (average MFI  $85.3\pm 2.4$  SD) (Fig. 3a). When C-peptide was added to the 25 mmol/l glucose, the cell surface expression of VCAM-1 decreased (Fig. 3a). Statistical significance was reached with a C-peptide concentration of 0.5 nmol/l (average MFI  $80.5\pm 5.5$  vs  $117.5\pm 25.5$  in 25 mmol/l glucose alone;  $p<0.01$ ). The cytokine TNF- $\alpha$  stimulated VCAM-1 expression (average MFI  $305.3\pm 115.5$  SD) while heat-inactivated C-peptide did not have a significant effect on VCAM-1 (average MFI  $118.8\pm 23.2$  SD).

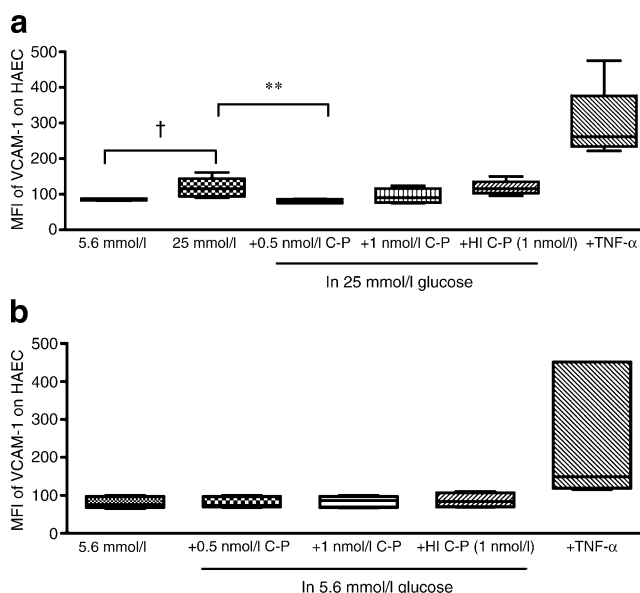


**Fig. 3** C-peptide reduces high glucose-stimulated VCAM-1 protein expression on HAEC. Boxplot graphs showing the median values (limits of the lines are the 5th and 95th centiles) of MFI of VCAM-1 expression in HAEC exposed to **a** 25 mmol/l glucose or **b** 5.6 mmol/l glucose with and without C-peptide (C-P) for 4 h as determined by flow cytometry ( $n=3$  independent experiments). **a** HAEC exposed to 25 mmol/l glucose significantly increased VCAM-1 expression;  $^{\dagger}p=0.03$  vs 5.6 mmol/l. This increase was significantly inhibited by 0.5 nmol/l C-peptide;  $^{**}p<0.01$ . No significant changes in VCAM-1 were observed when C-peptide was added to basal medium containing 5.6 mmol/l glucose (**b**). HI, heat-inactivated

When C-peptide was added to low glucose medium, it did not cause a significant change in VCAM-1 expression (Fig. 3b).

Because C-peptide at a dose of 0.5 nmol/l demonstrated a significant reduction in high glucose-induced VCAM-1 expression, we conducted all further experiments using this dose only.

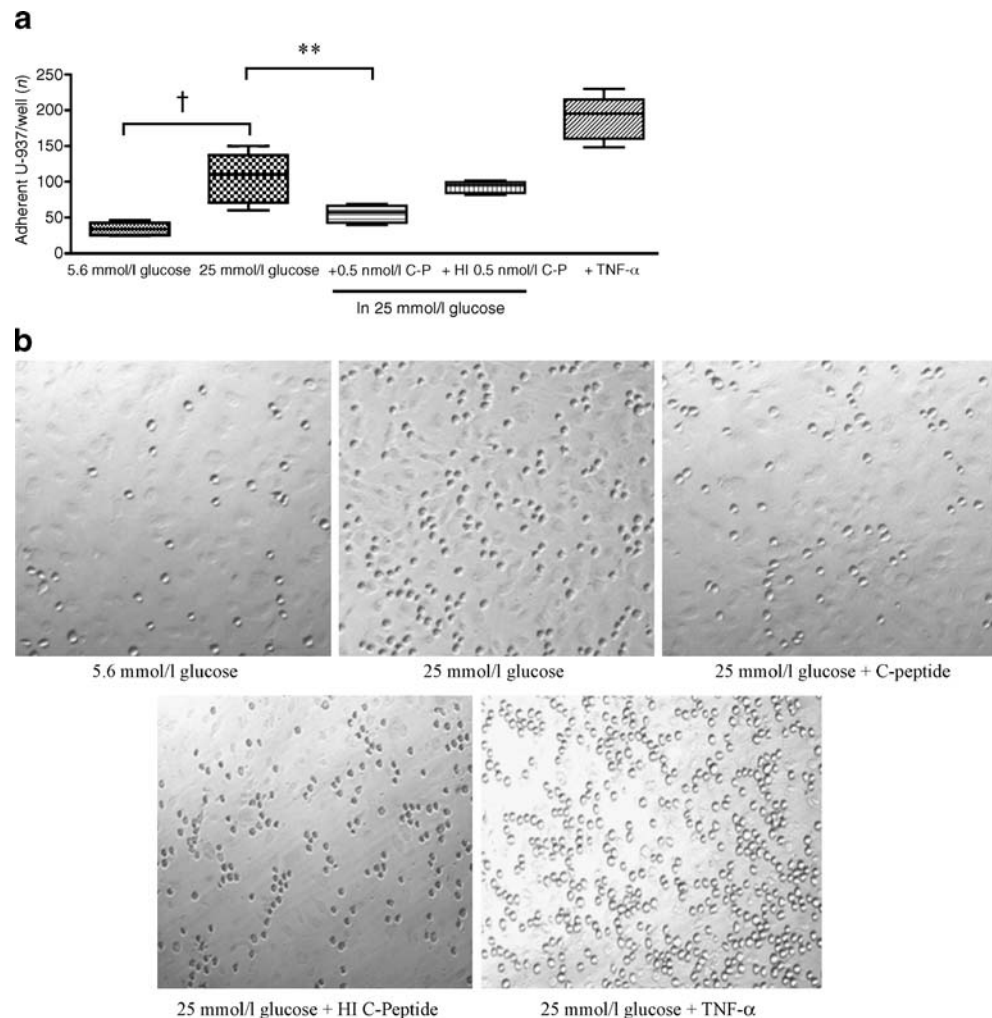
**C-peptide inhibits U-937 cells adhesion to endothelial cells** To determine whether the C-peptide-induced inhibition of VCAM-1 expression on HAEC was associated with a decrease in U-937 adherence, we assessed U-937 adhesion on HAEC exposed to C-peptide under high glucose conditions. There was a threefold increase in the number of adherent U-937 under high glucose ( $106 \pm 32$ ) as compared with 5.6 mmol/l glucose ( $34 \pm 8$ ;  $p=0.004$ ) (Fig. 4a). When C-peptide was added to the high glucose medium, the number of adherent U-937 cells was reduced ( $56 \pm 11$ ;  $p<0.01$  vs 25 mmol/l glucose; Fig. 4a). Addition of heat-inactivated C-peptide did not significantly alter the number of adherent

cells ( $93 \pm 5$ ) as compared with 25 mmol/l glucose alone. As expected, TNF- $\alpha$ , which activates endothelial cells, produced a fivefold increase in U-937 adherence in comparison with HAEC exposed to normal glucose (Fig. 4a). The adhesion of U-937 to HAEC under the different conditions was also photographed (Fig. 4b).

When we evaluated the adherence of U-937 to HAEC exposed to normal glucose and with C-peptide added, we did not observe a significant change as compared with normal glucose alone (ESM Fig. 1).

**C-peptide inhibits IL-8 and MCP-1 secretion by HAEC** Another factor possibly affecting U-937 adherence to HAEC in the presence of C-peptide is a downregulation of secreted chemoattractant molecules by endothelial cells. As expected, we found that secretion of IL-8 in the supernatant fraction of high glucose-stimulated HAEC significantly increased ( $751 \pm 99$  pg/ml) as compared with normal glucose ( $592 \pm 120$  pg/ml;  $p=0.04$ ; Fig. 5a), while addition of C-peptide reduced IL-8 concentrations to levels equivalent to normal

**Fig. 4** C-peptide reduces adhesion of U-937 to HAEC in condition of hyperglycaemia. HAEC were cultured in 25 mmol/l glucose in the presence or absence of 0.5 nmol/l of C-peptide (C-P) for 4 h. U-937 were added for 1 h and then counted. **a** Boxplot graphs showing the median values (limits of the lines are 5th and 95th centiles) of number of adherent U-937 per well ( $n=3$  sets of independent experiments). High glucose increased the number of adherent U-937;  $^{\dagger}p=0.004$  vs 5.6 mmol/l glucose. Addition of C-peptide reduced the number of adherent U-937;  $**p<0.01$  vs 25 mmol/l glucose alone. Heat-inactivated (HI) C-peptide (0.5 nmol/l) did not significantly alter adherence of U-937. TNF- $\alpha$  (10 ng/ml) produced more than a fivefold increase in adherent U-937 in comparison to normal glucose. **b** Photographic view of U-937 adherent to HAEC





glucose ( $p<0.05$ ; Fig. 5b). The heat-inactivated C-peptide control had no significant effect (Fig. 5b). The high glucose-induced IL-8 secretion by HAEC was mediated by NF- $\kappa$ B activation since treatment with PDTC (10  $\mu$ mol/l), an NF- $\kappa$ B inhibitor, reduced IL-8 secretion to basal levels also detected in normal glucose ( $p<0.01$  vs 25 mmol/l glucose; Fig. 5b).

Similarly, when HAEC were stimulated with high glucose for 4 h, secretion of MCP-1 increased ( $472\pm 89$  pg/ml) as compared with normal glucose ( $329\pm 152$  pg/ml;  $p=0.01$ ; Fig. 6a). Addition of C-peptide, decreased MCP-1 concentrations to those found with normal glucose levels ( $p<0.05$ ; Fig. 6b). Here, too, the specific-NF- $\kappa$ B inhibitor PDTC ( $\mu$ mol/l) decreased MCP-1 levels dramatically ( $p<0.01$  vs 25 mmol/l glucose; Fig. 6b).

C-peptide added to regular medium containing low glucose failed to significantly modify IL-8 and MCP-1 secretion compared with basal medium without C-peptide (ESM Fig. 2).

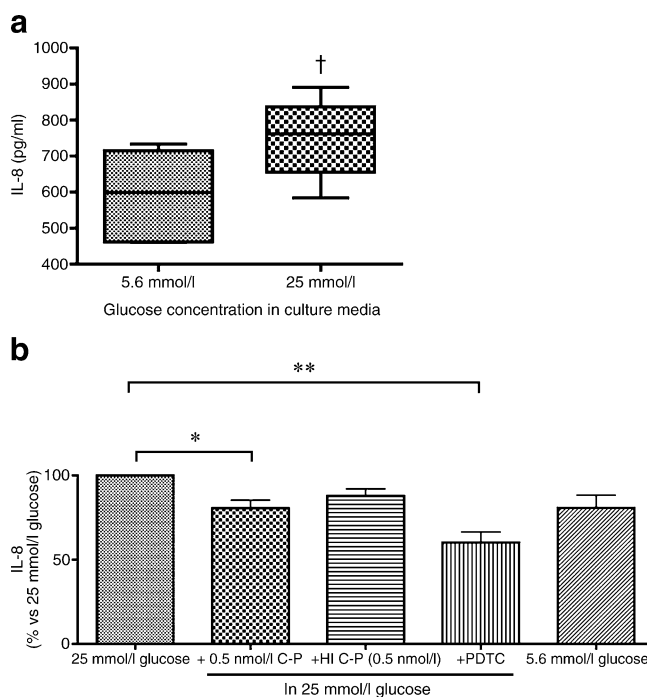


**Fig. 5** C-peptide decreases high glucose-stimulated IL-8 secretion by HAEC. HAEC were cultured with high glucose (HG; 25 mmol/l) alone or combined with C-peptide (C-P; 0.5 nmol/l) for 4 h and secretion of IL-8 in the supernatant fraction was assessed by ELISA. **a** Boxplot graph showing the median values (limits of the lines are 5th and 95th centiles) of secreted IL-8 in the supernatant fraction of HAEC exposed to HG compared with low glucose (5.6 mmol/l);  $\dagger p=0.04$ . **b** Levels of IL-8 in supernatant fraction of C-peptide-treated HAEC expressed as per cent versus the appropriate control at 25 mmol/l. HAEC treated with high glucose+C-peptide showed a decrease in secreted IL-8, approaching levels measured in low glucose;  $*p<0.05$  vs high glucose. A significant decrease in secreted IL-8 was also found in the presence of the NF- $\kappa$ B inhibitor PDTC (10  $\mu$ mol/l);  $**p<0.01$ . The average $\pm$ SD of a set of three independent experiments run in triplicate are shown. HI, heat-inactivated

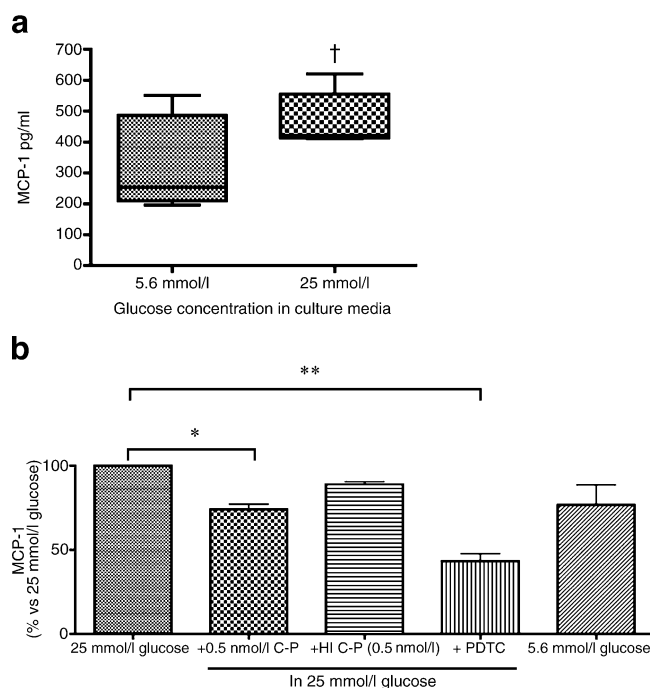


**Fig. 6** C-peptide decreases high glucose-stimulated MCP-1 secretion by HAEC. HAEC were cultured with high glucose (HG; 25 mmol/l) alone (**a**) or combined (**b**) with C-peptide (C-P; 0.5 nmol/l) for 4 h and secretion of MCP-1 in the supernatant fraction was assessed by ELISA. **a** Boxplot graph showing the median values (limits of the lines are 5th and 95th centiles) of secreted MCP-1 in the supernatant fraction of HAEC exposed to HG compared with low glucose (5.6 mmol/l);  $\dagger p=0.04$ . **b** Levels of MCP-1 in supernatant fraction of C-peptide-treated HAEC expressed as per cent versus the appropriate control at 25 mmol/l. When cells were treated with HG+C-peptide the secretion of MCP-1 decreased;  $*p<0.05$  vs HG. A dramatic decrease in MCP-1 secretion was obtained with the NF- $\kappa$ B inhibitor PDTC (10  $\mu$ mol/l);  $**p<0.01$ . The average $\pm$ SD of a set of three independent experiments run in triplicate are shown. HI, heat-inactivated

*C-peptide decreases high glucose-induced NF- $\kappa$ B translocation in HAEC* The signal transduction pathway leading to mRNA synthesis of adhesion molecules and chemokines involves activation of NF- $\kappa$ B. To determine whether C-peptide affected high glucose-induced NF- $\kappa$ B nuclear translocation in HAEC, immunoblot analysis and NF- $\kappa$ B-specific ELISAs were performed with nuclear extracts from stimulated-HAEC. As shown in Fig. 7a, exposure of HAEC to 25 mmol/l for 4 h induced an increase in NF- $\kappa$ B nuclear translocation in comparison to 5.6 mmol/l glucose. A twofold increase in NF- $\kappa$ B p65 activation was found after 24 h incubation with 25 mmol/l glucose ( $p=0.03$  vs 5.6 mmol/l; Fig. 7a). Addition of C-peptide to high glucose decreased NF- $\kappa$ B p65 nuclear translocation to that found with normal glucose levels, while heat-inactivated C-peptide did not suppress NF- $\kappa$ B activity (Fig. 7a). Densitometric analysis of this NF- $\kappa$ B p65 immunoblot demonstrated that C-peptide reduced NF- $\kappa$ B p65 nuclear translocation by twofold as compared with high glucose alone ( $p<0.05$ ; Fig. 7c).

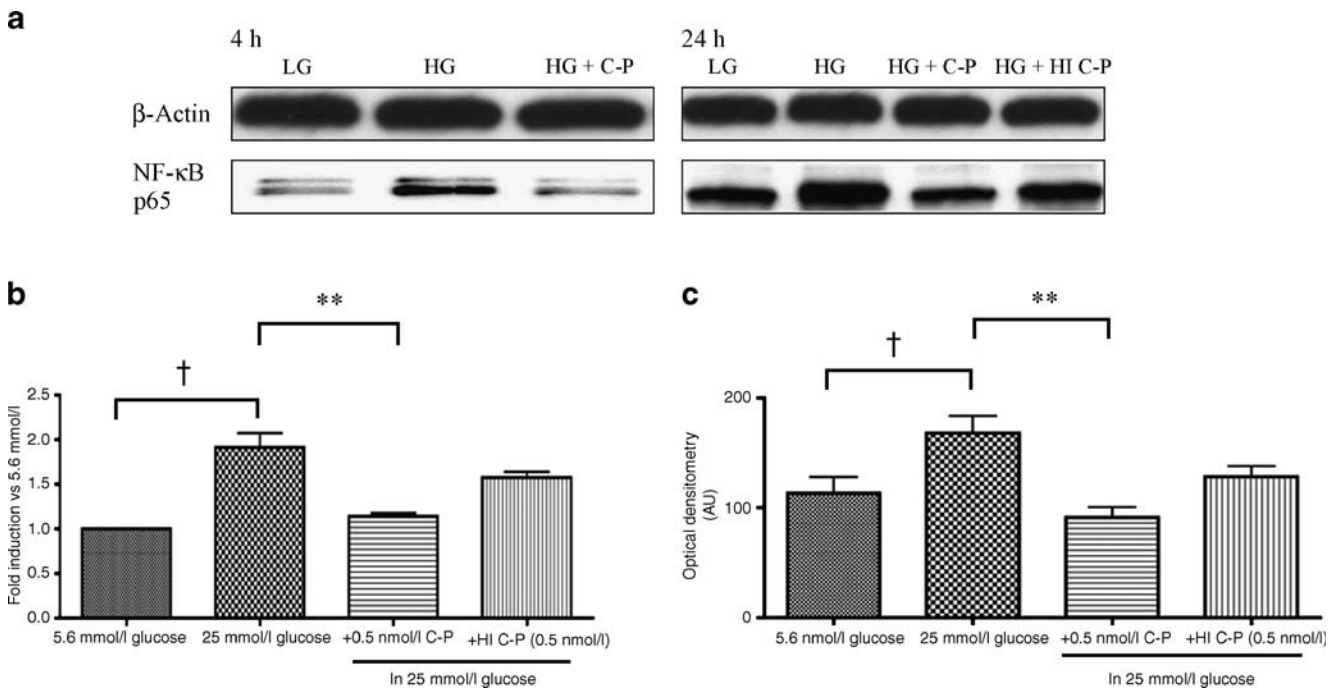


**Fig. 7** C-peptide reduces levels of NF- $\kappa$ B p65/p50 in HAEC cultured in high glucose. HAEC were cultured in low glucose (LG; 5.6 mmol/l) or high glucose (HG; 25 mmol/l) in the presence or absence of 0.5 nmol/l C-peptide (C-P) for 4 and 24 h. Cellular nuclear extracts were subjected to **a** Western immunoblotting to detect the 65 kDa band of the p65 subunit after 4 and 24 h. **b** Detection of the NF- $\kappa$ B p50 binding activity by ELISA after 24 h. Results are expressed as fold induction of NF- $\kappa$ B p50 activity in respect to 5.6 mmol/l glucose. In cells exposed to HG there was a twofold increase in NF- $\kappa$ B p50 nuclear translocation compared with cells in LG;  $^{\dagger}p=0.002$ . A

decrease in NF- $\kappa$ B p50 nuclear translocation was observed in the presence of 0.5 nmol/l C-peptide (C-P);  $^{**}p<0.01$  vs HG alone. **c** Bar graph showing the densitometric quantification in arbitrary units (AU) of the bands at 24 h. In cells exposed to HG there was a twofold increase in NF- $\kappa$ B p65 nuclear translocation compared with cells in LG;  $^{\dagger}p=0.03$ . A decrease in p65 nuclear translocation was observed in the presence of 0.5 nmol/l C-P;  $^{*}p<0.05$  vs HG alone. Results are expressed as means $\pm$ SD ( $n=3$ ). Heat-inactivated (HI) C-peptide was used as a control for C-peptide activity in all the experiments

Activation of the NF- $\kappa$ B p50 subunit in glucose-stimulated HAEC was assessed by ELISA. As shown in Fig. 7b, high glucose significantly induced NF- $\kappa$ B p50 activity in contrast to normal glucose ( $p=0.002$ ). High glucose-induced NF- $\kappa$ B p50 binding activity was efficiently ablated by the addition of C-peptide ( $p<0.01$ ).

## Discussion

Type 1 diabetes patients have an increased risk of developing atherosclerosis and microvascular complications compared with the non-diabetic population. This risk is in part associated with the difficulty in maintaining euglycaemic conditions even in the context of an appropriate exogenous insulin treatment [29]. Recombinant insulin does not contain C-peptide, a product of insulin protein biosynthesis that exerts beneficial effects on some of the microvascular complications associated with diabetes [30–32].

In this study, we investigated the impact of human C-peptide specifically in the early process of atherogenesis. The few studies available on the topic have tested the effect of C-peptide on low and high glucose-induced proliferative

activities of vascular smooth muscle cells, one major component involved in the formation of atherosclerotic plaque [33, 34]. Here, we wanted to expand upon these studies by evaluating the potential effects of C-peptide on the endothelial cell component of the vessel wall during hyperglycaemia.

The adhesion and migration of circulating monocytes into the subendothelial space is one of the key events in the early stages of atherogenesis [35]. This process is in part regulated by the expression of adhesion molecules, such as VCAM-1, on the surface of endothelial cells [36], and by the release of chemotactic factors, including IL-8 and MCP-1 [17]. We found that in vitro C-peptide exerts an inhibitory effect on high glucose-induced upregulation of the adhesion molecule VCAM-1 on HAEC. C-peptide at the physiological concentration of 0.5 nmol/l reduced high glucose-induced expression of VCAM-1 to basal levels observed under normal glucose conditions. This effect was observed as early as 4 h after C-peptide addition to the high glucose medium and was still detected after 24 h incubation. The decrease in high glucose-induced VCAM-1 expression by C-peptide on HAEC was detected both at the mRNA and protein level. Conversely, when C-peptide was added to the



medium containing normal glucose levels, it failed to significantly reduce VCAM-1 expression. These results are in line with findings from another group demonstrating that C-peptide reduced expression of the adhesion molecules P-selectin and intercellular adhesion molecule-1 on the rat microvascular endothelium during acute endothelial dysfunction *in vivo* [22]. In another model of vascular injury, C-peptide was shown to decrease polymorphonuclear leucocyte infiltration into the myocardium thereby improving cardiac dysfunction [25]. Overall, these data seem to point to an anti-inflammatory effect of C-peptide on the endothelium, especially in conditions of insult. This hypothesis is supported by recent *in vivo* data showing that survival rates of mice following endotoxic shock is improved after C-peptide administration [37]. In these mice, plasma levels of the pro-inflammatory cytokines TNF- $\alpha$  and MCP-1 were also decreased, suggesting a decreased generalised inflammatory response [37]. In the context of type 1 diabetes patients, upregulation of endothelial VCAM-1 and inflammation are early events in the course of the disease [2, 38–40]. These patients are insulin-dependent and take exogenous insulin to manage their blood glucose levels. It might well be that addition of physiological levels of C-peptide to the traditional exogenous insulin therapy could be a means of ‘counteracting’ the insult of high glucose on the endothelial cells of diabetic patients.

Another component of endothelial dysfunction affected by C-peptide is the secretion of IL-8 and MCP-1, chemokines that facilitate leucocyte-endothelial interactions. In support of other investigators [5, 6, 16], we observed an increased secretion of both chemokines in the supernatant fraction of endothelial cells under high glucose. Unique to this study, however, is the finding that C-peptide reduced high glucose-stimulated IL-8 and MCP-1 secretion by endothelial cells to near or below the basal levels measured under normal glucose concentrations. Based on our findings, it seems that C-peptide might exert its most meaningful biological effects on the endothelium in conditions of insult, as C-peptide did not significantly change chemokine secretion by HAEC when added to normal glucose-containing medium. In addition, adhesion of U-937 cells to high glucose-stimulated HAEC decreased after addition of C-peptide, an effect not detected when C-peptide was heat-inactivated. C-peptide at 0.5 nmol/l suppressed U-937 attachment to HAEC exposed to 25 mmol/l glucose by 50% due to a C-peptide-mediated inhibitory effect on VCAM-1, IL-8 and MCP-1 secretion by endothelial cells. Although in this study we focused on the effects of C-peptide on high glucose-induced endothelial dysfunction, another likely cellular target of C-peptide action in diabetes could be the immune cells. Previous studies from our laboratory [41] and others [42] have shown that phenotypic changes suggestive of cellular activation are present in circulating

monocytes of recently diagnosed type 1 diabetes patients. It is tempting to speculate that in conditions of hyperglycaemia and the underlying inflammation typical of diabetes, C-peptide might exert beneficial effects on both endothelial and immune cell dysfunction, thereby decreasing the overall risk of developing vascular lesions. The biological effect of C-peptide on immune cells is currently under investigation in our laboratory.

The mechanisms underlying the effects of C-peptide on the human vasculature, specifically on endothelial cells, are still largely unknown. Nevertheless, the signal transduction pathways that lead to the enhanced expression of genes encoding adhesion molecules and inflammatory cytokine secretion in endothelial cells require translocation of the transcription factor NF- $\kappa$ B [13]. Therefore, this study investigated C-peptide effects on NF- $\kappa$ B activation in high glucose-stimulated HAEC. In support of a previous study [5], we confirm that short-term high glucose exposure of endothelial cells stimulates NF- $\kappa$ B activation. However, our work has moved the paradigm forward by demonstrating that exogenous addition of C-peptide significantly reduced high glucose-induced nuclear translocation of canonical components of NF- $\kappa$ B, p65 and p50. The suppressive effect on NF- $\kappa$ B activation and high glucose-induced VCAM-1 expression as well as IL-8 and MCP-1 secretion in HAEC was specific for C-peptide, since heat-inactivated C-peptide was not able to elicit the same phenotype. Although we did not investigate the precise mechanism of action of C-peptide on the inhibition of NF- $\kappa$ B nuclear translocation in HAEC, evidence of cellular internalisation and binding to intracellular components has been recently demonstrated in Swiss 3 T3 and HEK-293 cells [43]. In the same study, interestingly, C-peptide was also shown to localise within the nuclei [43]. We can therefore speculate that the inhibitory action of C-peptide on NF- $\kappa$ B activation in HAEC could result from an effect on the phosphorylation of protein substrates in the cytoplasm and/or of a direct interaction of C-peptide with NF- $\kappa$ B p65/p50 subunits at the nuclear level, preventing DNA binding. In the lung of endotoxin-treated mice, C-peptide inhibited phosphorylation of extracellular signal-regulated kinase-1/2 followed by upregulation of nuclear levels and DNA binding of the nuclear transcription factor peroxisome proliferator-activated receptor- $\gamma$ , which plays an important role in the modulation of inflammation [37]. Currently, we are exploring which NF- $\kappa$ B-dependent upstream signalling events are affected by C-peptide in endothelial cells; examples are ROS generation and I $\kappa$ B kinase, an enzyme that elicits phosphorylation of the cytosolic NF- $\kappa$ B inhibitor I $\kappa$ B $\alpha$ . This latter upstream event regulates NF- $\kappa$ B translocation from the cytoplasm to the nucleus. In vascular smooth muscle cells we found that C-peptide reduced high glucose-induced phosphorylation of I $\kappa$ B $\alpha$  [44], a pathway likely to be also targeted in HAEC.

Inhibition of NF- $\kappa$ B would be suggestive of an anti-inflammatory effect of physiological concentrations of C-peptide at the endothelial cell level [19, 22] and would be consistent with a potential anti-atherosclerotic effect in type 1 diabetes. Higher supra-physiological levels of circulating C-peptide, such as those measured in type 2 diabetic patients with the hyperinsulinaemia associated with insulin resistance, might have deleterious effects on the vasculature. This view is supported by Walcher et al. [45], who found that higher concentrations of C-peptide, mimicking those found in the circulation of type 2 diabetic patients, produced maximal stimulation of lymphocyte chemotaxis in vitro. Future studies are required to further elucidate these issues.

Although this evidence in human endothelial cells is reported here for the first time, a protective effect of C-peptide on high glucose-induced vascular dysfunction has been invoked by other groups, who tested the efficacy of C-peptide in small clinical trials of type 1 diabetic patients [30–32, 46]. In addition to endothelial cells, vascular smooth muscle cells also appear to be the target of beneficial effects of C-peptide on the vasculature in conditions of hyperglycaemia [33, 44]. Physiological concentrations of C-peptide attenuate glucose-induced hyperproliferation of vascular smooth muscle cells [33, 44], a phenomenon associated, at least in part, with a specific inhibitory effect on NF- $\kappa$ B [44].

In conclusion, our findings support the hypothesis that C-peptide has major physiological effects on the inhibition of endothelial dysfunction under high glucose conditions. It does this by interfering with NF- $\kappa$ B activation and its effect on the reduced production of pro-inflammatory cytokines and chemokines. These findings underscore a role of C-peptide in endothelial cell functions, especially in conditions of diabetic insult to the vasculature. Our results support the idea of prolonged administration of physiological quantities of C-peptide to type 1 diabetes patients in an effort to lessen endothelial dysfunction and complications that may potentially arise during the course of the disease.

**Acknowledgements** This study was supported by the Henry Hillman Endowment Chair in Pediatric Immunology (to M. Trucco) and by grants DK 024021-24 from the National Institute of Health and NIH 5K12 DK063704 (to P. Luppi and M. Trucco) and W81XWH-06-1-0317 from the Department of Defense (M. Trucco)

**Duality of interest** The authors declare that there is no duality of interest associated with this manuscript.

## References

1. Zatz R, Brenner BM (1986) Pathogenesis of diabetic microangiopathy: The hemodynamic view. *Am J Med* 80:443–453
2. Jarvisalo MJ, Raitakari M, Toikka JO et al (2004) Endothelial dysfunction and increased arterial intima-media thickness in children with type 1 diabetes. *Circulation* 109:1750–1755
3. Schmidt AM, Crandall J, Hori O, Cao R, Lakatta E (1996) Elevated plasma levels of vascular cell adhesion molecule-1 (VCAM-1) in diabetic patients with microalbuminuria: a marker of vascular dysfunction and progressive vascular disease. *Br J Hematol* 92:747–750
4. Jude EB, Douglas JT, Anderson SG, Young MJ, Boulton AJ (2002) Circulating cellular adhesion molecules ICAM-1, VCAM-1, P- and E-selectin in the prediction of cardiovascular disease in diabetes mellitus. *Eur J Intern Med* 13:185–189
5. Piga R, Naito Y, Kokura O, Yoshikawa T (2007) Short-term high glucose exposure induces monocyte-endothelial cells adhesion and transmigration by increasing VCAM-1 and MCP-1 expression in human aortic endothelial cells. *Atherosclerosis* 193:328–334
6. Haubner F, Lehle K, Munzel D, Schmid C, Bimbaum D, Preuner JG (2007) Hyperglycemia increases the levels of vascular cellular adhesion molecule-1 and monocyte-chemoattractant-protein-1 in the diabetic endothelial cell. *Biochem Bioph Res Commun* 360:560–565
7. Inoguchi T, Li P, Umeda F et al (2000) High glucose level and free fatty acid stimulate reactive oxygen species production through protein kinase C-dependent activation of NAD(P)H oxidase in cultured vascular cells. *Diabetes* 49:1939–1945
8. Yano M, Hasegawa G, Ishii M et al (2004) Short-term exposure of high glucose concentration induces generation of reactive oxygen species in endothelial cells: implication for the oxidative stress associated with postprandial hyperglycemia. *Redox Rep* 9:111–116
9. Janssen-Heininger YM, Poynter ME, Baeuerle PA (2000) Recent advances towards understanding redox mechanisms in the activation of nuclear factor kappaB. *Free Radic Biol Med* 28:1317–1327
10. Nishikawa T, Edelstein D, Dux XL et al (2000) Normalizing mitochondrial superoxide production blocks three pathways of hyperglycaemic damage. *Nature* 404:787–790
11. Soares MP, Muniappan A, Kaczmarek E et al (1998) Adenovirus-mediated expression of a dominant negative mutant of p65/RelA inhibits proinflammatory gene expression in endothelial cells without sensitizing for apoptosis. *J Immunol* 161:4572–4582
12. Viatour P, Merville MP, Bours V, Chariot A (2005) Phosphorylation of NF-kappaB and IkappaB proteins: implications in cancer and inflammation. *Trends Biochem Sci* 30:43–52
13. Tak PP, Firestein GS (2001) NF-kB: a key role in inflammatory diseases. *J Clin Invest* 107:7–11
14. Harada C, Okumura A, Namekata K et al (2006) Role of monocyte chemotactic protein-1 and nuclear factor kappa B in the pathogenesis of proliferative diabetic retinopathy. *Diabetes Res Clin Practice* 74:249–256
15. Srinivasan S, Yeh M, Danzinger EC et al (2003) Glucose regulates monocyte adhesion through endothelial production of interleukin-8. *Cir Res* 92:371–377
16. Wilcox JN, Nelken NA, Coughlin SR, Gordon D, Schall TJ (1994) Local expression of inflammatory cytokines in human atherosclerotic plaques. *J Atheroscler Thromb* 1(Suppl 1):S10–S13
17. Gerszten RE, Garcia-Zepeda EA, Lim Y-C et al (1999) MCP-1 and IL-8 trigger firm adhesion of monocytes to vascular endothelium under flow conditions. *Nature* 398:718–723
18. Wahren J, Ekberg K, Jornvall H (2007) C-peptide is a bioactive peptide. *Diabetologia* 50:503–509
19. Steffes MW, Sibley S, Jackson M, Thomas W (2003) Beta-cell function and the development of diabetes-related complications in the diabetes control and complications trial. *Diabetes Care* 26:832–836
20. Lee TC, Barshes NR, Agee EE, O'Mahoney CA, Brunicaudi FC, Goss JA (2006) The effect of whole organ pancreas transplantation and PIT on diabetic complications. *Curr Diab Rep* 6:323–327
21. Shapiro AM, Ricordi C, Hering BJ et al (2006) International trial of the Edmonton protocol for islet transplantation. *N Engl J Med* 355:1318–1330

22. Scalia R, Coyle KM, Levin BL, Booth G, Lefer AM (2000) C-peptide inhibits leukocyte endothelium interaction in the microcirculation during acute endothelial dysfunction. *FASEB J* 14:2357–2364
23. Gauthier TW, Scalia R, Murohara T, Guo JP, Lefer AM (1995) Nitric oxide protects against leukocyte-endothelium interactions in the early stages of hypercholesterolemia. *Arterioscl Thromb Vasc Biol* 15:1652–1659
24. De Caterina R, Libby P, Peng HB et al (1995) Nitric oxide decreases cytokine-induced endothelial activation. Nitric oxide selectively reduces endothelial expression of adhesion molecules and proinflammatory cytokines. *J Clin Invest* 96:60–68
25. Young LH, Ikeda Y, Scalia R, Lefer AM (2000) C-peptide exerts cardioprotective effects in myocardial ischemia-reperfusion. *Am J Physiol Heart Circ Physiol* 279:H1453–H1459
26. Rigler R, Pramanik A, Jonasson P et al (1999) Specific binding of proinsulin C-peptide to human cell membranes. *Proc Natl Acad Sci U S A* 96:13318–13323
27. Grabner R, Till U, Heller R (2000) Flow cytometric determination of E-selectin, Vascular cell adhesion molecule-1, and intercellular cell adhesion molecule-1 in formaldehyde-fixed endothelial cell monolayers. *Cytometry* 40:238–244
28. Tse HM, Milton MJ, Piganelli JD (2004) Mechanistic analysis of the immunomodulatory effects of a catalytic antioxidant on antigen-presenting cells: implication for their use in targeting oxidation-reduction reactions in innate immunity. *Free Radic Biol Med* 36:233–247
29. Diabetes Control and Complications Trial Research Group (1993) The effect of intensive treatment of diabetes on the development and progression of long-term complications in insulin-dependent diabetes mellitus. *N Engl J Med* 329:977–986
30. Johansson BL, Borg K, Fernqvist-Forbes E, Kernell A, Odergren T, Wahren J (2000) Beneficial effects of C-peptide on incipient nephropathy and neuropathy in patients with type 1 diabetes: a three-month study. *Diabet Med* 17:181–189
31. Ekberg K, Brismar T, Johansson BL et al (2007) C-Peptide replacement therapy and sensory nerve function in type 1 diabetic neuropathy. *Diabetes Care* 30:71–76
32. Hansen A, Johansson BL, Wahren J, von Bibra H (2002) C-peptide exerts beneficial effects on myocardial blood flow and function in patients with type 1 diabetes. *Diabetes* 51:3077–3082
33. Kobayashi Y, Naruse K, Hamada Y et al (2005) Human proinsulin C-peptide prevents proliferation of rat aortic smooth muscle cells cultured in high-glucose conditions. *Diabetologia* 48:2396–2401
34. Walcher D, Babiak C, Poletsek P et al (2006) C-peptide induces vascular smooth muscle cell proliferation: Involvement of Src-kinase, phosphatidylinositol 3-kinase, and extracellular signal-regulated kinase 1/2. *Circulation Res* 99:1181–1187
35. Gerrity RG (1981) The role of the monocyte in atherogenesis: II. Migration of foam cells from atherosclerotic lesions. *Am J Pathol* 103:191–200
36. Dansky HM, Barlow CB, Lominska C et al (2001) Adhesion of monocytes to arterial endothelium and initiation of atherosclerosis are critically dependent on vascular cell adhesion molecule-1 gene dosage. *Arterioscler Thromb Vasc Biol* 21:1662–1667
37. Vish M, Mangeshkar P, Piraino G et al (2007) Proinsulin C-peptide exerts beneficial effects in endotoxic shock in mice. *Crit Care Med* 35:1348–1355
38. Elhadd TA, Kennedy G, Hill A et al (1999) Abnormal markers of endothelial cell activation and oxidative stress in children adolescents and young adults with type 1 diabetes with no clinical vascular disease. *Diabetes Metab Res Rev* 15:405–411
39. Toivonen A, Kulmala P, Savola K, Akerblom HK, Knip M, The Childhood Diabetes In Finland Study Group (2001) Soluble adhesion molecules in preclinical type 1 diabetes. The Childhood Diabetes in Finland Study Group. *Pediatr Res* 49:24–29
40. Devaraj S, Cheung AT, Jialal I et al (2007) Evidence of increased inflammation and microcirculatory abnormalities in patients with type 1 diabetes and their role in microvascular complications. *Diabetes* 56:2790–2796
41. Cifarelli V, Libman IM, DeLuca A, Becker D, Trucco M, Luppi P (2007) Increased expression of monocyte CD11b (Mac-1) in overweight recent-onset type 1 diabetic children. *Rev Diabet Stud* 4:112–117
42. Kunt T, Forst T, Fruh B et al (1999) Binding of monocytes from normolipidemic patients with type 1 diabetes to endothelial cells is increased in vivo. *Exp Clin Endocrinol Diabetes* 107:252–256
43. Lindahl E, Nyman U, Melles E et al (2007) Cellular internalization of proinsulin C-peptide. *Cell Mole Life Sci* 64:479–486
44. Cifarelli V, Luppi P, Tse MT, He J, Piganelli J, Trucco M (2008) Human proinsulin C-peptide reduces high glucose-induced proliferation and NF- $\kappa$ B activation in vascular smooth muscle cells. *Atherosclerosis*. DOI [10.1016/j.atherosclerosis.2007.12.060](https://doi.org/10.1016/j.atherosclerosis.2007.12.060)
45. Walcher D, Aleksie M, Jerg V et al (2004) C-peptide induces chemotaxis of human CD4-positive cells: involvement of pertussis toxin-sensitive G-proteins and phosphoinositide 3-kinase. *Diabetes* 53:1664–1670
46. Johansson BL, Wahren J, Pernow J (2003) C-peptide increases forearm blood flow in patients with type 1 diabetes via a nitric oxide-dependent mechanism. *Am J Physiol Endocrinol Metab* 285: E864–E870